Transoesophageal Echocardiography in Anaesthesia and Intensive Care Medicine

Second edition

Edited by

Jan Poelaert

Clinical Director, Cardiac Anaesthesia and Postoperative Cardiac Surgical Intensive Care Unit, Gent University Hospital, Gent, Belgium

Karl Skarvan

Professor of Anaesthesiology, University of Basel, Kantonsspital Basel, Basel, Switzerland

BMJ Books

Transoesophageal Echocardiography in Anaesthesia and Intensive Care Medicine

Second edition

Transoesophageal Echocardiography in Anaesthesia and Intensive Care Medicine

Second edition

Edited by

Jan Poelaert

Clinical Director, Cardiac Anaesthesia and Postoperative Cardiac Surgical Intensive Care Unit, Gent University Hospital, Gent, Belgium

Karl Skarvan

Professor of Anaesthesiology, University of Basel, Kantonsspital Basel, Basel, Switzerland

BMJ Books

First published in 2000
by BMJ Books, BMA House, Tavistock Square,
London WC1H 9JR

First edition 2000
Second edition 2004

www.bmjbooks.com

British Library Cataloguing in Publication Data

A catalogue record for this book is available from the British Library

ISBN 0 7279 1796 X

Typeset by SIVA Math Setters, Chennai, India
Printed and bound in Malaysia by Times Offset

Contents

Contributors

Ruggero Amà
Research Fellow, Cardiac Anaesthesia and Postoperative Surgical ICU, Department of Intensive Care, University Hospital, Gent, Belgium

Dominique Bettex
Assistant Professor of Anaesthesiology, Division of Cardiac Anaesthesia, Institute of Anaesthesiology, University Hospital (USZ) Zürich, Switzerland

Michael K Cahalan
Professor of Anesthesiology and Chairman, Department of Anesthesiology, University of Utah, Salt Lake City, USA

Pierre-Guy Chassot
Associated Professor of Anaesthesia, Head of Cardiac Anaesthesia Division, Department of Anaesthesiology, CHUV, Lausanne, Switzerland

Fiona Clements
Professor of Anesthesiology, Heart Center, Duke University, Durham, USA

Stefan G De Hert
Professor of Anaesthesiology, Director of the Division of Cardiothoracic and Vascular Anaesthesia, University Hospital, Antwerp, Belgium

Joachim M Erb
Staff Anaesthesiologist, Head Intraoperative Echocardiography, Deutsches Herzzentrum Berlin, Anaesthesiology Clinic, Berlin, Germany

Raimund Erbel
Professor of Cardiology, Director of Division of Cardiology, Zentrum Für Innere Medizin, Medizinische Klinik und Poliklinik, Universitätsklinikum Essen, Hufelandstrasse, Germany

Miodrag Filipovic
Assistant Professor of Anaesthesiology, Department of Anaesthesia, University of Basel, Kantonsspital Basel, Basel, Switzerland

Clemens-Alexander Greim
Professor of Anaesthesiology, Clinic of Anaesthesiology, University of Würzburg, Würzburg, Germany

Frank Hinder
Associate Professor of Anaesthesiology, Department of Anaesthesiology and Surgical Intensive Care Medicine, University Hospital UKM, Münster, Germany

Bijoy K Khandheria
Professor of Medicine, Mayo Medical School Consultant, Cardiovascular Diseases and Internal Medicine, Mayo Clinic and Chair, Information Management and Technology Committee, Mayo Clinic, Rochester, Minnesota, USA

John D Kneeshaw
Consultant Anaesthetist, Department of Anaesthesia and Critical Care, Papworth Hospital, Papworth Everard, UK

Steven N Konstadt
Professor of Anesthesiology, Department of Anesthesiology, Co-director, Division of Cardiothoracic Anesthesia, Mount Sinai School of Medicine, New York, USA

Heinz M Loick
Professor of Anesthesiology, Director, Clinic of Anaesthesiology and Operative Intensive Care Medicine, Marien Hospital, Euskirchen, Germany

Herman FJ Mannaerts
Associate Professor of Cardiology, Department of Cardiology, VU Medical Center, Amsterdam, the Netherlands

Isabelle Michaux
Associate Professor, Department of Intensive Care Medicine, Mont-Godinne University Hospital, Université Catholique de Louvain, Yvoir, Belgium

Yasu Oka
Professorial Lecturer, Department of Anesthesiology, Division of Cardiothoracic Anesthesia, Mount Sinai Medical Center, New York, USA

Kazumasa Orihashi
Associate Professor, First Department of Surgery, Hiroshima University School of Medicine, Hiroshima, Japan

Jan Poelaert
Professor and Clinical Director, Cardiac Anaesthesia and Postoperative Cardiac Surgical Intensive Care Unit, University Hospital, Gent, Belgium

Norbert Roewer
Professor of Anaesthesiology, Director, Clinic of Anaesthesiology, University of Würzburg, Würzburg, Germany

Christoph Schmidt

Associate Professor of Anaesthesiology, Department of Anaesthesiology and Surgical Intensive Care Medicine, University Hospital UKM, Münster, Germany

Manfred D Seeberger
Associate Professor of Anaesthesiology, Head of Cardiac Anaesthesia Division, University of Basel, Kantonsspital Basel, Based, Switzerland.

Jack S Shanewise
Professor of Anesthesiology, Division of Cardiothoracic Anesthesiology, Emory University School of Medicine, Atlanta, Georgia, USA

Karl Skarvan
Professor of Anaesthesiology, Department of Anaesthesia, University of Basel, Kantonsspital Basel, Basel, Switzerland

Daniel M Thys
Professor of Anesthesiology, Chairman, Department of Anesthesiology, St Luke's-Roosevelt Hospital Center and Department of Anesthesiology, College of Physicians and Surgeons, Columbia University, New York, USA

Hugo Van Aken

Professor of Anaesthesiology, Chairman, Department of Anaesthesiology and Surgical Intensive Care Medicine, University Hospital UKM, Münster, Germany

Cees A Visser
Professor of Cardiology, Chairman, Department of Cardiology, University Hospital, Free University of Amsterdam, Amsterdam, the Netherlands

Thomas Wichter
Associate Professor of Internal Medicine, Department of Cardiology, University Hospital UKM, Münster, Germany

Preface

The four years that have passed since the first edition of this textbook represent only a short period of the twenty-year history of perioperative transoesophageal echocardiography (TOE). Nevertheless, the new information obtained through research and educational activity in this field during the last four years justifies an updated second edition of this textbook. The new title of our textbook, TOE in Anaesthesia and Intensive Care Medicine, reflects the present wide deployment of TOE in cardiac and non-cardiac surgical patients as well as in non-surgical critically ill patients. The chapters from the first edition have been revised, updated or completely rewritten to incorporate the numerous new publications generated in the field of perioperative TOE.

Important developments in the field of ultrasound technology, such as three-dimensional echocardiography, contrast echocardiography, and tissue doppler imaging, have entered the practice of echocardiography during these last four years. We considered including new chapters that would comprehensively cover these techniques; however, we believe that the present impact of these methods on the practice of perioperative TOE does not yet justify extensive coverage in the present textbook. Nonetheless, we do feel that contrast echocardiography, tissue doppler imaging, and three-dimensional echocardiography are promising additions to perioperative TOE and their principles as well as clinical applications are covered in Chapters 1, 7, and 11. We have also added a new chapter covering the use of TOE during mechanical ventricular assistance, implantation of an artificial heart, and heart transplantation (Chapter 15) in response to the suggestions of our readers.

Our goal is to provide the present and future practitioners of TOE with a comprehensive and updated review of perioperative TOE. We believe that it would have been wrong to restrict the material to only the technical and sonographic aspects of TOE. Therefore, the TOE findings are not presented in isolation, but are accompanied by relevant physiological and clinical data. We hope that this additional information helps the readers to better understand the findings and that it will help them integrate TOE into the diagnostic process in both the operating theatre and in the intensive care unit.

The method of TOE in its existing form satisfies the needs of both anaesthetists and intensivists. Therefore, the main emphasis can now be shifted from the acquisition of new and highly sophisticated techniques to training and certification of physicians who care for cardiac, critically ill, or traumatized patients in operating theatres, intensive care units, and emergency wards. Today a critical and timely diagnosis need never again be missed because of the unavailability of a physician who is certified in TOE. Important guidelines for training and certification of physicians in perioperative TOE were recently published and are included in Chapters 17 and 18. Whereas in the first edition only the certification process in the USA was described, in this edition, we have added a review of the present educational situation of perioperative TOE in Europe and its future prospects are presented.

A prerequisite for proper documentation of perioperative findings is the use of universally accepted terminology for TOE imaging. Chapter 2 describes the practice of perioperative TOE and the whole potential of multiplane TOE imaging in the traditional way. Nevertheless, the twenty TOE images that were recommended in the guidelines for comprehensive intraoperative TOE examination by the American Society of Anesthesiologists and the Society of Cardiovascular Anesthesiologists Task Force are also presented and the corresponding terminology is used throughout this edition. Some structures cannot be interrogated or correctly imaged in the selected views because of anatomic or pathologic causes. Therefore, the knowledge of alternative views that can be made possible by multiplane TOE imaging remains important.

The findings obtained by perioperative TOE must be stored and readily available to the physicians who might subsequently need them. Comprehensive TOE documentation, including stored images and written reports based on the recommendation mentioned above, may not be feasible in every institution or in every situation. Therefore, we also provide an example of a more realistic TOE report based on a minimum set of TOE images.

Our textbook is the result of a collective effort, and therefore some overlaps are inevitable. Examples are the assessment of intracardiac pressures or of ventricular filling patterns. These techniques and findings are discussed in several chapters in accordance with the respective context. We accepted such minor overlaps when the information appeared useful for the structure of these chapters.

We greatly appreciate the contribution of all the authors to this revised edition and thank them for their willing cooperation. We also extend our thanks to Joan Etlinger of the Department of Anaesthesia in Basel for her invaluable support, to Christina Karaviotis at BMJ Books for her outstanding editorial work and Mary Banks for her ongoing encouragement.

Jan Poelaert
Karl Skarvan

Abbreviations

2D	two-dimensional
3D	three-dimensional
ABD	automated border detection
AR	aortic regurgitation
ARDS	acute respiratory distress syndrome
AS	aortic stenosis
ASD	atrial septal defect
AV	aortic valve
AVA	aortic valve area
BVAD	biventricular assist device
CABG	coronary artery bypass grafting
CAD	coronary artery disease
CF	colour flow
CI	cardiac index
CPB	cardiopulmonary bypass
CS	coronary sinus
CT	computed tomography
CW	continuous wave
CVP	central venous pressure
EAC	endoaortic clamp
ECG	electrocardiogram/electrocardiography
EDA	end-diastolic area
EDD	end-diastolic diameter
EDV	end-diastolic volume
ESA	end-systolic area
ESD	end-systolic diameter
ESV	end-systolic volume
FAC	fractional area change
FVR	flow velocity ratio
IABP	intraaortic balloon pump
IAS	interatrial septum
ICU	intensive care unit
IVC	inferior vena cava
IVCT	isovolumic contraction time
IVRT	isovolumic relaxation time
IVS	interventricular septum
LA	left atrium/left atrial
LAA	left atrial appendage
LAD	left anterior descending coronary artery
LAP	left atrial pressure
LAX	long axis
LCX	left circumflex coronary artery
LLPV	left lower pulmonary vein
LUPV	left upper pulmonary vein
LV	left ventricle/left ventricular
LVAD	left ventricular assist device
LVOT	left ventricular outflow tract
MOE	mid-oesophageal
MPI	myocardial performance index
MR	mitral regurgitation
MRI	magnetic resonance imaging
MVG	myocardial velocity gradient
PA	pulmonary artery
PCWP	pulmonary capillary wedge pressure
PFO	patent foramen ovale
PISA	proximal isovelocity surface area
PM	papillary muscle
PRF	pulse repetition frequency
PW	pulsed wave
PWR_{max}	maximal ventricular power
RAP	right atrial pressure
RCA	right coronary artery
RLPV	right lower pulmonary vein
RUPV	right upper pulmonary vein
RV	right ventricle/right ventricular
RVAD	right ventricular assist device
RVIT	right ventricular inflow tract
RVOT	right ventricular outflow tract
SAX	short axis
SR	strain rate
SV	stroke volume
SVC	superior vena cava
SWMA	systolic wall motion abnormality
TAH	total artificial heart
TAPSE	tricuspid annular plane systolic excursion
TDI	tissue Doppler imaging
TG	transgastric
TOE	transoesophageal echocardiography
TOF	tetralogy of Fallot
TR	tricuspid regurgitation
TTE	transthoracic echocardiography
UOE	upper oesophageal
VAD	ventricular assist device
VSD	ventricular septal defect
VTI	velocity time integral

1 Physical principles of ultrasound

Pierre-Guy Chassot

Definitions

Ultrasound represents a mechanical pressure disturbance propagating as waves through materials that are dense enough to transmit the fast oscillations imparted on molecules (Figure 1.1). Their frequencies are much higher than those perceptible to the human ear; for medical purposes they range from 2 to 12 MHz (1 MHz = 10^6 Hz).[1] Ultrasound waves have certain properties:

- they can be orientated like beams
- they follow the physical laws of reflection and refraction
- they are reflected by dense materials
- they propagate freely in liquids but very poorly through air.

A wave is defined by three physical terms: its velocity (c), its frequency (f), and its wavelength (λ). They are linked together by a simple relationship:

$$c = f \times \lambda \qquad (1.1)$$

In human soft tissues the speed of ultrasound (c) is assumed to be fairly constant; its mean value is 1540 m/s.[2] The equation above implies that frequency and wavelength vary in an opposite manner; the lower the frequency, the longer the wavelength. The spatial resolution, which is the minimum distance between two objects at which they can be differentiated, is increased when the frequency is higher; this is because the wavelength must be shorter than this distance if the two objects are to be distinguished from each other. The resolution is higher along the travelling axis (axial resolution) than it is perpendicularly because it depends only on the physical properties of the ultrasound wave; this resolution is in the 0·5–1 mm range.[3] In the lateral direction images are

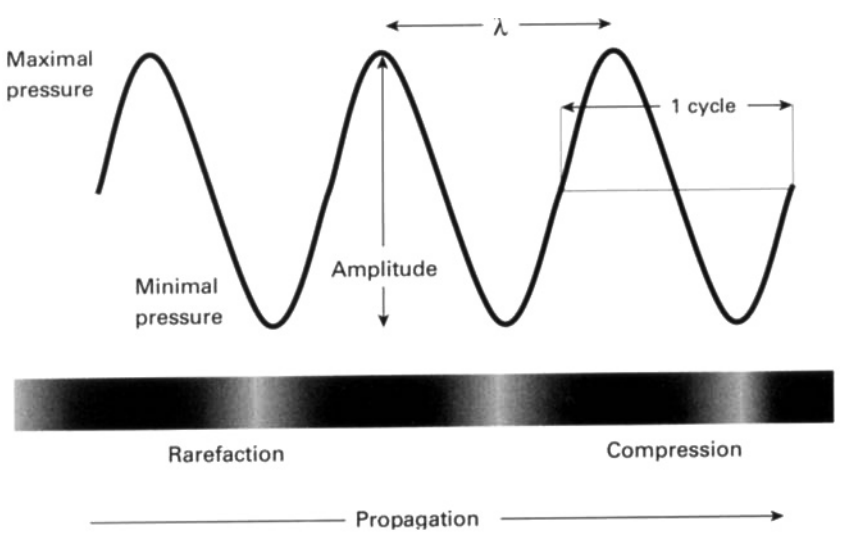

Figure 1.1 Ultrasound wave. The wave amplitude defines its intensity (in decibels [dB]). One cycle consists of one compression and one rarefaction. The wavelength is the distance between two maximal pressure values. Frequency is the number of cycles per second (1 cycle/s = 1 Hz).

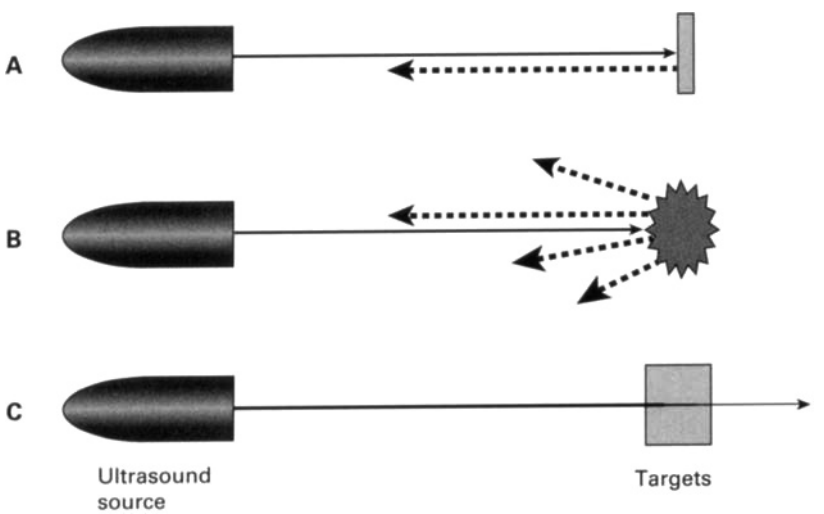

Figure 1.2 Interference between an ultrasound wave and a target. **(A)** Specular reflection: a flat, perpendicular object reflects completely the beam back to the transducer. If the angle between the beam and the target is too great then the echo is reflected away from the transducer and the object is not visible. **(B)** Scattering: the target is irregular and small compared with the wavelength; the beam is scattered in multiple directions, and some waves travel back to the transducer. **(C)** Attenuation: the tissue absorbs the energy of the ultrasound beam, the power of which decreases as it crosses the object. Natural structures are inhomogenous; they behave as a mixture of specular reflection, scattering, and attenuation.

obtained by summing up the scanning lines of the apparatus (121–484 lines/90° field); the precision depends on the electronic properties of the system, and is usually 1–3 mm. On the echo image a tiny structure may be missed if it is parallel to the ultrasound beam, although it is visible when it is perpendicular to the axis of propagation.

In order to provide an image the ultrasound wave must be reflected at the interface between two materials that are of different densities, representing an acoustic impedance mismatch;[4] the greater this difference, the stronger the echo. When an ultrasound beam hits an acoustic interface, three main phenomena become apparent (Figure 1.2).

- Specular reflection. The surface of the object is smooth and large compared with the emitted wavelength. When the plane is orthogonal to the direction of sound propagation, the incident energy is reflected back to the transducer; its amplitude depends only on the difference in acoustic impedance. When the interface is not orthogonal to the incident beam, the angle of reflection is the reciprocal of the angle of the incident beam; if this angle is too large then the direction of the reflected beam might be away from the emission source, and the object will not be visible.
- Diffused scatterers. When the surface is irregular and the reflectors small in comparison with the emitted wavelength, the energy is diffused or scattered in multiple directions. Only a small fraction of this radiation travels back toward the imaging transducer. These rough surfaces are typical of anatomical edges; because of the scattering, they are visualised even if they are not perpendicular to the direction of the ultrasound beam.
- Attenuation. The ultrasound waves impose vibrations on the tissues, in which frictional forces absorb energy. The beam loses power by travelling through the tissues; this is known as attenuation. It varies exponentially with distance, and increases linearly with emitting frequency. Transducers of higher frequencies (7–12 MHz) provide images with finer resolution, but they attenuate more easily and do not penetrate as deeply as do ultrasound waves of lower frequencies (< 5 MHz). Thus, attenuation introduces a trade-off between the depth of penetration and the image resolution.

Attenuation can be defined as the distance that ultrasounds can travel through the milieu before losing half of their power. For water this distance is 380 cm, for blood it is 15 cm, and for air it is 0·08 cm.[2] This illustrates the fact that ultrasound waves do not propagate through air and are strongly reflected by bubbles, which appear as bright spots.

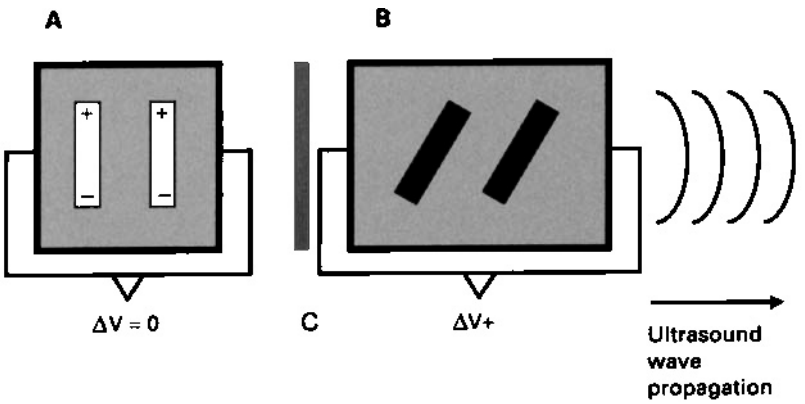

Figure 1.3 Piezoelectric crystal. **(A)** No current is applied and the crystal is at rest. **(B)** When stimulated by an electrical current (Δ V +), the molecules of the piezoelectric crystal change their orientation, the size of the crystal expands, and ultrasound waves are emitted. A strong backing (C) absorbs waves emitted in any direction other than to the front of the transducer.

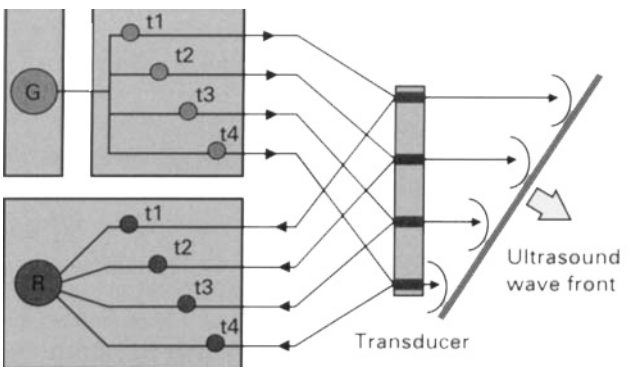

Figure 1.4 Phased-array transducer. The direction of the beam constructed by waves of different elements of the transducer is determined by the delay in stimulation of these elements imparted by the pulse generator (G). This delay is regulated by an electronic clock. The same delay is imposed at the reception by the receiving device (R), which allows the image to be reconstructed by the computer.

Transducers

Transducers are made of piezoelectric crystals, which have the property of changing shape and expanding when they are stimulated by an electrical current (Figure 1.3). Applying an alternating voltage through the crystal causes the element to vibrate and produce ultrasound waves. Inversely, it generates an electric field when it receives a pressure wave. It acts as a converter between pressure energy and electrical energy, and can function as both emitter and receiver. Transoesophageal transducers are of the phased-array type. These transducers are made of a group of 64–256 piezoelectric crystals. The wave front of simultaneously stimulated crystals is flat, perpendicular to the beam direction, and parallel to the surface of the transducer. In order to scan an area the beam is steered by exciting the individual crystals at slightly different time points. When a time delay is introduced into the excitation of successive crystals, the resulting beam can be aimed in a given direction (Figure 1.4). The resulting wavefront is still a flat one but at a defined angle with respect to the array surface; this angle depends only on the time intervals between the emissions from individual crystals.[5] The beam can be steered in a stepwise manner over an area without mechanical rotation of the transducer. It is also possible to focus the beam by exciting the peripheral elements before the central ones; the wavefront is concave toward a focal point. To increase the length of the parallel beam, some scanners can generate multiple focal zones. With focalisation at reception, or dynamic focusing, the signals received from each element are delayed by a variable amount of time from periphery to centre in order to reconstruct a concave wavefront coming from the focal area.

Similar to the light from a torch, the ultrasound is confined to a beam that diverges progressively. The narrow proximal part is composed of parallel individual beams, in which the energy and the precision are higher than in the diverging far field (Figure 1.5A). The length of the proximal field can be increased by increasing the dimension or the frequency of the transducer. The beam has a two-dimensional (2D) shape, the thickness of which (controlled by vertical focusing) determines the slice thickness of the imaging plane (Figure 1.5B).

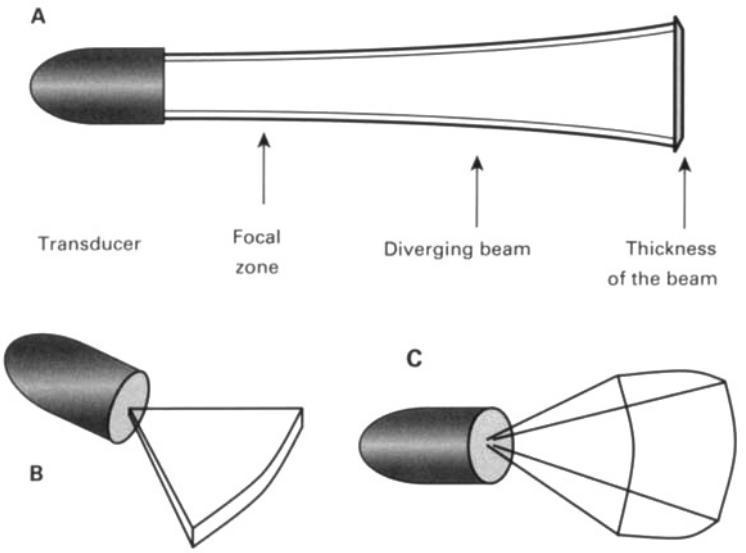

Figure 1.5 Transducer beam. **(A)** The proximal part of the beam is concentric and parallel; beyond the focal zone it diverges. **(B)** The spatial configuration of the beam is bidimensional; the quality of the anatomical slice of tissue appearing on the screen is inversely proportional to its thickness. **(C)** Pyramidal volume of a three-dimensional matrix transducer.

Working rates

Ultrasound images are constructed by sending small pulses of ultrasound waves into the organism and listening to the echoes reflected back by anatomical structures. The core of an echo scanner is a timer; the time lag between the start pulse and the received echo (Δt) is proportional to the distance (D) between the transducer and the reflecting object, because the speed of the ultrasound is constant through the blood and tissues.[6] The ultrasound pulse travels twice the distance because it must hit the object and return to the transducer.

$$\Delta t = \frac{2D}{c} \qquad (1.2)$$

$$D = \frac{\Delta t \times c}{2} \qquad (1.3)$$

For cardiac examination from the oesophagus or the chest wall, this time delay is 0·02–0·3 ms. Setting the depth of scanning on the instrument consists of modifying the time delay at reception.

The duration of the ultrasound packet is called the pulse length (or width), and the time interval between the pulses of emission is the pulse repetition frequency (PRF). The transducer uses only 1 or 2 μs for emission and waits 0·25 ms for the returning echoes; it spends 99·99% of its working time receiving. The rate of this cycle is 1000 to 6000 per second.[7] The deeper the reflecting object, the longer the time needed for the echoes to reach the transducer and the lower the PRF. On the other hand, the PRF increases when the ultrasound frequency diminishes; it is higher for a 2-MHz than for a 7-MHz probe. The PRF also increases when the pulse length, or duration, decreases. These shorter ultrasound pulses provide better axial resolution but their tissue penetration is poorer than that of longer pulses.

The frame rate is the frequency of image renewal on the screen; it varies from 5 to 120 images per second. The time taken to complete each scan line depends on the depth of the tissue examined, the width of the field, and any additional processing of the data, such as simultaneous Doppler analysis. If we assume a depth range of 18 cm, then the reception time for all echoes is 240 μs. Because the delay between emissions is about 60 μs, the total duration of one analysis is 300 μs. This can be done 3333 times per second, and this is the PRF. On a 90° field with 120 scan lines, this must be done 120 times successively: 120×300 μs = 36 000 μs = 36 ms. This can be achieved 28 times per second. The frame rate is thus 28 images per second.[5] The frame rate can be increased by narrowing the field and reducing the depth of interrogation. At a depth of 8 cm with a field of 20° the frame rate is 120 images per second, but at a depth of 24 cm and with a field of 90° the frame rate slows to 30 images per second. Adding processing time, such as colour Doppler added to the whole screen, further reduces the frame rate to 8 images per second.[8] The image appears jerky (like an old movie) when the frame rate is lower than 15 images per second. If the observer requires a continuous motion image to observe a fast moving structure, it is of the

utmost importance to reduce the field and the depth, and maintain the colour Doppler window to the minimum size.

Electronic processing

In order to obtain an accurate image on the screen, the raw data from the transducer must be processed in many ways. These procedures occur both before (preprocessing) and after (postprocessing) acquisition of digital data by the central processor of the apparatus.[9] An analogue–digital converter feeds the data into the computer's central memory, where the data are organised into 121–484 axial scan lines and 128–512 horizontal lines, for a total amount of 15 000–240 000 pixels.

Preprocessing

Many different controls must be adjusted correctly in order to provide useful images on the screen.

- Transmission. This control allows the emitting power of the instrument to be specified (in dB).
- Gain. The gain control allows the strength of all returning echoes to be modified.
- Compression. This control modifies the grey scale on the screen by reducing the intensity scale according to a non-linear curve by compressing the ultrasound spectrum from 0–100 dB to 0–40 dB.
- Filter. The filter allows elimination of low frequency (<200 Hz) and high amplitude (>80 dB) echoes during Doppler examination; these echoes correspond to wall motion but not to blood flow.
- Reject control. The reject control allows one to set the acoustic level below which weak echoes are eliminated; the remaining echoes retain their full amplitude.
- Time–gain compensation. This control electronically amplifies the signals received in proportion to their depth, in order to compensate for loss of energy due to absorption by the tissues; the echoes are selectively amplified by slices of depth in order to provide the same intensity for the whole field.
- Lateral gain compensation. This control allows selective amplification by axial scan sectors.

Postprocessing

In order to provide a simultaneous image of the entire field explored by the transducer, the computer must store in memory the echoes from the closest structures while it awaits receipt of signals from deeper objects. This time delay is mandatory if a coherent picture on the screen is to be achieved. Thereafter, the digitised images can be processed in several ways without imposing a reduction in frame rate.

- Dynamic focusing. (See under Transducers, above.)
- Remapping. The brightness levels of grey shades (128 or 256 different values) are non-linearly processed into a different scale, which amplifies weak echoes and dampens strong ones.
- Grey scale. The intensity of the different grey values can be adjusted.
- Convolution. Each pixel is combined to the eight surrounding ones to form a kernel; this process smoothes the image by an algorithm that fills the gaps between the different dots.
- Freezing. The on-line memory of the processor (2 GB RAM) stores images of the past few seconds; they can be frozen and displayed frame by frame.
- Cine-loop. Cardiac cycles gated on the electrocardiogram are stored and played continuously. With a split-screen display, they can be compared side by side with the real-time image.

Many reconstructions and calculations can be performed after storage of the digitised images, such as automated endocardial border delineation, colourisation of movements, or regional contraction rates.

Two-dimensional, Three-dimensional, and M-mode images

The 2D display provides conventional anatomical tomography of the structures with a field of up to 90°. Three-dimensional (3D) images of the heart can be reconstructed off-line. A series of electrocardiographically gated views are recorded; this sequential acquisition is achieved by automatic rotation of a multiplane transducer or by longitudinal travelling of a single plane

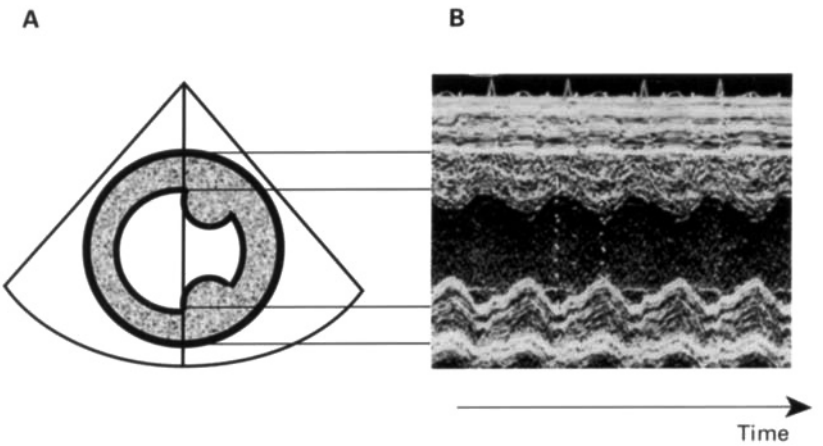

Figure 1.6 M-mode image. **(A)** Two-dimensional view of the short axis of the left ventricle; the M-mode axis cuts the cavity through its largest diameter. **(B)** M-mode image. The image recorded along the axis scrolls on the screen; contraction and relaxation of anterior and posterior walls appear as they occur along the time axis.

probe along the oesophagus. The data points obtained are digitised, decomposed according to their timing in the cardiac cycle, and reconstructed according to their position in space; the gaps are filled by geometric interpolation.[10] The 3D model of the heart corresponds to one cardiac cycle, like a cine-loop, and can be explored or cut along virtual planes. Acquisition and processing take a few minutes. With the increasing power of computers and with parallel processing technology, on-line 3D reconstruction of echo images is now possible with a matrix transducer made from 24×24 crystals, which insonifies a pyramidal volume (Figure 1.5C).[11] This technology exists only for transthoracic probes.

The motion mode, or M-mode, allows time–motion study of intracardiac structures with high temporal resolution. It interrogates the tissues along a single beam, and displays the cross-section of the heart in one dimension; on the screen the second dimension is the time (Figure 1.6). The high pulse repetition frequency (1000 cycles/s) is the main advantage of this mode, which has a high degree of precision for measuring dimensions and timing. Its interpretation is more difficult than that of the usual 2D image. To make recognition easier, M-mode analysis can be superimposed on the standard 2D image. For this purpose, the transducer shares the images between the 2D mode and the M-mode functions. In order to maintain the highest frame rate for M-mode images, the 2D frame rate is considerably reduced.

Doppler effect

In 1842 the Austrian physicist Johann-Christian Doppler described mathematically a well known phenomenon that is exemplified by the sound of a train whistle, which is high pitched when the train approaches and becomes lower as it moves away, although the emitting frequency is constant. A shift of frequency in recorded waves occurs when a luminous or acoustic source is in relative motion compared with the stationary observer (Figure 1.7). Whatever the speed of the source might be, the velocity of the sound is constant relative to the source and is determined by the characteristics of the medium through which it travels. When the source is approaching the receiver, following the generation of one wave, the sound source has moved slightly toward the receiver before sending the next wave; the two wave peaks are thus closer together, and the wavelength is shortened and the frequency increased.[7] This happens because the product of wavelength (λ) and frequency (f) is constant ($c = f \times \lambda$). If the source is moving away, the opposite is true; the wavelength increases and the frequency decreases. The Doppler shift is the difference between the frequency generated by the source and the frequency observed by the listener:

$$\Delta f = f_{observed} - f_{generated} \qquad (1.4)$$

This shift is proportional to the ratio of the speed of the object (V), to the velocity of the sound (c) and to the generated frequency, but is independent of the amplitude of the wave: the

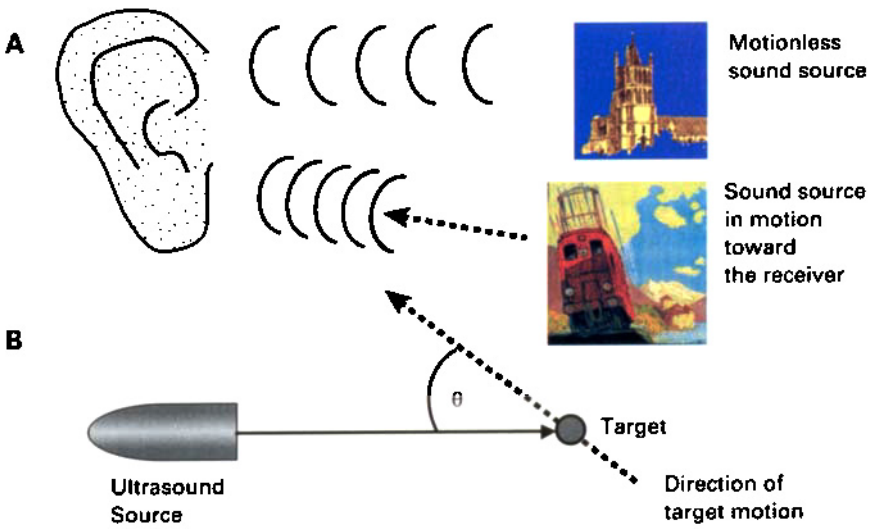

Figure 1.7 Doppler effect. **(A)** In contrast to the emission of sound from a motionless belfry, the sound waves from the horn of a train moving toward the receiver are compressed; thus, the frequency is increased and the pitch is higher. **(B)** Angle θ between the direction of movement of the target and the ultrasound beam axis.

$$\Delta f = \frac{V}{c} \times f_{generated} \qquad (1.5)$$

frequency shift can be positive or negative depending on whether the emitter is moving toward or away from the receiver. The same phenomenon occurs if a moving object is the target of an ultrasound wave emitted by a fixed source; the emitted echo wave and the echo wave returning to the transducer have different frequencies. They are also linked by the Doppler equation cited above but the frequency shift occurs twice, in the emitted and in the reflected wave:

$$\Delta f = \frac{V}{c} \times 2f_{generated} \qquad (1.6)$$

The formula is completed by an angle correction because the maximal shift is observed when the transducer orientation is parallel to the blood flow (Figure 1.7B). It can be rearranged to determine the velocity (V) of the target (equation 1.1):

$$V = \frac{c \times (\pm \Delta f)}{2f_{generated} \times \cos \theta} \qquad (1.7)$$

where θ is the angle between the direction of the target and the interrogating beam.

If the angle is 0 then the cosine is 1 and the Doppler effect is maximal. Perpendicular orientation of the interrogating beam to the axis of flow yields no Doppler shift, because the cosine of 90° is 0. Up to 20° (cosine 0·94), the underestimation induced by the angle in the measurement of velocity is smaller than 6% (approximately 5 cm/s) and is considered negligible for clinical purposes.[7] Although ultrasound systems can perform a correction for the angle of incidence in the Doppler formula calculation, this measurement is done in the displayed bidimensional plane only; there is no control on the perpendicular plane. Therefore, this angle correction is not recommended because it creates illusory precision.[12]

With respect to the usual blood flow velocities (0·2–6·0 m/s), to the speed of the ultrasound in tissues (1540 m/s), and to the emitting frequencies of the cardiac transducers (2–10 MHz), the Doppler shift falls within the range audible to the human ear (4–10 KHz) and can be heard through a loudspeaker. This sound is mathematically reproduced by addition or multiplication of emitted and received waves. The product of this operation is a new wave with a frequency equal to the Doppler shift.[4] Echocardiography is based on the time delay measurement between the emission of a short pulse of ultrasound and the detected echo. Doppler echo analyses variations in frequency, whereas 2D echo is based on variations in amplitude (or intensity) of returning waves. Therefore, Doppler analysis and 2D display require different conditions for optimal results. The best bidimensional image is obtained with a high frequency transducer (>5 MHz) and an interrogating beam perpendicular to the structure. The Doppler shift is maximal when the

ultrasound beam is parallel to the flow and when the emitting frequency is low (1–2 MHz).[8] In clinical practice, the setup of the echocardiographic machine must be adjusted appropriately for each function.

Instrumentation

Two Doppler systems are utilised for blood flow evaluation, both of which have specific characteristics: the continuous wave (CW) and the pulsed wave (PW) Doppler. Their analysis can be displayed on the screen using two different modes: spectral display or colour flow mapping. The beam axis, the sampling volume, and the colour image are overlayed on standard 2D images (duplex scanning) in order to localise anatomically the examined blood flow. Before we describe these systems, it is important to explain a phenomenon termed aliasing.

Aliasing

Any pulsating system observing an oscillating object will record anomalous images if its sampling rate is close to the vibration frequency of the observed structure. The Doppler effect generated by moving blood cells ($\Delta f = 4000$ to 10 000 cycles/s) has an oscillating frequency approaching the PRF of the observing instrument (PRF = 1000 to 6000 impulses/s). This proximity induces an artefact due to insufficient sampling, called aliasing. It is well illustrated by the apparent counter-rotation of a carriage wheel in a Western movie, which occurs when its number of rotations per second is superior to the number of images per second taken by the movie camera.[13] When the wheel rotation rate is much slower than the camera frame rate, the image is accurate. When the wheel rotates at a speed that is half the camera frame rate, the direction of rotation is no longer discernible, because the wheel spokes are at 180° on each neighbouring frame. If the rotation rate equals the sampling rate, then the film will catch the spokes of the wheel at the same point in each cycle and the wheel will appear motionless. Finally, when rotation rate exceeds the sampling rate, the wheel seems to be counter-rotating at an inaccurate and slow speed (Figure 1.8).

This sampling phenomenon introduces a limit above which the precision of movement is lost; the maximum frequency shift measurement is equivalent to one half of the sampling frequency. This limit is called the Nyquist limit:

$$\text{Nyquist limit} = \frac{\text{PRF}}{2} \qquad (1.8)$$

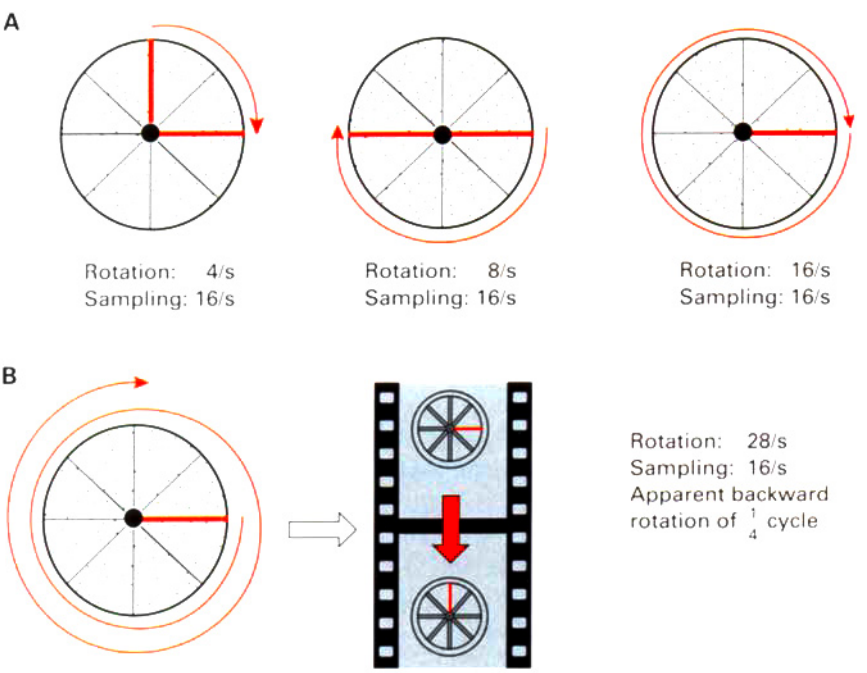

Fig. 1.8 Aliasing in a movie. **(A)** When the wheel rotation rate is much less than the camera frame rate, the image is accurate. When the wheel rotates at a speed that is half the camera frame rate, the direction of rotation is no longer discernible because the wheel spokes are at 180° on each neighbouring frame. If the rotation rate equals the sampling rate, then the film will catch the spokes of the wheel at the same position in each cycle and the wheel appears motionless. **(B)** Aliasing occurs when the rotation rate exceeds the sampling rate; the wheel appears then to be counter-rotating at an inaccurate and slow speed. (Adapted from Chassot.[38])

To represent a frequency signal (fs) correctly, it must be sampled at least twice for each cycle of the signal. The pulse repetition frequency of the computer must be superior to two oscillating periods of the observed wave, in this instance the Doppler shift Δ f (Figure 1.9):[14]

$$PRF \geq 2fs \text{ or } PRF \geq 2\ \Delta f \qquad (1.9)$$

If the Doppler frequency shift is superior to one half of the PRF, then aliasing occurs. The instrument reports a spurious value equal to the true Doppler shift minus the PRF. On the spectral frame the velocity curve appears as artificially reversed on the other side of baseline (see Figure 1.13, below). In colour flow, aliasing appears as an area of reversed colour (see Figure 1.16, below). By increasing the PRF the Nyquist limit can be raised, and thus the ability to obtain high velocity recordings is also increased. This is done by the technique called high-PRF PW Doppler.

Aliasing can be limited by reducing the emitting frequency of the transducer or by increasing the PRF. The presence of aliasing in a flow does not mean turbulence but rather indicates increased velocity; the flow may stay laminar.

Continuous and pulsed wave Doppler

The CW Doppler equipment transmits and receives the ultrasound signal continuously and simultaneously using two separate crystals, one for emission and one for reception (Figure 1.10A). It records all velocities in the area of overlap between the emitted and the returning beams, at any depth and at any frequency shift. There are no limitations on analysis of high velocities because the emission is continuous and therefore has an infinite pulse repetition frequency. However, it lacks the spatial resolution necessary to determine the exact depth from which the measurement was obtained; because emission and reception are continuous, the computer cannot define when, and therefore where, the emitted waves are reflected by the moving target.

In PW Doppler the transducer emits a short burst of ultrasound waves (3–6 waves) and awaits the return of the reflected waves (Figure 1.10B). Because it alternates between transmitting bursts of ultrasound energy and receiving echoes, it is able to calculate the time delay for the echoes to arrive at the transducer, and can interrogate the blood flow in a specific region. It waits until the echo from a prespecified location reaches the transducer, whereupon it opens an electronic gate to read the signal; the gate shuts after reading the signal for a fixed duration.[15] The duration of this gate opening determines the length of the exploring window, or sample volume (Figure 1.10C). This volume appears as brackets that can be moved along the Doppler cursor on the screen (depth of the sample) and the window length can be modified (duration of echo listening). The sensitivity rises when the dimension of this

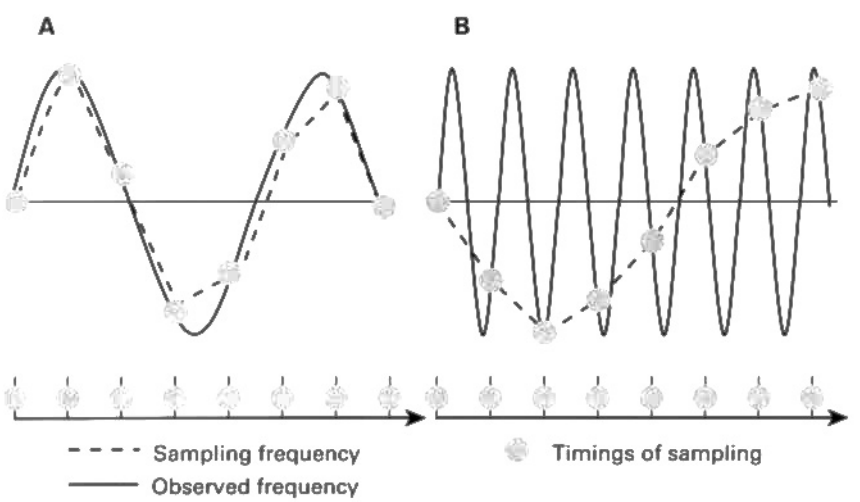

Figure 1.9 Aliasing in computer sampling. **(A)** When the pulse repetition frequency (PRF) of the sampling device (dotted line) is greater than the oscillatory frequency of the observed phenomenon (full line), the sampling is adequate and no aliasing occurs. **(B)** When the PRF is much slower then the oscillatory frequency of the object, the sampling is inadequate and aliasing occurs; the frequency of the sampling curve (dotted line) in inappropriately low in comparison with the real frequency of the phenomenon (full line).

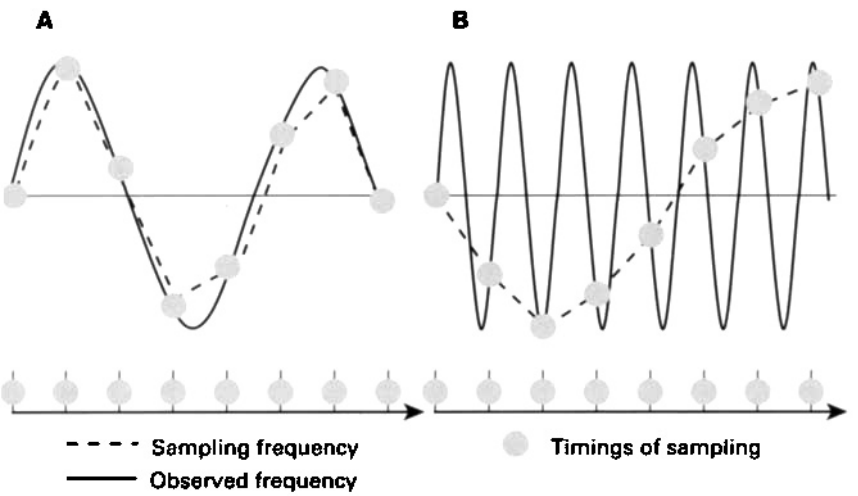

Figure 1.10 Continuous wave (CW) and pulsed wave (PW) Doppler instruments. **(A)** CW transducer emits and receives simultaneously through two different crystals; the zone of overlap between the emitted and reflected beams is the sampled volume. **(B)** At t1 the PW transducer emits bursts of ultrasound toward the moving target and awaits receipt of their reflection at t2. **(C)** The reception delay defines the depth of observation; the sampling volume is determined by the duration of observation. (Adapted from Chassot.[38])

window increases, because a larger sample volume contains more blood cells and produces stronger signals, but the axial resolution diminishes because the location is less precise. The delay (Δt) defines the depth (D) of the target; it is the time necessary for the ultrasound of known speed (c) to make a roundtrip between the transmitter and its target:

$$D = \frac{c \times \Delta t}{2} \qquad (1.10)$$

This precision in the location of the source of frequency shift has a drawback; it limits the velocity range that the instrument can read. Three facts account for this phenomenon.

- The sampling rate. The frequency overlap between PRF and Doppler shift gives rise to aliasing.
- The emitting frequency of the probe, which is in the denominator of equation 1.7 (see above). At the same PRF, the maximum recordable velocity with a 5-MHz probe is half the velocity determined by a 2·5-MHz probe.[3]
- The depth of the sampling gate. The deeper the interrogated target, the longer the waiting time between two pulse emissions. The maximum recordable velocity diminishes when the PRF decreases; it is 2·3 m/s at 8 cm with a 2·5-MHz probe, but at 16 cm with a 5-MHz probe it is only 0·65 cm/s.[8]

In order to enable the measurement of higher velocities, a modification called high-PRF has been implemented on most echo machines. In this system the PRF is multiplied by 1–4. A new burst of ultrasound waves is sent before the electronic receiving gate is opened to returning echoes. It therefore increases the number of sampling sites, but it introduces a range ambiguity because it is not possible for the computer to determine the gate from which each echo was received.[7] Fortunately, the gates are pictured over the bidimensional images, and the examiner can assume which sample volume lies where the recorded flow velocity is expected. The actual PRF is determined by the most proximal sample volume, but the most distal one is used for sampling flow in the zone of interest.[12]

An additional problem occurs with PW technology. The bursts of ultrasound waves are produced at a certain rhythmic period; this introduces an additional frequency into the emission (i.e. the frequency of bursts of ultrasound waves). This frequency is also Doppler shifted by the moving blood, and the resultant velocity profile is less clearcut than in CW Doppler and is affected by significant spectral broadening.[16]

Spectral display

In order to display Doppler information, the apparatus must reproduce the spectrum of frequency shifts, and this spectrum must be updated regularly during the cardiac cycle. The Doppler signal is a complex wave, containing information about the motion of all blood cells and tissues moving at a variety of velocities. In

the spectral mode, this shift is visually displayed as a power spectrum of frequency against time. The signal is processed in segments of 1–5 ms duration by the computer, and a mathematical calculation termed fast Fourier transform is performed on each segment to resolve the Doppler signal into its individual component frequencies. This spectrum represents the relative magnitude of each frequency component. Calculation of velocity, using the Doppler equation (equation 1.6), from these frequency shifts is done automatically by the computer.[13]

The spectral display of the Doppler trace presents time on the horizontal axis and flow velocity on the vertical axis; the grey scale of the trace is proportional to the number of blood cells moving at that speed; the darker the trace, the greater the number of blood cells (Figure 1.11). Usually, 16–32 shades of grey are used because the human eye cannot discern more than 32 shades of grey. The width of the trace is proportional to the spread of frequency; with little difference in velocity the band is narrow, whereas multiple velocities produce a wide spectral spread and a large trace on the screen. By convention, the flow toward the transducer is depicted above the baseline and the flow away from it below the baseline. On the spectral frame, the CW Doppler appears as a filled grey curve, showing all of the velocities encountered on the ultrasound beam, whereas the PW velocity curve has a thin envelope representing the blood flow at a determined location (Figure 1.12). The maximal velocity measurement must be done at the outer edge of the trace. In order to display the entire flow curve, it is frequently necessary to displace the baseline in the direction opposite to flow. In the case of aliasing, the velocity curve appears as artificially reversed on the other side of the baseline (Figure 1.13); for a blood flow towards the transducer it will be plotted below the zero line as a negative shift. For high velocities, this wrapping around may occur many times, so that the peak of the spectrum is buried in the superimposed traces and the maximal velocity is impossible to determine. By repositioning the baseline in the direction opposite to flow, some degree of aliasing may be unwrapped because higher velocities can be recorded in the direction of flow.

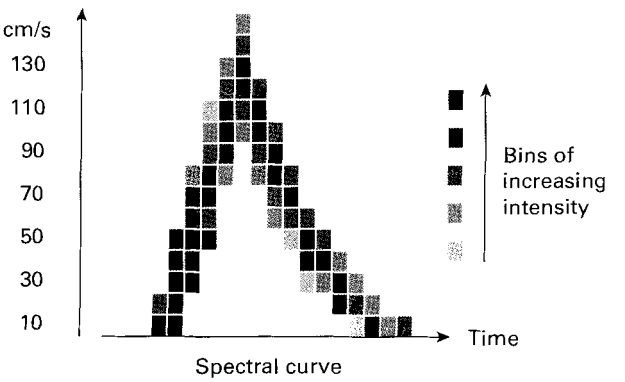

Figure 1.11 Spectral Doppler display: I. With use of fast Fourier transformation, the processor reconstructs a curve that is the summation of all sampled velocities, unfolded in time. Each segment of 5–10 ms is assigned to a stack of vertical bins, the intensity of which is proportional to the strength of the signal (i.e. it is proportional to the number of blood cells flowing within the range of velocities represented by each bin). The width of the trace, or "envelope", is proportional to the spread of frequencies, which represents the range of different velocities in the bloodstream. (Adapted from Chassot.[38])

Colour Doppler

PW Doppler analyses the complete spectrum of blood flow velocities at a single point. The technique can be expanded to analyse several samples along a line of interest. This multigate Doppler technique allows flow mapping by measuring returning echoes sequentially at different successive times after transmission of a single burst of ultrasound. The scan line is interrogated a number of times, ranging from three to sixteen; this number of times each line is sampled, called the packet size, is selected by the examiner or indicated by the manufacturer.[17] Each time a scan line is interrogated, an algorithm stores the Doppler data at each sample site along the line. After having interrogated one scan line, the beam direction is changed to the next scan line, and so on for the entire field. Depending upon the ultrasound system, the spacing between scan lines can be modified; this spacing is called line density. The spatial resolution increases with greater density of scan line, but the frame rate decreases in parallel because processing times are longer. The number of sample sites per scan line varies among instruments (usually 128), whereas the number of scan lines is determined by the colour sector width and the line density.

Despite the power of modern microprocessors, this large amount of information lowers significantly the frame rate of the images displayed on the screen. Therefore, rather than determining the complete spectrum of frequencies, as in the PW spectral display, an

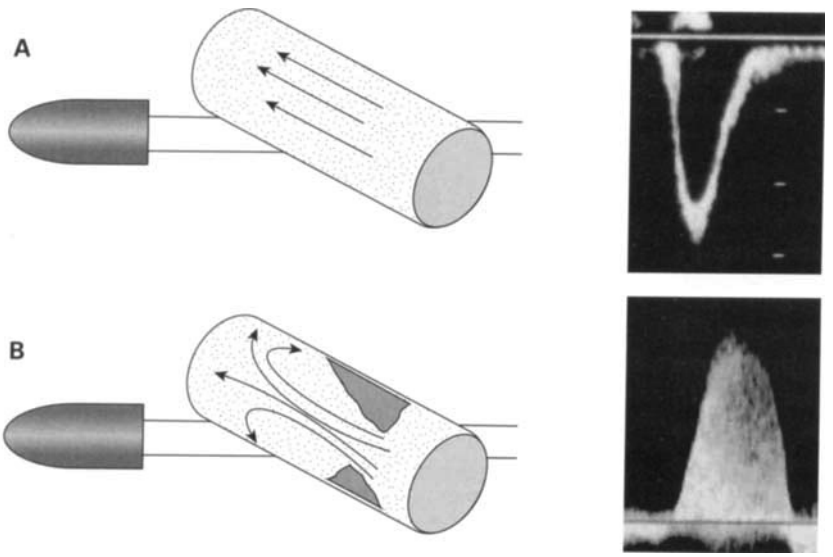

Figure 1.12 Spectral Doppler display: II. **(A)** In laminar flow the velocity is homogenous in the bloodstream; the spectral display of the pulsed wave (PW) Doppler shows a clear and well defined envelope. **(B)** In turbulent flow the trace is full and there is no envelope, with both PW and continuous wave Doppler.

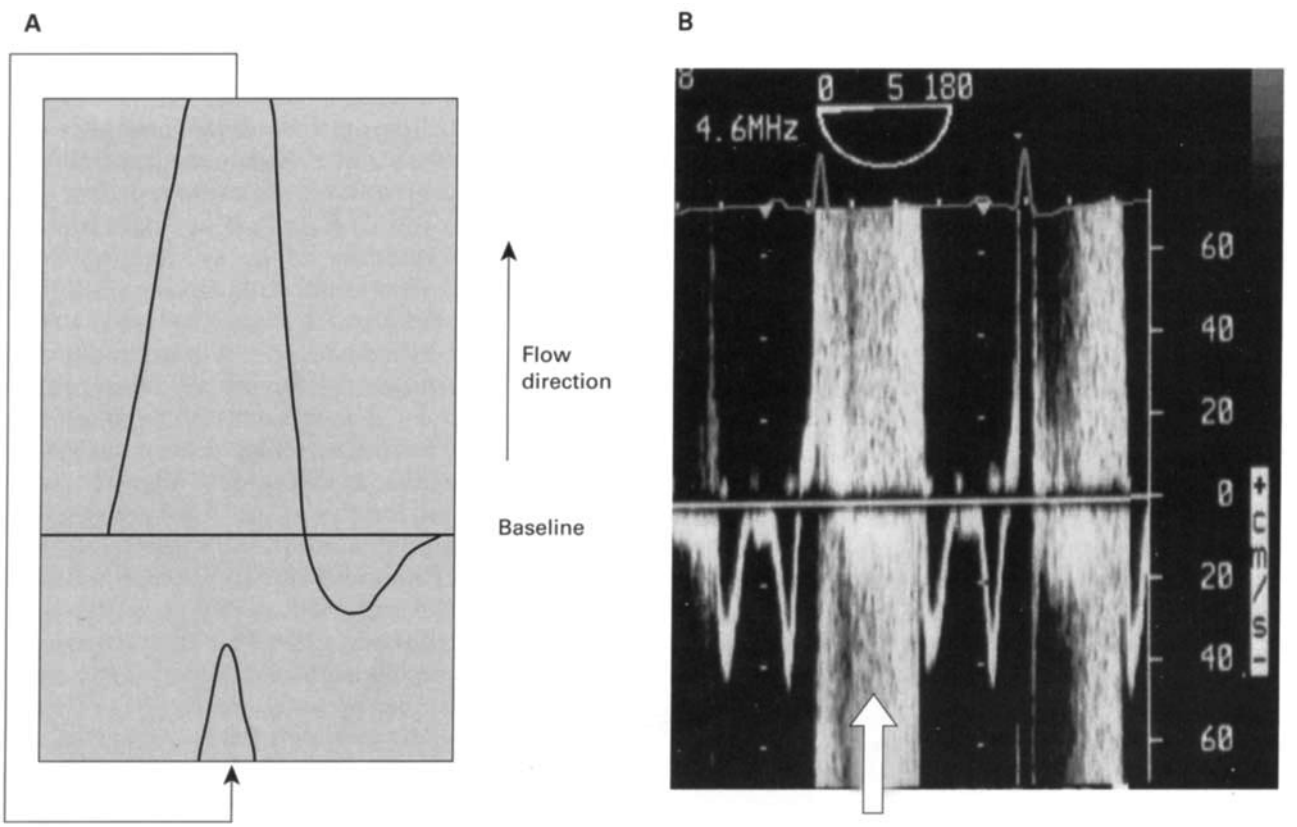

Figure 1.13 Aliasing in pulsed wave (PW) spectral display. **(A)** The velocity above the Nyquist limit appears reversed on the other side of the baseline. The flow toward the transducer is partially plotted below the 0 line. By repositioning the baseline in the direction opposite to flow, some degree of aliasing may be unwrapped because higher velocities can be recorded in the flow direction. **(B)** For a mitral regurgitation (V > 5 m/s) this wrapping around may occur many times, so that the peak of the spectrum is buried in the superposed traces (arrow), and the maximal velocity impossible to determine. (Adapted from Chassot.[38])

autocorrelator analyses the resultant phase shift between the emitted and received waveforms to generate a modal frequency, which represents the velocity of the majority of blood cells.[18] Echoes from subsequent pulses are correlated with echoes from previous pulses to determine the mean Doppler shift and its variance, which is the difference between the highest and the lowest returning frequencies, or the frequency spread of the spectrum. The modal frequency can be used in the Doppler equation to determine mean velocities and variance; for laminar flows the value of the mean velocity is approximately the same as the peak velocity.[19]

By converting the calculated values of mean velocity into colours, the blood flow velocity image can be overlayed onto a bidimensional greyscale display. Blood flow moving toward the transducer is usually displayed in red, and blood flow moving away from the transducer is coloured blue (Figure 1.14). Colour maps are the patterns of colours in use, and are illustrated by a colour bar appearing on the screen. This shows the properties of these colours, such as hue (the degree to which each of the primary colours is represented), the saturation (amount of white contained), and intensity (brightness). Lower velocities are indicated by dark colours, situated close to the baseline of the bar. Higher velocities are displayed in bright tones, near the end of the scale. Laminar flow appears as an homogenous smooth pattern of red or blue, whereas turbulent flow is depicted as a disorganised multicolour pattern termed a mosaic, indicating the many different speeds and directions at each sample site (Figure 1.14D). The numbers seen at the extremities of the colour scale bar represent the limit of the recordable mean velocity, or Nyquist limit, and not peak velocity estimates such as those from PW or CW Doppler (Figure 1.15). Above this limit, aliasing appears as colour reversal; the blood flowing toward the transducer, for example, changes abruptly from yellow to bright blue. By displacing the baseline of the colour bar in the direction opposite to flow, the recordable velocity is increased in the flow direction but diminished in the opposite direction. Under normal circumstances intracardiac flows are laminar; turbulence appears in pathological flows or abnormally high velocities (Figure 1.16).

Calculations imposed by data processing are proportional to the dimensions of the field of investigation. The wider the sector, the greater the number of lines that must be sampled; the deeper the sector, the more time that is necessary for the echoes to return to the transducer. Decreasing the width and depth of the sector decreases the processing time and increases the frame rate, which consequently varies from 6 to 90 images per second. This is critical for patients with rapid heart rates; important information can be missed if the frame rate is too low. Therefore, it is always advantageous to keep the colour sector as small as possible. Another way to increase the frame rate is to increase the PRF by

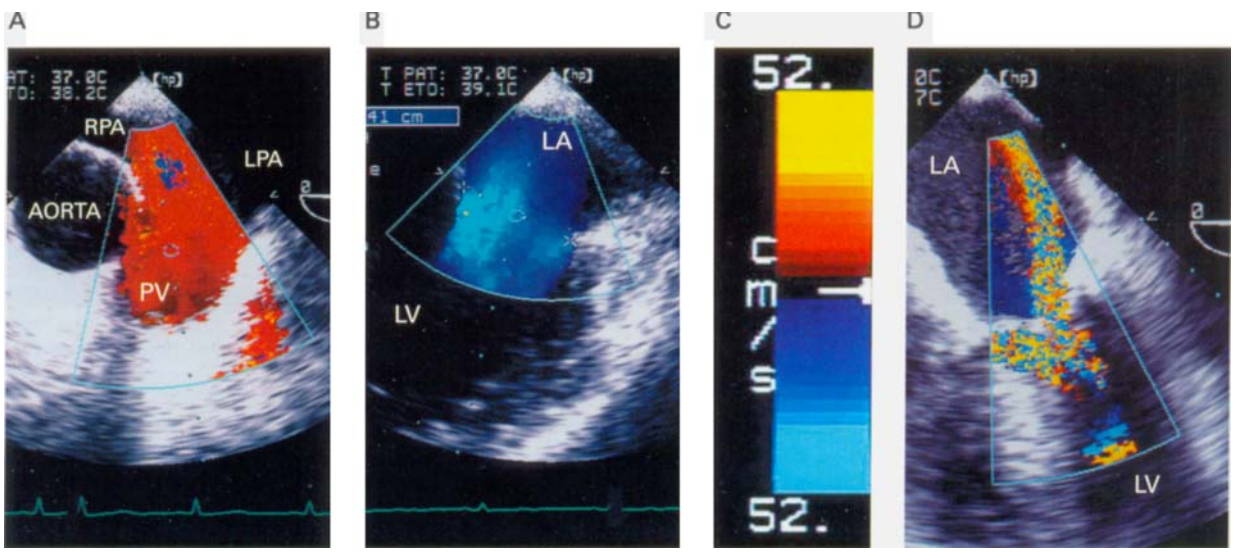

Figure 1.14 Colour Doppler flow. **(A)** Blood flow in pulmonary artery: it is depicted in red since it flows toward the transducer. **(B)** Diastolic flow through the mitral valve: it appears in blue because it is moving away from the transducer. **(C)** Colour bar: in enhanced colour maps the red gradually changes to yellow and the blue to an intense luminous shade as the velocity increases; this display is advantageous in operating rooms because it increases the contrast with the surrounding light. **(D)** Mitral regurgitation: turbulent flow is represented by a mosaic of disorganised multicoloured dots. LA = left atrium, LV = left ventricle, LPA = left pulmonary artery, PV = pulmonary valve, RPA = right pulmonary artery. (Adapted from Chassot.[38])

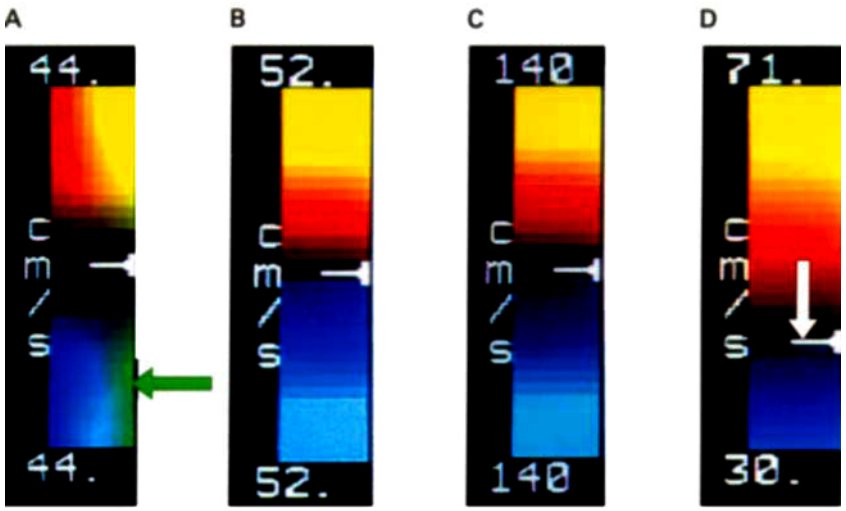

Figure 1.15 Colour coding, scale, and baseline. **(A)** Variance: to indicate the degree of turbulence, an orthogonal colour (usually green; green arrow) can be overlaid across the standard red and blue velocity bar. An algorithm calculates the variance between the individual velocities at each sample site, and adds the green colour if the irregularity is above a predetermined level. This particular display shows the advantage of mapping the turbulent areas inside the colour flow. **(B)** The numbers represent the highest mean velocity (cm/s) that can be depicted without aliasing; it increases with increasing pulse repetition frequency (PRF), decreasing the emitting frequency of the transducer and decreasing the depth of analysis. **(C)** The colour scale can be modified within the physical limits of the situation; in this case the aliasing velocity is 140 cm/s. **(D)** By lowering the baseline in the opposite direction to the blood flow (white arrow), the aliasing velocity can be raised in the direction of flow.

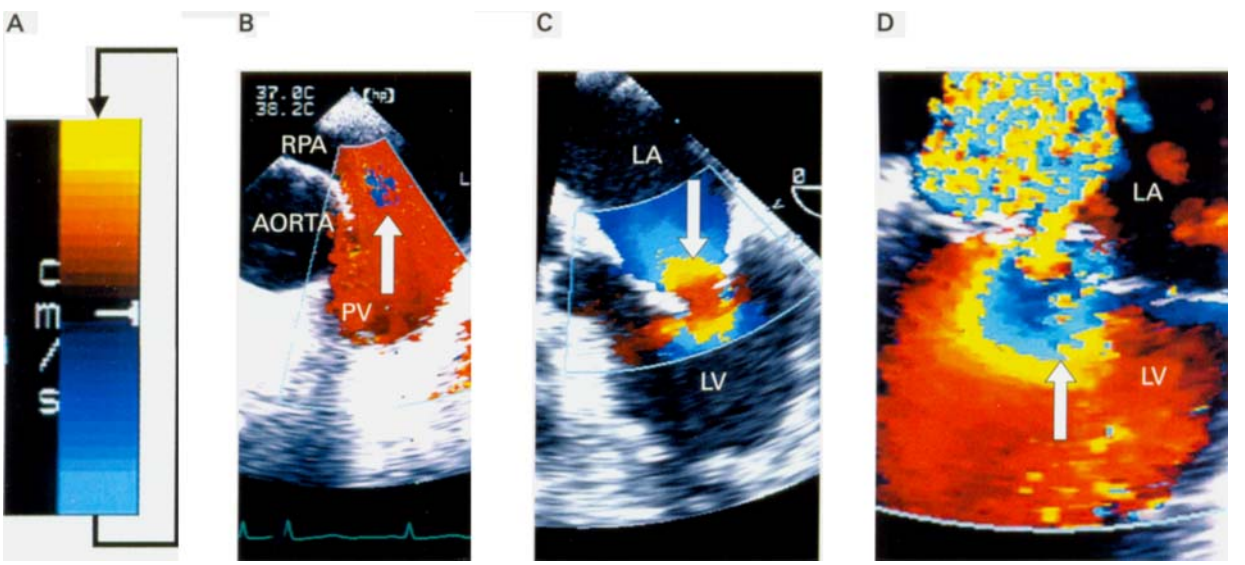

Figure 1.16 Aliasing with colour flow. **(A)** Aliasing appears as a colour reversal; when the blood flow velocity increases above Nyquist limit it appears with the brightest value of the opposite colour. **(B)** As the flow accelerates in the centre of the pulmonary artery, the colour is locally reversed to blue. **(C)** Diastolic flow has an increased velocity through a mitral stenosis; the blood acceleration appears as a complete reversal of colour, going from bright blue to bright yellow and to a darker red. **(D)** Systolic concentric acceleration zone on the ventricular side of a mitral regurgitation depicting aliasing from red to blue and further to yellow again, as the blood accelerates through the regurgitant orifice. LA = left atrium, LV = left ventricle, PV = pulmonary valve, RPA = right pulmonary artery. (Adapted from Chassot.[38])

adjusting the colour scale to a higher mean velocity, but this decreases the sensitivity to low velocity blood flow (Figure 1.15C). Using a transducer of lower frequency (<5 MHz) or reducing the emitting frequency of the probe also increases the PRF and the maximum velocity measurement capability at any depth; it decreases the tissue attenuation because lower frequencies lose less energy than do high frequency waves when travelling through the organ. The depth to

which transmission can interrogate, the number of scan lines, the probe frequency, the PRF, and the frame rate are interdependent. It is the responsibility of the observer to identify the optimal combination of these settings to obtain the most accurate information regarding flow.

Sometimes the interrogating beam can record frequency shifts due to rapid wall motions, and colours can be assigned to blood close to fast moving structures. This phenomenon is termed ghosting. It is minimised by setting the velocity scale at a higher value, which attenuates the signals of low velocity that correspond to tissues. However, this eliminates the low-velocity blood flow images. This dropout in low-velocity flow leads to a decrease in the size of a colour flow jet, and makes it appear smaller than it actually is. On the other hand a velocity scale set too low will yield flow images flooded with excessive aliasing.

The colour gain must be properly adjusted. Setting the gain control too low prevents detection of low amplitude signals, and blood flow patterns appear smaller than they are. A gain set too high causes much colour noise, which appears as random multicoloured specks sprayed over cardiac chambers and tissues. The proper gain is obtained by increasing the control until noise becomes obvious, and then decreasing it to the point where the noise just disappears. The gain of the greyscale, which displays the 2D tissue image on which the flow is superimposed, must be kept low otherwise it generates noise and restricts the dimensions of the colour flow. Like all Doppler data, the colour flow accuracy is dependent on the angle between the flow direction and the beam axis. If this angle is too wide (>20°) then the speed is misinterpreted as being too low; if the beam and the flow are perpendicular then there is no Doppler effect and no colour picture. The adjustment of transducer focal zone is important in multigate Doppler systems because sensitivity and spatial resolution decreases when the focal zone is set in the near field; the area of flow can appear larger than it actually is because Doppler data are collected in the divergent part of the ultrasound beam. When using colour flow, the focal zone must be kept at or below the interrogated area.[7]

It is important to remember that the colour flow display is a velocity map and not an actual blood volume measurement. Its area and brightness on the screen are determined only by the local speed of blood, which is the consequence of the instantaneous pressure gradient between the upstream and the downstream cavities.[3] A small mitral regurgitation orifice in the presence of normal left ventricular function will create a high-velocity jet (6 m/s) into the left atrium, which appears larger than the real regurgitant blood volume because of the displacement of left atrial blood by the jet. On the other hand the colour image of a large mitral insufficiency with poor left ventricular function will underestimate the amount of regurgitant blood because of the smaller pressure gradient. Moreover, the velocity measured locally in a vessel does not take into account the real flow profile, which is not flat except close to the root of great vessels; most of the time the flow profile is parabolic and presents accelerating zones in the centre of the flow or near curvatures. This fact limits the accuracy of velocity measurements, particularly when integrated into calculations such as cardiac output. Different positions of the Doppler sample volume in the main pulmonary artery cross-sectional area, for example, introduce errors of ± 35% in cardiac output measurements.[20]

Doppler tissue imaging

All moving structures and elements can induce a Doppler shift when they are hit by an ultrasound wave. Usually, only blood cell velocities are of interest to the clinician. They present as high frequency, low amplitude signals in comparison with the surrounding tissues; in contrast, the latter are characterised by high amplitude (>80 dB) and low frequency (<200 Hz) echoes because they are dense but move slowly compared with blood. Echoes from heart structures are considered noise in conventional Doppler systems and are eliminated by a high-pass filter. They appear only when the colour gain is too high or when filters are set at frequencies that are too low. However, this drawback can be used to identify parietal movements and wall kinetics if the low amplitude, high frequency signals of blood cells are properly filtered. With this technique, called tissue Doppler imaging (TDI), velocities as low as 0·1 cm/s are recorded. Depth resolution is inferior to that with conventional Doppler because velocity mapping requires longer pulses to be transmitted and longer gate times (0·5–1 cm).[21] Like conventional Doppler, TDI is angle dependent. Different modalities are in use, including pulse wave (PW) TDI with spectral display, velocity colour mapping (colour TDI), and colour M-mode. Postprocessing computation allows calculation of parameters such as myocardial strain and strain rate.

Pulse wave tissue Doppler imaging

The spectral display of the PW analysis of a tissue sample can be used to identify local movements such as mitral ring displacement or myocardial thickening. The transducer is of lower frequency (≤4 MHz), the gain and the velocity scale are set at low values (10–20 cm/s), and the sample volume is set at 0·5–1 cm.[22] The systolic and diastolic mitral ring motions are well depicted with this technique (Figure 1.17). The sampling volume can also be placed in a myocardial wall. Mitral annular systolic descent velocity correlates well with left ventricular ejection fraction, and basal lateral wall velocity with peak ventricular dP/dt.[23] However, the translation and rotation movements of the heart hamper considerably the precision of the measurements.

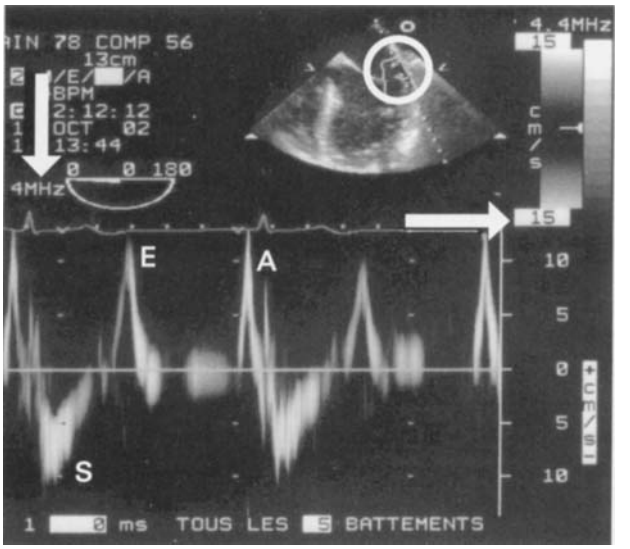

Figure 1.17 Pulsed wave tissue Doppler of the mitral ring. The transducer is in the lower range of frequency (vertical arrow), the maximal velocity is set at 15 cm/s (horizontal arrow), and the sampling volume is 0·5 cm (circle). The systolic descent (S) of the mitral ring is visible in systole, whereas two components (E and A) appear in diastole. The direction is opposite to the direction of blood flow; with the transoesophageal probe the systolic motion is away from the transducer, whereas the diastolic components move toward the transducer.

Colour tissue Doppler imaging

By plotting the spectrum of velocities, the mean velocity can be calculated and encoded in colour; a map of myocardial velocities is obtained, which allows assessment of the velocity and direction of regional myocardial contraction and relaxation.[24] Subepicardial layers usually have velocities lower than subendocardial ones; longitudinal motion decreases in amplitude from base to apex. Encoded in colour, these instantaneous velocity gradients within the walls appear in shades of red for motions toward the transducer and of blue for motions away from the transducer. Areas of no contraction are encoded green (Figure 1.18).[25,26]

Strain and strain rate

Strain (ε) is defined as the deformation of an object, normalised to its original shape. Variation in dimension L is expressed as a percentage of its original length (L0):

$$\varepsilon = \frac{L - L0}{L0} \ (\%) \qquad (1.11)$$

Lengthening has a positive value for strain, whereas shortening has a negative value. Strain rate is the temporal derivative of strain; it is the speed (V) at which deformation occurs, or the shortening/lengthening velocity per fibre length (L). It is expressed as unit per second:

$$\text{Strain rate} = \frac{\Delta\varepsilon}{\Delta t} = \frac{\Delta V}{\Delta L} \ (s^{-1}) \qquad (1.12)$$

If an object of 2 cm lengthens by 0·4 cm in 2 seconds, then the 20% strain is divided by 2 seconds (0·2 ÷ 2) to yield a strain rate of 0·1 s^{-1} (Figure 1.19). Strain rate has a linear relationship with myocardial dP/dt_{max} at the place at which it is measured, and it is independent of heart rate. The strain rate of the local wall motions also exhibits systolic and diastolic peaks (Figure 1.20).[27,28]

Because strain rate expresses the difference in velocities at both ends of the myocardial segment L, it can also be expressed as the spatial gradient of velocities within the sampling volume, and therefore colour coded. Each pixel of the frame includes two items of information: the mean velocity and the motion direction.[25] Strain rate can be extracted by postprocessing the real-time, digitally stored myocardial data sets of local instantaneous myocardial velocities. By temporal integration, strain is further extracted from strain rate.[28] The modern technology of postprocessing allows data collection along curved lines in order to follow the curvature of heart walls.

Compared with conventional methods, strain and strain rate analysis allows study of regional shortening and lengthening independently of heart rotation and translation movements. It

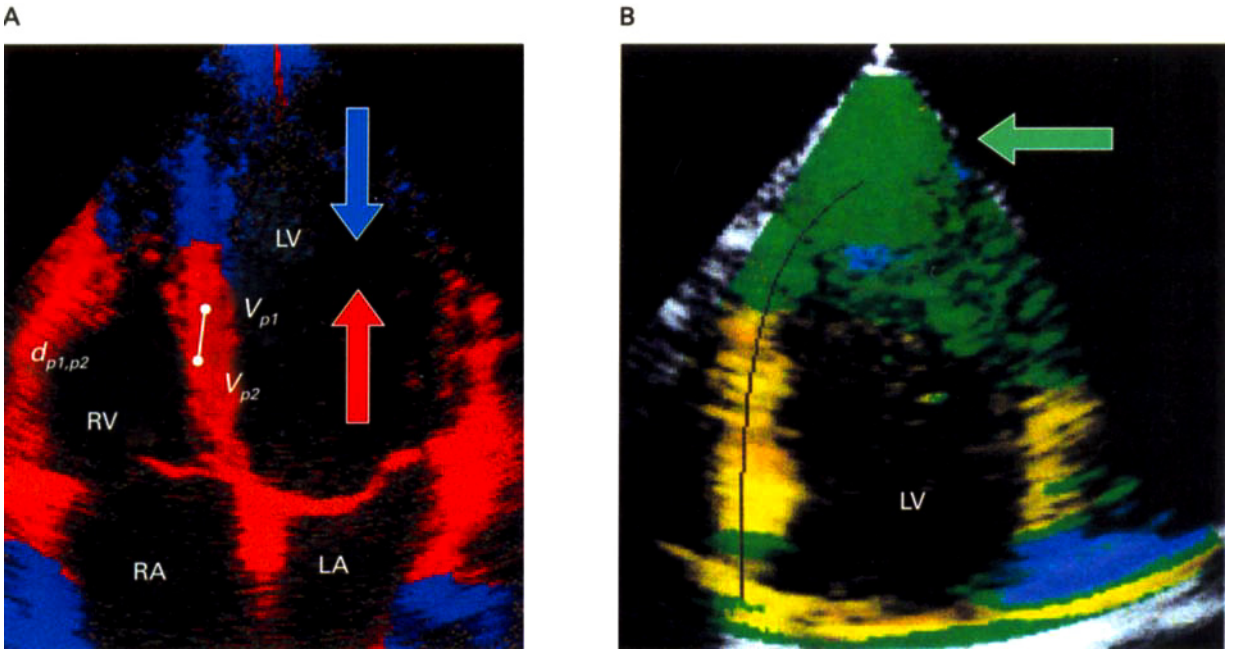

Figure 1.18 Colour tissue Doppler (transthoracic apical images). **(A)** During systole, the left ventricle contracts longitudinally. In this apical four chamber view, the apex moves away from the transducer and is coloured blue. The base moves toward the transducer because of the descent of the mitral ring; it therefore appears red. **(B)** A large akinetic area at the apex of the left ventricle is coloured green. $d_{p1,p2}$ = distance between points p1 and p2, LA = left atrium, LV = left ventricle, RA = right atrium, RV = right ventricle, v_{p1} = velocity of contraction at point p1, v_{p2} = velocity of contraction at point p2. (Adapted from Voigt *et al.*[25] and Heimdal *et al.*,[26] with permission.)

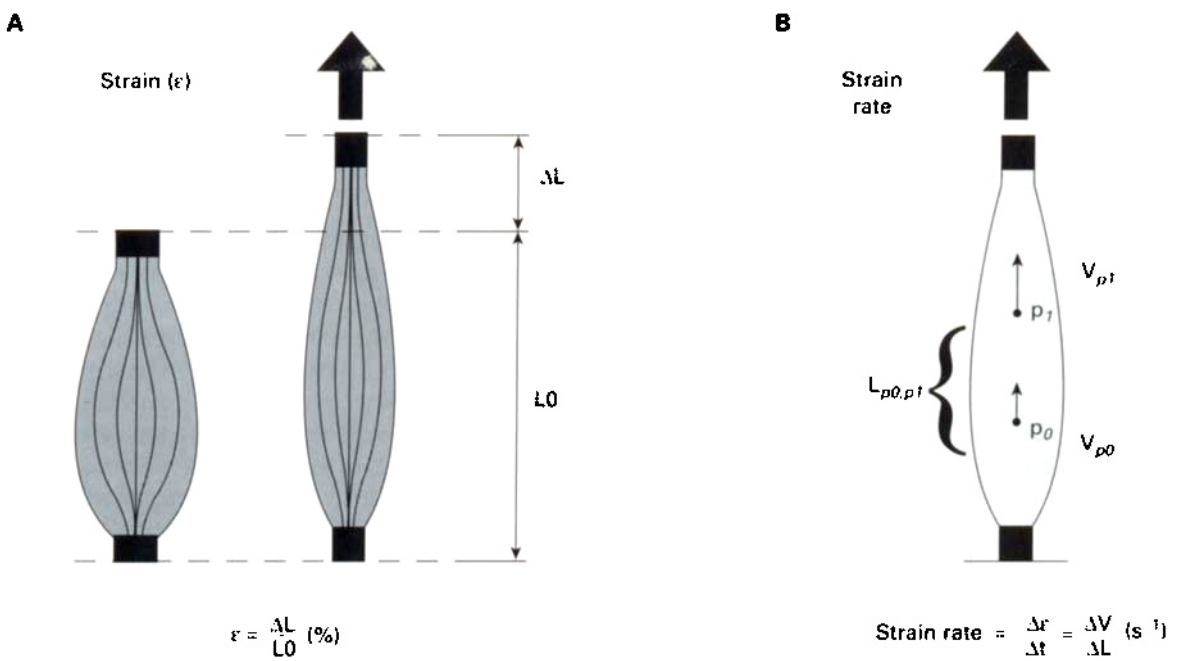

Figure 1.19 Strain and strain rate. **(A)** Strain (ε) is defined as the deformation of an object, normalised to its original shape. The variation in dimension L of the muscle is expressed as a percentage of its original length (L0). **(B)** Strain rate (SR) is the temporal derivative of strain; it is the speed (V) at which deformation occurs, or the shortening/lengthening velocity per fibre length (L). It is expressed in s^{-1}. $L_{p0,p1}$ = distance between points p0 and p1, v_{p0} = velocity of contraction at point p0, v_{p1} = velocity of contraction at point p1. (Adapted from Voigt *et al.*[25])

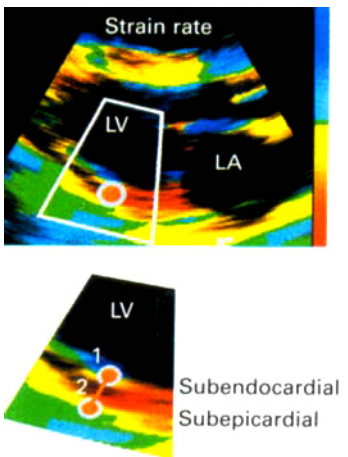

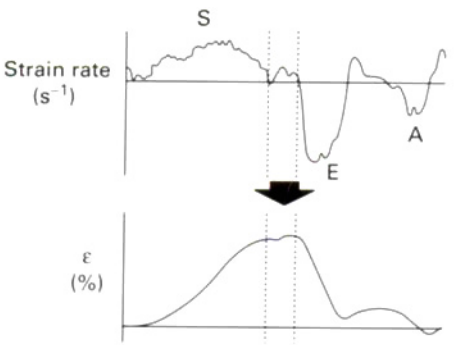

Figure 1.20 Colour tissue Doppler. Radial strain rate and strain are derived from colour Doppler myocardial imaging data from the left ventricular wall. Strain rate is calculated from myocardial velocity gradients between subendocardial (1) and subepicardial (2) points, normalised by the distance between points 1 and 2. Strain rate presents systolic (S) and diastolic (E and A) peaks corresponding to the maximal wall motion velocities. Strain (ε) is the time integral of strain rate. The dashed lines represent aortic valve closure and mitral valve opening. Ao = aorta, LA = left atrium, LV = left ventricle. (Adapted from Jamal *et al.*[28])

exploits the phase shift of the frequency signals rather than their amplitude, resulting in a better ratio of signal to noise. Its spatial resolution is intrinsically better and is not dependent on the definition of endocardial and epicardial borders, which are frequently difficult to identify properly.

Second harmonic

When ultrasound waves travel through tissues they are subjected to attenuation and distortion, and their echoes are progressively contaminated by new waves, the frequencies of which are multiples of the emitted frequency. They are called harmonics, and are coaxial to the main frequency beam.[29] The second harmonic is an echo wave with a frequency that is the double of the frequency emitted by the transducer. By filtering echoes at reception, the computer can construct the image based only on second harmonic wave analysis (Figure 1.21). The second harmonic technology, primarily developed to ameliorate the visibility of contrast products, adds considerable improvement to the definition of endocardial borders on normal 2D images. Moreover, these images present with much fewer artefacts because most artefacts, like reverberations and side lobes (see below), are produced in the nearest part of the field, whereas harmonics are generated in the depth of the tissue. To produce readable harmonics, the transducer must emit at rather high power (>70 dB) and low frequency (1·5–4 MHz), and have a broad band for reception. This technology is now available on some transoesophageal probes.

Contrast echocardiography

Contrast echocardiography is based on the use of microbubbles that can scatter ultrasound. Ultrasound waves induce alternative changes in pressure in the medium they travel through; microbubbles alternately contract and expand because they are more compressible than the tissues or the blood.[30] These pressure changes are quantified with a mechanical index proportional to the output power of the transducer, and inversely proportional to the square root of the emitted frequency.[31] When hit by ultrasound, microbubbles produce signals at the same frequency if the mechanical index is low, but when the transducer power is increased the expansion is greater than the contraction, and harmonics are produced as a result of non-linear oscillations (Figure 1.22). By filtering the emitted frequency at reception, an enhanced signal of microbubble-rich medium can be obtained from the second harmonic frequency. The intensity of harmonics increases with increasing power, and waves of high mechanical index will destroy microbubbles with emission of a brief, intense, wide-band acoustic signal. Being incompressible, tissues exhibit only linear oscillations, and can therefore be differentiated from compressible microbubbles because of their non-linear oscillations.

Hand-agitated saline or dextrose was the first contrast product to be used, but microbubbles of

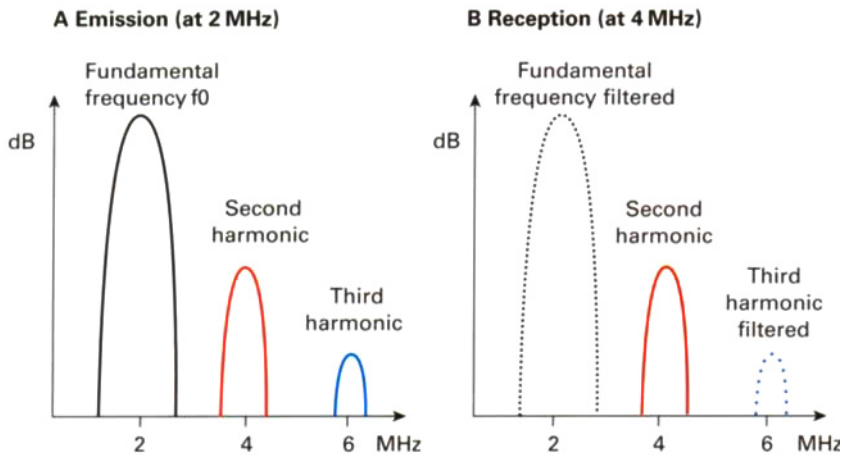

Figure 1.21 Second harmonic technology. **(A)** During emission at 2 MHz harmonics are generated as waves progress through tissues; there frequencies are multiples of the emitted frequency (f0). **(B)** At reception f0 is filtered out, as is the third, weakest harmonic; the second harmonic only is used to reconstruct the two-dimensional image.

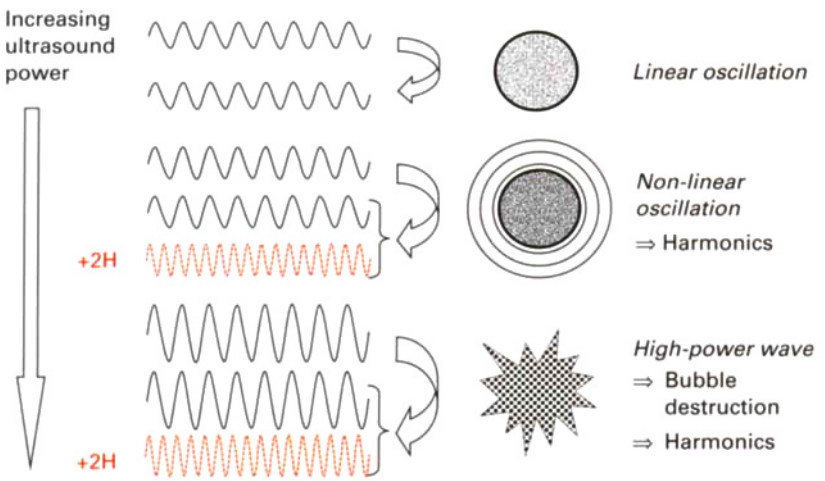

Figure 1.22 Contrast echocardiography. At low power of ultrasound (low mechanical index), microbubble oscillations are linearly correlated with ultrasound wave amplitude. With increasing power (local pressure >0·1 MPa), harmonics are produced. At high mechanical index (local pressure >0·2 MPa) the microbubble is destroyed, with emission of a short burst of high amplitude ultrasound waves. 2H = second harmonic.

air are rather large, do not cross the pulmonary capillaries, and have a short half-life. The first generation of contrast agents consisted of sonicated albumin or saccharide containing air. The diffusibility of air limits the persistence of microbubbles in the blood.[31] The second generation of contrast agents use poorly soluble, high-molecular-weight gases such as perfluorocarbon, pentafluoropentane, and sulphur hexafloride. These newer agents are capable of transpulmonary passage, and can opacify the left heart chambers and myocardial microcirculation after intravenous administration or continuous perfusion.[32] Their microbubbles are less than 7 μm; they cross capillaries but not membranes.

Tissue perfusion images have a spatial resolution of 1 mm and a high temporal resolution (30–100 Hz); the technique is without risk and is inexpensive. By postprocessing substraction, the 256 grey shades are converted to colour codes, which are easier to read for the human eye (Figure 1.23).[33] With temporal reduction in ultrasound exposure by triggering frame rates to once every cardiac cycle (intermittent imaging), lesser amounts of contrast agent are needed and a time–intensity curve representing microbubble washout is obtained; the flow in a region of interest can be quantified within myocardial tissue.[33,34]

Power Doppler

When a short pulse of ultrasound is reflected from a sample of moving blood cells and an echo signal detected by the transducer, two different

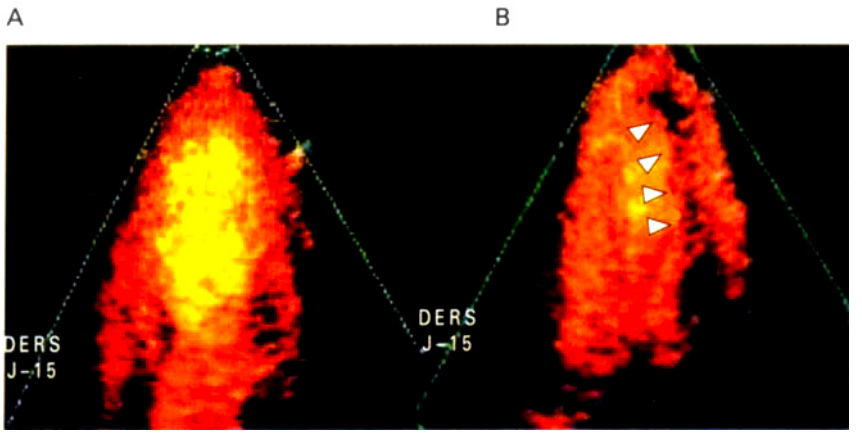

Figure 1.23 Contrast stress echocardiography: transthoracic two chamber view of the left ventricle at two different times during dobutamine stress echocardiography after intravenous injection of pentafluoropentane. **(A)** At rest: the intraventricular cavity is filled with contrast, and the ventricular walls are homogenously perfused. **(B)** Under dobutamine perfusion, a lateral wall defect appears as black spots with no perfusion by contrast agent. (From Porter *et al.*,[33] with permission.)

data are acquired: the frequency shift, which is determined by the speed of the target; and the amplitude of the echo signal, which is related to the number of blood cells in the sampling volume. Instead of indicating velocities, power Doppler imaging shows the instantaneous amount of blood cells by transforming the variations in amplitude of the returning echoes into a colour scale of varying brightness.[35] It uses high power emission and high pulse repetition frequency in order to decrease artefacts due to tissue motion. Because it does not measure velocity or flow direction, it is not sensitive to aliasing or to the angle between the flow and the ultrasound beam. Power Doppler is particularly useful for measurement of flow in blood vessels.

Artefacts

Numerous artefacts caused by the physical properties of ultrasound or by instrument settings can mislead the examiner. Aliasing and ghosting are referred to above. Strong reflectors such as prosthetic material or calcium deposits can mask all of the structures situated behind them and create shadowing. Close to the transducer, an acoustic noise is generated by high-amplitude oscillations of the piezoelectric elements and this prevents visualisation of any reflector; this is called near-field clutter.[3] More important are reverberations; when an ultrasound beam is strongly reflected by a nearby object, the front side of the transducer may function as another reflecting surface. The echo beam is then sent back to the object, which is hit a second time by the same ultrasound beam. This second journey travelled by the same burst produces a second signal, and is interpreted as a second object at twice the distance from the first because it took twice the time to return to the transducer (Figure 1.24). This pattern can be repeated two or three times, and can also occur between strong reflectors deeper in the field, such as calcium deposits or catheters. When the source of reverberation is moving, its amplitude of motion is twice as great as that of the original echo. Colour Doppler is subject to the same artefact; the flow of a sclerotic descending aorta, very close to the transoesophageal transducer, might be reproduced a second time in front of the aorta, as though a second vessel was present with the same arterial pulse.

With phased-array transducer, extraneous accessory beams of low intensity (<20 dB) may be produced by the edges of the transducer in the periphery of the main ultrasound beam; they normally do not interfere with 2D images. Nevertheless, if a strong echogenic target is in their field during the sweep of the beams, it will induce an image that is pictured on the screen as a bow-like shadow, called a side lobe (Figure 1.25). This shadow is concentric to the transducer and crosses anatomical boundaries.[3]

Usually, these artefacts can be recognised because they are independent of actual heart structures; they cross anatomical walls and cavities without any relationship to natural borders, and flow can appear in an area where there is no vessel. They usually disappear with readjustment of depth, angle or emitting frequency of the transducer, or by use of the second harmonic.

Understanding the physical concepts underlying ultrasound technology must be clearly understood by the examiner, because they have a crucial role

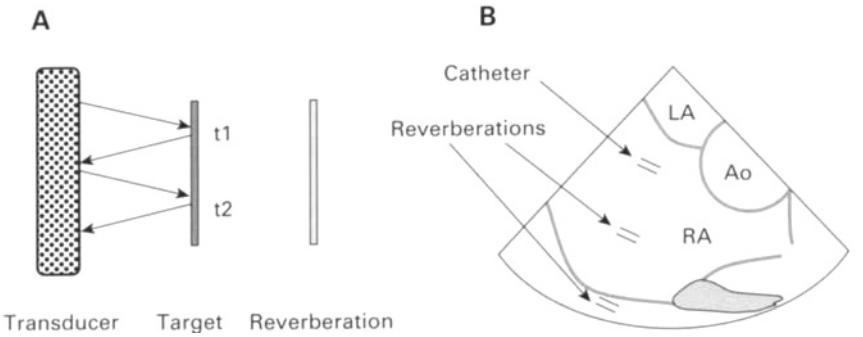

Figure 1.24 Reverberation. **(A)** When a strong reflector is close to the transducer, the front part of the transducer will partially reflect the echo from the structure; this wave will make a second round trip to the structure and back to the transducer. The time t1 determines the position of the structure in terms of depth. The second echo, at time t2, corresponds to a structure that twice distance from the transducer because t2 is twice t1. This phantom structure appears on the screen as a reproduction of the first structure at double the distance, and this is called reverberation. **(B)** A strong reflector in the field can also induce the same phenomenon. Shown is the image of a catheter in the right atrium and its reverberation. Ao = aorta, LA = left atrium, RA = right atrium. (Adapted from Bettex and Chassot.[8])

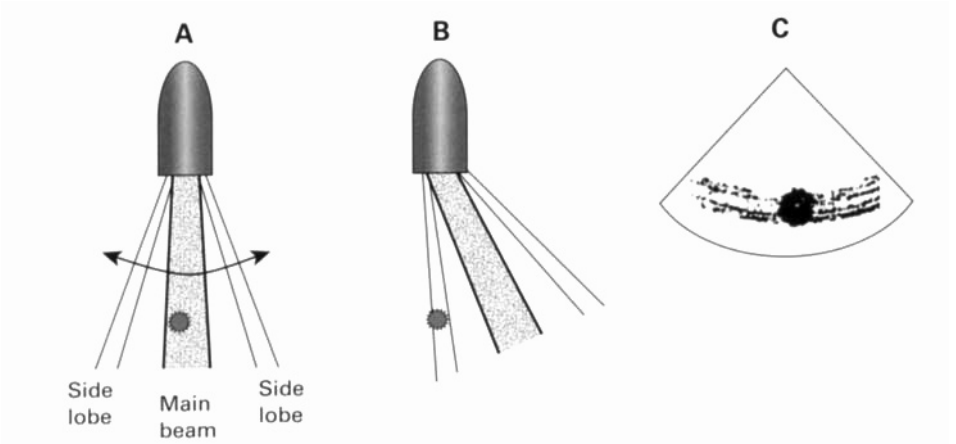

Figure 1.25 Side lobe. **(A)** A strongly reflective target is in the main beam of the transducer, and appears as a dark round image on the screen. The side lobes give no image. **(B)** Scanning by phased array transducer: the highly reflective target is now perceived by the weak lateral side lobes when it is out of the main beam. **(C)** The perception of the strong reflector by the weak side lobes gives the image of a grey shadowy bow superimposed on the real structures.

to play in generating the images that appear on the screen. Ignoring them can lead to an incorrect diagnosis.

REFERENCES

1 Geiser EA. Echocardiography: physics and instrumentation. In: Marcus M, ed. *Cardiac imaging: a companion to Braunwald's heart disease.* Philadelphia: WB Saunders, 1991, pp. 348–64.

2 Goldman DE, Jueter DF. Tabular data of the velocity and absorption of high-frequency sound in mammalian tissues. *J Acoust Soc Am* 1956;**28**:35.

3 Feigenbaum H. Instrumentation. In: Feigenbaum H, ed. *Echocardiography.* Philadelphia: Lea & Febiger, 1994, pp. 1–67.

4 Sehgal CM. Principles of ultrasonic imaging and Doppler ultrasound. In: St John Sutton MG, ed. *Textbook of echocardiography and Doppler in adults and children.* Cambridge: Blackwell Science, 1996, pp. 3–30.

5 Somer JC. Principles of phased-array imaging. In: Roelandt JRTC, ed. *Cardiac ultrasound.* Edinburgh: Churchill Livingstone, 1993, pp. 21–32.

6 Bom N. Ligtvoet CM. Principles of cardiac ultrasound. In: Roelandt JRTC, ed. *Cardiac ultrasound.* Edinburgh: Churchill Livingstone, 1993, pp. 9–20.

7 Labovitz AJ, Williams GA. *Doppler echocardiography. The quantitative approach,* 3rd ed. Philadelphia: Lea & Febiger, 1992.

8 Bettex D, Chassot PG. Principes physiques de l'échocardiographie. In: Bettex D, Chassot PG, eds. *Transoeosophageal echocardiography in anaesthesia and resuscitation* [in French]. Paris: Masson, 1997, pp. 13–39.

9 Kahn RA, Konstadt SN, Louie EK, Aronson S, Thys DM. Intraoperative echocardiography. In: Kaplan JA, ed. *Cardiac anesthesia*. Philadelphia: WB Saunders, 1999, pp. 401–84.

10 Seward JB, Belohlavek M, Foley DA, *et al.* Three-dimensional reconstruction by transesophageal echocardiography. In: Freeman WK, ed. *Transesophageal echocardiography*. Boston: Little Brown Co., 1994, pp. 577–85.

11 Shung KK. The principle of multidimensional array. *Eur J Echocardiography* 2002;**3**:149–53.

12 Quinones MA, Otto CM, Stoddard M, Wagooner A, Zoghbi WA. Recommendations for quantification of Doppler echocardiography: a report from the Doppler quantification Task Force of the Nomenclature and Standards Committee of the American Society of Echocardiography. *J Am Soc Echocardiogr* 2002;**15**:167–84.

13 DeMaria E. *Cardiac Doppler: the basics*. Andover, MA: Hewlett Packard Co., 1984, pp. 1–35.

14 Bom K, Boo J, Rijsterborgh H. On the aliasing problem in pulsed Doppler cardiac studies. *J Clin Ultrasound* 1984;**12**:559–63.

15 Baker DW, Rubenstein SA, Lorch GS. Pulsed Doppler echocardiography: principles and applications. *Am J Med* 1977;**63**:69–74.

16 Cannon SR, Richards KL. Principles and physics of Doppler. In: Markus M, ed. *Cardiac imaging: a companion to Braunwald's heart disease*. Philadelphia: W.B. Saunders Co., 1991, pp. 365–73.

17 Pandian N. *Cardiac Doppler: color flow imaging*. Andover, MA: Hewlett-Packard Co., 1993, pp. 1–34.

18 Wells PNT. Colour flow mapping: principles and limitations. In: Roelandt JRTC, ed. *Cardiac ultrasound*. Edinburgh: Churchill Livingstone, 1993, pp. 43–51.

19 Nanda NC. Basics in Doppler echocardiography. In: Nanda NC. *Atlas of color Doppler echocardiography*. Philadelphia: Lea & Febiger, 1989, pp. 1–5.

20 Muhiudeen IA, Kuecherer HF, Lee E, Cahalan MK, Schiller NB. Intraoperative estimation of cardiac output by transesophageal pulsed Doppler echocardiography. *Anesthesiology* 1991;**74**:9–14.

21 Desco M, Antoranz JC, Technical principles of Doppler tissue imaging. In: Garcia-Fernandez MA, Zamorano J, Azevedo J. *Doppler tissue imaging echocardiography*. Madrid: McGraw-Hill, 1998, pp. 7–21.

22 Sutherland GR, Stewart MJ, Groundstroem KWE, *et al.* Color Doppler myocardial imaging: a new technique for the assessment of myocardial function. *J Am Soc Echocardiogr* 1994;**7**:441–58.

23 Gorcsan III J. Tissue Doppler echocardiography. *Curr Opin Cardiology* 2000;**15**:323–9.

24 Trambaiolo P, Tonti G, Salustri A, Fedele F, Sutherland G. New insight into regional systolic and diastolic left ventricular function with tissue Doppler echocardiography: from qualitative analysis to quantitative approach. *J Am Soc Echocardiogr* 2001;**14**:85–96.

25 Voigt JU, Arnold MA, Karlsson M, *et al.* Assessment of regional longitudinal myocardial strain rate derived from Doppler myocardial imaging indexes in normal and infarcted myocardium. *J Am Soc Echocardiogr* 2000;**13**: 588–98.

26 Heimdal A, Stoylen A, Torp H, Skaerpe T. Real-time strain rate imaging of the left ventricle by ultrasound. *J Am Soc Echocardiogr* 1998;**11**:1013–9.

27 D'hooge J, Heimdal A, Jamal F, *et al.* Regional strain and strain rate measurements by cardiac ultrasound: Principles, implementation and limitations. *Eur J Echocardiography* 2000;**1**:154–70.

28 Jamal F, Kukulski T, Strotman J, *et al.* Quantification of the spectrum of changes in regional myocardial function during acute ischemia in closed chest pigs: an ultrasonic strain rate and strain study. *J Am Soc Echocardiogr* 2001;**14**:874–84.

29 Martin RW. Interaction of ultrasound with tissue, approaches to tissue characterization, and measurement accuracy. In: Otto CM, ed. *The practice of clinical echocardiography*, 2nd ed. Philadelphia: WB Saunders Co., 2002, pp. 183–201.

30 Paelinck BP, Kasprzak JD. Contrast-enhanced echocardiography: review and current role. *Acta Cardiol* 1999;**54**:195–201.

31 Kaul S. Myocardial contrast echocardiography: basic principles. *Progr Cardiovasc Dis* 2001;**44**: 1–11.

32 Mayer S, Grayburn PA. Myocardial contrast agents: advances and future directions. *Progr Cardiovasc Dis* 2001;**44**:33–44.

33 Porter RT, Noll D, Xie F. Myocardial contrast echocardiography. Methods, analysis and applications. In: Otto CM, ed. *The practice of clinical echocardiography*. Philadelphia: WB Saunders Co., 2002, pp. 159–82.

34 Wei K, Jayaweera AR, Firoozan S, *et al.* Quantification of myocardial blood flow with ultrasound-induced destruction of microbubbles administered as a constant venous infusion. *Circulation* 1998;**97**:473–83.

35 McDicken WN, Anderson T. The difference between colour Doppler velocity imaging and power Doppler imaging. *Eur J Echocardiography* 2002;**3**:240–4.

36 Hatle L, Brubackk A, Tromsdal A, Angelsen B. Non-invasive assessment of pressure drop in mitral stenosis by Doppler ultrasound. *Br Heart J* 1978;**40**:131–8.

37 Weyman AE, Griffin BP. Left ventricular outflow tract: the aortic valve, aorta, and subvalvular outflow tract. In: Weyman AE, ed. *Principles and practice of echocardiography*. Philadelphia: Lea & Febiger, 1994, pp. 498–574.

38 Chassot PG. Basic principles of Doppler ultrasounds. In: Denault AY, ed. *Perioperative transesophageal echocardiography*. New York: Marcel Dekker Inc., 2004, in press.

2 Perioperative transoesophageal echocardiography

Karl Skarvan, Jan Poelaert

Introduction

Echocardiography is a non-invasive imaging modality that has evolved to become a primary diagnostic tool in the routine practice of cardiology. In its standard transthoracic form, echocardiography encounters serious obstacles when it is deployed in patients undergoing surgery and in critically ill patients in intensive and emergency care units. Proper placement of the transducer and positioning of the patient are difficult if not impossible because of their interference with surgery. Because of the need for repeated positional adjustment of the hand-held transducer, the transthoracic method is not suitable for continuous monitoring of cardiac function. Intubated patients in the intensive care unit are often ventilated with large tidal volumes and positive expiratory pressure, and therefore they have poor acoustic windows. Moreover, surgical dressings and drains in the chest may be responsible for poor image quality. By contrast, a transducer introduced into the oesophagus or the stomach is in the immediate vicinity of the heart and the aorta, and there is no lung or bone tissue in the way of the ultrasound waves. Continuous monitoring of heart structures in the same imaging plane is feasible because the transducer can be kept in the required position by the locking mechanism of the transoesophageal probe.

Originally developed for echocardiographic studies in patients with poor image quality, transoesophageal echocardiography (TOE), not surprisingly, very soon became used widely during the perioperative period, both as a diagnostic tool and as a monitor of cardiac function.[1] A recent survey among cardiac anaesthetists demonstrated that TOE has become a common part of perioperative care in cardiac surgery, and that it is mostly performed and interpreted by the anaesthetists themselves.[2] In cardiac surgery TOE provides new and important information regarding cardiac pathology in many patients, and results in significant changes in both surgical and anaesthetic management.[3–5] The avoidance of unnecessary operations on the basis of intraoperative TOE findings further underscores the benefit and the cost-effectiveness of routine TOE in cardiac surgery.[6] The impact of TOE on the clinical management of patients undergoing non-cardiac surgery appears to be of equivalent importance.[7]

Prerequisites to the proper use of TOE are a comprehensive knowledge of cardiac anatomy, physiology, and ultrasound technology, and acquisition of essential technical skills (for more information on training in TOE, see Chapters 17 and 18). The present chapter focuses on the technique of two-dimensional TOE examination and related issues.

Originally, a monoplane probe was used for TOE. Because of rapid progress in ultrasound technology, a biplane probe was introduced early in the 1990s, which was soon replaced by the multiplane probe.[8] This device is now the most widely used and marketed. In addition to the standard multiplane probes used in adult TOE, smaller paediatric probes were developed. Furthermore, a miniaturised monoplane TOE has been tested in patients. The latter can be easily inserted transnasally in awake patients and allows for monitoring of ventricular function during induction of anaesthesia or in the intensive care unit.[9] In this chapter, only the method of multiplane TOE is described.

Routine diagnostic TOE in the echocardiography laboratory is performed in awake patients under topical anaesthesia of the oropharynx and in the left lateral decubitus position. By contrast, perioperative TOE is usually performed in anaesthetised and intubated, sedated, or unconscious patients in the operating theatre, postanaesthesia recovery room, intensive care unit, or emergency room, with the patient positioned supine. It can be also conducted out in awake patients or during resuscitative efforts. In most cases, however, perioperative TOE is an

elective diagnostic and monitoring procedure, and the probe is inserted following the induction of anaesthesia and endotracheal intubation.

Preinsertion check

The following checks should always be carried out:

- Is the probe intact?
- Are the control wheels working and unlocked?
- Ensure there are no contraindications to TOE.
- Is the probe disinfected?
- Is the patient prepared for TOE?
- Inspect the mouth.

The probe is basically a gastroscope equipped with ultrasound instead of fibreoptic technology. The phased-array transducer is integrated into the flexible tip of the probe. The dimensions of the tip transducer vary between 10 and 15 mm in diameter and between 20 and 45 mm in length. The shaft of the probe is 9–10 mm wide and about 100 cm long. Before insertion the probe must be inspected for any damage to its outer surface to prevent any mechanical, thermal, chemical, or electric injury to the patient. Regular checks of the electrical safety of the probes by maintenance personnel are warranted. By rotating the two steering wheels at the handle of the probe, the position of the flexible tip of the probe can be varied. As a rule, 90° of anteflexion and 90° of retroflexion are possible with the help of the major wheel, whereas the minor wheel directs left and right lateral flexion (Figure 2.1). The function of these mechanical controls must be checked before the probe is inserted. The wheels (and consequently the flexion of the tip of the probe) can be locked in an optimal position for monitoring purposes. During insertion and removal of the probe, the steering wheels must never be locked.

Protective latex sheaths for TOE probes are available. Use of these sheaths can save up to two-thirds of the time required for the standard disinfectant bath,[10] and there is no evidence that the risk for infection with sheaths is any greater than with the use of unprotected but properly disinfected probes. Four per cent of the latex sheaths were found to be defective after use by means of an air-tightness test. Thus, each used latex cover must be checked after the examination for perforations in order to avoid the spread of germs from one patient to the next via contaminated probes.[10] Before insertion of the probe, the operator must still ensure that there are no contraindications to the investigation (Box 2.1) and must inspect the oropharynx for proper position and fixation of the endotracheal tube, and for loose teeth, lacerations, or any other injuries.

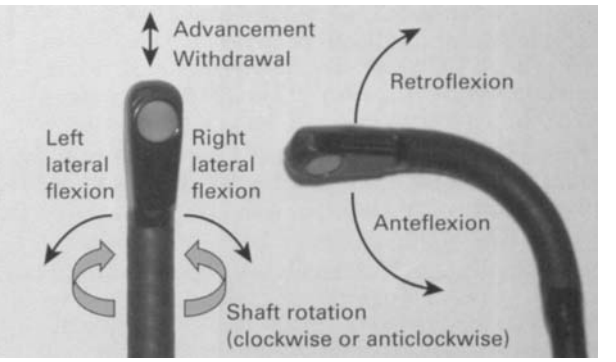

Figure 2.1 Tip of the multiplane transoesophageal echocardiography probe carrying the ultrasound transducer. The possible movements of the probe are indicated by arrows.

Absolute

- Oesophageal stenosis or stricture
- Oesophageal tumour
- Oesophageal diverticulum
- Ulcerous oesophagitis
- Bleeding oesophageal varices
- Gastric bleeding
- Suspicion of oesophageal or gastric perforation
- Recent pharyngeal/oesophageal/gastric surgery
- Difficult swallowing of unknown cause

Relative

- Oesophageal varices
- Reflux oesophagitis
- Severe cervical spondylosis
- Hiatal hernia
- Therapeutic thrombolysis
- Facial and oral injuries
- Loose teeth

Box 2.1 Contraindications to transoesophageal echocardiography

Insertion of the probe

No force must be applied during insertion of the TOE probe. In our hands, insertion in anaesthetised patients with the help of an

assistant proved to be both fast and safe. The assistant stands behind the head of the patient, opens the patient's mouth, and lifts his or her jaw. The (right-handed) operator assumes a position at the left side of the patient and uses the left hand to hold the handle of the scope and to adjust the flexion of the tip, if necessary, while the right hand (with finger tips!) gently introduces the tip of the probe into the oropharynx, then the oesophagus, and finally the stomach (Figure 2.2). Usually, no or only slight anteflexion of the tip is required to gain entry into the oesophagus. Gentle rotation of the shaft can also facilitate passage of the probe through the oropharynx into the oesophagus. Some operators use the index and middle fingers of the left hand to guide the probe through the pharynx. A biting block is inserted into the mouth either before or after (in paralysed patients) passage of the probe. In edentulous patients a biting block is not necessary and may cause a pressure sore in the mouth. Lidocaine jelly or lubricant spray applied to the tip of the probe facilitates insertion. This blind technique is almost always successful, safe, and does not increase the incidence of dysphagia or sore throat postoperatively. The probe is advanced approximately 40–42 cm from the teeth down into the gastric fundus, the mouth is checked for possible injury, the bite block and the probe secured, and the probe is connected to the ultrasound machine.

Because the probe is not connected to the ultrasound system until it is in position in the stomach, the mediastinal structures cannot be visualised during insertion of the probe. However, the operator can better concentrate on the insertion, and handling of the unconnected probe is easier. The indwelling gastric tube or oesophageal stethoscope may interfere with the insertion and cause ultrasound artefacts. For optimal imaging conditions the stomach should be aspirated and the gastric tube removed before TOE. Rarely, the TOE probe cannot be inserted. Increased jaw and chin lift or slight rotation of the head to the left may be helpful. If resistance is encountered in the oropharynx (probe entering fossa piriformis or coiling up), then laryngoscopy usually helps in navigating the tip of the probe into the oesophagus. A resistance occurring high in the oesophagus may be due to a hyperinflated cuff of the tracheal tube, abnormalities in the cervical spine, diverticulum, or compression of the oesophageal lumen by tumour or aneurysm. In the lower oesophagus the probe may encounter

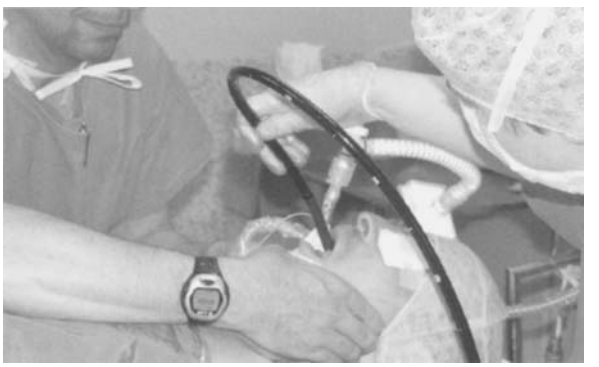

Figure 2.2 Insertion of the transoesophageal echocardiography probe in an anaesthetised and intubated patient. The operator stands to the left of the patient and uses the right hand for insertion while the left hand holds the handle of the probe. The assistant facilitates the insertion by lifting the jaw (Esmarch's manoeuvre).

stenoses or strictures due to benign or malignant processes or hiatal hernia. Any application of force in these conditions carries a risk for perforation and should prompt the operator to re-evaluate the indication or to call upon the gastroenterologist for help. A buckling of the probe can occur during insertion. If the probe becomes kinked in extreme anteflexion or retroflexion then this makes manipulation and image acquisition impossible, and the probe must be advanced into the stomach for unfolding before it is withdrawn.[11]

During imaging and in relation to the amount of energy emitted, the temperature of the transducer increases. In order to prevent any thermal injuries to the oesophagus and stomach, the temperature of the tip of the probe is continuously monitored. If the temperature of the transducer exceeds the preset limit, then the probe is automatically shut down. It is important that during continuous monitoring the ultrasound output (gain) is kept as low as possible and prolonged use of Doppler techniques is avoided. In patients with high fever the temperature sensor can disturb and interrupt the TOE examination because the transducer may remain turned off unless the temperature limits are adjusted or the oesophagus cooled with iced saline injected into the gastric tube.

The optimal setup in the operating theatre may vary according to the local conditions. Usually, the ultrasound machine is positioned behind the patient's head at the left side. Although this position, opposite to the anaesthetic machine and other monitors, facilitates handling of the probe

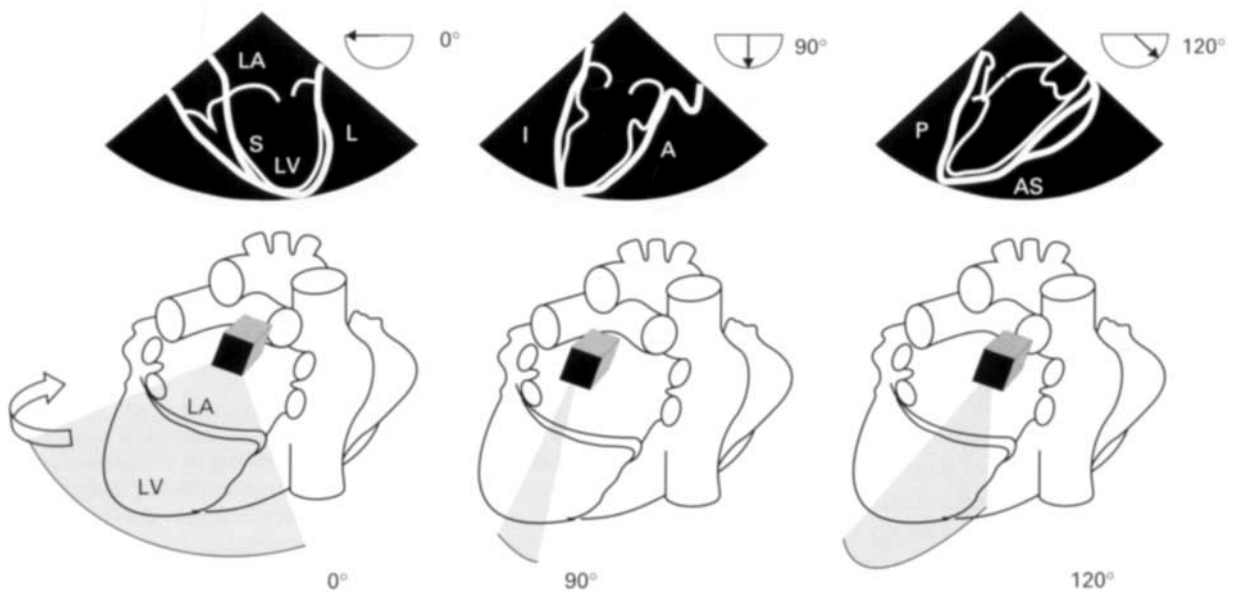

Figure 2.3 Principle of transoesophageal multiplane imaging of the heart. The transoesophageal echocardiography transducer is positioned behind the left atrium at the mid-oesophageal level. By appropriate retroflection of the tip of the probe, the imaging sector is directed toward the left ventricular (LV) apex. At 0° the imaging plane transects first the left atrium (displayed at the top) and further away the LV (displayed in the lower part of the screen). The lateral LV wall is displayed on the right, and the septum and the right ventricle on the left of the screen. By clockwise rotation of the imaging plane (arrow), the left margin of the imaging sector moves from the lateral to the anterior LV wall, whereas the right margin posteriorly traverses the septum and proceeds to the inferior wall. At 90° the anterior wall is displayed on the right and the inferior wall on the left of the screen. Further rotation of the imaging plane (to 120°) moves the original left margin to the anteroseptal wall, which is displayed on the right side of the screen. The opposing posterior wall is displayed on the left side. Thus, the entire LV can be imaged in longitudinal views without changing the position of the probe. The degree of rotation of the transducer is indicated by the displayed value of the angle (0–180°) and by the position of the arrow in the semicircular images. A = anterior, AS = anteroseptal, I = inferior, L = lateral, LA = left atrium, LV = left ventricle, P = posterior, S = septum.

and manipulation of the controls, it may result in decreased vigilance for changes in other monitored variables.[12]

Manipulation of the probe

The handling of the multiplane probe and the original monoplane or biplane probe differs. The monoplane probe provides images only in the transverse plane and is cumbersome to manipulate. Using the biplane probe, the operator alternatively switches on the horizontal (transverse) or the longitudinal (vertical) transducer and rotates the shaft of the probe to obtain the desired images. With the multiplane probe the steering of the ultrasound beam is automated (usually by pressing a knob on the handle), thus limiting the manual manipulation of the probe. The probe is moved downward (advanced) and upward (withdrawn) in the oesophagus and/or the stomach in order to obtain standard cross-sectional views at different levels. The whole probe can be rotated to the right (clockwise) and to the left (anticlockwise). The tip of the probe can be flexed anteriorly (anteflexion), posteriorly (retroflexion), and laterally (right or left lateral flexion). One usually starts the multiplane TOE at each standard level with the ultrasound beam in the transverse (horizontal) plane. A small semicircular icon on the screen displays the position of the imaging plane between 0° and 180°. The standard transverse plane corresponds to 0°. After initial imaging in the transverse plane, by pushing the appropriate knob the ultrasound beam is rotated clockwise (looked at from the patient's head) through 90° (longitudinal plane) to 180°, the latter being the mirror image of the 0° transverse plane. The left margin of the imaging plane that rotates up to 90° and down toward 180° is displayed on the right side of the screen. A second knob drives the beam back (anticlockwise) from 180° to 0°. This operation is illustrated in Figure 2.3.

Standard imaging procedure

Every TOE examination should be complete and performed according to a standard protocol. The standardised procedure minimises the risk for missing important abnormal findings. Of course, in life-threatening situations and emergencies, identification and immediate treatment of the culprit lesion have priority.

The complete TOE examination is performed at different levels between the stomach and the upper oesophagus. These standard imaging levels are defined in Table 2.1. A great number of images or views can be obtained by the multiplane TOE at these levels. Although many of them are not useful in routine perioperative TOE, the echocardiographer should be aware of the complete imaging potential of the multiplane TOE in order to draw the correct conclusions in special and difficult situations. The required information about a given cardiac structure can usually be derived from more than one view. This becomes important when the standard views cannot be obtained. TOE lacked a standardised terminology until the Task Force of the American Society of Echocardiography and the Society of Cardiovascular Anesthesiologists labelled the 20 most important intraoperative TOE views in a way that is consistent with the terminology used for transthoracic echocardiography[13] (Box 2.2). Throughout this chapter, these now standardised views are highlighted in bold. There is still some disagreement in differentiating between the mid- and upper oesophageal views. For didactic reasons, we describe the views according to the traditional classification.

Table 2.1 Multiplane transoesophageal echocardiography: imaging planes

Imaging level	*Distance from teeth to tip of the probe*
Transgastric levels	38–45 cm
Gastro-oesophageal junction	34–37 cm
Lower and middle oesophagus	29–33 cm
Upper oesophagus	24–28 cm

Recommended views

- MOE four chamber
- MOE two chamber
- MOE LAX
- TG mid SAX
- TG two chamber
- TG basal SAX
- MOE mitral commissural
- MOE AV SAX
- MOE AV LAX
- TG LAX
- Deep TG LAX
- MOE bicaval
- MOE RV inflow – outflow
- TG RV inflow
- MOE ascending aortic SAX
- MOE ascending aortic LAX
- Descending aortic SAX
- Descending aortic LAX
- UOE aortic arch LAX
- UOE aortic arch SAX

AV = aortic valve, LAX = long axis, MOE = midoesophageal, RV = right ventricular, SAX = short axis, TG = transgastric, UOE = upper oesophageal.

Box 2.2 Comprehensive intraoperative multiplane transoesophageal echocardiography examination: American Society of Echocardiography/Society of Cardiovascular Anesthesiologists Guidelines[13]

Transgastric views

Transgastric short-axis views

We prefer to begin the TOE examination in the stomach with the imaging of the left ventricle (LV). The depth control of the ultrasound imaging system is set at 12–15 cm (starting the imaging with lower magnification facilitates the orientation of the operator at the start of the study), and the compress control and the gain are adjusted until the structures surrounding the transducer are clearly visualised. Initially the imaging plane is kept at 0°. At the top of the imaging sector, hepatic tissue (left liver lobe) and diaphragm can be seen. By rotating the probe along its long axis to the left and anteflecting the tip (by rotating the large wheel clockwise), the transducer is brought into contact with the gastric wall adjacent to the diaphragmatic (inferior) wall of the LV, which is visualised in its cross-section. Some adjustment of the insertion depth and anteflexion of the tip will be necessary to obtain a standard short-axis view of the LV at the mid-papillary muscle level (Figure 2.4). The average distance from the teeth to the tip of the probe associated with this view is 43 cm (range 38–42 cm, depending on the height of the

patient). The standard transgastric short-axis view of the LV at mid-papillary muscle level (**TG mid SAX**) is circular and symmetrical; both papillary muscles (anterolateral and posteromedial) have a semicircular form and attach to the ventricular wall by a broad base. The standard orientation of the image shows the inferior LV wall at the top of the sector, close to the transducer, and the anterior wall at the bottom. The septum is located on the left of the image, and opposite to it on the right is the lateral wall. On the left of the LV septum is found the right ventricle (RV), in its crescent-like cross-section or short-axis view.

With slight changes to both the depth of insertion and anteflexion of the probe, additional short-axis views of the LV are obtained; starting from the mid-papillary muscle level toward the apex, the low papillary muscle level where the papillary muscle insertion is still just visible comes into view, followed by the apical view (with minimum anteflexion) below the insertion of the papillary muscles. Toward the base of the ventricle the high papillary muscle view, with papillary muscles separated from the wall and circular in cross-section, can be obtained. A little more cranially, the chordae tendineae appear instead of the papillary muscles in the ventricular cavity (chordal view), only to be replaced shortly after by the mitral valve leaflets in this basal or mitral valve short-axis view (**TG basal SAX**). The posterior leaflet is seen at the top right and the anterior leaflet at the bottom left of the sector. The anterolateral commissure is situated at about the 5 o'clock position, and the posteromedial commissure at about the 10 o'clock position of the sector.

Visual on-line evaluation of these short-axis images offers the anaesthetist very useful

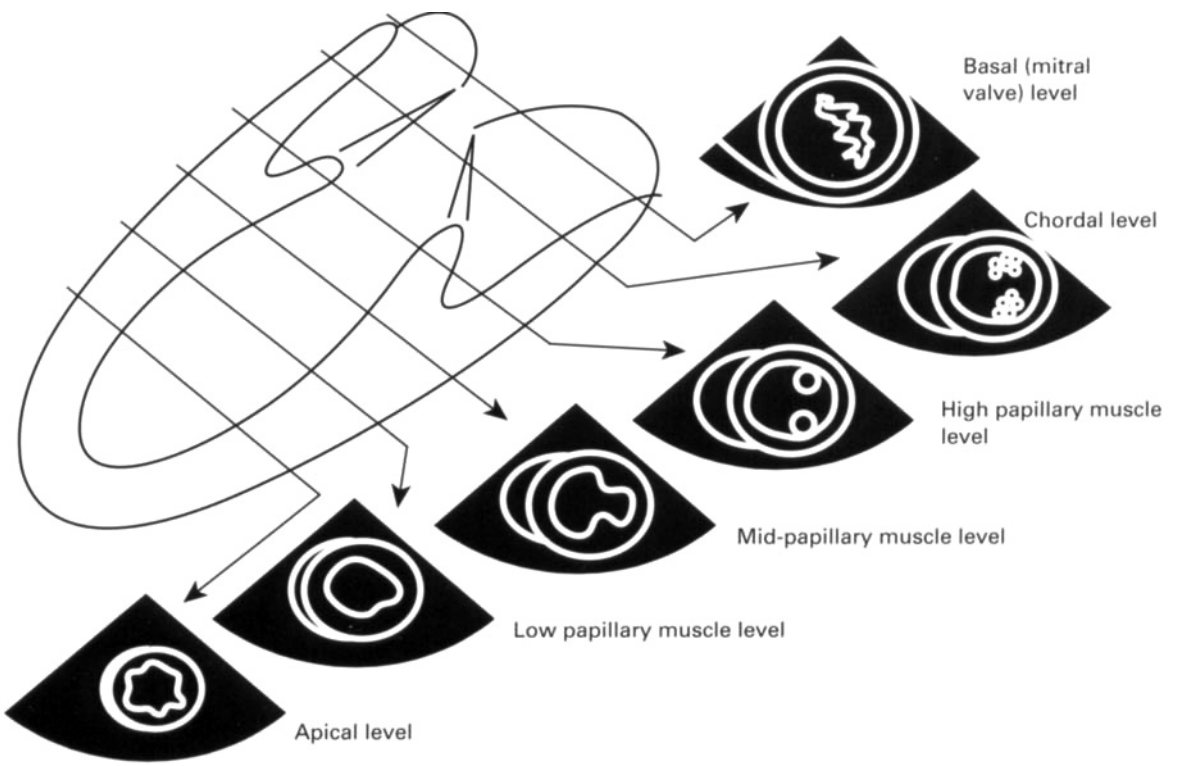

Figure 2.4 Transgastric views I. The cross-sectional views of the left ventricle can be obtained at different levels between the mitral valve annulus and the apex. The standard short-axis view shows the left ventricle at the level between the origin and the tip of the papillary muscles (mid-papillary muscle level). Here, both papillary muscles appear as semicircular structures still attached with their base to the left ventricular wall. The posteromedial papillary muscle occasionally presents with two heads. The optimal imaging of the right ventricle in its short axis requires a slight rotation of the shaft to the right. The basal short-axis view displays the cross-section of the mitral valve, with the anterior leaflet on the left and the posterior leaflet on the right of the screen. The anterolateral commissure is displayed down and to the right of the screen, and the posteromedial commissure on the top left of the screen.

Table 2.2 Left ventricular dimension and function in anaesthetised and ventilated individuals free of cardiovascular disease, as obtained by transoesophageal echocardiography[14]

Transgastric short-axis view	Men		Women	
	cm^2	cm^2/m^2	cm^2	cm^2/m^2
EDA	16·1 ± 3·7	8·2 ± 1·9	12·7 ± 2·7	7·1 ± 1·6*
ESA	6·7 ± 2·2	3·4 ± 1·1	4·9 ± 1·4	2·7 ± 0·7*
EDD_{ap}	4·4 ± 0·5	2·2 ± 0·3	3·9 ± 0·5	2·2 ± 0·3
ESD_{ap}	2·9 ± 0·6	1·5 ± 0·3	2·5 ± 0·5	1·4 ± 0·2
FAC%	59 ± 8		62 ± 6	
FS%	34 ± 9		37 ± 7	

*$P < 0·05$ versus men. ap = anteroposterior, EDA = end-diastolic area, EDD = end-diastolic diameter, ESA = end-systolic area, ESD = end-systolic diameter, FAC% = fractional area change, FS% = fractional shortening. Values are mean ± SD (Data from Skarvan *et al.*[15])

information on the size (normal, small, or dilated), structure (normal or hypertrophic), and systolic function (global and regional) of the LV and RV. In addition, the relative sizes of both ventricles and the shape of the interventricular septum and pericardium can be evaluated. The characteristic semicircular appearance of both papillary muscles arising with their broad base from the free LV wall allows the operator to return to this plane and to reproduce this image after the probe has been moved to another level. Both TG mid and basal SAX views are a part of the 16-segment model of the LV used for evaluation of regional LV wall motion and detection of myocardial ischaemia (see Chapter 11).

The information obtained by the operator visually (using the "naked eye") should be confirmed by measurements in images frozen in end-diastole and end-systole using the measurement software of the given ultrasound system. The standard measurements include end-diastolic area (EDA) and end-systolic area (ESA), and corresponding diameters (end-diastolic diameter [EDD] and end-systolic diameter [ESD]) at the mid-papillary muscle level as measures of LV size. EDA and ESA measurements enable calculation of fractional area change (FAC%):

$$FAC\% = ([EDA - ESA]/EDA) \times 100$$

FAC% is the TOE analogue of the radionuclide or contrast ventriculography based ejection fraction, and is used as an index of global LV function. An alternative index of global systolic function is the fractional shortening (FS%):

$$FS\% = ([EDD - ESD]/EDD) \times 100$$

The end-diastolic image is the frame synchronous with the R wave of the electrocardiogram, whereas the end-systolic frame is that with the smallest size of the LV cavity. For standard measurements of the area (or diameters), the papillary muscles are included in the LV cavity. Several techniques for measurements in echocardiography have been proposed; the leading edge to leading edge or the black–white interface technique is used by most institutions.[14] Normal values for LV size and global function obtained in anaesthetised and ventilated patients without cardiovascular disease, based on the transgastric short-axis view, are given in Table 2.2. The LV size is smaller than in awake patients, reflecting the redistribution of blood volume associated with controlled ventilation. The cross-sectional area of the LV is smaller in women, even after correction for body surface area.[15]

Transgastric longitudinal views

Starting out from the mid-papillary level and rotating the imaging plane to 90°, the LV transgastric two-chamber view (**TG two chamber**) is obtained (Figure 2.5). This longitudinal cross-section shows the inferior wall at the top and the anterior wall at the bottom of the sector, whereas on the right we see the left atrium and the mitral valve, and on the left the distal parts of the LV. The true apex can only rarely be imaged because the longitudinal imaging plane tends to run either in front of or behind the apex through the adjacent wall. By slight rotation of the shaft, the longitudinal cross-sectional views of the papillary muscles and the subvalvular structures can be examined. Further rotation of the plane toward 120°–130° brings the LV outflow tract,

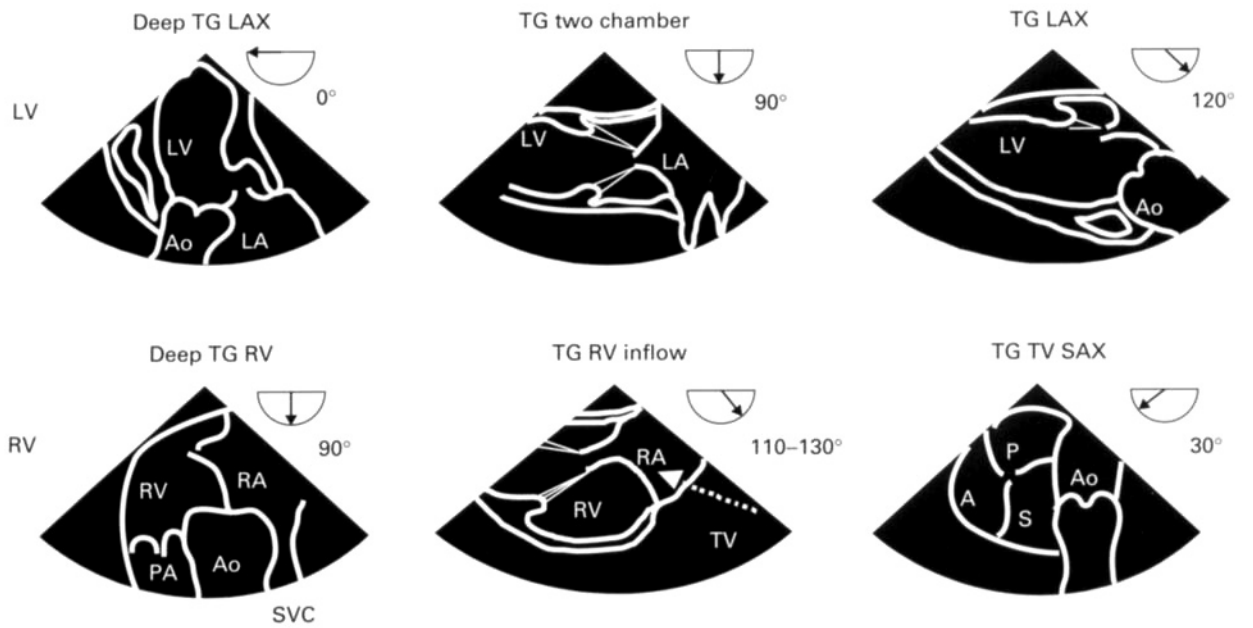

Figure 2.5 Transgastric views II. The deep transgastric left ventricular long-axis (deep TG LAX) view resembles the transthoracic apical view and requires maximal anteflexion of the transoesophageal echocardiography probe tip. The transgastric two chamber (TG two chamber) view allows for evaluation of the basal and middle anterior and inferior wall motion and the mitral valve apparatus, including both papillary muscles in their long axes. The transgastric long-axis (TG LAX) view offers good alignment of ultrasound beam and blood flow across the aortic valve, which is a prerequisite for reliable Doppler measurements of aortic flow velocity. Alternatively, aortic blood flow velocity can also be measured in the deep transgastric planes, particularly in the deep TG right ventricular (RV) view. Flows in the RV outflow tract, across the pulmonary valve, and in the pulmonary artery can also be measured here using Doppler. The tricuspid valve can be interrogated in the transgastric RV inflow (TG RV inflow) view in its long axis and at approximately 30° in its short axis (TG TV SAX). A = anterior, Ao = aorta, LA = left atrium, LV = left ventricle, P = posterior leaflet of the tricuspid valve, PA = pulmonary artery, RA = right atrium, RV = right ventricle, S = septal leaflet of the tricuspid valve, SVC = superior vena cava, TV = tricuspid valve.

aortic valve, and a variable part of the ascending aorta into view. This cross-section is called the transgastric long-axis view (**TG LAX**), and it is important for measurements of blood flow velocity in the LV outflow tract and across the aortic valve using Doppler techniques. By rotating the shaft of the probe to the right the long-axis view of the RV (**TG RV inflow**), showing the right atrium (on the right of the display), tricuspid valve, and RV, is obtained. A short-axis view of the tricuspid valve with all three leaflets can be also obtained at this level.

Distal (deep) transgastric views

By advancing the probe deeper into the gastric fundus and maximising the anteflexion of its tip with the beam at 0°, a modified transgastric 'apical' or five-chamber view of the heart can be obtained (Figure 2.5). At the top of the screen both ventricles (usually foreshortened) and at the bottom both atria can be seen. The RV is on the left and the LV is on the right of the screen. With minor adjustment, the view can be modified into a three-chamber view or deep transgastric long-axis view (**deep TG LAX**) with the para-apical region of the LV at the top, the left atrium at the bottom, and the LV outflow tract, aortic valve, and a proximal portion of the ascending aorta in the centre (on the left of the left atrium). This view allows excellent alignment of the ultrasound beam with the blood flow out of the LV, which is a prerequisite to any quantitative Doppler measurements in the outflow tract and across the aortic valve. By clockwise rotation of the imaging plane, the right heart structures can be evaluated. The aorta remains in the centre of the sector, and on its right the RV outflow tract with the pulmonary valve and the proximal main pulmonary artery will appear. The right atrium and tricuspid valve are localised on the left of the aortic cross-section. This view is useful for Doppler measurements of blood flow

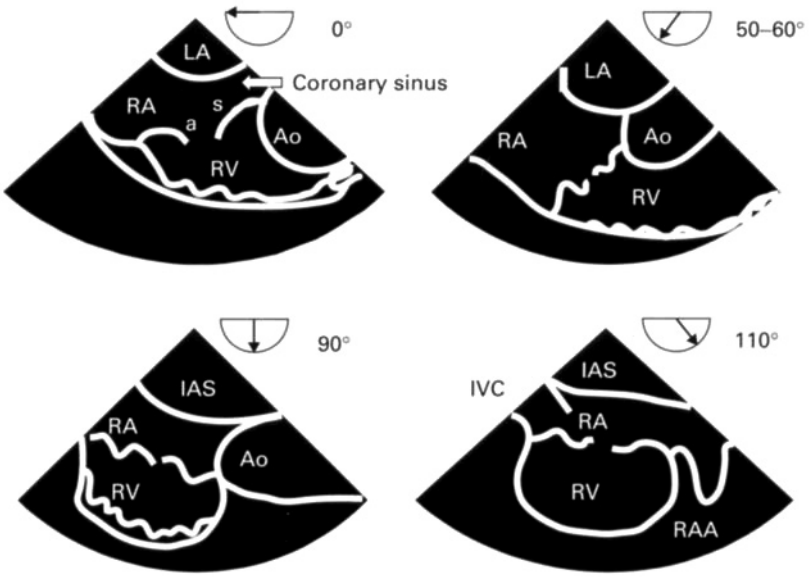

Figure 2.6 Gastro-oesophageal junction views. These views are obtained during withdrawal of the probe from the proximal gastric level to the low oesophageal level and by rotating the imaging plane from 0° to 110°. These views are useful in the evaluation of right heart anatomy, function, and pathology. The function of the right ventricular free wall, as well as the morphology of coronary sinus, atrial septum, tricuspid valve, and right atrial appendage, can be assessed. At 90° the velocity of tricuspid regurgitation can be measured as required for the estimation of right ventricular systolic pressure. The views are also useful for detection of masses (thrombi, vegetations) and for localisation of catheters, cannulas, and electrodes in the right heart. a = anterior leaflet of the tricuspid valve, Ao = aorta, IAS = atrial septum, IVC = inferior vena cava, LA = left atrium, RA = right atrium, RAA = right atrial appendage, RV = right ventricle, s = septal leaflet of the tricuspid valve.

velocity across the RV outflow tract and the pulmonary valve.

Gastro-oesophageal junction views

Withdrawing the probe back to the level of the gastro-oesophageal junction (usually by 4–5 cm) and rotating the shaft slightly clockwise, informative images of the right heart can be obtained (Figure 2.6). At 0° the right atrium at the top and the anterolateral free wall of the RV at the bottom of the sector can be seen. At the bottom on the right side of the sector an oblique section of the posterior portion of the interventricular septum is seen. Anterior (on the left) and septal leaflets of the tricuspid valve are well visualised. To the right and above the septal leaflet of the tricuspid valve, the coronary sinus is seen entering the right atrium at the end of its course in the atrioventricular groove. At 50–60° the left atrium appears at the top with the right atrium and an oblique section of the aorta below it. The position of the tricuspid valve now allows alignment of the Doppler beam with both the forward and regurgitant tricuspid blood flows for reliable flow velocity measurements across the tricuspid valve. At 90° the structure and form of the interatrial septum in its almost horizontal course can easily be assessed, and shunting of blood at the atrial level can be examined by colour Doppler imaging. The inferior and superior venae cavae are seen entering the right atrium. This bicaval view can also be obtained at the mid-oesophageal level as the **MOE bicaval** view. Finally, by rotating the imaging plane to 100–110°, the junction of the inferior vena cava, with the right atrium on the left and the right atrial appendage on the right, can be seen. The fine linear and usually quite mobile structure arising from the junction is Eustach's valve.

Mid-oesophageal views

By withdrawing the probe toward the middle of the left atrium and, for the first time, retroflecting it with the imaging plane kept between 0° and 20°, the standard four-chamber view (**MOE four chamber**) with both atria and both ventricles is obtained (Figure 2.7). The lateral free walls of both ventricles and the posterior portion of the interventricular septum are visualised in this view. The mitral valve is now close to the

transducer positioned behind the left atrium and can be zoomed in and examined in great detail. The anterior mitral valve leaflet is displayed on the left and the posterior leaflet on the right. Because the imaging plane often misses the apex, the ventricles may be foreshortened in this view, and consequently the true apex cannot be visualised. A slight withdrawal of the probe and a reduced retroflexion allows imaging of the LV outflow tract, aortic valve, and to a variable extent the ascending aorta, resulting in the three-chamber and five-chamber views. The left-sided boundary of the ventricle is now the anterior septum and the right-sided structure is its posterolateral wall.

By rotating the plane from about 30° toward 60°, the left-sided wall of the ventricle on the screen now becomes the inferior septum, whereas the anterolateral wall emerges on the right of the screen. At about 60° the mitral valve leaflets exchange their respective positions on the screen; the anterior leaflet appears on the right and posterior leaflet on the left. Similarly, the anterior wall is displayed on the right and the inferior wall on the left of the screen. Approximately between 60° and 70° the imaging plane runs parallel to the line connecting the anterolateral and posteromedial commissures of the mitral valve, resulting in visualisation of both coaptation points. The corresponding mitral commissural view (**MOE mitral commissural**) shows the posterior leaflet both on the right (segment or scallop P1) and on the left (segment P3) of the sector, with the middle segment of the anterior leaflet (A2) between them. At 90° the LV two-chamber view (**MOE two chamber**) is obtained, displaying the anterior wall on the right and the inferior wall on left of the screen. The left atrial appendage and the left upper pulmonary vein entering the atrium can be visualised above

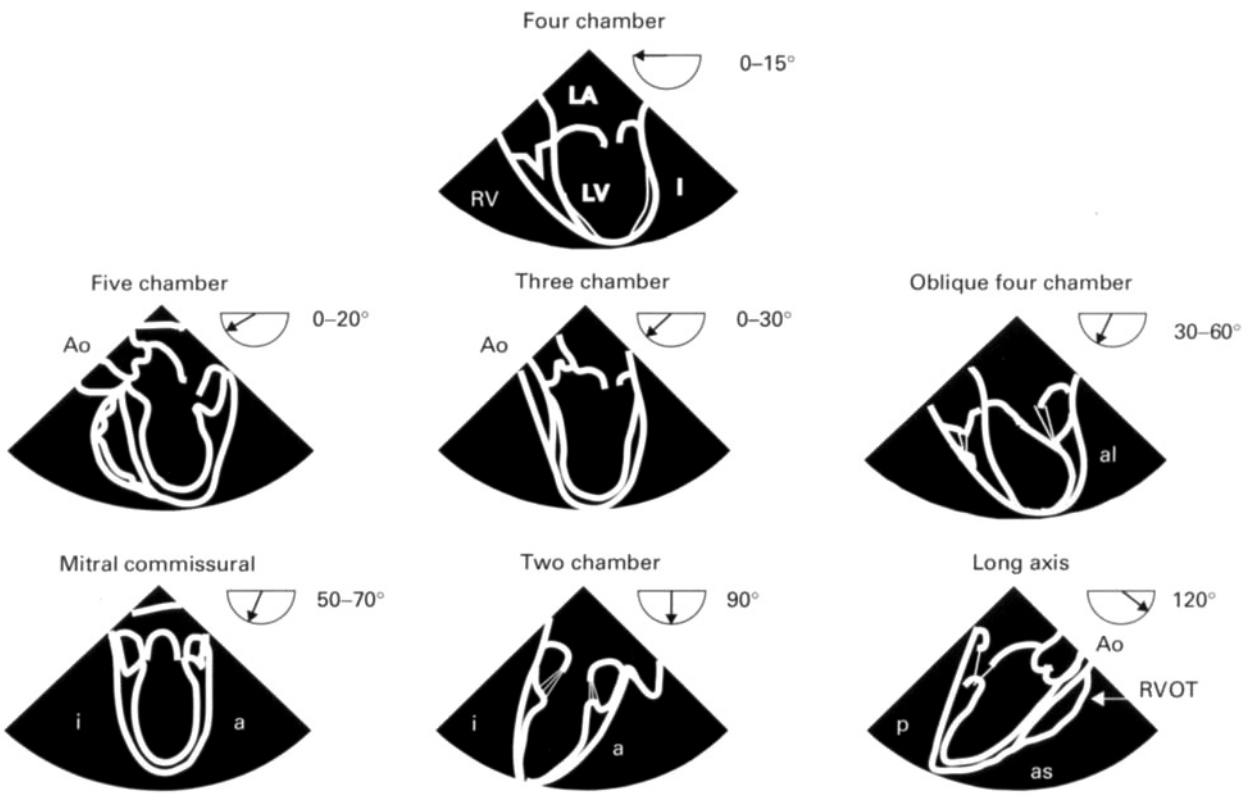

Figure 2.7 Lower and mid-oesophageal views: I. This series of longitudinal views allow comprehensive evaluation of global and regional left ventricular functions and the mitral valve. The four-chamber view is the starting point of mid-oesophageal imaging. It is indispensable for assessing the relative size of the four chambers, overall cardiac function, and geometry of atrial and ventricular septa. The slightly anteriorly located three-chamber and five-chamber views are obtained by decreasing the degree of tip retroflection and/or by slightly withdrawing the probe from the four-chamber level. The morphology and motion of the aortic valve can be also evaluated in these views. a = anterior, al = anterolateral, Ao = aorta, as = anteroseptal, i = inferior, l = lateral, LA = left atrium, LV = left ventricle, p = posterior, RV = right ventricle, RVOT = right ventricular outflow tract.

the LV anterior wall. Further rotation to about 130° finally produces the mid-oesophageal LV long-axis view (**MOE LAX**), with the left atrium and LV on the left and the LV outflow tract with the aortic valve, aortic root, and a portion of the ascending aorta on the right. The posterior and posterolateral wall now forms the left-sided boundary and the anteroseptal wall the right-sided boundary of the LV chamber. The non-coronary or left coronary (upper) and right coronary (lower) cusps of the aortic valve are visible.

The examination at the mid-oesophageal level is completed by imaging the interatrial septum and various structures of the right heart (Figure 2.8). For this purpose, some degree of rotation of the shaft to the right is necessary. The interatrial septum should be interrogated at different levels and plane angles (from 0° to 130°). The longitudinal views of the RV allow evaluation of the RV inflow and outflow tracts and the pulmonary valve. In order to measure blood flow velocities across the tricuspid valve by Doppler, the best alignment between the ultrasound beam and blood flow is usually found at 40–50°. The bicaval view displays the inferior and superior venae cavae entering the right atrium on the left and right of the screen, respectively. The variable Eustachian valve marking the insertion of the inferior vena cava must not be mistaken for thrombus or foreign body.

Upper oesophageal views

Aortic views

The American Society of Echocardiography/ Society of Cardiovascular Anesthesiologists guidelines designate these views as mid-oesophageal.[13] A series of important images is obtained at this level by slight adjustments of the transducer depth and rotation of the ultrasound beam. These views are characterised by the central position of the aortic root and the left atrium occupying the top of the screen (Figure 2.9). At 0–30° an oblique section of the aortic root appears on the screen. At 40–60° the characteristic short-axis view of the aortic valve (**MOE AV SAX**) is obtained. The right coronary cusp and sinus are located at the bottom, contiguous with the RV wall; the non-coronary sinus lies on the left and the left coronary sinus on the right. On the right side the left atrial appendage can be imaged. At 60–100° the cross-sectional view of the aorta still remains in the middle of the image whereas, from left to right, the right atrium, tricuspid valve, RV, pulmonary valve, and main pulmonary artery become visible as they wind around the aorta. This view is called mid-oesophageal RV inflow–outflow view (**MOE RV inflow–outflow**) and is indispensable for evaluating the right heart and congenital lesions involving the RV and pulmonary artery. Rotation

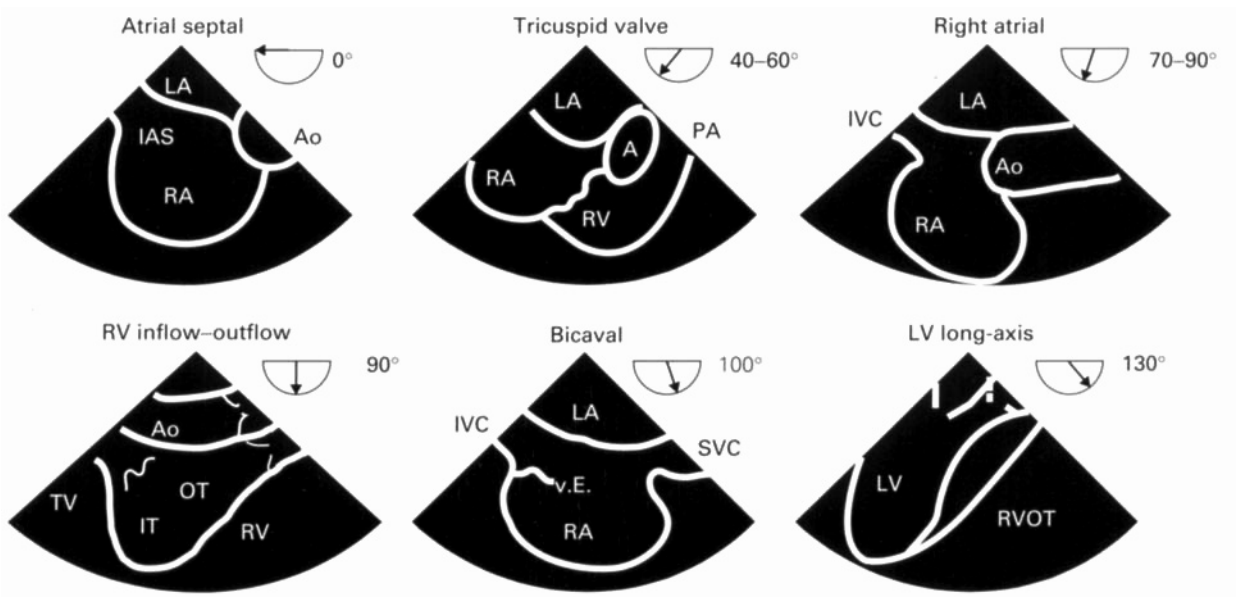

Figure 2.8 Lower and mid-oesophageal views: II. In addition to the gastro-oesophageal junction views, important right heart structures can also be interrogated at this level. Ao/A = aorta, IAS = atrial septum, IT = inflow tract, IVC = inferior vena cava, LA = left atrium, LV = left ventricle, OT = outflow tract, PA = pulmonary artery, RA = right atrium, RV = right ventricle, RVOT = right ventricular outflow tract, SVC = superior vena cava, TV = tricuspid valve, v.E. = valvula Eustachi.

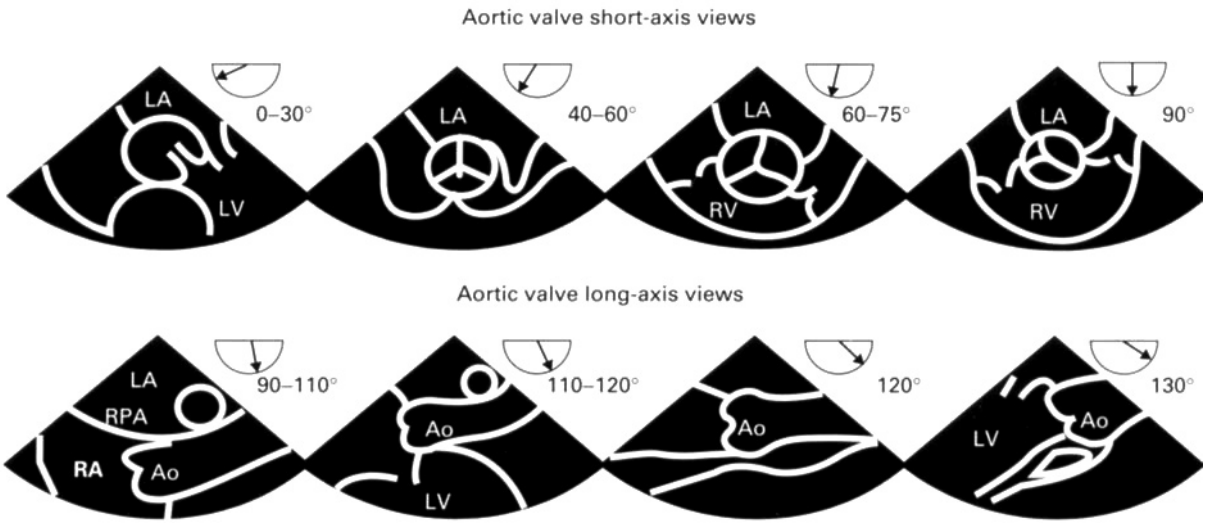

Figure 2.9 Upper oesophageal views I: aortic views. These views allow for a comprehensive evaluation of the aortic valve in its short (0–90°) and long axes (90–130°). In the short-axis views the individual aortic valve cusps and the origins of the right and left coronary arteries can be evaluated. Furthermore, the opening area of the aortic valve can be measured. In the longitudinal views the width of the aortic valve annulus, aortic root, and sinotubular connection can be measured and the proximal part of the ascending aorta examined (e.g. for dissecting membranes, atheroma, aneurysm). In the 60–75° view the left coronary cusp of the aortic valve is seen on the viewer's right, the non-coronary cusp on the left, and the right coronary cusp at the bottom. In the long-axis views the right coronary cusp is displayed toward the bottom, the superiorly displayed cusp is the left coronary cusp if the probe tip is rotated anticlockwise or the non-coronary cusp if the probe is rotated clockwise. Ao = aorta, LA = left atrium, LV = left ventricle, RA = right atrium, RPA = right pulmonary artery, RV = right ventricle.

of the imaging plane beyond 110–120° displays the most distal part of the LV outflow tract (on the left), and the aortic valve and ascending aorta (on the right) in their longitudinal axes (**MOE AV LAX** and **MOE ascending aortic LAX**). The short axis of the right pulmonary artery is visible between the posterior wall of the aorta and the top of the sector. At approximately this level and at 0–40° plane rotation, the left main coronary artery can be found originating from the left coronary sinus and can be followed further beyond its division into the left anterior descending artery (running downward) and circumflex artery (running horizontally). The ostium of the right coronary artery can be found at the bottom of the right coronary cusp.

Pulmonary artery views

When the probe is further withdrawn at 0°, the main pulmonary artery appears in the centre of the sector, branching at the top of the sector into the right (on the left of the sector) and left pulmonary arteries (**MOE ascending aortic SAX**; Figure 2.10). In this view the patent ductus arteriosus can be diagnosed with the help of colour Doppler imaging. Colour Doppler shows a turbulent flow entering the pulmonary artery, and by rotating the imaging plane it allows one to identify the mouth of the duct. This view is suitable for Doppler measurement of pulmonary artery flow velocity. On the left of this long-axis view of the pulmonary artery are the cross-sections of the ascending aorta and superior vena cava. Rotating the plane toward 30–50° allows interrogation of most of the right pulmonary artery in its long axis. The imaging of the left pulmonary artery beyond the bifurcation is usually not possible because of the interference with air in the left main bronchus. At 120–150° the right pulmonary artery is imaged in its short axis, appearing above the ascending aorta.

Pulmonary vein views

From the upper oesophagus the pulmonary veins can be imaged as they enter the left atrium from their respective sides. The upper and lower pulmonary veins enter the atria at slightly different angles; the lower pulmonary veins run more in the

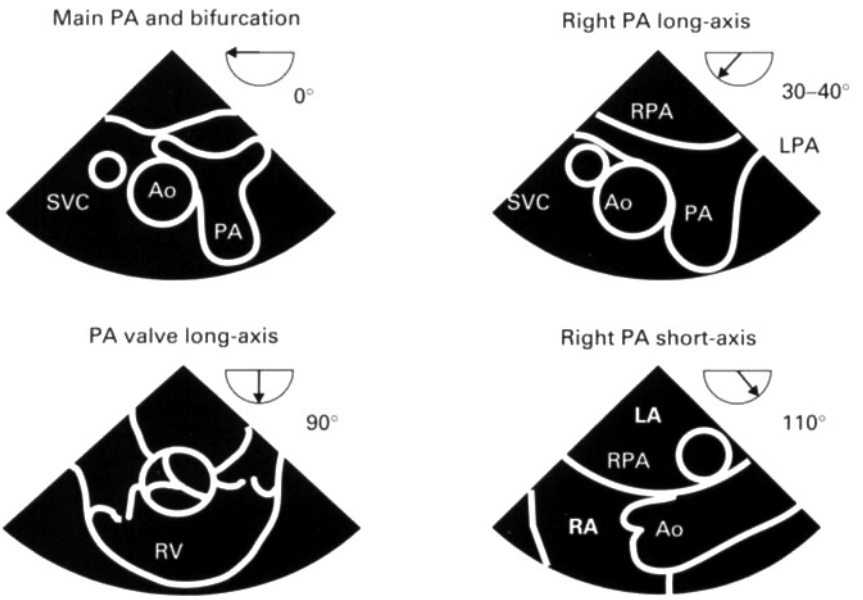

Figure 2.10 Upper oesophageal views II: pulmonary artery. These views are important for evaluating the size of the main pulmonary artery and its two branches, and the structure and function of the pulmonary valve. The comparison of diameters of pulmonary artery and aorta provides simple yet valuable information about the pulmonary vascular bed (dilation, hypoplasia). Blood flow velocity in the main pulmonary artery can be measured using an optimal insonation angle. In these views the search for thrombi in the superior vena cava and in the right heart or for pulmonary artery emboli initiated in the gastro-oesophageal junctional and lower oesophageal views is completed. The position of the central venous and pulmonary artery catheters can also be determined. Ao = aorta, LA = left atrium, LPA = left pulmonary artery, PA = pulmonary artery, SVC = superior vena cava, RA = right atrium, RPA = right pulmonary artery, RV = right ventricle.

posteromedial direction and the upper veins more in the anteromedial direction. In addition, the lower veins exhibit a more horizontal course and the upper veins a slightly vertical course. The left upper pulmonary vein is found easily at 0–30° between the left atrial appendage and the descending aorta (Figure 2.11). In order to image the left lower pulmonary vein, the probe is slightly advanced and rotated to the left (anticlockwise). Localisation of the pulmonary veins is facilitated by colour Doppler imaging. If two left pulmonary veins are imaged simultaneously, then the vein adjacent to the left atrial appendage is the left upper pulmonary vein. By rotating the imaging plane toward 90°, the left upper pulmonary vein can be found below the left pulmonary artery (in its short axis), entering the left atrium just above the anterolateral atrioventricular groove. The right upper and lower pulmonary veins can be visualised on the left of the sector at 0–40° as they enter the left atrium from the right. Rotation of the imaging plane to 80–100° facilitates the interrogation and improves the alignment of blood flow with the ultrasound beam, as required for Doppler flow velocity measurements. In the short axis, the right pulmonary vein adjacent to the superior vena cava is the right upper pulmonary vein; the latter lies next to the right pulmonary artery (in its short axis) in the longitudinal views. Again, colour Doppler is helpful for identifying these veins. Measurement of pulmonary venous blood flow velocity is useful for assessing LV diastolic function (LV filling) and to grade mitral regurgitation. In the presence of asymmetrical high-velocity mitral regurgitation jets, interrogation of all four pulmonary veins may be warranted.

Aortic arch and descending aortic views

The ascending aorta can be imaged all the way from the deep transgastric position up to the upper oesophagus (UOE), both in its short and long axes. In the upper oesophagus the short axis of the ascending aorta is obtained at 0–40°, with the right pulmonary artery appearing above and the superior vena cava to the left of the aorta. The longitudinal view of the ascending aorta is obtained by rotating the imaging plane to 110–120°. In this view the short axis of the right pulmonary artery is seen just above the posterior aortic wall. However, because of

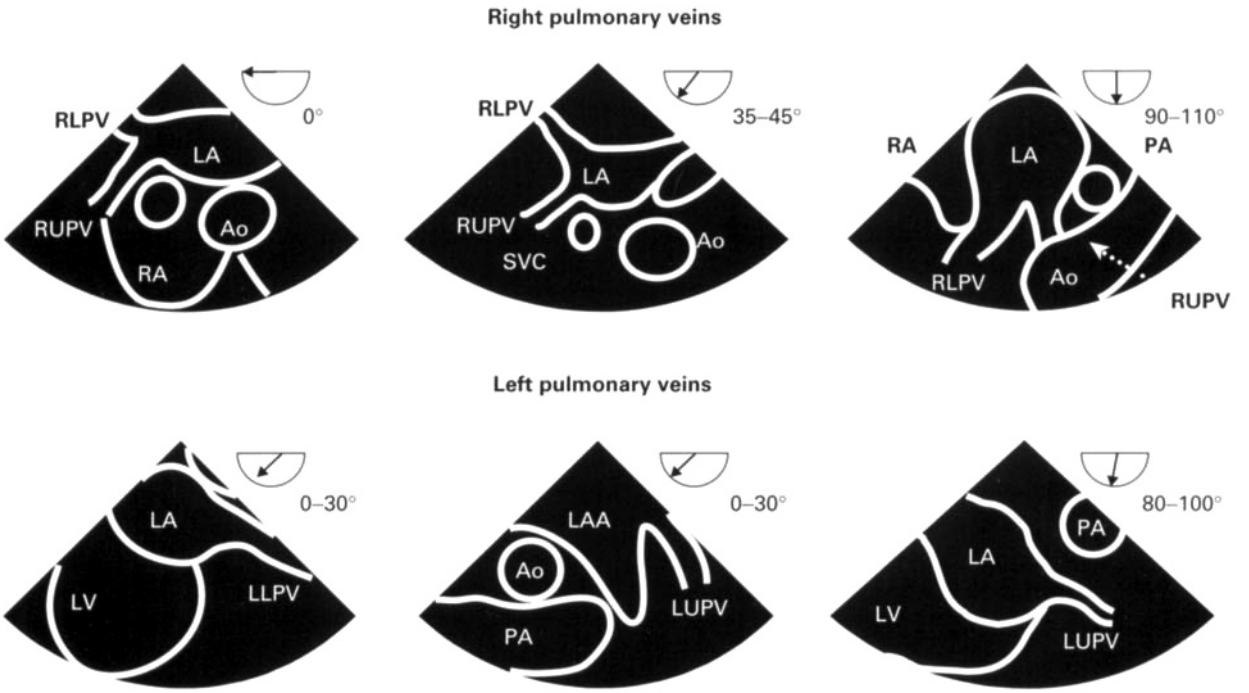

Figure 2.11 Upper oesophageal views III: pulmonary veins. Identification of the right-sided pulmonary veins can be difficult and is best done with the help of colour Doppler. The search for left-sided pulmonary veins is easier and it is usually at the left upper pulmonary vein, adjacent to the left atrial appendage, that the blood flow velocity is measured using pulsed Doppler. The pulmonary venous flow pattern is helpful in evaluating left ventricular diastolic function and in the grading of mitral valve regurgitation. In the presence of asymmetrical mitral regurgitation jets, the flow pattern in all four pulmonary veins should be assessed. This requires a careful search for an optimum insonation angle for the individual veins. The left atrial appendage must be meticulously scrutinised for thrombi. Ao = aorta, LA = left atrium, LAA = left atrial appendage, LLPV = left lower pulmonary vein, LUPV = left upper pulmonary vein, LV = left ventricle, PA = pulmonary artery, RA = right atrium, RLPV = right lower pulmonary vein, RUPV = right upper pulmonary vein, SVC = superior vena cava.

interference with air in the trachea and in the left main bronchus, the distal ascending aorta and the proximal arch represent blind spots for TOE. With the help of multiplane technology the blind area is reduced, and in many cases even arched vessels can be visualised.

In the upper mediastinum the aortic arch runs obliquely backward and to the left, whereas the oesophagus descends posteriorly and to the right. Therefore, by rotating the shaft of the probe to the left and keeping the imaging plane at 0°, an oblique longitudinal view of the arch (**UOE aortic arch LAX**) can be obtained with the proximal portion on the left lower and the distal portion on the right upper side of the sector (Figure 2.12). The systolic flow direction on the screen is from the left to the right, and is therefore coded red by colour Doppler. In front of the arch (below its anterolateral wall on the screen) the anonymous vein becomes visible. By rotating the imaging plane to 90°, the short-axis view of the arch (**UOE aortic arch SAX**) is obtained. Its posteromedial wall is on the top and its superior wall (where the arch branches originate) on the right of the screen. By carefully adjusting the depth of the probe, the left subclavian artery can be visualised. Below and to the right of the arch the left subclavian vein appears on the screen. Colour Doppler is very helpful in finding the arch vessels and for identification of the adjacent veins. The origin of the left subclavian artery represents an important landmark for localisation of the aortic isthmus at the junction of the arch and the descending aorta. This is the site of important pathologies such as aortic coarctation and traumatic rupture. A small dimple representing the ligamentum arteriosum can be usually found on the inferior aspect of the arch. The upper thoracic aorta runs downward and to the left of the midline in front of the vertebral column. During its downward course the descending aorta moves rightward and reaches the midline at the level of the diaphragm. The

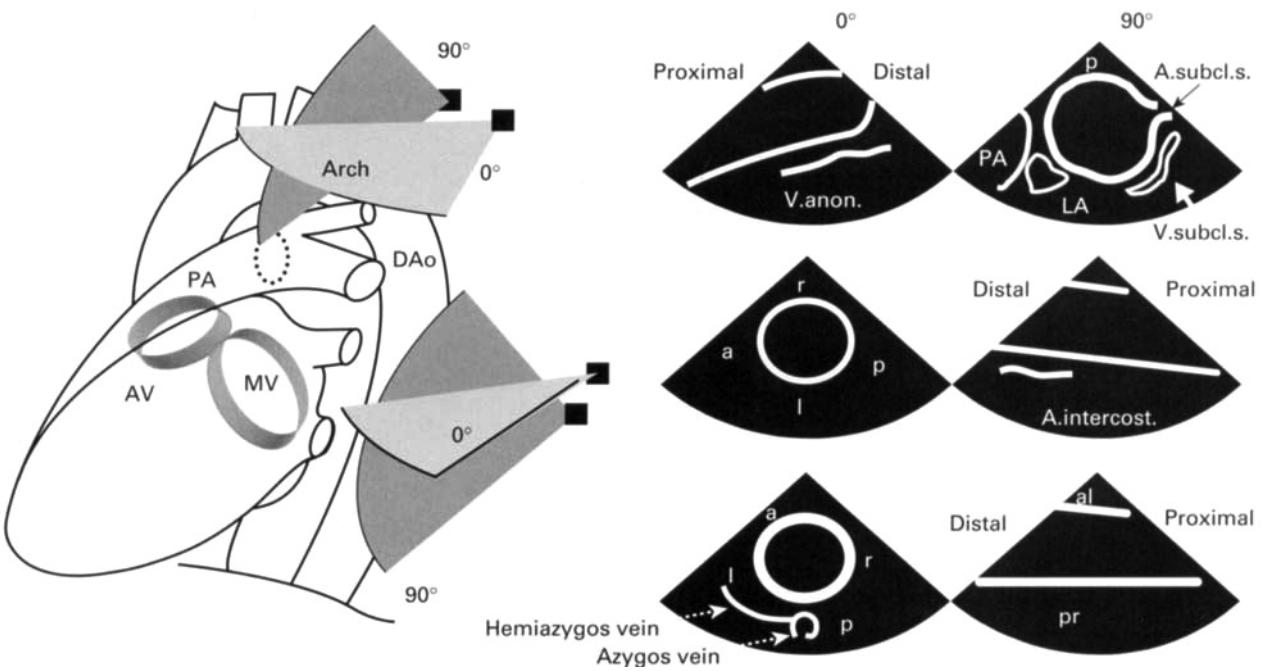

Figure 2.12 Aortic arch and descending aortic views. In the upper mediastinum, the oesophagus lies in front of the vertebral column and behind the aortic arch. The latter runs in an oblique plane from the front right to the back left. Thus, the distal part of the arch projected at 0° to the right on the display is closer to the transducer, and it is therefore displayed toward the top of the display. The short-axis view (at 90°) of the distal arch allows imaging of the origin of the left subclavian artery. The artery serves as a landmark for localisation of the aortic isthmus – a site of important pathologies (coarctation, traumatic rupture). In the middle of the chest the oesophagus lies to the right of the aorta and, consequently, the transoesophageal echocardiography transducer looks toward the right wall of the aorta. In the lower chest, both oesophagus and aorta approach the midline with the oesophagus in front of the aorta. At the level of gastric fundus, the aorta again moves slightly to the left of the vertebral column. The extent of left-hand rotation of the probe necessary to image the descending aorta increases as the probe is advanced toward the diaphragm. a = anterior, A.intercost. = intercostal artery, al = left anterior, A.subcl.s. = left subclavian artery, AV = aortic valve, DAo = descending aorta, l = left, LA = left atrium, MV = mitral valve, p = posterior, PA = pulmonary artery, pr = right posterior aortic wall, Prox = proximal, r = right, V.anon. = anonymous vein, V.subcl.s. = left subclavian vein.

oesophagus is partially twisted around the descending aorta and lies to the right of it in the upper mediastinum and in front of it in the lower mediastinum. This spatial relationship between the oesophagus and the descending aorta must be considered in order to localise correctly any aortic pathology on the TOE image. At 0° a cross-sectional image of the descending aorta (**descending aortic SAX**) is obtained, with its right wall at the top and its anterior wall on the left of the screen. Above the diaphragm, as the oesophagus becomes situated in front of the aorta, the aortic anterior wall will be found at the top and its left wall on the left of the sector. By rotating the plane from 0° to 90° the long axis of the descending aorta (**descending aortic LAX**) will appear, with the proximal portion situated on the right and the distal portion on the left of the screen.

Comprehensive intraoperative TOE examination

Multiplane technology allows a detailed interrogation of almost all parts of the heart and the great vessels. Although any of the described views can be important, it is not always necessary and usually impracticable to obtain and store all possible TOE views during routine perioperative studies. On the other hand, a minimal set of views should be defined to ensure that a significant pathology is not missed. Because of this the American Society of Echocardiography and the Society of Cardiovascular Anesthesiologists guidelines selected 20 two-dimensional views that should be obtained and stored during the performance of every comprehensive intraoperative

multiplane TOE examination.[13] These views and their respective nomenclature are presented in Figures 2.13–2.17. This standardisation has proven most useful both in reporting TOE findings and in teaching. However, the recording and storage of all of these 20 standard views is still difficult to achieve in practice (particularly if the echocardiographer-anaesthetist is also responsible for the management of anaesthesia) and may result in incomplete and non-systematic documentation. In addition, most of the intraoperative TOE studies also comprise pulsed, continuous, and colour Doppler examinations that further increase the number of images and loops to be stored. Therefore, a further reduction in routine TOE recordings to those views that are really essential is inevitable. Such a basic intraoperative examination based on eight cross-sections has recently been validated in the setting of cardiac surgery. Even this abridged TOE resulted in a pre-bypass view acquisition and storage rate of only 81% and a diagnostic accuracy rate of 79% among eight faculty anaesthetists. In repeated examinations the view acquisition rate decreased further.[16] Clearly, there is still considerable potential for improvement in diagnostic performance and documentation, and thus an important need for programmes that continuously improve the quality of perioperative TOE.[17]

Based on these published reports and our own experience, for a baseline perioperative TOE study we recommend a set of 10 two-dimensional views that provide adequate information on the structure and function of atria, ventricles, valves, and great vessels (Tables 2.3 and 2.4). In MOE four and two chamber, MOE LAX, MOE AV LAX, and MOE RV inflow–outflow views, colour Doppler is applied in order to evaluate the function of all four cardiac valves. Velocities of blood flow across the mitral and aortic valves are measured by Doppler in MOE four chamber and TG LAX views, respectively. Should a need for more information arise, then additional views will have to be obtained. Follow-up examinations (e.g. after cardiopulmonary bypass or at the end of surgery) are often limited to views with abnormal findings at baseline, but of course such an approach runs a risk for missing new abnormalities.

Documentation of perioperative transoesophageal echocardiography studies

It is essential that TOE records be archived in a way that allows quick identification and easy comparison with previous findings. Digital storage (optical discs) has, in comparison with videotapes, the advantages of better image quality and minimised storage space, and they are faster to access than previous records. Every TOE study must be completed with a written report that becomes a part of the patient's medical file. The customised reporting forms in use vary from simple to exhaustive. The items reported most often are listed in Box 2.3. Recently, a task force of

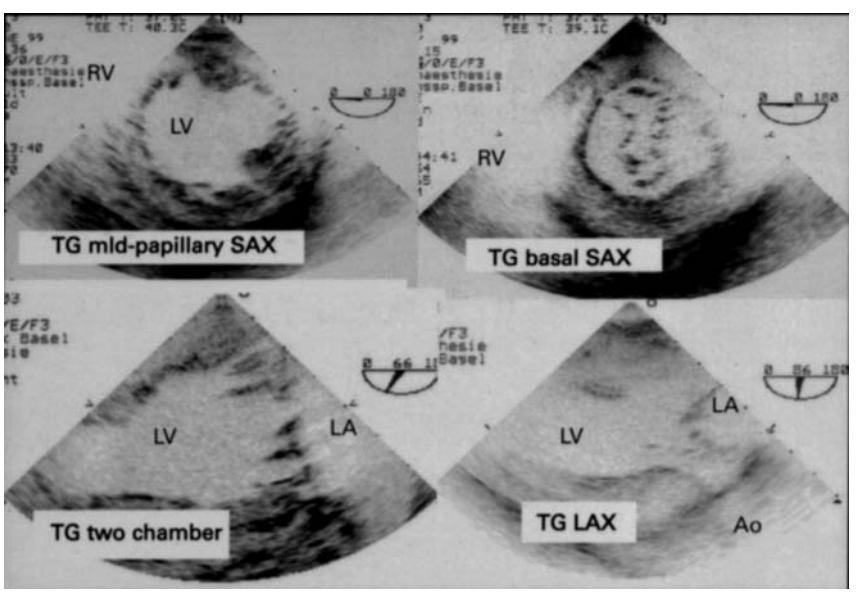

Figure 2.13 Comprehensive intraoperative transoesophageal echocardiography examination I: transgastric short-axis (TG SAX) and long-axis (TG LAX) views. Ao = aorta, LA = left atrium, LV = left ventricle, RV = right ventricle.

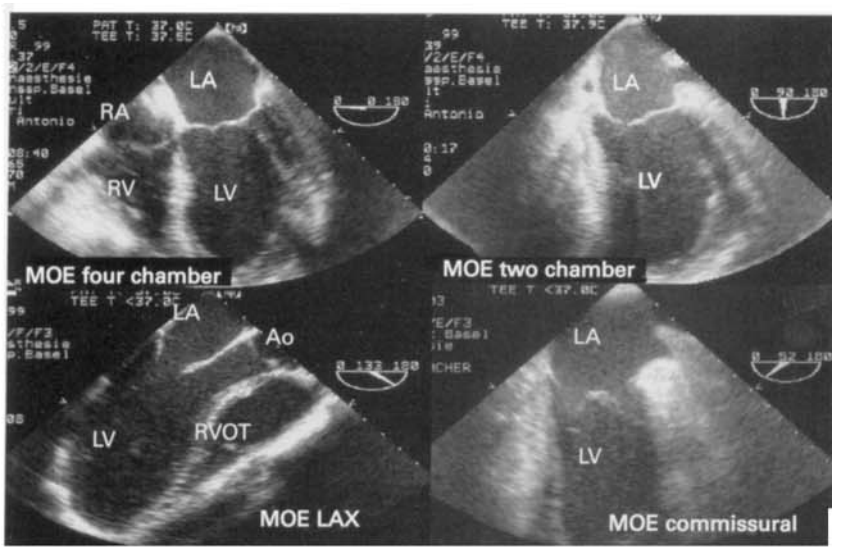

Figure 2.14 Comprehensive intraoperative transoesophageal echocardiography examination II: mid-oesophageal (MOE) longitudinal views. Ao = aorta, LA = left atrium, LAX = long-axis, LV = left ventricle, RA = right atrium, RV = right ventricle, RVOT = right ventricular outflow tract.

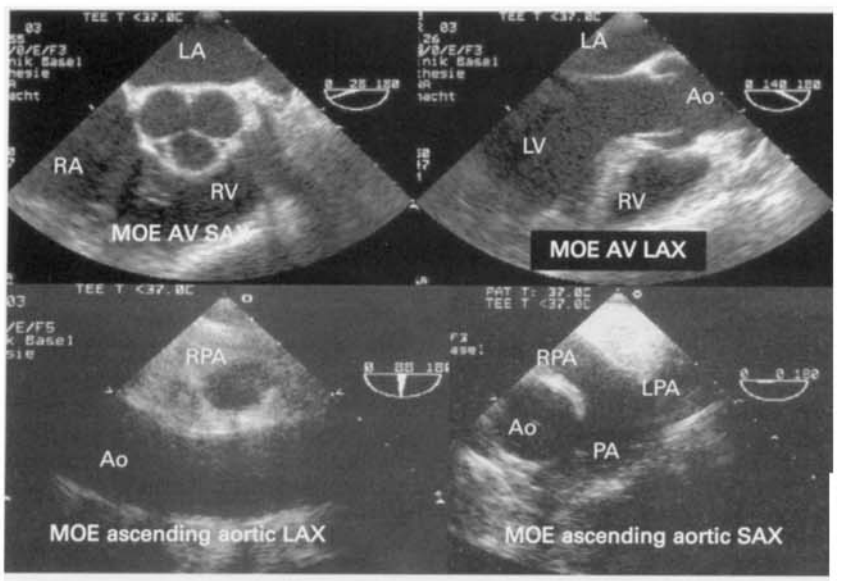

Figure 2.15 Comprehensive intraoperative transoesophageal echocardiography examination III: mid-oesophageal (MOE) aortic views. Ao = aorta, AV = aortic valve, LA = left atrium, LAX = long-axis, LPA = left pulmonary artery, LV = left ventricle, RA = right atrium, RPA = right pulmonary artery, RV = right ventricle, SAX = short-axis.

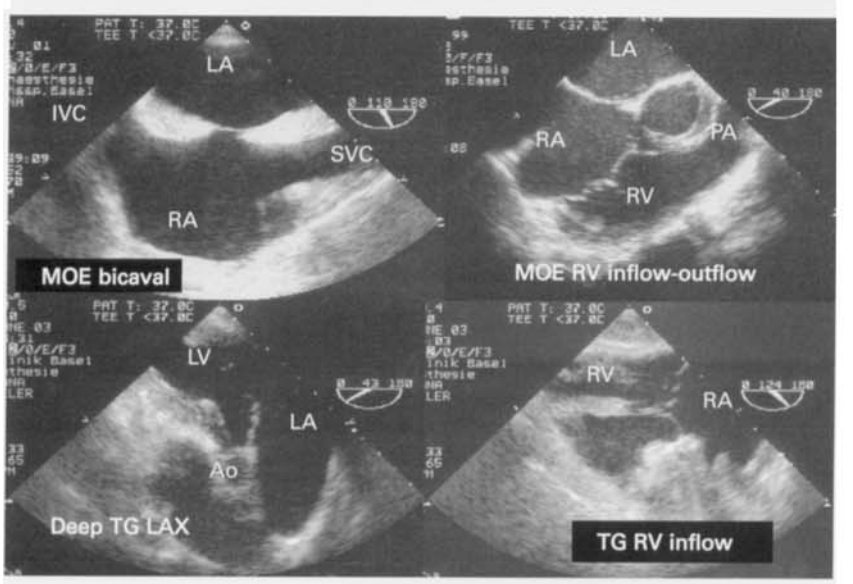

Figure 2.16 Comprehensive intraoperative transoesophageal echocardiography examination IV: mid-oesophageal (MOE) right heart views, deep transgastric left ventricular long-axis (deep TG LAX) view and transgastric right ventricular inflow (TG RV inflow) view. Ao = aorta, IVC = inferior vena cava, LA = left atrium, LV = left ventricle, PA = pulmonary artery, RA = right atrium, RV = right ventricle, SVC = superior vena cava.

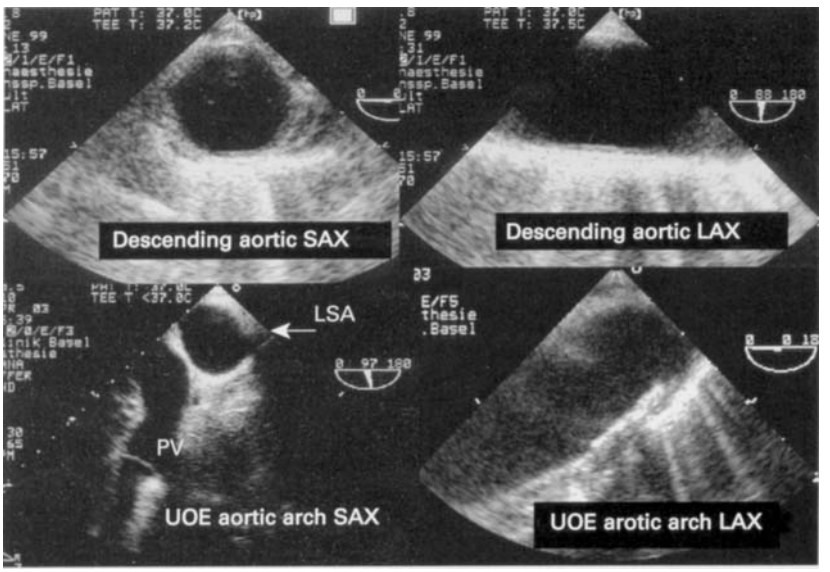

Figure 2.17 Comprehensive intraoperative transoesophageal echocardiography examination V: aortic arch and descending aortic views. LAX = long-axis, LSA = left subclavian artery, PV = pulmonary valve, SAX = short-axis, UOE = upper oesophagus.

Table 2.3 Minimal perioperative transoesophageal echocardiography study: I

TOE view		*Structures seen*	*Information provided*
	TG mid SAX	RV free wall; ventricular septum; LV anterior, lateral, inferior, posterior wall	Global and regional LV and RV function, wall thickness. Hypertrophy? Preload?
	TG LAX	LV posterior wall, anterior septum, papillary muscles, mitral valve, LVOT, aortic valve	Global and regional LV function, aortic flow (Doppler*). LVOT obstruction? Aortic stenosis? Aortic regurgitation?
	MOE four chamber	RA, tricuspid valve, RV, atrial and ventricular septum, LA, mitral valve, LV lateral wall	Global and regional RV and LV function, LA, RA size, function, masses, septal shape, transmitral flow (Doppler*). Tricuspid, mitral regurgitation? Mitral stenosis? SAM?
	MOE two chamber	LA, LA appendage, mitral valve, LV inferior and anterior wall	Global and regional LV function, transmitral flow (Doppler*). Mitral regurgitation, stenosis?
	MOE LAX	LA, mitral valve, LVOT, aortic valve, LV anteroseptal and posterior wall	Global and regional LV function, SAM? Aortic stenosis, regurgitation?

*Pulsed wave, continuous wave, and colour Doppler. LA = left atrium/atrial, LAX = long axis, LV = left ventricle/ventricular, LVOT = LV outflow tract, MOE = mid-oesophageal, RA = right atrium, RV = right ventricle/ventricular, SAM = systolic anterior motion of the mitral valve, SAX = short axis, TG = transgastric, TOE = transoesophageal echocardiography.

the Society of Cardiovascular Anesthesiologists and the American Society of Echocardiography proposed a standardised, one-page report for adult perioperative TOE (www.scahq.org). The wide use of such standardised forms would be helpful both in training and in quality control, and would facilitate communication among physicians.

Imaging difficulties

Poor image quality is mostly caused by the following factors:

- false control settings
- abnormal position of the heart

Table 2.4 Minimal perioperative transoesophageal echocardiography study: II

TOE view		Structures seen	Information provided
	MOE AV SAX	AV, cusps, sinuses of Valsalva, coronary ostia	Tricuspid or bicuspid valve? Cusp mobility, valve opening area. Aortic stenosis? Vegetations?
	MOE AV LAX	AV, cusps, aortic root, sinotubular junction, ascending aorta, right pulmonary artery SAX	Aortic dimensions, wall composition, cusp mobility. Aortic stenosis, regurgitation? Dissection? Aneurysma? Atheroma?
	MOE RV inflow–outflow	RA, tricuspid valve, RV inflow and outflow tract, pulmonary valve, main pulmonary artery LAX	RV global and regional function. Tricuspid, pulmonary regurgitation? RV systolic pressure (Doppler), thrombi? Foreign bodies?
	MOE bicaval	LA, atrial septum, inferior and superior caval veins, RA	Septum shape and motion. Open foramen ovale? Atrial septum defect? Thrombi?
	Descending aortic SAX	Aortic wall and lumen, posterior mediastinum	Aneurysm? Dissection? Rupture? Atheroma? Intramural/periaortic haematoma? Effusion?

AV = aortic valve, LA = left atrium, LAX = long axis, LV = left ventricle/ventricular, MOE = mid-oesophageal, RA = right atrium, RV = right ventricle/ventricular, SAX = short axis.

Demographic data and patient-specific information

- Patient's name, identification number, age, sex, weight
- Indication for TOE, specific questions regarding TOE, date/time of study, examiner, echo system, probe, identification number of tape/disc

Findings and measurements

- Left ventricle and right ventricle (size, morphology, global and regional function)
- Left atrium, right atrium (size, masses, foreign bodies)
- Atrial and ventricular septum (morphology, defects, shunts)
- Mitral, aortic, tricuspid, and pulmonary valves (leaflet morphology, leaflet motion, annulus size, prosthetic valve, stenosis, regurgitation transmitral flow pattern, pulmonary venous flow pattern)
- Pericardium
- Aortic arch, ascending and descending aorta (atherosclerosis, dissection, aneurysm)

Postintervention study (results of surgery)

Comments/recommendations

New findings/impact of TOE on therapy

Summary

Complications

Box 2.3 Report of perioperative transoesophageal echocardiography study

- air in the stomach/oesophagus
- lung hyperinflation
- pneumothorax
- foreign bodies (surgical tools).

The quality and reproducibility of perioperative TOE depends on the quality of the TOE images. Acquisition of the standard views has become easier since the introduction of the multiplane probe. However, there still may be dropouts of endocardial borders, usually in the lateral and/or septal regions, due to poor lateral resolution. The image can be optimised by appropriate settings for the various controls, such as frequency, focus, lateral gain, time compensation, border facilitation, and others. Intravenous injection of new echo contrast media can be used for better demarcation of the cardiac chambers and endocardial borders. In patients with abnormal forms of the stomach, dilated and horizontally positioned hearts, elevated diaphragms, or morbid obesity, it may be difficult to obtain anatomically correct views of the LV. Other causes for poor image quality are the presence of air in the stomach, interposition of gas-filled intestine between the gastric fundus and left diaphragm, hyperinflated lung compressing the heart, or hiatal and paraoesophageal hernia.[18,19] During open-heart surgery and wide retraction of the sternum and the rib cage, the heart surface may

lose contact with the parietal pericardium and air may get in the way of the ultrasound beam. This can happen particularly during off-pump cardiac surgery with the heart lifted and fixed, and under such circumstances it is impossible to obtain the transgastric views. Surgical instruments and a pleural or pericardial drainage tube can cast acoustic shadows on the heart. With increasing experience with the multiplane probe, however, the inability to obtain the standard views is rare. In order to obtain a correct transgastric short-axis view, it can be helpful to image during a brief inflation hold or during application of positive expiratory pressure. These manoeuvres can move the LV into the imaging plane. An important part of TOE training is the recognition of false, inadequate images and the detection of artefacts to avoid erroneous interpretation and false diagnoses. For instance, an oblique non-standard cross-section might mimic a regional wall motion abnormality, wall thinning, pathological mass, or asymmetrical hypertrophy.

Care of the transoesophageal echocardiography probe after use

The following procedure should be followed:

- clean and wash
- check for damage
- disinfect
- rinse
- dry
- store
- conduct regular electrical safety checks.

Before removing the probe from the stomach or oesophagus, the control wheels must be unlocked in order to avoid injuries to the upper gastrointestinal tract and damage to the probe. The shaft of the removed probe is inspected for any damage and cleaned of secretions with warm water and soap. Detergent or enzymatically active solutions can also be used for mechanical cleaning and washing. The control wheels and knobs and the cable are wiped with 70% alcohol. The handle and steering controls of the probe must never be immersed in water or disinfectant solution. The shaft of the probe is then put into the disinfectant bath. The duration of the disinfecting procedure depends on the type of agent used. The guidelines issued by the providers of the TOE probes should be carefully read and followed. The disinfectants used most often are 2–2·4% glutaraldehyde-based solutions. An alternative agent is the ortho-phthalaldehyde, used as a 0·55% solution. This compound appears to have superior disinfectant activity compared with glutaraldehyde, and it is less volatile and therefore less irritating. However, a chemical burn injury to the upper digestive tract caused by disinfectant residue on the surface of the probe was recently reported.[20] The efficacy of the recommended disinfectant methods has been confirmed even in patients with AIDS.[21] Solutions containing hydrogen superoxide as well as sterilisation procedures such as autoclaving, ultraviolet light, gamma radiation, gas, vapour, or heat must not be used. After the disinfectant bath the shaft of the probe is rinsed for 10–15 minutes in tap water, dried, and hung up on a rack. A minimum of 20 minutes should be allowed for evaporation of the glutaraldehyde residue before the next use.

Although the protection of the patient is of utmost importance, care of expensive TOE probes must not be neglected. Such care comprises storage in dedicated holders, protection of the probe connector, and use of suitable holders when the probe is in use or is being disinfected.[22]

Complications of transoesophageal echocardiography

The following complications can occur during TOE:

- dental injures
- pressure lesions
- vocal cord injury
- thermal injuries
- chemical burn injury
- upper gastrointestinal tract bleeding
- perforation
- airway obstruction
- aspiration
- myocardial ischaemia
- arrhythmia.

In large clinical series TOE was shown to be a safe method, with morbidity and mortality comparable with those of other similar endoscopic

techniques.[23,24] The risk for injury to the upper alimentary tract with major bleeding, as well as that for perforation, can be minimised by knowing the precise history of the patient (contraindications) and by using an atraumatic technique. In a retrospective case series of 7200 adult cardiac surgical patients, no TOE-related mortality and a morbidity of 0·2% was reported. The most common complication was severe odynophagia (0·1%), followed by dental injury (0·03%), endotracheal tube malpositioning (0·03%), upper gastrointestinal tract haemorrhage (0·03%), and oesophageal perforation (0·01%).[25] One report suggested that the complication rate with TOE performed in emergency departments might be higher.[26] Isolated cases of hypopharynx or oesophagus perforation requiring immediate surgery have been reported.[27–29] Cases of profuse bleeding after intraoperative TOE have also been reported. The bleeding usually originates from the gastro-oesophageal junction (Mallory–Weiss tears) and requires an immediate endoscopic intervention.[30,31] It is likely that the risk for bleeding is increased when the probe is inserted in fully heparinised or thrombolysed patients.[31] A discrepancy in size between the probe and the adjacent structures can cause airway, aortic, or pulmonary artery compression, particularly in paediatric TOE.[32–34]

Heavy sedation in spontaneously breathing patients can cause hypoxaemia and hypotension during or after TOE. Conversely, the stimulus of insertion and manipulation of the probe in patients under inadequate local or general anaesthesia may give rise to hypertension, tachycardia, myocardial ischaemia, and arrhythmias. A transient sore throat can follow a TOE examination, but the intensity of complaints is similar to that in patients undergoing endotracheal intubation only.[35] Respiratory complications can also occur, including aspiration of gastric contents in sedated patients with an unprotected airway, bronchospasmus, laryngospasmus, vocal cord injury, and recurrent laryngeal nerve palsy.[36] Overall, TOE examination in intubated patients under general anaesthesia appears to be associated with fewer complications, and it is therefore possibly safer. However, the prolonged monitoring and manipulation of the probe during long operations has caused some concern regarding the potential for pressure and thermal injuries. The maximum surface contact pressure between the oesophagus and fully flexed TOE probe was measured both in dogs and humans by pressure recording from a flat balloon fitted to the end of the probe.[37] The pressures were low (< 20 mmHg) despite maximal rotation of the control wheels, and no signs of oesophageal damage were observed. The possible damaging effects of continuous imaging and probe manipulation were studied in dogs. Up to 7 hours of imaging, which included the period of cardiopulmonary bypass with heparinisation, caused no traumatic or thermal injury.[38] However, in some cases potentially dangerous pressure may be generated, and so locking the TOE probe in an extreme flexed position for a long time should be avoided.

The incidence of bacteraemia during TOE is low (2%), but a transient subfebrile increase in temperature was reported in some patients. During follow up of these patients, however, no cases of endocarditis developed.[39,40] Routine prophylactic antibiotic administration is therefore not required, except for patients who are considered to be at very high risk for endocarditis (e.g. history of previous endocarditis). Because patients undergoing surgery as well as those treated in the intensive care unit are usually already receiving antibiotics, no further measures are necessary.

Contraindications to transoesophageal echocardiography

Contraindications to TOE are absolute and relative, and they are presented in Box 2.1. Frequently, TOE is performed as an emergent procedure and/or in patients who are unable to answer questions, and the operator may be unaware of the existing oesophageal pathology. It is therefore important that any force during probe insertion is strictly avoided and the examination aborted should any unexpected resistance be encountered. In case of relative contraindications the physician must weigh the risks associated with the procedure against the benefit of arriving at a diagnosis.

Indications for transoesophageal echocardiography

Initially introduced into the operating theatre as a monitor of LV function and praised as the 'gold standard' for monitoring of regional wall

Haemodynamic instability, refractory hypotension, low cardiac output

- Evaluation of left ventricular global and regional functions
- Evaluation of valvular structure and function
- Evaluation of right ventricular global and regional functions
- **Look for the following**: left ventricular failure, right ventricular failure, biventricular failure, myocardial ischaemia, myocardial infarction, hypovolaemia, cardiac tamponade, acute valvular regurgitation, acute left-right shunt, pulmonary embolism, severe aortic stenosis, dynamic left ventricular outflow tract obstruction, hyperdynamic circulation of sepsis

Cardiac surgery

- Cardiac valve reconstruction
- Correction of congenital heart disease
- Cardiac valve replacement
- Aortic dissection
- Myotomy for hypertrophic cardiomyopathy
- Resection of intracardiac tumours and thrombi
- Pulmonary embolectomy and thrombectomy
- Total endoscopic, robotic, or minimal access cardiac surgery
- Implantation of ventricular assist devices and artificial heart
- Myocardial revascularisation (in patients with poor ventricular function, unstable angina, acute or impeding infarction, aneurysmectomy, ventricle reduction surgery, after resuscitation)
- Minimally invasive and off-pump cardiac surgery in high risk patients
- Heart transplantation
- Myocardial laser revascularisation
- Localisation of intracardiac foreign bodies, electrodes, catheters, stents, filters, and other devices
- Detection and guiding elimination of intracardiac air

Non-cardiac surgery

- Vascular surgery: thoracic and thoraco-abdominal aortic surgery; abdominal aortic surgery in patients with severe coronary artery disease and/or poor ventricular function
- Endoluminal stent: graft repair of aortic aneurysm
- Major non-cardiac surgery in patients with poor ventricular function, heart failure, or high risk for myocardial ischaemia
- Major non-cardiac surgery in patients with severe valvular heart disease
- Liver transplantation
- Emergency surgery in cardiac patients without preoperative cardiological examination
- Contraindication or impracticality of invasive monitoring

Trauma

- Closed and penetrating chest trauma
- Control of volaemia/preload
- Detection of haemothorax, cardiac tamponade
- Detection of cardiac contusion and other cardiac traumatic lesions
- Traumatic rupture of the aorta

Sepsis

- Endocarditis
- Search for cardiac source of septic emboli
- Evaluation of ventricular function and filling

Assessment of haemodynamic function

- Measurement of stroke volume, cardiac output, pulmonary artery systolic and diastolic pressures, and estimation of left ventricular filling by means of pulsed and continuous wave Doppler

Other

- Donor heart evaluation (if transthoracic echo is not feasible)
- Refractory hypoxaemia from patent foramen ovale and right to left shunt

Box 2.4 Indications for perioperative transoesophageal echocardiography

motion and myocardial ischaemia, TOE has also been deployed in other perioperative situations and has proven to be safe and useful in many of them. All evidence regarding the effectiveness of TOE during the perioperative period reported up to the year 1996 was reviewed by the Task Force on Practice Parameters for Perioperative Transesophageal Echocardiography appointed by the American Society of Anesthesiologists and the Society of Cardiovascular Anesthesiologists.[41] Evaluation of the literature along with expert opinions from the Task Force resulted in guidelines for the use of TOE during the perioperative period, including a list of indications for TOE. The Task Force divided the indication into three categories based on the published evidence and expert opinions. Category I indications are those supported by the strongest evidence or expert opinion that TOE improves outcome. These indications include severe perioperative haemodynamic disturbances, valve repair, repair of congenital cardiac lesions,

hypertrophic obstructive cardiomyopathy, endocarditis, and aortic dissection.[41] Category II and category III indications are supported by less convincing evidence. The formulation of the guidelines allows for adequate flexibility in their application and future updating according to new evidence and experience. Large prospective randomised studies of the utility and safety of TOE in clearly defined patient populations are needed but cannot be expected in the near future. Box 2.4 summarises the indications for perioperative TOE, which reflect both the published evidence and the practices used by the authors' institutions.

References

1 Thys DM. Echocardiography and anesthesiology successes and challenges. *Anesthesiology* 2001;**95**: 1313–4.

2 Morewood GH, Gallagher ME, Gaughan JP, Conlay LA. Current practice patterns for adult perioperative transesophageal echocardiography in the United States. *Anesthesiology* 2001;**95**:1507–12.

3 Click RL, Abel MD, Schaff HV. Intraoperative transesophageal echocardiography: 5-year prospective review of impact on surgical management. *Mayo Clin Proc* 2000;**75**:241–7.

4 Couture P, Denault AY, McKenty S, *et al.* Impact of routine use of transesophageal echocardiography during cardiac surgery. *Can J Anaesth* 2000;**47**:20–6.

5 Mishra M, Chauhan R, Sharma KK, *et al.* Real-time intraoperative transesophageal echocardiography: How useful? Experience of 5,016 cases. *J Cardiothorac Vasc Anesth* 1998;**12**:625–32.

6 Fanshaw M, Ellis C, Habib S, Konstadt SN, Reich DL. A retrospective analysis of the costs and benefits related to alterations in cardiac surgery from routine intraoperative transesophageal echocardiography. *Anesth Analg* 2002;**95**:824–7.

7 Denault AY, Couture P, Mc Kenty S, *et al.* Perioperative use of transesophageal echocardiography by anesthesiologists: impact in noncardiac surgery and in the intensive care unit. *Can J Anesth* 2002;**49**:287–93.

8 Seward JB, Khandheria BK, Freeman WK, *et al.* Multiplane transesophageal echocardiography: image orientation, examination technique, anatomic correlations, and clinical applications. *Mayo Clin Proc* 1993;**68**:523–51.

9 Zimmermann P, Greim C, Trautner H, *et al.* Echocardiographic monitoring during induction of general anesthesia with a miniaturized esophageal probe. *Anesth Analg* 2003;**96**:21–7.

10 Fritz S, Hunt MH, Ochs C, *et al.* Use of latex cover sheath for transesophageal echocardiography (TEE) instead of regular disinfection of the echoscope? *Clin Cardiol* 1993;**16**:737–40.

11 Orihashi K, Sueda T, Matsuura Y, Yamanoue T, Yuge O. Buckling of transesophageal echocardiography probe: a pitfall at insertion in an anesthetized patient. *Hiroshima J Med Sci* 1993; **42**:155–7.

12 Weinger MB, Herndon OW, Gaba DM. The effect of electronic record keeping and transesophageal echocardiography on task distribution, workload, and vigilance during cardiac anesthesia. *Anesthesiology* 1997;**87**:144–55.

13 Shanewise JS, Cheung AT, Aronson S, *et al.* ASE/SCA Guidelines for Performing a Comprehensive Intraoperative Multiplane Transesophageal Examination: Recommendations of the American Society of Echocardiography Council for Intraoperative Echocardiography and the Society of Cardiovascular Anesthesiologists Task Force for Certification in Perioperative Transesophageal Echocardiography. *Anesth Analg* 1999;**89**:870–84.

14 Schiller NB. Two-dimensional echocardiographic determination of left ventricular volume, systolic function, and mass. *Circulation* 1991;**85(suppl I)**: I-280–7.

15 Skarvan K, Lambert A, Filipovic M, Seeberger M. Reference values for left ventricular function in subjects under general anaesthesia and controlled ventilation assessed by two-dimensional transoesophageal echocardiography. *Eur J Anaesth* 2001;**18**:713–22.

16 Miller JP, Lambert A-S, Shapiro WA, *et al.* The adequacy of basic intraoperative transesophageal echocardiography performed by experienced anesthesiologists. *Anesth Analg* 2001;**92**:1103–10.

17 Mathew JP, Fontes ML, Garwood S, *et al.* Transesophageal echocardiography interpretation: a comparative analysis between cardiac anesthesiologists and primary echocardiographers. *Anesth Analg* 2002;**94**:302–9.

18 Freedberg RS, Weinreb J, Gluck M, Kronzon I. Paraesophageal hernia may prevent cardiac imaging by transesophageal echocardiography. *J Am Soc Echocardiogr* 1989;**2**:202–3.

19 Cooke RA, Chambers JB. Failure to obtain a transoesophageal echocardiographic window because of a rolling hiatal hernia. *Heart* 1996;**76**: 88–9.

20 Venticinque SG. Oral, pharyngeal, and digestive tract chemical burn injury secondary to intraoperative transesophageal echocardiography: a case report. *Anesth Analg* 2003;**96**:SCA78.

21 Hanson PJV, Gor D, Clarke JR, *et al.* Contamination of endoscopes used in AIDS patients. *Lancet* 1989; **2**:86–8.

22 Taillefer J, Couture P, Sheridan P, *et al.* A comprehensive strategy to avoid transesophageal echocardiography probe damage. *Can J Anesth* 2002;**49**:500–2.

23 Daniel WG, Erbel R, Kasper W, *et al.* Safety of transesophageal echocardiography: a multi-centre survey of 10 419 examinations. *Circulation* 1991; **83**:817–21.

24 Seward JB, Khandheria BK, Oh JK, Freeman WK, Tajik AJ. Critical appraisal of transesophageal echocardiography: limitations, pitfalls and complications. *J Am Soc Echocardiogr* 1992;**5**: 288–305.

25 Kallmeyer IJ, Collard CD, Fox JA, Body SC, Shernan SK. The safety of intraoperative transesophageal echocardiography: a case series of 7200 cardiac surgical patients. *Anesth Analg.* 2001; **92**:1126–30.

26 Gendreau MA, Triner WR, Bartfield J. Complications of transesophageal echocardiography in the ED. *Am J Emerg Med* 1999;**17**: 248–51.

27 Spahn DR, Schmid S, Carrel T, Pasch T, Schmid ER. Hypopharynx perforation by a transesophageal echocardiography probe. *Anesthesiology* 1995; **82**:581–3.

28 Badaoui R, Choufane S, Riboulot M, Bachelet Y, Ossart M. Esophageal perforation after transesophageal echocardiography [In French]. *Ann Fr Anesth Reanim* 1994;**13**:850–2.

29 Kharash ED, Sivarajan M. Gastroesophageal perforation after intraoperative transesophageal echocardiography. *Anesthesiology* 1996;**85**:426–8.

30 Dewhirst WE, Stragand JJ, Fleming BM. Mallory–Weiss tear complicating intraoperative transoesophageal echocardiography in a patient undergoing aortic valve replacement. *Anesthesiology* 1990;**73**:777–8.

31 St-Pierre J, Fortier LP, Couture P, Hebert Y. Massive gastrointestinal hemorrhage after transoesophageal echocardiography probe insertion. *Can J Anaesth* 1998;**45**:1196–9.

32 Arima H, Sobue K, Tanaka S, *et al.* Airway obstruction associated with transesophageal echocardiography in a patient with a giant aortic pseudoaneurysm. *Anesth Analg* 2002;**95**:558–60.

33 Lunn RJ, Oliver WC, Hagler DJ, Danielson GK. Aortic compression by transesophageal probe in infants and children undergoing cardiac surgery. *Anesthesiology* 1992;**92**:587–90.

34 Preisman S, Yusim Y, Mishali D, Perel A. Compression of the pulmonary artery during transesophageal echocardiography in a pediatric cardiac patient. *Anesth Analg* 2003;**96**:85–7.

35 Oewall A, Stahl L, Settergren G. Incidence of sore throat and patient complaints after intraoperative transesophageal echocardiography during cardiac surgery. *J Cardiothorac Vasc Anesth* 1992;**6**:15–6.

36 Zwetsch G, Filipovic M, Skarvan K, Todorov A, Seeberger MD. Transient recurrent pharyngeal nerve palsy after failed placement of a transesophageal echocardiographic probe in an anesthetized patient [case report]. *Anesth Analg* 2001;**92**:1422–3.

37 Urbanowicz JH, Kernoff RS, Oppenheim G, Parnagian E, Billingham ME, Popp RL. Transesophageal echocardiography and its potential for esophageal damage. *Anesthesiology* 1990;**72**:40–3.

38 O'Shea JP, Southern JF, d'Ambra MN, *et al.* Effects of prolonged transesophageal echocardiographic imaging and probe manipulation on the esophagus: an echocardiographic–pathologic study. *J Am Coll Cardiol* 1991;**17**:1426–9.

39 Steckelberg JM, Khandheria BK, Anhalt JP, *et al.* Prospective evaluation of the risk of bacteraemia associated with transesophageal echocardiography. *Circulation* 1991;**84**:177–80.

40 Roudaut R, Lartigue MC, Texler-Maugein J, Dallocchio M. Incidence of bacteraemia or fever during transoesophageal echocardiography: a prospective study of 82 patients. *Eur Heart J* 1993;**14**:936–40.

41 American Society of Anesthesiologists and the Society of Cardiovascular Anesthesiologists Task Force on Transoesophageal Echocardiography. Practice guidelines for perioperative transesophageal echocardiography. *Anesthesiology* 1996;**84**:986–1006.

3 Global left ventricular systolic function

Christoph Schmidt, Frank Hinder, Hugo Van Aken, Jan Poelaert

Introduction

For more than two decades transoesophageal echocardiography (TOE) has been undergoing unparalleled evolution as a contributor to the diagnosis and monitoring of critically ill patients at the bedside. The rapidly increasing impact of TOE in the perioperative setting stems from its inherent ability to provide information regarding cardiac geometry and dimensions. Its ability to assess global heart function by direct measurement of chamber dimensions, rate of shortening of the left ventricular (LV) or right ventricular (RV) walls, and variations in thickness of the ventricular wall throughout the cardiac cycle has been well recognised in recent years. This potential of cardiac ultrasound prompted the establishment of correlative indices of cardiac structure and function.[1] In particular, analysis of global LV systolic function, which (apart from heart rate) is governed by three major parameters, namely preload, afterload, and contractility, is considerably enhanced by integrating geometrical aspects.[2,3] Combination of conventional pressure measurements with Doppler echocardiographic flow data and dimensional information derived from imaging echocardiography results in a quantitative description of global LV systolic function in terms of its three major determinants. This chapter specifies the application of TOE as a non-invasive tool for independent assessment of preload, afterload, and contractile performance of the left ventricle, thus allowing discrimination of ventricular loading conditions from inotropic properties.

The crucial importance of the echocardiographic evaluation of LV systolic function arises from the fact that LV function is vital for and predictive of survival both in cardiac surgical patients and in patients with increased risk undergoing non-cardiac surgery during the perioperative phase and on the intensive care unit.[4–6] Despite advances in patient assessment and care, cardiac morbidity continues to be the leading cause of perioperative death.[7–10] In view of the clear and undisputed advantages of TOE as a monitor of LV systolic function, TOE was judged by the Task Force on Perioperative Transesophageal Echocardiography (American Society of Anesthesiologists/Society of Cardiovascular Anesthesiologists Task force 1996) to improve frequently clinical outcomes in patients suffering from unexplained hypotension.[11] In the guidelines released by the Task Force, the indication "perioperative evaluation of acute, life-threatening hemodynamic disturbances" is assigned to category I (in addition to four other indications).

Therefore, anaesthesiologists and intensive care specialists should be able to assess LV function by means of TOE in order to determine the appropriate treatment modalities and thus improve outcomes. Moreover, recent concerns about both the safety of pulmonary artery catheters and the use of data derived from them[12,13] increase pressure to progress echocardiography as an essential tool with which to manage critically ill patients.[14]

Preload

Monitoring of preload has important implications in clinical medicine. Insufficient LV preload due to hypovolaemia accounts for most cases of decreased stroke volume and unexplained hypotension in critically ill patients in the intensive care unit.[4–6,15]

LV preload can be defined as the stretch imposed on the myocardial fibres at end-diastole. Myocardial fibre stretch and fibre length depend on ventricular volume at the macroscopic level. LV end-diastolic volume (LVEDV) is therefore a

clinical variable that is used in assessing preload. The importance of preload is demonstrated by the Frank–Starling effect, whereby preload is a determinant of stroke volume and hence cardiac output. Changes in LVEDV correlate well with changes in stroke volume, as long as all the other factors that determine LV function remain constant. The Frank–Starling law of the heart was originally extrapolated from in vitro studies on isolated cardiac muscle fibres; increasing their stretch resulted in a greater velocity of shortening. In vivo, the intrinsic ability of the ventricle to adapt its performance to rapid changes in preload is the most important mechanism by which stroke volume can be increased in normal hearts. The degree to which preload can improve systolic function via the Frank–Starling mechanism depends on the position and the form of the diastolic pressure–volume curve. Ventricular pressure is related to ventricular volume in a non-linear manner according to a compliance curve. With increasing preload the ventricle becomes stiffer. For an equal increase in ventricular volume, the rise in ventricular pressure is lesser at low preload than it is if preload is high to begin with.

The clinical setting will determine whether pressure or volume is the best marker of preload. In the case of pulmonary oedema, the pressure transmitted to the pulmonary venous system is required. On the other hand, if cardiac output is to be to optimised then volume may be a better marker, because ventricular performance depends on myocardial fibre stretch and length.

More recently it was stressed that the traditional pressure and/or volume measures of preload do not reliably differentiate between preload responsiveness (i.e. fluid challenge leads to an increase in cardiac output) and preload unresponsiveness (i.e. fluid challenge leads to no change or a decrease in cardiac output) in patients with acute circulatory failure.[16–21] This emphasises the need for factors that can predict whether volume expansion will be effective in order to select those patients who will benefit from volume expansion and avoid ineffective or even deleterious fluid therapy (worsening of pulmonary oedema or haemodilution). Therefore, in patients receiving mechanical ventilation, the magnitude of variation in stroke volume over a respiratory cycle has been employed to detect preload responsiveness more precisely than is possible with conventional haemodynamic pressure measurements, and even echocardiographic estimates of end-diastolic LV dimension.[22–25] As surrogates of stroke volume variation, cyclic respiratory variations in systemic arterial pressure[21,26] or in aortic Doppler velocity (using TOE) have been reported to predict fluid responsiveness.[24,25] These dynamic parameters for preload assessment contrast with traditional static measurements.

Pulmonary capillary wedge pressure

Pulmonary capillary wedge pressure (PCWP) has been used as an estimate of LV preload. During recording of PCWP with a pulmonary artery catheter, pulmonary artery inflow is blocked by a balloon just below the tip of the catheter. PCWP measured distally to the balloon is therefore regarded as the pressure in the capillary bed after equilibration with the pulmonary venous system. Pressure gradients between pulmonary veins and left atrium on one side, and left atrium and left ventricle on the other side are negligible during diastole in normal persons.[27] PCWP was therefore commonly used as an estimate of LV end-diastolic pressure, which changes with alterations in LVEDV in normal hearts. PCWP under these conditions can provide useful information during a volume challenge. Using PCWP as an estimate of LVEDV, it was found that misinterpretation of LVEDV occurs to some degree because of the curvilinear nature of the diastolic pressure–volume relationship. This relationship is exponential when end-diastolic pressures are varied over a wide range, but it may be approximated by a linear relation during low filling pressures.

However, when PCWP is not measured in spontaneously breathing persons with physiological cardiovascular function, but rather, for example, in critically ill patients, the above mentioned relations between PCWP and LVEDV are altered by various factors, including pharmacological intervention, increased ventricular stiffness during cardiac ischaemia, mitral valve insufficiency, and increased intrathoracic pressure.[28] In such cases, PCWP ceases to be a measure of preload.[29,30] In other words, the relation between PCWP and LVEDV is governed by the diastolic compliance of the left ventricle, which is subject to frequent changes in critically ill patients.[31,32] Thus, direct volumetric assessment of cardiac filling is superior to PCWP in the perioperative setting because the delicate assumption that ventricular compliance remains unchanged is avoided.

Preload using volumetric methods

Currently, echocardiography provides direct visualisation of the cardiac chambers and an opportunity to measure end-diastolic ventricular dimensions at the bedside. Two-dimensional echocardiography yields several measures for the evaluation of LV preload.

Qualitative analysis

A first qualitative impression of LV filling can rapidly be gained when both cardiac ventricles are visualised in the transgastric short-axis view (Figure 3.1). Usually, during hypovolaemia both ventricles appear small. The sign of "kissing papillary muscles" or "kissing walls" may become evident. This phrase describes a low LV filling state, in which the anterolateral and the posteromedial papillary muscles come into contact when the ventricle has expelled most of its stroke volume (Figure 3.2). At end-systole the LV cavity may even disappear completely (end-systolic obliteration).[33]

Position and movements of the atrial and ventricular septa can be analysed in the four chamber view. Deviations of the atrial septum may be caused by increased preload in one of the cardiac ventricles. Pathologically elevated RV preload during RV failure, for instance, will lead to increased right atrial pressure and consequent bulging of the atrial septum and even the ventricular septum to the left side (Figure 3.3).[34]

Quantitative analysis

Several measures have been proposed for quantitative assessment of LV preload, with the precision of the approximation of true LV volume increasing with the number of dimensions included. The end-diastolic transverse diameter of the left ventricle at the

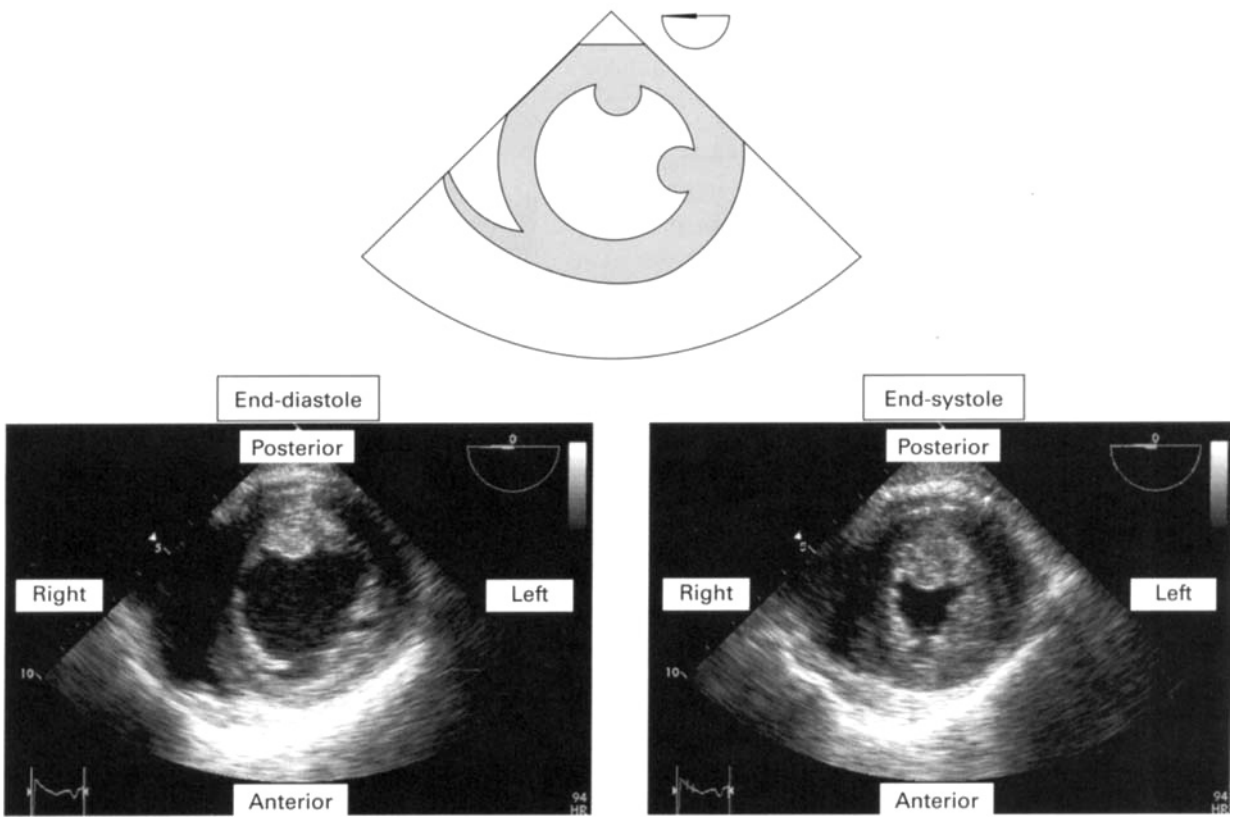

Figure 3.1 Transgastric short-axis view of the left ventricle at end-diastole and end-systole. The papillary muscles serve as an internal landmark. This cross-sectional view forms the basis for rapid appreciation of preload, afterload, and contractile performance. The American Society of Echocardiography (Council for Intraoperative Echocardiography) and the Society of Cardiovascular Anesthesiologists (Task Force for Certification in Perioperative Transesophageal Echocardiography) refer to this anatomically directed cross-sectional image as the transgastric mid-papillary short-axis (TG mid SAX) view.

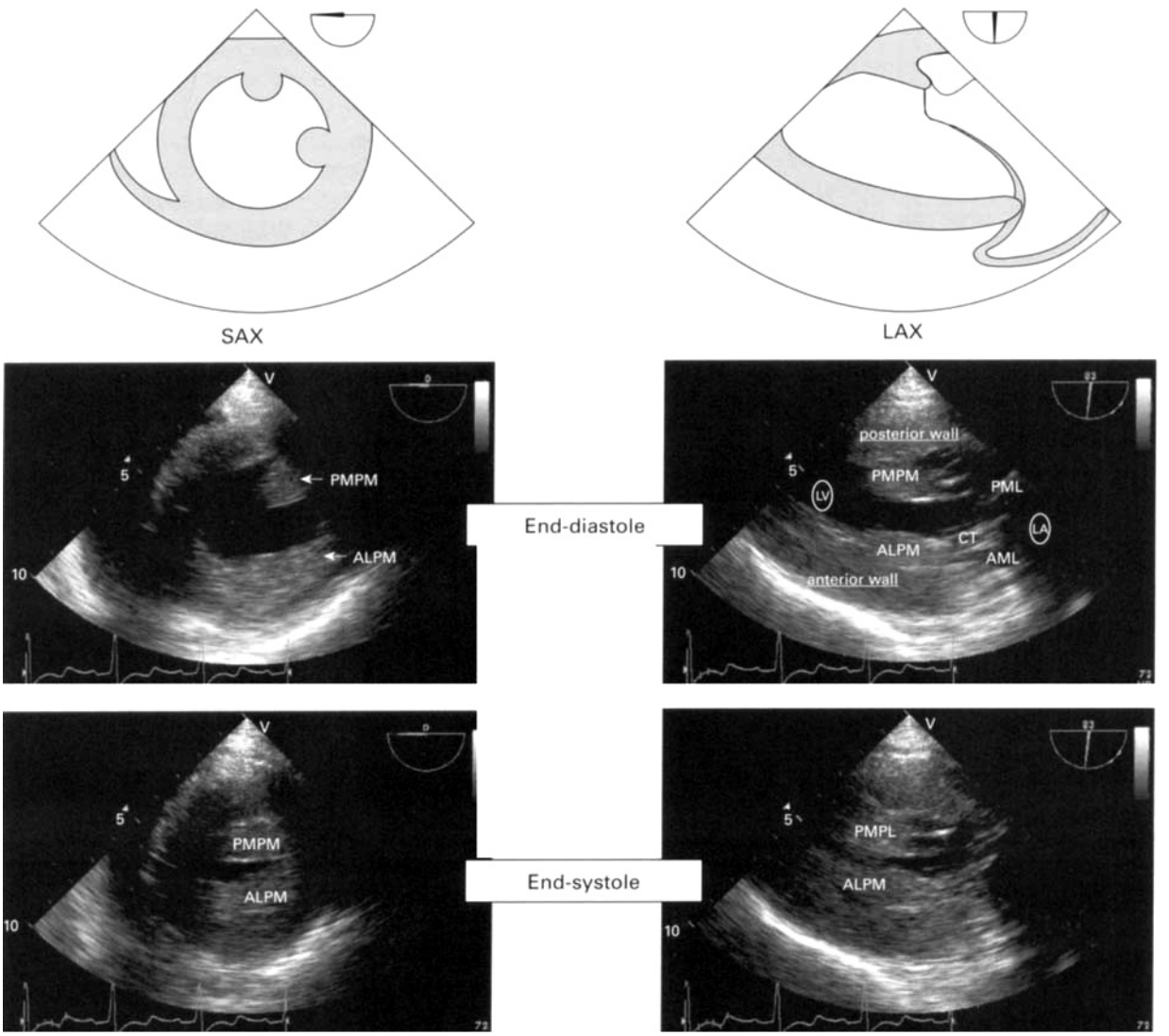

Figure 3.2 Transgastric short-axis and long-axis views of the left ventricle at end-diastole and end-systole. Papillary muscles come into contact at end-systole, illustrating a low left ventricular filling state. The transgastric views of the left ventricle are acquired by advancing the probe into the stomach and anteflexing the tip until the heart comes into view. At a multiplane angle of 0°, a short-axis (SAX) view of the left ventricle will appear. The transgastric mid SAX view is used for assessing left ventricular chamber size and wall thickness. The longitudinal transgastric two chamber view (long-axis [LAX]) is developed by rotating the multiplane angle forward to approximately 90°, until the apex and the mitral annulus come into view. ALPM = anterolateral papillary muscle, AML = anterior mitral leaflet, CT = chordae tendineae, LA = left atrium, LV = left ventricle, PML = posterior mitral leaflet, PMPM = posteromedial papillary muscle.

level of the papillary muscles (LV end-diastolic diameter [LVEDD] = 2·3–3·2 cm/m^2) and the end-diastolic mid-papillary cross-sectional area (LV end-diastolic area [LVEDA] = 7·5–10 cm^2/m^2) are commonly employed as one- and two-dimensional parameters of ventricular preload (see Figure 3.1). Unlike LVEDD and LVEDA, which are measured directly from the echocardiographic image, the three-dimensional LVEDV (50–70 ml/m^2) is reconstructed from various two-dimensional cross-sectional views using appropriate geometrical and mathematical models. The two approaches most commonly applied are the prolate ellipse method (area–length method) and the Simpson's rule method.

Prolate ellipse method (area–length method)

For this method it is assumed that the left ventricle is of prolate ellipsoid shape and contracts uniformly. The volume of the left

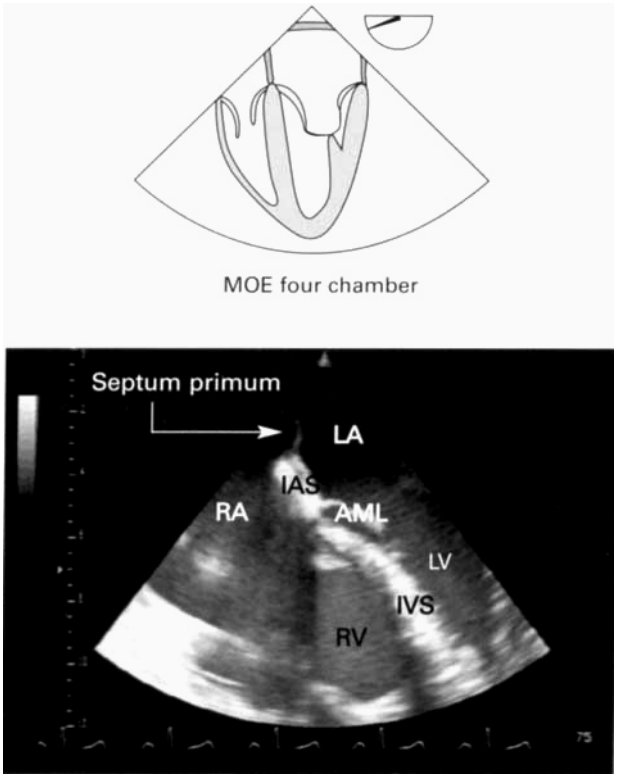

Figure 3.3 Deviation of interatrial septum and interventricular septum in right sided heart failure. Both the interatrial septum and the interventricular septum bulge to the left, as a result of increased preload of the right ventricle. AML = anterior mitral leaflet, IAS = interatrial septum, IVS = interventricular septum, LA = left atrium, LV = left ventricle, MOE = mid-oesophageal, RA = right atrium, RV = right ventricle.

ventricle is then calculated from a single geometrical figure for which two imaging planes (the mid-oesophageal four chamber view for the long-axis and the mid-papillary short-axis view for the cross-sectional area) are viewed. The fact that two planes are needed for calculation is a disadvantage. Moreover, the left ventricle often does not resemble a prolate ellipsoid, particularly if aneurysms or segmental wall motion abnormalities are present. Last but not least, with TOE it may be difficult to obtain a true long-axis image of the left ventricle because it may be technically impossible to direct the ultrasound beam through the apex within the constraints of the oesophagus.

Simpson's rule method

According to Simpson's rule, which has been validated against angiography, the left ventricle is divided into 20 individual slices of different diameter but equal thickness.[35] LVEDV is then calculated as the sum of the volumes of the cylindrical slices (Figure 3.4). Simpson's rule has been implemented into the computer software of most new generation ultrasonographic systems and can be used to estimate LVEDV from a four chamber view or from a mid-oesophageal two chamber view of the left ventricle in a longitudinal imaging plane. Clear advantages of this method are its validity when the ventricular geometry is markedly disturbed[36] and that Simpson's rule can be applied to only one image plane. The true LVEDV may, however, be underestimated if the visualised apex is not the anatomical apex.

Left ventricular end-diastolic area

LVEDA, measured at the mid-papillary short-axis level, has become the parameter most frequently used to estimate LV preload by echocardiography in the clinical setting. It has been assessed in vascular and cardiac surgical patients.[31,33,37,38] It has also been measured in critically ill patients with haemodynamic disturbances on the intensive care unit.[39–42] LVEDA does not measure LVEDV directly, but changes in LVEDA consistently reflect changes in LVEDV.[43–45] This can in part be explained by the finding that 90% of stroke volume results from shortening of the ventricular short-axis, whereas only 10% of the stroke volume is generated by ventricular shortening in the long-axis. LVEDA is measured by the leading edge-to-leading edge technique, using the borders of the echocardiographic image of the endocardium that are closer to the transducer. The papillary muscles are included in this outline. They serve as easily discernible anatomical landmarks, thus allowing for reproducible determinations of LVEDA.

LVEDA should be measured during expiration at end-diastole. End-diastole can be identified by electrocardiography at the beginning of the QRS wave or as the last frame before closure of the mitral valve. For practical reasons, however, the R wave is usually used, which corresponds to the first frame with the mitral valve closed while the aortic valve has not yet opened. It is generally accepted that at least three heart cycles during sinus rhythm and five to eight cycles during arrhythmia must be analysed and averaged.

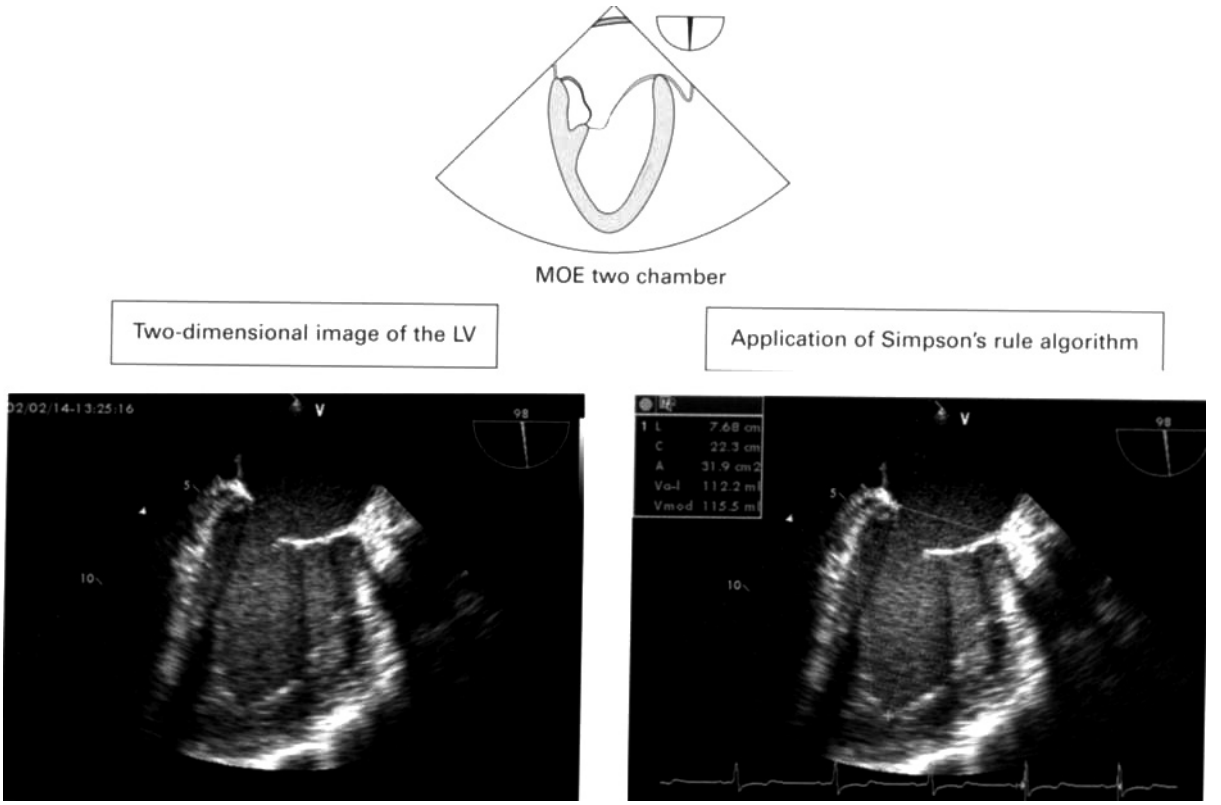

Figure 3.4 Simpson's rule to determine left ventricular volume offline. Computer assisted planimetry is used to outline endocardial borders in a longitudinal view, which is classified as mid-oesophageal two chamber view (MOE two chamber). The software of the ultrasonograph subsequently dissects the outlined surface in a series of 20 ellipsoid cylinders of equal height. The sum of the volumes of the individual slices gives the total chamber volume. The two chamber view is developed from a mid-oesophageal probe position by rotating the multiplane angle forward to between 80 and 100°. This cross-section shows the basal, mid, and apical segments in each of the anterior and inferior walls.

Acoustic quantification technique to determine left ventricular end-diastolic area

The acoustic quantification technique is a hardware based algorithm that processes superimposed acoustic data before they are compressed into video format. The technique is based on the different ultrasound scattering properties of blood and myocardial tissue. Imaging of the backscatter profile and further processing of the acoustic information by a so-called automated boundary detection (ABD) system makes it possible to demarcate blood and myocardium. Thus, online assessment of cardiac preload and derived variables on a beat-to-beat basis is facilitated (Figure 3.5). The investigator can use a trackball to outline a particular region of interest in which ABD will be activated. The resultant area of blood, for example representing the LV cross-sectional area in the transgastric short-axis view, can then be displayed in real-time. TOE with an ABD system for automatic detection of the endocardial border displays the following online: waveforms for LV cavitary areas or volumes; (optionally) waveforms for the derivatives of these area or volume curves; beat-to-beat digital values for EDA, EDV, end-systolic area, end-systolic volume, fractional area change (area), or ejection fraction (volume); and some new parameters gathered from the waveforms of the derivatives, such as peak filling rate.[36]

ABD is highly dependent on the quality of the image. Correct gain settings to produce a high resolution image with distinct endocardial borders are critical for successful performance of this method. When interpreting preload data obtained by acoustic quantification, it must be taken into account that the papillary muscles are usually included in the area measurements by the conventional manual technique, but that ABD excludes them. The practical value of ABD in the

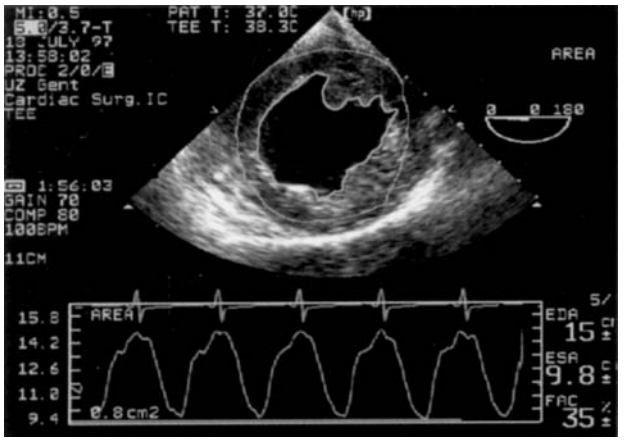

Figure 3.5 Transgastric short-axis view with activated automated boundary detection system and outlined region of interest (split screen image). Instantaneous changes in ventricular short-axis dimension are displayed as a waveform. End-systolic area (ESA) and end-diastolic area (EDA), as well as fractional area change (FAC), are indicated numerically.

perioperative setting has not yet been fully evaluated.

Left ventricular end-diastolic area in the clinical setting

A linear relationship was found between changes in LVEDA and acute changes in circulating blood volume in patients undergoing coronary artery surgery, confirming the usefulness of LVEDA for the evaluation of preloading conditions.[31] Changes in LVEDA in this study correlated well with graded acute hypovolaemia both in patients with normal LV function and in those presenting with segmental wall motion abnormalities. LVEDA was significantly reduced after only 1·75 ml/kg blood loss and continued to decrease with further venesection. The authors found a linear decrease in LVEDA (0·3 cm^2 per 1% loss of estimated blood volume) in response to graded acute blood volume deficits. These results emphasise the quantitative character of LVEDA. These findings were confirmed in dogs by Swenson *et al.*,[45] who demonstrated that changes in LVEDA were closely related to changes in cardiac output. This relationship was used to identify the intravascular volume associated with maximum cardiac output. Reich *et al.*[38] identified changes in LVEDA by manipulating blood volume in paediatric patients. LVEDA detected even small decreases in circulating blood volume with a sensitivity of 90% and a specificity of 80%. A similar result was reported by Dalibon and coworkers[46] when they analysed the ability of echocardiography derived preload to detect hypovolaemia. Those investigators subjected pigs to graded hypovolaemia and subsequent retransfusion. LVEDA correlated well with blood loss ($r = 0·96$) and was significantly reduced after 5 ml/kg blood loss. Furthermore, a correlation coefficient of 0·87 was found between indexed LVEDA and intrathoracic blood volume (blood volume between the right atrium and the distal aorta) perioperatively in patients undergoing coronary artery bypass grafting.[30]

Clearly, LVEDA is a reliable measure for detecting acute volume changes in patients in whom a baseline LVEDA is known. In the presence of normal RV and LV function, as well as normal pulmonary vascular resistance, low LVEDA can even be relied on to identify hypovolaemia, which cannot be confirmed on the basis of abrupt shifts in intravascular volume. In all of the above studies, the LVEDA was derived from the transgastric short-axis view of the left ventricle at the level of the mid-papillary muscles. Although volumetric methods seem to perform well in detecting decreased ventricular EDVs and hypovolaemia, their use in conditions of high preload and fluid overload may not be as reliable. This is due to the shape of the LV compliance curve, which means that when the ventricle is under-filled volume changes are large for a given change in pressure. In contrast, when the ventricle is well filled the volume changes are less for a given pressure change.

A further approach is to look at the effect of increasing preload on stroke volume, assuming that the two will increase along the Frank–Starling curve. Both EDAs and EDVs correlate well ($r = 0·91$ for both) with thermodilution cardiac index in patients undergoing coronary artery grafting.[47] During liver transplantation, LVEDA again correlated well with cardiac output, but neither correlated with PCWP.[48]

A number of studies have compared echocardiographic estimates of preload with PCWP. In 32 patients with septic shock, LVEDV was compared with PCWP as an index of preload.[49] The two methods showed only a mild inverse correlation. The authors concluded that it was PCWP that was a poor measure of preload. Clements *et al.*[50] compared PCWP with both echocardiography derived LVEDA and radionuclide derived EDA. PCWP correlated poorly with the other two variables, which were well correlated ($r = 0·84$). In patients undergoing

laparoscopy, there was also poor correlation between LVEDA and PCWP with pneumoperitoneum and changes in posture.[51] The effects of increased intra-abdominal and intrathoracic pressure are important because they have the potential to increase filling pressure while simultaneously reducing volumes.

Limitations of left ventricular end-diastolic area

It is more difficult to discriminate hypovolaemia from other causes of haemodynamic instability by determining LVEDA, and to predict whether stroke volume will increase in response to volume loading if LVEDA is within the "normal physiological range" and if LVEDA is the only echocardiographic parameter evaluated. In a recent study conducted in patients with sepsis induced hypotension, the accuracy of several indicators of the response of stroke volume to a fluid challenge was tested by receiver operating characteristic curve analysis.[21] The delta down of the systolic pressure variation component was found to have the highest positive and negative predictive values. The area under the receiver operating characteristic curve was 0·97 for delta down but only 0·77 for indexed LVEDA. The authors speculated that the interindividual variation in LVEDA and a possible dilation of the heart in septic patients during fluid administration might explain the only modest predictive value of LVEDA.

Interindividual variations in LVEDA were demonstrated by Leung and colleagues.[33] LVEDAs under baseline conditions were 18 ± 4 cm^2 in 17 anaesthetised patients with normal ventricular function and 23 ± 5 cm^2 in those with segmental wall motion abnormalities. Also, patients with dilated cardiomyopathy have even stronger elevated LVEDA in order to generate sufficiently high stroke volumes. On one hand, the appropriate preload may therefore be underestimated in patients requiring high preload if only LVEDA is evaluated. On the other hand, both RV failure with severe tricuspid regurgitation and LV diastolic dysfunction (see the respective chapters) may be associated with a low LVEDA in the presence of pulmonary and systemic venous congestion, respectively. For this reason, parallel assessment of RV function and LV diastolic function by echocardiography is strongly recommended to avoid misinterpretation of the low LVEDA in these patient populations. Likewise, LVEDA may appear to be within the normal range in a hypovolaemic patient if the volume loss is masked by a high vascular tone due to the administration of vasoconstrictive substances. Therefore, an apparently normovolaemic state should always be questioned in the presence of vasoconstrictor therapy.

Dynamic measurements for preload using heart-lung interaction

As outlined above, even if echocardiography derived measures of end-diastolic LV dimensions are accurate, they still do not satisfactorily differentiate between preload responsiveness and unresponsiveness in patients with acute circulatory failure.[20,52] This may not be a weakness but may reflect the fact that preload responsiveness and absolute, single point estimates of end-diastolic LV dimensions are different physiological concepts. Measuring alterations in preload provides more information with respect to fluid responsiveness than do single point estimates of LVEDA alone. For this reason it was proposed that static pressure and volume measurements be complemented by dynamic monitoring consisting of assessment of fluid responsiveness using respiratory variations in systolic arterial pressure, arterial pulse pressure, or aortic Doppler velocity induced by positive pressure ventilation.[20,22]

Systolic pressure variation (the difference between the maximal and minimal values of systolic pressure during one mechanical breath) has been shown to be a valuable variable of cardiac preload in several clinical studies.[19,21,53] Pulse pressure variation (the maximal pulse pressure below the minimum pulse pressure divided by the average of these two pressures) can more accurately reflect changes in LV stroke volume than systolic pressure variation because it is not influenced by intrathoracic pressure induced changes in arterial pulse.[26,54,55] A similar method for continuous assessment of fluid responsiveness is offered by TOE. Comparable to systolic pressure variation and pulse pressure variation, respiratory variations in aortic Doppler velocity reflect ventilation induced changes in LV stroke volume, and the magnitude of respiratory changes in the aortic velocity time integral (VTI_{Ao}) can be used as a reliable indicator of volume depletion and responsiveness.[24,25] To calculate dynamic respiratory changes in VTI_{Ao} (ΔVTI_{Ao}), maximal and minimal values of VTI_{Ao} are determined over a single respiratory cycle:

$$\Delta VTI_{A0}\,(\%) = 100 \times \frac{VTI_{A0}max - VTI_{A0}min}{(VTI_{A0}max + VTI_{A0}min) \div 2} \quad (3.1)$$

By increasing pleural pressure and transpulmonary pressure, mechanical insufflation decreases RV filling and impairs RV ejection by an increase in pulmonary vascular resistance.[56] Therefore, RV stroke volume decreases during the inspiratory period, leading to a reduction in LV preload during the expiratory period because of the long pulmonary transit time of blood.[57] These respiratory changes in LV preload induce cyclic changes in LV stroke volume.[57,58] Interestingly, the cyclic changes in RV preload induced by mechanical ventilation should result in greater cyclic changes in RV stroke volume when the right ventricle operates on the steep rather than on the flat portion of the Frank–Starling curve. The cyclic changes in RV stroke volume, and hence in LV preload, also should result in greater cyclic changes in LV stroke volume when the left ventricle operates on the ascending portion of the Frank–Starling curve.[59,60] Thus, the magnitude of the respiratory changes in LV stroke volume should be an indicator of biventricular preload dependence (Figure 3.6). In other words, a patient is a responder to volume expansion only if both ventricles operate on the ascending portion of the Frank–Starling curve (biventricular preload dependence). In contrast, if one or both ventricles operate on the flat portion of the curves, then the patient is a non-responder, and his or her stroke volume will not increase significantly in response to volume challenge.[52]

TOE allows beat-to-beat measurement of the aortic blood flow velocity profile. Because the integral of aortic blood flow velocity over time (VTI_{Ao}) is directly proportional to LV stroke volume, analysis of the respiratory changes in aortic blood velocity serves as an accurate estimation of the respiratory changes in LV stroke volume, and thus can be used to assess biventricular preload dependence and fluid responsiveness.[25] An example of a simultaneous recording of the airway pressure curve and aortic blood flow is shown in Figure 3.7. To perform measurements of aortic blood flow, the transoesophageal ultrasound probe is positioned deep in the stomach. A deep TG LAX of the LV outflow tract (LVOT), the aortic valve, and the ascending aorta is obtained by moving the tip of the probe anteriorly and turning it to the left. This modification of the classical transgastric short-axis view enables arrangement of the LVOT, aortic valve, and ascending aorta in an almost vertical direction. Aortic blood flow velocities are measured using a pulsed wave Doppler beam focused at the level of the aortic valve. Doppler signals are judged to be optimal when the greatest amplitude and clarity of the spectral waveform is achieved through adjustment of the beam position and gain settings. Consecutive velocity waveforms are then recorded over one respiratory cycle, stored in the cine-loop memory of the echocardiographic system, and measured by planimetry using the software routines of the ultrasonograph to generate the different values for VTI_{Ao}. Up to this point, the approach for measuring cardiac output at the level of the aortic valve and that for calculating respiratory changes in aortic blood flow velocity (ΔVTI_{Ao}) are

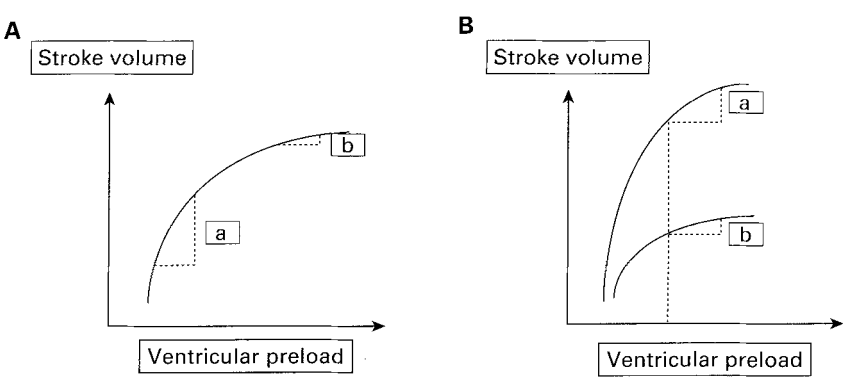

Figure 3.6 Frank–Starling relationships between ventricular preload and stroke volume. **(A)** A Frank–Starling curve is shown (a) before and (b) after volume expansion in the same patient. After volume expansion the same magnitude of change in preload recruits less stroke volume because the plateau of the curve is reached, which characterises a condition of preload independency. **(B)** The relationship in (a) a normal heart and (b) in a failing heart. A given value of preload can be associated with preload dependence in a normal heart or with preload independence in a failing heart.

essentially the same. Maximal and minimal values for VTI_{Ao} are finally determined over the designated respiratory cycle and are inserted into equation cited above to calculate ΔVTI_{Ao}.

Two recent studies strikingly demonstrate the superiority of dynamic measurements of aortic Doppler velocity as opposed to traditional static measurements of pressure and end-diastolic dimension, whenever accurate evaluation of cardiac preload dependence is the issue. Feissel *et al.*[25] demonstrated that the magnitude of respiratory variations in aortic blood flow velocity was a more accurate method than measurement of LV dimensions for predicting the haemodynamic effects of volume expansion. Those investigators studied 19 patients receiving mechanical ventilation and with septic shock. All patients received mechanical ventilation in a volume controlled mode with a tidal volume of 8–10 ml/kg. Measurements were performed in duplicate, first before volume expansion and then immediately after volume expansion using 8 ml/kg 6% hydroxyethylstarch over 30 minutes. Indexed LVEDA and respiratory changes in aortic blood flow velocity were compared. In 12 mechanically ventilated and anaesthetised rabbits, Slama *et al.*[24] compared dynamic and static echocardiographic indices of ventricular preload during stepwise hypovolaemia and after retransfusion. During hypovolaemia, they demonstrated a progressive reduction in ventricular preload indices as well as an increased magnitude of ΔVTI_{Ao}. However, during the sequential retransfusion of blood, only the ΔVTI_{Ao} correlated with the increase in systemic blood flow, suggesting that the dynamic parameter of preload responsiveness is more reliable than static parameters for assessing the haemodynamic response to volume infusion.

Echocardiographic estimation of left ventricular filling pressure

As opposed to the case in LV systolic failure, in the presence of diastolic dysfunction LVEDA is expected to be low in spite of markedly increased filling pressures. The coincidence of low filling volumes and high filling pressures has been termed the "paradox of the stiff heart".[61] In the context of diastolic dysfunction the non-invasive assessment of LV filling pressure may be a helpful adjunct in predicting the development of pulmonary oedema. Surprisingly, TOE provides practical ways to estimate LV filling pressure.[62]

By using pulsed Doppler, the pattern of flow through the mitral valve during diastole is typically biphasic. An early (E) wave is followed by a subsequent (A) wave, which corresponds to filling during atrial systole. A number of techniques have been used to estimate LV end-diastolic pressure from these filling waveforms. The ratio of E/A peak mitral velocity was first correlated with PCWP in 1986.[63] A ratio greater than 2 was associated with LV end-diastolic pressure above 20 mmHg in 20 patients with ischaemic heart disease. In another group of 132 patients, a regression equation using E/A ratios was able to predict PCWP with reasonable accuracy ($r = 0{\cdot}92$).[64] Even more accurate information can be derived by analysing pulmonary venous flow velocity spectra. By

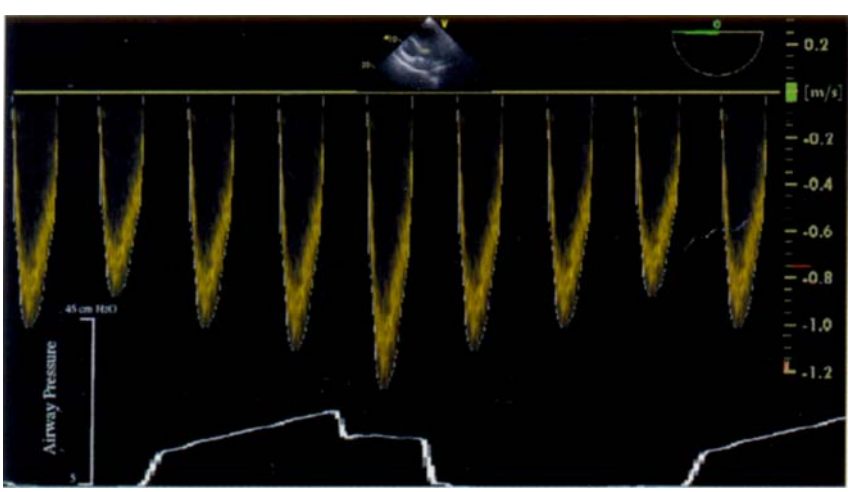

Figure 3.7 Cyclic respiratory changes in airway pressure and in aortic Doppler velocity. Beat-to-beat measurement of the aortic velocity–time integral (VTI_{Ao}) allows determination of VTI_{Ao}max and VTI_{Ao}min over a single respiratory cycle. The ΔVTI_{Ao} is then calculated as the difference between VTI_{Ao}max and VTI_{Ao}min divided by the mean of the two values and is expressed as a percentage.

placing the pulsed Doppler cursor at the junction of the left atrium and left superior pulmonary vein, it could be demonstrated that the systolic fraction of the pulmonary venous flow into the left atrium was inversely correlated with left atrial pressure.[65] Pulmonary venous flow is phasic, with antegrade peaks during ventricular systole and diastole and retrograde flow during atrial contraction (Figure 3.8).[66] A systolic fraction of flow of less than 55% was a specific and sensitive marker of left atrial pressure greater than 15 mmHg.

Other Doppler parameters have been suggested for the estimation of filling pressure. Rossvoll and Hatle[67] described a new Doppler variable: the difference in duration between pulmonary venous atrial regurgitation wave and mitral A wave. With atrial contraction, blood is ejected from the atrium into the left ventricle and also backward into the pulmonary veins. As a result of atrial contraction, an antegrade A wave is displayed on the pulsed Doppler flow velocity profile of transmitral inflow and a retrograde atrial regurgitation wave on the pulmonary venous flow velocity pattern. Under normal circumstances the amount and duration of transmitral flow exceeds reverse flow into the pulmonary veins. However, with elevated filling pressures the duration of transmitral flow at atrial contraction is shortened and the duration of flow backward into the pulmonary veins is lengthened. In 50 patients undergoing cardiac catheterisation, Rossvoll and Hatle demonstrated that a pulmonary venous atrial regurgitation wave flow reversal that exceeded the duration of mitral A wave predicted a LV end-diastolic pressure greater than 15 mmHg with a sensitivity of 85% and a specificity of 79%. Hence, TOE cannot

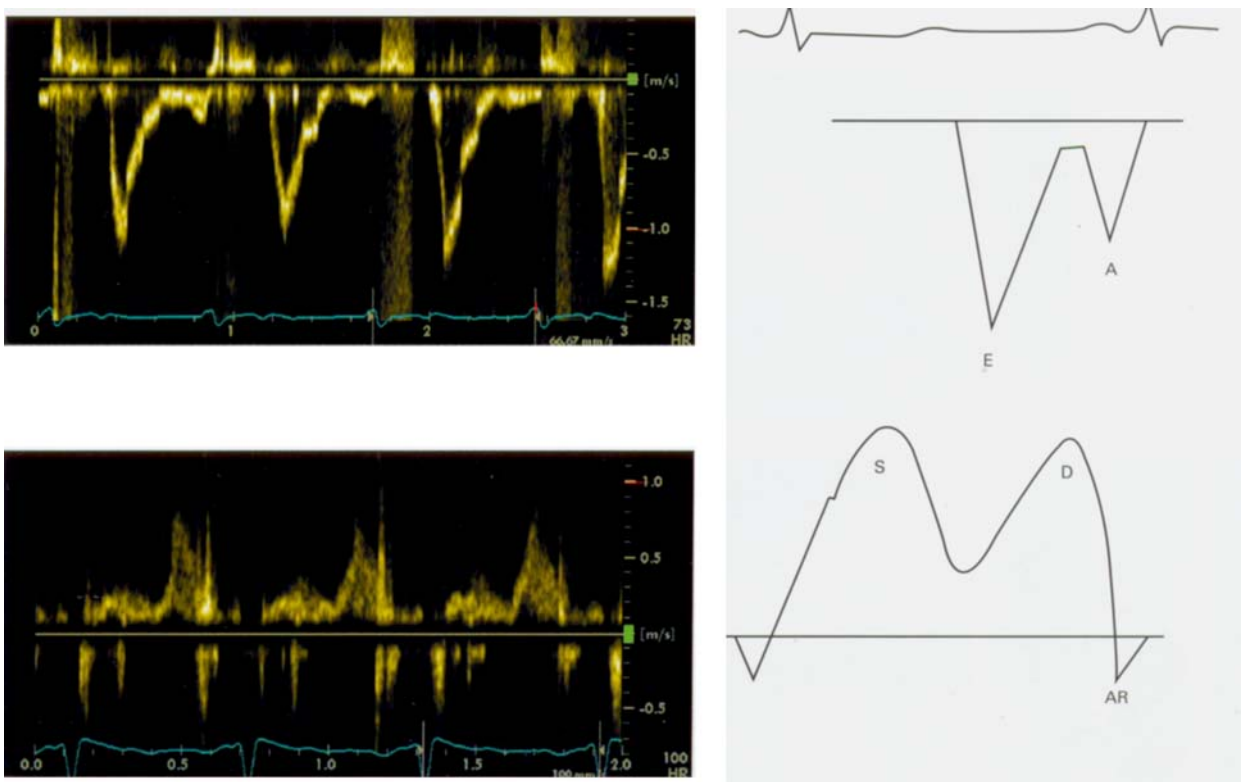

Figure 3.8 Pulsed Doppler echocardiographic recording of transmitral and pulmonary venous flow velocity profiles. The depicted transmitral and pulmonary venous flow pattern are indicative of elevated end-diastolic left ventricular pressures. Transmitral flow during diastole is typically biphasic with an early (E) filling wave and a subsequent atrial (A) wave, corresponding to atrial contraction. The ratio of E/A peak transmitral velocity is age dependent, but in normal adult patients it is close to 1. In the pulmonary veins blood flow is antegrade throughout systole (S wave) and diastole (D wave). Most normal adult patients exhibit a prominent systolic flow and a systolic-to-diastolic ratio greater than 1. Retrograde flow occurs during atrial contraction (pulmonary AR wave). Integration of instantaneous pulmonary flow velocities during systole and diastole allows for calculation of the systolic and diastolic fraction, respectively. See text for further details.

quantitatively measure LV filling pressure, but appears able to identify clinically significant elevations reliably.

More recently the study of myocardial relaxation has led to the development of novel indices of LV filling pressure, which are relatively stable in the face of changes in ventricular loading conditions. As a byproduct, these can be used to obtain a measure of preload from the LV filling pattern. After the mitral valve opens in diastole, flow propagates from the atrium, through the valve, toward the apex. The rate at which this flow is propagated into the left ventricle (V_p) depends on the relaxation rate of the ventricle, and it appears to be independent of preload. Imaging from the mitral valve to the apex with colour M-mode Doppler echocardiography, transmitral flow appears as a jet directed into the left ventricle.[68–70] Although standard pulsed wave Doppler echocardiography provides the temporal distribution of blood flow velocities in a specific location, colour M-mode Doppler echocardiography provides the spatiotemporal distribution of these velocities across a vertical scan line. Thus, the information displayed in a colour M-mode recording of transmitral inflow is comparable to that given by multiple simultaneous pulse Doppler tracings obtained at different levels from the mitral orifice to the apex of the left ventricle.

Figure 3.9 demonstrates the typical pattern displayed by patients in sinus rhythm. A first wave propagates from the left atrium to the LV apex corresponding to early filling (E), and a second wave follows atrial contraction (A). The velocity at which flow propagates within the ventricle (V_p) is given by the slope of the colour wavefront of early filling. V_p is dependent on intraventricular pressure gradients, which are responsible for the mechanism of suction in ventricles with normal relaxation.

The ratio of peak early diastolic filling velocity/flow propagation velocity (E/V_p) by colour M-mode Doppler provides a better estimate of PCWP than either transmitral or

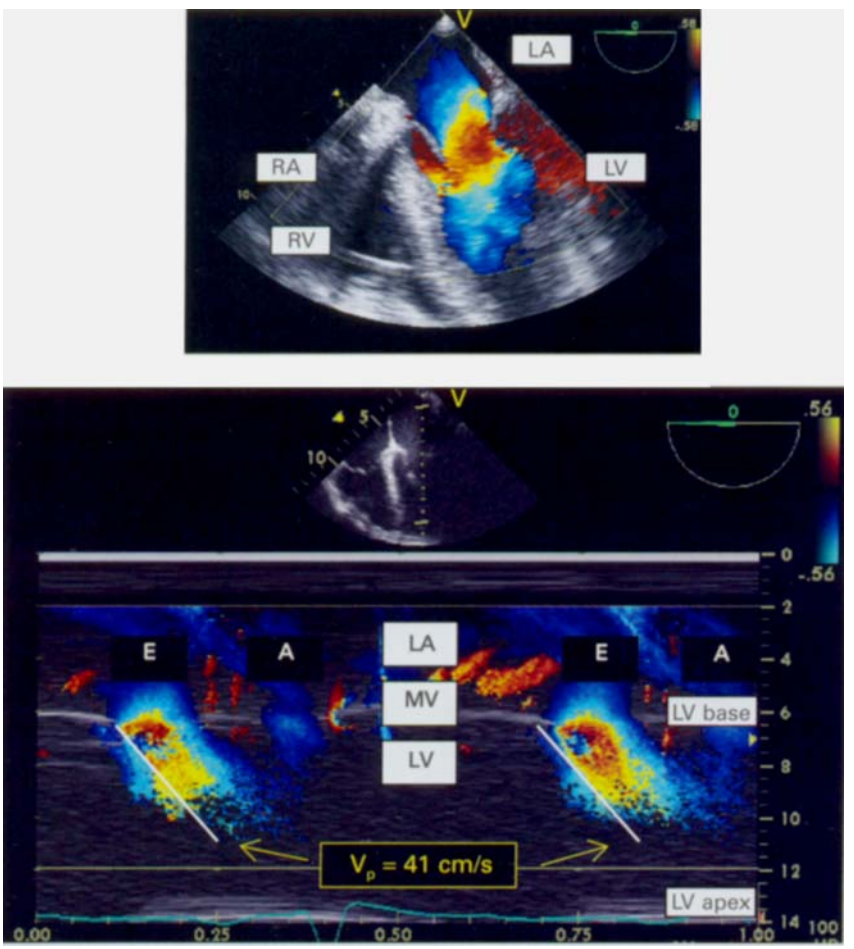

Figure 3.9 Colour Doppler and colour M-mode Doppler images of the transmitral inflow obtained by transoesophageal echocardiography from a mid-oesophageal four chamber view. On the colour M-mode Doppler tracing the early (E) and atrial contraction (A) waves are shown. Flow propagation velocity (V_p) is given by the slope of the colour wavefront. LA = left atrium, LV = left ventricle, MV = mitral valve, RA = right atrium, RV = right ventricle.

pulmonary venous flow alone. In 45 patients in intensive care, estimated PCWP by E/V_p showed good agreement with measured PCWP, over-reading by 1 ± 6·2 mmHg (bias ± 2 standard deviations) at a mean PCWP of 15 mmHg.[71] In patients with hypertrophic obstructive cardiomyopathy, E/V_p still predicted PCWP with reasonable accuracy (0 ± 7·8 mmHg; bias ± 2 standard deviations) at a mean PCWP of 14 mmHg.[72] In patients with acute myocardial infarction, E/V_p by colour M-mode Doppler during early LV filling provided a better estimate of PCWP than transmitral or pulmonary venous flow. This was demonstrated by Ueno *et al.*[73] in a group of patients suffering from acute myocardial infarction. Those investigators measured transmitral flow velocity indices and the deceleration time of diastolic pulmonary venous flow and E/V_p, and compared these variables with PCWP measured using a pulmonary artery catheter. E/V_p was strongly correlated with PCWP ($r = 0·89$). The sensitivity of an E/V_p of 2·0 or more for predicting a PCWP 18 mmHg or more was 95%, and the specificity was 98%.

Summary

Echocardiography provides important information for diagnosis and monitoring of LV preload. Exclusive monitoring of LVEDA appears sufficient in patients with normal cardiovascular function. The additional consideration of ΔVTI_{Ao} and of a non-invasive Doppler index of LV filling pressure (i.e. E/V_p) is advisable in patients with abnormal cardiac function in order to obtain all information necessary to make correct decisions for optimisation of cardiac preload.

Afterload

It is relatively easy to define afterload for the isolated muscle preparation. Afterload is the force that resists muscle shortening. It is the weight or load that a contracting muscle must overcome before shortening.[74] Similar to preload, the weight must be normalised to the cross-sectional diameter of the muscle preparation, and afterload is therefore quantified in terms of force per unit cross-sectional area or stress during the contraction phase. In isolated muscle an inverse relationship exists between the velocity of myocardial fibre shortening and afterload.

In the intact heart it is more complex to characterise afterload. The ventricle does not lift an ordinary weight, but accelerates and moves a viscous fluid (stroke volume of blood) into a viscoelastic system (distensible arterial tree) at a certain pressure. Thus, the afterload on an intact ventricle is not a simple quantity. One attempt to delineate afterload is to regard the arterial system itself as the ventricular afterload. In that case the properties of the arterial system may be expressed by a simple but incomplete variable, such as systemic vascular resistance (SVR), or by the input impedance of the systemic arteries. The latter variable fully represents the properties of the arterial bed but it necessitates an intricate analysis of instantaneous pressure and flow in the frequency domain.[75,76] An alternative way to describe afterload is to look at it at the level of the ventricle, and to consider it as the stress imposed on the ventricular wall during systole.[77,78] This wall stress concept incorporates both the pressure and ventricular geometric components of the Laplace relation.[79] By analogy with the velocity of fibre shortening in experiments on cardiac muscle strips, the overall performance of the intact ventricle is inversely related to the existing stress within the ventricular walls.[80,81] Thus, for the intact ventricle, in many respects the wall stress concept represents a straightforward extrapolation of the afterload definition for the papillary muscle preparation.

Systemic vascular resistance

Similar to the definition given by Ohm's law for electrical resistance, vascular resistance is calculated as the ratio of driving pressure to flow. Vascular resistance indicates the physical opposition to flow accurately, if the system obeys Poiseuille's law. The applicability of Poiseuille's law requires several preconditions: flow must be laminar, the tube must be cylindrical in shape, the fluid must have Newtonian viscosity, and flow must be non-pulsatile.[76] None of these conditions is satisfied in the integrated cardiovascular system. Nevertheless, the calculation of vascular resistance as the ratio of mean pressure to mean flow is useful in its application to whole vascular beds, for example to the entire systemic circulation. In fact, the physiological significance of SVR is its ability to detect constriction and dilation in the systemic circulation. Therefore, SVR is used in clinical medicine as an indicator of vasomotor tone.[82] SVR is calculated according to the following formula:

$$SVR = \frac{(MAP - CVP)}{CO} \times 80 \text{ (dyne} \cdot \text{s} \cdot \text{cm}^{-5}) \quad (3.2)$$

where MAP is the mean arterial pressure, CVP is the central venous pressure, and CO is the cardiac output. This equation can be resolved by linking pressure data to Doppler echocardiographic measurements of volumetric aortic flow. Pressures are measured in millimetres of mercury, cardiac output is given in litres per minute, and 80 is a conversion factor. Mean arterial pressure can be derived either from cuff blood pressure or invasive pressure measurements. Because mean central venous pressure is low relative to mean arterial pressure, it is frequently neglected in the calculation. Fortunately, substantial research using Doppler has established that TOE can measure cardiac output at the level of the LVOT with exceptional precision.[83–85] The advances in Doppler echocardiographic estimation of cardiac output are extensively reviewed later in this text.

It should again be emphasised that the problem with SVR is that it reflects only the non-pulsatile component of peripheral load. SVR does not account for the impact of wave reflections, arterial impedance, or ventricular ejection gradients. However, each of these phenomena augments LV afterload independently of peripheral vascular resistance or arterial pressure.[79] With ageing, hypertension, or aortic stiffening the added pulsatile load becomes more and more prominent.[86,87] For that reason SVR alone is an incomplete description of the real arterial load that the ventricle must carry.

Left ventricular end-systolic meridional wall stress

As mentioned above, afterload can be considered the force that is present in the ventricular wall during systole. This force is defined as stress and expressed as dyne·cm^{-2}. Because the stress within the ventricular wall must exactly balance the forces acting on the wall, LV systolic wall stress is a quantitative index of true myocardial afterload.[78] It reflects the combined effects of peripheral loading conditions and factors within the heart.[88] Wall stress can be derived from the basic Laplace relationship as follows:

$$\sigma = \frac{P \times r}{2h} \text{ (dyne} \cdot \text{cm}^{-2}) \quad (3.3)$$

where σ is wall stress, P is the intraventricular pressure throughout systole, r is the corresponding chamber radius, and h is the wall thickness. Thus, LV wall stress incorporates both pressure and ventricular geometric components. As evidenced by the Laplace relation, at similar systolic pressures a larger ventricle will have greater wall stress than a smaller one. Because of the instantaneous changes of its three determinants (intraventricular pressure, ventricular radius, and wall thickness) during the ejection phase of the cardiac cycle, wall stress varies markedly. Peak ventricular wall stress occurs within the first third of ejection. Then wall stress declines to its end-systolic value, which is less than 50% of the peak value.[89] There are different opinions as to which phase of the stress–time cycle should be employed as the index of LV afterload.[90,91] Peak, mean, total systolic (stress–time integral), and end-systolic stress have all been proposed. Each of these components has different physiological significance, and the choice of index depends on the question to be answered; total stress predicts myocardial oxygen consumption, and peak stress correlates closely with the progress of hypertrophy, but end-systolic stress provides the most suitable parameter of afterload.[92]

Apart from the timing of appropriate measurements and the choice of the parameter, it is important to differentiate the circumferential (σ_c) and meridional (σ_m) components of wall stress. The circumferential stress acts along the minor axis of the left ventricle, whereas the meridional stress represents forces acting along the longitudinal axis. For a sphere, the circumferential stress will equal the meridional stress. However, for an ellipsoid model of the left ventricle, circumferential stress at end-systole is 2·57 times higher than the meridional stress. In heart failure, as the ventricle becomes more spherical, the ratio decreases toward a value of 1.[93]

Assessment of instantaneous wall stress throughout the ejection phase necessitates continuous micromanometer LV pressure recordings, and continuously digitised echocardiograms. However, at end-systole, as demonstrated by Reichek *et al.*,[94] meridional wall stress can be determined totally non-invasively. Reichek's method is based on M-mode measurements of end-systolic diameter and posterior wall

thickness. Using TOE these measurements are taken from a mid-papillary transgastric short-axis view of the left ventricle. They are combined with cuff systolic arterial pressure, and inserted into an angiographically proven equation reported by Grossman *et al.*[77] In Reichek's investigation non-invasive stress correlated well with invasively derived values ($r = 0{\cdot}97$; $n = 31$). The equation for M-mode meridional end-systolic wall stress is as follows:

$$\text{LV ESWS} = \frac{0{\cdot}334 \times P_{syst} \times \text{LVESD}}{\text{ESWT} \times \left(1 + \frac{\text{ESWT}}{\text{LVESD}}\right)} \ (10^3 \cdot \text{dyne} \cdot \text{cm}^{-2}) \qquad (3.4)$$

where ESWS is the end-systolic meridional wall stress, P_{syst} is the cuff systolic blood pressure, LVESD is the left ventricular internal diameter, ESWT is the end-systolic posterior wall thickness, and 0·334 is the conversion factor from millimetres of mercury to dyne·cm^{-2}.

Using TOE with a system for automatic detection and outlining of endocardial borders (i.e. ABD; see above), it may be more appropriate to calculate meridional wall stress from two-dimensional echo recordings of the transgastric short-axis view. However, the two-dimensional method requires tracing of both endocardial and epicardial LV borders to account for myocardial area. Although the endocardial border is automatically available with ABD, epicardial structures are often poorly reproducible, revealing a drawback of the two-dimensional method. On the other hand, an average value of ventricular wall thickness is inserted, obviating the assumption of uniformity of myocardial wall thickness. When averaging ventricular wall thickness, normal two-dimensional values are found to differ from those of M-mode recordings ($86{\cdot}0 \pm 16$ dyne·cm^{-2} and $64{\cdot}8 \pm 19{\cdot}5$ dyne·cm^{-2}, respectively).[93] Fortunately, the various equations yield results that are qualitatively similar in spite of quantitative differences.[95] The equation for two-dimensional meridional end-systolic wall stress is as follows:

$$\sigma_{m(es)} = 1{\cdot}33 \times \text{SBP} \times \frac{A_c}{A_m} \ (\text{dyne} \cdot \text{cm}^{-2}) \qquad (3.5)$$

where $\sigma_{m(es)}$ is the end-systolic meridional wall stress, SBP is the cuff systolic blood pressure, A_m is the myocardial area (end-systolic epicardial area – end-systolic endocardial area), and A_c is the LV end-systolic cavity area in the short-axis view.

Just recently Greim and coworkers[96] tested TOE for its ability to assess acute alterations in afterload in patients requiring cardiovascular support with noradrenaline or nitroglycerine. They derived end-systolic meridional wall stress from M-mode as well as from two-dimensional echocardiograms at the level of the mid-papillary cross-section of the left ventricle, and they concluded that acute changes in afterload were clearly indicated by the two-dimensional method, whereas M-mode measurements remained inconclusive. The same group presented a further simplified wall stress estimation, which was carefully designed to match the specific needs of the perioperative setting.[97] Greim *et al.* calculated the end-systolic pressure–area product by multiplying systolic arterial pressure by the end-systolic LV cavity area obtained by TOE:

$$\text{End-systolic pressure–area product} = \text{SBP} \times \text{LVESA}$$

where SBP is the cuff systolic blood pressure, and LVESA is the end-systolic cross-sectional LV area. If it is assumed that the cross-sectional myocardial area does not change markedly during perioperative alterations in afterload, then the use of the end-systolic pressure–area product circumvents redundant measurements of end-systolic cavity and myocardial dimensions. Greim *et al.* reported a close correlation between baseline values in the end-systolic pressure–area product and M-mode derived end-systolic wall stress ($r = 0{\cdot}85$; $n = 30$). Changes in the end-systolic pressure–area product by more than 10% reflected end-systolic meridional wall stress changes with a sensitivity of 88% and a specificity of 94%. Greim concluded that, "The ES [end-systolic] pressure–area product seems suitable for the detection of intraoperative LV wall stress changes."

Although quantitative indices of true myocardial afterload are readily at hand by combining TOE and pressure data, clinical assessment still relies on SVR and systolic blood pressure. This practice promotes misinterpretation.[98] A concrete clinical example may illustrate the limitations of SVR. It is assumed that a normal left ventricle will dilate after the onset of myocardial ischaemia.[99] Moreover, it is assumed that mean arterial pressure and cardiac output will remain constant, because the left ventricle shifts to the right on its Starling curve, thus exploiting its preload reserve. As shown in

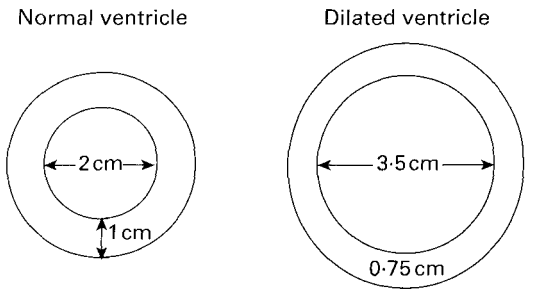

P_{syst}	100 mmHg	100 mmHg
P_{mean}	75 mmHg	75 mmHg
CO	5 l·min^{-1}	5 l·min^{-1}
SVR	1200 mmHg·s·cm^{-5}	1200 mmHg·s·cm^{-5}
M-mode σ	45·0 dyne·cm^{-2}	126·0 dyne·cm^{-2}

Figure 3.10 Comparison of systemic vascular resistance (SVR) and end-systolic meridional wall stress as indications of left ventricular afterload for a normal ventricle and a dilated ventricle. SVR does not change when pressure and cardiac output remain constant, despite the presence of a pathophysiological process that increases afterloading conditions. CO = cardiac output, M-mode σ = M-mode meridional wall stress at end-systole, P_{mean} = mean arterial pressure, P_{syst} = systolic arterial pressure (cuff pressure), SVR = systemic vascular resistance.

Figure 3.10, SVR will not change because the increase in ventricular dimensions occur in the presence of unchanged pressure and cardiac output. At the same time, meridional end-systolic wall stress indicates an increase by a factor of 2·8. This apparent discrepancy highlights the importance of implementing geometrical factors into analysis of afterloading conditions.

Summary

In summary, the addition of the wall stress concept to the perioperative monitoring of critically ill patients makes it possible to:

- identify the presence of excessively increased afterload as a component of LV dysfunction
- rule out myocardial oxygen demand, which is governed by the integral of wall stress throughout systole
- account for drug induced alterations in ventricular loading conditions
- study individuals under different loading conditions
- distinguish different groups of patients (for example those with normal hearts and those with congestive cardiomyopathy or aortic regurgitation).

Contractile performance

A variety of indices have been developed to characterise the contractile performance of the left ventricle.[100,101] Many of these indices have proven to be clinically useful. They can principally be distinguished into two groups: those that display marked dependence on ventricular loading, and those that reflect more or less the inotropic properties of the myocardium.[2,3,102] Over recent years, new refinements in echocardiography (such as Doppler tissue imaging[103–107] and colour kinesis technology[108,109]) and the renewal of old concepts (such as the analysis of isovolumic time intervals[110–113]) have been introduced into clinical medicine. Thus, a new group of echocardiography specific parameters should be added to the classical variables of ventricular performance. Indices that can be obtained by means of TOE are summarised in Table 3.1.

The following text discusses in more detail the echocardiographic determination of stroke volume and cardiac output; mean rate of LV pressure rise; fractional area change; load-independent preload-adjusted maximal power; and myocardial performance index (MPI). At present the potential usefulness of these parameters appears to be greatest in the perioperative setting.

Cardiac index

Cardiac output is usually corrected for body size and is expressed as the cardiac index (CI; cardiac output per square meter of body surface area). CI can be looked upon as the net result of ventricular systolic performance, which mirrors the complex interaction of loading conditions and inotropic properties. The normal range for CI in the basal state is wide (2·5–4·2 l/min per m^2). This broad normal range makes the resting CI insensitive in detecting mild to moderate impairment in cardiac function. However, a cardiac index of less than 2·5 l/min per m^2 usually represents a marked disturbance of cardiovascular performance and is always manifested clinically. Thus, CI provides a valuable measure of the integrated function of the

Table 3.1 Transoesophageal echocardiographically determined parameters that reflect contractile performance of the left ventricle

Type of Index	Details
Load-dependent indices of overall LV systolic performance	Isovolumic phase indices: • mean rate of LV pressure rise[114] • isovolumic contraction time[115] Ejection phase indices: • stroke volume, cardiac output[84] • percentage fibre shortening (ejection fraction, fractional area change, fractional diameter shortening)[35] • mean velocity of circumferential fibre shortening[116] • E-point septal separation[117]
Load-independent indices of myocardial inotropy	End-systolic pressure-dimension relationship[2,118] End-systolic meridional wall stress rate corrected mean velocity of fibre shortening relationship[90] Preload adjusted maximal power[119]
Echocardiography-specific indices of ventricular contractile function	Myocardial performance index (MPI)[112] Doppler tissue imaging, tissue tracking, strain rate imaging[106,107] Colour kinesis technology[109]

LV = left ventricular.

cardiovascular system,[82] especially in critically ill patients.

The approaches most commonly applied to estimate CI in the clinical setting comprise Fick's principle of measurement, indicator dilution techniques, and angiographic methods. They all require the insertion of catheters into the central circulation. Furthermore, these methods are burdened with theoretical limitations and practical drawbacks.[120] Different from these invasive techniques, echocardiography represents a non-invasive means to assess volumetric flow.[121,122] Two different echocardiographic approaches are currently available.[123–125] The first is based on two-dimensional imaging of the heart. Cross-sectional areas and diameters are measured at specific locations of the heart. LV volumes are then calculated by applying predetermined geometric models. The most popular and accurate geometrical model calculates the total LV volume according to Simpson's rule (see above). Simpson's rule is incorporated into modern ultrasound equipment and can be used in conjunction with acoustic quantification technology.[36] In this way online estimations of LV end-systolic volume and EDV become possible and provide beat-to-beat values for stroke volume.[126] The full clinical potential of this technology, however, has yet to be defined. Although many studies have validated acoustic quantification estimates, the results remain highly operator dependent, and Doppler echocardiography is generally believed to produce more reliable measurements of volumetric flow in the clinical scenario.

Doppler echocardiographic estimation of volumetric flow through the aortic valve

The Doppler method can be used to measure flow through all cardiac valves. Irrespective of the sampling site, certain well recognised preconditions must be fulfilled to qualify any particular location for measurement of volumetric flow.

- Blood flow should be laminar.
- The velocity profile should be flat.
- It should be possible to orientate the Doppler beam parallel to the direction of blood flow.
- The measurement of the cross-sectional area at the level of the sampling site should be practicable.
- The cross-sectional area of the orifice should be constant throughout the region of blood flow.

With regard to these preconditions, former efforts at Doppler estimation employed the pulmonary artery and the mitral valve as sampling sites but showed high failure rates.[123] Fortunately, substantial research using TOE has now established that CI can be measured at the level of the aortic valve with a high degree of reproducibility and accuracy.[127] This sampling site became popular following the description of a modification of the classical transgastric view, visualising the long-axis of the heart from an apical aspect (Figure 3.11).[83–85,127,128] The view is anatomically referred to as the deep transgastric long-axis (deep TG LAX) view of the left ventricle.[129] In order to obtain this view, the TOE probe is advanced deep into the stomach. The probe's tip is fully moved anteriorly and to the left. Careful withdrawal of the flexed probe then results in the tip being positioned close to the apex of the left ventricle. The exact position of the probe and transducer is more difficult to determine and control deep in the stomach, but some trial and error flexing, turning, advancing, withdrawing, and rotating of the probe develops this view in almost all patients. In the deep TG LAX view, the aortic valve is located in the far field at the bottom of the display with LV outflow directed away from the transducer (see Figure 3.11). Detailed assessment of valve anatomy is not advisable in this view because the LVOT and aortic valve are so far from the transducer, but the view is perfectly suitable for Doppler quantification of blood flow velocities because of the ability to align blood flow almost parallel through the LVOT, the aortic valve, and the ascending aorta to a Doppler beam.[127]

Figure 3.12 illustrates how the Doppler echocardiographic method can be employed to calculate volumetric flow, and hence stroke volume, across the aortic valve as the product of the integral over time of flow velocities occurring at the sampling site and the effective systolic orifice area of the aortic valve.

The Doppler recording is obtained with the scan plane aligned parallel to the long-axis of the LVOT. The pulsed Doppler sample volume is positioned in the middle of the LVOT just at the aortic leaflet coaptation point. With Doppler data, velocity is shown in the form of a spectral display per unit time, conventionally in centimetres per second. Consecutive velocity waveforms are recorded and stored in the cine loop memory of the echocardiographic system. Then, the contours of the spectral Doppler signals are measured by planimetry using the software routines of the echocardiographic system. As a result the integral velocity over time (VTI) will automatically be displayed on the screen in units of centimetres. The VTI can be thought of as the distance travelled by the blood column during each ejection.[122]

Following the measurement of blood flow velocities, a mid-oesophageal short-axis scan (MOE AV SAX) is taken to depict the effective systolic orifice area of the aortic valve. The multiplane transducer is rotated to about 30–60° in order to transsect the valve's plane perpendicularly and to achieve a geometrically symmetrical image.[129] This cross-section is the only view that provides a simultaneous image of all three cusps of the aortic valve. The cusp adjacent to the atrial septum is the non-coronary

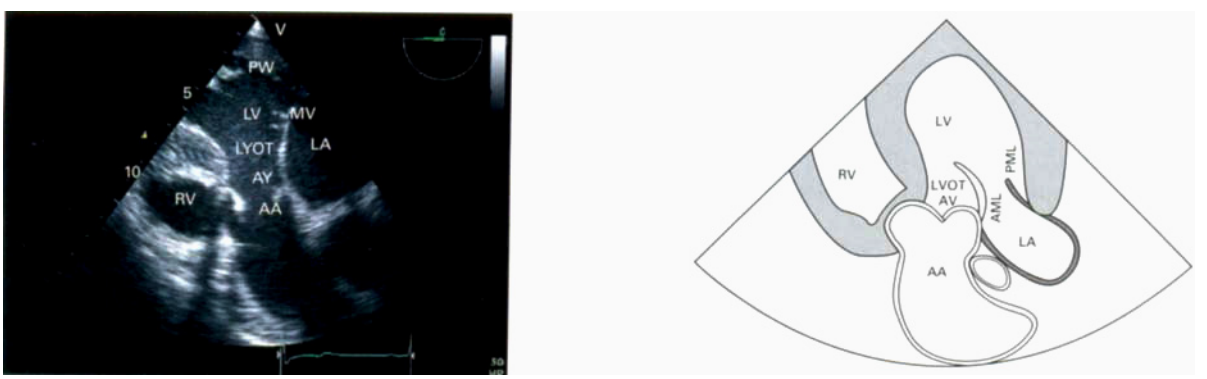

Figure 3.11 Deep transgastric long-axis view of the left ventricle (LV) for Doppler quantification of flow velocities through the aortic valve (AV). The echo probe is advanced deep into the stomach and anteflexed to get contact to the apical aspect of the LV. The left ventricular outflow tract (LVOT), the AV, and the ascending aorta (AA) are aligned almost parallel to the Doppler beam. For this reason Doppler quantification of blood flow velocities through the LVOT and AV are best performed using this view. AML = anterior mitral leaflet, IVS = interventricular septum, LA = left atrium, PML = posterior mitral leaflet, PW = posterior wall of the LV, RV = right ventricle.

cusp, the most anterior cusp is the right coronary cusp, and the other is the left coronary cusp. Proceeding on the assumption that time averaged aortic valve area (AVA) during systole can be considered an equilateral triangle, it can be calculated as follows:

$$AVA = 0{\cdot}5 \times \cos 30^\circ \times L^2 = 0{\cdot}433 \times L^2\ (cm^2) \quad (3.6)$$

where L is the average length of the three sides of the triangle (cm). For the evaluation of AVA a mid-systolic stop frame is chosen, in which the aortic valve appears precisely as an equilateral triangle. The length of each cusp is measured, and the average value taken for inclusion in the above equation (see Figure 3.12).[84,85] In most studies the orifice of the aortic value is considered to be circular, with the annulus diameter taken in the five chamber view or in the longitudinal view of the ascending aorta.[83] The circular shape of the orifice represents the maximal value of the instantaneously changing orifice area (fully opened orifice). In contrast the triangular shape of the orifice assumes a time averaged valve area. This explains why the circular orifice overestimates stroke volume and cardiac output. Compared with the usual circular model, the correlation coefficient improved from 0·88 to 0·93, when the triangular AVA was used.[84]

As the final step, volumetric flow is derived from the product of VTI, cross-sectional area, and heart rate. CI is then calculated as follows:

$$CI = VTI \times AVA \times HR \times BSA^{-1}\ (ml/min\ per\ m^2) \quad (3.7)$$

$$CI = VTI \times (0{\cdot}433 \times L^2) \times HR \times BSA^{-1}\ (ml/min\ per\ m^2) \quad (3.8)$$

where VTI is the velocity–time integral (cm), AVA is the time averaged aortic valve area, HR is the heart rate (beats/min), BSA is the body surface area (m^2), L is the average length of the aortic valve's cusps (cm), and $0{\cdot}433 = 0{\cdot}5 \times \cos 30^\circ$.

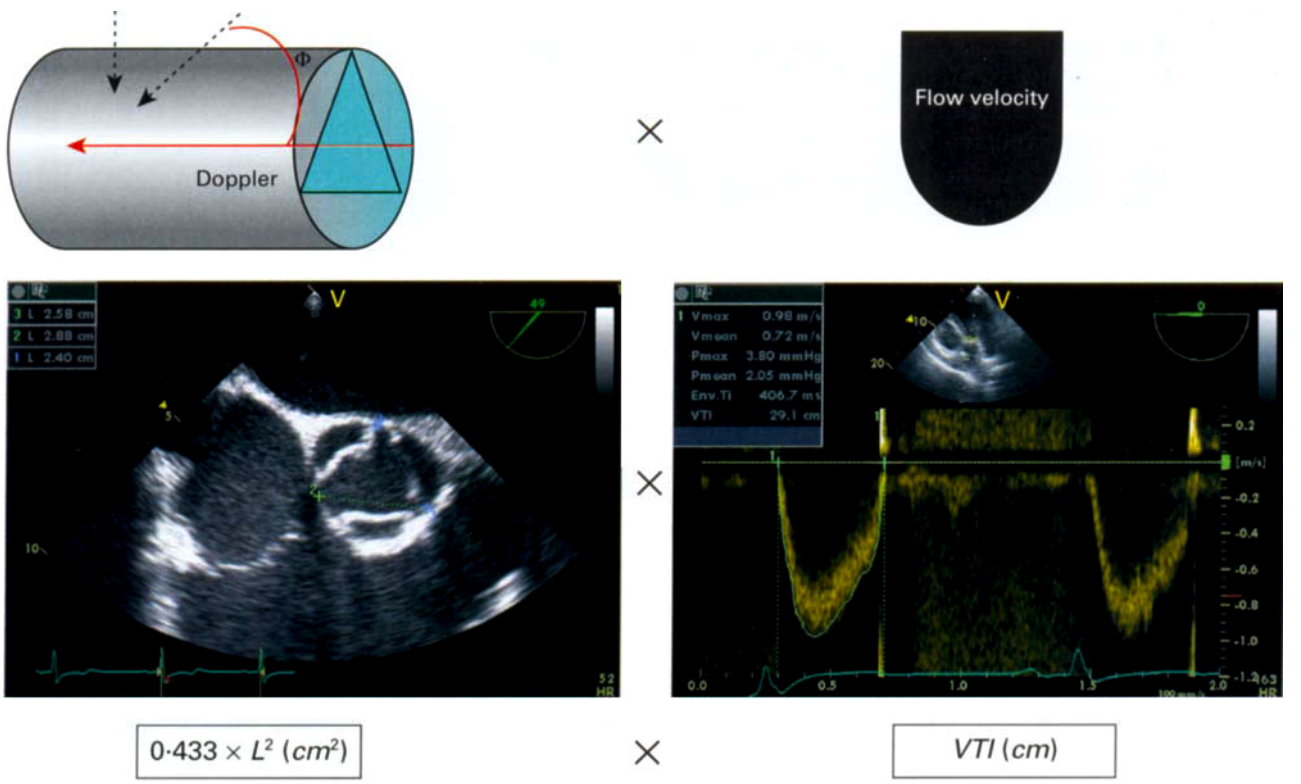

Figure 3.12 Doppler echocardiographic method to calculate volumetric flow across the aortic valve. Schematic diagrams and correlating echocardiographic recordings and corresponding equations are plotted one below the other.

At present the Doppler method should be regarded as the state of the art in non-invasive quantification of blood flow through the heart and in the great vessels. Nevertheless, future developments may provide further progress in this field, particularly with respect to automation and to the determination of the exact flow area, which is the major source of error when using the Doppler method.[130] Among these promising new techniques, cardiac output measurements by spatiotemporal integration of colour Doppler data[131,132] and three-dimensional imaging of the heart are most important.[133,134]

Mean rate of left ventricular pressure rise

The search for an indicator of contractile performance at first concentrated on the maximal rate of rise in intraventricular pressure (dP/dt_{max}), because interventions that were believed to improve contractility increased this parameter.[100,135] For example, Lee *et al.*[136] found that dP/dt_{max} was as effective at defining increases in contractility as was the end-systolic pressure–volume relationship.[136]

Invasive measurement of dP/dt_{max} requires insertion of an intraventricular catheter with a micromanometer at its tip. The LV pressure is recorded continuously while an electronic differentiator automatically calculates the first derivative of pressure, which is dP/dt (mmHg/s). The highest value throughout systole is designated dP/dt_{max}, and it is expected to be proportional to contractility.[74] Under normal conditions dP/dt_{max} occurs before the opening of the aortic valve during the isovolumic phase of contraction. Thus, it is not affected by alterations in afterload. On the other hand, as the developed strength of contraction is dependent on the initial length of the muscle fibres, it is predictable that dP/dt_{max} is very sensitive to changes in preload. The marked preload dependence and the wide normal range (1200–2000 mmHg/s) limit the usefulness of dP/dt_{max} for assessing basal contractility. Nevertheless, this parameter is of great advantage for following directional changes during acute interventions.[82]

The clinical utility of dP/dt_{max} is noticeably hampered, however, by the fact that its computation conventionally requires an intraventricular catheter.[137] Hence, there is interest in a reliable and widely applicable method for the non-invasive measurement of dP/dt_{max}. Non-invasive evaluation is possible with continuous wave Doppler echocardiography in patients with mitral regurgitation. The velocity profile of the regurgitant jet can be recorded, and each point on the velocity curve can be converted to a left ventriculo-atrial pressure gradient using the modified Bernoulli equation.[114,138,139] The pressure gradient curve can be digitised and differentiated to give instantaneous values for dP/dt and to identify dP/dt_{max}. Such curves have been demonstrated to correlate closely with those obtained invasively in experimental models ($r = 0{\cdot}92$).[138,139]

Although the derivation of a complete dP/dt curve necessitates the employment of refined computer hardware and software, and elaborate offline analysis of data, the estimation of dP/dt as the mean rate of pressure rise (dP/dt_{mean}) from the steepest rising segment of the Doppler regurgitant velocity spectrum is of proven benefit in the clinical setting.[78] The calculation of dP/dt_{mean} is illustrated in Figure 3.13. The figure combines a schematic presentation and an original Doppler registration of a mitral regurgitant velocity profile recorded with a sufficiently high sweep speed of more than 100 mm/s. At 1 m/s and at 3 m/s on the rising part of the velocity curve, two points are marked. Based on the modified Bernoulli-equation, these two points correspond to left ventriculo-atrial pressure gradients of 4 mmHg and 36 mmHg, respectively. Assisted by the software of the echocardiograph, the time interval between the two points is measured, which represents the time needed by the ventricle to augment its pressure by 32 mmHg. The following equations further clarify the calculation of dP/dt_{mean}.

$$dP/dt_{mean} = \frac{\Delta p\ (mmHg)}{\Delta t\ (s)} \qquad (3.9)$$

$$dP/dt_{mean} = \frac{4 \times (V_2^2 - V_1^2)}{\Delta t} \qquad (3.10)$$

$$dP/dt_{mean} = \frac{4 \times (3^2 - 1^2)}{\Delta t} \qquad (3.11)$$

$$dP/dt_{mean} = \frac{32}{\Delta t}\ (mmHg/s) \qquad (3.12)$$

The non-invasively assessed dP/dt_{mean} underestimates dP/dt_{max} to some extent but correlates well with invasive dP/dt_{max} data ($r = 0{\cdot}87$).[139] dP/dt_{mean} is readily at hand, but the technique has some substantial limitations.

- Mitral regurgitation must be present.
- The maximal velocity profile must be recorded, which is often difficult.

- Because of regurgitation, the early part of systole is not truly isovolumic.[78]

Fractional area change

The most commonly used non-invasive method for clinical evaluation of contractile performance is percentage fibre shortening.[90] As an ejection phase index it must exhibit clear afterload dependence, whereas preload dependence is not expected to be prominent.[100] Despite this limitation the measurement of percentage fibre shortening has become established as a good clinical estimate of LV function, most convincingly in the preoperative evaluation of anaesthetised patients, and it has proved to be most helpful as a prognostic outcome variable.[140] In particular, when ventricular function is reduced the parameter serves the clinician well in its sensitivity to changes in contractility.[141]

Percentage fibre shortening can be assessed as percentage of volume change (ejection fraction) or dimension change (fractional area change [FAC], fractional shortening). It relates to the following equation:

$$\%\Delta D = \frac{Dim_{dia} - Dim_{syst}}{Dim_{dia}} \times 100 \qquad (3.13)$$

where $\%\Delta D$ is the percentage fibre shortening, Dim_{dia} is the end-diastolic dimension or volume, and Dim_{syst} is the end-systolic dimension or volume.

In the perioperative setting FAC is routinely used to obtain a rough impression of contractile performance. In numerous studies FAC has exhibited good correlations with ejection fraction using alternative methods.[50,142] The major advantage of FAC is that it can be derived from the transgastric mid-papillary short-axis view (TG mid SAX) of the left ventricle. The same image

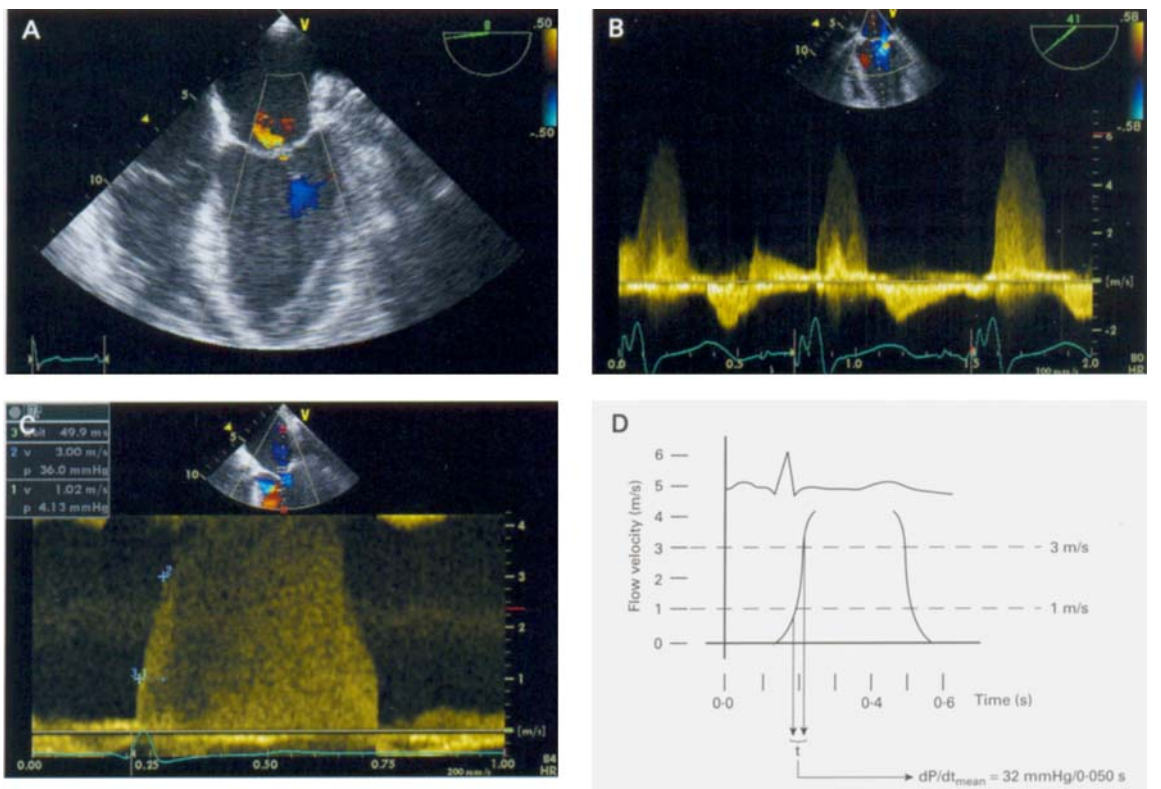

Figure 3.13 Doppler echocardiographic determination of the mean rate of left ventricular pressure rise (dP/dt_{mean}) from the steepest rising segment of a mitral regurgitant jet. The figure combines **(D)** a schematic presentation and an example with original Doppler registrations. **(A)** A mitral insufficiency jet is identified by colour Doppler echocardiography in the mid-oesophageal four chamber view. **(B)** Guided by the colour Doppler display, the flow velocity profile of the insufficiency jet is recorded by continuous wave Doppler echocardiography. **(C)** The sweep speed is increased to 100 mm/s or more, and the velocity range is adjusted from baseline to 4 m/s. Two points are marked at 1 m/s and at 3 m/s on the rising part of the continuous wave velocity curve. The time interval between the two points is measured. It is noteworthy that all measurements can be performed easily on screen.

also forms the basis of the quantitative analysis of preload and afterload. For this reason the short-axis plane of the left ventricle should be considered the anaesthesiologist's key to ventricular systolic performance (see Figure 3.1).[34,143] Determination of FAC from the short-axis image can be done either offline, using computer assisted planimetry, or online, relying on the newer acoustic quantification technology (see above).

Preload adjusted maximal power as a load independent measure of left ventricular contractility

Altered loading conditions may cause a divergence between the function of the heart as a systolic pump and the intrinsic inotropic state of the myocardium. In many clinical situations and disease states an apparent difference exists between what the muscle is capable of doing (its inotropic state) and what it actually does under a specific set of loading conditions.[76] For example, it is possible to have abnormal systolic performance despite normal contractility when ventricular afterload is excessive. Alternatively, LV systolic performance may be nearly normal despite decreased myocardial contractility if LV afterload is low, as occurs in some patients with mitral regurgitation. Thus, altered loading conditions by themselves have the potential to result in severe LV dysfunction, at a time when the heart's intrinsic contractile state may be normal, depressed, or perhaps supranormal. For this reason it is recommended that abnormalities in load and contractility be carefully differentiated from each other whenever severe LV dysfunction presents.[82,102]

The most useful approaches to assessing contractility involve two fundamental physiological principles. The first is based on the ventricle's pressure–volume loop, specifically the end-systolic pressure–volume relation.[144,145] The second principle that yields an index of contractility is derived from the myocardial force–velocity relation.[2,91,119,146] TOE allows translation of these principles into three different non-invasive techniques for measuring contractility. The three techniques are listed in Table 3.1 (i.e end-systolic pressure-dimension relationship and end-systolic meridional wall stress/rate corrected mean velocity of fibre shortening relationship, preload-adjusted maximal power), and have all been applied to clinical medicine and have their own merits.[147] Nevertheless, serial assessment of LV contractility is still uncommon in clinical practice because of the methodological complexity of the techniques. This may change with the introduction of preload-adjusted maximal power, which is relatively easy to obtain.[148,149]

Ventricular power can be directly extended from the isolated muscle to the intact ventricle. For the intact ventricle, power is analogous to the area under a force–velocity curve for isolated muscle. The close relationship to the force–velocity curve strongly suggests that power reflects contractile strength of the ventricle. Power, the rate at which the ventricle performs external work, can be calculated from simultaneous records of ventricular pressure and rate of volume change. In the absence of valvular lesions, the rate of ventricular volume change equals aortic volumetric flow, and ventricular pressure can be closely approximated by aortic pressure. By combining Doppler echocardiographic aortic flow velocity measurements and invasive aortic blood pressure, the maximal value of power can hence be expressed as follows:

$$PWR_{max} = [P_{A0}(t) \times V_{A0}(t)]_{max} \times AVA \times 1{\cdot}333 \times 10^{-4} \text{ (w)} \quad (3.14)$$

where PWR_{max} is the maximal ventricular power, P_{Ao} is the maximum aortic pressure, V_{Ao} is the maximum aortic blood flow velocity, AVA is the effective aortic valve orifice area, and $1{\cdot}333 \times 10^{-4}$ is a factor to convert PWR_{max} units to watts (mmHg·ml/s per 10^4).

The calculation of PWR_{max}, based on the above formula, is demonstrated in Figure 3.14. Although exhibiting marked stability in the face of changes in afterload, PWR_{max} is sensitive to preloading conditions. To generate an index that exclusively quantifies contractile properties of the left ventricle, normalisation of PWR_{max} to the square of LVEDV was found to be appropriate.[119,148–150] Other investigators used regional approximations of $LVEDV^2$ to correct for preload, such as $LVEDA^{3/2}$ or $LVEDD^2$.[151,152] Regardless of the parameter chosen (PWR_{max}/EDV^2, $PWR_{max}/EDA^{3/2}$, or PWR_{max}/EDD^2), preload-adjusted power appeared to be a physiologically significant method for serial quantification of LV contractility.

Myocardial performance index (Tei index)

As detailed above, LV systolic function is usually described in terms of stroke volume,

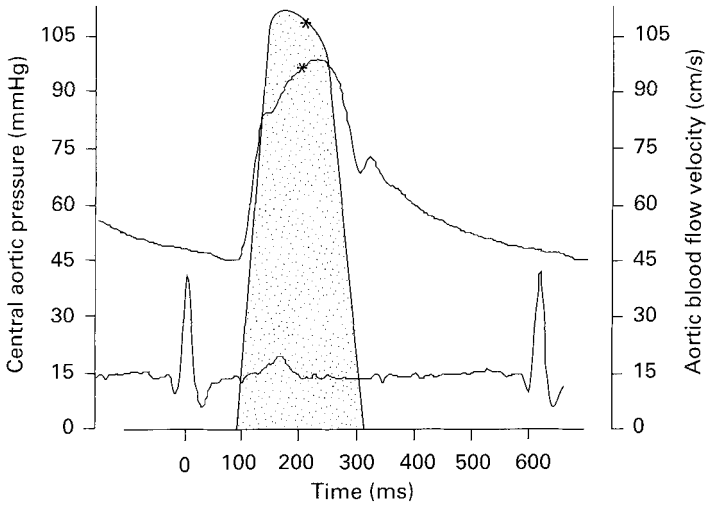

Figure 3.14 Schematic diagram depicting electrocardiogram, central aortic pressure, and aortic blood flow velocity. Original tracings of a representative patient are plotted together. For a more concise illustration, flow velocity waveform is flipped around its horizontal axis. An asterisk indicates the maximal pressure–flow velocity product. Multiplication of the product by aortic valve orifice area results in maximal power (from Schmidt *et al.*[149]; reproduced with permission).

cardiac output, or percentage fractional shortening. LV diastolic function, on the other hand, is primarily defined by Doppler measures of mitral inflow during early and late diastole, duration of the myocardial relaxation phase, and flow velocity pattern in the pulmonary veins (see respective chapters).[66,153–155] Intuitively, a measure of LV myocardial performance combining both systolic and diastolic function would be most useful in assessing cardiac function because disturbances in systolic and diastolic function often coexist in patients with heart disease.[156] Consequently, a new Doppler index of combined systolic and diastolic myocardial performance of the left ventricle has been reported and subsequently introduced into clinical medicine.[112,157] This index is defined as the sum of the isovolumetric contraction time (IVCT) and isovolumetric relaxation time (IVRT) divided by ejection time (ET; Figure 3.15).[158,159] It is named MPI or, after its pioneer, the "Tei index".[160–162] The MPI is easily obtained, reproducible, has a narrow range in normal individuals, does not depend on LV geometry, and correlates well with invasively obtained measures of systolic and diastolic cardiac function.[112,163]

The method for measurement of the MPI is summarised in Figures 3.15 and 3.16. It can simply be determined from two time intervals by Doppler echocardiographic registration of mitral and aortic flow velocity profiles. Using TOE the LV outflow velocity curve is recorded from the deep transgastric long-axis (deep TG LAX) view of the left ventricle, or from the transgastric long-axis view (TG LAX), which is developed from the transgastric mid-papillary short axis view (TG mid SAX) by rotating the multiplane angle forward to 90–120° until the aortic valve comes into view to the right side of the far field. LV outflow is registered with the pulsed wave Doppler sample volume positioned just below the aortic valve. The mitral inflow is recorded from the mid-oesophageal four chamber view (MOE four chamber view) with the pulsed wave Doppler sample volume positioned at the tips of the mitral leaflets during diastole.[112] Care should be taken to perform these studies with the ultrasound beam parallel to the direction of blood flow without the necessity of angle correction of the Doppler signal, and signals should be acquired at a sweep speed of 100 mm/s or even higher. The mitral inflow and LV outflow velocity curves are interpreted with respect to time intervals "a" and "b" (see Figure 3.15).[113,157] The interval "a" from cessation to onset of mitral inflow is equal to the sum of IVCT, ET, and IVRT. Left ventricular ejection time "b" is measured from the duration of the LV outflow velocity curve. The sum of IVCT and IVRT is obtained by subtracting "b" from "a". Each Doppler profile is analysed by digital tracing and Doppler measurements should be calculated from an average of three to five consecutive cardiac cycles. Finally, the MPI is calculated, as shown in Figure 3.16.

Systolic time intervals measured by phonocardiography and pulse tracing or M-mode echocardiography have long been used as parameters of LV systolic function.[110,164–166]

Mancini and coworkers[111,167] reported the use of an isovolumetric index for the assessment of systolic and diastolic function obtained from the simultaneous carotid artery pulse tracing and M-mode echocardiography of the mitral valve. However, there has been little clinical application of these indices because of methodologic difficulties in obtaining values. It required the development of Doppler echocardiography before measurements of systolic time intervals were routinely used in the assessment of ventricular function.[168] Since then it was found that Doppler measurement of IVCT exhibits excellent correlation with dP/dt_{max}. Furthermore, this interval is relatively independent of afterload but is heart rate dependent.[161,162] ET also correlates with dP/dt_{max} and is closely related to heart rate.[110] Thus, a ratio of IVCT and ET (both heart rate dependent) normally requires no correction for heart rate and is highly correlated with dP/dt_{max}.[112,164] On the other hand, IVRT correlates well with invasive measures of the diastolic phase of the cardiac cycle, such as the time constant of relaxation, and ET is related to the maximal rate of LV pressure decline.[112] Thus, a ratio of IVRT divided by ET correlates best with measures of diastolic function. This ratio is also relatively independent of normal heart rate and blood pressure in comparison with IVRT or ET alone. Because myocardial contractility and relaxation are energy dependent,[169] myocardial dysfunction results in prolongation of both isovolumic time intervals, and the summation of IVCT and IVRT is a reasonable measurement of overall systolic and diastolic function. On the other hand, left ventricular ET has been shown to correlate with dP/dt_{max} and to become progressively shorter with worsening ventricular function. For this reason the MPI ([IVCT + IVRT]/ET) proved to be a better discriminator of each functional group than the sum of isovolumic time intervals alone.

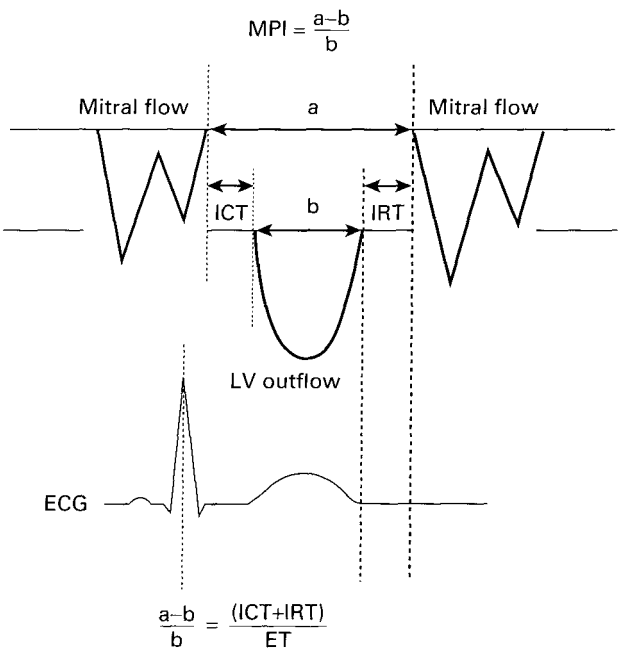

Figure 3.15 Estimation of myocardial performance index (MPI, or Tei index). MPI is derived as (a – b)/c, where a is the interval between cessation and onset of mitral inflow, (a – b) is the sum of isovolumetric contraction time (IVCT) and isovolumetric relaxation time (IVRT), and b is ejection time of left ventricular outflow (ET).

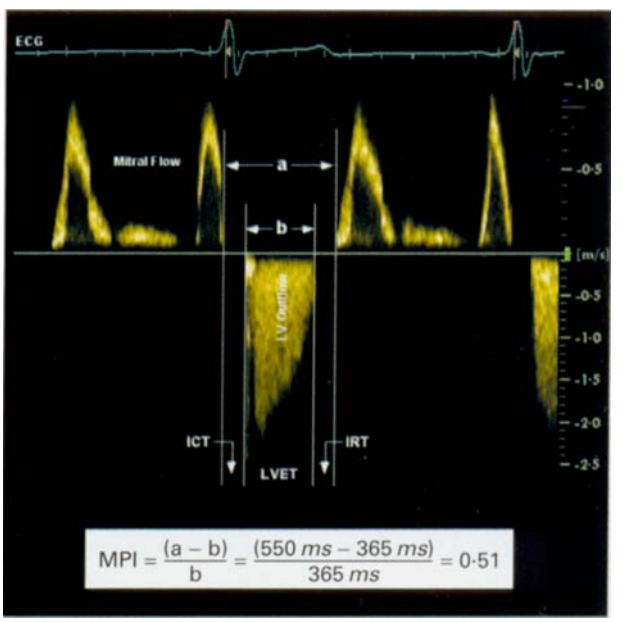

Figure 3.16 Typical example of a measurement of myocardial performance index (MPI, or Tei index) simply from two time intervals by Doppler echocardiographic registration of mitral and aortic flow velocity profiles. For illustrative purposes, original Doppler tracings of mitral inflow and left ventricular outflow are plotted together. The velocity profiles of mitral inflow are flipped around their vertical axis for the same reason. Intervals are as follows: a, from cessation to next onset of mitral flow; and b, from onset to cessation of aortic flow. Time intervals a and b are indicated in milliseconds (ms). MPI can easily be calculated as (a – b)/b. ECG = electrocardiogram, IVCT = isovolumetric contraction time, IVRT = isovolumetric relaxation time, LVET = left ventricular ejection time.

Tei *et al.*[112] were the first group to document that the MPI correlates well with simultaneous invasive measurements of LV pressure. More recently LaCorte *et al.*[163] compared the Tei index with load independent estimates of LV function in a porcine model. Those investigators obtained pressure volume loops from 10 pigs (32–45 kg) with a micromanometer and a conductance catheter placed in the LV cavity. An ischaemic insult was induced by ventricular fibrillation to alter myocardial performance. Invasive indices included preload recruitable stroke work and ventricular stiffness constant (β). The authors demonstrated a statistically significant inverse correlation between percentage change in preload recruitable stroke work (load independent measure of systolic function) and the percentage change in Tei index. They also found a significant linear correlation between Tei index and β, which is an assessment of the diastolic properties of the left ventricle. Although the absolute values of the Tei index did not exhibit a statistically significant correlation with the absolute values of preload recruitable stroke work and β, once LV function was altered the percentage changes did have a statistical correlation. LaCorte *et al.* concluded that this has clinical implications because the use of the MPI is appropriate in following up a patient serially, and that the index is a reliable measure of global LV function. Again in an animal model, Broberg *et al.*[170] validated the MPI by echocardiography in mice. A total of 29 anaesthetised mice with LV pressure catheters underwent echocardiography at baseline and during manipulation of β-adrenergic tone, preload, and afterload. The MPI and the ratio of fractional shortening to MPI was compared with dP/dt_{max}. MPI correlated strongly with dP/dt_{max} ($r = 0{\cdot}779$). The ratio of fractional shortening to MPI showed the best correlation. MPI differed significantly with contractility, preload, and afterload manipulation. It was concluded from the results that the MPI is a good non-invasive index of LV function using dP/dt_{max} as a reference standard, that the index distinguishes a wide range of functional states, and that it is simple, independent of ventricular geometry, and completely non-invasive. Nevertheless, it was demonstrated in that study that the MPI exhibited both preload and afterload sensitivity.

Dependence on heart rate, preload, and afterload is always an important issue when discussing parameters of LV function. Poulsen *et al.*[171] studied the influence of heart rate changes on MPI. Thirty patients with sick sinus syndrome treated with a pacemaker with a right atrial lead were included in the protocol. The patients were paced at increasing rates from 50 to 100 beats/min. The MPI increased on average $0{\cdot}02 \pm 0{\cdot}03$ per 10 beats/min increase in rate. The correlation between MPI and heart rate was only weak. The small increase in MPI during increasing heart rate was judged by the authors to be without clinical importance. Thus, that study supports previous findings that heart rate has no major impact on MPI.[161] The effects of preload alterations on MPI were addressed by Moller and coworkers.[172] Doppler echocardiography was performed during Valsalva manoeuvre, passive leg lifting, and after sublingual administration of nitroglycerine in 50 healthy volunteers (group 1) and 25 patients (group 2) with previous myocardial infarction. MPI was significantly lower in group 1 ($0{\cdot}34 \pm 0{\cdot}04$) than in group 2 ($0{\cdot}52 \pm 0{\cdot}14$). In group 1 MPI was significantly increased during preload manipulations. The greatest change in MPI was induced by nitroglycerine. In group 2 no significant changes in MPI were found. It was concluded that the MPI is influenced by changes in preload in normal individuals but it is less influenced by changes in preload in patients with previous myocardial infarction. Moreover, at baseline and during loading stages, MPI effectively differentiated individuals in a healthy control group from patients with previous infarction. Only limited information is available on afterload sensitivity of the MPI. Data on chronic afterload in human beings with aortic stenosis demonstrate that MPI varies with LV function[173,174] and surgical repair.[175] Other studies showed increased MPI of the right ventricle from pulmonary hypertension[176] and RV volume overload.[177] Furthermore, because dP/dt_{max} is afterload sensitive to some extent, it may be anticipated that MPI follows dP/dt_{max} in this quality.[170]

Apart from theoretical considerations of load sensitivity, the MPI has already been proved to have merits in clinical medicine because it reflects severity and prognosis in various heart diseases. These include dilated cardiomyopathy,[113,157,178,179] symptomatic heart failure,[180] cardiac amyloidosis,[162] ischaemic heart disease,[181] acute myocardial infarction,[158,159,182,183] congenital heart disease,[177,184] or RV dysfunction.[185] The power of MPI to discriminate distinct degrees of severity and to delineate prognosis in such a wide variety of different heart disorders is attributable to its

unique ability to integrate in one measurement functional aspects of both ventricular filling and ejection. In summary:

- MPI is a Doppler-derived index that is easily obtained, with excellent interobserver and intraobserver reproducibility because it measures relatively large time intervals
- MPI is relatively stable in the face of changes in loading conditions (as compared with traditional measures of LV function) and has been shown to be independent of heart rate
- MPI does not depend on LV geometry, which makes it theoretically superior to standard measures of myocardial performance in ventricles during the remodelling process
- MPI improvement correlates with higher exercise capacity – an overall clinical indicator of cardiac reserve – in patients with LV dysfunction
- MPI is non-invasively derived either by transthoracic or transoesophageal echocardiography, and it can be used perioperatively or on the intensive care unit for serial tracking of changes in LV function at the patient's bedside.

References

1 Feigenbaum H. Evolution of echocardiography. *Circulation* 1996;**93**:1321–7.

2 Kass DA. Clinical ventricular pathophysiology: a pressure–volume view. In: Warltier DC, ed. *Ventricular function.* Baltimore, Philadelphia, Hong Kong, London, Munich, Sydney, Tokyo: Williams & Wilkins, 1995.

3 Opie LH. Mechanisms of cardiac contraction and relaxation. In: Braunwald E, ed. *Heart disease. A textbook of cardiovascular medicine, 5th edn.* Philadelphia, London, Toronto, Montreal, Sydney, Tokyo: W.B. Saunders Company, 1997.

4 Heidenreich PA, Stainback RF, Redberg RF, Schiller NB, Cohen NH, Foster E. Transesophageal echocardiography predicts mortality in critically ill patients with unexplained hypotension. *J Am Coll Cardiol.* 1995;**26**:152–8.

5 Heidenreich PA, Foster E, Cohen NH. Prediction of outcome for critically ill patients with unexplained hypotension. *Crit Care Med* 1996;**24**:1835–40.

6 Brown JM. Use of echocardiography for hemodynamic monitoring. *Crit Care Med* 2002;**30**: 1361–4.

7 Roger VL, Ballard DJ, Hallett JJ, *et al.* Influence of coronary artery disease on morbidity and mortality after abdominal aneurysmectomy: a population-based study, 1971–1987. *J Am Coll Cardiol* 1989;**14**:1245–52.

8 Mangano DT. Perioperative cardiac morbidity. *Anesthesiology.* 1990;**72**:153–84.

9 Mangano DT, Browner W, Hollenberg M, London M, Tubau J, Tateo I, for The Study of Perioperative Ischemia Research Group. Association of perioperative myocardial ischemia with cardiac morbidity and mortality in men undergoing noncardiac surgery. *N Engl J Med.* 1990;**323**: 1781–8.

10 Poldermans D, Boersma E, Bax J, *et al,* for the Dutch Echocardiographic Cardiac Risk Evaluation Applying Stress Echocardiography Study Group. The effect of bisoprolol on perioperative mortality and myocardial infarction in high-risk patients undergoing vascular surgery. *N Engl J Med* 1999;**341**:1789–94.

11 American Society of Anesthesiologists and Society of Cardiovascular Anesthesiologists Task Force on Transesophageal Echocardiography. Practice guidelines for perioperative transesophageal echocardiography. *Anesthesiology* 1996;**84**: 986–1006.

12 Connors AF Jr, Speroff T, Dawson NV, *et al.* The effectiveness of right heart catheterization in the initial care of critically ill patients. SUPPORT Investigators. *JAMA* 1996;**276**:889–97.

13 Sandham JD, Hull RD, Brant RF, *et al.* A randomized, controlled trial of the use of pulmonary-artery catheters in high-risk surgical patients. *N Engl J Med* 2003;**348**:5–14.

14 Ritchie JL, Cheitlin MD, Eagle KA, *et al.* ACC/AHA guidelines for the clinical application of echocardiography. A report of the American College of Cardiology/American Heart Association Task Force on Practice Guidelines (Committee on Clinical Application of Echocardiography). *Circulation* 1997;**95**:1686–744.

15 Poelaert JI, Trouerbach J, De Buyzere M, Everaert J, Colardyn FA. Evaluation of transesophageal echocardiography as a diagnostic and therapeutic aid in critical care setting. *Chest* 1995;**107**:774–9.

16 Michard F, Boussat S, Chemla D, *et al.* Relation between respiratory changes in arterial pulse pressure and fluid responsiveness in septic patients with acute circulatory failure. *Am J Respir Crit Care Med* 2000;**162**:134–8.

17 Michard F, Ruscio L, Teboul JL. Clinical prediction of fluid responsiveness in acute circulatory failure related to sepsis. *Intensive Care Med* 2001;**27**:1238.

18 Michard F, Mangin I, Ruyer O, Faller JP, Teboul JL. Using heart-lung interactions to assess fluid responsiveness during mechanical ventilation. *Chest* 2001;**119**:867–73.

19 Michard F, Teboul JL. Predicting fluid responsiveness in ICU patients: a critical analysis of the evidence. *Chest* 2002;**121**:2000–8.

20 Gunn SR, Pinsky MR. Implications of arterial pressure variation in patients in the intensive care unit. *Curr Opin Crit Care* 2001;**7**:212–7.

21 Tavernier B, Makhotine O, Lebuffe G, Dupont J, Scherpereel P. Systolic pressure variation as a

guide to fluid therapy in patients with sepsis-induced hypotension. *Anesthesiology* 1998;**89**:1313–21.

22 Bendjelid K, Romand JA. Fluid responsiveness in mechanically ventilated patients: a review of indices used in intensive care. *Intensive Care Med* 2003;**29**:352–60.

23 Berkenstadt H, Margalit N, Hadani M, *et al.* Stroke volume variation as a predictor of fluid responsiveness in patients undergoing brain surgery. *Anesth Analg* 2001;**92**:984–9.

24 Slama M, Masson H, Teboul JL, *et al.* Respiratory variations of aortic VTI: a new index of hypovolemia and fluid responsiveness. *Am J Physiol Heart Circ Physiol* 2002;**283**:H1729–33.

25 Feissel M, Michard F, Mangin I, Ruyer O, Faller JP, Teboul JL. Respiratory changes in aortic blood velocity as an indicator of fluid responsiveness in ventilated patients with septic shock. *Chest* 2001;**119**:867–73.

26 Michard F, Boussat S, Chemla D, *et al.* Relation between respiratory changes in arterial pulse pressure and fluid responsiveness in septic patients with acute circulatory failure. *Am J Respir Crit Care Med* 2000;**162**:134–8.

27 O'Quinn R, Martini JJ. Pulmonary artery occlusion pressure: clinical physiology, measurement, and interpretation. *Am Rev Respir Dis* 1983;**128**: 319–26.

28 Tuman KJ, Carroll GC, Ivankovich AD. Pitfalls in interpretation of pulmonary artery catheter data. *J Cardiothorac Anesth* 1989;**3**:625–41.

29 Hansen RM, Viquerat CE, Matthay MA, *et al.* Poor correlation between pulmonary arterial wedge pressure and left ventricular end-diastolic volume after coronary artery bypass graft surgery. *Anesthesiology* 1986;**64**:764–70.

30 Hinder F, Poelaert JI, Schmidt C, *et al.* Assessment of cardiovascular volume status by transoesophageal echocardiography and dye dilution during cardiac surgery. *Eur J Anaesthesiol* 1998;**15**:633–40.

31 Cheung AT, Joseph SS, Weiss SJ, Aukburg SJ, Berlin JA. Echocardiographic and hemodynamic indexes of left ventricular preload in patients with normal and abnormal ventricular function. *Anesthesiology* 1994;**81**:376–87.

32 Kalman PG, Wellwood MR, Weisel RD, *et al.* Cardiac dysfunction during abdominal aortic operation: the limitations of pulmonary wedge pressure. *J Vasc Surg* 1986;**3**:773–81.

33 Leung JM, Levine EH. Left ventricular end-systolic cavity obliteration as an estimate of intraoperative hypovolemia. *Anesthesiology* 1994;**81**:1102–9.

34 Poelaert J, Schmidt C, Colardyn F. Transoesophageal echocardiography in the critically ill. *Anaesthesia* 1998;**53**:55–68.

35 Smith MD, MacPhail B, Harrison MR, Lenhoff SJ, DeMaris AN. Value and limitations of transesophageal echocardiography in determination of left ventricular volumes and ejection fraction. *J Am Coll Cardiol* 1992;**19**: 1213–22.

36 Bednarz JE, Marcus RH, Lang RM. Technical guidelines for performing automated border detection studies. *J Am Soc Echocardiogr* 1995;**8**:293–305.

37 Coriat P, Vrillon M, Perel A, Baron J, Le Bret F, Saada M, Viars P. A comparison of systolic blood pressure variations and echocardiographic estimates of end-diastolic left ventricular size in patients after aortic surgery. *Anesth Analg* 1994;**78**:46–53.

38 Reich DL, Konstadt SN, Nejat M, Abrams HP, Bucek J. Intraoperative transesophageal echocardiography for the detection of cardiac preload changes induced by transfusion and phlebotomy in pediatric patients. *Anesthesiology* 1993;**79**:10–5.

39 Feltes TF, Pignatelli R, Kleinfert S, Mariscalco M. Quantitated left ventricular systolic mechanics in children with septic shock utilizing noninvasive wall-stress analysis. *Crit Care Med* 1994;**22**: 1647–58.

40 Axler O, Tousgnant C, Thompson CR, *et al.* Small hemodynamic effect of typical rapid volume infusions in critically ill patients. *Crit Care Med* 1997;**25**:965–70.

41 Vedrinne JM, Duperret S, Decaillot F, *et al.* Haemodynamic changes induced by two I:E ratios: a transoesophageal echocardiographic study. *Can J Anaesth* 1997;**44**:354–9.

42 Wolrab C, Weber T, Tschernich H, *et al.* Assessment of left ventricular preload: transoesophageal echocardiography versus filling pressure. *Acta Anaesthesiol Scand* 1997;**111**:283–6.

43 Clements FM, De Bruijn NP. Perioperative evaluation of regional wall motion by transesophageal two-dimensional echocardiography. *Anesth Analg* 1987;**66**:249–61.

44 Liu N, Darmon PL, Saada M, *et al.* Comparison between radionuclide ejection fraction and fractional area changes derived from transesophageal echocardiography using automated border detection. *Anesthesiology* 1996;**85**:468–74.

45 Swenson JD, Harkin C, Pace NL, Astle K, Bailey P. Transesophageal echocardiography: an objective tool in defining maximum ventricular response to intravenous fluid therapy. *Anesth Analg* 1996;**83**:1149–53.

46 Dalibon N, Schlumberger S, Saada M, *et al.* Haemodynamic assessment of hypovolaemia under general anaesthesia in pigs submitted to graded haemorrhage and retransfusion. *Br J Anaesth* 1999;**82**:97–103.

47 Thys DM, Hillel Z, Goldman ME, Mindich BP, Kaplan JA. A comparison of hemodynamic indices derived by invasive monitoring and two-dimensional echocardiography. *Anesthesiology* 1987;**67**:630–4.

48 Tuchy GL, Gabriel A, Muller C, *et al.* Titrating the preload by using the rapid infusion system: use of echocardiography during orthotopic liver transplantation. *Transplant Proc* 1993;**25**:1858–60.

49 Jardin F, Valtier B, Beauchet A, *et al.* Invasive monitoring combined with two-dimensional echocardiographic study in septic shock. *Intensive Care Med* 1994;**20**:550–4.

50 Clements FM, Harpole DH, Quill T, Jones RH, McCann RL. Estimation of left ventricular volumes and ejection fraction by two-dimensional echocardiography: comparison of short axis imaging and simultaneous radionuclide angiography. *Br J Anaesth* 1990;**64**:331–6.

51 Gannedahl P, Odeberg S, Brodin LA, *et al.* Effects of posture and pneumoperitoneum during anae thesia on the indices of left ventricular filling. *Acta Anaesthesiol Scand* 1996;**40**:160–6.

52 Michard F, Teboul JL. Using heart-lung interactions to assess fluid responsiveness during mechanical ventilation. *Crit Care* 2000;**4**:282–9.

53 Perel A. Assessing fluid responsiveness by the systolic pressure variation in mechanically ventilated patients. *Anesthesiology* 1998;**89**: 1309–10.

54 Michard F, Chemla D, Richard C, *et al.* Clinical use of respiratory changes in arterial pulse pressure to monitor the hemodynamic effects of PEEP. *Am J Respir Crit Care Med* 1999;**159**:935–9.

55 Michard F, Mercat A, Chemla D, Richard C, Teboul J. Non invasive assessment of respiratory changes in arterial pulse pressure by infrared photoplethysmography in mechanically ventilated patients. *Am J Respir Crit Care Med* 1999;**159**:A520.

56 Jardin F, Delorme G, Hardy A, *et al.* Reevaluation of hemodynamic consequences of positive pressure ventilation: emphasis on cyclic right ventricular afterloading by mechanical lung inflation. *Anesthesiology* 1990;**72**:966–70.

57 Jardin F, Farcot J, Gueret P, Prost J, Ozier Y, Bourdarias J. Cyclic changes in arterial pulse during respiratory support. *Circulation* 1983;**68**:266–74.

58 Robotham JL, Cherry D, Mitzner W, *et al.* A re-evaluation of the hemodynamic consequences of intermittent positive pressure ventilation. *Crit Care Med* 1983;**11**:783–93.

59 Guyton AC. *Textbook of medical physiology, 8th edn.* Philadelphia, PA: WB Saunders, 1991.

60 Berne RM, Levy MN. *Physiology, 4th edn.* St. Louis, MO: Mosby, 1998.

61 Dodek A, Kassebaum DG, Bristow JD. Pulmonary edema in coronary-artery disease without cardiomegaly: paradox of the stiff heart. *N Engl J Med* 1972;**286**:1347–50.

62 Yamamoto K, Nishimura RA, Burnett JC Jr, Redfield MM. Assessment of left ventricular end-diastolic pressure by Doppler echocardiography: contribution of pulmonary venous versus mitral flow velocity curves at atrial contraction. *J Am Soc Echocardiogr* 1997;**10**:52–9.

63 Channer KS, Culling W, Wilde P, *et al.* Estimation of left ventricular end-diastolic pressure by pulsed Doppler ultrasound. *Lancet* 1986;**1**:1005–7.

64 Vanoverschelde JL, Robert AR, Gerbaux A, *et al.* Noninvasive estimation of pulmonary artery wedge pressure with Doppler transmitral flow velocity pattern in patients with known heart disease. *Am J Cardiol* 1995;**75**:383–9.

65 Kuecherer HF, Muhiudeen IA, Kusumoto FM, *et al.* Estimation of mean left atrial pressure from transesophageal pulsed Doppler echocardiography of pulmonary venous flow. *Circulation* 1990;**82**: 1127–39.

66 Appleton CP. Doppler assessment of left ventricular diastolic function: the refinements continue. *J Am Coll Cardiol* 1993;**21**:1697–700.

67 Rossvoll O, Hatle LK. Pulmonary venous flow velocities recorded by transthoracic Doppler ultrasound: relation to left ventricular diastolic pressures. *J Am Coll Cardiol* 1993;**21**:1687–96.

68 Garcia MJ, Ares MA, Asher C, Rodriguez L, Vandervoort P, Thomas JD. Color M-mode flow velocity propagation: an index of early left ventricular filling that combined with pulsed Doppler peak E velocity may predict capillary wedge pressure. *J Am Coll Cardiol* 1997;**29**:448–54.

69 Garcia MJ, Thomas JD, Klein AL. New Doppler echocardiographic applications for the study of diastolic function. *J Am Coll Cardiol* 1998;**32**:865–75.

70 Garcia MJ, Palac RT, Malenka DJ, Terrell P, Plehn JF. Color M-mode Doppler flow propagation velocity is a relatively preload-independent index of left ventricular filling. *J Am Soc Echocardiogr* 1999;**12**:129–37.

71 Garcia MJ, Ares MA, Asher C, Rodriguez L, Vandervoort P, Thomas JD. An index of early left ventricular filling that combined with pulsed Doppler peak E velocity may estimate capillary wedge pressure. *J Am Coll Cardiol* 1997;**29**:448–54.

72 Nagueh SF, Lakkis NM, Middleton KJ, Spencer WH, Zoghbi WA, Quinones MA. Doppler estimation of left ventricular filling pressures in patients with hypertrophic cardiomyopathy. *Circulation* 1999;**99**:254–61.

73 Ueno Y, Nakamura Y, Kinoshita M, Fujita T, Sakamoto T, Okamura H. Noninvasive estimation of pulmonary capillary wedge pressure by color M-mode Doppler echocardiography in patients with acute myocardial infarction. *Echocardiography* 2002;**19**:95–102.

74 Thys DM, Dauchot PJ. Advances in cardiovascular physiology. In: Kaplan JA, ed. *Cardiac anesthesia, 3rd edn.* Philadelphia, London, Toronto, Montreal, Sydney, Tokyo: W. B. Saunders Company, 1993.

75 Milnor WR. Arterial impedance as ventricular afterload. *Circ Res* 1975;**36**:565–70.

76 Milnor WR. *Cardiovascular physiology.* New York, Oxford: Oxford University Press, 1990.

77 Grossman W, Jones D, McLaurin LP. Wall stress and patterns of hypertrophy in the human left ventricle. *J Clin Invest* 1975;**56**:56–64.

78 Vuille C, Weyman AE. Left ventricle I: General considerations, assessment of chamber size and function. In: Weyman AE, ed. *Principles and practice of echocardiography, 2nd ed.* Philadelphia, Baltimore, Hong Kong, London, Munich, Sydney, Tokyo: Lea & Febiger, 1994.

79 Devereux RB. Toward a more complete understanding of left ventricular afterload. *J Am Coll Cardiol.* 1991;**17**:122–4.

80 Braunwald E, Ross JJ. Control of cardiac performance. In: Berne RM, Sperclakis N, Geiger SR, eds. *Handbook of physiology: the cardiovascular system.* Baltimore: Williams and Wilkins, 1979.

81 Braunwald E, Sonnenblick E, Ross J. Mechanisms of cardiac contraction and relaxation. In: Braunwald E, ed. *Heart Disease.* Philadelphia: WB Saunders Company, 1988:383–425.

82 Little WC, Braunwald E. Assessment of cardiac function. In: Braunwald E, ed. *Heart disease. A textbook of cardiovascular medicine, 5th edn.* Philadelphia, London, Toronto, Montreal, Sydney, Tokyo: W.B. Saunders Company, 1997.

83 Katz WE, Gasior TA, Quinlan JJ, Gorcsan JI. Transgastric continuous-wave Doppler to determine cardiac output. *Am J Cardiol.* 1993;**71**: 853–7.

84 Darmon PL, Hillel Z, Mogtader A, Mindich B, Thys DM. Cardiac output by transesophageal echocardiography using continuous-wave Doppler across the aortic valve. *Anesthesiology* 1994;**80**: 796–805.

85 Darmon PL, Hillel Z, Mogtader A, Thys DM. A study of the human aortic valve orifice by transesophageal echocardiography. *J Am Soc Echocardiogr* 1996;**9**:668–74.

86 Morita S, Kuboyama I, Asou T, *et al.* The effect of extraanatomic bypass on aortic input impedance studied in open chest dogs. *J Thorac Cardiovasc Surg* 1991;**102**:774–83.

87 Sunagawa K, Maughan WL, Sagawa K. Stroke volume effect of changing arterial input impedance over selected frequency range. *Am J Physiol* 1985;**248**:H477–84.

88 Gould KL, Lipscomb K, Hamilton GW, Kennedy JW. Relation of left ventricular shape, function, and wall stress in man. *Am J Cardiol* 1974;**34**:627–35.

89 Kolev N, Huemer G, Zimpfer M. *Transesophageal echocardiography. A new monitoring technique.* Wien, New York: Springer Verlag, 1995.

90 Colan SD. Noninvasive assessment of myocardial mechanics: a review of analysis of stress-shortening and stress velocity. *Cardiol Young* 1992;**2**:1–13.

91 Colan SD, Borow KM, Neumann A. Left ventricular end systolic wall stress-velocity of fiber shortening relation: a load independent index of myocardial contractility. *J Am Coll Cardiol* 1984;**4**:715–24.

92 Carabello BA, Spann JF. The uses and limitations of end-systolic indexes of LV function. *Circulation* 1984;**69**:1058–67.

93 Douglas PS, Reichek N, Plappert T, Muhammad A, St. John Sutton MG. Comparison of echocardiographic methods for measurement of left ventricular shortening and wall stress. *J Am Coll Cardiol* 1987;**9**:945–9.

94 Reichek N, Wilson J, St. John Sutton M, Plappert TA, Goldberg S, Hirshfeld JW. Noninvasive determination of left ventricular end-systolic stress: Validation of the method and initial application. *Circulation* 1982;**65**:99–108.

95 Huisman RM, Sipkema P, Westerhof N, Elzinga G. Comparison of models used to calculate left ventricular wall force. *Med Biol Eng Comput* 1980;**18**:133–44.

96 Greim C, Roewer N, Meißner C, Bause H, Schulte am Esch J. Estimation of acute ventricular afterload alterations in ventilated patients by transesophageal echocardiography. *Anaesthetist* 1995;**44**:108–115.

97 Greim CA, Roewer N, Schulte am Esch J. Assessment of changes in left ventricular wall stress from the end-systolic pressure-area product. *Br J Anaesth* 1995;**75**:583–587.

98 Lang RM, Borow KM, Neumann A, Janzen D. Systemic vascular resistance: an unreliable index of left ventricular afterload. *Circulation* 1986;**74**: 1114–23.

99 JS, Roizen MF, Cahalan MK, *et al.* Does anesthetic technique make a difference? Augmentation of systolic blood pressure during carotid endarterectomy: effects of phenylephrine versus light anesthesia and of isoflurane versus halothane on the incidence of myocardial ischemia. *Anesthesiology* 1988;**69**:846–53.

100 Kass DA, Maughan WL, Guo AM, Kono A, Sunagawa K, Sagawa K. Comparative influence of load versus inotropic states on indexes of ventricular contractility: experimental and theoretical analysis based on pressure–volume relationships. *Circulation* 1987;**76**:1422–36.

101 Kass DA, Maughan WL. From "Emax" to pressure–volume relations: a broader view. *Circulation* 1988;**77**:1203–12.

102 Little WC, Cheng C, Peterson T, Vinten-Johansen J. Response of the left ventricular end-systolic pressure–volume relation in conscious dogs to a wide range of contractile states. *Circulation* 1988;**78**:736–45.

103 Simmons LA, Weidemann F, Sutherland GR, *et al.* Doppler tissue velocity, strain, and strain rate imaging with transesophageal echocardiography in the operating room: a feasibility study. *J Am Soc Echocardiogr* 2002;**15**:768–76.

104 Williams RI, Haaverstad R, Sianos G, Vourvouri E, Fraser AG. Perioperative tissue Doppler echocardiography and bypass graft flowmetry in patients undergoing coronary revascularization: predictive power for late recovery of regional myocardial function. *J Am Soc Echocardiogr* 2002;**15**:1202–10.

105 Fedele F, Trambaiolo P, Magni G, De Castro S, Cacciotti L. New modalities of regional and global left ventricular function analysis: state of the art. *Am J Cardiol* 1998;**81**:49G–57G.

106 Miyatake K, Yamagishi M, Tanaka N, *et al.* New method for evaluation left ventricular wall motion by color-coded tissue Doppler imaging: in vitro and in vivo studies. *J Am Coll Cardiol* 1995;**25**:717–24.

107 Nagueh SF, Kopelen HA, Lim DS, *et al.* Tissue Doppler imaging consistently detects myocardial contraction and relaxation abnormalities, irrespective of cardiac hypertrophy, in a transgenic rabbit model of human hypertrophic cardiomyopathy. *Circulation* 2000;**102**:1346–50.

108 Bednarz J, Vignon P, Mor-Avi VV, *et al.* Color kinesis: principles of operation and technical guidelines. *Echocardiography* 1998;**15**:21–34.

109 Mor-Avi V, Lang RM. Recent advances in echocardiographic evaluation of left ventricular anatomy, perfusion, and function. *Cardiol Rev* 2001;**9**:146–59.

110 Weissler AM, Harris WS, Schoenfeld CD. Systolic time intervals in heart failure in man. *Circulation* 1968;**37**:149–59.

111 Mancini GB, Friedman HZ, Hramiec JE, DeBoc SF. The hemodynamic determinants of the isovolumic index. *Am Heart J* 1986;**112**:791–9.

112 Tei C, Nishimura RA, Seward JB, Tajik AJ. Noninvasive Doppler-derived myocardial performance index: correlation with simultaneous measurements of cardiac catheterization measurements. *J Am Soc Echocardiogr* 1997;**10**: 169–78.

113 Dujardin KS, Tei C, Yeo TC, Hodge DO, Rossi A, Seward JB. Prognostic value of a Doppler index combining systolic and diastolic performance in idiopathic-dilated cardiomyopathy. *Am J Cardiol* 1998;**82**:1071–6.

114 Chen C, Rodriguez L, Lethor J, *et al.* Continuous wave Doppler echocardiography for noninvasive assessment of left ventricular dP/dt and relaxation time constant from mitral regurgitant spectra in patients. *J Am Coll Cardiol* 1994;**23**:970–6.

115 Huemer G, Kolev N, Kurz A, Zimpfer M. Influence of positive end-expiratory pressure on right and left ventricular performance assessed by Doppler two-dimensional echocardiography. *Chest* 1994;**106**:67–73.

116 Kikura M, Ikeda K. Comparison of effects of sevoflurane/nitrous oxide and enflurane/nitrous oxide on myocardial contractility in humans. Load-independent and noninvasive assessment with transesophageal echocardiography. *Anesthesiology* 1993;**79**:235–43.

117 Ohte N, Narita H, Hashimoto T, *et al.* Noninvasive evaluation of left ventricular performance by the shortest distance between mitral leaflets coaptation and interventricular septum at end-systole. *Clin Cardiol* 1992;**15**:656–9.

118 Gorcsan JI, Gasior TA, Mandarino WA, Deneault LG, Hattler BG, Pinsky MR. Assessment of the immediate effects of cardiopulmonary bypass on left ventricular performance by on-line pressure-area relations. *Circulation* 1994;**89**:180–90.

119 Kass DA, Beyar R. Evaluation of contractile state by maximal ventricular power divided by the square of end-diastolic volume. *Circulation* 1991;**84**:1698–708.

120 Schuster AH, Nanda NC. Doppler echocardiographic measurement of cardiac output: comparison with a non-golden standard. *Am J Cardiol* 1984;**53**: 257–9.

121 Stewart WJ, Jiang L, Mich R, Pandian N, Guerrero JL, Weyman AE. Variable effects of changes in flow rate through the aortic, pulmonary and mitral valves on valve area and flow velocity: impact on quantitative Doppler flow calculations. *J Am Coll Cardiol* 1985;**6**:653–62.

122 Marshall SA, Weyman AE. Doppler estimation of volumetric flow. In: Weyman AE, ed. *Principles and practice of echocardiography.* Philadelphia: Lea & Febiger, 1994.

123 Savino JS, Troinaos CA, Aukburg S, Weiss R, Riechek N. Measurement of pulmonary blood flow with transesophageal two-dimensional and Doppler echocardiography. *Anesthesiology* 1991; **75**:445–51.

124 Muhiudeen IA, Kuecherer HF, Lee E, Cahalan MK, Schiller NB. Intraoperative estimation of cardiac output by transesophageal pulsed Doppler echocardiography. *Anesthesiology* 1991; **74**:9–14.

125 Hozumi T, Shakudo M, Applegate R. Accuracy of cardiac output estimation with biplane transesophageal echocardiography. *J Am Soc Echocardiogr* 1993;**6**:62–8.

126 Marcus RH, Bednarz JE, Coulden R, Shroff S, Lipton M, Lang R. Ultrasonic backscatter system for automated on-line endocardial boundary detection: Evaluation by ultrafast computed tomography. *J Am Coll Cardiol* 1993;**22**:839–47.

127 Poelaert J, Schmidt C, Van Aken H, Hinder F, Mollhoff T, Loick HM. A comparison of transoesophageal echocardiographic Doppler across the aortic valve and the thermodilution technique for estimating cardiac output. *Anaesthesia* 1999;**54**:128–36.

128 Feinberg MS, Hopkins WE, Davila-Roman VG, Barzilai B. Multiplane transesophageal echocardiographic Doppler imaging accurately determines cardiac output measurements in critically ill patients. *Chest* 1995;**107**:769–73.

129 Shanewise JS, Cheung AT, Aronson S, *et al.* ASE/SCA guidelines for performing a comprehensive intraoperative multiplane transesophageal echocardiography examination: recommendations of the American Society of Echocardiography Council for Intraoperative Echocardiography and the Society of Cardiovascular Anesthesiologists Task Force for

Certification in Perioperative Transesophageal Echocardiography. *Anesth Analg* 1999;**89**: 870–84.

130 Van Camp G, Carlier S, *et al.* Quantification of mitral regurgitation by the automated cardiac output method: an in vitro and in vivo study. *J Am Soc Echocardiogr* 1998;**11**:643–51.

131 Sun JP, Pu M, Fouad F, Christian R, Stewart WJ, Thomas JD. Automated cardiac output measurement by spatiotemporal integration of color Doppler data: in vitro and clinical validation. *Circulation* 1997;**95**:932–9.

132 Kim WY, Poulsen JK, Terp K, Stasalsen NH. A new Doppler method for quantification of volumetric flow: in vivo validation using color Doppler. *J Am Coll Cardiol* 1996;**27**:182–92.

133 Siu SC, Rivera JM, Guerrero JL, *et al.* Three-dimensional echocardiography. In vivo validation for left ventricular volume and function. *Circulation* 1993;**88**:1715–23.

134 Pearlman AS. Measurement of left ventricular volume by three-dimensional echocardiography: present promise and potential problems. *J Am Coll Cardiol* 1993;**22**:1538–40.

135 Quinones MA, Gaasch WH, Alexander JK. Influence of acute changes in preload, afterload, contractile state, and heart rate on ejection and isovolumic indices of myocardial contractility in man. *Circulation* 1976;**53**:293–302.

136 Lee J, Tajimi T, Widmann TF, Ross JJ. Application of end-systolic pressure–volume and pressure–wall thickness relations in conscious dogs. *J Am Coll Cardiol* 1987;**9**:136–45.

137 Rhodes J, Udelson JE, Marx GR, *et al.* A new noninvasive method for the estimation of peak dP/dt. *Circulation* 1993;**88**:2693–9.

138 Chen C, Rodriguez L, Guerrero JL, *et al.* Noninvasive estimation of the instantaneous first derivative of left ventricular pressure using continuous-wave Doppler echocardiography. *Circulation* 1991;**83**:2101–10.

139 Bargiggia GS, Bertucci C, Recusani F, *et al.* A new method for estimating left ventricular dP/dt by continuous wave Doppler-echocardiography: validation studies at catheterization. *Circulation* 1989;**80**:1287–92.

140 Hammermeister KE, DeRouen TA, Dodge HT. Comparison of survival of medically and surgically treated coronary disease patients in Seattle heart watch: a nonrandomized study. *Circulation* 1982;**65(suppl II)**:53–9.

141 Robotham JL, Takata M, Berman M, Harasawa Y. Ejection fraction revisited. *Anesthesiology* 1991;**74**:172–83.

142 Urbanowicz JH, Shaaban MJ, Cohen NH, *et al.* Comparison of transesophageal echocardiographic and scintigraphic estimates of left ventricular end-diastolic volume index and ejection fraction in patients following coronary artery bypass grafting. *Anesthesiology* 1990;**72**: 607–12.

143 Poelaert J, Schmidt C, Van Aken H, Colardyn F. Transoesophageal echocardiography in critically ill patients. A comprehensive approach. *Eur J Anaesthesiol* 1997;**14**:350–8.

144 Suga H, Sagawa K, Shoukas A, Bakalar K. Load independence of the instantaneous pressure-volume ratio of the canine left ventricle and effects of epinephrine and heart rate on the ratio. *Circ Res* 1973;**32**:314–21.

145 Sagawa K, Suga H, Shouas A, Bakalar K. End-systolic pressure/volume ratio: a new index of ventricular contractility. *Am J Cardiol* 1977;**40**: 748–53.

146 Borow K, Neumann A, Arensman F, Yacoub M. Effects of simultaneous alterations in preload and afterload on measurements of left ventricular contractility in patients with dilated cardiomyopathy: comparisons of ejection phase, isovolumetric and end-systolic force-velocity indexes. *J Am Coll Cardiol* 1992;**20**:787–95.

147 Schmidt C, Hinder F, Van Aken H, Poelaert JI. Non-invasive assessment of left ventricular contractility by means of transoesophageal echocardiography. *Ballière's Clin Anaesthesiol* 1998;**12**:577–94.

148 Sharir T, Feldman MD, Haber H, *et al.* Ventricular systolic assessment in patients with dilated cardiomyopathy by preload-adjusted maximal power. Validation and noninvasive application. *Circulation* 1994;**89**:2045–53.

149 Schmidt C, Roosens C, Struys M, *et al.* Contractility in humans after coronary artery surgery. *Anesthesiology* 1999;**91**:58–70.

150 Kass DA, Van Anden E, Becker LC, Kasper EK, White WB, Feldman AM. Dose dependence of chronic positive inotropic effect of vesnarinone in patients with congestive heart failure due to idiopathic or ischemic cardiomyopathy. *Am J Cardiol* 1996;**78**:652–6.

151 Mandarino WA, Pinsky MR, Gorcsan JI. Assessment of left ventricular contractile state by preload-adjusted maximal power using echocardiographic automated border detection. *J Am Coll Cardiol* 1998;**31**:861–8.

152 Pagel PS, Nijhawan N, Warltier DC. Quantitation of volatile anesthetic-induced depression of myocardial contractility using a single beat index derived from maximal ventricular power. *J Cardiothorac Vasc Anesth* 1993;**7**:688–95.

153 Nishimura RA, Abel MD, Hatle LK, Tajik AJ. Relation of pulmonary vein to mitral flow velocities by transesophageal Doppler echocardiography. Effect of different loading conditions. *Circulation* 1990;**81**:1488–97.

154 Nishimura RA, Tajik J. Evaluation of diastolic filling of left ventricle in health and disease: Doppler echocardiography is the clinician's Rosetta Stone. *J Am Coll Cardiol* 1997;**30**:8–18.

155 Rockey R, Kuo LC, Zoghbi WA, Limacher MC, Quinones MA. Determination parameters of left ventricular diastolic filling with pulsed Doppler

echocardiography: comparison with cineangiography. *Circulation* 1985;**71**:543–50.

156 Grossman W. Diastolic dysfunction in congestive heart failure. *N Engl J Med* 1991;**325**:1557–64.

157 Dujardin KS, Tei C, Yeo TC, Hodge DO, Rossi A, Seward JB. New index of combined systolic and diastolic myocardial performance: a simple and reproducible measure of cardiac function: a study in normals and dilated cardiomyopathy. *J Cardiol* 1995;**26**:357–66.

158 Poulsen SH, Jensen SE, Tei C, Seward JB, Egstrup K. Value of the Doppler index of myocardial performance in the early phase of acute myocardial infarction. *J Am Soc Echocardiogr* 2000;**13**:723–30.

159 Poulsen SH, Jensen SE, Nielsen JC, Moller JE, Egstrup K. Serial changes and prognostic implications of a Doppler derived index of combined left ventricular systolic and diastolic myocardial performance in acute myocardial infarction. *Am J Cardiol* 2000;**85**:19–25.

160 Tei C. New non-invasive index for combined systolic and diastolic ventricular function. *J Cardiol* 1995;**26**:135–6.

161 Tei C, Ling LH, Hodge DO, *et al.* New index of combined systolic and diastolic myocardial performance: a simple and reproducible measure of cardiac function: a study in normals and dilated cardiomyopathy. *J Cardiol* 1995;**26**: 357–66.

162 Tei C, Dujardin KS, Hodge DO, Kyle RA, Tajik AJ, Seward JB. Doppler index combining systolic and diastolic myocardial performance: clinical value in cardiac amyloidosis. *J Am Coll Cardiol* 1996;**28**:658–64.

163 Lacorte JC, Cabreriza SE, Rabkin DG, *et al.* Correlation of the Tei index with invasive measurements of ventricular function in a porcine model. *J Am Soc Echocardiogr* 2003;**16**:442–7.

164 Stack RS, Lee CC, Reddy BP, Taylor ML, Weissler AM. Left ventricular performance in coronary artery disease evaluated with systolic time intervals and echocardiography. *Am J Cardiol* 1976;**37**:331–9.

165 Heikkila J, Luomanmaki K, Pyorala K. Serial observations on left ventricular dysfunction in acute myocardial infarction, II: systolic time intervals in power failure. *Circulation* 1971;**44**: 343–54.

166 Garrad CL, Weissler AM, Dodge HT. The relationship of alterations in systolic time intervals to ejection fraction in patients with cardiac disease. *Circulation* 1970;**42**:455–62.

167 Mancini GB, Costello D, Bhargava V, Lew W, LeWinter M, Karliner JS. The isovolumetric index: a noninvasive approach to the assessment of left ventricular function in man. *Am J Cardiol* 1982;**50**:1401–8.

168 Burwash IG, Otto CM, Pearlman AS. Use of Doppler-derived left ventricular time intervals for noninvasive assessment of systolic function. *Am J Cardiol* 1993;**72**:1331–3.

169 Gleason WL, Braunwald E. Studies on the first derivative of the ventricular pressure pulse in man. *J Clin Invest* 1962;**41**:80–91.

170 Broberg CS, Pantely GA, Barber BJ, *et al.* Validation of the myocardial performance index by echocardiography in mice: a noninvasive measure of left ventricular function. *J Am Soc Echocardiogr* 2003;**16**:814–23.

171 Poulsen SH, Nielsen JC, Andersen HR. The influence of heart rate on the Doppler-derived myocardial performance index. *J Am Soc Echocardiogr* 2000;**13**:379–84.

172 Moller JE, Poulsen SH, Egstrup K. Effect of preload alternations on a new Doppler echocardiographic index of combined systolic and diastolic performance. *J Am Soc Echocardiogr* 1999;**12**:1065–72.

173 Mugerwa JA, Kiatchoosakun S, Restivo J, Hoit BD. The myocardial performance index in patients with aortic stenosis. *Echocardiography* 2002;**19**: 267–72.

174 Bruch C, Schmermund A, Dagres N, Katz M, Bartel T, Erbel R. Severe aortic valve stenosis with preserved and reduced systolic left ventricular function: diagnostic usefulness of the Tei index. *J Am Soc Echocardiogr* 2002;**15**:869–76.

175 Haque A, Otsuji Y, Yoshifuku S, *et al.* Effects of valve dysfunction on Doppler Tei index. *J Am Soc Echocardiogr* 2002;**15**:877–83.

176 Tei C, Dujardin KS, Hodge DO, *et al.* Doppler echocardiographic index for assessment of global right ventricular function. *J Am Soc Echocardiogr* 1996;**9**:838–47.

177 Eidem BW, O'Leary PW, Tei C, Seward JB. Usefulness of the myocardial performance index for assessing right ventricular function in congenital heart disease. *Am J Cardiol* 2000;**86**: 654–8.

178 Eto G, Ishii M, Tei C, Tsutsumi T, Akagi T, Kato H. Assessment of global left ventricular function in normal children and in children with dilated cardiomyopathy. *J Am Soc Echocardiogr* 1999; **12**:1058–64.

179 Sato T, Harada K, Tamura M, Watanabe A, Ishii M, Takada G. Cardiorespiratory exercise capacity and its relation to a new Doppler index in children previously treated with anthracycline. *J Am Soc Echocardiogr* 2001;**14**:256–63.

180 Harjai KJ, Scott L, Vivekananthan K, Nunez E, Edupuganti R. The Tei index: a new prognostic index for patients with symptomatic heart failure. *J Am Soc Echocardiogr* 2002;**15**:864–8.

181 Lax JA, Bermann AM, Cianciulli TF, Morita LA, Masoli O, Prezioso HA. Estimation of the ejection fraction in patients with myocardial infarction obtained from the combined index of systolic and diastolic left ventricular function: a new method. *J Am Soc Echocardiogr* 2000;**13**:116–123.

182 Moller JE, Sondergaard E, Poulsen SH, Appleton CP, Egstrup K. Serial Doppler echocardiographic assessment of left and right ventricular performance after a first myocardial infarction. *J Am Soc Echocardiogr* 2001;**14**:249–55.

183 Moller JE, Egstrup K, Kober L, Poulsen SH, Nyvad O, Torp-Pedersen C. Prognostic importance of systolic and diastolic function after acute myocardial infarction. *Am Heart J* 2003; **145**:147–53.

184 Eidem BW, Tei C, O'Leary PW, Cetta F, Seward JB. Nongeometric quantitative assessment of right and left ventricular function: myocardial performance index in normal children and patients with Ebstein anomaly. *J Am Soc Echocardiogr* 1998;**11**:849–56.

185 Burgess MI, Mogulkoc N, Bright-Thomas RJ, Bishop P, Egan JJ, Ray SG. Comparison of echocardiographic markers of right ventricular function in determining prognosis in chronic pulmonary disease. *J Am Soc Echocardiogr* 2002;**15**:633–9.

4 Left ventricular diastolic function

Stefan G De Hert

Introduction

The clinical importance of diastolic function in normal and abnormal left ventricular (LV) performance has been recognised for many years.[1–6] Congestive heart failure is one of the most common heart problems in adults. The final common pathway in the development of symptoms of congestive heart failure is elevation in diastolic filling pressures. Diastolic dysfunction is therefore present in all patients with congestive heart failure. Progressive systolic dysfunction may lead to diastolic dysfunction and ultimately result in congestive heart failure. However, systolic performance is normal in as many as 40% of patients who present with congestive heart failure, indicating that primary diastolic dysfunction is the cause of LV heart failure.[7–9]

Systolic dysfunction manifests as a reduction in LV ejection fraction. Diastolic dysfunction manifests as increasing difficulty in filling the left ventricle, but with an initially normal LV ejection fraction. The causes of diastolic dysfunction are summarised in Box 4.1. The two main characteristic features of LV diastolic dysfunction are alterations in relaxation and changes in compliance. These two characteristics can accurately be assessed using invasive methodology. The rate of relaxation is determined by the time constant tau of isovolumic pressure decay,[10] and ventricular compliance is assessed from the slope of the diastolic pressure–volume relation.[11,12] This is very complicated and not practical in clinical routine assessment of LV function. Therefore, the use of non-invasive methodology has attracted much interest.[13,14] Non-invasive assessment of LV diastolic function focuses on determining the pattern of LV filling. However, this approach does not directly assess diastolic function but instead uses analysis of LV filling patterns to serve as markers of diastolic function. Therefore, it is essential to appreciate the sequence and the physiology of LV filling during the LV diastolic phase, in order to interpret correctly the LV filling patterns.

Mechanical factors

- Hypertrophy
- Scarring
- Pericardial restraint

Functional factors

- Delayed relaxation
- Abnormal relaxation patterns
- Tachycardia
- Changes in compliance

Box 4.1 Causes of diastolic dysfunction

Phases of diastole

Normal diastolic function implies that normal adequate filling of the left ventricle can occur without an abnormal increase in filling pressures. According to the Frank–Starling mechanism, normal diastolic function ensures adequate stroke volume both at rest and during increased work. LV diastolic filling consists of a series of haemodynamic events. Although diastole is the phase during which the ventricle is filled, it cannot be regarded as a passive phase in the cardiac cycle. Instead, it represents a phase during which myocardial properties are further modulated not only by creep and stress relaxation[15] but also by preload conditions,[16,17] by possible incomplete relaxation,[18–20] and by expression of nitric oxide.[21]

In clinical assessment, diastole is assumed to start with aortic valve closure. The first phase in the clinical assessment therefore considers isovolumic relaxation, which represents the time interval from aortic valve closure to mitral valve opening. This interval is determined primarily by the timing of mitral valve opening, which is influenced by the rate of LV relaxation and left atrial (LA) pressure.[22,23] In normal adults the duration of isovolumic relaxation is rather uniform, in the range of 60 ± 10 ms (mean ± standard deviation), with significantly lower values in children.[24]

The second phase is the rapid filling phase. When LV pressure falls below the LA pressure, the mitral valve opens and rapid early diastolic filling begins. The predominant determinant of the early diastolic filling driving force is LV elastic recoil and the rate of LV relaxation. In this phase, LA pressure is less important as a driving force. Approximately 80% of LV filling normally occurs during this phase. Opening of the mitral valve is the start of LV filling, which continues until the start of the next systole. The total time during which the mitral valve is open represents the time available for ventricular filling. At rest, ventricular filling time is between 400 and 500 ms at a heart rate of 60 beats/min.[25] With increasing heart rate, there is a disproportionate reduction in filling time from 150 to 200 ms at a rate of 120 beats/min to 100 ms or less at 160 beats/min. The peak rate of inflow normally occurs early in diastole and reaches a value of 500–700 ml/s. In normal conditions, the proportion of stroke volume entering the ventricle during the first third of diastole is 47 ± 15% at rest.[26]

That phase is followed by the phase of passive ventricular filling. This period starts when pressure and volume increase together at the end of the rapid filling phase and lasts until the start of atrial systole. Even when heart rate is slow, only 10–20% of the total stroke volume enters the ventricle during this phase.

The final phase of diastole is atrial systole. This phase accounts for approximately 20% of the stroke volume. The contribution of atrial systole to stroke volume may increase to up to 30% in patients with LV disease, although absolute volumes are not increased. Atrial contraction is associated with an increase in LV pressure in the range of 2–5 mmHg in normal persons but may be considerably increased in patients with LV disease.

Non-invasive assessment of left ventricular diastolic function

The proportions of LV filling during the different diastolic phases depend on the rate of myocardial relaxation, LV elastic recoil, chamber compliance, and LA pressure. These variable factors will determine the transmitral pressure gradient and consequently the transmitral flow pattern. Doppler echocardiography allows non-invasive assessment of the LV diastolic function. Analysis of transmitral flow velocities allows assessment of the LV diastolic filling pattern,[22,27] whereas analysis of the pulmonary venous flow velocity assesses the filling of the left atrium.[28,29] Assessment of diastolic filling is based mainly on measurements of transmitral and pulmonary venous flow patterns. The reason why more than one non-invasive measure is needed is that no single index has adequate sensitivity and specificity. More recently, the introduction of new technologies, such as tissue Doppler of the mitral annulus and colour M-mode, has allowed further refinement in the clinical assessment of diastolic function.

Transmitral flow

From a physiological point of view, LV diastolic filling is a function of the atrioventricular pressure gradient and the impedance of the mitral valve.[30,31] Figure 4.1 illustrates the pressure gradients between the left atrium and left ventricle, along with corresponding transmitral flow signals. The transmitral pressure gradient is determined not only by the rate of LV relaxation and LV compliance, but also by preload, afterload, and heart rate.[27,32–34] Therefore, heart rate and loading conditions must be taken into account when assessing transmitral filling.

Mitral flow velocities are obtained by pulsed wave Doppler echocardiography with the sample flow volume located between the tips of the mitral leaflets during diastole. The different phases of LV diastole can be assessed by analysis of the transmitral flow signal. Figure 4.2 shows the different variables that are used in the clinical assessment of transmitral flow signals. The following variables may be measured: LV isovolumic relaxation time, peak flow velocity in early diastole (E wave), flow velocity at the end of diastasis just before atrial contraction (E at A), peak velocity at atrial contraction (A wave), mitral deceleration time, and mitral A wave duration. Table 4.1 summarises the physiological meanings of the different variables of the mitral flow velocity profile. During the isovolumic relaxation time, the ventricular pressure falls rapidly. The mitral valve is still closed and no filling of the left ventricle occurs. When ventricular pressure drops below the atrial pressure, the mitral valve opens and the left ventricle fills rapidly with blood during the early

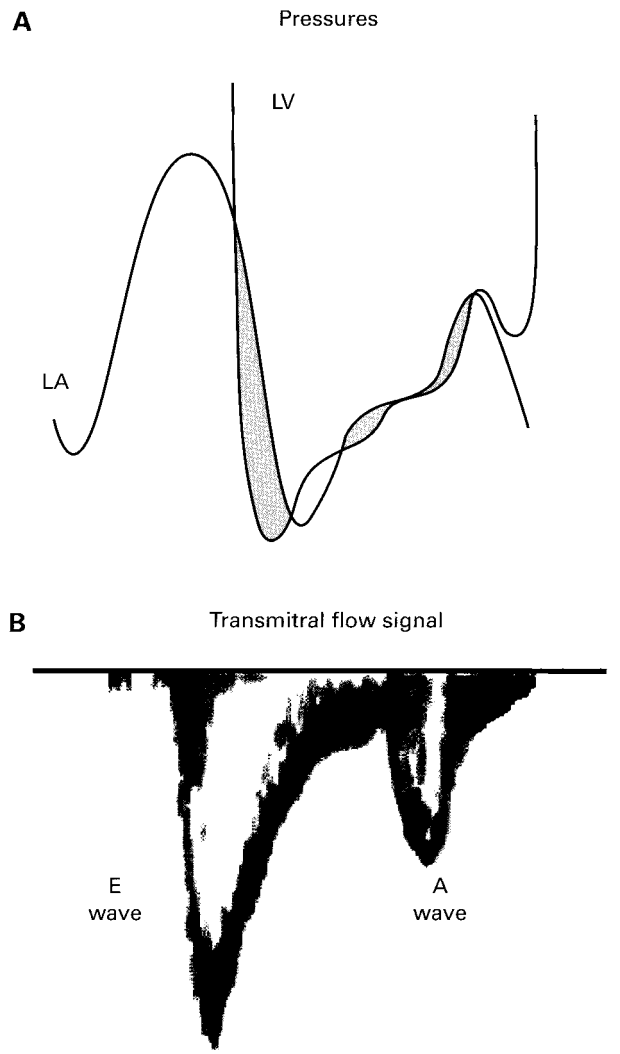

Figure 4.1 **(A)** Time course of left atrial (LA) and left ventricular (LV) pressure during diastole in the normal ventricle, and **(B)** the corresponding transmitral flow signal obtained by transoesophageal echocardiography. The transmitral flow pattern is the reflection of the transmitral pressure gradient. The transmitral flow signal consists of two distinct waves. When LV pressure drops below LA pressure, the mitral valve opens and the left ventricle fills rapidly. This phase presents as the E wave on the transmitral flow. During diastasis, LA and LV pressures are equalised and little filling is observed. With atrial contraction, late filling of the left ventricle occurs and this coincides with the A wave on transmitral flow.

diastolic filling phase. This phase presents as an E wave on transmitral flow. The inflow velocity accelerates to a peak early filling velocity and then decelerates at a measurable rate, which is called the deceleration time. During diastasis ventricular and atrial pressure equalise, and little filling is observed. Then atrial contraction increases the atrioventricular pressure gradient and late filling of the ventricle occurs. This phase presents as the A wave.

The E/A wave flow velocity ratio is an important parameter. This ratio is affected by age. Tachycardia and first degree atrioventricular block may result in fusion of E and A velocities. The A velocity may be relatively increased if it starts before the E velocity has declined to zero. If the E velocity is greater than 20 cm/s at the beginning of the A wave (E at A), then both the A velocity and E/A ratio are affected by the fusion of the two components.[35]

The diastolic flow pattern is also characterised by the deceleration time. Mitral deceleration time is measured by extending the deceleration slope from peak E wave velocity to the zero velocity baseline. This parameter is prolonged when relaxation abnormality is the predominant diastolic dysfunction. In the presence of impaired relaxation, it takes longer for LA and LV pressures to be equilibrated. The result is a slower fall in LV pressure until mid to late diastole, with a reduced rate of filling during early diastole. Deceleration time will be shortened when rapid filling occurs as a result of vigorous LV relaxation and elastic recoil. This phenomenon is observed in healthy normal persons. Shortened deceleration time may also occur when LV compliance is decreased. Decreased LV compliance will result in a more marked increase in LV pressure in early diastole. Both theoretically[36] and experimentally,[37] it was shown that mitral deceleration time is related to chamber compliance of the left ventricle. Clinical studies indicated that short mitral deceleration times (< 130 ms) were related to increased filling pressures in patients with coronary artery disease.[38,39] Short deceleration times were also suggested to have a prognostic value in patients with dilated[40–42] and restrictive cardiomyopathies,[43] as well as in patients with acute myocardial infarctions.[44] This possible prognostic implication makes deceleration time a very attractive parameter in Doppler assessment of diastolic function. However, compared with peak flow velocities, it is less reproducible[45,46] and is more subject to interobserver and intraobserver variability.[46]

Normal transmitral flow patterns

The rate of myocardial relaxation and compliance change with age.[38,47] Therefore, the different diastolic filling patterns are observed for the various age groups. The normal values

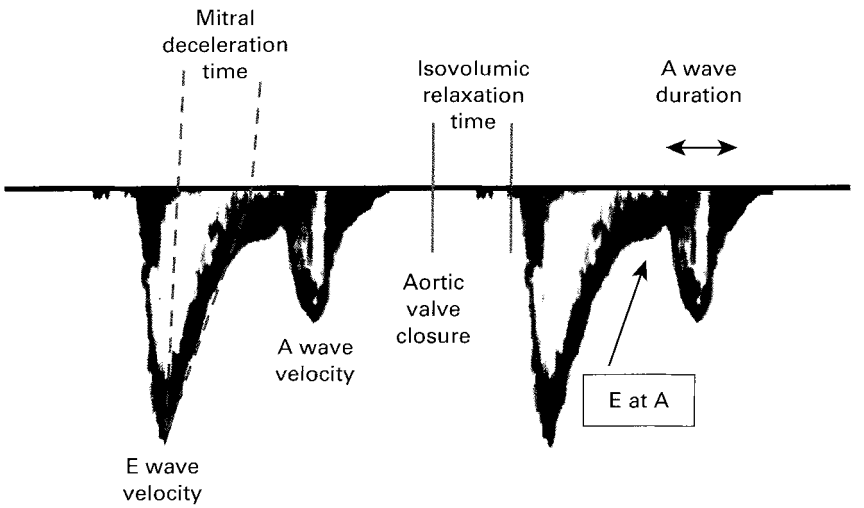

Figure 4.2 Variables that are measured during assessment of transmitral flow signals. These variables are as follows: peak mitral flow velocity in early diastole (E wave velocity), peak mitral flow velocity at atrial contraction (A wave velocity), mitral flow velocity at onset of atrial contraction (E at A), isovolumic relaxation time, mitral deceleration time, and duration of the mitral A wave.

Table 4.1 Physiological meaning of mitral flow velocity variables

Flow velocity variable	*Physiological meaning*
LV isovolumic relaxation time	Early or late mitral valve opening Relation between LV relaxation and left atrial pressure
E wave velocity	Reflects early diastolic transmitral pressure gradient
A wave velocity	Reflects late diastolic transmitral pressure gradient
E/A ratio	Type of LV filling pattern
E at A velocity	Effect of PR and RR interval
Mitral deceleration time	LV compliance in early diastole Prognostic value in dilated and restrictive cardiomyopathy
A wave duration	LV compliance in late diastole Left atrial stroke volume

LV = left ventricular.

for the transmitral variables are summarised in Table 4.2. The changing profiles of the normal transmitral flow pattern with age are shown in Figure 4.3A. With increasing age, the rate of myocardial relaxation and LV elastic recoil decrease. As a consequence, LV pressure decline and LV filling become slower. In the presence of a normal LA pressure, the pressure crossover between the left ventricle and the left atrium – which is the mitral valve opening – occurs later and the early transmitral pressure gradient is decreased. These physiological changes are manifested as an increase in LV isovolumic relaxation duration and a gradual decrease in E velocity with increasing age. When LV filling in early diastole is reduced, it will take longer before pressure equilibrium is reached between the left ventricle and the left atrium. As a consequence, deceleration time will increase. Secondly, because early LV filling is reduced, the contribution of atrial contraction to LV filling will become more important.[48] The result is a gradual increase in A velocity with ageing. At the age of 65 years, E velocity approaches A wave velocity, and in individuals older than 70 years the E/A ratio is usually less than 1. These changes appear to be independent of LV systolic function, which remains well preserved. Rather, these changes appear related in part to an age-associated increase in LV mass.

Abnormal transmitral flow patterns

Abnormal transmitral flow patterns may be caused by two distinct pathological processes. These are firstly the presence of an abnormal relaxation pattern and secondly the occurrence of

Table 4.2 Normal values for left ventricular diastolic filling parameters in different age groups

Parameter	21–40 years	41–60 years	>60 years
Isovolumic relaxation time (ms)	67 ± 8	74 ± 7	87 ± 7
E wave velocity (cm/s)	75 ± 13	71 ± 13	71 ± 11
A wave velocity (cm/s)	51 ± 11	57 ± 13	75 ± 12
E/A ratio	1·53 ± 0·40	1·28 ± 0·25	0·96 ± 0·18
Mitral deceleration time (ms)	166 ± 14	181 ± 19	200 ± 0·29
A wave duration (ms)	127 ± 13	133 ± 13	138 ± 19
PV_s velocity (cm/s)	44 ± 10	49 ± 8	52 ± 11
PV_d velocity (cm/s)	47 ± 11	41 ± 8	39 ± 11
PVa velocity (cm/s)	21 ± 8	23 ± 3	25 ± 9
PVa duration (ms)	96 ± 33	112 ± 15	113 ± 30
PVs/PV_d ratio	0·98 ± 0·32	1·21 ± 0·20	1·39 ± 0·47

Values are expressed as mean ± standard deviation. a = atrial reversal component, d = diastolic component, PV = pulmonary venous flow, S = systolic component. (Adapted from Oh *et al.*,[13] Appleton and Hatle,[38] and Klein *et al.*[47])

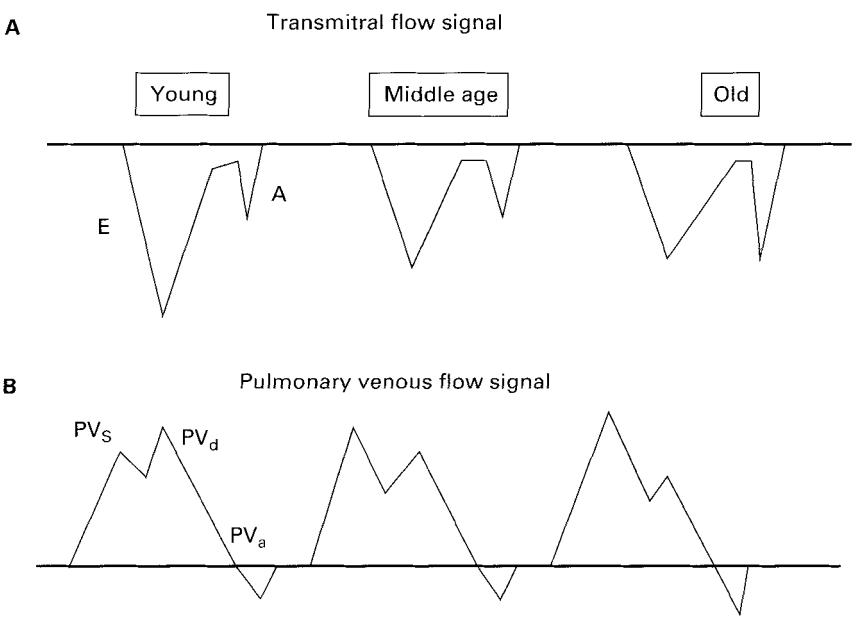

Figure 4.3 **(A)** Normal transmitral flow signals in different age groups. In young individuals the E wave predominates. With ageing E wave amplitude declines, whereas A wave amplitude increases. **(B)** Normal pulmonary venous flow signals in different age groups. In young individuals, the pulmonary venous systolic (PV_s) and diastolic (PV_d) flow velocities are nearly equal. With ageing, however, PV_d velocity declines and PV_s velocities increase. (Adapted from Oh *et al.*[13])

decreased LV compliance, resulting in a restrictive diastolic filling pattern. The different typical pathological flow velocity profiles are illustrated in Figure 4.4A.

Impaired myocardial relaxation pattern

Impaired myocardial relaxation is observed during the course of various cardiac pathologies, including LV hypertrophy, myocardial ischaemia and infarction,[49–52] various cardiomyopathies,[53,54] congestive heart failure,[19,55] and in patients undergoing coronary surgery.[20] Isovolumic relaxation time is prolonged because the LV pressure fall is slower. This slower LV pressure fall delays the timing of mitral valve opening for as long as the LV pressure remains normal. However, when LA pressures are increased, this phenomenon is no longer observed. E wave velocity is reduced and A velocity is increased. This results in an E/A ratio of less than 1 and in prolonged deceleration time.

Restrictive filling pattern

A restrictive diastolic filling pattern can be present in any heart disease, and results

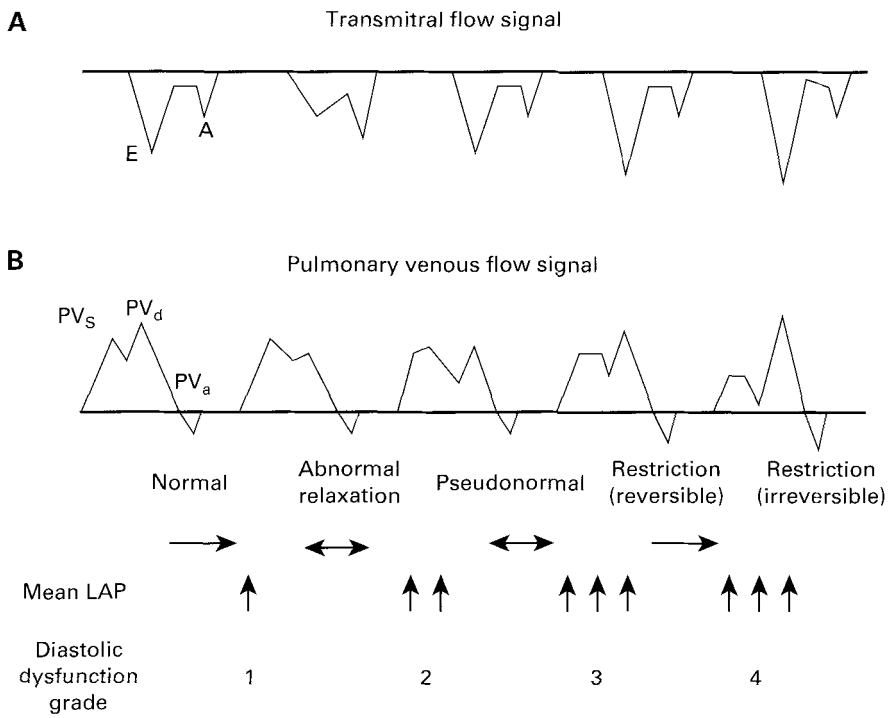

Figure 4.4 **(A)** Typical abnormal transmitral flow patterns. The two major abnormal flow patterns are the impaired myocardial relaxation pattern and the decreased compliance flow pattern. In the initial period of cardiac disease, the main diastolic abnormality is impaired myocardial relaxation. Only later does left ventricular compliance become affected (see text for a detailed description of the changes that take place in the different variables). **(B)** Typical abnormal pulmonary venous flow patterns. As for transmitral flows, the two major abnormal flow patterns are the impaired myocardial relaxation pattern and the decreased compliance flow pattern (see text for detailed description of the changes that take place in the different variables). LAP = left atrial pressure. (Adapted from Oh *et al.*[13])

in decreased LV compliance and increased LA pressure.[22,36,37,56] This may occur during decompensated congestive heart failure, severe coronary artery disease, aortic regurgitation, advanced restrictive cardiomyopathy, and constrictive pericarditis.[43,53,57–59] In the presence of an increased LA pressure, mitral valve opening will occur earlier. Therefore, isovolumic relaxation time will be shortened and the transmitral pressure gradient will be higher. This will result in a higher early transmitral flow with an increased E wave velocity. In the presence of a non-compliant left ventricle, this early diastolic flow causes a rapid increase in early LV diastolic pressure. This will result in a rapid equilibrium of LV and LA pressures, which manifests as shortened deceleration time. At the end of diastole, the atrial contraction will increase LA pressure. However, because of the non-compliant left ventricle and the restrictive filling pattern, LV pressure will increase even more rapidly. This abnormally rapid rise in LV pressure terminates mitral inflow prematurely, and little additional filling is seen in mid-diastole and at atrial contraction. The result is a decrease in A wave velocity and A wave duration. In extreme cases the rise in LV pressure overshoots LA pressure sufficiently to provoke mitral regurgitation in mid-diastole or after atrial contraction. A restrictive filling pattern is therefore characterised by a shortened isovolumic relaxation time, mitral flow velocities that exhibit increased E velocity and decreased A velocity, and finally the presence of a shortened deceleration time. The E/A ratio is typically greater than 2. This pattern is different from that observed with impaired myocardial relaxation. Nevertheless, myocardial relaxation is also impaired in patients with a restrictive filling pattern. The effects of impaired relaxation on the LV filling patterns are masked in these patients by the presence of decreased LV compliance and markedly elevated LA pressures. In the early phase of the disease, the restrictive flow pattern may still be reversible (e.g. by loading manipulations). Later in the process, however, the restrictive flow pattern becomes irreversible.

Pseudonormalised filling pattern

Abnormal or impaired relaxation is an early finding in nearly all cardiac diseases. With progression of the disease, LV compliance becomes reduced and filling pressures start to increase. During this transition, the elevated LA pressures increase the early transmitral pressure

gradient. This augments early transmitral flow, and thereby counteracts the effects of impaired relaxation. In this situation, the transmitral flow may resemble a normal diastolic filling pattern. This has been termed a pseudonormalised filling pattern and it represents a moderate stage of diastolic dysfunction.

A pseudonormal pattern can be distinguished from a true normal pattern by closer analysis of additional clinical and echocardiographic data. In the presence of an abnormal left ventricle size, systolic dysfunction, or increased wall thickness, abnormal relaxation is expected. When in such a patient a normal E/A ratio is observed, this suggests elevated LA pressures that mask the abnormal relaxation pattern. The presence of LA enlargement in the absence of mitral valve disease also indicates elevated LV diastolic and mean LA pressures. When forward mitral flow at atrial contraction is abbreviated or when a prolonged reversal of flow in the pulmonary vein exceeds forward mitral flow at atrial contraction, underlying pathology should also be suspected.

Finally, a dynamic evaluation with analysis of effects of a reduction in preload may also help to distinguish a true normal from a pseudonormal pattern.[60] Patients with a pseudonormal mitral flow pattern have a primary abnormality in LV relaxation combined with elevated mean LV filling pressure. Underlying impaired LV relaxation may be unmasked when preload is reduced and LA pressures decrease. When, with this manoeuvre, the E/A ratio is reduced to less than 1, this reveals the presence of a pseudonormalised pattern. In normal persons, both E and A velocities will decrease more proportionally when preload is reduced. A simple bedside technique to decrease LV preload is the Valsalva manoeuvre.

Pulmonary venous flow pattern

Analysis of pulmonary venous flow patterns may help in more accurate interpretation of diastolic filling patterns. Several studies have demonstrated that there is a close relationship between pulmonary venous flow and pressure in the left atrium, with venous peak velocities corresponding to troughs in the LA pressure.[61–64] LA pressure is influenced by LV function, particularly during diastole when the mitral valve is open. Therefore, patterns of pulmonary venous flow may contain information not only about LA function but also about LV function.

The haemodynamic determinants of pulmonary venous flow velocity have been extensively evaluated and variables quantified, which help in the interpretation of mitral flow patterns and in the estimation of LV filling pressures.[29,65–72] Figure 4.5 illustrates a pulmonary venous flow signal and relates the different components of this signal to the transmitral flow signal and the transmitral pressure gradients. Pulmonary venous Doppler recordings contain two systolic velocity components (PV_{S1} and PV_{S2}), one diastolic velocity component (PV_d), and an atrial flow reversal component (PV_a).[65–67] The first phase of the pulmonary venous waveform occurs following atrial systole, and therefore coincides with atrial diastole and ventricular systole. Because PV_{S1} occurs early in systole, it is related to atrial relaxation. During atrial relaxation, LA pressure decreases and flow from the pulmonary veins into the left atrium can occur. A second systolic flow (PV_{S2}) occurs in mid to late systole. This flow is produced by the increase in pulmonary venous pressure after right ventricular systole. In the presence of a normal atrioventricular conduction, both the systolic components are closely connected and a distinct PV_{S1} peak velocity may not be seen in 70% of cases.[13] After mitral valve opening when LA pressure declines, a forward flow velocity (PV_d) is observed in the pulmonary veins. Finally, during atrial contraction, the increase in LA pressure results in a flow reversal into the pulmonary vein (PV_A). The extent and duration of this flow component are related to LV diastolic pressure, LA compliance, and heart rate. The diastolic phase of the pulmonary venous flow coincides with early mitral E wave flow.

Analysis of pulmonary venous flow velocities complements assessment of mitral flow velocity pattern. This is especially true when there is a fusion of mitral E and A waves. In this situation, the ratio between pulmonary venous systolic and diastolic flow velocities can be helpful in characterising diastolic filling in patients with sinus rhythm. In the presence of atrial fibrillation, no PV_{S1} component is observed and PV_{S2} velocity is always smaller than that of PV_d. Both the peak velocity and duration of reversal of pulmonary venous atrial flow (PV_a) increase with higher end-diastolic pressure.[68,69] In patients with high LV end-diastolic pressure, the duration of PV_a therefore exceeds the duration of mitral A wave.

Pulmonary venous flow velocities exhibit similar changes with ageing as do transmitral

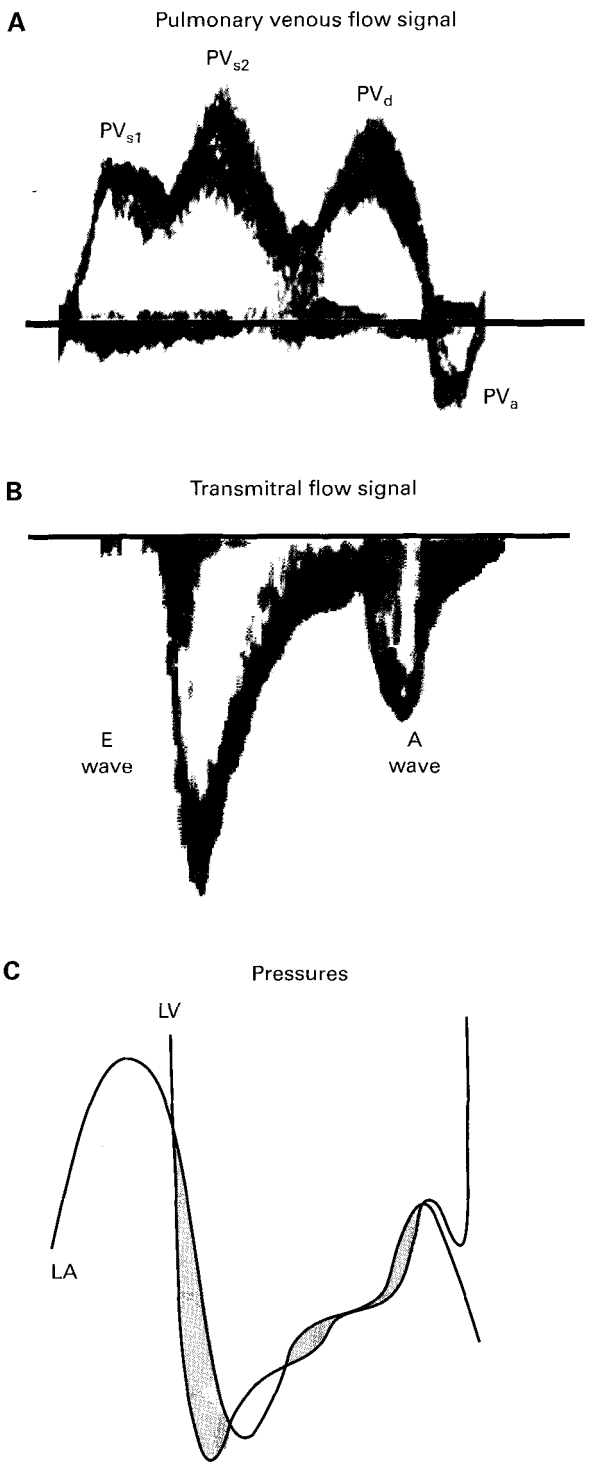

Figure 4.5 **(A)** Pulmonary venous flow signal, compared with **(B)** a simultaneous transmitral flow signal, and **(C)** the time course of changes in left atrial (LA) and left ventricular (LV) pressures during diastole. The different variables that are measured during assessment of pulmonary venous flow analysis include peak flow velocity in early ventricular systole (PV_{S1}), peak flow velocity later in systole (PV_{S2}), peak diastolic flow velocity (PV_d), peak reverse flow velocity at atrial contraction (PV_a), and duration of PV_a.

flow signals. The changing profiles of the normal pulmonary venous flow pattern with age are illustrated in Figure 4.3B. Because more LV filling occurs at atrial contraction, diastolic forward flow velocity (PV_d) becomes less and systolic forward flow velocity becomes more prominent with increasing age.[66]

Abnormal pulmonary venous flow patterns

The abnormal flow patterns discussed for transmitral flow also exist for pulmonary venous flow. The different typical pathological flow velocity profiles are shown in Figure 4.4B. Because the left atrium mainly functions as a passive conduit during early diastole, pulmonary diastolic flow closely parallels the changes in mitral E wave pattern. In the presence of abnormal relaxation, pulmonary diastolic forward flow is diminished with compensatory increased flow in systole. The duration of pulmonary venous atrial flow reversal and velocity is usually normal, but may be increased if LV end-diastolic pressure is high.

In the presence of a restrictive filling pattern, LA pressure is increased and LA compliance is decreased. Therefore, the systolic forward flow velocity in the pulmonary vein is reduced. Pulmonary venous forward flow stops at mid to late diastole, reflecting a rapid increase in LV pressure. At atrial contraction, the increase in LA pressure can result in a prolonged reversal of flow in the pulmonary veins. When pulmonary venous velocity is high as a result of tachycardia, PV_a may not be seen.

New advances in the echocardiographic assessment of diastolic function

The transmitral and pulmonary vein flow velocity patterns reflect a composite of interrelated physical properties, including the pressure gradients, the compliances at the different levels, and the rate and extent of myocardial relaxation, among others. The analysis of these flow patterns has proven useful in patients with systolic dysfunction. However, it becomes more difficult to determine the presence and severity of abnormalities of diastolic filling in patients with a normal LV ejection fraction. Indeed, normal persons with rapid ventricular

relaxation and a vigorous diastolic suction may have a transmitral flow velocity pattern that strongly resembles the flow velocity profile of a patient with diastolic dysfunction caused by a combination of abnormal relaxation (which causes a decrease in E wave velocity and lengthening of the deceleration time) and the presence of elevated LA pressures (which cause an increase in E wave velocity and shortening of the deceleration time). The assessment of diastolic function with differentiation between the normal and the pseudonormal patterns may therefore be difficult, certainly in patients with normal or near-normal LV systolic function.[73] It is exactly this group of patients in whom correct assessment of diastolic function is most important because more than one-third of elderly patients presenting with symptoms of heart failure have "isolated" LV diastolic dysfunction. Non-invasive assessment of myocardial relaxation, independent of loading conditions, is therefore an important goal in the field of "diastology" because it facilitates correct diastolic assessment. Recent studies have proposed new methods for analysing the rate of myocardial relaxation that would allow one to separate normal from pseudonormal flow velocity patterns.

Tissue Doppler of the mitral annulus

Doppler tissue imaging is an ultrasound modality that allows recording of velocities at the corners of the mitral annulus.[74,75] The tissue Doppler signal is easily obtained, of high amplitude and low velocity, and can be identified in more than 95% of patients.[76] The velocity of annular motion reflects shortening and lengthening of the myocardial fibres along a longitudinal plane. Basic haemodynamic principles indicate that the mitral annulus must move in the opposite direction to that of myocardial blood flow, with a speed that is proportional to the speed of blood flow.[77] The tissue Doppler image of the mitral annulus typically consists of a systolic velocity wave (Sa) and an early (Ea) and late (Aa) diastolic velocity wave (Figure 4.6). The systolic velocity wave appears to correlate well with ejection fraction.[78] The early diastolic velocity wave progressively declines with increasing age and is reduced in pathological conditions such as LV hypertrophy and restrictive cardiomyopathy.[74,75] These observations suggested that Ea could be used as an index of LV relaxation that may not be influenced by LA pressure. Several studies have since demonstrated that Ea can be used as a relatively load-insensitive estimator of myocardial relaxation.[78–80] Although Ea correlates well with tau, the most significant impact appears to be its combination with the transmitral blood flow E velocity. In fact, the E/Ea ratio provides another method to adjust the E wave velocity parameter for the effects of relaxation and to correct for the load dependency of E.[76]

The E/Ea ratio has been shown to be the best predictor of LV filling pressure. It appears to be independent of systolic function and can be used to identify easily those patients with high and low filling pressures. Patients with an E/Ea ratio greater than 15 have elevated LV filling pressures, whereas patients with an E/Ea ratio less than 8 tend to have low or normal filling pressures.[76] The E/Ea ratio also appears to correlate well with the pulmonary capillary wedge pressure (pulmonary capillary wedge pressure = 1·24 [E/Ea] + 1·9), with a difference between Doppler and invasive measurements of 0·1 ± 3·8 mmHg.[78] Of particular importance is the fact that the E/Ea ratio and its relationship to LV filling pressures remain valid in patients with normal systolic function, fused mitral flow inflow signals due to tachycardia, and in patients with atrial fibrillation.[80–82] Various reports have sampled different portions of the annulus (septal, lateral, average of several), but the relationship to the filling pressures is not significantly altered by the sample site.[76] Because of its ease of use in various patient groups, the E/Ea ratio may represent an important tool in the clinical echocardiographic assessment of diastolic function.

It should be remembered that no single Doppler parameter is sufficient for complete assessment of diastolic function. The combination of different variables, however, may help to assess diastolic function more accurately in the presence of different pathologies (Figure 4.7, Table 4.3).[83]

Colour flow propagation

Another possible approach to separate the normal from the pseudonormal mitral flow velocity pattern is to measure the rate of early diastolic flow propagation in the left ventricle. Colour M-mode is ideal for the study of mitral inflow propagation because of its high sampling rate and the ability to measure flow velocities both in a temporal and spacial distribution.

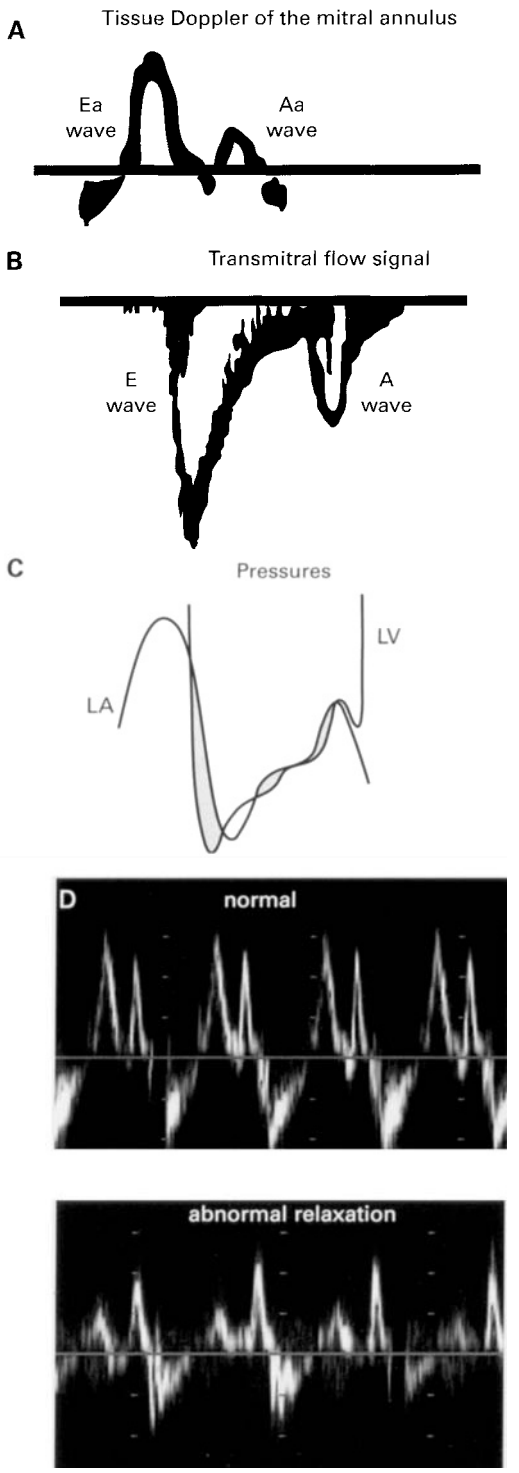

Figure 4.6 Transthoracic Echo-Tissue Doppler patterns. **(A)** Tissue Doppler signal of the mitral annulus, compared with **(B)** a simultaneous transmitral flow signal, and **(C)** the time course of changes in left atrial (LA) and left ventricular (LV) pressures during diastole. The different variables that are measured during assessment of mitral annulus Doppler analysis include peak Ea and Aa velocity. **(D)** A normal and an abnormal relaxation tissue Doppler pattern.

Indeed, whereas pulsed wave Doppler velocity measurements represent a temporal velocity variation throughout the cardiac cycle obtained at a single point in space, colour M-mode Doppler echocardiography interrogates all of the velocities along a scan line and provides a velocity map with a temporal resolution of 5 ms, a spatial resolution of approximately 0·3 mm, and a velocity resolution typically of 3 cm/s.[84]

An adequate recording of a colour M-mode Doppler image of LV filling starts with the placement of the M-mode line parallel to the direction of flow observed by two-dimensional colour Doppler echocardiography. The propagation velocity (Vp) is defined as the slope of the propagation image of the early filling flow in the ventricle (Figure 4.8). This velocity of flow propagation during early diastole has been shown to correlate well with the invasively measured time constant of isovolumic relaxation (tau).[85] A chamber with normal relaxation (small tau) exhibits a quick flow propagation into the cavity. On the contrary, a slowly relaxing ventricle (large tau) exhibits blunted flow propagation. Several studies have indicated that Vp is a relatively load-independent index of myocardial relaxation that is free of pseudonormalisation in evaluating LV diastolic dysfunction.[85–88] Different methods for measuring the rate of flow propagation have been described. Discussion of these methods is beyond the scope of this chapter, and the reader is referred to a recent excellent review on the subject.[89] It is important to note that these different methods result in different values of Vp (Table 4.4). Therefore, values obtained using the different methods cannot be unequivocally compared. In healthy young persons, a Vp greater than 55 cm/s is associated with normal diastolic function.[90] Impaired diastolic function associated with advancing age or pathophysiological conditions such as dilated and hypertrophic cardiomyopathy, hypertension, aortic stenosis, myocardial ischaemia and infarction, or LV hypertrophy has been reported to reduce Vp to less than 50 cm/s.[86,90–93] In coronary surgery patients, analysis of Vp was also reported to allow identification of abnormal diastolic function.[94]

E wave velocity is dependent on both filling pressure and myocardial relaxation. The use of the E/Vp ratio has been proposed as a method for adjusting the E wave velocity parameter for the effects of relaxation. In other words, Vp is believed to correct for the load-dependency of E. As such, the E/Vp ratio can be used as an index of

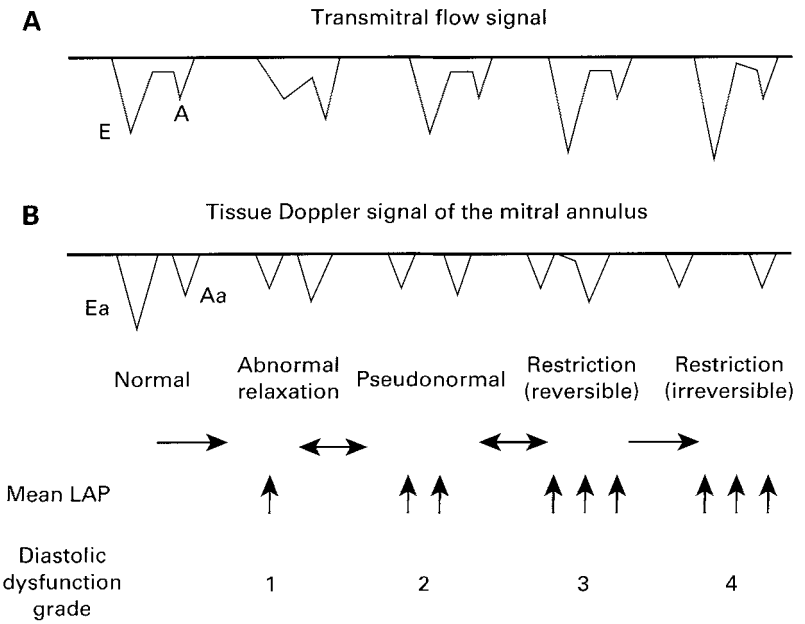

Figure 4.7 **(A)** Transmitral flow signals compared with **(B)** typical flow patterns of the tissue Doppler signal of the mitral annulus in different pathological conditions. The two major abnormal flow patterns are the impaired myocardial relaxation pattern and the decreased compliance flow pattern. In the initial period of cardiac disease the main diastolic abnormality is impaired myocardial relaxation. Only later does left ventricular compliance become affected (see text for a detailed description of the changes that take place in the different variables). LAP = left atrial pressure.

Table 4.3 Variables of diastolic function in relation to the different pathologies

Variable	*Normal*	*Abnormal relaxation*	*Pseudonormal filling*	*Restrictive filling*
E/A	>1	<1	1–2	>2
Deceleration time (ms)	<220	>220	150–200	<150
S/D	≥1	≥1	<1	<1
A rev (m/s)	<0·35	<0·35	≥0·35	≥0·35
Ea (m/s)	>0·08	<0·08	<0·08	<0·08

A rev = reverse flow velocity in the pulmonary vein during atrial contraction, Ea = early flow velocity obtained using tissue Doppler imaging of the mitral annulus, E/A = ratio of early to late filling of transmitral flow velocity, S/D = ratio of systolic to diastolic flow velocity in the pulmonary vein. (Adapted from Poelaert.[83])

LA pressure, LV end-diastolic pressure, or pulmonary capillary wedge pressure.[95–99] All studies propose a linear relationship of the form:

$$p = \alpha \times E/Vp + \beta$$

where p is filling pressure, and α and β are fitting constants. Apart from its ability to help in the diagnosis of diastolic dysfunction, analysis of the E/Vp ratio (E/Vp > 1·5) allows for prediction of in-hospital heart failure and even mortality in patients with myocardial infarction.[100]

It should be noted that, as for all aspects of echocardiographic assessment of cardiac function, there is a technical learning curve. There are different methods for measuring Vp, and the various techniques reported are not interchangeable. Finally, the influence of rapid heart rates with subsequent fusion of early and late diastolic flow is not yet completely understood.[101]

Colour kinesis

Colour kinesis is an echocardiographic technique based on acoustic quantification that tracks endocardial motion by colour encoding pixel transitions between blood and myocardial tissue in real time.[102] This technique generates an integrated display of magnitude and timing of endocardial motion in a single end-systolic or

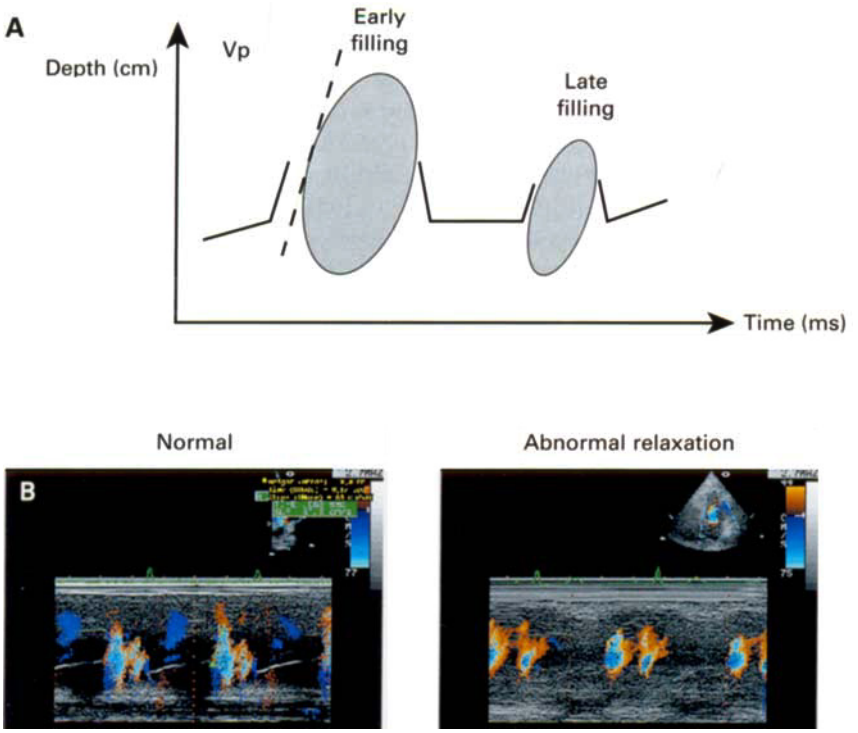

Figure 4.8 **(A)** Velocity of flow propagation (Vp) in the left ventricle by colour M-mode transthoracic echocardiography. The flow pattern in the left ventricle during diastole is illustrated, consisting of an early phase and a late filling phase. Vp is calculated using a slope of the early filling wave. Several methods for calculation of Vp have been described (see De Mey *et al.*[89]). **(B)** A normal and an abnormal relaxation M-mode echocardiographic image.

Table 4.4 Reported normal values of propagation velocity, obtained using different methods of measurement

Method	*Age (years)*	*Vp (cm/s)*	*Reference*
Brun	39 ± 13	84 ± 11	86
Brun	21–35	77 ± 25	142
Brun	36–50	70 ± 23	142
Brun	51–60	53 ± 15	142
Brun	> 60	43 ± 11	142
Duval-Moulin-Garcia	63 ± 11	76 ± 16	100
Duval-Moulin-Garcia	60 ± 11	74 ± 19	143
Duval-Moulin-Garcia	37 ± 9	54 ± 9	97
Takatsuji	58 ± 13	74 ± 17	88
Takatsuji	56 ± 10	73 ± 19	91

Values are expressed as mean ± standard deviation. Vp = propagation velocity.

end-diastolic frame. This allows objective evaluation of regional myocardial performance. Diastolic wall motion asynchrony constitutes a major mechanism responsible for impaired myocardial relaxation. By providing an objective tool to detect delayed diastolic endocardial motion, analysis of colour kinesis images has potential for identifying regional diastolic dysfunction and to help distinguish a normal from a pseudonormal mitral inflow signal.[103]

Estimation of left ventricular filling pressures

Optimal management of heart failure patients requires an accurate estimation of their haemodynamic status. Doppler echocardiography may play an important role in the non-invasive measurement of cardiac output, pulmonary artery pressures, and LV and right ventricular filling

pressures. The role of transoesophageal echocardiography in the non-invasive assessment of haemodynamics is addressed extensively in Chapter 10. In the present chapter, only the non-invasive estimation of LV filling pressures is addressed. These pressures determine LV filling during diastole, and in the clinical assessment of cardiac patients LV diastolic pressure is regarded as an indicator not only of diastolic function but also of the functional reserve of the ventricle.[19,20,55,104,105] Several Doppler methods have been described that can be used for predicting LV filling pressures and pulmonary capillary wedge pressure non-invasively.[39,69,80,95–100,106–109]

The modified Bernoulli equation (which allows for estimation of intravascular pressure gradients) can be used to estimate the LA pressure and the LV end-diastolic pressure in the presence of mitral and aortic regurgitation, respectively.[110,111] Using this equation, the peak velocity of the mitral regurgitant jet (v_{MR}; obtained with continuous wave Doppler) can be converted to the pressure gradient between the left ventricle and the left atrium during systole:

$$4v^2_{MR} = \text{LV systolic pressure} - \text{LA pressure}$$

Therefore:

$$\text{LA pressure} = \text{LV systolic pressure} - 4v^2_{MR}$$

Because the systolic blood pressure equals the LV systolic pressure (in the absence of outflow obstruction), the equation can be rewritten as:

$$\text{LA pressure} = \text{systolic blood pressure} - 4v^2_{MR}$$

Similarly, the end-diastolic velocity of the aortic regurgitant jet (V_{AR}) can be converted to the pressure gradient between the left ventricle and the aorta during diastole, and hence applied to estimation of LV end-diastolic pressure:

$$4v^2_{AR} = \text{aortic diastolic pressure} - \text{LV end-diastolic pressure}$$

Therefore:

$$\text{LV end-diastolic pressure} = \text{aortic diastolic pressure} - 4v^2_{AR}$$

This method assumes that comparable values of diastolic pressures are present in the aortic root and the peripheral artery where systemic pressures are measured.

It is important to note that this type of calculation may result in large overestimation errors of filling pressures if the exact peak velocity is not measured.[112] In addition, the above calculations can only be performed in the presence of either a mitral or an aortic regurgitant jet. Clearly, this is seldom the case in the presence of isolated diastolic dysfunction, and therefore other methods to estimate LV filling pressures should be used.

Several studies have demonstrated that, in the presence of systolic dysfunction, Doppler recordings of the mitral and pulmonary venous flow can reliably be used for estimation of LV filling pressures.[106–109] In patients with normal systolic function, however, this is far less accurate, particularly in those patients with either normal or markedly abnormal LV relaxation.[109,113]

The main determinant of transmitral flow is the diastolic transmitral pressure gradient. As previously discussed, the early diastolic flow (E wave) is directly related to the magnitude of the LA v wave and is inversely related to the minimal LV pressure. With impaired relaxation the LV minimal pressure is abnormally elevated, and consequently the E wave is reduced. Because of incomplete emptying of the left atrium in early diastole, the atrial volume before contraction is increased, which leads to increased emptying during atrial contraction (increased A wave). To maintain the stroke volume, LA pressure increases. This results in an increased transmitral pressure gradient, with a pseudonormalisation pattern of the transmitral flow signal. With further progression of the disease, LA and LV filling pressures increase further, resulting in a restrictive transmitral flow pattern. Therefore, the presence of a restrictive diastolic filling pattern usually indicates increased filling pressures. In the presence of a typical mitral pattern of impaired relaxation, normal filling pressures can be expected unless isovolumic relaxation time and deceleration time become shorter and exhibit a "normalised" duration. Exceptions may occur in patients with marked LV hypertrophy because of markedly prolonged relaxation in this subgroup of patients. Impaired relaxation can be expected in patients older than 70 years and in the presence of increased wall thickness, coronary artery disease, and systolic dysfunction. In these circumstances, elevated filling pressure should be suspected whenever E velocity is greater than A velocity.

Initial estimation of LV end-diastolic pressure and mean LA pressure obtained from mitral flow

velocity pattern should be checked by analysis of the pulmonary venous flow velocities. As the LA pressure increases, the systolic component of the pulmonary venous flow velocity pattern becomes reduced, with a predominance of the diastolic flow.[67–69,108,114] This happens because the atrium empties in diastole and therefore has a lower pressure than the pulmonary veins at that time. A significant increased LA and LV diastolic pressure was demonstrated when the systolic fraction of the forward pulmonary vein flow was less than 40%.[68] Pulmonary venous atrial flow velocity is usually less than 35 cm/s in normal persons. A higher velocity suggests increased filling pressure.[66] The most reliable feature suggesting LV end-diastolic pressure greater than 15 mmHg appears to be the comparison of pulmonary venous atrial flow reversal and mitral A wave duration.[68,69] Atrial reversal flow velocity and duration can indeed provide a reasonable assessment of filling pressures. As these pressures rise, both the velocity and the duration of the atrial reversal flow will increase. When the duration of the pulmonary venous atrial flow reversal flow is more than 30 ms longer than the duration of mitral A wave, then LV end-diastolic pressure can be expected to be elevated.[76] In addition, the presence of a prolonged Δ A duration (the difference between duration of mitral A wave and duration of the pulmonary venous reversal flow) is a strong predictor of 2-year mortality. When Δ A duration is greater than 30 ms, survival is only 37%, as compared with 86% when Δ A duration is less than 30 ms.[115] The difference in the duration of flow of these velocities also correlates well with the increase in LV pressure during atrial systole. When the ratio of mitral A wave duration to pulmonary venous atrial flow duration is 0·9 or less, an LV end-diastolic pressure of greater than 20 mmHg can be expected.[116]

The use of preload manipulations may also help to assess LV filling pressures.[60,76,117–119] The use of the Valsalva manoeuvre (or medical manipulation, e.g. nitroglycerine) to distinguish the pseudonormal from the normal transmitral flow pattern is discussed above. Several studies have recently examined the utility of the transmitral and transpulmonary flow signals during a Valsalva manoeuvre with respect to the estimation of LV filling pressures. The change in A wave velocity with the Valsalva manoeuvre has been shown to correlate well with LV end-diastolic pressure.[118] Valsalva decreases preload and LV filling in early and mid-diastole, which implies that LV pressure and operating compliance at atrial systole are improved and flow velocity at atrial contraction will increase. Another study found that a decrease in E/A ratio from rest to Valsalva of greater than 40%, and an increase in mitral A wave duration had diagnostic accuracies of 85% and 86%, respectively, for the presence of increased LV filling pressures.[117] It should also be emphasised that patients with an E/A ratio of less than 1 can also have elevated filling pressures and that this can be detected using the Valsalva manoeuvre. The diagnostic accuracy for the detection of an increased LV end-diastolic pressure was 88% using a decrease in E/A greater than 40%, and it was 90% using an increase in A wave duration for patients with resting E/A ratio less than 1.[117] Still another study found that the response to Valsalva could be used to predict the presence of elevated filling pressures if the E/A ratio decreased by an absolute 0·5.[76] Importantly, this finding appeared not to be altered by the degree of systolic function.

Finally, analysis of LA volumes can also help to estimate LV filling pressures. When maximal and minimal atrial volumes become larger, and atrial ejection fractions decrease, it can be assumed that filling pressures are increased.

In the presence of atrial fibrillation the usefulness of Doppler signals for evaluating LV filling pressures is reduced. Indeed, with atrial fibrillation, the A and A reversal waves are absent, and the E/A ratio cannot be used as a variable for the assessment of filling pressures. In addition, the lack of atrial contraction and relaxation will result in a reduction in pulmonary venous antegrade systolic flow in the absence of increased filling pressures. Nevertheless, the mitral inflow velocity variables (peak acceleration rate, isovolumic relaxation time, and deceleration time) and the pulmonary venous diastolic velocity can still be used to estimate filling pressures.

It should be borne in mind that it is not always easy to obtain reliable pulmonary vein flow signals. Several studies have demonstrated that a complete analysis of pulmonary vein flow signals, with all components, is possible in only 63–73% of patients.[76,115,117,120] Even in patients in whom adequate signals were obtained, the diagnostic accuracy of the non-invasively measured filling pressures ranged between 56% and 82% for the different variables.[76,117] This

means that even in optimal circumstances up to 20% of patients may be misclassified and a further 25% cannot be assessed by pulmonary vein flow analysis.[101] As discussed above, the use of tissue Doppler signals, alone or together with other Doppler derived variables, may help in the diagnosis of diastolic dysfunction and in the assessment of LV filling pressures.

Pitfalls and limitations in the assessment of diastolic Doppler analysis

Although cardiac echocardiography and Doppler analysis are widely used, it should be remembered that their clinical use in diagnosis, decision making, and treatment may be subject to difficulties in obtaining accurate and reproducible measurements from flow velocity recordings.[121] This is due to two main causes. The first is an under-appreciation of the importance of some technical aspects regarding the quality and reliability of signals, including ultrasound beam alignment to flow, Doppler audio and spectral characteristics, and ultrasound machine settings.[122] The second cause is the possible influence of a number of physiological variables on cardiac filling dynamics and Doppler velocity flow profiles.

Technical aspects

Suboptimal ultrasound machine settings can affect the quality and accuracy of Doppler signals markedly. Use of the smallest sample volume size and lowest Doppler gain will aid in optimising axial and lateral flow velocity resolution.[123] Large sample volumes and excessive Doppler gain result in coarse signals with spectral broadening of the velocity envelopes.[122] This phenomenon makes measurements of variables of flow velocities and flow duration difficult.

The most common technical pitfalls in Doppler assessment of LV diastolic dysfunction are caused by beam misalignment, misplacement of the sample volume, and suboptimal machine adjustments. All of these will result in poorly reliable signals of peak wave velocity and wave duration. This is particularly true for the mitral deceleration time and the isovolumic relaxation time. Because differences in flow duration of 20–40 ms can be of clinical significance,[41–44,68,69,124–126] it is clear that suboptimal machine settings may greatly influence timing measurements and lead to data that are poorly reproducible.

Physiological aspects

Age is an important physiological variable that may influence the diastolic filling profile. The E/A wave flow velocity ratio should be compared with age-adjusted normal values,[23,38,47,48,127–129] and only then will observed values allow initial qualification of the type of LV filling pattern.[22,38]

The second physiological variable that may affect Doppler profiles is heart rate. The velocity at the start of atrial contraction (E at A) will indicate whether the E/A ratio is affected by rapid heart rate,[35,130,131] delayed mitral valve opening,[38] or prolonged PR interval.[38,132] In the presence of tachycardia, diastolic filling period is shortened and atrial contraction may occur before the early diastolic filling phase is completed. In such cases, A wave velocity will be higher than at slower heart rates. When fusion of E and A mitral inflow velocities occurs, analysis of transmitral flow patterns may be obscured. Measurements of pulmonary venous forward flow velocity may then be helpful in the classification of diastolic filling patterns.

An abnormally long or short PR interval also influences mitral inflow velocities. If a PR interval is abnormally prolonged, then it produces an effect similar to that of tachycardia. When a PR interval is abnormally short, the A velocity is abbreviated as a result of the abrupt rise in LV systolic pressures.[13]

E wave and A wave velocities, E/A ratio, and deceleration time profile of the restrictive filling pattern can be similar to that in young healthy persons. The mechanism underlying the production of such diastolic filling patterns, however, is completely different. In young healthy individuals vigorous normal relaxation is the underlying mechanism, whereas in the presence of restrictive cardiac disease the high driving pressure is responsible for the observed diastolic filling pattern. Pulmonary venous diastolic flow velocity may be greater than systolic velocity in normal young persons, and the duration of the mitral A wave flow can also be short. However, it remains equal to or (usually) longer than that of pulmonary venous atrial flow reversal, whereas the opposite is true in patients with restrictive physiology.[13] Atrial size and contractility are normal in young healthy persons,

but contractility is decreased in patients with restrictive filling pattern and high filling pressure. Decreasing preload may unmask the underlying relaxation abnormality in patients with restrictive physiology, whereas both E and A velocities will decrease proportionally in patients with normal filling pressures.

Arrhythmia or atrioventricular conduction abnormalities may also cause problems in the interpretation of diastolic filling patterns. When there is atrioventricular block, E and A velocities of mitral inflow, and systolic and diastolic velocities of pulmonary venous flow vary according to the timing of the atrial contraction with respect to ventricular systole. Atrial contraction optimally occurs near the completion of or shortly after early diastolic filling, and should precede the onset of the QRS complex such that atrial filling is not terminated prematurely by ventricular systole. In the presence of a prolonged PR interval, diastolic mitral regurgitation will occur even without increased LV filling pressures. This is contrary to what occurs in the presence of a normal PR interval, where diastolic mitral regurgitation is indicative of high filling pressures.[13]

The systolic component of pulmonary venous flow decreases with increasing amounts of mitral regurgitation. This phenomenon depends on the degree of increase in LA systolic pressure. However, a decreased pulmonary venous systolic forward flow velocity does not necessarily imply significant mitral regurgitation. This phenomenon may also occur with a high LA filling pressure as a result of restrictive filling. However, frank reversal of pulmonary venous systolic flow usually indicates severe mitral valve regurgitation.[60,133]

With atrial fibrillation, lack of ventricular filling at atrial contraction will result in insignificant or even absent mitral atrial flow (A wave) and in reduced pulmonary venous forward flow during early systole. Variations in peak velocity of E wave, isovolumic relaxation time, and mitral deceleration time may impede accurate interpretation of diastolic filling. This variation tends to be more pronounced when LA pressure is low.[134]

How to interpret left ventricular diastolic filling patterns in clinical practice

In the analysis and interpretation of diastolic filling patterns, not only should the various aspects discussed above be taken into account, but also one should keep in mind the fact that a wide 95% confidence limit for normal values is present.[47,66,135]

The various LV diastolic filling patterns are summarised in Box 4.2. In the absence of cardiac symptoms and morphological abnormalities on echocardiography, it seems reasonable to assume that a normal-looking filling pattern also represents normal diastolic function. Therefore, the first step is the assessment of the patient's cardiac structural and functional status. This includes LV ejection fraction, regional wall motion abnormalities, wall thickness, LA size and contractility, valvular disease, and the pericardium. Only when these have been assessed will one be able to interpret fully the various diastolic filling patterns.

Analysis of diastolic flow patterns should be systematic. The easiest way to address this issue is to analyse the E/A wave ratio. In the absence of hypovolaemia, all patients with an E/A ratio less than 1 can be categorised as having abnormal LV relaxation. The degree of relaxation abnormality is then further judged by a quantification of the E/A ratio and the measurement of the mitral deceleration time. These become lower and longer, respectively, with increasing impairment. An uncomplicated relaxation abnormality is associated with normal LV filling pressures. However, increased filling pressure may be present with an E/A ratio less than 1·0 and a prolonged deceleration time. In this case, the longer duration of pulmonary venous atrial flow reversal compared with mitral A wave duration may permit identification of the diastolic filling pattern.

An E/A ratio greater than 2 usually indicates restrictive physiology in patients with symptoms of congestive heart failure and structural heart disease. Restrictive filling should be accompanied by LA enlargement and other features of elevated diastolic pressure. This can be confirmed by the presence of a predominant diastolic flow in the pulmonary veins and a shortened deceleration time. Diastolic mitral regurgitation in mid-diastole or after atrial contraction can be seen when LV diastolic pressure is markedly elevated. With an E/A ratio between 1 and 2, diastolic filling can be normal, pseudonormal, or restrictive. Additional data are needed to classify diastolic filling.

A change in diastolic function is one of the earliest haemodynamic manifestations in patients

Normal filling pattern

- Normal anatomy on TOE
- Deceleration time: 160–240 ms
- Mitral A wave duration ≥ PV_a duration
- $PV_{S2} \geq PV_d$
- Ea >8 cm/s
- Vp >55 cm/s

Abnormal relaxation

- Normal anatomy on TOE
- Prolonged isovolumic relaxation time
- Reduced E wave velocity; increased A wave velocity → E/A ratio <1
- Prolonged deceleration time
- Reduced PV_d flow
- Ea <8 cm/s
- Vp <50 cm/s

Pseudonormal filling pattern

- TOE signs of structural heart disease → decreased ejection fraction, increased LA size, left ventricular hypertrophy
- Deceleration time: 160–240 ms
- $PV_{S2} < PV_d$
- Mitral A wave duration < PV_a duration
- Reversal of E/A ratio with preload reduction
- Ea <8 cm/s
- Vp <50 cm/s

Restrictive filling pattern

- TOE signs of structural heart disease
- Deceleration time <160 ms
- $PV_{S2} \ll PV_d$
- Mitral A wave duration < PV_a duration
- Increased PVa velocity (≥35 cm/s)
- Decreased E/A ratio with preload reduction
- Ea <8 cm/s
- Vp <50 cm/s

Ea = early flow velocity obtained with tissue Doppler imaging of the mitral annulus, LA = left atrium, PV_a = pulmonary venous flow (atrial reversal component), PV_d = pulmonary venous flow (diastolic component), PV_{S2} = pulmonary venous flow (systolic component), TOE = transoesophageal echocardiography, Vp = flow propagation velocity. (Adapted from Oh *et al.*[13])

Box 4.2 Classification of left ventricular filling patterns

with myocardial ischaemic disease. Ischaemia results in decreased and impaired relaxation.[20,136,137] In patients with acute extensive myocardial infarction or severe coronary artery disease with important LV dysfunction, a pseudonormal or even restrictive pattern can be seen, despite the presence of impaired myocardial relaxation.[44] Changes in indices of diastolic transmitral flow velocity have been reported to be highly sensitive for detection of myocardial ischaemia in awake patients both during coronary angioplasty and during dobutamine stress echocardiography. However, these findings have been questioned by other studies. The relative diagnostic value of Doppler studies of diastolic transmitral flow velocity signals in the detection of perioperative myocardial ischaemia still is poorly understood. A recent study demonstrated that indices of transmitral flow velocity were of little help in detecting ischaemia in anaesthetised patients undergoing dobutamine stress echocardiography.[138] Whether the incorporation of the newer techniques for echocardiographic assessment of myocardial function can increase the accuracy of echocardiographic diagnosis of perioperative myocardial ischaemia remains to be elucidated. Manoeuvres that alter cardiac load have also been applied during the perioperative period. It has been demonstrated in coronary surgery patients that leg elevation allowed identification of a subset of patients with impaired length dependent regulation of myocardial function. These patients typically developed an increase in E wave velocity and a decrease in deceleration time on transmitral inflow analysis. These changes were suggestive of the development of a restrictive filling pattern when cardiac load was increased.[139]

Dilated cardiomyopathy is associated with increased LV end-systolic and end-diastolic volumes. These increased volumes result in decreased elastic recoil and reduced chamber compliance, and hence in impaired diastolic function. During the early stage of congestive heart failure, the main diastolic abnormality is slowing of LV relaxation with reduced early diastolic filling. As congestive heart failure progresses, the transmitral gradient increases with a return of mitral flow velocity to baseline, indicating a pseudonormalisation of the mitral flow pattern. During a more advanced stage, the transmitral pressure gradient increases further with progressive shortened deceleration time, resulting in a restrictive filling pattern.[37,140] This restrictive filling pattern is often seen during the decompensated stage of dilated cardiomyopathy. The initial deceleration time in these patients was shown to be a powerful predictor of long-term survival. Deceleration times of less than 130–150 ms were associated with increased mortality rates: 30% after 1 year and up to 50%

within 2 years.[39,42] Similarly, the presence of a prolonged Δ A duration of more than 30 ms (pulmonary venous flow A duration minus mitral inflow A duration) is a strong predictor of 2 year mortality.[115] In the initial phase of restrictive cardiomyopathy, systolic function is usually maintained whereas diastolic filling pattern becomes restrictive. Morphologically, the left ventricle is not dilated and systolic function is maintained until a later stage.[43,53,54]

With LV hypertrophy, LV myocardial mass is increased. This will result in a decrease in the rate of myocardial relaxation. Therefore, in most patients with LV hypertrophy, E wave velocity is decreased. Isovolumic relaxation time and mitral deceleration time are prolonged. A wave velocity is increased, and hence the E/A ratio becomes less than 1.[141] With increasing stiffness of the myocardium, the diastolic filling pattern evolves to a more pseudonormal and finally a restrictive pattern. With hypertrophic cardiomyopathy, a diastolic restrictive ventricular filling may occur in the presence of a normal or even hyperdynamic systolic function. In patients with hypertrophic cardiomyopathy, diastolic filling patterns have a poorer relationship with LV diastolic pressures.[133] This phenomenon is most likely the result of the more profound relaxation abnormalities in the presence of significant LV hypertrophy.

If heart failure is caused primarily by systolic dysfunction, then mitral and pulmonary venous flow Doppler velocities usually show restrictive physiology or pseudonormalised filling pattern because of elevated filling pressure in the decompensated stage. This represents the most common clinical situation of heart failure, usually occurring in patients with a significant coronary artery disease or dilated cardiomyopathy.

LV diastolic function can be assessed by analysis of mitral and pulmonary venous flow velocities using Doppler ultrasound. Different patterns of diastolic filling abnormalities may be observed. The classification of these patterns is summarised in Box 4.2. Grade 1 diastolic dysfunction reflects an impaired relaxation pattern and identifies patients with early stage heart disease. Grade 2 is the pseudonormalisation pattern and represents the transitional phase between abnormal relaxation and the restrictive filling pattern. With respect to grade 1, grade 2 implies increased diastolic pressures and decreased ventricular compliance. Finally, grades 3 and 4 represent the reversible and irreversible forms of restrictive filling pattern, respectively. These diastolic filling patterns are usually present in symptomatic heart disease with a poor prognosis.

Despite this classification, many patients will present with a mixed or indeterminate filling pattern. Additional echocardiographic evaluation and dynamic testing with alterations in loading conditions of the heart may be helpful in further diagnosis. Recent evidence suggested that analysis of changes in transmitral flow patterns during alterations in ventricular loading conditions may help to identify, during the intraoperative period, those patients with length dependent impairment in myocardial function.[139] Finally, the quality of the obtained signals (ultrasound beam alignment, sample volume, and gain settings) and the possible influences of physiological variables may critically affect the reliability of the signals, and hence the reliability and the reproducibility of calculations and diagnosis.

References

1 Grossman W. Diastolic dysfunction in congestive heart failure. *N Engl J Med* 1991;**325**:1557–64.

2 Lorell BH. Significance of diastolic dysfunction of the heart. *Annu Rev Med* 1991;**42**:411–36.

3 Bonow RO, Udelson JE. Left ventricular diastolic dysfunction as a cause of congestive heart failure. Mechanisms and management. *Ann Intern Med* 1992;**117**:502–10.

4 Pagel PS, Grossman W, Haering M, Warltier DC. Left ventricular diastolic function in the normal and diseased heart: perspectives for the anesthesiologist [first of two parts]. *Anesthesiology* 1993;**79**:836–54.

5 Pagel PS, Grossman W, Haering M, Warltier DC. Left ventricular diastolic function in the normal and diseased heart: perspectives for the anesthesiologist [second of two parts]. *Anesthesiology* 1993;**79**:1104–20.

6 Gaash WH. Diagnosis and treatment of heart failure based on left ventricular systolic or diastolic dysfunction. *JAMA* 1994;**271**:1276–80.

7 Dougherty AH, Naccarelli GV, Gray EL, Hicks CH, Goldstein RA. Congestive heart failure with normal systolic function. *Am J Cardiol* 1984;**54**:778–82.

8 Soufer R, Wohlgelernter D, Vita NA, *et al.* Intact systolic left ventricular function in clinical congestive heart failure. *Am J Cardiol* 1985;**55**:1032–36.

9 Vasan RS, Benjamin EJ, Levy D. Prevalence, clinical features and prognosis of diastolic heart failure: an epidemiologic perspective. *J Am Coll Cardiol* 1995;**26**:1565–74.

10 Thompson DS, Waldron CB, Coltart DJ, *et al.* Estimation of time constant of left ventricular relaxation. *Br Heart J* 1983;**49**:250–7.

11 Gaash WH, Apstein CS, Levine HJ. Diastolic properties of the left ventricle. In: Levine HJ, Gaash WH, eds. *The ventricle: basic and clinical aspects.* The Hague: Nijhoff, 1985, pp. 143–70.

12 Mirsky I. Assessment of diastolic function: suggested methods and future considerations. *Circulation* 1984;**69**:836–41.

13 Oh JK, Appleton CP, Hatle LK, Nishimura RA, Seward JB, Tajik AJ. The noninvasive assessment of left ventricular diastolic function with two-dimensional and Doppler echocardiography. *J Am Soc Echocardiogr* 1997;**10**:246–70.

14 European Study Group on Diastolic Heart Failure. How to diagnose diastolic heart failure. *Eur Heart J* 1998;**19**:990–1003.

15 Pouleur H, Karliner JS, Lewinter MM, Covell JW. Diastolic viscous properties of the intact left ventricle. *Circ Res* 1979;**45**:410–19.

16 Gillebert TC, Raes DF. Preload, length–tension relation and isometric relaxation in cardiac muscle. *Am J Physiol* 1994;**267**:H1872–79.

17 De Hert SG, Rodrigus IE, Haenen LR, De Mulder PA, Gillebert TC. Recovery of systolic and diastolic left ventricular function early after cardio-pulmonary bypass. *Anesthesiology* 1996;**85**: 1063–75.

18 Leite-Moreira AF, Gillebert TC. Myocardial relaxation in regionally stunned left ventricle. *Am J Physiol* 1996;**270**:H509–17.

19 Eichhorn EJ, Hatfield B, Marcoux L, Risser RC. Functional importance of myocardial relaxation in patients with congestive heart failure. *J Cardiac Failure* 1994;**1**:45–56.

20 De Hert SG, Gillebert TC, Ten Broecke PW, Mertens E, Rodrigus IE, Moulijn AC. Contraction–relaxation coupling and impaired left ventricular performance in coronary surgery patients. *Anesthesiology* 1999;**90**:748–57.

21 Paulus WJ, Vantrimpont PJ, Shah AM. Acute effects of nitric oxide on left ventricular relaxation and diastolic distensibility. *Circulation* 1994;**89**: 886–898.

22 Appleton CP, Hatle LK, Popp RL. Relation of transmitral flow velocity patterns to left ventricular diastolic function: new insights from a combined hemodynamic and Doppler echocardiographic study. *J Am Coll Cardiol* 1988; **12**:426–40.

23 Nishimura R, Housmans PR, Hatle LK, Tajik AJ. Assessment of diastolic function of the heart: background and current applications of Doppler echocardiography, part II: clinical studies. *Mayo Clinic Proc* 1989;**64**:181–204.

24 Chen W, Gibson DG. Relation of isovolumic relaxation to left ventricular wall movement in man. *Br Heart J* 1979;**42**:51–8.

25 Oldershaw PJ, Dawkins KD, Ward DE, *et al.* Effect of exercise on left ventricular filling in left ventricular hypertrophy. *Br Heart J* 1983;**49**: 568–73.

26 Reduto LA, Wickemeyer WJ, Young JB *et al.* Left ventricular diastolic performance at rest and during exercise in patients with coronary artery disease: assessment with first pass radionuclide angiography. *Circulation* 1981;**63**:1228–35.

27 Choong CY, Abascal VM, Thomas JD, *et al.* Combined influence of ventricular loading and relaxation on transmitral flow velocity profile in dogs measured by Doppler echocardiography. *Circulation* 1988;**78**:672–83.

28 Appleton CP, Gonzales ms, Basnight MA. Relation of left atrial pressure and pulmonary venous flow velocities: importance of baseline mitral and pulmonary venous flow patterns studied in lightly sedated dogs. *J Am Soc Echocardiogr* 1994;**7**: 264–75.

29 Nishimura RA, Abel MD, Hatle LK, Tajik AJ. Relation of pulmonary vein to mitral flow velocities by transesophageal Doppler echo-cardiography: effect of different loading conditions. *Circulation* 1990;**81**:1488–97.

30 Ishida Y, Meisner JS, Tsujioka K, *et al.* Left ventricular filling dynamics: influence of left ventricular relaxation and left atrial pressure. *Circulation* 1986;**74**:187–96.

31 Yellin EL, Nikolic S, Frater RWM. Left ventricular filling dynamics and diastolic function. *Prog Cardiovasc Dis* 1990;**32**:247–71.

32 Myreng Y, Smiseth OA. Assessment of left ventricular relaxation by Doppler echocardio-graphy: a comparison of isovolumic relaxation time and transmitral low velocities with the time constant of isovolumic relaxation. *Circulation* 1990;**81**:260–66.

33 Myreng Y, Smiseth OA, Risoe C. Left ventricular filling at elevated diastolic pressures: relationship between transmitral Doppler flow velocities and atrial contribution. *Am Heart J* 1990;**119**:620–26.

34 Thomas JD, Weyman AE. Echocardiographic Doppler evaluation of ventricular diastolic function: physics and physiology. *Circulation* 1991;**77**:977–90.

35 Appleton CP, Carucci MJ, Henry CP, Olajos M. Influence of incremental changes in heart rate on mitral flow velocity: assessment in lightly sedated, conscious dogs. *J Am Coll Cardiol* 1991;**17**:227–36.

36 Thomas JD. Physical basis for the mitral flow velocity curve in assessing mitral valve area and LV diastolic function. *Echocardiography* 1992;**9**: 301–12.

37 Ohno M, Cheng C-P, Little WC. Mechanism of altered filling patterns of left ventricular filling during the development of congestive heart failure. *Circulation* 1994;**89**:2241–50.

38 Appleton CP, Hatle LK. The natural history of left ventricular filling abnormalities: assessment by two-dimensional and Doppler echocardiography. *Echocardiography* 1992;**9**:437–57.

39 Giannuzzi P, Imparato A, Temporelli PL, *et al.* Doppler-derived mitral deceleration time of early

filling as a strong predictor of pulmonary capillary wedge pressure in postinfarction patients with left ventricular systolic dysfunction. *J Am Coll Cardiol* 1994;**23**:1630–37.

40 Pinamonti B, Di Lenardo A, Sinagra G, Camerini F. Restrictive left ventricular filling pattern in dilated cardiomyopathy assessed by Doppler echocardiography: clinical, echocardiographic and hemodynamic correlations and prognostic implications. *J Am Coll Cardiol* 1993;**22**:808–15.

41 Ortiz J, Matsumoto AY, Ghefter C, *et al.* Prognosis in dilated myocardial disease: influence of diastolic dysfunction and anatomic changes. *Echocardiography* 1993;**10**:247–53.

42 Rihal CS, Nishimura RA, Hatle LK, Bailey KR, Tajik AJ. Systolic and diastolic dysfunction in patients with clinical diagnosis of dilated cardiomyopathy. Relation to symptoms and prognosis. *Circulation* 1994;**90**:2772–79.

43 Klein AL, Hatle LK, Taliercio CP, *et al.* Prognostic significance of Doppler measures of diastolic function in cardiac amyloidosis. A Doppler echocardiographic study. *Circulation* 1991;**83**: 808–16.

44 Oh JK, Ding ZP, Gersh BJ, Bailey KR, Tajik AJ. Restrictive left ventricular diastolic filling identifies patients with heart failure after acute myocardial infarction. *J Am Soc Echocardiogr* 1992;**5**:497–503.

45 Benjamin EJ, Levy D, Anderson KM, *et al.* Determinants of Doppler indexes of left ventricular diastolic function in normal subjects (the Framingham Heart Study). *Am J Cardiol* 1992;**70**:508–15.

46 Valantine HA, Hatle LK, Appleton CP, Gibbons R, Popp RL. Variability of Doppler echocardiographic indexes of left ventricular filling in transplant recipients and in normal subjects. *J Am Soc Echocardiogr* 1990;**3**:276–84.

47 Klein AL, Burstow DJ, Tajik AJ, *et al.* Effects of age on left ventricular dimensions and filling dynamics in 117 normal persons. *Mayo Clin Proc* 1994;**69**:212–24.

48 Miyatake K, Okamoto M, Kinoshita N, *et al.* Augmentation of atrial contribution to left ventricular inflow with aging as assessed by intracardiac Doppler flowmetry. *Am J Cardiol* 1984;**53**:586–9.

49 Takenaka K, Dabestani A, Gardin JM, *et al.* Left ventricular filling in hypertrophic cardiomyopathy: a pulsed Doppler echocardiographic study. *J Am Coll Cardiol* 1986;**7**:1263–71.

50 Maron BJ, Spirito P, Green KJ, *et al.* Noninvasive assessment of left ventricular diastolic function by pulsed Doppler echocardiography in patients with hypertrophic cardiomyopathy. *J Am Coll Cardiol* 1987;**10**:743–7.

51 Labovitz AJ, Lewen MK, Kern M, *et al.* Evaluation of left ventricular diastolic dysfunction during transient myocardial ischemia produced by angioplasty. *J Am Coll Cardiol* 1987;**10**:748–55.

52 Spirito P, Maron BJ. Relation between extent of left ventricular hypertrophy and diastolic filling abnormalities in hypertrophic cardiomyopathy. *J Am Coll Cardiol* 1990;**15**:808–13.

53 Klein AL, Hatle LK, Burstow DJ, *et al.* Serial Doppler characterization of LV function in cardiac amyloidosis. *J Am Coll Cardiol* 1989;**13**:1017–26.

54 Klein AL Hatle LK, Taliercio CP, *et al.* Serial Doppler echocardiographic follow-up of LV diastolic function in cardiac amyloidosis. *J Am Coll Cardiol* 1990;**16**:644–55.

55 Eichhorn EJ, Willard JE, Alvarez L, *et al.* Are contraction and relaxation coupled in patients with and without congestive heart failure? *Circulation* 1992;**85**:2132–39.

56 Thomas JD, Choong CYP, Flachskampf FA, *et al.* Analysis of the early transmitral Doppler velocity curve: affect of primary physiologic changes and compensatory preload adjustment. *J Am Coll Cardiol* 1990;**16**:644–55.

57 Hatle LK, Appleton CP, Popp RL, *et al.* Differentiation of constrictive pericarditis and restrictive cardiomyopathy by Doppler echocardiography. *Circulation* 1989;**79**:357–70.

58 Oh JK, Hatle LK, Sinak LJ, Seward JB, Tajik AJ. Characteristic Doppler echocardiographic pattern of mitral inflow velocity in severe aortic regurgitation. *J Am Coll Cardiol* 1989;**14**:1712–17.

59 Oh JK, Hatle LV, Seward JB, *et al.* Diagnostic role of Doppler echocardiography in constrictive pericarditis. *J Am Coll Cardiol* 1994;**23**:154–62.

60 Dumesnil JG, Gaudreault G, Honos GN, *et al.* Use of the Valsalva maneuver to unmask left ventricular diastolic function abnormalities by Doppler echocardiography in patients with coronary artery disease or systemic hypertension. *Am J Cardiol* 1991;**68** 515–19.

61 Friend JA, Lee GJ, Ragajopalan B, Stallard T. Measurement of blood flow in the large pulmonary veins in dogs. *J Physiol* 1977;**269**:52–63.

62 Keren G, Sherez J, Megidish R, *et al.* Pulmonary venous flow pattern – its relationship to cardiac dynamics. A pulsed Doppler echocardiographic study. *Circulation* 1985;**6**:1105–12.

63 Smallhorn JF, Freedom RM, Olley PM. Pulsed Doppler echocardiographic assessment of extraparenchymal pulmonary vein flow. *J Am Coll Cardiol* 1987;**9**:573–9.

64 Keren G, Sonnenblick EH, LeJemtel TH. Mitral annulus motion. Relation to pulmonary venous and transmitral flows in normal subjects and in patients with dilated cardiomyopathy. *Circulation* 1988;**78**:621–9.

65 Basnight MA, Gonzalez MS, Kershenovich SC, Appleton CP. Pulmonary venous flow velocity: relation to hemodynamics, mitral flow velocity and left atrial volume, and ejection fraction. *J Am Soc Echocardiogr* 1991;**4**:547–58.

66 Klein Al, Tajik AJ. Doppler assessment of pulmonary venous flow in healthy subjects and

patients with heart disease. *J Am Soc Echocardiogr* 1991;**4**:379–92.

67 Kuecherer HF, Kusumoto F, Muhuideen IA, *et al.* Pulmonary venous flow patterns by transesophageal pulsed Doppler echocardiography: relation to parameters of left ventricular systolic and diastolic function. *Am Heart J* 1991;**122**:1683–93.

68 Rossvoll O, Hatle LK. Pulmonary venous flow velocities recorded by transthoracic Doppler, relation to LV diastolic pressures. *J Am Coll Cardiol* 1993;**21**:1687–96.

69 Appleton CP, Galloway JM, Gonzalez MS, Gaballa M, Basnight MA. Estimation of left ventricular pressures using two-dimensional and Doppler echocardiography in adult patients with cardiac disease: additional value of analyzing left atrial size, left atrial ejection fraction and the difference in duration of pulmonary venous and mitral flow velocity at atrial contraction. *J Am Coll Cardiol* 1993;**22**:1972–82.

70 Smiseth OA, Ldemel K, Riddervold F, Blaha M. Changes in pulmonary vein flow pattern during volume loading. *Cardiovasc Res* 1993;**21**:1687–96.

71 Steen T, Voss BM, Smiseth OA. Influence of heart rate and left atrial pressure on pulmonary venous flow pattern in dogs. *Am J Physiol* 1994;**255**:H2296–302.

72 Appleton CP. The hemodynamic determinants of Doppler pulmonary venous flow velocity components: new insights from studies in lightly sedated dogs. *J Am Coll Cardiol* 1997;**30**:1562–74.

73 Nishimura RA, Appleton CP. "Diastology": beyond E and A. *J Am Coll Cardiol* 1996;**27**:372–4.

74 Rodriguez L, Garcia M, Ares M *et al.* Assessment of mitral annular dynamics during diastole by Doppler tissue imaging: comparison with mitral Doppler inflow in subjects without heart disease and in patients with left ventricular hypertrophy. *Am Heart J* 1996;**131**:982–7.

75 Garcia MG, Rodriguez L, Ares M *et al.* Differentiation of constrictive pericarditis from restrictive cardiomyopathy: assessment of left ventricular diastolic velocities in longitudinal axis by Doppler tissue imaging. *J Am Coll Cardiol* 1996;**27**:108–14.

76 Ommen SR, Nishimura RA, Appleton CP *et al.* Clinical utility of Doppler echocardiography and tissue Doppler imaging in the estimation of left ventricular filling pressures: a comparative simultaneous Doppler – catheterization study. *Circulation* 2000;**102**:1788–94.

77 Lisauskas J, Singh J, Courtais M. The relation of the peak Doppler E-wave to peak mitral annulus velocity ratio to diastolic function. *Ultrasound Med Biol* 2001;**27**:499–507.

78 Nagueh SF, Middleton KJ, Kopelen HA, *et al.* Doppler tissue imaging: a noninvasive technique for evaluation of left ventricular relaxation and estimation of filling pressures. *J Am Coll Cardiol* 1997;**30**:1527–33.

79 Sohn DW, Chai IH, Lee DL, *et al.* Assessment of mitral annulus velocity by Doppler tissue imaging in the evaluation of left ventricular diastolic function. *J Am Coll Cardiol* 1997;**30**:474–80.

80 Nagueh SF, Mikati I, Kopelen HA, *et al.* Doppler estimation of left ventricular filling pressure in sinus tachycardia: a new application of tissue Doppler imaging. *Circulation* 1998;**98**:1644–50.

81 Sohn D, Kim Y, Kim H, *et al.* Evaluation of left ventricular diastolic function when mitral E and A waves are completely fused: role of assessing mitral annulus velocity. *J Am Soc of Echocardiogr* 1999;**12**:203–8.

82 Sohn D, Song J, Zo J, *et al.* Mitral annulus velocity in the evaluation of left ventricular diastolic function in atrial fibrillation. *J Am Soc of Echocardiogr* 1999;**12**:927–31.

83 Poelaert J. Diagnosis of diastolic dysfunction: importance of spectral Doppler imaging. *Anesth Analg* 2002;**94**:1043–4.

84 Thomas JD, Garcia MJ, Greenberg NL. Application of color Doppler M-mode echocardiography in the assessment of ventricular diastolic function: potential for quantitative analysis. *Heart Vessels* 1997;**12(suppl)**:135–7.

85 Garcia M, Smedira N, Greenberg N, *et al.* Color M-mode Doppler flow propagation velocity is a preload insensitive index of left ventricular relaxation: animal and human ventilation. *J Am Coll Cardiol* 1999;**35**:201–8.

86 Brun P, Tribouilly C, Duval A. Left ventricular flow propagation during early filling is related to wall relaxation: a color M-mode Doppler analysis. *J Am Coll Cardiol* 1992;**20**:420–32.

87 Stugaard M, Smiseth OA, Risoe C, Ihlen H. Intraventricular early diastolic filling during acute myocardial ischemia, assessment by multigated color M-mode Doppler echocardiography. *Circulation* 1993;**88**:2705–13.

88 Takatsuji H, Mikami T, Urasawa K, *et al.* A new approach for evaluation of left ventricular diastolic function: spatial and temporal analysis of left ventricular filling flow propagation by color M-mode Doppler echocardiography. *J Am Coll Cardiol* 1996;**27**:365–71.

89 De Mey S, De Sutter J, Vierendeels J, Verdonck P. Diastolic filling and pressure imaging: taking advantage of the information in a colour M-mode Doppler image. *Eur J Echocardiography* 2001;**2**:219–33.

90 Garcia MJ, Thomas JD, Klein AL. New Doppler echocardiographic applications for the study of diastolic function. *J Am Coll Cardiol* 1998;**32**:865–75.

91 Nishihara K, Mikami T, Takatsuji H, *et al.* Usefulness of early diastolic flow propagation velocity measured by color M-mode Doppler technique for the assessment of left ventricular diastolic function in patients with hypertrophic cardiomyopathy. *J Am Soc Echocardiogr* 2000;**13**:801–8.

92 Steine K, Flogstad T, Stugaard M, Smiseth OA. Early diastolic intraventricular filling pattern in acute myocardial infarction by color M-mode Doppler echocardiography. *J Am Soc Echocardiograph* 1998;**11**:119–25.

93 Moller JE, Poulsen SH, Sondergaard E, Egstrup K. Preload dependence of color M-mode Doppler flow propagation velocity in controls and in patients with left ventricular dysfunction. *J Am Soc Echocardiogr* 2000;**13**:902–9.

94 Djaiani GN, McCreath BJ, Ti LK, *et al.* Mitral flow propagation velocity identifies patients with abnormal diastolic function during coronary artery bypass graft surgery. *Anesth Analg* 2002;**95**:524–30.

95 Garcia MJ, Ares MA, Asher C, *et al.* An index of early left ventricular filling that combined with pulsed Doppler peak E velocity may estimate capillary wedge pressure. *J Am Coll Cardiol* 1997;**29**:448–54.

96 Gonzales-Vilchez F, Ares M, Ayuela J, Alonso L. Combined use of pulsed and color M-mode Doppler echocardiography for the estimation of pulmonary capillary wedge pressure: an empirical approach based on an analytical relation. *J Am Coll Cardiol* 1999;**34**:515–23.

97 Firstenberg M, Levine B, Garcia M, *et al.* Relationship of echocardiographic indices to pulmonary capillary wedge pressures in healthy volunteers. *J Am Coll Cardiol* 2000;**36**:1664–9

98 Nagueh SF, Kopelen HA, Quinones MA. Assessment of left ventricular filling pressures by Doppler in the presence of atrial fibrillation. *Circulation* 1996;**94**:2138–45.

99 Nagueh SF, Lakkis NM, Middleton KJ, *et al.* Doppler estimation of left ventricular filling pressures in patients with hypertrophic cardiomyopathy. *Circulation* 1999;**99**:254–61.

100 Moller J, Sondergaard E, Seward J, *et al.* Ratio of left ventricular peak E-wave velocity to flow propagation velocity assessed by color M-mode Doppler echocardiography in first myocardial infarction: prognostic and clinical implications. *J Am Coll Cardiol* 2000;**35**:363–70.

101 Ommen SR. Echocardiographic assessment of diastolic function. *Curr Opin in Cardiol* 2001;**16**: 240–5.

102 Lang R, Vignon P, Weinert L, *et al.* Echocardiographic quantification of regional left ventricular wall motion using color kinesis. *Circulation* 1996;**93**:1877–85.

103 Mor-Avi V, Vignon V, Lang RM. Clinical applications of color kinesis: facts versus hopes. In: Perez JE, Lang RM, eds. *Echocardiography and cardiovascular function: tools for the next decade.* Dordrecht, Boston, London: Kluwer Academic Publishers, 1997, pp. 221–40.

104 De Hert SG, Gillebert TC, ten Broecke PW, *et al.* Length-dependent regulation of left ventricular function in coronary surgery patients. *Anesthesiology* 1999;**91**:379–87.

105 Gillebert TC, Leite-Moreira AF, De Hert SG. Load dependent diastolic dysfunction in heart failure. *Heart Fail Rev* 2000;**5**:345–55.

106 Mulvagh S, Quinones MA, Kleiman NS, *et al.* Estimation of left ventricular end diastolic pressure from Doppler transmitral flow velocity in cardiac patients independent of systolic performance. *J Am Coll Card* 1992;**20**:112–9.

107 Nagueh SF, Kopelen HA, Zoghbi WA. Feasibility and accuracy of Doppler echocardiographic estimation of pulmonary artery occlusive pressure in the intensive care unit. *Am J Cardiol* 1995;**75**:1256–62.

108 Pozzoli M, Capomolla S, Pinna G, *et al.* Doppler echocardiography reliably predicts pulmonary artery wedge pressure in patients with chronic heart failure with and without mitral regurgitation. *J Am Coll Card* 1996;**27**:883–93.

109 Yamamoto K, Nishimura RA, Chaliki AP, *et al.* Determination of left ventricular filling pressure by Doppler echocardiography in patients with coronary artery disease. The critical role of left ventricular systolic function. *J Am Coll Cardiol* 1997;**30**:1819–26.

110 Nishimura RA, Tajik AJ. Determination of left-sided pressure gradients by utilizing Doppler aortic and mitral regurgitant signals: validation by simultaneous dual catheter and Doppler studies. *J Am Coll Card* 1988;**11**:317–21.

111 Gorcsan J III, Snow FR, Paulsen W, Nixon JV. Noninvasive estimation of left atrial pressure in patients with congestive heart failure and mitral regurgitation by Doppler echocardiography. *Am Heart J* 1991;**121**:858–63.

112 Nagueh SF. Noninvasive evaluation of hemodynamics by Doppler echocardiography. *Curr Opin in Cardiol* 1999;**14**:217–24.

113 Nishimura R, Appleton C, Redfield M, *et al.* Noninvasive Doppler echocardiographic evaluation of left ventricular filling pressures in patients with cardiomyopathies: a simultaneous catheterization and Doppler echocardiographic study. *J Am Coll Card* 1996;**26**:1226–33.

114 Kuecherer HF, Muhiudeen IA, Kusumoto FM, *et al.* Estimation of mean left atrial pressure from transesophageal pulsed Doppler echocardiography of pulmonary venous flow. *Circulation* 1990;**82**:1127–39.

115 Dini F, Michelassi C, Michele G, *et al.* Prognostic value of pulmonary venous flow Doppler signal in left ventricular dysfunction: contribution of the difference in duration of pulmonary venous and mitral flow at atrial contraction. *J Am Coll Card* 2000;**36**:1295–1302.

116 Cecconi M, Manfrin M, Zanoli R, *et al.* Doppler echocardiographic evaluation of left ventricular end-diastolic pressure in patients with coronary artery disease. *J Am Soc Echocardiogr* 1996;**9**: 241–50.

117 Brunner-LaRocca H, Rickli H, Attenhofer-Jost C, *et al.* Left ventricular end-diastolic pressure can be estimated by either changes in transmitral inflow pattern during Valsalva maneuver or analysis of pulmonary venous flow. *J Am Soc Echocardiogr* 2000;**13**:599–607.

118 Schwammenthal E, Popescu B, Popescu A, *et al.* Noninvasive assessment of left ventricular

end-diastolic pressure by the response of the transmitral A-wave velocity to a standardized Valsalva maneuver. *Am J Cardiol* 2000;**86**:169–74.

119 Hurrell DG, Nishimura RA, Ilstrup DM, *et al.* Utility of preload alteration in assessment of left ventricular filling pressure by Doppler echocardiography: a simultaneous catheterization and Doppler echocardiographic study. *J Am Coll Cardiol* 1997;**30**:459–67.

120 Farias C, Rodriguez L, Garcia M, *et al.* Assessment of diastolic function by tissue Doppler echocardiography: comparison with standard transmitral and pulmonary venous flow. *J Am Soc Echocardiogr* 1999;**12**:609–17.

121 Grodecki P, Klein A. Pitfalls in the echo-Doppler assessment of diastolic dysfunction. *Am J CV Ultrasound Allied Technol* 1993;**10**:213–34.

122 Appleton CP, Jensen JL, Hatle LK, Oh JK. Doppler evaluation of left and right ventricular diastolic function: a technical guide for obtaining optimal flow velocity recordings. *J Am Soc Echocardiogr* 1997;**10**:271–91.

123 Hatle L, Angelsen P. *Doppler ultrasound in cardiology. Physical principles and clinical applications*, 2nd ed. Philadelphia: Lea & Febiger, 1985.

124 Shen WF, Tribouilloy C, Rey JL, *et al.* Prognostic significance of Doppler-derived left ventricular diastolic filling variables in dilated cardiomyopathy. *Am Heart J* 1992;**124**:1524–33.

125 Xie GY, Berk MR, Smith MD, *et al.* Prognostic value of Doppler transmitral flow patterns in patients with congestive heart failure. *J Am Coll Cardiol* 1992;**24**:132–9.

126 Werner GS, Schafer C, Dirks R, Figulla HR, Kreuzer H. Prognostic value of Doppler echocardiographic assessment of left ventricular filling in dilated cardiomyopathy. *Am J Cardiol* 1994;**90**:2772–9.

127 Kuo LC, Quinones MA, Rokey R, Sartori M, Abinader EG, Zoghbi WA. Quantification of atrial contribution to left ventricular filling by pulsed Doppler echocardiography and the effect of age in normal and diseased hearts. *Am J Cardiol* 1987;**59**:1174–8.

128 Gardin JM, Rohan MK, Davidson DM, *et al.* Doppler transmitral flow velocity parameters: relationship between age, body surface area, blood pressure and gender in normal subjects. *Am J Non-invasive Cardiol* 1987;**1**:3–10.

129 Van Dam I, Fast J, de Boo T, *et al.* Normal diastolic filling patterns of the left ventricle. *Eur Heart J* 1988;**9**:165–71.

130 Smith SA, Stoner JE, Russell AE, Sheppard JM, Aylward PE. Transmitral velocities measured by pulsed Doppler in healthy volunteers: effects of acute changes in blood pressure and heart rate. *Br Heart J* 1989;**61**:344–7.

131 Harrison MR, Clifton GD, Pennel AT, DeMaria AN, Cater A. Effect of heart rate on left ventricular diastolic transmitral flow patterns assessed by Doppler echocardiography in normal subjects. *Am J Cardiol* 1991;**67**:622–7.

132 Masuyama T, Kodama K, Nakatani S, Kitabake A. Effects of atrioventricular interval on left ventricular diastolic filling assessed with pulsed Doppler echocardiography. *Cardiovasc Res* 1989;**23**:1034–42.

133 Symanski JD, Nishimura RA, Hurrell DH. Doppler parameters of left ventricular filling are poor predictors of diastolic performance in patients with hypertrophic cardiomyopathy. *Circulation* 1995;**92**:I–269.

134 Nagueh SF, Kopelen HA, Quinones MA. Doppler estimation of left ventricular filling pressures in the presence of atrial fibrillation. *Circulation* 1995;**92**:I–397.

135 Byrg RJ, Williams GA, Labovitz AJ. Effect of aging on left ventricular diastolic filling in normal subjects *Am J Cardiol* 1987;**59**:971–4.

136 Iliceto S, Amico A, Marangelli V, *et al.* Doppler echocardiographic evaluation of the effect of atrial pacing-induced ischemia on left ventricular filling in patients with coronary artery disease. *J Am Coll Cardiol* 1988;**11**:953–61.

137 Castello R, Pearson AC, Kern MJ, *et al.* Diastolic function in patients undergoing coronary angioplasty: influence of degree of revascularization. *J Am Coll Cardiol* 1990;**15**:1564–9.

138 Filipovic M, Seeberger MD, Rohlfs R, *et al.* Doppler indices of diastolic transmitral flow velocity are invalid indicators of myocardial ischemia during high-dose dobutamine infusion in anaesthetized patients. *Eur J Anaesth* 2002;**19**:789–95.

139 De Hert SG, Van der Linden PJ, ten Broecke PW, *et al.* Assessment of length-dependent regulation of myocardial function in coronary surgery patients using transmitral flow velocity patterns. *Anesthesiology* 2000;**93**:374–81.

140 Little WC, Ohno M, Kitzman D, *et al.* Determination of left ventricular chamber stiffness from the time for deceleration of early left ventricular filling. *Circulation* 1995;**92**:1933–40.

141 Douglas PS, Berko BB, Lesh M, *et al.* Alterations in diastolic function in response to progressive left ventricular hypertrophy. *J Am Coll Cardiol* 1989;**13**:461–7.

142 Mego DM, DeGeare VS, Nottestad SY, *et al.* Variation of flow propagation velocity with age. *J Am Soc Echocardiogr* 1998;**11**:20–5.

143 Moller J, Sondergaard E, Poulsen S, Egstrup K. Pseudonormal and restrictive filling patterns predict left ventricular dilation and cardiac death after a first myocardial infarction: a serial color M-mode Doppler echocardiographic study. *J Am Coll Cardiol* 2000;**36**:1841–6.

5 Mitral valve disease

Heinz M Loick, Thomas Wichter, Christoph Schmidt

Introduction

The diagnosis of a functionally important valve disease has an important impact on the therapy of critically ill patients, especially in those with unstable haemodynamics. Various technical applications, including M-mode, two-dimensional (2D) echocardiography, and spectral and colour Doppler technique, are powerful tools for defining the functional severity of the underlying disease.[1–4] The mitral valve has attracted great interest from users of transoesophageal echocardiography (TOE). This is because of the excellent anatomical visualisation, clear delineation of transmitral flow, and high sensitivity and specificity for detection of valve regurgitation. TOE therefore plays an important role in the differential diagnosis of anatomical and functional pathological patterns of the mitral valve apparatus.[5,6] This is particularly true for the diagnosis of valve dysfunction following valve replacement and repair, and for endocarditis of the mitral valve. Several studies have demonstrated the diagnostic value of TOE with respect to preoperative and postoperative evaluation of mitral valve function, thereby allowing evaluation of the surgical result.[5,7–9] Evaluation of the mitral valve apparatus requires a thorough knowledge of anatomical structures, with their functional components and pathophysiological changes (e.g. anatomical identification of a valve prolapse, annulus dilation, valve retraction, etc.). Precise echocardiographic verification of anatomical structures and functional changes in the mitral valve have an impact on the surgical procedure and thereby on perioperative morbidity.[5,8] Apart from the impact on the immediate surgical procedure, other TOE findings such as entrapped air and/or the assessment of the postoperative ventricular function provide essential information for successful weaning of patients from cardiopulmonary bypass.

This chapter outlines important clinical aspects of perioperative use of TOE for the evaluation of anatomy, physiology, and disorders of the mitral valve. It summarises the possibilities of surgical interventions and presents some haemodynamic conditions that are necessary for the evaluation of surgical success by TOE.

Anatomy/physiology

The mitral valve is suspended from the fibrous skeleton of the heart. It comprises the valvular apparatus and the tensor apparatus. The former consists of the mitral annulus, which demarcates the left atrium and the left ventricle, and two leaflets, namely the posterior and anterior leaflets. The tensor apparatus is composed of the chordae tendineae and the papillary muscles, namely the posteromedial and anterolateral papillary muscles. Their vulnerability to dysfunction depends on the location of coronary disease and degree of consequent diminished blood supply. Although only one coronary vessel, the posterior descending coronary artery, delivers the blood to the posteromedial papillary muscle, the anterolateral papillary muscle receives the blood from the circumflex and the left anterior descending coronary arteries. The chordae tendineae are composed of strong fibrous cords. They extend from the margins of both leaflets and converge toward the papillary muscles. During diastole they prevent the leaflets from prolapsing into the left atrium. The chordae tendineae are usually divided into first order if they insert into the free edge of the leaflet, second order if they insert into the ventricular side of the leaflet, and third order if they attach to the base of the mitral valve. The chordae from each papillary muscle insert into both leaflets. The anterior leaflet of the mitral valve has a semilunar shape and is divided into anterior (A1), middle (A2), and lateral (A3) scallops (Figure 5.1A). It occupies 35–40% of the annular circumference and almost two thirds of the orifice area. The posterior leaflet fills the remaining orifice of the mitral valve and is usually divided into the lateral (P1), middle (P2), and medial (P3) scallops. Up to the sector position of

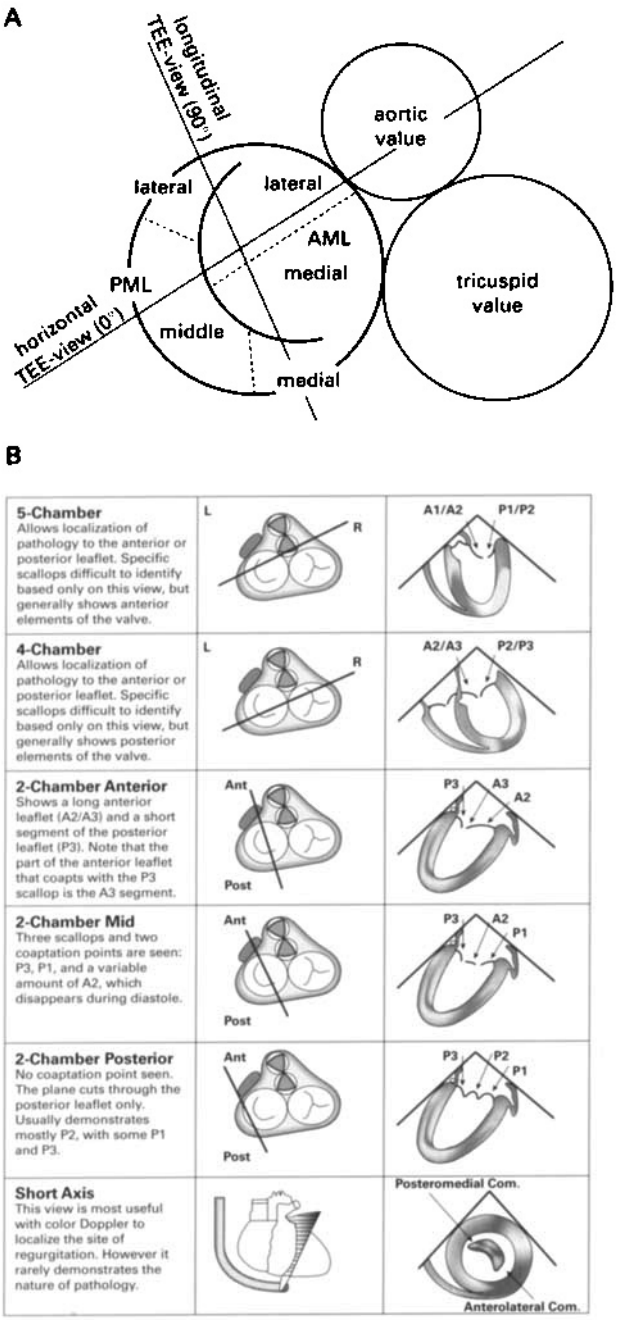

Figure 5.1 Anatomy and evaluation of the mitral valve. **(A)** Anatomical view of the mitral valve and its different scallops. AML = anterior mitral valve leaflet, PML = posterior mitral valve leaflet. **(B)** Systemic mitral valve examination. A1/A2/A3 = anterolateral/middle/posteromedial areas of the anterior mitral leaflet, P1/P2/P3 = anterolateral/middle/posteromedial scallop of the posterior mitral leaflet. (Reproduced with permission from Lambert A-S, Miller JP, Merrick SH, *et al.* Improved evaluation of the location and mechanism of mitral valve regurgitation with a systematic transesophageal echocardiography examination. *Anesth Analg* 1999;**88**:1205–12. Reproduced by permission of Lippincott, Williams & Wilkins.)

the transoesophageal scan, different scallops of the posterior or anterior leaflets are presented and can be studied by TOE (Figure 5.1B).

Diseases of the mitral valve

Morphology and function

Various illnesses such as ischaemic heart disease, myxomatous degeneration, and rheumatic valve disease affect the valve's morphology and thereby its function. Up to the underlying disease, the valve becomes stenotic or insufficient, or both. Stenotic valves are mostly the result of a rheumatic pathological mechanism. The leaflets are thick and often calcified, whereas the cordae tendineae are shortened and relatively immobile. The commissures are fused, resulting in a decreased mitral valve orifice with decreased mitral blood flow, and often an enlarged left atrium. In parallel with mitral stenosis, a huge number of patients also develop mitral insufficiency caused by inadequate coaptation of the leaflets. Mitral insufficiency leads to regurgitation of blood flow during systolic heart action. The underlying pathophysiology includes, as mentioned above, rheumatic disease, myocardial ischaemia, rupture of the chordae tendineae, and mitral valve prolapse. The latter is caused by a displacement of the leaflets toward the left atrium beyond the annulus during systole. It results in a gap between the leaflets in the TOE view. The regurgitant jet is directed through this gap to the opposite side of the prolapsed leaflet (Figure 5.2). The underlying mechanism is characterised by systolic dysfunction of the concomitant papillary muscle. Flail leaflet is another phenomenon that leads to mitral regurgitation; in contrast to mitral valve prolapse, the leaflet is depicted high in the left atrium during systole (Figure 5.3). There are various underlying pathological mechanisms, including myocardial ischaemia and endocarditis. The valve dysfunction that is noted during TOE is a systolic regurgitant blood flow that is directed toward the opposite side of the flail leaflet.

Whenever mitral insufficiency is obvious, there is potential for pathology in the atrium, especially if mitral regurgitation has existed for a long time. In such cases TOE demonstrates an enlarged left atrium and a dilated mitral annulus.

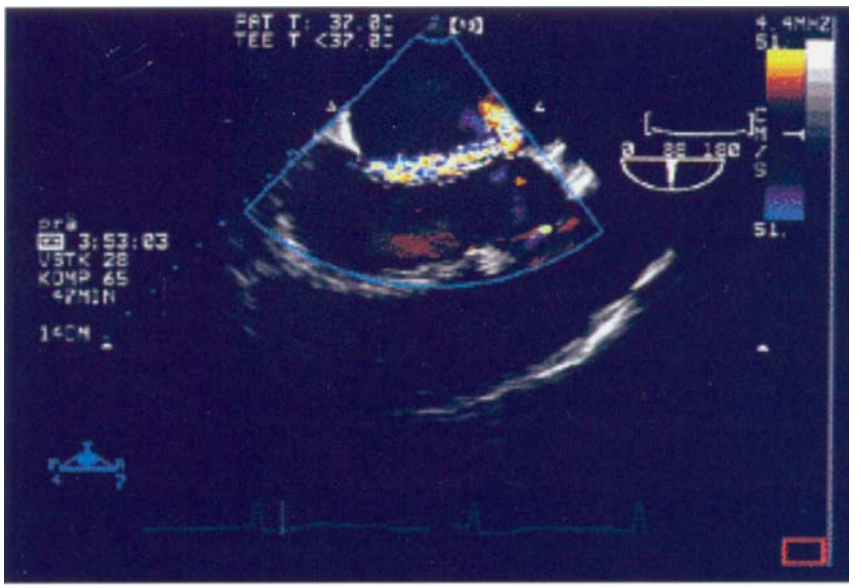

Figure 5.2 Eccentric mitral regurgitation jet, caused by a prolapse of the posterior mitral valve (MOE-LAX).

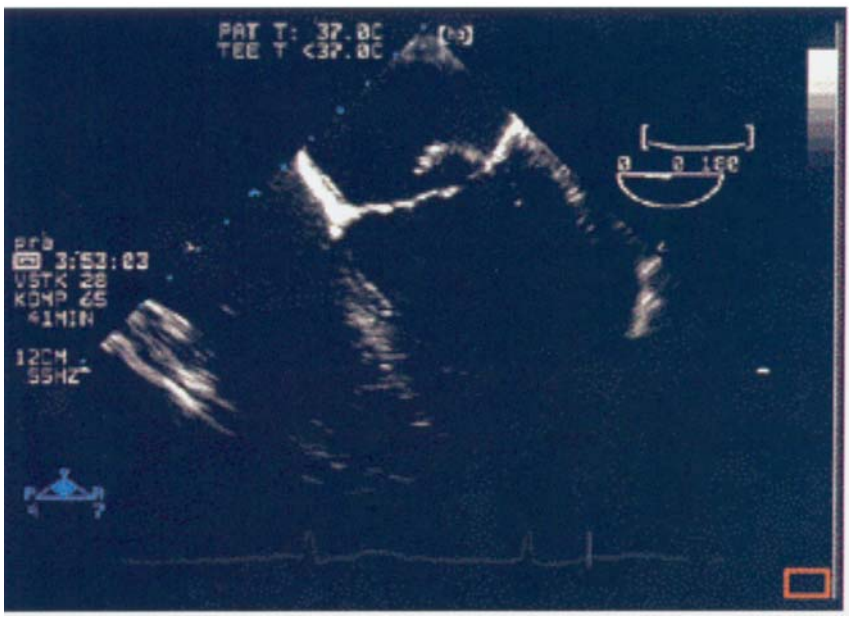

Figure 5.3 MOE four chamber view in a patient with a flail leaflet of the posterior mitral valve.

Epidemiology

Mitral stenosis in adults is most predominately caused by rheumatic fever (77%).[10] Although the prevalence of rheumatic fever has decreased over recent years in industrialised countries, the disease has an important impact on the development of mitral disease in underdeveloped areas. Mitral stenosis in young adults often results from a severe mitral episode or from recurrent episodes of rheumatic fever. In older patients the mitral stenosis is mostly the result of gradual progression of the valvular disease. Because of the different time course of valvular disease, the latency between the rheumatic fever and clinical symptoms of mitral valve obstruction ranges from 11 to 21 years.[10] Mitral insufficiency is not pathological in every case. Taams *et al.*[11] detected mitral regurgitation in 36% of healthy volunteers who were examined using TOE. The detected regurgitant jet was holosystolic, short (< 30 mm) and narrow (< 10 mm), and was considered to be physiological. Pathological mitral insufficiency develops in almost 7% of the population, with 42% suffering from rheumatic valve disease and 44% exhibiting degenerative valvular disease.

Only 3% have a history of endocarditis or congenital valve malformation. In their study of 140 patients who had undergone mitral valve surgery, Cohn and coworkers[12] concluded that mitral insufficiency was due to an ischaemic pathological mechanism in 27% of the patients. Other causes for mitral insufficiency were myxomatous degeneration (41%), rheumatic valve disease (12%), endocarditis (13%), and congenital valve disease (3%).

Diagnostic tools of transoesophageal echocardiography and classification of valve dysfunction

In mitral valve disease the severity of valvular dysfunction can be roughly assessed by clinical symptoms and exercise capacity (New York Heart Association [NYHA] functional class). More detailed information on the morphology, characteristics, severity, and haemodynamic consequences of the valvular lesion may be obtained using echocardiography or invasive cardiac catheterisation. The optimal echocardiographic assessment should be quick, reliable, simple to use, and relatively unaffected by haemodynamic conditions. Although mitral stenosis can be reliably quantified using 2D echocardiographic planimetry and spectral Doppler, quantification of mitral regurgitation using these techniques has proved to be more difficult and less accurate and reliable. However, accurate assessment of valvular function is a prerequisite for clinical decision making for medical management, surgical intervention, and intraoperative assessment of surgical results or residual valvular lesions.

Mitral regurgitation

Recent improvements in and widespread availability of mitral valve repair have expanded the indications for mitral valve surgery. Today, patients with mitral regurgitation may be operated on earlier in the course of their disease. In addition, asymptomatic patients may be operated on based on the magnitude of mitral regurgitation and the appearance of occult left ventricular dysfunction. It is therefore of major importance that mitral regurgitation is quantified accurately, so that surgery may be timed appropriately. Also, accurate intraoperative quantification of residual mitral regurgitation is essential during mitral valve repair surgery. The major determinant of the severity of mitral regurgitation is the effective regurgitant orifice area, which may be fixed (rheumatic disease, endocarditis, mitral valve prolapse) or dynamic (ischaemia induced or functional regurgitation). In addition, the resulting regurgitant volume is affected by left atrial compliance, left ventricular function, concomitant aortic valve disease, peripheral vascular resistance, and other factors. Most frequently, mitral regurgitation is assessed semiquantitatively as mild, moderate, or severe, which works surprisingly well for many clinical applications. Unfortunately, although a variety of quantitative methods derived from echocardiography, angiography, and nuclear and magnetic resonance imaging are available to characterise the severity of regurgitation in more detail, in routine clinical practice these are applied with significant inconsistency.

Haemodynamic and angiographic assessment

Angiographic assessment of mitral regurgitation requires invasive cardiac catheterisation, during which additional information on haemodynamics (pressures, cardiac output, and other parameters), left ventricular function, and coronary anatomy can be obtained. The regurgitation of contrast across the mitral valve during left ventricular angiography is categorically classified as mild, moderate, or severe, or as grade I–IV.[13] These subjective and semiquantitative interpretations are only two of the several methodological limitations inherent to angiographic quantification of mitral regurgitation.[14] However, despite all of its limitations, angiography is still an accepted and widely used method for assessing mitral regurgitation. Haemodynamic information may also be helpful in assessing the severity of a regurgitant mitral lesion. An elevated left atrial pressure with a prominent systolic v wave and elevated pulmonary artery pressures indicate that mitral regurgitation is haemodynamically significant. The recording of pulmonary capillary wedge pressure (PCWP) is widely used as a substitute for left atrial pressure to avoid transseptal puncture during catheterisation, but it has proved to be less reliable. In cases with low

systemic vascular resistance, depressed left ventricular function or a large left atrium, the left atrial pressure and PCWP tracings are not as characteristic and may significantly underestimate the severity of mitral regurgitation.

Echocardiography

The assessment of mitral regurgitation is still among the most challenging problems in echocardiography. 2D echocardiography, particularly the transoesophageal approach, generally provides excellent visualisation of the mitral valve. Apart from providing a structural description of the mitral valve apparatus, measures such as left atrial size and compliance may be helpful in characterising and quantifying mitral regurgitation. However, significant overlap of left atrial size occurs in varying degrees of mitral regurgitation. Moreover, the coexistence of atrial fibrillation diminishes the usefulness of left atrial size as an index of disease severity. In order to move beyond the simple categorical assessment of severity of mitral regurgitation, a variety of echocardiographic techniques have been developed during recent years, including the following:

- quantitative Doppler
- colour Doppler flow mapping
- visualisation of the vena contracta
- proximal flow convergence (proximal isovelocity surface areas [PISAs])
- pulmonary venous flow pattern.

Quantitative Doppler

Flow across an orifice can be calculated from the product of cross-sectional area (πr^2) and flow velocity integral across the orifice.[15] Mitral stroke volume is calculated as the product of mitral annular area and the flow velocity integral obtained from the pulsed wave Doppler waveform in the mitral annular region. In the setting of mitral regurgitation, the regurgitant volume can be calculated as the difference between mitral and aortic stroke volumes, and the regurgitant fraction as the regurgitant volume divided by mitral stroke volume.[16] In patients with severe mitral regurgitation, the regurgitant volume and fraction usually exceed 40 ml and 40%, respectively. The effective regurgitant orifice area may be calculated by dividing the regurgitant volume by the regurgitant time–velocity integral using continuous wave Doppler.[17] In the presence of severe mitral regurgitation, the regurgitant orifice area generally exceeds 35–40 mm^2. Although a strong correlation exists between the effective regurgitant orifice area and the regurgitant fraction, a wide range of orifice sizes are observed for regurgitant fractions greater than 40%, underscoring the added utility of this measurement in the assessment of the severity of mitral regurgitation.

However, quantitative Doppler is time consuming and requires meticulously accurate measurements from multiple imaging windows, because an error in any of the measurements is propagated throughout all subsequent calculations. The largest sources of error in Doppler quantification of mitral regurgitant volume occur with the need to subtract one stroke volume from another and with determination of the mitral annular area, resulting in a tendency toward overestimation of the severity of mitral regurgitation. In addition, quantitative Doppler cannot distinguish the severity of mitral regurgitation from that of aortic regurgitation in patients with both entities.

Colour Doppler flow mapping

Colour Doppler flow mapping of regurgitant jets potentially provides the simplest method for quantifying valvular regurgitation. Initial observations indicated a good correlation between the area of the colour regurgitant jet into the left atrium and the severity of mitral regurgitation assessed by left ventriculography.[2,18] However, the suitability of the jet area method for the quantification of mitral regurgitation depends largely on the regurgitation mechanism and is limited by a variety of haemodynamic and technical factors. Apart from the severity of mitral regurgitation (regurgitant volume, regurgitant orifice size), the area of the mitral regurgitant jet may also be influenced by echocardiography equipment settings, wall impingements or fluid entrainment of the regurgitant jet, differences between left atrial and left ventricular pressures, and left atrial dimensions.[19–22] Therefore, use of jet size alone for the assessment of severity of mitral regurgitation is frequently unreliable and exhibits only a modest correlation with calculated regurgitant volumes ($r = 0{\cdot}63$) and regurgitant orifice areas ($r = 0{\cdot}60$) assessed by quantitative Doppler.[23] For example, a large

Table 5.1 Different colour Doppler measurements for the angiographic grades I-IV of mitral regurgitation

Parameter	Grade I	Grade II	Grade III	Grade IV
JA (cm^2)	3·9 ± 2·5	5·9 ± 2·3	4·6 ± 2·3	8·9 ± 5·5
JL (cm)	3·2 ± 1·1	4·2 ± 0·9	3·9 ± 1·5	5·0 ± 1·8
JA% (%)	13 ± 8	18 ± 7	14 ± 7	25 ± 15
rv28 (mm)	3·8 ± 2·0	6·7 ± 2·8	13·0 ± 4·8	21·6 ± 8·0
rv41 (mm)	2·1 ± 1·9	4·8 ± 2·3	9·6 ± 3·4	15·6 ± 5·8

Values are expressed as mean ± standard deviation. JA = jet area, JA% = relation of jet area to left atrial area, JL = jet length, rv28 (rv41) = proximal isovelocity surface area–radius for the flow velocity of 28 cm/s (41 cm/s). (Data from Grossmann *et al.*[24])

centrally directed jet may be observed in patients with only small regurgitant volume because of entrainment of surrounding blood. By contrast, the regurgitant jets are frequently eccentric (approximately 70%) in patients with organic and severe mitral regurgitation.[24] In these cases, the size of eccentric jets appears to underestimate consistently the severity of mitral regurgitation because of energy loss due to impingement against the left atrial wall.[19,22] Technical factors that affect jet area include (among others) inappropriate gain settings, transducer carrier frequency, pulse repetition frequency, and interobserver variability. Table 5.1 provides different colour Doppler measurements for the angiographical grades I–IV of mitral regurgitation.

Visualisation of the vena contracta

The regurgitant orifice area has been proposed as a marker of lesion severity in valvular regurgitation. Although direct visualisation of the mitral regurgitant orifice area is difficult, it can closely be approximated by measurement of the width of the vena contracta, defined as the narrowest cross-sectional area of the jet at the regurgitant orifice.[23,25] Hall *et al.*[23] reported good correlations of vena contracta width with regurgitant volume ($r = 0{\cdot}86$) and regurgitant orifice area ($r = 0{\cdot}86$) as assessed using quantitative volumetric Doppler (Table 5.2). Vena contracta widths greater than 0·5 cm were associated with severe mitral regurgitation (regurgitant volume > 60 ml, regurgitant orifice area > 0·4 cm^2), whereas those less than 0·3 cm indicated mild regurgitation. Intermediate sized vena contracta (0·3–0·5 cm) would require additional methods such as quantitative Doppler to further clarify the severity of the valvular lesion.[23] The proximal jet width, which has also been proposed as a marker of the severity of mitral regurgitation,[26,27] may differ significantly from the vena contracta width and may therefore overestimate mitral regurgitation. Careful transducer angulation, zoom mode, adjustment of colour Doppler gain, and high frame rates (> 15/s) are helpful in accurate identification of the vena contracta zone and distinction from the proximal convergence zone and the rapidly expanding distal jet. Several studies have suggested that measurement of the vena contracta width is simple and quick, is relatively independent of haemodynamic variables, orifice geometry and instrument settings (gain, carrier frequencies), and is associated with a low interobserver variability.[28–30] Therefore, it is capable of reliable and accurate prediction of regurgitant volume and regurgitant orifice area in mitral regurgitation.[23]

Proximal isovelocity surface area method

Flow through a regurgitant orifice converges toward the orifice in a series of proximal isovelocity hemispheres (i.e. PISAs). In the presence of mitral regurgitation, this flow convergence region can be demonstrated by Doppler as a colour mosaic on the ventricular side of the mitral valve. Regurgitant flow and effective regurgitant orifice can be calculated by manipulating the Nyquist limit of the colour flow and measuring the radius of the flow convergence zone. The baseline of the Doppler colour bar is shifted downward in the direction of the flow to magnify the larger isovelocity contours with lower velocity and reduce error in measurement of radial distance.

Table 5.2 Vena contracta width, regurgitant volume, and effective regurgitant orifice area in relation to severity of mitral regurgitation[23]

Parameter	Degree of mitral regurgitation		
	Mild	Moderate	Severe
VC width (cm)	<0·3	0·3–0·5	>0·5
Rvol (ml)	<40	40–60	>60
EROA (cm^2)	<0·2	0·2–0·4	>0·4

EROA = effective regurgitant orifice area, Rvol = regurgitant volume, VC = vena contracta. (Data from Hall *et al.*[23])

The regurgitant flow rate is calculated as $2\pi r^2 v$, where r is the distance to a contour of velocity v, typically defined by the change in colour at the aliasing boundary. Calculated peak instantaneous flow rates exceeding 500 ml/s are consistently associated with severe mitral regurgitation. The regurgitation volume can be derived by measurement of the maximal regurgitation velocity (Vmr) and the time velocity integral (VTImr):

$$\text{regurgitation volume} = 2\pi r^2 \times Va/Vmr \times VTImr$$

(where Va is the aliasing velocity). The regurgitant orifice area can be calculated by dividing the peak flow rate by the maximal velocity through the orifice (obtained by continuous wave Doppler).[17,31] A regurgitant orifice less than 0·1 cm^2 is usually negligible, whereas those greater than 0·3 cm^2 will impose a significant volume load on the heart and those greater than 0·5 cm^2 typically correspond to a regurgitant fraction in excess of 50% and will usually require surgery. A simplified version of the proximal convergence formula to calculate the regurgitant orifice area has been proposed.[32,33] Assuming that the pressure difference between the left ventricle and the left atrium is 100 mmHg (producing a 5 m/s regurgitation jet), then if the aliasing velocity is set to 40 cm/s the regurgitant orifice area can be calculated as $r^2/2$, where r is the distance to the aliasing contour.[32]

Accurate measurement of the flow convergence region is possible in more than 95% of patients,[24] and it has been shown to be advantageous over the use of the distal regurgitant colour jet size because it is less influenced by factors other than the regurgitant volume.[24,34,35] When compared with angiographical findings, the proximal flow convergence method was reported to differentiate reliably between mild-to-moderate and severe mitral regurgitation in all patients with organic mitral valve disease.[24] The correlation coefficient was less in the subgroup of patients with functional mitral regurgitation and a centrally directed regurgitant jet. However, the proximal convergence method is subject to geometric complexities of the regurgitant orifice that require correction factors. Particularly in severe regurgitation, mitral valve prolapse, and eccentric jets, non-optimal visualisation of the flow convergence region may limit the accuracy of the flow convergence method. It is important to note that errors in the measurement of the flow convergence radius are squared in the flow equation. Flattening of the isovelocity surface in the immediate vicinity of the orifice may result in underestimation of flow and can be avoided by lowering the colour aliasing velocities to increase the measured radius.[36] Additional but clinically less relevant limitations include the temporal variability in the size of the jet and the assumption of a hemispheric surface in the presence of a non-hemispheric flow convergence region.[37]

Pulmonary venous flow pattern

Pulmonary vein flow velocity obtained by transthoracic or transoesophageal pulsed wave Doppler has recently been used more widely in the assessment of the severity of mitral regurgitation.[38] In normal persons, pulmonary vein flow demonstrates forward systolic and diastolic flow and retrograde diastolic flow with atrial contraction. Under normal conditions, systolic pulmonary vein velocity is higher than diastolic velocity. Forward systolic flow exhibits an inverse relation to the severity of mitral regurgitation, resulting in a progressive impairment in systolic pulmonary vein flow velocity with increasing degrees of mitral regurgitation and flow reversal in severe regurgitation. Compared with angiography, pulmonary vein flow velocity had a sensitivity of 86% and a specificity of 81%.[38] However, apart from the severity of mitral regurgitation (regurgitant volume), patterns of pulmonary venous blood flow are strongly influenced by other factors, including left atrial pressure and compliance, left ventricular systolic and diastolic function, peripheral vascular resistance, age, and cardiac rhythm. Furthermore, mitral regurgitation may be underestimated in patients with eccentric regurgitant jets, despite sampling both right and left superior pulmonary veins. For these reasons, pulmonary venous flow should not be taken as an

isolated parameter in the evaluation of mitral regurgitation. A combination of the systolic pulmonary vein flow velocity and the left atrial filling volume has recently been proposed as a means to estimate reliably the regurgitant volume in mitral regurgitation,[39] but it has not been well validated thus far.

Mitral regurgitation index

Thomas *et al.*[40] suggested that the mitral regurgitation index may be used as a severity score for mitral insufficiency. The index includes the following:

- size of regurgitant jet
- regurgitation volume, as assessed using the proximal convergence method
- quantitative Doppler analysis
- profile of the pulmonary venous flow
- pressure gradient within the pulmonary vessels
- dimension of the left atrium.

Each of the parameters is scored between 0 and 3. The total is divided by the number of evaluated parameters, to yield the mitral regurgitation index. An index greater than 2·2 is judged to be severe, whereas an index less than 1·7 is judged to be low with respect to the extent of mitral insufficiency.

Miscellaneous

The regurgitation volume can be calculated as the difference of transmitral and transaortic stroke volumes. The ratio of regurgitation volume and transmitral stroke volume describes the regurgitation fraction. Severe mitral insufficiency can be assumed in the case of rupture to a papillary muscle.

Summary

Intraoperative echocardiographic assessment of mitral regurgitation should be quick, reliable, simple, and relatively unaffected by haemodynamics. For quantification of mitral regurgitation, visualisation of the vena contracta and the proximal flow convergence method (PISAs) are relatively quick and simple methods that give accurate and reliable results. Pulmonary venous flow reliably indicates severe mitral regurgitation in the presence of systolic flow reversal, but it should not be taken as an isolated parameter for the assessment of mitral regurgitation because it depends on several haemodynamic variables and conditions. Assessment of jet size and area by colour Doppler flow mapping is quick and simple but it has insufficient accuracy and reliability in the quantification of mitral regurgitation. By contrast, quantitative Doppler assessment is accurate and reliable, but it is complicated, time consuming, and difficult to apply. In Figure 5.4 the various methods of quantifying mitral regurgitation are depicted. Figure 5.5 provides an example of transoesophageal colour Doppler flow echocardiography in a patient with severe mitral regurgitation.

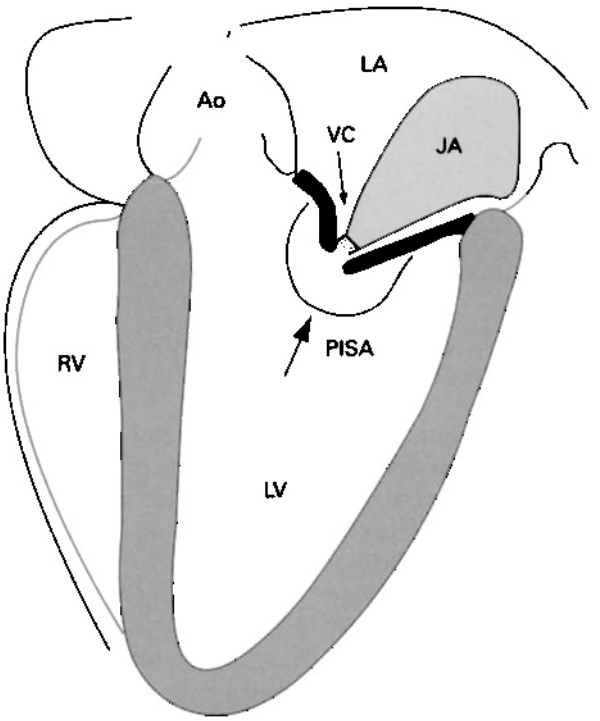

Figure 5.4 Schematic transoesophageal view of the left atrium (LA), the mitral valve, and the left ventricle (LV). Different methods of quantification of mitral regurgitation are depicted: Jet area (JA) and jet length, proximal isovelocity surface area (PISA) according to the flow convergence method, and measurement of the vena contracta width (VC). See text for details. Ao = aorta ascendens, RV = right ventricle.

Mitral stenosis

Improvements in and increasing availability of percutaneous mitral balloon valvotomy for the treatment of mitral stenosis has expanded the number of therapeutic options in patients with

mitral stenosis. The majority of patients with pure or predominant mitral stenosis may be successfully treated using this catheter based intervention with low procedure related risk, thus avoiding cardiac surgery. Therefore, since the introduction of balloon mitral valvotomy, the indications for intervention have expanded from highly symptomatic patients (NYHA functional class III) to patients with moderate degrees of initial stenosis, with the intention being to preserve physical activity and/or sinus rhythm. However, in a subset of patients with severe valvular or subvalvular destruction or calcification, significant concomitant mitral regurgitation, and technical problems or contraindications to percutaneous valvotomy, surgical treatment of mitral stenosis is still indicated. In these cases, valve replacement will frequently be necessary because of unsuitable valve morphology for surgical mitral commissurotomy. It is therefore essential to assess mitral valve morphology and to quantify mitral stenosis accurately so that appropriate therapeutic decisions can be made.

The major determinant of the severity of mitral stenosis is the effective mitral valve orifice area, which is 4·0–5·0 cm^2 in the normal mitral valve. Narrowing of the mitral valve area to below 2·5 cm^2 must occur before symptoms will develop. The subsequent diastolic transmitral pressure gradient results from elevation in left atrial pressure, which is reflected back into the pulmonary venous circulation causing dyspnoea as the major symptom. The transmitral pressure gradient is influenced by heart rate (duration of diastole), transmitral flow (cardiac output), cardiac rhythm (atrial contraction), left ventricular diastolic function (inflow resistance), and other factors. For example, sinus tachycardia or atrial fibrillation with rapid ventricular response results in shortened duration of diastole with subsequent increase in the mitral valve gradient and symptoms.

Haemodynamic and angiographic assessment

Haemodynamic assessment of mitral stenosis using invasive cardiac catheterisation includes right and left heart catheterisation. Right heart catheterisation determines the effects of mitral stenosis on pulmonary circulation and right ventricular function by measuring pulmonary artery and right ventricular pressures, cardiac output, and pulmonary vascular resistance. In addition, subsequent functional tricuspid regurgitation can be evaluated by right atrial pressure tracings or right ventricular angiography. Investigations during exercise may reveal severe

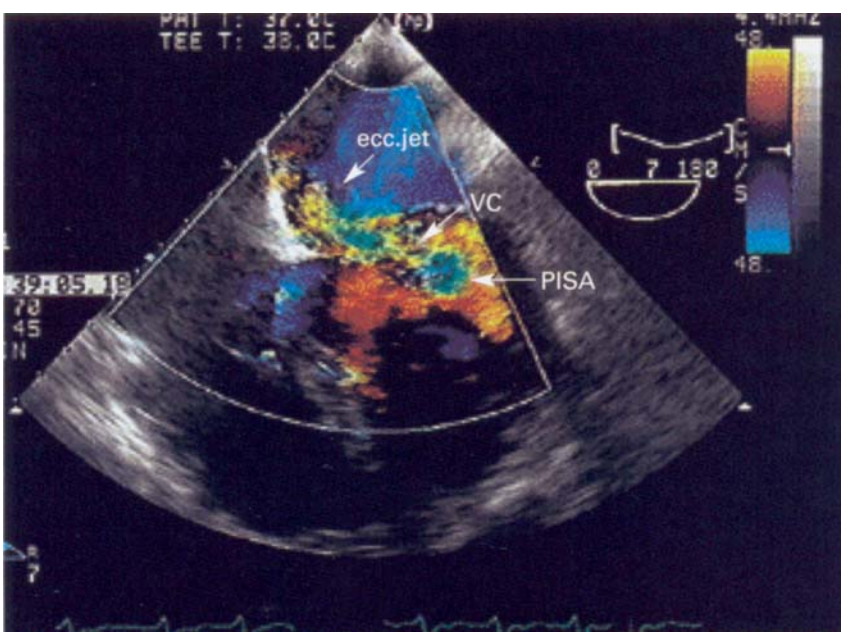

Figure 5.5 Transoesophageal colour Doppler flow echocardiography in a patient with severe mitral regurgitation. The eccentric regurgitant jet impinges against the left atrial septal wall, resulting in an underestimation of the jet size. The vena contracta (VC) and proximal isovelocity surface area (PISA) are visualised and allow quantification of regurgitant flow. See text for details.

mitral stenosis in patients with near normal haemodynamics at rest but with rapidly worsening haemodynamics during increases in heart rate and/or cardiac output induced by exercise. Left heart catheterisation enables measurement of the transmitral gradient by simultaneous recording of left atrial and left ventricular pressures during diastole. However, access to the left atrium is provided only by transseptal puncture, which carries a small risk for pericardial effusion and tamponade. Therefore, some investigators prefer to use the PCWP as a substitute, which is less accurate and less reliable. The transmitral gradient is directly influenced by the effective valve orifice, but also by haemodynamic variables such as the transmitral flow, which is determined by cardiac output and the duration of diastole (heart rate), left ventricular diastolic function, and other factors. Calculations of the mitral valve area from haemodynamic measurements according to Gorlin's formula[41–43] carry several potential sources of error, and therefore these lack accuracy and reliability.

For routine clinical use, several methods for echocardiographic assessment of the mitral valve area have been developed and proved to be accurate and reliable; these are described below.

Echocardiography

2D visualisation with planimetry and the mitral pressure half-time derived from spectral Doppler are currently the most widely used techniques for the assessment of mitral valve area in patients with mitral stenosis. However, a variety of echocardiographic methods have been developed for assessing of mitral stenosis, including the following:

- 2D echocardiography
- transmitral pressure gradient
- planimetry
- flow area
- continuity equation
- proximal flow convergence (PISAs)
- pressure half-time.

Two-dimensional echocardiography

Mitral stenosis is generally diagnosed by 2D echocardiography and is characterised by an increased echo production from the thickened, deformed mitral leaflets, abnormal diastolic leaflet motion, fusion of the commissures, an reduction in mitral orifice area. Consequently, le atrial dimensions are enlarged, sometime resulting in the demonstration of spontaneou echo contrast or left atrial thrombi (Figure 5.6A) Using 2D echocardiography, a semiquantitativ score has widely been used to quantify th morphological alterations of stenotic mitra valves and to assess eligibility for balloon mitra valvotomy.[44,45] The score semiquantitatively (grade 1–4) assesses mitral valve thickness mobility, calcification, and involvement of th subvalvular apparatus. According to the severity of abnormal mitral valve morphology, the resulting score values range between 4 and 16. Similar score systems for mitral valve morphology have been proposed by other groups.[46]

Transmitral pressure gradient

The peak instantaneous and mean transmitral pressure gradients (dp) can reliably be measured from peak and mean diastolic flow velocities (v) across the mitral valve using continuous wave spectral Doppler and the modified Bernoulli equation: $dp = 4v^2$ (Figure 5.6B).[47] However, it should be borne in mind that the transmitral pressure gradient underlies several haemodynamic variables that affect transmitral flow, including heart rate, cardiac output, valvular regurgitation, and ventricular diastolic function. In addition, pressure gradients can be underestimated if the angle between the sampling beam and the flow vector is too large. By contrast, gradients can also be overestimated in patients with concomitant aortic regurgitation because of contamination of the mitral flow stream with the higher velocity aortic regurgitant flow. For these reasons, measurements of the transmitral pressure gradient appear to be less accurate and reliable in determining the severity of mitral stenosis than those of the effective mitral valve orifice area.

Planimetry

2D echocardiographic visualisation of the valve orifice and subsequent planimetry of the mitral valve area from short-axis planes has excellent correlation with the anatomical orifice size.[48,49] However, in patients with less than optimal echocardiographic conditions, planimetric measurement of mitral valve area is less reliable.

Improper imaging plane orientation, inappropriate receiver gain settings, movement of the valve into the short-axis plane, or severe calcification may affect the accuracy of orifice measurements, among other factors.

Flow area

As an alternative to visualising the stenotic mitral orifice by 2D planimetry, measurement of the flow area using colour Doppler has been proposed.[50] The flow area is defined as the width of the central laminar core of the jet in two perpendicular scan planes (e.g. apical long axis and 90° perpendicular) with determination of a minor (a) and a major (b) diameter of the ellipse forming the valve orifice. Valve area is then calculated by applying the equation for the area of an ellipse: $(\pi/4) \times (a \times b)$. Measurement of flow area has good correlation with cardiac catheterisation, direct planimetry, and pressure half-time. It is unaffected by mitral or aortic regurgitation, and should not be influenced by ventricular function or atrial pressure. However, a recent study showed that the flow area method underestimates the anatomical orifice size, as determined from excised valve specimens, and

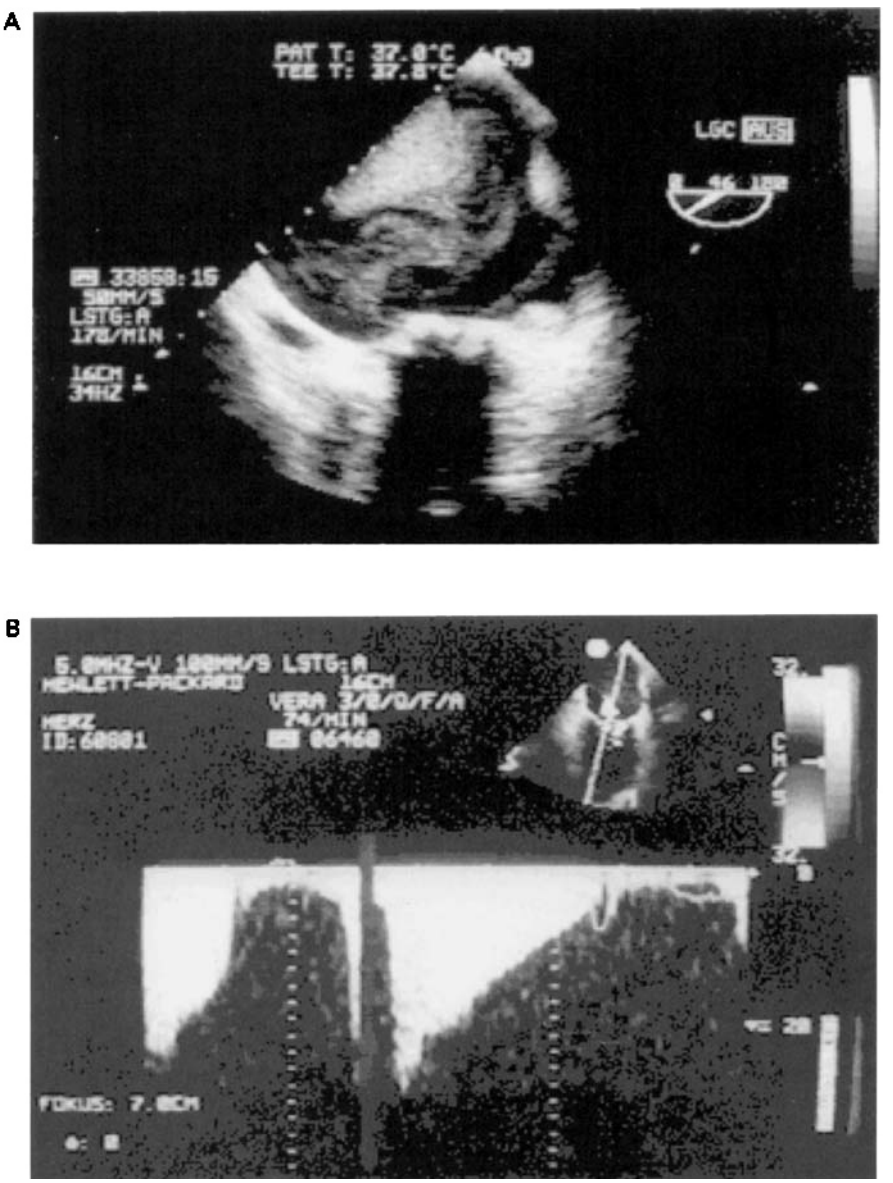

Figure 5.6 Transoesophageal echocardiography in severe mitral stenosis. (**A**) The enlarged left atrium is filled with massive spontaneous echo contrast. The stenotic and immobile mitral valve is severely thickened and calcified. (**B**) Continuous wave Doppler showing a peak instantaneous pressure gradient of 27 mmHg. The pressure half-time is prolonged, resulting in a calculated mitral valve area of 1·0 cm^2.

was less accurate than pressure half-time and proximal convergence methods.[48]

Continuity equation

The continuity equation is based on the principle of conservation of mass and energy. This means that the flow at all points along a tube is constant and is equal to the product of the mean velocity and the cross-sectional area. The mitral valve area can be calculated according as $A_1 \times v_1/v_2$, where A_1 is the reference valve area, v_1 is the reference valve velocity integral, and v_2 is the velocity integral at the stenotic mitral valve.[51] It is important to appreciate that the continuity equation gives the effective and not the anatomical orifice area, and that concomitant regurgitation of the mitral or reference valve results in invalid calculations of the mitral valve area because the equation requires that flows through both the reference and the mitral valve are the same.

Flow convergence method

Based on the continuity equation, the proximal flow acceleration or flow convergence method has also proved to be useful for the determination of mitral valve area in patients with mitral stenosis.[52] In principle, the approach is based on the observation that flow converges uniformly and radially toward an orifice that is small relative to the proximal chamber, thus forming PISAs. The flow convergence method, similar to the continuity equation, predicts the valve area at the point where the velocity of the jet is highest. The mitral orifice area can be determined by dividing instantaneous flow ($2\pi r^2 \times Va \times \alpha/180$) by peak transmitral velocity recorded by continuous wave Doppler, where $2\pi r^2$ is flow through an hemispheric surface, Va is the aliasing velocity, and $\alpha/180$ is the factor that accounts for the inflow angle. Several studies confirmed a good correlation between the flow convergence method and the size of the anatomical mitral orifice area, without systematic underestimation of the valve area.[48,52,53]

Pressure half-time method

The pressure half-time method for assessing mitral valve orifice area follows the haemodynamic concept that in patients with mitral stenosis, the rate of left atrial depressurisation is inversely related to the narrowing of the anatomical orifice: mitral valve area = 220/pressure half-time (ms).[54,55] However, there are variations in this relationship with exercise, changes in heart rate, left atrial compliance, and after balloon mitral valvotomy.[56] In addition, the pressure half-time is dependent on the inflow resistance because of the funnel shape of the mitral apparatus as a whole, including both orifice and non-orifice components. Additional resistance within a stenotic subvalvular apparatus may therefore further slow the rate of pressure decline, leading to smaller calculated area than that delimited by the edges of the stenotic valve leaflets itself. Thus, the valve area measured by pressure half-time is usually smaller than that measured by 2D planimetry and tends to underestimate the anatomical orifice area. The difference between the two methods might represent the quantifiable contribution of the subvalvular apparatus to the obstruction. By contrast, mitral valve area may be overestimated in patients with aortic regurgitation in whom the pressure half-time is decreased.[51,57]

Pulmonary venous flow pattern

Some patients with severe mitral valve stenosis with or without mitral regurgitation exhibit systolic flow reversal. This phenomenon was closely correlated with the presence of atrial fibrillation. Among patients with mitral regurgitation and in atrial fibrillation, flow reversal timing was shorter in patients with significant mitral regurgitation than in patients with mild or no mitral regurgitation.[58]

Summary

For measurement of mitral valve area, echocardiographic planimetry requires no assumptions, and is accurate and reliable when the orifice can be clearly depicted. As an alternative, the pressure half-time method is simple and has the least interobserver variability. However, it is affected by various haemodynamic variables such as atrial and ventricular compliance. Continuity based methods are more difficult and complicated to apply but yield accurate results in appropriate cases. Haemodynamic measurements based on the Gorlin equation are probably less accurate than echo Doppler methods. Table 5.3 provides a quantification of mitral stenosis by 2D echocardiography and continuous wave Doppler.

Table 5.3 Quantification of mitral stenosis by two-dimensional echocardiography and continuous wave Doppler

Parameter / Grade	Grade I	Grade II	Grade III	Grade IV
MVA (cm^2)	>2·5	>1·5–2·5	>1·0–1·5	≤1·0
Gradient (mean)	≤5	>5–10	>10–15	>15

Mitral valve area (MVA) may be measured by planimetry or calculated by pressure half-time, continuous equation, proximal flow convergence, or flow area method. See text for details.

Surgical management

Developments in surgical and interventional techniques have continuously broadened the spectrum of treatment options in patients with acquired valvular lesions, including mitral valve disease. This has also changed therapeutic strategies and expanded the indications for interventional (mitral valvotomy/valvuloplasty) or surgical (mitral valve repair) treatment to improve the patient's condition. However, this approach requires accurate quantification of the valvular lesion so that surgery or catheter based interventions may be timed appropriately. In addition, various procedures such as mitral valve repair, surgical commissurotomy, or balloon valvotomy require assessment of valvular function during the intervention as an essential precondition for successful treatment. To meet these requirements, echocardiography, particularly using the transoesophageal approach, has developed as a major diagnostic tool, providing qualitative and quantitative information on the morphology and function of the mitral valvular lesion.

Mitral regurgitation

The optimal timing for surgery in mitral regurgitation is still a challenge and remains controversial. The development and refinement of surgical techniques and the low perioperative risk associated with mitral valve repair have expanded the indications for surgery in mitral regurgitation from highly symptomatic patients in NYHA functional classes III and IV to include all patients with severe mitral regurgitation, even those who are asymptomatic. The magnitude of mitral regurgitation and the appearance of occult left ventricular dysfunction now represent the principal events that trigger surgical intervention. Left ventricular dysfunction may occur even in asymptomatic patients with mitral regurgitation, but it worsens long-term prognosis even after successful mitral valve repair or replacement. Therefore, early surgery for severe mitral regurgitation has been suggested in patients with no or minor symptoms and normal left ventricular ejection fraction in order to minimise the risk for postoperative left ventricular failure. As a consequence, the safest indication for surgery should no longer be based on symptoms or left ventricular function, but rather on an accurate estimation of the severity of mitral regurgitation.

Mitral stenosis

The timing of intervention for mitral stenosis can be roughly predicted by the patient's symptoms and functional status (NYHA functional class). In most cases mitral valve stenosis can be relieved by balloon mitral valvotomy (valvuloplasty), which offers results comparable to those with open commissurotomy, as shown in several randomised trials.[59] For these reasons, balloon mitral valvotomy has widely replaced surgical commissurotomy for the treatment of mitral valve stenosis. Surgery is reserved for those cases in which valve anatomy is unfavourable for balloon valvotomy or in which balloon valvotomy has been attempted and failed. In most of these cases, the unfavourable anatomy for balloon valvotomy will also be unfavourable for surgical commissurotomy. Therefore, when mitral valve surgery is considered for the treatment of mitral stenosis, valve replacement is usually indicated and necessary. When surgery is performed before severe pulmonary hypertension develops, operative mortality is 1–3%, even with the insertion of a prosthesis.

Surgical procedure

Mitral valve repair

Mitral valve repair is the operation of choice in patients with mitral regurgitation when the valve is suitable for repair, and appropriate surgical skill and expertise are available. Mitral valve repair preserves the patient's native valve without a prosthesis, and it therefore avoids the risks

associated with chronic anticoagulation and prosthetic valve failure. In addition, mitral valve repair reduces surgical risk and improves long-term functional results because of the maintenance of normal left ventricular geometry and function through preservation of the valve–chordal–papillary muscle complex. However, mitral valve repair is technically more demanding than mitral valve replacement, it may require longer extracorporal circulation time, and it may occasionally fail. Severe valve calcification, subvalvular involvement, and anterior leaflet involvement decrease the likelihood that repair will be feasible, whereas uncalcified posterior leaflet disease is almost always repairable. A variety of surgical techniques have been developed for mitral valve repair. Among other procedures, the spectrum of techniques includes direct repair of leaflets, chordal replacement with Gore-Tex suture in mitral valve prolapse, and mitral annuloplasty with or without insertion of a prosthetic annuloplasty ring in patients with a severely enlarged and dilated mitral annulus. It is essential that the sonographer knows exactly what the surgeon has done in order to evaluate the structural and functional results of mitral valve repair intraoperatively, as well as during long-term follow up.

Mitral commissurotomy

Closed commissurotomy remains the surgical technique of choice for the treatment of mitral stenosis in many developing countries. Open commissurotomy was an accepted surgical procedure because it allows direct inspection of the mitral valve apparatus and, under direct vision, division of the commissures, splitting of fused chordae tendineae and papillary muscles, and debridement of calcium deposits. However, it has widely been replaced by interventional percutaneous balloon mitral valvulotomy (valvuloplasty), which offers comparable acute and long-term results and low complication rates.

Mitral valve replacement

Mitral valve replacement is an accepted surgical procedure for patients with severe mitral stenosis or regurgitation who are not candidates for surgical valve repair, commissurotomy, or percutaneous mitral valvotomy. In the presence of significant calcification, fibrosis and subvalvular fusion of the mitral valve apparatus, surgi valve repair or commissurotomy a percutaneous mitral balloon valvulotomy is l likely to be successful. The risk associated w mitral valve replacement is dependent on vario factors, including functional status, age, l ventricular function, cardiac output, a concomitant coronary artery disease or oth medical problems. Mortality rates range fr below 5% in young and otherwise healt patients to 10–20% in older patients wi concomitant medical problems or pulmona hypertension. Major complications of val replacement include prosthetic valve thrombos dysfunction, endocarditis, thromboembolis and structural failure (leaflet degeneration) bioprosthetic valves.

Perioperative transoesophageal echocardiographic monitoring

The diagnosis of a functionally importa valve disease has an important impact on t therapy of critically ill patients, especially those with unstable haemodynamics. The mitr valve has attracted great interest from users TOE. This is because of the excellent anatomic visualisation, the clear delineation of transmitr flow, and the high sensitivity and specifici for the detection of valve regurgitation. TC therefore plays an important role in distinguishi between anatomical and functional pathologic patterns of the mitral valve apparatus.[5,6] Th is especially true for the diagnosis of valv dysfunction following valve replacement an repair.

Compared with transthoracic echocardiograph (TTE), TOE has an outstanding positio intraoperatively. TTE or epicardial scannin cannot be performed continuously, and it therefore unable to deliver "online" informatio on the working heart. Several studies hav demonstrated the high diagnostic value TOE with respect to the preoperative an postoperative evaluation of valve functio thereby allowing evaluation of the surgic result.[5,7–9,60] Precise echocardiographic verificatio of anatomical structures and functional change has an important impact on the surgic procedure and perioperative morbidity.[5,8] Fc instance, in a study conducted by Sheik *et al.*,[5] 1 out of 154 patients who were scheduled for valv surgery suffered an unsatisfactory surgical resul

Those patients underwent a second pump run for revision. Patents in whom intraoperative TOE revealed an unsatisfactory result, and in whom no surgical revision was performed, had higher postoperative morbidity than did those patients whose surgical result was judged to be satisfactory. Apart from the impact on the immediate surgical procedure, other TOE findings such as entrapped air and/or assessment of the postoperative ventricular function provide important information for successful weaning of patients from cardiopulmonary bypass.

As well as having a thorough knowledge of anatomical structures, it is necessary to appreciate the haemodynamic situation when interpreting TOE findings. For instance, TOE findings of mitral insufficiency are dependent on myocardial afterload. This aspect is especially true during valve repair procedures, where the myocardial afterload is often low following the surgical procedure. In this circumstance, afterload must be increased pharmacologically in order to provide similar haemodynamic conditions to those preoperatively for judging the surgical result. Keeping this in mind, TOE is a valuable diagnostic tool in the perioperative setting of mitral valve surgery.

Evaluation of the mitral valve using three dimensional TOE

In most centres, 3D images of heart structures are computerised reconstructions from 2D images. Real-time 3D performance is still under evaluation. The mitral valve structure is highly complex, and 3D TOE provides an excellent overview of anatomy and pathophysiology in mitral valve disease. In mitral valve insufficiency, the ability to visualise the colour Doppler regurgitant jet in three dimensions using this technique offers an additional option for evaluating mitral valve pathophysiology (Figure 5.7). Using digital subtraction methods, the mitral valve annulus can be clearly evaluated in the extracted 3D image of the annuloplasty ring in patients following mitral valve reconstruction.[61]

Costs and benefits of TOE in mitral valve surgery

Benson and Cahalan[62] calculated the costs of routine intraoperative TOE in mitral valve surgery. They found savings of US$450 per case where TOE was used in patients undergoing mitral valve repair, but they identified additional costs of US$150 where TOE was performed in mitral valve replacement. A recent study conducted by Fanshawe *et al.*[63] investigated the costs and benefits of TOE in a cohort of patients undergoing cardiac surgery. Those investigators reported a change in the surgical procedure as a result of intraoperative TOE examinations in 24 cases out of 430 patient records. Five of these cases involved disease of the mitral valve, one case involved the tricuspid valve, and in the remaining 18 patients the presence of a patent foramen ovale was identified intraoperatively. A cost–benefit analysis based on the six valvular diagnoses revealed savings of US$230 per patient. Both studies demonstrated that routine intraoperative TOE in mitral valve repair surgery is justified not only medically but also economically.

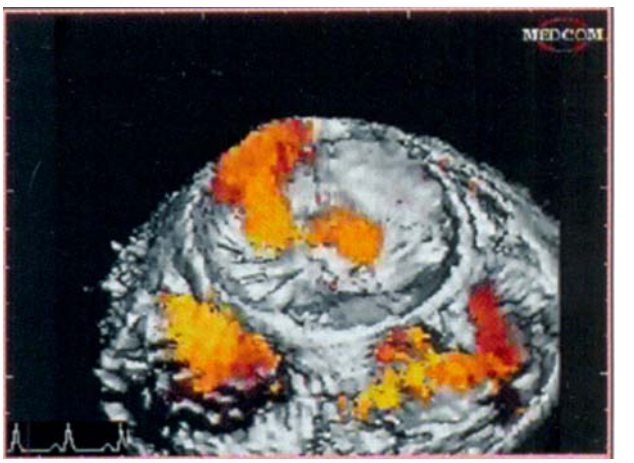

Figure 5.7 Central mitral regurgitation jet in a three-dimensional image (left atrial view).

References

1 Loick HM, Poelaert J, Van Aken H. Transesophageal echocardiography in anesthesia and intensive care. The diagnostic importance of transesophageal echocardiography [in German]. *Anaesthetist* 1997; **46**:504–14.

2 Helmcke F, Nanda NL, Hsiung MC, *et al.* Color Doppler assessment of mitral regurgitation with orthogonal planes. *Circulation* 1987;**75**:175–83.

3 Hatle L. Doppler echocardiographic evaluation of mitral stenosis. *Cardiol Clin* 1990;**8**:233–47.

4 Pieper EPG, Hellemans IM, Hamer HPM, *et al.* Biplane transoesophageal color-flow Doppler imaging in assessing severity of mitral regurgitation: influence of hemodynamic circumstances and mechanism of regurgitation. *J Cardiothorac Vasc Anesth* 1996;**10**:748–55.

5 Sheikh KH, de Bruijn NP, Rankin JS, *et al.* The utility of transesophageal echocardiography and Doppler color flow imaging in patients undergoing cardiac valve surgery. *J Am Coll Cardiol* 1990;**15**:363–72.

6 Seward JB, Khandheria BK, Abel MD, *et al.* Transesophageal echocardiography: technique, anatomical correlations, implementation, and clinical applications. *Mayo Clin Proc* 1988;**63**: 649–80.

7 Sheikh KH, Bengtson JR, Rankin JS, de Bruijn NP, Kisslo J. Intraoperative transesophageal Doppler color flow imaging used to guide patient selection and operative treatment of ischemic mitral regurgitation. *Circulation* 1991;**84**:594–604.

8 Freemann WK, Schaff HV, Khandheria BK, *et al.* Intraoperative evaluation of mitral valve regurgitation and repair by transesophageal echocardiography: incidence and significance of systolic anterior motion, *J Am Coll Cardiol* 1992;**20**:599–609.

9 Czer LS, Maurer G, Bolger A, *et al.* Tricuspid valve repair. Operative and follow-up evaluation by Doppler color flow mapping. *J Thorac Cardiovasc Surg* 1989;**98**:101–10.

10 Horstkotte D, Niehues R, Strauer BE. Pathomorphological aspects, aetiology and natural history of acquired mitral valve stenosis. *Eur Heart J* 1991;**12(suppl B)**:55.

11 Taams MA, Gussenhoven EJ, Cahalan MK, *et al.* Transesophageal Doppler color flow imaging in the detection of native and Björk–Shiley mitral valve regurgitation. *J Am Coll Cardiol* 1989;**13**:95–9.

12 Cohn LH, Kowalker W, Bhatia S, *et al.* Comparative morbidity of mitral valve repair versus replacement for mitral regurgitation with and without coronary artery disease. *Ann Thorac Surg* 1988;**45**:284–90.

13 Sellers RD, Levy MJ, Amplatz K, Lillehei CW. Left retrograde cardioangiography in acquired cardiac disease: technique, indications and interpretation in 700 cases. *Am J Cardiol* 1964;**14**:437–47.

14 Croft CH, Lipscomb K, Mathisk K, *et al.* Limitations of qualitative angiographic grading in aortic or mitral regurgitation. *Am J Cardiol* 1984; **53**:1593–8.

15 Lewis JF, Fuo LC, Nelson JG, Limacher MC, Quinones MA. Pulsed Doppler echocardiographic determination of stroke volume and cardiac output: clinical validation of two new methods using the apical window. *Circulation* 1984;**70**: 425–31.

16 Enriquez-Sarano M, Bailey KR, Seward JB, *et al.* Quantitative Doppler assessment of valvular regurgitation. *Circulation* 1993;**87**:841–8.

17 Enriquez-Sarano M, Seward JB, Bailey KR, Tajik AJ. Effective regurgitant orifice area: a noninvasive Doppler development of an old hemodynamic concept. *J Am Coll Cardiol* 1994;**23**:443–51.

18 Miyatake K, Okamoto M, Kinoshita N, *et al.* Semi-quantitative grading of severity of mitral regurgitation by real-time two-dimensional Doppler flow imaging technique. *J Am Coll Cardiol* 1986;**7**:82–8.

19 Chen C, Thomas J, Anconina J, *et al.* Impact of impinging wall jet on color Doppler quantification of mitral regurgitation. *Circulation* 1991;**84**: 712–20.

20 Castello R. Quantitation of mitral regurgitation by transesophageal echocardiography with Doppler color flow mapping: correlation with cardiac catheterization. *J Coll Cardiol* 1992;**19**:1516–21.

21 Sahn DJ. Instrumentation and physical factors related to visualization of stenotic and regurgitant jets by Doppler color flow mapping. *J Am Coll Cardiol* 1988;**12**:1354–65.

22 Enriquez-Sarano M, Tajik A, Bailey K, Seward J. Color flow imaging compared with quantitative Doppler assessment of severity of mitral regurgitation: influence of eccentricity of jet and mechanism of regurgitation. *J Am Coll Cardiol.* 1993;**21**:1211–19.

23 Hall SA, Brickner ME, Willett WL, Irani WN, Afridi I, Grayburn PA. Assessment of mitral regurgitation severity by Doppler color flow mapping of the vena contracta. *Circulation* 1997;**95**:636–42.

24 Grossmann G, Giesler M, Schmidt A, *et al.* Influence of the mechanism of regurgitation on the quantification of mitral regurgitation by proximal flow convergence method and the jet area method. *Eur Heart J* 1996;**17**:1256–64.

25 Yoganathan AP, Cape EG, Sung HW, Williams FP, Jimoh A. Review of hydrodynamic principles for the cardiologist: applications to the study of blood flow and jets by imaging techniques. *J Am Coll Cardiol.* 1988;**12**:1344–53.

26 Mele D, Vanderpoort P, Palacios I, *et al.* Proximal jet size by Doppler color flow mapping predicts severity of MR. *Circulation* 1995;**91**:746–54.

27 Tribouilloy C, Shen W, Quere J, *et al.* Assessment of severity of mitral regurgitation by measuring regurgitant jet width at its origin with transesophageal Doppler color flow imaging. *Circulation* 1992;**85**:1248–53.

28 Baumgartner H, Schima H, Kuhn P. Value and limitations of proximal jet dimensions for the quantification of valvular regurgitation: an *in vitro* study using Doppler flow imaging. *J Am Soc Echocardiogr* 1991;**4**:57–66.

29 Hoit B, Jones M, Eidbo E, Elias W, Sahn D. Sources of variability for Doppler color flow mapping of regurgitant jets in an animal model of mitral regurgitation. *J Am Coll Cardiol* 1989;**13**:1631–6.

30 Grayburn PA, Fehske W, Omran H, Brickner ME, Luderitz B. Multiplane transesophageal echocardiographic assessment of mitral regurgitation

by Doppler color flow mapping of the vena contracta. *Am J Cardiol* 1994;**74**:912–17.

31 Vandervoort PM. Application of color Doppler flow mapping to calculate effective regurgitant orifice area. *Circulation* 1993;**88**:1150–6.

32 Thomas JD. How leaky is that mitral valve? Simplified Doppler methods to measure regurgitant orifice area. *Circulation* 1997;**95**: 548–50.

33 Rossi A, Dujardin K, Sarano M, Seward JB. Rapid estimation of regurgitant volume by proximal isovelocity surface area: can continuous wave Doppler be omitted? *J Am Soc Echocardiogr* 1998;**11**:138–48.

34 Bargiggia GS, Tronconi L, Sahn DJ, *et al.* A new method for quantification of mitral regurgitation based on color flow Doppler imaging of flow convergence proximal to regurgitant orifice. *Circulation* 1991;**84**:1481–9.

35 Yoshida K, Yoshikawa J, Akasaka T, Nishigami K, Minagoe S. Value of acceleration flow signals proximal to the leaking orifice in assessing the severity of prosthetic mitral valve regurgitation. *J Am Coll Cardiol* 1992;**19**:333–8.

36 Rodriguez L, Anconina J, Flachskampf FA, Weyman AE, Levine RA, Thomas JD. Impact of finite orifice on proximal flow convergence: implications for Doppler quantification of valvular regurgitation. *Circ Res* 1992;**70**:923–30.

37 Schwammenthal E, Chen C, Benning F, *et al.* Dynamics of mitral regurgitant flow rate and orifice area: physiological application of the proximal flow convergence method: clinical data and experimental testing. *Circulation* 1994;**90**: 307–22.

38 Klein AL, Obarski TP, Stewart WJ, *et al.* Transesophageal Doppler echocardiography of pulmonary vein flow: a new marker of mitral regurgitation severity. *J Am Coll Cardiol* 1991;**18**: 518–26.

39 Rossi A, Golia G, Gasparini G, *et al.* Left atrial filling volume can be used to reliably estimate the regurgitant volume in mitral regurgitation. *J Am Coll Cardiol* 1999;**33**:212–17.

40 Thomas L, Foster E, Hoffman JL, Schiller NB. The mitral regurgitation index: an echocardiography guide to severity. *J Am Coll Cardiol* 1999;**33**: 2016–22.

41 Gorlin R, Gorlin G. Hydraulic formula for calculation of area of stenotic mitral valve, other cardiac valves and central circulatory shunts. *Am Heart J* 1951, **41**:1–12.

42 Cohen MV, Gorlin R. Modified orifice equation for calculation of mitral valve area. *Am Heart J* 1972;**84**:839–40.

43 Gorlin WB, Gorlin R. A generalized formulation of the Gorlin formula for calculating the area of the stenotic mitral valve and other stenotic cardiac valves. *J Am Coll Cardiol* 1990;**15**:246–7.

44 Wilkins GT, Weyman AE, Abascal VM, Block PC, Palacios IF. Percutaneous mitral valvotomy: an analysis of echocardiographic variables related to outcome and the mechanism of dilatation. *Br Heart J* 1988;**60**:299–308.

45 Abascal VM, Wilkins GT, Choong CY, Palacios IF, Block PC, Weyman AE. Echocardiographic evaluation of mitral valve structure and function in patients followed for at least 6 months after percutaneous balloon mitral valvuloplasty. *J Am Coll Cardiol* 1988;**12**:606–15.

46 Iung B, Cormier B, DucimetiËre P, *et al.* Immediate results of percutaneous mitral commissurotomy. A predictive model on a series of 1514 patients. *Circulation* 1996;**94**:2124–30.

47 Holen J, Aaslic R, Landmark K, Simonsen S. Determination of pressure gradient in mitral stenosis with Doppler echocardiography. *Br Heart J* 1979;**41**:529.

48 Faletra F, Pezzano Jr A, Fusco R, Mantero A, *et al.* Measurement of mitral valve area in mitral stenosis: four echocardiographic methods compared with direct measurement of anatomical orifices. *J Am Coll Cardiol* 1996;**28**:1190–7.

49 Henry WL, Griffith JM, Michaelis LL, McIntosh CL, Morrow AG, Epstein SE. Measurement of mitral orifice area in patients with mitral valve disease by real-time two-dimensional echocardiography. *Circulation* 1975;**51**:827–31.

50 Kawahara T, Yamagishi M, Seo, *et al.* Application of Doppler color flow imaging to determine valve area in mitral stenosis. *J Am Coll Cardiol* 1991;**18**:85–92.

51 Nakatani S, Masuyama T, Kodama K, Kitabatake A, Fujii K, Kamada T. Value and limitations of Doppler echocardiography in the quantification of stenotic mitral valve area: comparison of the pressure half-time and continuity equation methods. *Circulation* 1988;**77**:78–85.

52 Rodriguez L, Thomas JD, Monterroso V, *et al.* Validation of the proximal flow convergence method: calculation of orifice area in patients with mitral stenosis. *Circulation* 1993;**88**:1157–65.

53 Rifking RD, Harper K, Tighe D. Comparison of proximal isovelocity surface area method with pressure half-time and planimetry in evaluation of mitral stenosis. *J Am Coll Cardiol* 1995;**26**:458–65.

54 Libanoff AJ, Rodbard S. Atrioventricular pressure half-time: measure of mitral valve area. *Circulation* 1968;**38**:144–50.

55 Hatle L, Angelsen B, Tromsdal A. Noninvasive assessment of atrioventricular pressure half time by Doppler ultrasound. *Circulation* 1979, **60**:1096–104.

56 Thomas JD, Weyman AE. Doppler mitral pressure half-time: a clinical tool in search of theoretical justification. *J Am Coll Cardiol* 1987;**10**:923–9.

57 Flachskampf FA, Weyman AE, Gillum L, Chun-Ming L, Abacal VM, Thomas JD. Aortic regurgitation shortens Doppler pressure half-time in mitral stenosis: clinical evidence, *in vitro* simulation, and theoretical analysis. *J Am Coll Cardiol* 1990;**16**:396–404.

58 Palileo RA, Santos RJ. Transesophageal echocardiographic Doppler study of the pulmonary venous flow pattern in severe mitral stenosis with variable degrees of mitral regurgitation. *J Am Soc Echocardiogr* 1997;**10**:540–540.

59 Reyes VP, Raju BS, Wynne J, *et al.* Percutaneous balloon valvuloplasty compared with open surgical commissurotomy for mitral stenosis. *N Engl J Med* 1994;**331**:961–7.

60 Stewart WJ, Currie PJ, Salcedo EE, *et al.* Evaluation of mitral leaflet motion by echocardiography and jet direction by Doppler color flow mapping to determine the mechanism of mitral regurgitation. *J Am Coll Cardiol* 1992;**20**:1353–61.

61 Yamaura Y, Yoshida K, Hozumi T, Akasaka T, Morioka S, Yoshikawa J. Evaluation of the mitral annulus by extracted three-dimensional images in patients with an annuloplasty ring. *Am J Cardiol* 1998;**82**:534–536.

62 Benson MJ, Cahalan MK. Cost benefit analysis of transesophageal echocardiography in cardiac surgery. *Echocardiography* 1995;**12**:171–83.

63 Fanshawe M, Ellis C, Habib S, Konstadt SN, Reich DL. A retrospective analysis of the costs and benefits related to alterations in cardiac surgery from routine intraoperative transesophageal echocardiography. *Anesth Analg* 2002;**95**:824–7.

6 Aortic valve

Jack S Shanewise

Introduction

A careful and complete assessment of the aortic valve should be part of every transoesophageal echocardiographic (TOE) examination. This chapter reviews TOE examination of the aortic valve, echocardiographic assessment of haemodynamic lesions of the aortic valve, and common pathological states that affect the aortic valve encountered in the perioperative period.

Normal anatomy and function of the aortic valve

The aortic valve is located between the left ventricle and the ascending aorta. It normally opens without resistance, permitting the left ventricle to eject blood into the systemic circulation during systole, and closes during diastole to prevent regurgitation of blood from the aorta into the left ventricle. The aortic valve is a semilunar valve with three, symmetrical cusps of similar size. Each cusp is attached to the aortic root at its lower edge along a U-shaped line, with its upper free edge protruding into the lumen of the aorta. Behind each cusp is a pocket-like dilation of the aortic root called the sinus of Valsalva. During diastole the cusps meet in the centre of the aortic root along a line close to their free edges. Each cusp has small fibrous nodule of thickening at the central point of coaptation called the node of Arantius, and a 2–3 mm fringe of thin tissue called the lunula distal to the line of coaptation that may be perforated. The three cusps of the aortic valve are named according to their relationship with the coronary arteries: the left cusp is adjacent to the origin of the left coronary artery, and the right cusp is adjacent to the origin of the right coronary artery. The most posterior of the three cusps is not associated with the origin of a coronary artery and is therefore called the non-coronary cusp.

The aortic valve is located deep within the central portion of the heart and is related to several important structures around its annulus, where the three cusps meet the left ventricular outflow tract (LVOT). The adjacent portions of the left and non-coronary cusps are in continuity with the base of the anterior leaflet of the mitral valve. The atrioventricular portion of the membranous septum is adjacent to the right half of the non-coronary cusp, and the interventricular membranous septum to the posterior part of the right cusp. The anterior halves of the right and left cusps are in contact with the muscular interventricular septum. Distally, the region where the aortic valve joins the cylindrical portion of the ascending aorta at the superior edge of the sinuses of Valsalva is called the sinotubular junction.

Examination of the aortic valve

Evaluation of the aortic valve with TOE should include two-dimensional (2D) images from multiple transducer locations and angles, as well as colour flow (CF) Doppler and spectral Doppler displays.[1] There are two main types of 2D views of the aortic valve: short-axis and long-axis (Figure 6.1). In short-axis views of the aortic valve the imaging plane is perpendicular to the direction of flow through the valve, creating an image that appears as though one is looking directly down onto the valve from the ascending aorta. In long-axis aortic valve views the LVOT, aortic valve, and proximal ascending aorta are aligned and visible in the image, as though one is looking at the valve from the side. Because the aortic valve and the outflow from the left ventricle are orientated at oblique angles to the sagittal and coronal planes of the body in most people, short-axis and long-axis views of the aortic valve are usually obtained with oblique rather than vertical or horizontal imaging planes, and are most easily developed using a multiplane TOE transducer.

The aortic valve is easily located by advancing the TOE probe into the mid-oesophagus, approximately 30 cm from the teeth, until the superior portion of the left atrium is seen in the

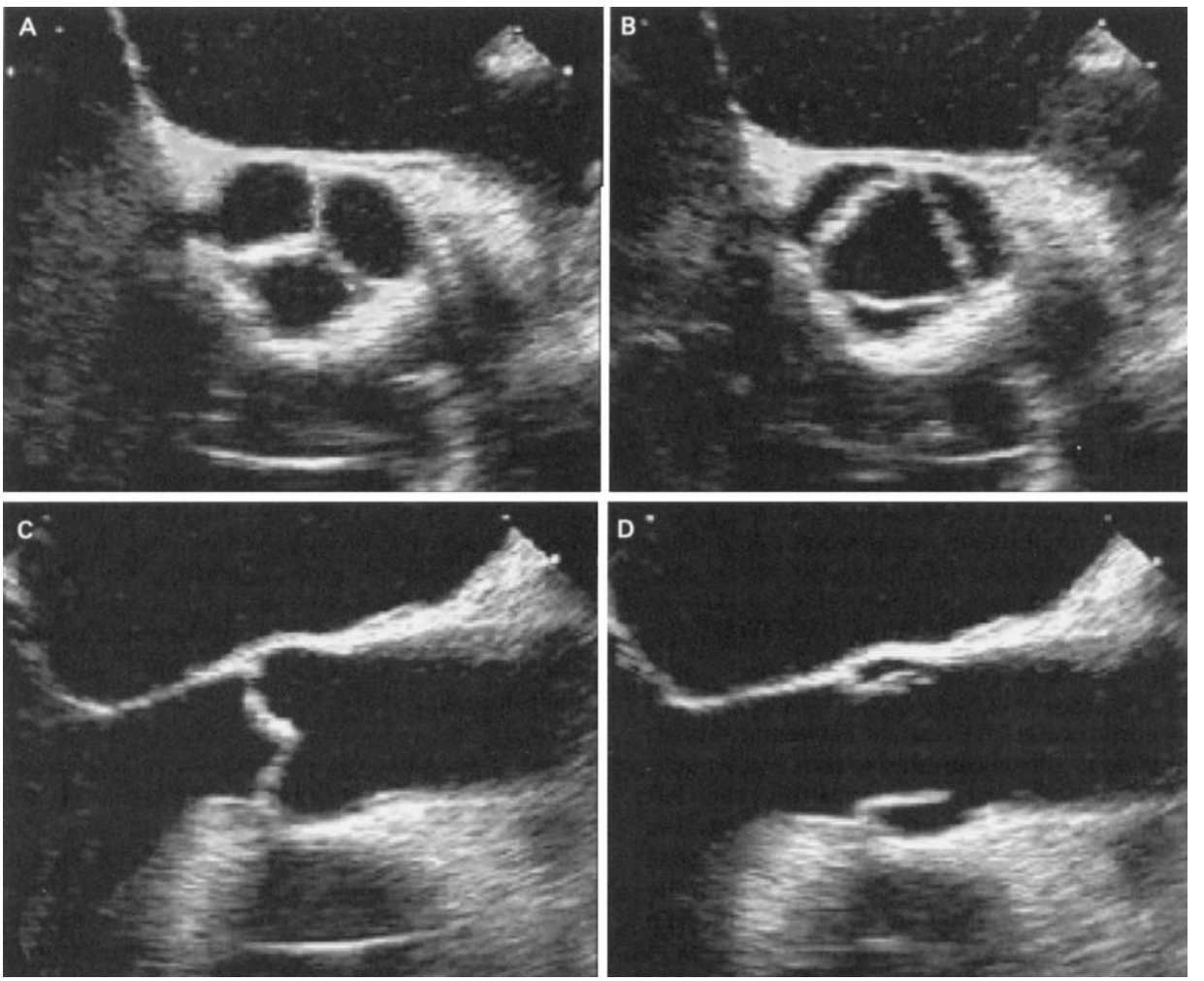

Figure 6.1 Mid-oesophageal views of the aortic valve. **(A)** Short-axis view during diastole with the aortic valve closed; multiplane angle 40°. **(B)** Short-axis view during systole with aortic valve open; multiplane angle 40°. **(C)** Long-axis view during diastole with the aortic valve closed; multiplane angle 130°. **(D)** Long-axis view during systole with aortic valve open; multiplane angle 130°.

near field of the image. The probe is advanced or withdrawn until the aortic valve comes into view, and it is then rotated to the left or the right as needed until the aortic valve is in the centre of the display. The image depth is adjusted to bring the aortic valve to the mid range of the display, usually 10–12 cm. Next, the multiplane angle is increased from 0° until a symmetrical image of the three cusps of the aortic valve comes into view, usually at about 30–60°. This is the mid-oesophageal short-axis view of the aortic valve (Figure 6.1A, B). This view can be approximated with a biplane TOE probe by flexing the tip of the probe to the patient's left in the horizontal plane or to the right in the vertical plane. The mid-oesophageal short-axis view of the aortic valve is the only view that provides a simultaneous image of all three cusps. The cusp adjacent to the atrial septum is the non-coronary cusp, the most anterior cusp is the right coronary cusp, and the cusp to the right side of the display from the other two is the left coronary cusp. The probe is withdrawn slightly to move the imaging plane superiorly just distal to the aortic valve cusps to bring the right and left coronary ostia and then the sinotubular junction into view. The probe is then advanced through, and then inferior to the aortic valve to produce a short-axis view of the LVOT. The short-axis view of the aortic valve at the level of the free edges of the cusps is used to measure the area of the aortic valve orifice during systole by planimetry. CF Doppler is applied in

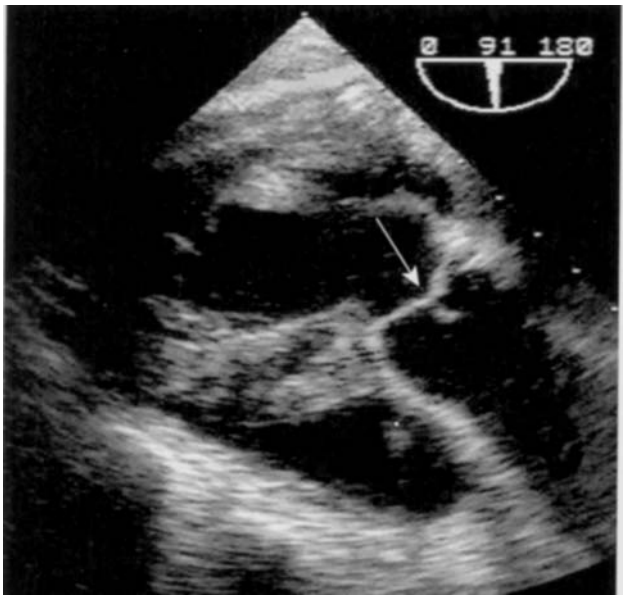

Figure 6.2 Transgastric long-axis view of the aortic valve; multiplane angle 91°. The arrow indicates the point of coaptation of the aortic valve cusps. This view is developed from the transgastric mid-papillary short-axis view by increasing the multiplane angle from 0° and is most useful for making spectral Doppler measurements of aortic valve flow.

this view to detect aortic regurgitation (AR) and to estimate the size and location of the regurgitant orifice.

Then, from the short-axis view, the mid-oesophageal long-axis view of the aortic valve is developed by keeping the valve in the centre of the display while increasing the multiplane angle until the LVOT, aortic valve, and proximal ascending aorta line up in the image, usually between 120° and 160° (Figure 6.1C, D). This view can be approximated with a biplane TOE probe by flexing the tip of the probe to the patient's right in the horizontal plane or to the left in the vertical plane. The LVOT appears toward the left of the display and the proximal ascending aorta toward the right. Only two of the three cusps appear simultaneously in the mid-oesophageal long-axis view of the aortic valve. The right coronary cusp always appears anteriorly or toward the bottom of the display in this view, but the cusp that appears posteriorly may be either the left or the non-coronary cusp, depending on the exact location of the imaging plane as it passes through the valve. The probe is rotated to the patient's left and right in order to examine the entire aortic valve in long-axis planes. The mid-oesophageal long-axis view of the aortic valve is used to assess the size of the aortic root by measuring the diameters of the aortic valve annulus, sinuses of Valsalva, sinotubular junction, and proximal ascending aorta, adjusting the probe position to maximise these dimensions in the image. The diameter of the aortic valve annulus is measured during systole at the points of attachment of the aortic valve cusps to the LVOT. CF Doppler is applied to the mid-oesophageal long-axis view of the aortic valve to assess flow through the LVOT, aortic valve, and proximal ascending aorta and it is especially useful for detecting and quantifying AR. Turbulent systolic flow through a stenotic aortic valve into the ascending aorta is also easily seen with CF Doppler.

There are two transgastric views of the aortic valve; the transgastric long-axis view (Figure 6.2) and the deep transgastric long-axis view (Figure 6.3). The primary purpose of these views is to make pulsed wave (PW) and continuous wave (CW) Doppler measurements by directing the ultrasound beam parallel to the flow through the aortic valve, which is not possible from the mid-oesophageal views. They also provide good images of the ventricular aspect of the aortic valve in some patients. These views are more difficult to obtain than are mid-oesophageal views of the aortic valve and cannot be developed in all patients, but one or the other can usually be achieved in most patients.

The transgastric long-axis view of the aortic valve is developed by starting from the transgastric mid-papillary short-axis view of the left ventricle. From that point the multiplane angle of the imaging plane is increased from 0° until the aortic valve appears in the right side of the far field of the image, usually between 90° and 120°. Sometimes, rotating the probe slightly to the patient's right is needed to achieve the desired view. This view can be approximated with a biplane TOE probe by flexing the tip of the probe to the patient's left from the vertical plane. In the transgastric long-axis view the left ventricular outflow is directed away from the transducer.

The deep transgastric long-axis view is obtained by advancing the probe deep into the stomach and positioning the probe adjacent to the apex of the left ventricle with the multiplane angle at 0°. The probe is then flexed anteriorly until the imaging plane is directed superiorly toward the base of the heart and the aortic valve

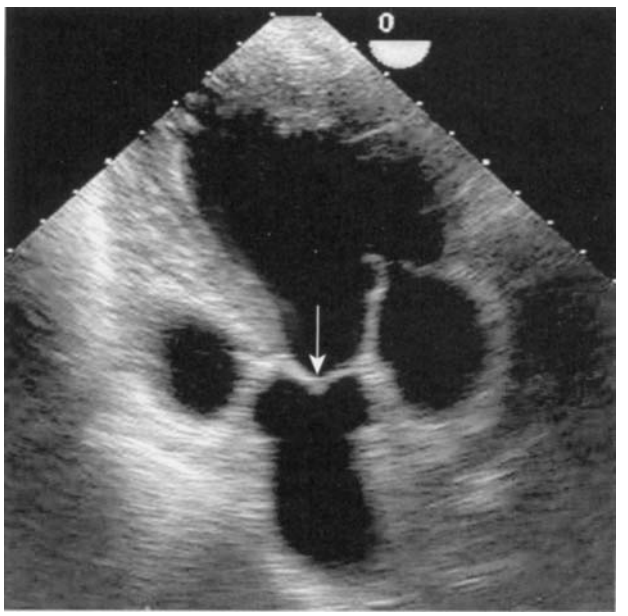

Figure 6.3 Deep transgastric long-axis view of the aortic valve; multiplane angle 0°. The arrow indicates the point of coaptation of the aortic valve cusps. This view is developed by advancing the TOE probe deep into the stomach and flexing the tip anteriorly and to the patient's left. It is most useful for making spectral Doppler measurements of aortic valve flow.

comes into view. Simultaneously flexing the tip of the probe to the patient's left is sometimes helpful in developing this view. The exact position of the probe and transducer is more difficult to determine and control deep in the stomach, but with some trial and error flexing, rotating, advancing, withdrawing, and angle adjusting, this view can be acquired in many patients. In the deep transgastric long-axis view, the aortic valve is located in the far field at the bottom of the display with left ventricular outflow directed away from the transducer. Detailed assessment of valve anatomy is difficult in this view because the LVOT and aortic valve are so far from the transducer, but Doppler quantification of flow velocities in these structures is usually possible.

Doppler quantification of outflow velocities through the LVOT and aortic valve is performed from either the transgastric long-axis view or the deep transgastric long-axis view by directing the spectral Doppler cursor through the middle of the aortic valve as parallel to the direction of flow as possible. CF Doppler imaging of the LVOT and aortic valve is helpful in directing the Doppler beam through the area of maximum flow when making these velocity measurements. Peak outflow velocity at the aortic valve is measured most easily with CW Doppler, assuming that there is no obstruction to outflow proximal to the valve such as a subaortic membrane or hypertrophic obstructive cardiomyopathy. Blood flow velocity in the LVOT is measured by positioning the PW Doppler sample volume in the centre of the LVOT just inferior to the aortic valve cusps. Normal LVOT and aortic valve outflow velocities are less than 1·5 m/s. AR can be seen with CF Doppler from the transgastric mid long-axis and deep transgastric long-axis views and can be used to facilitate the placing of the CW Doppler cursor through the regurgitant jet to obtain a spectral display of the regurgitation.

Assessment of the severity of aortic stenosis

In aortic stenosis (AS) pathological changes of the aortic valve obstruct the outflow from the left ventricle, creating a pressure gradient between the left ventricle and the aorta during systole. Severity of AS is best judged by measuring the aortic valve area (AVA). The area of the normal aortic valve orifice is 2·5–5 cm^2. AS is considered to be significant when the valve area is 1·2 cm^2 or less, and severe when it is less than 0·7 cm^2. Complete TOE assessment of the severity of AS includes 2D imaging with and without CF Doppler, and spectral Doppler measurements of aortic valve flow velocities. Multiple measurements of each parameter are made and averaged to account for beat-to-beat variation and to minimise measurement errors. Ideally, multiple echocardiographic modalities are used to assess AS, looking for consistency to increase confidence in the diagnosis.

The first step in assessing a patient for AS with TOE is to perform a careful 2D examination of the valve with short-axis and long-axis views. The aortic valve cusps in significant AS are usually thickened with markedly limited mobility, and although the presence of three thin, normally mobile cusps excludes the diagnosis of valvular AS, it is surprising how bad an aortic valve can look on 2D examination and yet be only mildly or moderately stenotic. Bicuspid valves are often but not necessarily stenotic, and congenitally unicuspid valves (which are much less common than bicuspid valves) may be severely stenotic but still appear thin and mobile. Often, a short-axis view of the aortic valve at the level of the

cusps provides a direct image of the restricted systolic orifice that can be directly measured with planimetry.[2–5] The imaging plane is moved through the valve to locate the narrowest orifice to avoid underestimation of the severity of AS. This technique is best applied by acquiring a digital loop or clip of the aortic valve and scrolling through the images to mid-systole and tracing around the orifice with the planimetry function of the echocardiograph. In many patients with AS, however, calcification of the cusps and annulus creates acoustic shadows, which obscures the orifice making planimetry unfeasible.[6] Nonetheless, when carefully applied in appropriate patients, AVAs measured with this technique correlate well with other methods such as those applied in the catheterisation laboratory.

The most reliable and commonly used echocardiographic means to assess severity of AS is to measure the velocity of flow through the aortic valve with Doppler. AS increases this velocity beyond the Nyquist limit of PW Doppler, and so CW Doppler must be used. The primary difficulty in measuring aortic valve outflow velocity with TOE is directing the ultrasound beam relatively parallel to the flow in order to avoid significant underestimation. This cannot be done with the mid-oesophageal views, and requires developing either the transgastric long-axis view or the deep transgastric long-axis view. The CW Doppler cursor should be directed through the LVOT and across the aortic valve into the ascending aorta, keeping the angle between the direction of the flow and the beam less than 20° to limit underestimation of the velocity to less than 6%.

Velocity measurements are converted to pressure gradients using the simplified Bernoulli equation ($\Delta P = 4V^2$, where ΔP is pressure gradient [mmHg] and V is the velocity [m/s]). When the peak velocity is used, it gives the peak instantaneous gradient, which is considered to be severe if greater than 64 mmHg (peak aortic valve outflow velocity greater than 4 m/s). Tracing of the outflow velocity profile of the aortic valve to obtain the mean velocity allows calculation of the mean gradient, which is considered to be severe if greater than 50 mmHg.

The gradient across a stenotic aortic valve is not simply a function of the severity of AS, but it is also affected by the volume of flow through the valve. It is possible for the aortic valve gradient to decrease in the end stages of disease because left ventricular function deteriorates and the stroke volume decreases, and so the finding of a moderate aortic valve gradient does not exclude severe AS. Also, increased stroke volume due to aortic regurgitation (AR) or a high cardiac output state such as anaemia or sepsis can increase the gradient in mild or moderate AS.[7] Therefore, it is preferable to measure AVA rather than rely on pressure gradients alone when assessing the severity of AS.[8]

AVA is most commonly measured with echocardiography by applying the continuity equation to velocity measurements made at the LVOT and the aortic valve.[9–12] The continuity equation states that the same amount of flow passes through the aortic valve and the LVOT with each stroke. Flow rate is equal to the velocity of the flow multiplied by the area through which the flow occurs (flow = V × area) and, by the continuity equation, is the same at the aortic valve and at the LVOT, yielding the following:

$$\text{Flow}_{AV} = \text{Flow}_{LVOT}$$

$$V_{AV} \times \text{Area}_{AV} = V_{LVOT} \times \text{Area}_{LVOT}$$

By rearranging, we obtain the following:

$$\text{Area}_{AV} = (V_{LVOT} \times \text{Area}_{LVOT})/V_{AV}$$

The area of the LVOT is obtained from the mid-oesophageal long-axis view of the aortic valve by measuring its diameter (D) during systole and applying the formula for the area of a circle:

$$\text{Area}_{circle} = \pi \times r_2 = \pi(D/2)^2 = (\pi/4) \times D^2 = 0{\cdot}785D^2$$

V_{LVOT} is measured using PW Doppler by placing the sample volume just proximal to the aortic valve in the LVOT, and V_{AV} is measured by directing the CW Doppler through the stenotic valve. It is most convenient to use units of cm/s and cm in order to obtain the AVA in units of cm^2 (Figure 6.4). Common pitfalls in using the continuity equation to measure AVA are underestimation of the LVOT diameter (an error that is squared in the calculation) and underestimating the peak aortic valve velocity because of a large angle between the direction of the flow and the Doppler beam. It is often necessary to make small adjustments in the direction of the CW Doppler until it is directed through the small stenotic orifice to detect the true peak aortic valve velocity. The key is to make

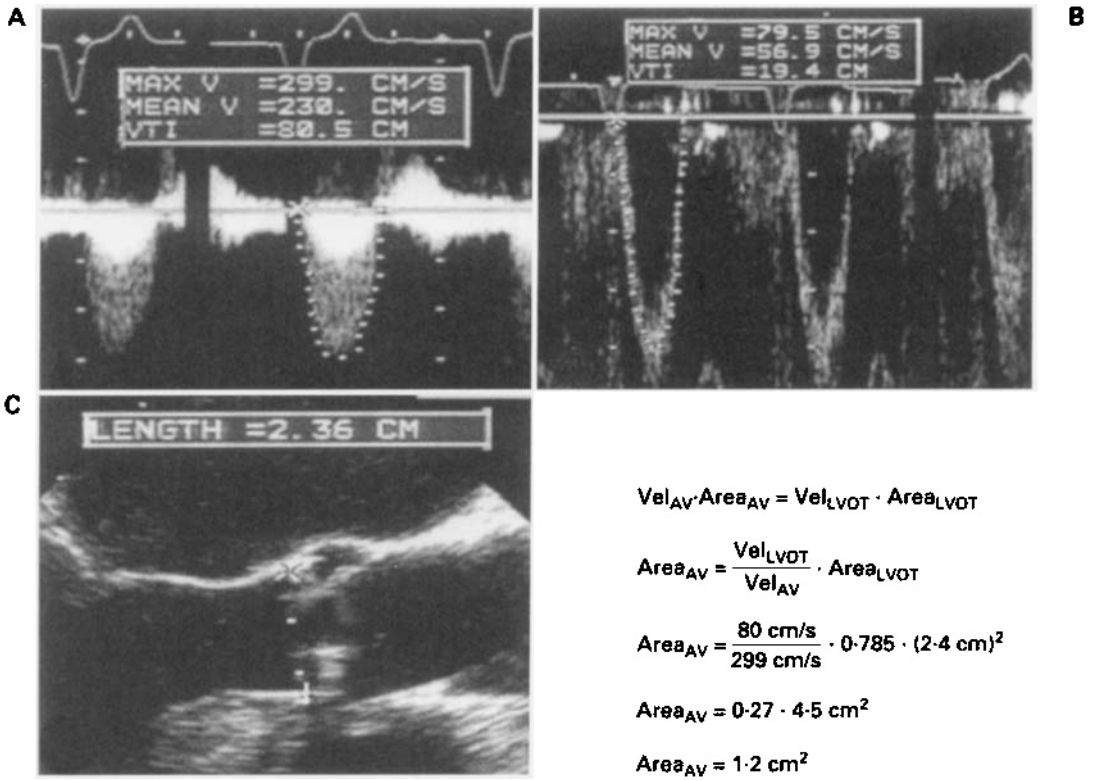

Figure 6.4 Calculation of aortic valve area (AVA) using the continuity equation. **(A)** Spectral display of continuous wave Doppler directed through a stenotic aortic valve from the transgastric mid long-axis view. Scale is 100 cm/s between marks. Peak aortic valve velocity is 299 cm/s. **(B)** Spectral display of pulsed wave Doppler made from the same view as in panel A with the sample volume located in the left ventricular outflow tract (LVOT) just proximal to the aortic valve. Scale is 20 cm/s between marks. Peak LVOT velocity is 80 cm/s. **(C)** Mid-oesophageal long-axis view of the stenotic aortic valve during systole. The LVOT diameter is 2·4 cm. The equations show calculation of the AVA using these three measurements in the continuity equation.

multiple attempts and measurements, looking for results consistent with the appearance of the valve on 2D examination. It is also possible to mistake the velocity profile of mitral regurgitation (MR) for AS if the CW Doppler is inadvertently directed through a MR jet.

Application of CF Doppler to images of the aortic valve can provide some information about the presence of AS,[13] but it does not help to quantify its severity. High velocity, turbulent systolic flow can be seen with CF Doppler in the ascending aorta, and often the narrowness of the orifice can be appreciated in the short-axis view, but mild, moderate, and severe AS produces similar changes with CF Doppler, making their distinction difficult on the basis of CF Doppler findings alone. It is also helpful to look for secondary effects of AS such as hypertrophy and dilation of the left ventricle. Such findings are not specific for AS but they may help confirm the diagnosis in unclear cases.

Assessment of the severity of aortic regurgitation

In AR pathological changes in the aortic valve or aortic root cause imperfect closure of the valve cusps, allowing blood to flow from the aorta retrograde into the left ventricle during diastole. Echocardiographic assessment of the severity of AR is based on the 2D appearance of the valve, CF Doppler images of the regurgitant jet, CW Doppler measurements of the AR flow, and detection of other effects of AR on the heart and great vessels. AR is usually rated on a semiquantitative, 4-point scale ranging from none to trace (0+), mild (1+), moderate (2+), moderately severe (3+), and severe (4+) AR. The clinical significance of AR is not solely determined by the amount of regurgitation present but by its acuity as well; the same amount of AR that developed slowly and is well tolerated in one patient may cause pulmonary oedema when appearing acutely in another.

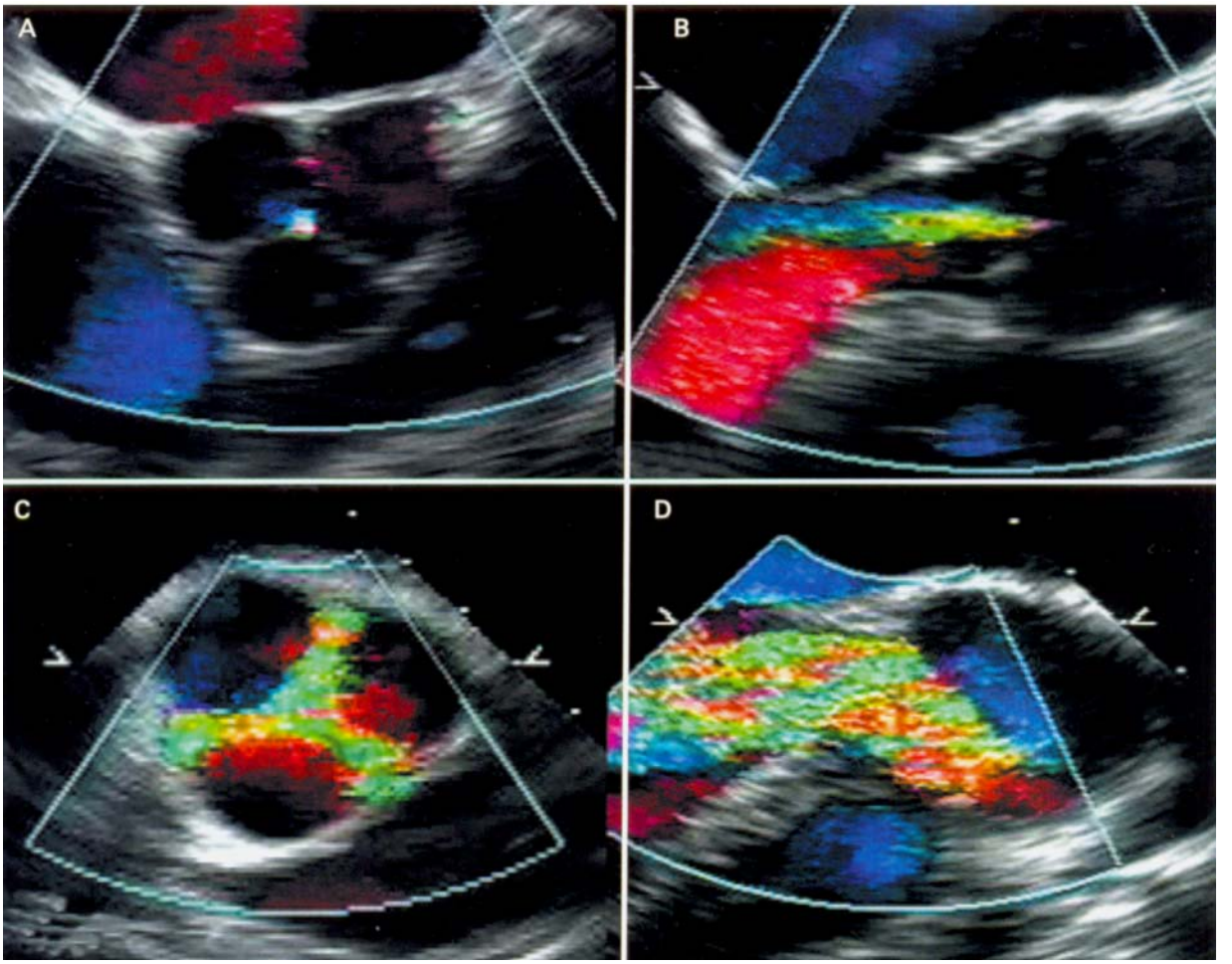

Figure 6.5 Colour flow Doppler of aortic regurgitation (AR). **(A)** Mid-oesophageal short-axis view of an aortic valve with mild (I+) AR showing a small, central regurgitant orifice. **(B)** Mid-oesophageal long-axis view of the same valve as in panel A, showing a narrow jet of AR confined to the left ventricular outflow tract. **(C)** Mid-oesophageal short-axis view of an aortic valve with severe AR due to annular dilation. There is regurgitation visible through the entire surface of cusp coaptation. **(D)** Mid-oesophageal long-axis view of the same aortic valve as in panel C, showing a wide jet of AR extending into the left ventricle. This view was made to optimise the image of the AR and does not show the true diameter of the aortic valve annulus, which was 3·5 cm.

Assessment of AR begins with a careful 2D examination of aortic valve in short-axis and long-axis views, looking for imperfections in coaptation of the cusps due to prolapse, perforations, or annular dilation. Visible gaps between cusps are usually accompanied by regurgitation, which is often significant. The examination is then repeated with CF Doppler, focusing attention on the regurgitant orifice at the level of the valve and the regurgitant jet in the LVOT. The size and location of the regurgitant orifice are assessed by applying CF Doppler to the short-axis view of the aortic valve, positioning the imaging plane just distal to the valve cusps and then moving it slowly into the valve until the holodiastolic, high velocity regurgitant flow just comes into view. A small, central regurgitant orifice usually is associated with mild AR and larger or eccentric orifices with more severe AR (Figure 6.5). The length of the regurgitant jet is best assessed with the mid-oesophageal long-axis view, moving the imaging plane from the left border of the LVOT across its centre to the right border to avoid missing an eccentric jet. There is a correlation between the size of the regurgitant jet as seen with CF Doppler and the amount of AR,[14] but the relationship is complex and influenced by factors other than severity of AR. One way to assess the size of the jet is to compare the width at its origin at the valve with the width

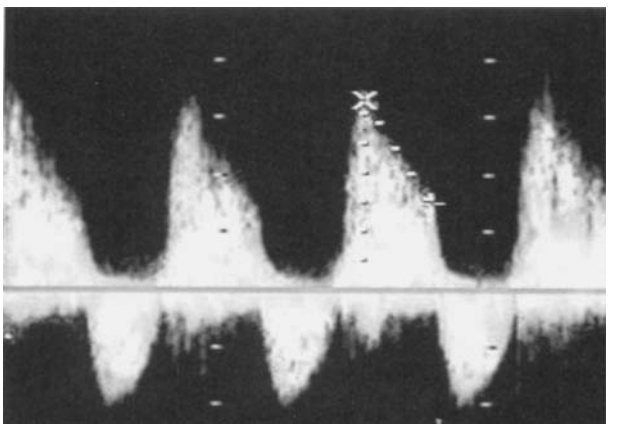

Figure 6.6 Spectral display of continuous wave Doppler made through a regurgitant aortic valve from the deep transgastric long-axis view. Aortic regurgitation (AR) flow is toward the transducer and above the baseline, and systolic outflow through the aortic valve is away from the transducer and below the baseline. Scale is 100 cm/s between each mark. The steep slope of the AR profile suggests severe AR.

of the LVOT measured in the mid-oesophageal long-axis view of the aortic valve. A ratio greater than 0·4 correlates with severe AR as graded with angiography.[15] Exceptions may occur, however, such as when a mild but eccentric jet of AR sprays across the LVOT after striking the ventricular septum or the anterior leaflet of the mitral valve. Colour M-mode can be used to facilitate this measurement and helps to distinguish diastolic regurgitant flow in the LVOT from systolic outflow when tachycardia is present. The depth to which the AR jet extends into the LV should also be considered. A narrow jet of AR that does not extend beyond the LVOT is usually not severe. On the other hand, a jet seen to strike and spray off of the posterior wall of the left ventricle is likely to be significant, especially if it is visible in the transgastric views. In patients with mitral stenosis or a mitral prosthesis it is possible to confuse the turbulent mitral inflow seen by CF Doppler with AR. Both appear as turbulent flow moving toward the apex of the left ventricle during diastole, but only AR is visible in the LVOT.

The CW Doppler profile of an AR jet is made from the transgastric mid long-axis view or the deep transgastric long-axis view and has an easily recognisable shape (Figure 6.6). The flow is diastolic and toward the transducer, with an early peak velocity between 3 and 5 m/s decreasing at a steady rate from the peak until the onset of systole. The intensity or brightness of the profile is a function of the amount of regurgitant flow encountered by the ultrasound beam and is greater with more severe AR. The rate of decrease or slope of the velocity profile is also influenced by the severity of AR, decreasing more rapidly with more severe and acute AR.[16,17] One measure of this slope is the pressure half-time of the AR CW Doppler profile, which suggests significant AR if it is less than 200 ms and mild AR if it is greater than 400 ms. Most echocardiographs have an automated function to facilitate making this measurement. In extreme cases of acute, severe AR, the left ventricular and aortic pressures equalise during diastole, causing the velocity of the AR jet to rapidly fall to 0.

Another approach to assessing severity of AR with TOE is to measure and compare the forward stroke flow of the aortic valve and mitral valve by multiplying the time velocity integral of each valve's flow profile obtained with spectral Doppler by its area from 2D images.[18] In the presence of AR without MR, the difference between the two is the AR regurgitant volume, which is considered severe if it is greater than 50% of the total forward stroke volume of the aortic valve, and mild if it is less than 20%.

AR can cause other changes within the heart and great vessels that are detectable with TOE. Diastolic flow reversal in the descending thoracic aorta may be due to severe AR and is measured with TOE by placing the PW Doppler sample volume in the descending thoracic aorta.[19,20] Early diastolic flow reversal is normal, but holodiastolic flow reversal is a sign of severe AR (Figure 6.7). Another echocardiographic sign of severe AR is presystolic closure of the mitral valve.[21] The rapid rise in left ventricular diastolic pressure caused by AR can close the mitral valve before ventricular systole, and in some cases even cause diastolic MR to appear. This is most easily detected by acquiring a digital loop or clip of the mid-oesophageal long-axis view simultaneously showing the aortic valve and mitral valve with CF Doppler, and scrolling through each diastolic frame looking for closure of the mitral valve and/or MR before the AR jet disappears with the onset of ventricular systole. Presystolic MR may also be detected with CW Doppler from the mid-oesophageal position by directing the ultrasound beam through the mitral valve and looking for flow toward the transducer (MR) before the QRS complex appeals on the electrocardiogram. When present, presystolic closure of the mitral valve and diastolic MR are reliable signs of severe AR.

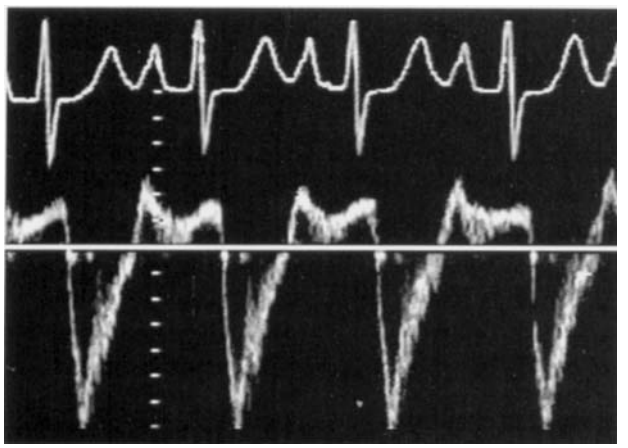

Figure 6.7 Holodiastolic flow reversal in the descending thoracic aorta due to severe aortic regurgitation. Spectral display of pulsed wave Doppler with sample volume located in mid-descending thoracic aorta. Antegrade flow is below the baseline, and retrograde flow reversal is above the baseline. Scale is 10 cm/s between each mark.

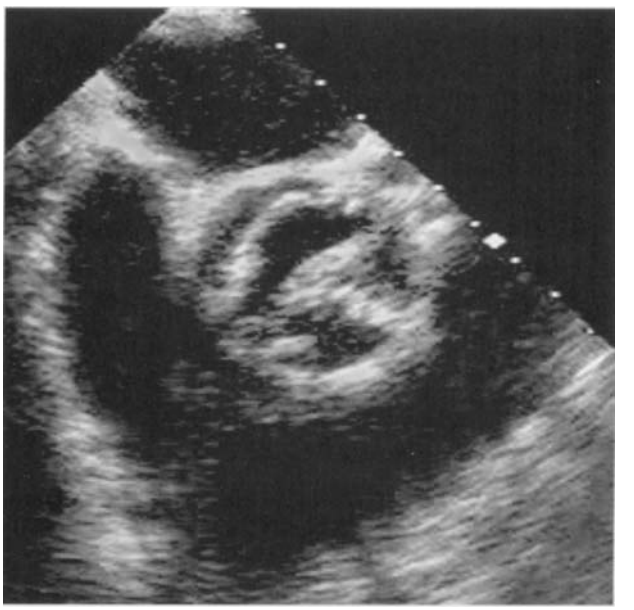

Figure 6.8 Mid-oesophageal short-axis view of a congenitally malformed, bicuspid aortic valve during systole with moderate thickening of the leaflets and stenosis. The orifice of the valve is more elliptical than triangular. A typical raphe is visible in the anterior cusp, and the valve appeared to have three cusps when closed during diastole.

Because the heart compensates for regurgitation by enlarging, left ventricular size is an important indicator of the significance of AR and is easily measured with TOE.[22–24] Patients with AR referred for valve replacement whose left ventricular end-systolic diameter is less than 55 mm are more likely to have preserved left ventricular function postoperatively and to have a better long-term prognosis than those with larger ventricles.[25] The finding by TOE of a dilated left ventricle is consistent with, but not specific for, significant AR.

Specific diseases of the aortic valve

Congenital malformations of the aortic valve

Bicuspid aortic valve is the most common congenital heart defect, with an incidence of 1–2% reported in autopsy series,[26] and it has been shown to occur in familial clusters.[27] Most bicuspid aortic valves function normally in the first few decades of life and then develop stenosis because of accelerated calcification and thickening of the cusps, typically presenting for surgery in the fifth or sixth decade of life.[28] Some bicuspid valves present in earlier adulthood with AR due to degeneration and prolapse of a cusp.[29] Bicuspid aortic valve also predisposes to infective endocarditis, which causes AR by destruction of the cusps and valve annulus.

The hallmark echocardiographic feature of a bicuspid aortic valve is an elliptical rather than the normal triangular opening during systole (Figure 6.8). The two cusps of the valve are located anteriorly and posteriorly in about half of cases, and to the right and to the left in the other half. Approximately half of bicuspid aortic valves have a raphe or ridge in one cusp, usually the anterior or the right, and can appear to have three cusps when closed during diastole.

Unicuspid congenitally malformed aortic valves are much less common than bicuspid and usually present in childhood or early adulthood with stenosis. Echocardiographic features include a single, mobile cusp with a small, circular or elliptical orifice that domes toward the aorta during systole. The valve area is measured by planimetry with the short-axis view by moving the imaging plane through the valve until the minimal orifice is seen, which is then traced at mid-systole. There are two recognised forms, unicommissural with a raphe visible in the short-axis view and a commissural without a raphe.[30]

Calcific aortic stenosis

The most common cause of significant AS is calcific degeneration of a previously normal valve. This process can be seen in its early stages by TOE with mild, sclerotic changes of the cusps as areas of nodularity and thickening accompanied by mild restriction of movement.[31] As the process progresses and the cusps thicken more and move less, the stenosis becomes more severe. Calcific AS of a previously normal valve usually presents later in life than bicuspid valve AS, typically in the seventh and eighth decades. The principle echocardiographic challenge is to accurately assess the severity of the stenosis, usually by measuring the AVA with the continuity equation.

Echocardiographic features of calcific AS include the presence of three separate cusps with areas of increased echo density and thickness associated with limited movement and opening during systole. Each of the three cusps remains distinct until the late stages of the disease. As calcifications accumulate on the valve, however, acoustic shadowing makes it difficult to obtain detailed images of the cusps, and it may not be possible to distinguish calcific AS from bicuspid aortic valve disease by echocardiographic appearance alone. Severely stenotic valves typically show minimal movement of the cusps during systole. On the other hand, it is surprising how thickened and distorted the cusps can appear in calcific AS and yet be only mildly stenotic as long there is some movement of the cusps. The calcific thickening is often seen to extend from the aortic valve into the base of the anterior leaflet of the mitral valve, but it usually spares the distal portions of the leaflet, rarely causing significant haemodynamic lesions of the mitral valve. AR may accompany calcific AS, but it is usually at most mild to moderate in severity.

Rheumatic aortic valve disease

Rheumatic heart disease, the chronic sequela of acute rheumatic endocarditis, may involve the aortic valve, but it preferentially affects the mitral valve, and so rheumatic aortic valve disease almost always coexists with rheumatic mitral stenosis and/or regurgitation. Typical echocardiographic findings of rheumatic aortic valve disease are fusion of the commissures and thickening of the cusps, resulting in a fixed orifice with mixed AS and AR (Figure 6.9). In the late stages rheumatic degeneration of the aortic valve may be difficult to distinguish from calcific AS other than by the associated rheumatic changes in the mitral valve.

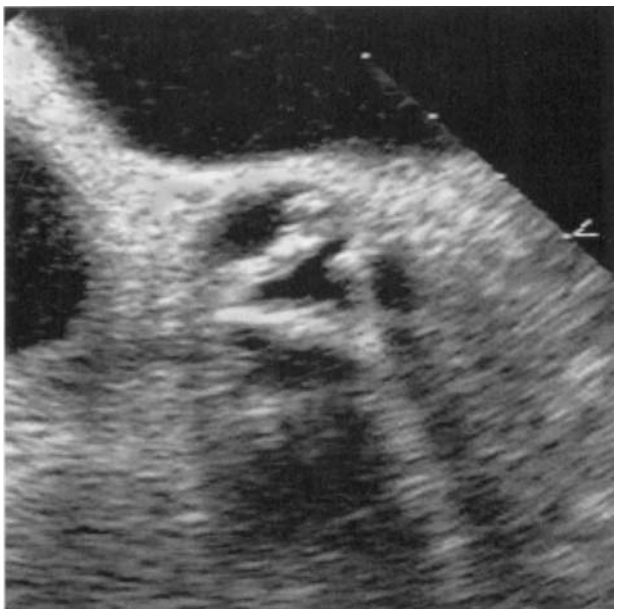

Figure 6.9 Mid-oesophageal short-axis view of a rheumatic aortic valve during systole with moderate thickening of the leaflets and stenosis. The orifice of the valve is triangular but narrowed. There is fusion of the cusps at all three commissures, which is typical of rheumatic aortic valve disease.

Dilation of the aortic root

Dilation of the aortic root can cause significant AR by distorting the normal geometry of the aortic valve. The free edge of the valve cusps must be at least as long as the diameter of the sinotubular junction in order to reach the central point of coaptation and are normally 1·2 times this diameter. If the diameter of the aortic valve annulus or the sinotubular junction enlarges beyond this length, the aortic valve cusps fail to meet, resulting in central AR. Diseases such as hypertension, cystic medial necrosis, and Marfan's syndrome can cause annular dilation sufficient to cause AR. Aneurysmal dilation of the ascending aorta can also cause AR without annular enlargement if the sinotubular junction is involved. Measurements of the aortic valve annulus and the sinotubular junction are best made with TOE from the mid-oesophageal long-axis view during systole. The normal values in adults depend on the patient's size and sex.[32] The upper limit of normal for the diameter of the

aortic valve annulus is 2·6 cm and for the sinotubular junction 3·4 cm.[33]

Aortic dissection

Aortic dissections involving the proximal portion of the ascending aorta can cause AR either by dilating the aortic root resulting in central AR or by separating one or more of the valve commissures from the outer layers of the aorta causing eccentric AR. Occasionally the intimal flap of the dissection lays across and obstructs the aortic valve during diastole, masking the severity of the AR. AR due to annular dilation usually requires valve replacement, but commissural separation can be repaired in some cases by resuspension of the valve.[34] Other important features to look for in aortic dissections with TOE are extension of the intimal flap into the coronary arteries and pericardial effusion.

Infective endocarditis of the aortic valve

Infective endocarditis of the aortic valve usually occurs in the setting of a pre-existing abnormality such as a bicuspid, stenotic, or regurgitant valve.[35] The hallmark echocardiographic feature of infective endocarditis is the vegetation – a mass that consists of fibrin, blood cells, and micro-organisms. Aortic valve vegetations appear on echocardiography as independently mobile echo-dense masses adherent to the cusps, typically on the ventricular aspect, often prolapsing into the LVOT during diastole (Figure 6.10). They range in size from microscopic, below the resolution of TOE, to several centimetres in length. The higher sensitivity of TOE over transthoracic echocardiography in detecting infective endocarditis is due primarily to its ability to identify smaller vegetations.[36] As infective endocarditis progresses, the cusps are damaged, resulting in increasing degrees of AR, which can suddenly become severe. In one-third to one-half of cases of infective endocarditis of the aortic valve, the infection extends to the perivalvular tissues, forming an abscess or mycotic aneurysm of the aortic root.[37] TOE is much better at identifying these lesions than transthoracic echocardiography.[38]

TOE examination of the aortic valve for infective endocarditis includes careful imaging with short-axis and long-axis views, moving the imaging plane through the entire extent of the valve to avoid missing eccentrically located vegetations or abscesses. CF Doppler is used to detect AR and flow into mycotic aneurysms. Often, off-axis imaging planes are needed to best display the serpiginous paths of regurgitation, aneurysms, and fistulas caused by infective endocarditis. The other valves should be examined carefully for evidence of involvement as well.

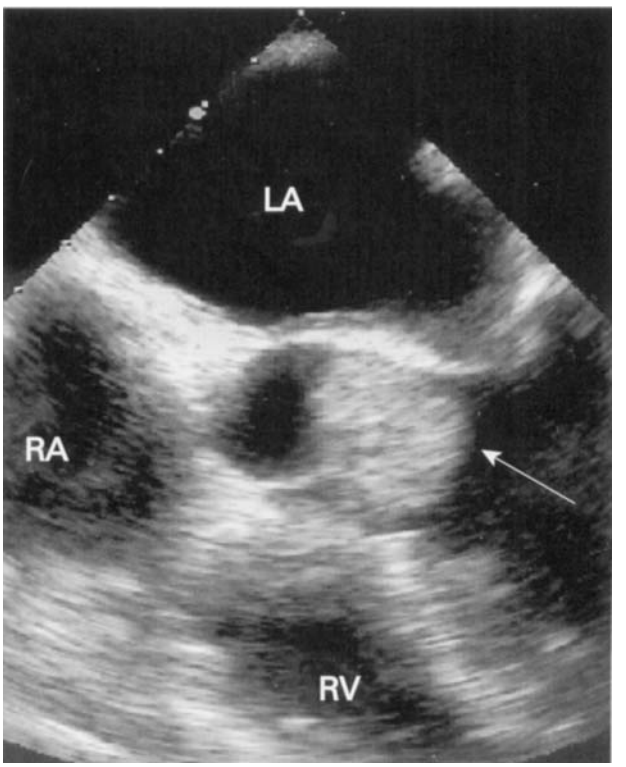

Figure 6.10 Infective endocarditis of the aortic valve. Mid-oesophageal view of the aortic valve at a multiplane angle of 0° (horizontal plane), showing a large vegetation (arrow) adherent to the ventricular aspect of the aortic valve prolapsing into the left ventricular outflow tract during diastole. Colour flow Doppler revealed severe aortic regurgitation. LA = left atrium, RA = right atrium, RV = right ventricle.

Not all independently mobile echo-dense masses of the aortic valve are active vegetations. Other possibilities include old, healed endocarditis, degenerative changes called Lambl's excrescences, papillary fibroelastomae, and non-infective vegetations due to systemic lupus erythematosus or marantic disease.[35]

Trauma to the aortic valve

Blunt trauma to the chest has been reported to injure the aortic valve resulting in significant AR.[39,40] The mechanism of injury is thought to be a sudden increase in intrathoracic pressure while the

aortic valve is closed during diastole, avulsing one or more of the cusps. Echocardiographic features of these injuries are prolapse of the damaged cusps into the LVOT during diastole, along with CF Doppler and CW Doppler evidence of AR.

References

1 Shanewise JS, Cheung AT, Aronson S, *et al.* ASE/SCA Guidelines for Performing a Comprehensive Intraoperative Multiplane Transesophageal Echocardiography Examination: Recommendations of the American Society of Echocardiography Council for Intraoperative Echocardiography, and the Society of Cardiovascular Anesthesiologists Task Force for Certification in Perioperative Transesophageal Echocardiography, *Anesth Analg* 1999;**89**:870–84.

2 Okura P, Yoshida K, Hozumi T, Akasaka T, Yoshikawa J. Planimetry and transthoracic two-dimensional echocardiography in non-invasive assessment of aortic valve area in patients with valvular aortic stenosis. *J Am Coll Cardiol* 1997;**30**:753–9.

3 Kim CJ, Berglund H, Nishioka T, Luo H, Siegel RJ. Correspondence of aortic valve area determination from transesophageal echocardiography, transthoracic echocardiography, and cardiac catheterization. *Am Heart J* 1996;**132**:1163–72.

4 Hoffmann R, Flachskampf FA, Hanrath P. Planimetry of orifice area in aortic stenosis using multiplane transesophageal echocardiography. *J Am Coll Cardiol* 1993;**22**:529–34.

5 Stoddard MF, Arce J, Liddell NE, Peters G, Dillon S, Kupersmith J. Two-dimensional transesophageal echocardiographic determination of aortic valve area in adults with aortic stenosis. *Am Heart J* 1991;**122**:1415–22.

6 Cormier B, Iung B, Porte JM, Barbant S, Vahanian A. Value of multiplane transesophageal echocardiography in determining aortic valve area in aortic stenosis. *Am J Cardiol* 1996;**77**:882–5.

7 Grayburn PA, Smith MD, Harrison MR, Gurley JC, DeMaria AN. Pivotal role of aortic valve area calculation by the continuity equation for Doppler assessment of aortic stenosis in patients with combined aortic stenosis and regurgitation. *Am J Cardiol* 1988;**61**:376–81.

8 Harrison MR, Gurley JC, Smith MD, Grayburn PA, DeMaria AN. A practical application of Doppler echocardiography for the assessment of severity of aortic stenosis. *Am Heart J* 1988;**115**:622–8.

9 Otto CM, Pearlman AS, Gardner CL, Kraft CD, Fujioka MC. Simplification of the Doppler continuity equation for calculating stenotic aortic valve area. *J Am Soc Echocardiogr* 1988;**1**:155–7.

10 Richards KL, Cannon SR, Miller JF, Crawford MH. Calculation of aortic valve area by Doppler echocardiography: a direct application of the continuity equation. *Circulation* 1986;**73**:964–9.

11 Otto CM, Pearlman AS, Comess KA, Reamer RP, Janko CL, Huntsman LL. Determination of the stenotic aortic valve area in adults using Doppler echocardiography. *J Am Coll Cardiol* 1986;**7**: 509–17.

12 Skjaerpe T, Hegrenaes L, Hatle L. Noninvasive estimation of valve area in patients with aortic stenosis by Doppler ultrasound and two-dimensional echocardiography. *Circulation* 1985;**72**:810–18.

13 Fan PH, Kapur KK, Nanda NC. Color-guided Doppler echocardiographic assessment of aortic valve stenosis. *J Am Coll Cardiol* 1988;**12**:441–9.

14 Bouchard A, Yock P, Schiller NB, *et al.* Value of color Doppler estimation of regurgitant volume in patients with chronic aortic insufficiency. *Am Heart J* 1989;**117**:1099–105.

15 Zarauza J, Ares M, Vilchez FG, *et al.* An integrated approach to the quantification of aortic regurgitation by Doppler echocardiography. *Am Heart J* 1998;**136**:1030–41.

16 Teague SM, Heinsimer JA, Anderson JL, *et al.* Quantification of aortic regurgitation utilizing continuous wave Doppler ultrasound. *J Am Coll Cardiol* 1986;**8**:592–9.

17 Masuyama T, Kodama K, Kitabatake A, *et al.* Noninvasive evaluation of aortic regurgitation by continuous-wave Doppler echocardiography. *Circulation* 1986;**73**:460–6.

18 Rokey R, Sterling LL, Zoghbi WA, *et al.* Determination of regurgitant fraction in isolated mitral or aortic regurgitation by pulsed Doppler two-dimensional echocardiography. *J Am Coll Cardiol* 1986;**7**:1273–8.

19 Touche T, Prasquier R, Nitenberg A, de Zuttere D, Gourgon R. Assessment and follow-up of patients with aortic regurgitation by an updated Doppler echocardiographic measurement of the regurgitant fraction in the aortic arch. *Circulation* 1985;**72**:819–24.

20 Takenaka K, Dabestani A, Gardin JM, *et al.* A simple Doppler echocardiographic method for estimating severity of aortic regurgitation. *Am J Cardiol* 1986;**57**:1340–3.

21 Meyer T, Sareli P, Pocock WA, Dean H, Epstein M, Barlow J. Echocardiographic and hemodynamic correlates of diastolic closure of mitral valve and diastolic opening of aortic valve in severe aortic regurgitation. *Am J Cardiol* 1987;**59**:1144–8.

22 Siemienczuk D, Greenberg B, Morris C, *et al.* Chronic aortic insufficiency: factors associated with progression to aortic valve replacement. *Ann Intern Med* 1989;**110**:587–92.

23 Gaasch WH, Carroll JD, Levine HJ, Criscitiello MG. Chronic aortic regurgitation: prognostic value of left ventricular end-systolic dimension and end-diastolic radius/thickness ratio. *J Am Coll Cardiol* 1983;**1**:775–82.

24 Fioretti P, Roelandt J, Bos RJ, *et al.* Echocardiography in chronic aortic insufficiency. Is valve replacement too late when left ventricular end-systolic dimension reaches 55 mm? *Circulation* 1983;**67**:216–21.

25 Bonow RO, Lakatos E, Maron BJ, Epstein SE. Serial long-term assessment of the natural history of asymptomatic patients with chronic aortic regurgitation and normal left ventricular systolic function. *Circulation* 1991;**84**:1625–35.

26 Roberts WC. The congenitally bicuspid aortic valve. A study of 85 autopsy cases. *Am J Cardiol* 1970;**26**:72–83.

27 Huntington K, Hunter AG, Chan KL. A prospective study to assess the frequency of familial clustering of congenital bicuspid aortic valve. *J Am Coll Cardiol* 1997;**30**:1809–12.

28 Beppu S, Suzuki S, Matsuda H, Ohmori F, Nagata S, Miyatake K. Rapidity of progression of aortic stenosis in patients with congenital bicuspid aortic valves. *Am J Cardiol* 1993;**71**:322–7.

29 Stewart WJ, King ME, Gillam LD, Guyer DE, Weyman AE. Prevalence of aortic valve prolapse with bicuspid aortic valve and its relation to aortic regurgitation: a cross-sectional echocardiographic study. *Am J Cardiol* 1984;**54**:1277–82.

30 Weyman AE, Griffin BP. Left ventricular out flow tract: the aortic valve, aorta, and subvalvular outflow tract. In: Weyman AE, ed. *Principles and practice of echocardiography, 2nd edn.* Philadelphia: Lea & Febiger, 1994:511.

31 Lindroos M, Kupari M, Heikkila J, Tilvis R. Prevalence of aortic valve abnormalities in the elderly: an echocardiographic study of a random population sample. *J Am Coll Cardiol* 1993;**21**: 1220–5.

32 Vasan RS, Larson MG, Levy D. Determinants of echocardiographic aortic root size. The Framingham Heart Study. *Circulation* 1995; **91**:734–40.

33 Weyman AE, ed. Normal cross-sectional echocardiographic measurements. In: *Principles and practice of echocardiography,* 2nd edn. Philadelphia: Lea & Febiger, 1994:1290.

34 Mazzucotelli JP, Deleuze PH, Baufreton C, *et al.* Preservation of the aortic valve in acute aortic dissection: long-term echocardiographic assessment and clinical outcome. *Ann Thorac Surg* 1993;**55**:1513–17.

35 Shanewise JS, Martin RP. Assessment of endocarditis and associated complications with transesophageal echocardiography. *Crit Care Clin* 1996;**12**:411–27.

36 Shapiro SM, Young E, De Guzman S, *et al.* Transesophageal echocardiography in diagnosis of infective endocarditis. *Chest* 1994;**105**:377–82.

37 Karalis DG, Bansal RC, Hauck AJ, *et al.* Transesophageal echocardiographic recognition of subaortic complications in aortic valve endocarditis. Clinical and surgical implications. *Circulation* 1992;**86**:353–62.

38 Daniel WG, Mugge A, Martin RP, *et al.* Improvement in the diagnosis of abscesses associated with endocarditis by transesophageal echocardiography. *N Engl J Med* 1991;**324**:795–800.

39 Gay JA, Gottdiener JS, Gomes MN, Patterson RH, Fletcher RD. Echocardiographic features of traumatic disruption of the aortic valve. *Chest* 1983;**83**:150–1.

40 Munshi IA, Barie PS, Hawes AS, Lang SJ, Fischer E. Diagnosis and management of acute aortic valvular disruption secondary to rapid-deceleration trauma. *J Trauma* 1996;**41**:1047–50.

7 Prosthetic valves

Herman FJ Mannaerts, Cees A Visser

Introduction

Accurate evaluation of prosthetic heart valves by transoesophageal echocardiography (TOE) is complex for several reasons. Several different types and sizes of prosthetic valves can be implanted in any of the four valve positions. Each of these valves and each size have unique flow characteristics. Furthermore, the ultimate haemodynamic characteristics of a prosthetic valve also largely depend on various physiological (for example, the patient's body size) and pathological processes and concomitant changes in function, pressures, and compliance of atria, ventricles and aorta or pulmonary artery. In spite of this complexity, the great majority of pathological conditions that affect both biological and mechanical valve prostheses can be accurately diagnosed by TOE.[1] Quantitative evaluation of prosthetic valvular stenosis (in terms of gradients and effective orifice areas [EOAs]) and prosthetic aortic regurgitation, however, can best be performed by transthoracic echocardiography (TTE), with concomitant use of spectral Doppler and colour flow imaging.[2–8] By using a combined approach of TTE and TOE, prosthetic heart valves can be well investigated.

Pathological conditions that can affect both biological and mechanical valve prostheses are those that lead to stenosis, thrombosis, regurgitation, haemolysis, endocarditis, and others such as fistula or pseudoaneurysm formation. Mechanical valve prostheses share the same pathological conditions, albeit that strut fracture is a problem specific to mechanical prostheses. On the other hand, valve stenosis and regurgitation, due to degeneration, is specific to bioprostheses.

Although TOE provides a higher image resolution (1 mm), TTE and TOE are complementary for the assessment of prosthetic valve morphology and function (obstruction as well as regurgitation).[2–12] Thus, if transthoracic acoustic windows are available, then TTE should be performed mainly for the accurate assessment of gradients and the calculation of valve areas. However, morphological evaluation by TTE can be helpful, for example, in the evaluation of the ventricular side of a mitral valve prosthesis. Reverberations and shadowing by TTE and TOE occur on opposite sides of prosthetic valves, so that abnormalities masked by one technique may be revealed by the other. This is also true in the case of flow masking if colour Doppler flow imaging is used. With both the TTE and TOE approaches, the sewing ring should always be visualized in order to identify dehiscence as well as the moving parts. In the case of a bioprosthesis, the leaflets should be inspected for thickening, calcification, abnormal apposition, and reduced opening. In addition, the stents of these valves should be identified.[13]

With two-dimensional (2D) TTE or 2D TOE, multiple ultrasound reverberations are observed in mechanical prostheses, caused by the metal disk or ball. Nevertheless, poppet or disk motion can be assessed by observing the motion pattern of the reverberations. Furthermore, the abnormal closing motion causes an abnormal motion pattern that can be precisely recorded by M-mode echocardiography.[14] Abnormal mass lesions, such as thrombus or vegetations, paraprosthetic abscesses, or fistulas or pseudoaneurysms associated with the prostheses, should be looked for.[15–20] Substantial improvement in imaging of prosthetic valves has been achieved with the introduction of three-dimensional (3D) TOE, especially for mechanical prostheses in the mitral position.[21] In the vast majority of patients the opening and closing of the leaflets in a mechanical prosthesis can be directly observed. Accurate mechanical prosthetic valve area can thus be assessed, as well as obstruction to flow by pannus, thrombus, or vegetations, which can be directly seen. Similarly, dehiscence of the sewing ring of the prosthetic valve, for example in the case of endocarditis with paravalvular regurgitation, can be directly assessed.

Colour flow imaging provides a velocity map of forward and regurgitant flow across the prosthesis. Each type of prosthesis has a characteristic colour map for both forward flow

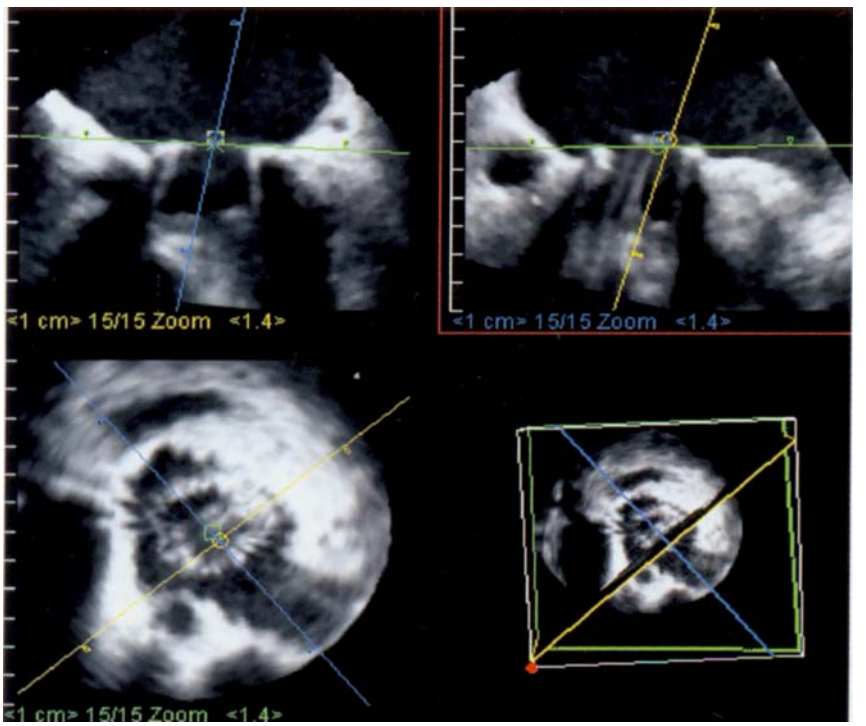

Figure 7.1 This figure shows the first step in three-dimensional planimetry of the orifice area of a St. Jude prosthesis in the mitral position. From two perpendicular long axes of the prosthesis (upper tiles), an accurate short axis at the level of the inner prosthetic ring is defined (left lower panel), from which the orifice area can be measured precisely.

and regurgitation. Being familiar with normal flow imaging for various prostheses is mandatory if one is to conduct a quick screen for prosthetic valvular stenosis and abnormal regurgitation.[9–12] In addition, colour flow imaging is useful for guiding placement of the continuous wave cursor for guided measurement of prosthetic valve gradients. Figures 7.1 and 7.2 illustrate the way in which the orifice area is measured using 3D TOE planimetry and provide examples of monoleaflet (i.e. tilting disc (Medtronic Hall) and bileaflet (St. Jude Medical, Carbomedics) valve prostheses.[21]

Spectral Doppler imaging provides complete assessment of forward flow haemodynamics and can aid in the detection and timing of regurgitation (in the cardiac cycle). Continuous wave (CW) Doppler imaging is used to measure prosthetic valve gradients,[22] whereas the combination of pulsed wave (PW) and CW Doppler echocardiography is used for measurement of EOAs (using the continuity equation).[23,24] During the transthoracic study, CW Doppler imaging is also used to screen for prosthetic valvular regurgitation. In general, the amount of regurgitation is proportional to the intensity of CW Doppler signals.

Prostheses in aortic position

Forward flow characteristics

The forward flow characteristics across prostheses in the aortic position provide an assessment of the degree of obstruction. All prosthetic valves are inherently obstructive to some degree. In general, bioprosthetic valves, and especially the homograft, with normal function are less obstructive than are their mechanical counterparts. For imaging of aortic prostheses TOE is superior to TTE. For Doppler measurement of the forward flow velocity and gradient, however, the opposite is true. This is mainly because of difficult alignment of the CW Doppler cursor parallel to flow through the aortic prosthesis, which can occasionally be accomplished by a long-axis transgastric TOE approach. Also, far field attenuation by the prosthesis is an important limitation, even with good alignment. Fortunately, complete haemodynamic assessment of prosthetic aortic valves can almost always be achieved using TTE, usually from the apical or right parasternal or right supraclavicular views.[2–8] The maximal Doppler

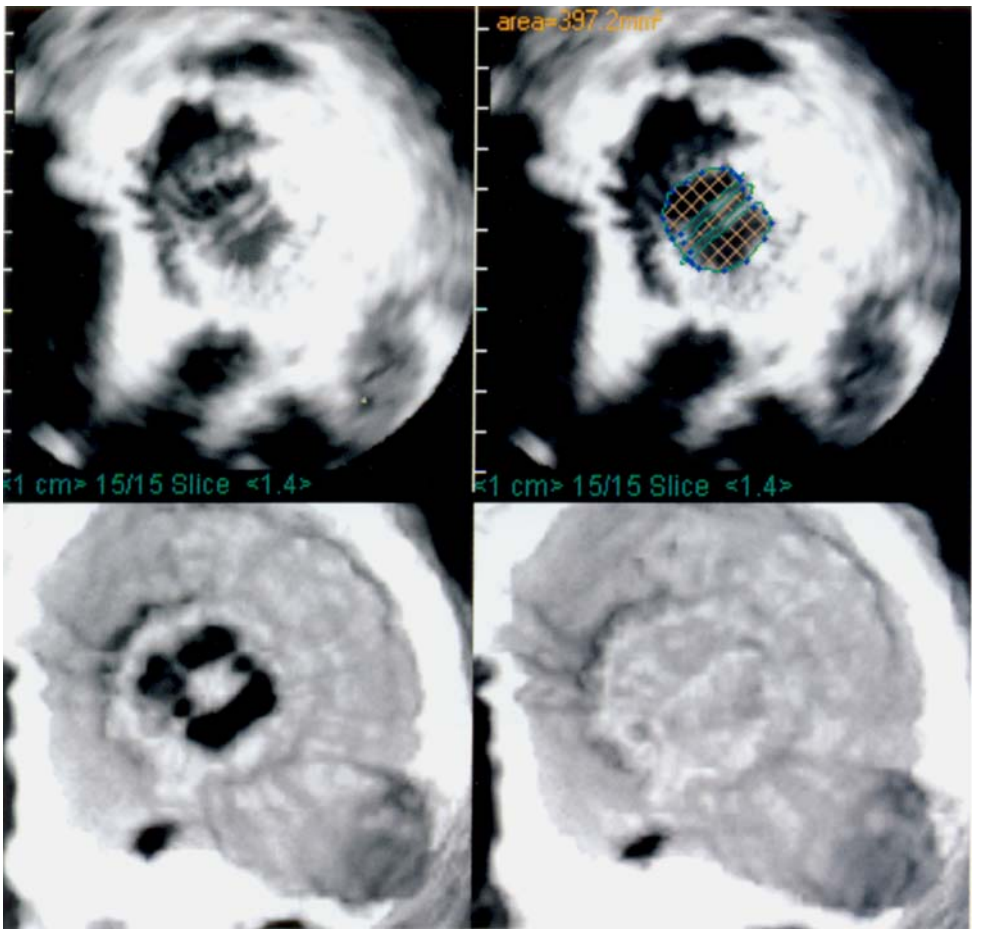

Figure 7.2 The second step in mechanical valve area measurement is shown with two anyplane images at the level of the inner prosthetic ring (i.e. cross-sectional two-dimensional images, obtained from electronic cross-section of the three-dimensional dataset) in the upper panels. Two corresponding volume rendered images from the so-called unroofed left atrial view (or surgical view), looking from above on the prosthesis, are also shown, with visible prosthetic opening and closure. The left atrial appendage can be seen at the "5 o'clock" position.

spectrum should be selected for calculation of the maximal and mean gradients. For patients who are in regular sinus rhythm three to five beats are averaged, and for patients in atrial fibrillation five to ten beats should be averaged.[2–8]

Ball-in-cage type prostheses such as the Starr–Edwards prostheses have a significantly higher mean gradient than do heterograft (bioprosthetic), Bjork–Shiley (tilting disc type), and St. Jude Medical (bileaflet type) valves. Homograft aortic valves have the lowest mean gradient.[25] During the past few years stentless bioprostheses have been implanted in the aortic position, and they also have very favourable flow characteristics, especially in small aortic roots.[26] Furthermore, pressure gradients decrease with larger valve sizes.[27] Also, left ventricular (LV) function and the patient's size are important determinants of the pressure gradient measured by CW Doppler. With poor systolic LV function the gradient will be underestimated,[28] and pathological obstruction caused by thrombus, pannus formation, or degeneration may be masked. This problem may be solved by calculating the EOA of the aortic prosthesis using the continuity equation, in which both PW Doppler (for the velocity in the LV outflow tract [LVOT]) and CW Doppler (for the velocity across the aortic prosthesis) are used. This method also has some limitations, which are mainly caused by inaccuracies in the measurement of the LVOT radius, which is squared in the formula of the continuity equation; a calculated EOA below 1 cm^2 tends to be associated with an obstructed aortic prosthesis at surgery or autopsy.[24,29] EOA data obtained using the continuity equation correlates well with those obtained by catheterization (Gorlin formula).[24] Flow velocity ratio (FVR; i.e. LVOT velocity/velocity across the aortic prosthesis) is a simplified way to measure the degree of obstruction, and obviates the need for LVOT diameter measurement. A FVR below 0·25 is also a useful indicator of pathological obstruction in the symptomatic patient.[30] Figure 7.3 is a 3D TOE

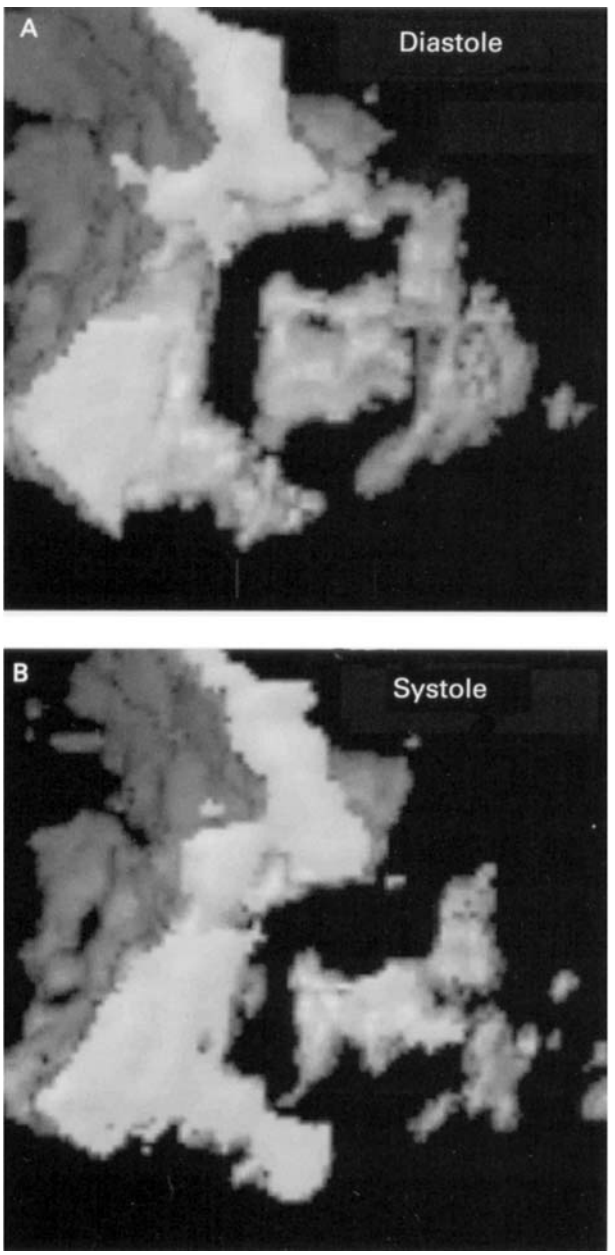

Figure 7.3 Three-dimensional transoesophageal echocardiographic volume rendered image of a severely obstructed Medtronic Hall valve in the aortic position, viewed from the left ventricular outflow tract, in **(A)** diastole and **(B)** systole. Note the central mass, which hardly changes between systole and diastole, and the irregular borders of the inner prosthetic ring caused by pannus ingrowth.

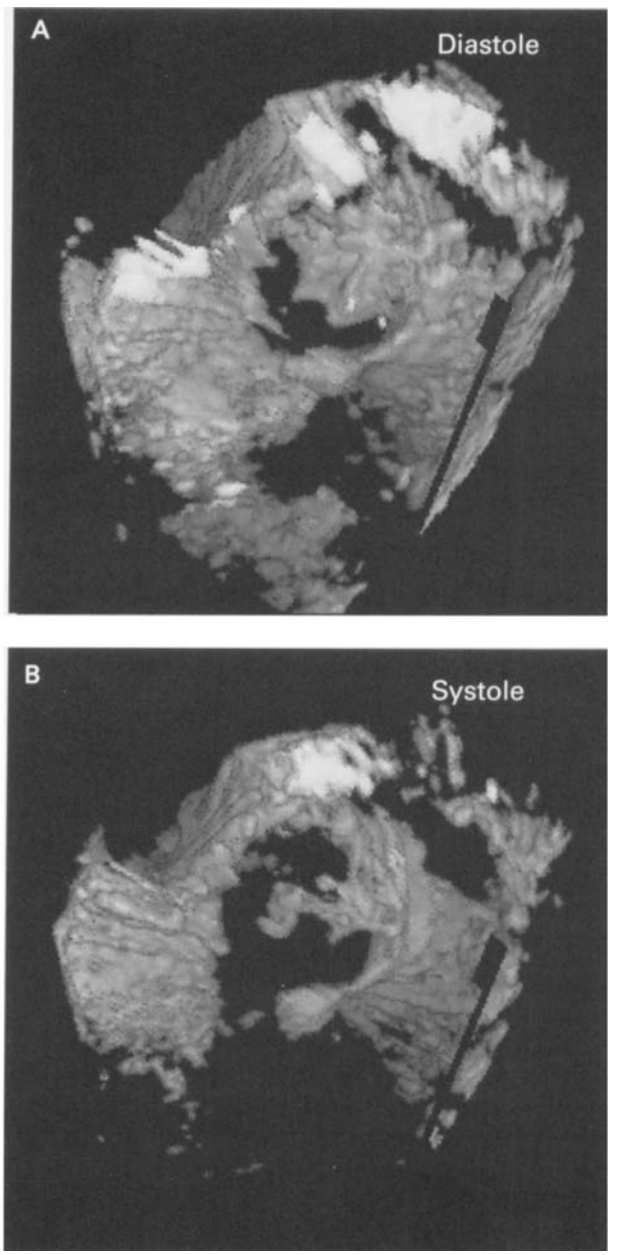

Figure 7.4 Three-dimensional transoesophageal echocardiographic volume rendered image of a normally functioning Medtronic Hall valve in the aortic position in **(A)** diastole and **(B)** systole. In systole the central hinge and part of the disc can be seen. In diastole the tilting disc seals of inner ring. Because of the settings used, this cannot entirely be seen as they were optimised for the central hinge part. The margins of the inner ring appear less irregular than in Figure 7.4.

example of a Medtronic Hall prosthesis.[21] Shown is a valve prostheses in the aortic position in a patient with rapidly progressive yet asymptomic prosthetic valve stenosis with a maximal gradient increase in 3 years from 36 mmHg to 135 mmHg, presumably due to pannus ingrowth (the patient has not yet undergone surgery). For comparison another patient with a Medtronic Hall prosthesis 27 in the aortic position with a peak gradient of 25 mmHg is shown in Figure 7.4.

Patient–valve mismatch occurs if a prosthesis is implanted that is too small relative to the patient's body surface area (i.e. the EOA is too small for the relatively higher cardiac output needed in a large patient), which generates large pressure gradients, possibly even within the range encountered in patients with severe aortic stenosis.[31] Because all normally functioning prosthetic valves have some intrinsic obstruction, an elevated pressure gradient is virtually always present to some extent. Patients without symptoms, even with the same prosthesis type and size (especially in the aortic position), exhibit an extensive variation in transprosthetic gradients.[25] This is mainly due to variations in cardiac output and transprosthetic pressures. Therefore, there is a wide range of normal values. Severe forms of patient–valve mismatch (with EOAs < 1 cm^2, and FVRs $< 0{\cdot}25$) can occur, especially in the smaller valve sizes – numbers 19 and 21 – of mechanical valves, and might be responsible for a lack of symptomatic improvement after prosthetic valve implantation or possible development of heart failure in the long term.

Regurgitation characteristics

A small amount of regurgitation is observed in normal prosthetic valves. Blood is displaced back into the receiving chamber, in this case the left ventricle, because of the closure of the moving parts of the prosthesis. This referred to as "closure backflow". Once the valve has been closed, "leakage backflow" also occurs through the hinges and between the cusps and the inner prosthetic valve ring of mechanical bileaflet and tilting disc prostheses.[10] Leakage backflow does not occur in normally functioning Starr–Edwards valves because the ball in the closed position effectively seals the inner prosthetic valve ring. Prosthetic regurgitation can be divided into transprosthetic and paraprosthetic (also termed periprosthetic) regurgitation. Closure and leakage backflow are transvalvular and non-pathological. The resultant regurgitation is usually mild, but may be more than 20% of the forward stroke volume in normally functioning prostheses in the aortic position.[32] Pathological transvalvular prosthetic regurgitation may occur in the case of a torn cusp of an aortic bioprosthesis and in the case of strut fracture with resulting disc embolisation of a mechanical valve. Paravalvular or periprosthetic regurgitation may be caused by dehiscence of the prosthesis, which in turn may be a sequela of endocarditis.

Prosthetic aortic regurgitation can be semiquantitatively assessed both with TTE and with biplane or multiplane TOE by measuring the jet width (or area in the short axis) and dividing it by the LVOT diameter (or area in the short axis), and expressing it as one of three classes ($< 25\%$, $25–45\%$, and $> 45\%$ indicate none-to-mild, moderate, and severe aortic regurgitation, respectively).[29,33] Trivial or mild regurgitation is considered normal. TTE is usually sufficient for assessing prosthetic aortic regurgitation by colour flow imaging, because of the proximity and direction of jets of either transvalvular or perivalvular prosthetic aortic regurgitation relative to the transthoracic transducer. These jets occur just below the transducer positioned in the left parasternal position, and they are directed toward the transducer positioned at the apex. TOE may even underestimate the severity of aortic regurgitation by colour flow because of acoustic shadowing.

In a study conducted by Mohr Kahaly *et al.*,[9] TOE was more sensitive for detecting prosthetic aortic regurgitation except in the case of Bjork–Shiley prostheses. However, for all types of aortic prostheses, the regurgitant jet width was larger when evaluated by TTE than by TOE. This factor has important implications for grading the severity of prosthetic aortic regurgitation by TOE colour flow imaging alone. Nevertheless, TOE is particularly useful for intraoperative studies or when transthoracic imaging is technically inadequate. TOE provides high resolution images of the prosthesis itself, allowing identification of structural defects causing the regurgitation, such as degeneration of aortic heterograft cusps. TOE is also proving to be especially useful in diagnosing whether an aortic regurgitation jet is prosthetic or periprosthetic, as is the case with dehiscence of prostheses in the aortic position. Jets of aortic regurgitation are most completely defined when multiplane (or biplane) transducers are used. The amount of diastolic flow reversal in the descending thoracic aorta can be used for semiquantitation of the degree of prosthetic aortic regurgitation.[34] Holodiastolic reversal is a marker of severe prosthetic transvalvular aortic regurgitation. This can be investigated by TTE from the suprasternal notch with either colour flow imaging or PW Doppler,

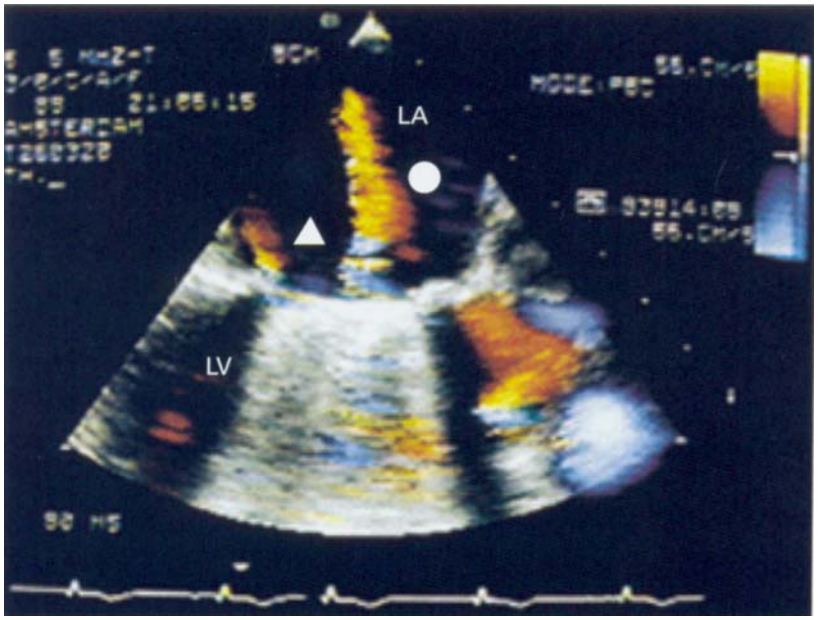

Figure 7.5 Transoesophageal echocardiographic colour Doppler flow image from a patient with a normal Medtronic Hall prosthesis in the mitral position. The white circle indicates an apparent central jet starting after valve closure. One of the two small peripheral jets is also visualized in this plane (triangle). LA = left atrium, LV = left ventricle. (Reproduced from Van den Brink *et al.* 1989,[10] with permission from Excerpta Medica Inc., and the first author.)

or from a subcostal transducer position examining the abdominal aorta, or by TOE of the aortic arch.[34]

For complete assessment of the amount of aortic regurgitation, not only colour flow imaging but also PW and CW Doppler examinations are necessary. The latter modality allows calculation of the pressure half-time of the regurgitant jet, which in the absence of high end-diastolic pressures is also a useful marker for the severity of acute aortic regurgitation. The latter is severe if the pressure half-time is less than 300 ms.[35] Periprosthetic jets can only be identified when the origin of the periprosthetic jet is identified outside the boundary of the prosthesis.[29] This is particularly applicable to bioprostheses because tears and perforations of the cusps frequently occur near the point of attachment to the sewing ring. Echocardiographic identification of the sewing ring is therefore important in differentiating between prosthetic and periprosthetic regurgitation.

Mitral and tricuspid prostheses

Forward flow characteristics

Several aspects of Doppler echocardiography can be employed for assessing pathological obstruction. TOE is ideally suited to assessment of the opening and closing motion of a prosthesis in the mitral position. In terms of morphological details (thrombus, pannus, abcesses, or vegetations), the atrial site of the prosthesis is better evaluated using TOE because of its proximity to that part of the prosthesis and the absence of reverberation/shadowing (usually present from the transthoracic approach). Also, the presence of spontaneous echo contrast can readily be appreciated by TOE. This phenomenon occurs if there is slow flow across a native or prosthetic mitral valve due to either obstruction or atrial fibrillation, or both. It often coincides with thrombi in the left atrium or left atrial appendage, especially if the PW Doppler velocity in the left atrial appendage is less than 20 cm/s.[36] However, with 2D TOE the ventricular side is obscured by shadowing, and can be better evaluated through a parasternal or apical transthoracic view. 3D TOE allows direct visualisation of obstructive pannus, thrombus, or vegetations; these often interfere with the opening (angle) and closing of the mechanical leaflets by reducing the opening angle or by preventing complete closure, with concomitant pathological valvular leakage. The latter is usually directly visible with 2D TOE.

Colour Doppler will show turbulent inflow in the case of a mechanical prosthesis, which can best be assessed by transthoracic (apical or parasternal) echocardiography. The TOE guided CW cursor can be guided across mitral prostheses with the use of either four chamber or

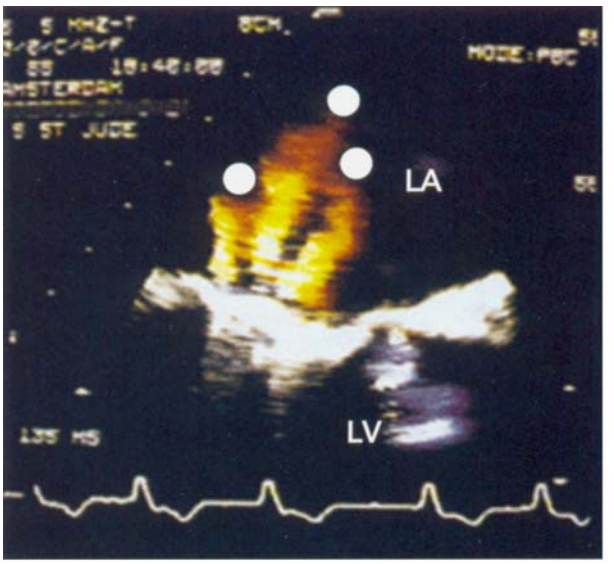

Figure 7.6 Transoesophageal echocardiographic colour Doppler flow image obtained in another patient with a St. Jude Medical prosthesis in the mitral position. Three systolic regurgitant jets (white circles) are present in the left atrium (LA). LV = left ventricle. (Reproduced from Van den Brink *et al.* 1989,[10] with permission from Excerpta Medica Inc., and the first author.)

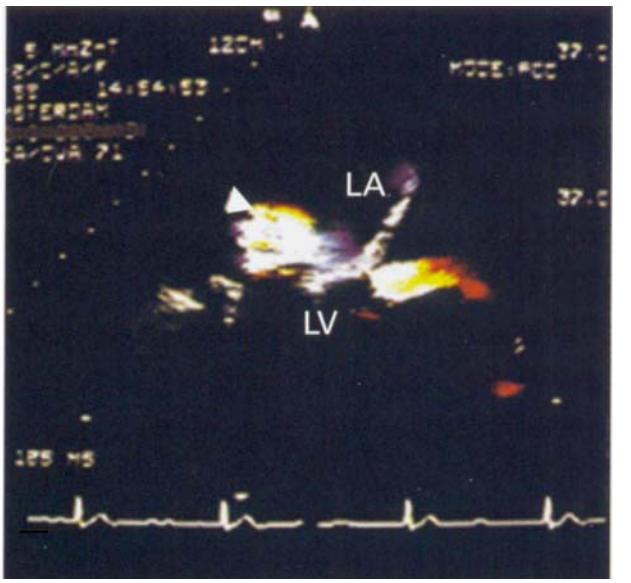

Figure 7.8 Transoesophageal echocardiographic colour Doppler flow image from a patient with a normal Starr–Edwards mitral valve prosthesis, obtained 105 ms after onset of the R wave. The two confluent jets in the left atrium (triangle) are due to "closure backflow". LA = left atrium, LV = left ventricle. (Reproduced from Van den Brink *et al.* 1989,[10] with permission from Excerpta Medica Inc., and the first author.)

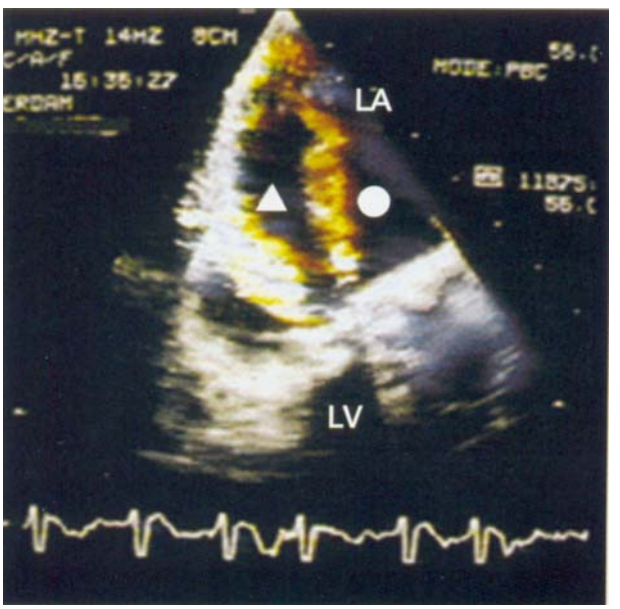

Figure 7.7 Transoesophageal echocardiographic colour Doppler flow image obtained in another patient with a St. Jude Medical prosthesis in the mitral position. Note the normal jet (white circle) caused by leakage backflow, and the bright, extensive jet (triangle) that arises outside the prosthetic valve ring (paraprosthetic regurgitation jet). LA = eft atrium, LV = left ventricle. (Reproduced from Van den Brink *et al.* 1989,[10] with permission from Excerpta Medica Inc., and the first author.)

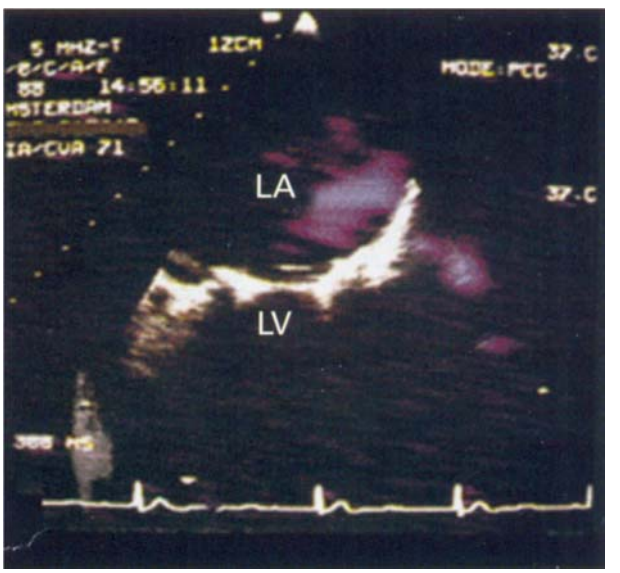

Figure 7.9 Transoesophageal echocardiographic colour Doppler flow image (obtained from the same patient as Figure 7.9) 300 ms after the R wave. There is no leakage backflow after valve closure. LA = left atrium, LV = left ventricle. (Reproduced from Van den Brink *et al.* 1989,[10] with permission from Excerpta Medica Inc., and the first author.)

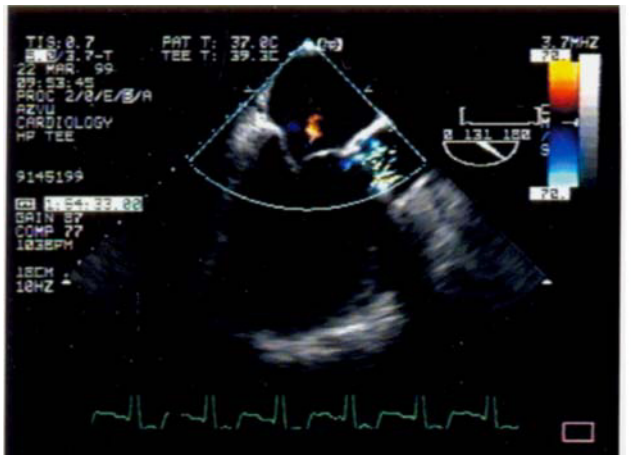

Figure 7.10 Transoesophageal echocardiographic colour flow image of a Duromedics prosthetic valve in the aortic position (systolic frame). The two tilting discs of this bileaflet valve prosthesis can clearly be observed.

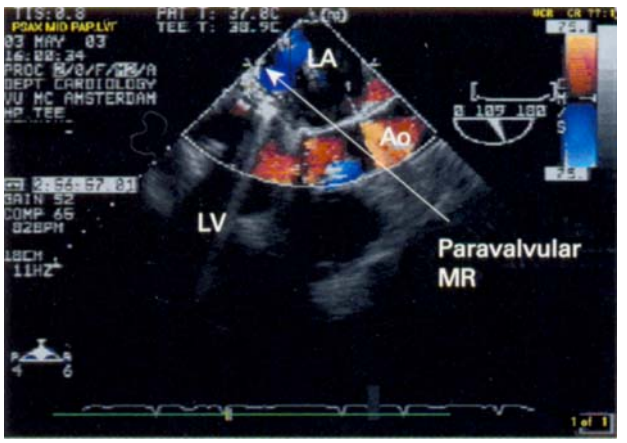

Figure 7.11 Two-dimensional colour transoesophageal echocardiographic image in systole showing a thickened valve prosthesis with irregular margins (vegetations), and clear signs of dehiscence with a severe resulting paravalvular mitral regurgitation (MR; arrow). Ao = aorta, LA = left atrium, LV = left ventricle.

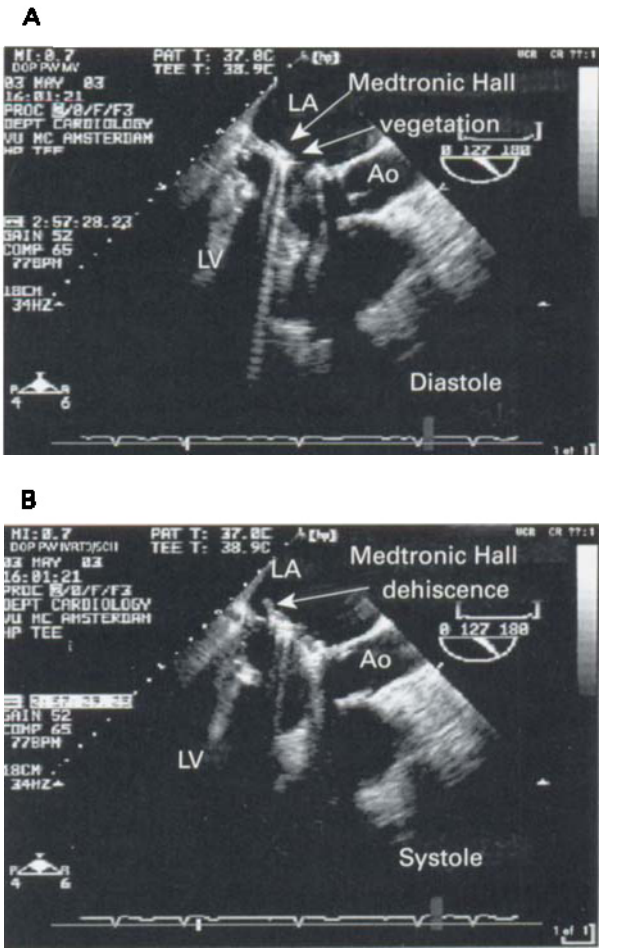

Figure 7.12 The corresponding three-dimensional transoesophageal echocardiographic images for Figure 7.12 in **(A)** diastole with an irregular orifice of the inner prosthetic ring (arrow), and **(B)** a clear zone of dehiscence posterior (arrow) in systole. Ao = aorta, LA = left atrium, LV = left ventricle.

longitudinal plane two-chamber views. This approach is supplemented by colour flow mapping to align the cursor directly parallel to mitral inflow. In both TOE and TTE, CW Doppler can be used to quantify peak and mean velocities and gradients, pressure half-time, and EOA. The pressure half-time for mitral and tricuspid prostheses is best reported as an independent measure of obstruction without converting it to an EOA,[37] as is often performed using the well known formula by Hatle *et al.*[38] The EOA can better be measured using the continuity equation method.[39] Pathological obstruction in mitral prostheses tends to be associated with a pressure halftime in excess of 160 ms and a mean transprosthetic gradient greater than 16 mmHg, provided that the heart rate is within normal limits (i.e. < 100 beats per minute).[2–4]

Regurgitation

Virtually every mechanical valve prosthesis in the mitral or tricuspid position exhibits closure

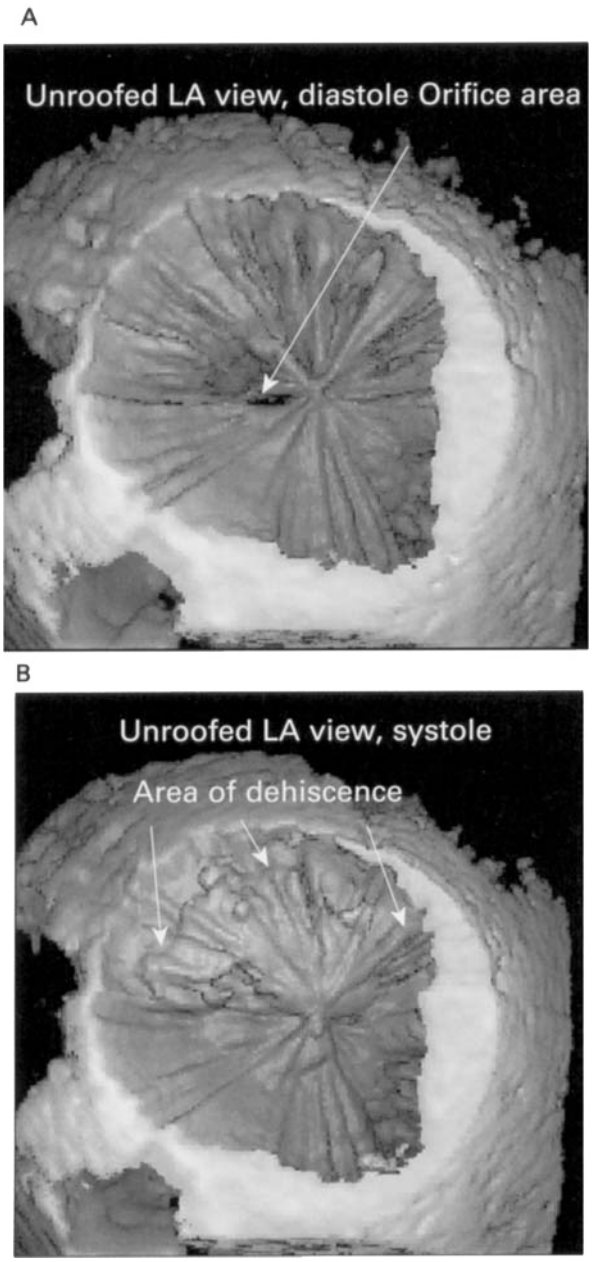

Figure 7.13 Volume rendered three-dimensional transoesophageal echocardiographic image, showing an unroofed left atrial view with an irregular aspect of the prosthetic orifice in **(A)** diastole due to obstruction by vegetations and **(B)** the area of dehiscence in systole.

and leakage backflow, except for the Starr–Edwards prosthesis, which only exhibits closure backflow. Each type of prosthesis generates a specific jet pattern with colour Doppler. Depending on the orientation of the TOE imaging plane, two or three small jets can be visualized, which are usually 1–2 cm in length and are non-turbulent (Figures 7.5–7.10).[10] In contrast, pathological regurgitant jets are more extensive, turbulent, and crescent shaped in comparison with jets caused by normal closure and leakage backflow (Figure 7.11).[10] They usually originate outside the valvular ring, and they are therefore periprosthetic. Often, dehiscence due to endocarditis can clearly be observed with 2D/3D TOE (Figures 7.12 and 7.13). There is great variability among patients with comparable mechanical valve prostheses, and it is therefore very important to assess the specific regurgitation pattern for each mitral valve prosthesis shortly after implantation, because this "signature" can serve as a control for future follow up of the patient.[10]

Conclusion

2D TOE is a very valuable tool, especially for morphological assessment of prosthetic valves and for assessment of regurgitation characteristics of prosthetic valves in the mitral position. 3D TOE provides additional information with respect to orifice area, prosthetic obstruction, dehiscence, or prosthetic valve endocarditis. Additional TTE with Doppler is needed for in-depth assessment of forward flow characteristics of prosthetic valves in the aortic position. Because of the individual variability in Doppler measurements of both forward flow and regurgitation characteristics, a TOE/TTE study conducted shortly after implantation of a prosthetic valve is indicated to serve as a control for later follow up of the patient.

References

1 Mohr-Kahaly S, Kupferwasser I, Erbel R. Transesophageal echocardiography for the evaluation of prosthetic valve function. In: Roelandt JRTC, Sutherland GR, Iliceto S, Linker DT, eds. *Cardiac ultrasound*, 1st ed. Edinburgh: Churchill Livingstone, 1993. pp. 335–42.

2 Williams GA, Labovitz AJ. Doppler hemodynamic evaluation of prosthetic (Starr–Edwards and Bjork–Shiley) and bioprosthetic (Hancock and Carpentier Edwards) cardiac valves. *Am J Cardiol* 1985;**56**:325–32.

3 Labovitz AJ. Assessment of prosthetic heart valve function by Doppler echocardiography: a decade of experience. *Circulation* 1989;**80**:707–9.

4 Sagar KB, Wann LS, Paulsen WH, Romhilt DW. Doppler echocardiographic evaluation of Hancock and Bjork-Shiley prosthetic valves. *J Am Coll Cardiol* 1986;**7**:681–7.

5 Cooper DM, Stewart WJ, Schiavone WA, *et al.* Evaluation of normal prosthetic valve function by Doppler echocardiography. *Am Heart J* 1987; **114**:576–82.

6 Ramirez ML, Wong M. Reproducibility of stand alone continuous wave Doppler recordings of aortic flow velocity across bioprosthetic valves. *Am J Cardiol* 1985;**55**:1197–9.

7 Panidis IP, Ross J, Mintz GS. Normal and abnormal prosthetic valve function as assessed by Doppler echocardiography. *J Am Coll Cardiol* 1986;**8**: 317–26.

8 Weinstein IR, Marbarger JP, Perez JE. Ultrasonic assessment of the St. Jude prosthetic valve: M-mode, two-dimensional, and Doppler echocardiography. *Circulation* 1983;**68**:897–905.

9 Mohr Kahaly S, Kupferwasser I, Erbel R, *et al.* Regurgitant flow in apparently normal valve prostheses: improved detection and semiquantitative analysis by transesophageal two-dimensional color-coded Doppler echocardiography. *J Am Soc Echocardiogr* 1990;**3**:187–95.

10 Van den Brink RB, Visser CA, Basart DC, Duren DR, de Jong AP, Dunning AJ. Comparison of transthoracic and transesophageal color Doppler flow imaging in patients with mechanical prostheses in the mitral valve position. *Am J Cardiol* 1989;**63**:1471–4.

11 Taams MA, Gussenhoven EJ, Cahalan MK, *et al.* Transesophageal Doppler color flow imaging in the detection of native and Bjork–Shiley mitral valve regurgitation. *J Am Coll Cardiol* 1989;**13**:95–9.

12 Lange HW, Olson JD, Pederson WR, *et al.* Transesophageal color Doppler echocardiography of the normal St Jude Medical mitral valve prosthesis. *Am Heart J* 1991;**122**:489–94.

13 Alam M, Serwin JB, Rosman HS, *et al.* Transesophageal echocardiographic features of normal and dysfunctioning bioprosthetic valves. *Am Heart J* 1991;**121**:1149–55.

14 Cunha CLP, Guliani ER, Callahan JA, Pluth JR. Echophonocardiographic findings in patients with prosthetic heart valve malfunction. *Mayo Clin Proc* 1980;**55**:231–42.

15 Sutton MSJ, Lee RT. Diagnosis and medical management of infective endocarditis: transthoracic and transesophageal echocardiography. *J Card Surg* 1990;**5**:39–43.

16 Taams MA, Gussenhoven EJ, Bos E, *et al.* Enhanced morphological diagnosis in infective endocarditis by transoesophageal echocardiography. *Br Heart J* 1990;**63**:109–13.

17 Pedersen WR, Walker M, Olson JD, *et al.* Value of transoesophageal echocardiography as an adjunct of transthoracic echocardiography in evaluation of native and prosthetic valve endocarditis. *Chest* 1991;**100**:351–6.

18 Daniel WG, Mugge A, Martin RP, *et al.* Improvement in the diagnosis of abscesses associated with endocarditis by transoesophageal echocardiography. *N Engl J Med* 1991;**324**:795–800.

19 Bansal RC, Graham BM, Jutzy KR, *et al.* Left ventricular outflow tract to left atrial communication secondary to rupture of mitral-aortic intervalvular fibrosa in infective endocarditis: diagnosis by transesophageal echocardiography and color flow imaging. *J Am Coll Cardiol* 1990;**15**:499–504.

20 Meyerowitz CB, Jacobs LE, Kotler MN, *et al.* Four year follow-up of a pseudoaneurysm of the mitral aortic fibrosa. *Am Heart J* 1991;**122**:589–92.

21 Mannaerts H, Li Y, Kamp O, Valocik G, *et al.* Quantitative assessment of mechanical prosthetic valve area by 3-dimensional transesophageal echocardiography. *J Am Soc Echocardiogr* 2001;**14**: 723–31.

22 Burstow DJ, Nishimura RA, Bailey KR, *et al.* Continuous wave Doppler echocardiographic measurement of prosthetic valve gradients: a simultaneous Doppler-catheter correlative study. *Circulation* 1989;**80**:504–14.

23 Skjaerpe T, Hegrenaes L, Hatle L. Non-invasive estimation of valve area in patients with aortic stenosis by Doppler ultrasound and two-dimensional echocardiography. *Circulation* 1985;**72**:810–19.

24 Rothbart RM, Castriz JL, Harding LV, *et al.* Determination of aortic valve area by two-dimensional and Doppler echocardiography in patients with normal and stenotic bioprosthetic valves. *J Am Coll Cardiol* 1990;**15**:817–24.

25 Weyman AE. *Principles and practice of echocardiography*, 2nd ed. Philadelphia: Lea & Febiger, 1994.

26 Baur LHB, Braun J, Kappetein AP, *et al.* Stentless bioprostheses are perfect for the small root [abstract]. *J Am Coll Cardiol* 1999;**33**:553A.

27 Chafizadeh ER, Zoghbi WA: Doppler echocardiographic assessment of the St. Jude Medical prosthetic valve in the aortic position using the continuity equation. *Circulation* 1991;**83**: 213–23.

28 Ren JF, Chandrasekaran K, Mintz GS, Ross J, Pennock RS, Frankl WS. Effect of depressed left ventricular function on hemodynamics of normal St. Jude Medical prosthesis in the aortic valve position. *Am J Cardiol* 1990;**65**:1004–9.

29 Kapur KK, Fan P, Nanda NC, Yoganathan AP, Goayal RG. Doppler color flow mapping in the evaluation of prosthetic mitral and aortic valve function. *J Am Coll Cardiol* 1989;**13**:1561–71.

30 Oh JK, Taliercio CP, Holmes DR Jr, *et al.* Prediction of the severity of aortic stenosis by Doppler aortic valve area determination: prospective Doppler-catheterization correlation in 100 patients. *J Am Coll Cardiol* 1988;**11**:1227–34.

31 Rahimtoolah SH. The problem of valve prosthesis-patient mismatch. *Circulation* 1978;**58**:20–5.

32 Dellsperger KC, Wieling DW, Baehe DA, Bard RJ, Brugger JP, Harrison E. Regurgitation of prosthetic

heart valves: dependence on heart rate and cardiac output. *Am J Cardiol* 1983;**51**:321–9.

33 Perry GJ, Helmcke F, Nanda NC, Byard C, Soto B. Evaluation of aortic insufficiency by Doppler color flow mapping. *J Am Coll Cardiol* 1987;**9**:952–9.

34 Touche T, Prasquier R, Nitenberg A, *et al.* Assessment and follow-up of patients with aortic regurgitation by an updated Doppler echocardiographic measurement of the regurgitant fraction in the aortic arch. *Circulation* 1985;**72**:819–24.

35 Teague SM, Heinsimer JA, Anderson JL, *et al.* Quantification of aortic regurgitation utilizing continuous wave Doppler ultrasound. *J Am Coll Cardiol* 1986;**57**:692–4.

36 Kamp O, Verhorst PM, Welling RC, Visser CA. Importance of left atrial appendage flow as a predictor of thromboembolic events in patients with atrial fibrillation. *Eur Heart J* 1999;**20**:979–85.

37 Chambers J, Deverall P. Limitations and pitfalls in the assessment of prosthetic valves with Doppler ultrasonography. *J Thorac Cardiovasc Surg* 1992; **104**:495–501.

38 Hatle L, Angelsen B, Tromsdal A. Non-invasive assessment of atrioventricular pressure half time by Doppler ultrasound. *Circulation* 1979;**60**:1096–104

39 Bitar JN, Lechin ME, Salazar G, Zoghbi WA. Doppler echocardiographic assessment with the continuity equation of St. Jude Medical mechanical prostheses in the mitral valve position. *Am J Cardiol* 1995;**76**:287–93.

8 Right ventricle

Isabelle Michaux, Miodrag Filipovic, Karl Skarvan

Introduction

Information about the structure and function of the right heart, including right ventricle, right atrium, pulmonary artery (PA), tricuspid and pulmonary valves, and the great veins (superior vena cava [SVC] and inferior vena cava [IVC]), can be of vital importance during the perioperative period. During this time mechanical ventilation, with an increase in intrathoracic pressure and various adverse factors such as hypoxaemia, acidosis, embolism, release of mediators, and volume overload, may produce important alterations in right ventricular (RV) preload and afterload, and affect RV function. Perioperative RV failure can be secondary to pre-existing RV dysfunction, new ischaemia or myocardial infarction, intraoperative myocardial injury, chest trauma, or an acute increase in pulmonary vascular resistance. The right ventricle also plays a pivotal role in patients with congenital heart disease undergoing cardiac or non-cardiac surgery (see Chapter 12). Perioperative RV failure has an important impact on outcome, and rapid diagnosis followed by specific therapy is a prerequisite for favourable outcome. Although the PA catheter is an invaluable continuous monitor of right heart function, its diagnostic value is limited because similar pressure and global flow data can be associated with various pathologies.[1,2] Because transthoracic echocardiography may not be feasible in ventilated patients with poor acoustic windows, transoesophageal echocardiography (TOE) often becomes the diagnostic method of choice. The search for a cause of haemodynamic instability and refractory hypotension represents a category I indication for perioperative TOE (Task Force 1996).[3] For instance, in a joint medical and surgical intensive care unit, TOE was used in this indication and found RV failure to be the cause of haemodynamic instability in 18% of patients.[4]

Apart from assessment of RV function, TOE provides invaluable information on the presence of intracardiac shunts, thrombi, vegetations, foreign bodies or valvular dysfunction, and allows non-invasive estimation of systolic and diastolic PA pressures as well as RV stroke volume by Doppler techniques.

Anatomy of the right heart

The systemic venous return enters the right atrium via SVC and IVC, and the coronary venous blood via the coronary sinus. The hepatic veins insert into the IVC 2–3 cm distally from the insertion of the latter into the right atrium. A muscular ridge extending downward and rightward from the SVC toward the IVC is called the crista terminalis and marks the border between the posterior, smooth walled part and the anterior, trabeculated part of the right atrium. The right atrial (RA) appendage is located medially on the top of the right atrium adjacent to the ascending aorta. Anterior to the insertion of the IVC, a rudimentary but variable valve (Eustachian valve) can be seen. Occasionally, this valve is large and perforated, giving rise to a lace-like structure known as network of Chiari. Another small valvular structure is located at the orifice of the coronary sinus. The tricuspid valve is formed by anterior, posterior, and septal leaflets that are connected to anterior, posterior, and medial papillary muscles, respectively.[5]

The right ventricle can be depicted as a tetrahedron in which tricuspid ostium, interventricular septum, and anterior and inferior parts of the free wall represent the four walls, and margo acutus is the connection between the anterior and inferior walls.[6] A strong muscle band divides the RV cavity into two parts: the RV inflow tract and the RV outflow tract. This U-shaped band is called crista supraventricularis and extends from the upper interventricular septum along the anterior tricuspid annulus into the RV free wall. A smaller (moderator) band also connects the distal interventricular septum with the free wall of the right ventricle. In contrast to the trabeculated inner wall of the inflow tract, the surface of the outflow tract (remnant of the bulbus cordis) is smooth. The outflow tract is separated

from the trunk of the PA by the pulmonary valve with right, left, and anterior cusps. The bifurcation of the PA is located to the left of the ascending aorta, with the right PA traversing toward the right hilus behind the aorta.

Physiology of the right heart

Most of the venous return collected in the right atrium during RV systole enters the right ventricle in early diastole, immediately after opening of the tricuspid valve. The RA contraction completes the RV diastolic filling. The right ventricle operates as a low pressure, thin walled volume pump, moving the blood across the low resistance pulmonary bed into the left heart. After the onset of RV contraction, the RV pressure quickly exceeds the diastolic PA pressure, and consequently the time between the closure of the tricuspid valve and the opening of the pulmonary valve (isovolumic contraction period) is very short. The peak RV pressure is reached early during ejection, which – in contrast to left ventricular (LV) ejection – continues even during the late systolic decline in RV pressure. Therefore, the isovolumic relaxation period is also short and often absent. The global systolic function of the right ventricle is determined by RV preload (according to the Frank–Starling law), afterload, and contractility. The thin and compliant wall of the normal right ventricle allows a large increase in end-diastolic volume (preload) without a corresponding increase in RV end-diastolic and RA mean pressures. During acute increase in RV volume it is not only the RV wall but also the pericardium that increasingly opposes further filling and causes a steep increase in right filling pressures. The impedance of the pulmonary vascular bed represents the afterload of the right ventricle. The low pressure pump of the right ventricle is very sensitive to any increase in afterload, and thus there is a close correlation between pulmonary vascular resistance and systolic function of the right ventricle. It is difficult to assess RV contractility directly at the bedside because it requires construction of RV pressure–volume or pressure–area loops, and calculation of RV end-systolic elastance.[7] An improvement in wall motion associated with increase in stroke volume, decrease in RV size, and unchanged or decreasing filling pressures can be interpreted as indirect evidence of increased contractility.

The contraction of the right ventricle follows a specific, "peristaltic" pattern with the outflow tract contracting 25–50 ms after the inflow, giving rise to an intraventricular systolic pressure gradient between the proximal and distal parts of the right ventricle. The crista supraventricularis plays an important role during RV ejection by pulling in most of the RV free wall from margo acutus and anterior interventricular sulcus toward the apex. The effects of its contraction include systolic narrowing of the tricuspid orifice and displacement of the RV free wall toward the septum.[6] The right and left ventricles operate in series, and the function of one ventricle affects the function of the other. This phenomenon is called ventricular interdependence ("cross-talk") and takes place in both systole and diastole. Because the ventricles share common myocardial fibres in the septal region, the contraction of one ventricle contributes to the force of contraction of the other. Naturally, the "help" of the left ventricle is much stronger. Both ventricles compete for space within the pericardium, and therefore the filling of one ventricle affects, by septal shift, the filling of the other. For instance, a marked dilatation of the right ventricle shifts the septum toward the left ventricle and impairs LV compliance and diastolic filling.

The upstream position of the right ventricle renders its pump function sensitive to changes in intrathoracic pressure and lung volume. During spontaneous inspiration, venous return, filling of the right heart, early and late diastolic filling velocities, RV end-diastolic volume, PA flow, and consequently RV stroke volume all increase. In maximal inspiration, even an increase in RV ejection fraction is observed. The respiratory variation in transtricuspid flow velocity (early [E] and late [A] waves) during quiet breathing is in the range 13–17%, whereas excessive variation (> 50%) is an important sign of cardiac tamponade.[8] Opposite changes occur during mechanical ventilation. The intrathoracic pressure increase associated with the mechanical inspiration impairs venous return, reduces RV filling (E and A velocities), PA flow, and RV stroke volume. This inspiratory decrease in RV preload can combine with an increase in RV afterload (by compression of the pulmonary vascular bed due to high inspiratory pressures and/or additional positive end-expiratory pressure) to impair RV ejection.[9]

Normal RV function implies transfer of venous return across pulmonary circulation into the left

Table 8.1 Transoesophageal echocardiographic examination of the right heart

Methods	*Indications*
Two-dimensional TOE	Dimensions of cavities Geometry and wall motion evaluation of the right ventricle Evaluation of the valves' structure Research of thrombi or foreign bodies
Doppler	
PW Doppler	Flow velocity and flow pattern: tricuspid valve, pulmonary artery, hepatic veins
CW Doppler	Velocity of regurgitant flow: tricuspid and pulmonary regurgitation
Colour flow Doppler	Visualisation of regurgitant and shunt flows
TDI	Tricuspid lateral annulus velocities
Contrast	Enhancement of tricuspid regurgitant flow Research of patent foramen ovale

CW = continuous wave, PW = pulsed wave, TDI = tissue Doppler imaging, TOE = transoesophageal echocardiography

heart with physiological right heart volumes and pressures. RV dysfunction means that the right ventricle is still able to fulfil its physiological pumping function but only by activating its reserve or compensatory mechanisms, basically by the Frank–Starling mechanism as well as by development of myocardial hypertrophy in the long term. RV dysfunction is suggested by symptoms and signs occurring under exercise or other forms of stress, and it is confirmed by haemodynamic and/or echocardiographic measurements. RV failure develops when the right ventricle is unable to function properly despite fully activated compensatory mechanisms and causes systemic venous congestion, underfilling of the left ventricle, low cardiac output syndrome, or cardiogenic shock.

Transoesophageal echocardiographic evaluation of the right heart

Two-dimensional TOE and Doppler techniques are used to study the structures and function of the right heart. Application of these techniques is summarised in the Table 8.1.

Two-dimensional examination of the right heart

Right ventricle and tricuspid valve

The right ventricle can be visualised by TOE in four main views that were described in Chapter 2. They include the MOE four chamber view at 0° focused on the tricuspid valve, obtained from the mid-oesophageal (MOE) four chamber view by slightly advancing and turning the probe to the right until the tricuspid valve appears in the centre of the display. This view shows the anterior and septal leaflets of the tricuspid valve and the anterior part of the free wall, with its apical segment on the right, and the basal segment on the left of the display. The MOE RV inflow–outflow view at 60–75° (Figure 8.1B) shows the inferior part of the free wall on the left of the display (basal and apical), and the RV outflow tract on the right of the display. From the stomach we obtain the transgastric short-axis view of the right ventricle (TG RV SAX; Figure 8.1C), which permits evaluation of the basal segments of the anterior (lower part of the display) and inferior (upper part of the display) free wall. Finally, the TG RV inflow view at 120° (Figure 8.1D) provides a view of the inferior free wall (basal and apical segments at the upper part of the display), the anterior free wall (at the lower part of the display), and the tricuspid valve. In this view the anterior and posterior leaflets of the tricuspid valve can be observed, as can the chordae tendineae.

Right atrium and vena cava

The right atrium and the atrial septum can be studied in the MOE four chamber view (see Figure 8.1A) as well as in the *MOE bicaval view* (plane at 110°; Figure 8.2A). The utility of these two views is in searching for patent foramen ovale (using colour Doppler and echo contrast) and thrombi. In the MOE four chamber view,

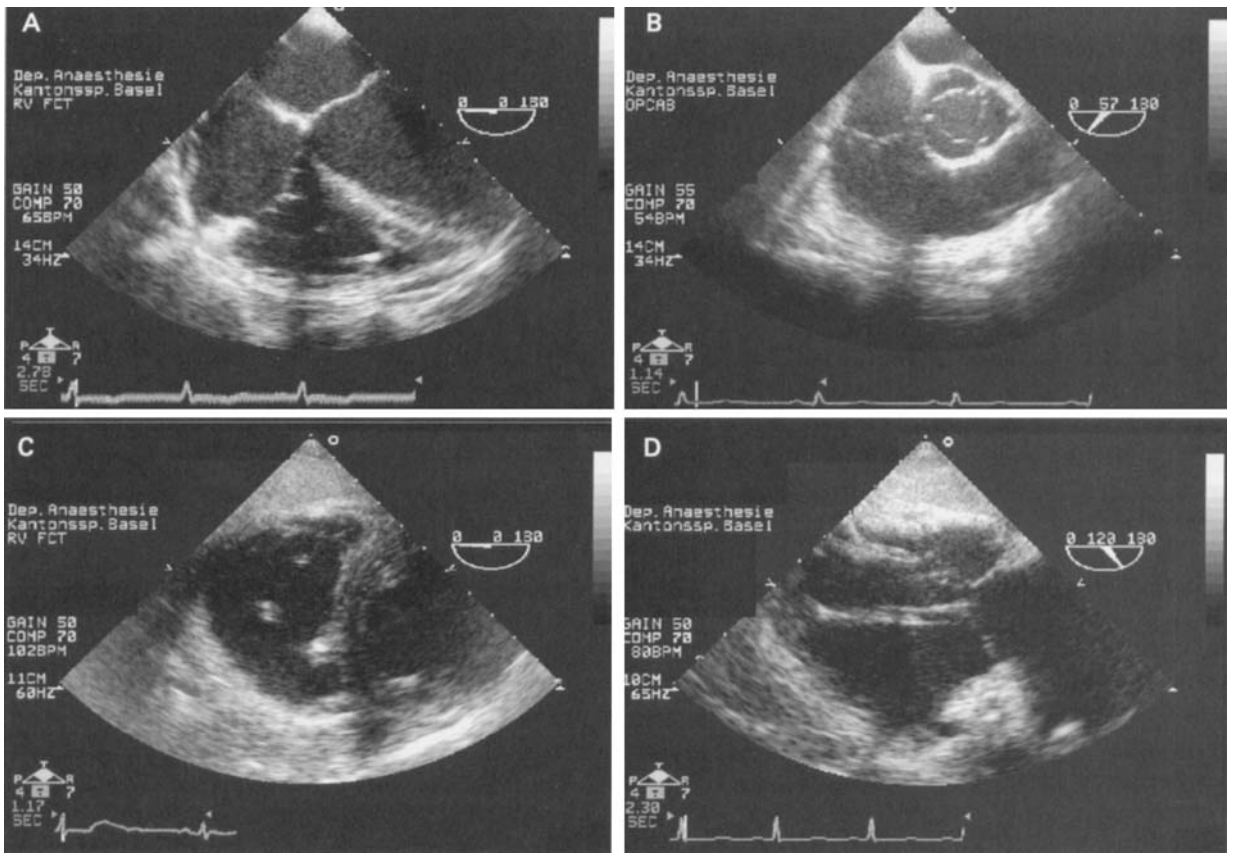

Figure 8.1 Two-dimensional images of the right heart: Four main two-dimensional views of the right ventricle: **(A)** MOE four chamber view (plane at 0°), focused on the tricuspid valve; **(B)** mid-oesophageal right ventricular inflow–outflow (MOE RV inflow–outflow) view; **(C)** transgastric short-axis (TG SAX) view; and **(D)** TG RV inflow view (plane at 120°).

focused on the tricuspid valve, one can also see the coronary sinus, visualisation of which can be helpful in guiding the placement of catheters or pacing leads. On the MOE bicaval view, the SVC is displayed on the right and the IVC on the left. The SVC can also be seen in the upper oesophageal (UOE) SAX view of the ascending aorta (see Chapter 2). These views are also helpful in localising catheters or pacing leads within the right atrium and central parts of caval veins, and in detecting vegetations or thrombi attached to these foreign bodies.

Hepatic veins

From the MOE four chamber view, focused on the tricuspid valve, by rotating the probe to the right, we visualise the junction between the IVC and the three hepatic veins in the liver: the left vein on the right, the right vein on the left, and the middle vein between them (Figure 8.2B). The use of the colour Doppler, with a reduced Nyquist limit, can help to localise the hepatic veins.

Right ventricular outflow tract and the pulmonary artery

The RV outflow tract and the pulmonary valve can be observed on the MOE RV inflow–outflow view (see Figure 8.1B) as well as on the deep TG view of the right ventricle. The PA is interrogated in the UOE views, with the plane at 0° or 90° (Figure 8.2C, D). The UOE view at 0° shows the main trunk of the PA as well as the bifurcation and the right branch. This view is of great interest in case of suspected proximal pulmonary emboli because it allows detection of the thrombi at the bifurcation and/or in the right PA. The UOE SAX view of the aortic arch (plane at 90°) shows the main trunk of the PA.

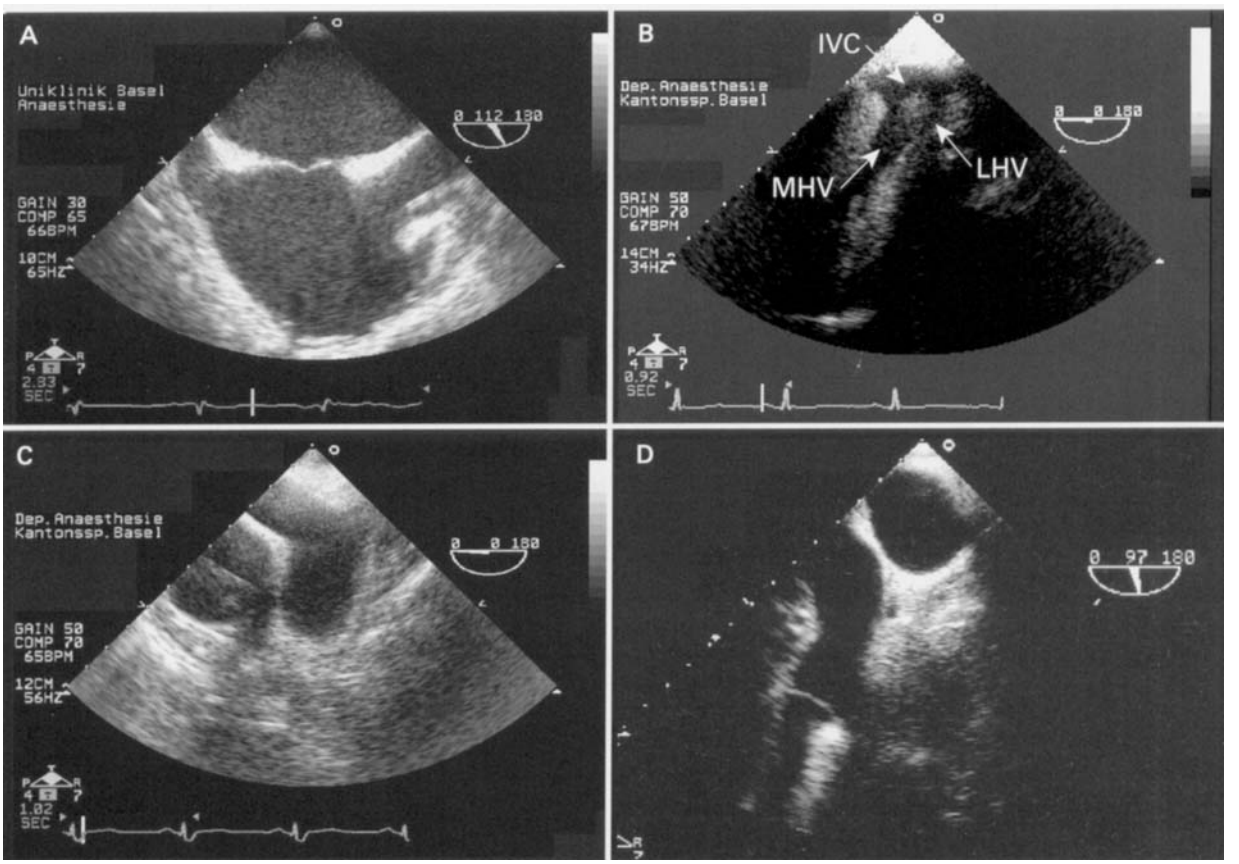

Figure 8.2 Two-dimensional images of the right heart: II. **(A)** Mid-oesophageal bicaval (MOE bicaval) view (plane at 110°) showing the right atrium and the junction of the two venae cavae with the right atrium. **(B)** Junction between the inferior vena cava (IVC) and the hepatic veins(left hepatic vein [LHV] and median hepatic vein [MHV]). **(C)** Upper oesophageal view at 0° showing the main trunk and the right branch of the pulmonary artery. **(D)** Upper oesophageal view at 90° showing a longitudinal view of the pulmonary artery.

Evaluation of right ventricular function

Because of the cyclic changes in RV size and function associated with respiration, a simultaneous recording of respiration is advised in mechanically ventilated patients. Furthermore, all right sided Doppler signals should be recorded at end-expiration. The normal values for RV size and function were derived by transthoracic echocardiography (TTE) in awake and spontaneously breathing individuals (Table 8.2). Our data obtained by TOE in anaesthetised and mechanically ventilated patients free of cardiovascular and pulmonary disease are presented in Table 8.3.

Systolic function

RV fractional shortening expresses the change in RV diameter (free wall to septum) between diastole and systole as a percentage. It is calculated as follows: RV fractional shortening (%) = ([RV EDD–RV ESD]/RV EDD) × 100, where RV EDD is the RV end-diastolic diameter, and RV ESD is the RV end-systolic diameter. The diameters are measured in the MOE four chamber view just below the tricuspid valve and perpendicular to the major axis of the right ventricle. Normal values for RV fractional shortening are in excess of 30%.

The area of the right ventricle can be measured by planimetry in the MOE four chamber view or TG RV SAX view (see Table 8.3). The RV/LV end-diastolic area ratio, which is measured on the MOE four chamber view, is more important for the diagnosis of RV dilation than the absolute RV dimensions.[10] In acute pulmonary embolism, a RV/LV end-diastolic area ratio between 0·6 and 1 indicates mild RV dilation, whereas a ratio greater than 1 is associated with severe dilation.[11]

Table 8.2 Normal right ventricular dimensions (transthoracic values)

Dimension	*View*	*Normal range*
RV diameter	TG SAX (free wall to mid-septum)	EDD 3 ±0·4 cm ESD 2·6 ±0·3 cm
	MOE four chamber view	EDD 3·5 ±0·4 cm ESD 2·9 ±0·4 cm
RV length	MOE four chamber view	EDL 7·1 ±0·8 cm ESL 5·5 ±0·8 cm
RV outflow tract		Diameter 2·5 ±0·4 cm

EDD = end-diastolic diameter, EDL = end-diastolic length, ESD = end-systolic diameter, ESL = end-systolic length, MOE = mid-oesophageal, RV = right ventricular, SAX = short-axis, TG = transgastric. (Data from Weyman.[55])

Table 8.3 Right heart two-dimensional and pulsed wave Doppler transoesophageal echocardiography values obtained in subjects free of cardiovascular disease under general anaesthesia and mechanical ventilation

Number	*Men 25*	*Women 18*
2D MOE four-chamber view		
RVEDA (cm^2)	16 ± 4	14 ± 3
RVESA (cm^2)	10 ± 2	8 ± 2
RV FAC (%)	40 ± 10	42 ± 10
2D TG SAX		
RVEDA (cm^2)	12 ± 5	10 ± 3
RVESA (cm^2)	7 ± 4	5 ± 2
RV FAC (%)	43 ± 14	51 ± 12
RVEDA/LVEDA	0·55 ± 0·1	0·59 ± 0·2
PW Doppler transtricuspid flow velocity		
E (cm/s)	34 ± 10	35 ± 9
A (cm/s)	23 ± 7	22 ± 5
E/A	1·5 ± 0·6	1·7 ± 0·5
PW Doppler pulmonary artery flow velocity		
V_{max} (cm/s)	77 ± 18	72 ± 20
VTI (cm)	18 ± 7	17 ± 5
Acceleration (cm/s^2)	749 ± 286	745 ± 370
Time to peak (ms)	108 ± 24	111 ± 35
Pre-ejection time (ms)	85 ± 31	81 ± 18
Ejection time (ms)	371 ± 62	384 ± 36
PEP/ET	0·23 ± 0·08	0·21 ± 0·06

E and A = early and late transtricuspid peak flow velocity, EDA = end-diastolic area, ESA = end-systolic area, ET = ejection time, FAC = fractional area shortening, PEP = pre-ejection period, RV = right ventricular, V_{max} = pulmonary artery peak flow velocity, VTI = velocity–time integral of pulmonary flow signal. (Data from Lambert-Lintner.[56])

The RV fractional area change (FAC) is calculated as (RV EDA–RV ESA)/RV EDA, where EDA is the end-diastolic area, and RV ESA the end-systolic area. A RV FAC under 35% before coronary artery bypass graft surgery is associated with increased postoperative mortality.[12] The wide range of normal values for RV FAC (40–74%)[13] and its poor relationship with the severity of haemodynamic instability limit its use in daily practice.

Measurement of the RV end-diastolic and end-systolic volumes is difficult because of the complex shape of the right ventricle. Several models of the right ventricle were proposed.

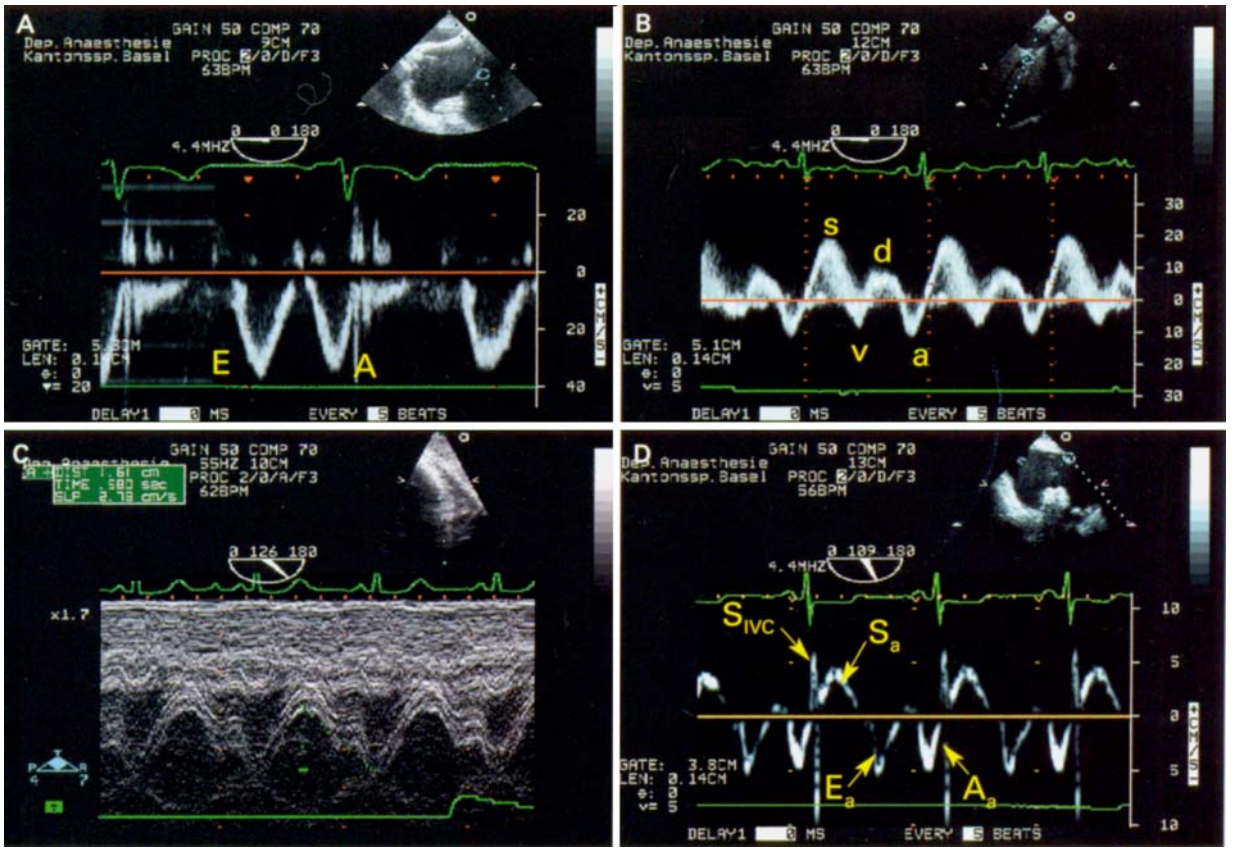

Figure 8.3 Doppler and M-mode examination of the right heart. **(A)** Tricuspid inflow, with early (E) and late (A) waves shown. **(B)** Hepatic venous flow: a = atrial reverse wave, d = diastolic wave, s = systolic wave, v = late systolic reverse wave. **(C)** Tricuspid annular plane systolic excursion, measured in M-mode on the tricuspid lateral annulus using the transgastric right ventricular inflow (TG RV inflow) view. **(D)** Tissue Doppler imaging of the tricuspid lateral annulus: Aa = atrial myocardial wave, Ea = early myocardial diastolic wave, Sa = systolic myocardial wave, S_{IVC} = isovolumic contraction.

Using a formula based on a crescentic model, the RV volume can be calculated as $2/3 \times$ (RV area $\times$ RV long axis), where the area is measured in the MOE four chamber view and the long-axis as the distance between the tricuspid valve and the pulmonary valve on the MOE RV inflow–outflow view. Taking these measurements at end-diastole and end-systole, one can calculate the RV end-diastolic and end-systolic volumes, as well as the RV ejection fraction. This model, however, has never been validated in TOE, and its use is limited to research studies.

The tricuspid annular plane systolic excursion (TAPSE) is the maximal systolic excursion of the tricuspid lateral annulus, which is measured in M-mode at the lateral annulus (Figure 8.3C). To reduce the angle between the ultrasound beam and the longitudinal displacement of the annulus, we recommend that it be recorded in the TG RV inflow view. In TTE there is good correlation between the TAPSE and the RV ejection fraction measured by radionuclide ventriculography or right heart catheterisation; a TAPSE in excess of 14 mm differentiates normal from reduced RV function.[14,15]

Tissue Doppler imaging (TDI) of the tricuspid lateral annulus measures the systolic and diastolic velocities of the lateral annulus of the tricuspid valve. In our experience, the TG RV inflow view allows recording of the tricuspid TDI with the narrowest angle between the probe and the longitudinal movement of the annulus (Figure 8.3D). The typical RV velocity pattern is characterised by two systolic velocity and two diastolic velocity peaks. The first systolic wave is recorded during isovolumic contraction and the second during RV ejection (Sa). The first diastolic wave reflects the early (Ea) and the second wave (Aa) late RV filling. From these TDI signals various time intervals can be derived, such as pre-ejection time, time to peak, and ejection time.

The peak systolic velocity of the tricuspid annulus (Sa) appears to be a useful measure of global RV function. For instance, a systolic velocity below 11·5 cm/s predicts a RV ejection fraction under 45% in patients with dilated cardiomyopathy with a sensitivity of 90% and a specificity of 85%.[16] Peak systolic velocity is lower in patients with an inferior than in those with an anterior myocardial infarction. Furthermore, the systolic velocity is even more reduced in patients with an inferior myocardial infarction with RV involvement.[17] The published data on RV TDI are based on TTE, and the utility of TDI in perioperative TOE is still under investigation.

The PA flow can be recorded with pulsed wave Doppler in the UOE or TG views in the long-axis of the PA. A normal flow pattern exhibits a gradual acceleration and deceleration, with a peak velocity occurring close to the mid-ejection (symmetrical shape). By measuring the velocity–time integral (VTI) of the PA flow signal and the diameter of the PA, it is possible to calculate RV stroke volume (ml) as PA_{VTI} (cm) multiplied by cross-sectional area (cm^2) of the main trunk of the PA. The measurement of the diameter can be improved by the use of colour Doppler to mark off the arterial walls. In our experience it appears that a PA_{VTI} greater than 15 cm indicates normal RV output (see Table 8.3).

Wall motion reading

Because of asymmetrical geometry, smaller degree of systolic shortening, and thinner wall, RV wall motion abnormalities are more difficult to detect than those of the LV wall. Although no segmental model of the right ventricle has yet been validated, the RV free wall is usually divided into four segments: anterobasal, inferobasal, anteroapical, and inferoapical. In addition, the wall motion must be evaluated in the RV outflow tract and in the ventricular septum. Whereas the anterior segments are best evaluated in the MOE four chamber view focused on the tricuspid valve (0°), the inferior segments and the outflow tract are interrogated in the MOE RV inflow–outflow view. Basal and mid-ventricular segments can also be evaluated in the TG SAX view. The grading scale for visual assessment of wall motion of the free wall is as follows: 1 = normal, 2 = hypokinetic, 3 = akinetic, and 4 = dyskinetic).[18]

Diastolic function

The tricuspid inflow velocities (Figure 8.3A) can be recorded from the MOE four chamber view, focused on the tricuspid valve, and from the TG RV inflow view, where the optimal alignment between flow and Doppler beam can usually be found. The velocities across the tricuspid valve are lower than those across the mitral valve. Regarding the mitral inflow, the tricuspid inflow shows E and A waves. Similar to the measurements of transmitral velocities, peak E and A velocities, corresponding VTIs, deceleration time of the E wave, and ratio of peak E/A velocities can be determined (see Table 8.3).

The tricuspid inflow changes with increasing age, as does the mitral inflow; E wave decreases and A wave increases, leading to a gradual decrease in the E/A ratio and an increase in the E wave deceleration time.[19] The E/A ratio increases in the case of elevation in central venous pressure (CVP), in severe tricuspid regurgitation, and in RV dysfunction (RV infarction or advanced restrictive myocardial disease).[20] In pulmonary hypertension associated with RV hypertrophy, E velocity decreases and A velocity increases, resulting in a low E/A ratio. The simultaneously prolonged E deceleration time allows for qualification of these findings as an abnormal relaxation pattern. A colour Doppler superimposed on the RV inflow and tricuspid valve is used to detect tricuspid regurgitation (see Figure 8.5A), which is a common finding in mechanically ventilated patients. By placing the cursor line of continuous wave Doppler in the tricuspid regurgitant jet, the maximal velocity (V_{max}) of the regurgitation can be measured and the systolic RV pressure estimated (see below).

Placing the sampling volume of pulsed wave Doppler in one of the three hepatic veins, with a filter reduced to 50 Hz, allows recording of hepatic venous flow. The hepatic venous flow pattern has four components (Figure 8.3B): a biphasic forward flow with a systolic and a diastolic wave, and two reverse flows – one occurring during the atrial contraction and the other in late systole. The systolic wave (s) is produced by RA relaxation and RV contraction with an increase in RA volume because of the descent of the tricuspid annulus to the apex. The diastolic (d) component occurs with the opening of the tricuspid valve and RV filling. The atrial reverse wave (a) is a backflow in the hepatic veins due to atrial contraction. Finally, the late systolic

reverse flow, called the V wave (v), can be explained by atrial overfilling. The normal hepatic pattern is a biphasic forward flow with systolic dominance and two small reverse waves. The systolic forward velocity decreases with elevation in CVP,[21] or in the presence of tricuspid regurgitation or inferior myocardial infarction.[22] In the case of severe tricuspid regurgitation, a systolic flow reversal may be observed. Using peak hepatic vein flow velocities or their VTI values, one can calculate the systolic filling fraction (SFF) as systolic velocity/(systolic + diastolic velocity) (peak or VTI values). In TTE there is a good correlation between the SFF and CVP.[21] In a prospective study, the equation CVP = 21·6 – 24 SFF was validated in intensive care unit patients with and without mechanical ventilation, and it was found to be clinically useful. The reverse flow/forward flow ratio, calculated as $(VTI_a + VTI_v)/(VTI_s + VTI_d)$ increases with increases in CVP.[23]

The diastolic function indices derived from TDI of the tricuspid lateral annulus are Ea, Aa, Ea/Aa ratio, and isovolumic relaxation time (IVRT) measured between the end of systolic and onset of early diastolic motion. Once again, only TTE data have been validated. The Ea/Aa ratio decreases with age, in cases of inferior myocardial infarction, and in pulmonary and systemic hypertension.[24] There is a strong correlation between the CVP and the tricuspid E/Ea ratio in patients with and without mechanical ventilation. A E/Ea ratio greater than 6 predicts a CVP greater than 10 mmHg with a sensitivity of 79% and a specificity of 73%.[25] This relationship between E/Ea and CVP was also found in heart transplant recipients.[26] Such a non-invasive estimate of CVP may be very useful because CVP elevation is an early sign of graft rejection. The IVRT is generally very short or absent, but for pulmonary or systemic hypertension, or in the case of hypertrophic cardiomyopathy, the IVRT increases significantly and can easily be measured.[24]

Myocardial performance index (Tei index) applied to the right ventricle

The myocardial performance index (MPI), first described by Tei *et al.*[27] in 1995, allows combined evaluation of the systolic and diastolic functions.[27] The MPI is a ratio of the sum of the two isovolumic intervals (IVRT and isovolumic contraction time [IVCT]) divided by the ejection

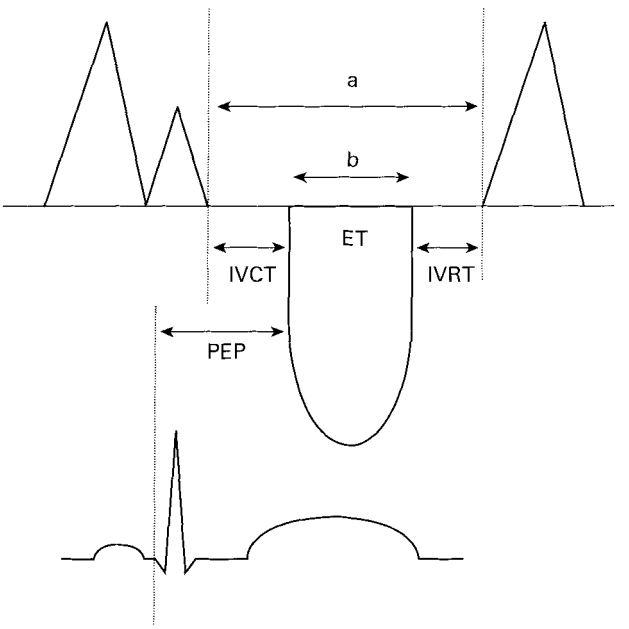

Figure 8.4 Doppler intervals used to calculate the myocardial performance index (MPI), or Tei index. MPI = (a–b)/b where "a" is the time between cessation and onset of the two consecutive tricuspid inflows and "b" is the ejection time (ET) of the right ventricle. IVCT = isovolumic contraction time, IVRT = isovolumic relaxation time, PEP = pre-ejection period. (According to the Figure published by Eidem.[28])

time (Figure 8.4). These three intervals are important energy dependent periods of the cardiac cycle. For the calculation of this index, Doppler velocity recordings of tricuspid inflow and PA outflow are required, and the following intervals are measured: time between cessation and onset of two consecutive tricuspid inflows (time a) and time between the onset and cessation of pulmonary flow (ejection time, time b). The index is then calculated as MPI = (a – b)/b (see Figure 8.4). In systolic dysfunction, the IVCT increases whereas the ejection time decreases, and consequently the MPI increases. In diastolic dysfunction there is a prolongation in the IVRT that also results in an increased MPI. This index was validated by TTE in congenital heart disease[28] and in chronic respiratory disease,[29] and is the strongest predictor of adverse outcome in patients with primary pulmonary hypertension.[30] Preliminary data suggest that the RV MPI determined by TOE is feasible during cardiac surgery.[31,32]

Although the MPI can easily be calculated, it has some limitations in clinical practice. These

limitations include the phenomenon of pseudonormalisation in patients with severe RV dysfunction,[33] heart block, and arrhythmias. The pseudonormalisation of the MPI is caused by significant shortening of the IVCT for severe RV dysfunction. Finally, the effect of loading conditions and heart rate on the MPI is still unknown. When the two intervals are measured sequentially on two separate Doppler recordings (i.e. during two different cardiac cycles), there can be a significant fluctuation in the RR interval, which can compromise the accuracy of the calculated MPI. Therefore, some authors propose simultaneous measurement of these two intervals during one cardiac cycle, using the TDI signal of the tricuspid annulus.[34] The MPI is derived from the TDI signal as $(a' - b')/b'$, where (a') is the time between the end of Aa and onset of Ea and (b') is the duration of Sa. There is good correlation between the different times measured on pulsed Doppler signals and on TDI signals, and between the TDI MPI and the MPI determined by pulsed wave Doppler.

Measurement of pulmonary artery pressure

Echocardiography offers non-invasive access to the pressures in the right heart. When a tricuspid regurgitation (Figure 8.5A) is present, which is quite common in mechanically ventilated patients as well as in patients with abnormal RV function, it is possible to measure the maximal velocity of the regurgitant jet by continuous wave Doppler (Figure 8.5B). By application of the simplified Bernoulli's equation ($\Delta P = 4V^2$), the peak pressure gradient between the right ventricle and right atrium can be calculated. RV systolic pressure then equals this gradient plus CVP. In the absence of pulmonary valve stenosis, the PA systolic pressure is equivalent to the RV systolic pressure. The accuracy of this pressure estimation depends on the recording of a complete envelope of the regurgitant velocity by continuous wave Doppler. The Doppler signal can be enhanced by intravenous injection of an echocardiographic contrast agent. Similarly, in the presence of pulmonary regurgitation (Figure 8.5C), visualised by colour Doppler on the deep TG view of the right ventricle, the diastolic pulmonary pressure can be calculated as the end-diastolic pressure gradient across the pulmonary valve plus CVP (Figure 8.5D). A summary of calculations that may be used to estimate PA pressures is presented in Box 8.1.

In pulmonary hypertension the flow pattern resembles that of aortic ejection, with a short acceleration time and early peak (asymmetrical shape). An abrupt decrease in velocity in mid-systole (notch) can be observed in some patients with severe pulmonary hypertension. In these patients a late systolic flow reversal may also be present. Total RV ejection time and acceleration time (time to peak) are shortened, whereas RV IVRT (time between the closure of pulmonary valve and opening of the tricuspid valve) and pre-ejection time (time between the onset of QRS and the onset of pulmonary ejection flow) are prolonged. One can make use of the negative correlation between the RV acceleration time of the PA flow signal and the PA pressure. An RV acceleration time under 80 ms was indicative of increased PA pressure in a transthoracic study.[35] The RV IVRT corrected for heart rate and obtained by transthoracic Doppler can also be used to estimate PA pressure and to detect pulmonary hypertension.[36] Finally, the index of RV acceleration time divided by RV ejection time also correlates with the PA pressure.

Patients with pulmonary hypertension often present an abnormal tricuspid flow pattern with prolonged deceleration time of the E velocity and low E/A ratio. The right atrium and right ventricle are dilated as a result of the increased RV afterload. The presence of RV hypertrophy allows differentiation between acute and chronic pulmonary hypertension. The diastolic RV wall thickness is measured by M-mode echocardiography, using the MOE RV inflow–outflow view or the TG RV inflow view. RV hypertrophy can be considered if RV wall thickness is in excess of 6 mm.[37] In acute pulmonary hypertension the RV thickness is typically below 6 mm, with clear visualisation of the RV trabeculations. In chronic pulmonary hypertension the RV hypertrophy is more pronounced, with a RV wall thickness of about 10 mm.

Preload and afterload of the right ventricle

The right ventricle typically dilates in response to an increase in preload or afterload, or in both. Because the two ventricles share myocardial fibres of the common septum and are enclosed in the same stiff pericardium, any change in RV filling can affect the diastolic function of the left ventricle (diastolic interdependence). TOE provides valuable information on the shape and motility of the interventricular septum, which is a mediator in this ventricular interaction.

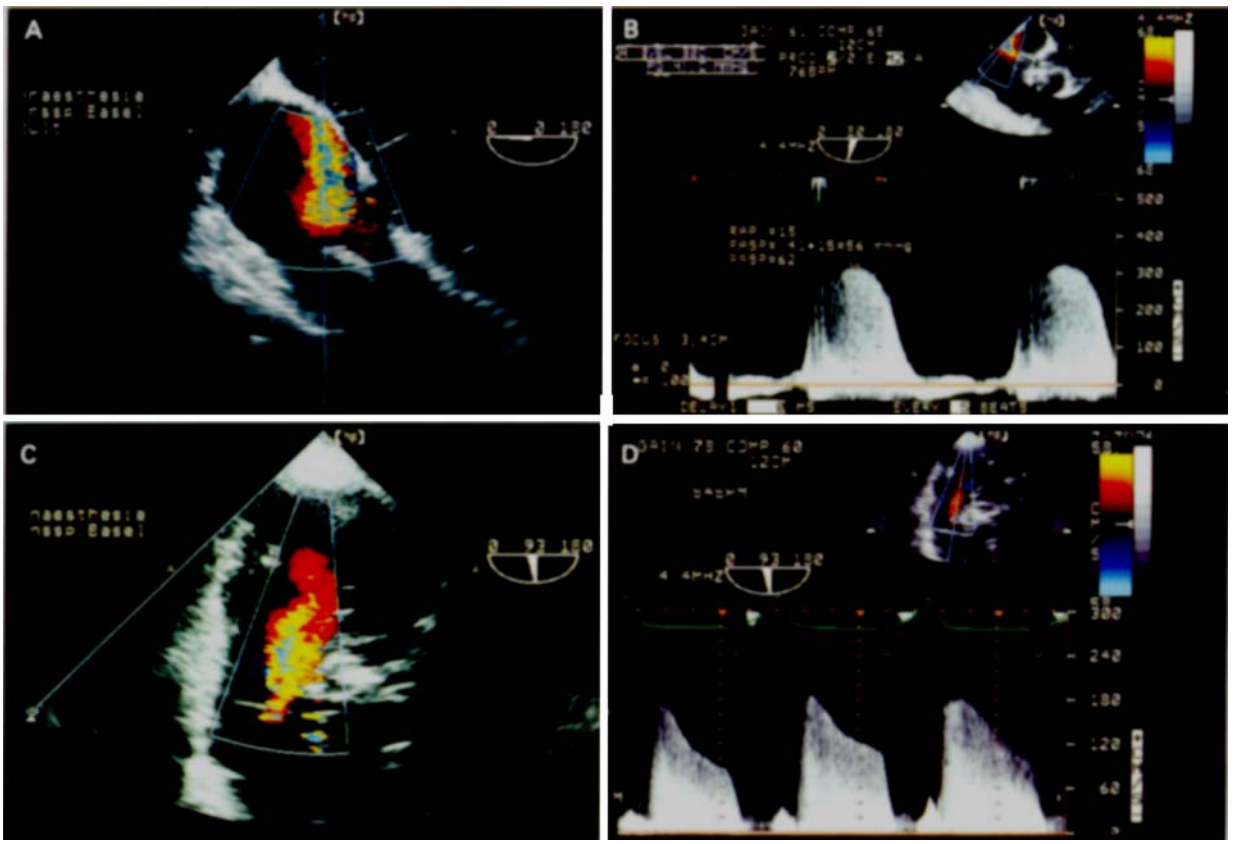

Figure 8.5 Measurements of the pulmonary pressures. **(A)** Moderate tricuspid regurgitation detected by colour Doppler, with **(B)** recording of the tricuspid regurgitation velocity by continuous wave Doppler. **(C)** Pulmonary regurgitation detected by colour Doppler, with **(D)** recording of the pulmonary regurgitation velocity by continuous wave Doppler.

- Systolic pulmonary pressure = $4 \times V^2_{TR} + CVP$
- Diastolic pulmonary pressure = $4 \times ED\ V^2_{PR} + CVP$

CVP = central venous pressure, ED = end-diastolic, PR = pulmonary regurgitation, TR = tricuspid regurgitation, V = velocity.

Box 8.1 Estimation of pulmonary artery pressures from regurgitant velocities by continuous wave Doppler

Volume overload

With increasing intensity of RV volume overload, the RV end-diastolic pressure equals and eventually exceeds the LV end-diastolic pressure. The septum follows the abnormal diastolic transseptal pressure gradient and becomes flat and even bows toward the left ventricle in end-diastole. In diastole, in the TG SAX view, the right ventricle assumes a circular shape, whereas the left ventricle becomes crescentic. These changes are more pronounced if the pericardium is closed. During systole, when the pressure generated by the left ventricle exceeds RV pressure, the septum moves swiftly toward the right ventricle and the left ventricle resumes its normal circular shape. This abnormal early systolic outward movement is called paradoxical septum motion (Figure 8.6).

Pressure overload

For pressure overload, the high RV end-diastolic pressure and volume affect LV filling and shape in the same way as the volume overload during diastole. However, in severe pulmonary hypertension the RV pressure may exceed the LV pressure even during systole. In this case, the abnormal shift of the septum toward the left ventricle persists throughout systole (see Figure 8.6).

Right ventricle in cardiac surgery

Impairment in RV function after cardiac surgery was originally documented by

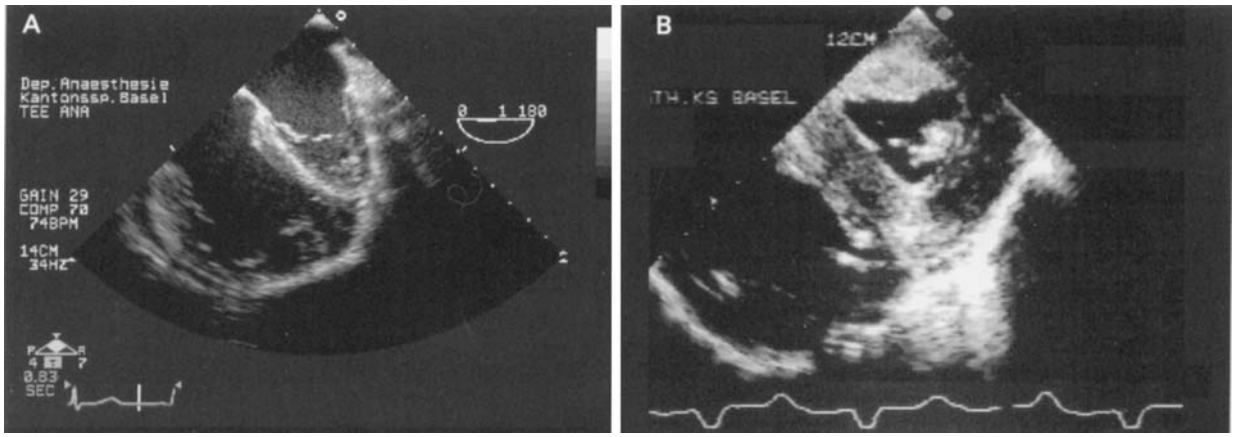

Figure 8.6 Right ventricular overload. **(A)** Mid-oesophageal four chamber (MOE four chamber) view of a dilated right ventricle caused by volume overload due to atrial septum defect. **(B)** Transgastric short-axis (TG SAX) view of a dilated right ventricle caused by pressure overload, with clear flattening of the septum.

radionuclide ventriculography.[38,39] The multiple factors responsible for postoperative abnormal RV systolic and diastolic functions include mechanical injury (RA cannulation, RA traction and compression), inadequate myocardial protection (particularly in the presence of right coronary artery stenosis), myocardial ischaemia (failed revascularisation, coronary artery spasm), perioperative myocardial infarction, increase in RV afterload, and, later, formation of adhesions. In patients who develop refractory hypotension and/or low cardiac output syndrome after cardiac surgery, isolated RV failure (Box 8.2) was identified by using TOE in 22% and 23% of cases, respectively.[1,2] In addition, RV failure combined with LV failure (biventricular failure) was found in 12% and 28% of cases, respectively. Most patients with postoperative RV failure have a severe tricuspid regurgitation that can interfere with haemodynamic measurements.[2] The finding of RV failure is associated with a high hospital mortality rate of 44%.[2] This emphasises the importance of rapid and accurate diagnosis as a starting point for optimal therapy. The right ventricle does not appear to benefit much from improvements in intraoperative myocardial protection. Even after retrograde cold blood cardioplegia, worsening in tricuspid regurgitation (17%), new RV wall motion abnormalities (8%), and RV failure (6%) were revealed by TOE.[40] The RV failure following cardiac surgery is likely to represent the "tip of the iceberg" because distinct changes in RV systolic and diastolic function occur even after an uneventful aortocoronary bypass operation. They include decreases in RV major and minor axis shortening, fractional area shortening, and tricuspid annular excursion.[22,41]

- Dilated right ventricle: ratio of right to left ventricular EDA >0·6[11]
- Right ventricular FAC <25%[2] or 35%[12]
- Severe hypokinesis or akinesis in two or more right ventricular segments[2]

EDA = end-diastolic area, FAC = fractional area shortening.

Box 8.2 Definition of right ventricular failure

The RV filling pattern can also be markedly altered after cardiac surgery. In the hepatic veins there is a decrease in systolic forward flow (s) associated with an increase in late systolic reverse flow (v), and a decrease in late diastolic reverse flow (a). This results in a fall in systolic to diastolic forward flow ratio as well as in an increase in the ratio of the reverse to forward flow.[22,23,42] Similar changes were also observed in SVC flow pattern.[43] Although tricuspid regurgitation is associated with lower systolic to diastolic forward flow ratio, this alone does not explain the marked changes in the systemic venous flow pattern.[23] Although a gradual return to preoperative values was noted during follow up, after 6 months the recovery of the filling pattern and the tricuspid annular motion was still

incomplete.[43] This alteration in RV diastolic function appears to be related to the method of intraoperative myocardial protection. It occurs when hypothermic crystalloid cardioplegia is used but not after normothermic blood cardioplegia.[44]

Right ventricular infarction

The clinical syndrome of RV infarction combines manifestations of an acute myocardial infarction with systemic venous congestion but with clear lung fields (absent pulmonary congestion). An isolated RV infarction is rare; usually it accompanies inferior, posterior, inferolateral, and inferoseptal infarctions. Nevertheless, the extent of wall motion abnormalities in the right ventricle is more pronounced than in the left ventricle (predominant RV infarction). The ratios of RV to LV dimensions and volumes at end-diastole and end-systole are markedly increased as evidence of RV dilation, and the RV ejection fraction is more depressed than the LV ejection fraction.[45] This RV dilation is accompanied by tricuspid annulus dilation and, together with papillary muscle dysfunction, it is responsible for the tricuspid regurgitation that is usually present. Because the infarcted right ventricle can no longer generate a normal pressure gradient between the right ventricle and the right atrium, the measured transtricuspid pressure gradient is low. RV dysfunction can be accompanied by impaired function of the right atrium that can be detected by RA dilation, decrease in RA FAC, and reduction in tricuspid A wave velocity.[46] The inversion of the normal atrial septum convexity (leftward shift) in the setting of acute inferior infarction is evidence of right sided filling pressures exceeding filling pressures on the left side. This finding is associated with increased incidences of hypotension, atrioventricular block, and increased mortality.[47] RV infarction can progress into a cardiogenic shock, which has long been considered to be potentially reversible. However, recent data from the SHOCK registry[48] showed that the mortality with predominant RV shock is almost as high as that with LV shock. Furthermore, a persisting RV dysfunction (defined as RV FAC $< 32\%$) after myocardial infarction was shown to be an independent predictor of cardiovascular mortality and heart failure.[49] Thus, an early echocardiographic diagnosis of predominant RV infarction in the setting of cardiogenic shock is important because it allows immediate therapy to be instituted, with the goal being to reopen the right coronary artery and save the RV myocardium.

Right heart in non-cardiac surgical intensive care unit patients

In non-cardiac, mechanically ventilated, surgical patients, the two most important causes of RV dysfunction or failure are acute pulmonary embolism and acute respiratory distress syndrome (ARDS). In these two situations the right ventricle in non-cardiac surgical intensive care unit patients faces a sudden increase in its afterload that can be further intensified by the use of positive end-expiratory pressure.[50] The impediment in RV ejection is responsible for an increase in RV end-diastolic and end-systolic volumes, a reduced RV stroke volume, and RV FAC.[11] The RV dilation may be less apparent in hypovolaemia and there may be an additional reduction in venous return with positive end-expiratory pressure. The notion of "acute cor pulmonale" was recently introduced to describe the dilatation of the right ventricle, defined as a ratio of RV to LV end-diastolic area (measured in the MOE four chamber view) greater than 0·6 in combination with the abnormal RV end-diastolic shape in the TG short-axis view.[11] In both clinical situations the Doppler patterns of pulmonary hypertension can be found (i.e. an asymmetrical pulmonary ejection flow with an eventual mid-systolic notching, a tricuspid flow showing a large A wave, and a prolonged deceleration time of the E wave). The colour flow Doppler detects a moderate or severe tricuspid regurgitation due to the dilation of the tricuspid annulus. The measurement of the regurgitant jet velocity allows the degree of pulmonary hypertension to be quantified.

Acute pulmonary embolism in ventilated patients is difficult to diagnose because of the absence of clinical signs such as dyspnoea, chest pain, or hyperventilation. For peripheral pulmonary embolism, not only can RV dilation be absent but also the Doppler signs of pulmonary hypertension. In massive pulmonary embolism (i.e. occlusion of at least two lobar arteries), RV failure can be so severe that RV contraction can no longer generate a normal pressure gradient between atrium and ventricle. Despite the finding of severe tricuspid regurgitation in colour

Doppler, continuous wave Doppler often does not produce a distinct tricuspid regurgitation envelope. Using the definition of acute cor pulmonale mentioned above,[11] Vieillard-Baron *et al.*[51] found a 61% incidence of echocardiographic acute cor pulmonale in patients with acute pulmonary embolism. There is a good correlation between the extent of obstruction of the pulmonary vascular bed and the magnitude of RV dilation and the decrease in RV FAC.[52] Recently, the usefulness of acceleration time/RV ejection time in the diagnosis of acute pulmonary embolism was confirmed. After therapy, persisting low values of this index suggest the presence of residual thrombi.[53] For central embolism, the UOE view at 0° can detect the thrombus inside the main PA or in the right branch. The signs of RV dilation and pulmonary hypertension regress or even normalise in the following 2–3 weeks because of spontaneous fibrinolysis. After thrombolytic therapy, the regression is usually much faster.

In patients with ARDS who are undergoing mechanical ventilatory support, TOE often provides more reliable information on RV function than does TTE because of the poor transthoracic window. The aetiology of the pulmonary hypertension in ARDS is multifactorial; intravascular obstruction, pulmonary vasoconstriction (provoked by hypoxaemia, permissive hypercapnia, and administration of catecholamines), and high intrathoracic pressure (usually with positive end-expiratory pressure), all combine and result in an increase in RV afterload in both inspiration and expiration.[9] In a recent prospective study, Vieillard Baron *et al.*[54] studied the incidence of acute cor pulmonale in ventilated ARDS patients under a protective ventilator strategy (airway pressure limitation). There was an incidence of 25% at 3 days after the beginning of mechanical ventilation.

In patients with sepsis or septic shock, TOE provides useful information about preload, presence of pulmonary hypertension, and biventricular function. In addition, an outbreak of sepsis in patients with indwelling central venous catheters or leads should prompt a search for tricuspid or pulmonary endocarditis and for vegetations enclosing the venous foreign bodies. The discovery of a thrombus in the SVC in the context of sepsis suggests septic thrombophlebitis.

The anterior position and the attachment of the great veins make the right heart very sensitive to blunt chest trauma. Myocardial contusion of the free wall or of the septum manifests as wall motion abnormality (akinesia or dyskinesia). Intracavitary thrombi can be seen attached to the injured endocardium. It is mandatory to search for other traumatic injuries to the right heart because if they are not recognised and immediately treated they can be lethal. These injuries include rupture of the right atrial or ventricular wall leading to acute heart tamponade; caval vein tears; atrial and ventricular septum defects; rupture of valve leaflets, chordae, and papillary muscles causing tricuspid regurgitation; and injury to the right coronary artery.

During a TOE examination in ventilated patients with pulmonary embolism or ARDS and hypoxaemia, a patent foramen ovale should be sought by colour Doppler and contrast echocardiography, accompanied by Valsalva's manoeuvre. Until the left atrial pressure remains higher than the RA pressure the valve of the foramen remains closed, but as soon as RA pressure exceeds left atrial pressure the foramen may reopen, creating a right-to-left shunt and causing a severe, oxygen refractory hypoxaemia. In pulmonary embolism, the presence of a patent foramen ovale represents a risk for paradoxical systemic embolism.

References

1 Reichert CL, Visser CA, Koolen JJ, *et al.* Transesophageal echocardiography in hypotensive patients after cardiac operations. Comparison with hemodynamic parameters. *J Thorac Cardiovasc Surg* 1992;**104**:321–6.

2 Davila-Roman VG, Waggoner AD, Hopkins WE, Barzilai B. Right ventricular dysfunction in low output syndrome after cardiac operations: assessment by transesophageal echocardiography. *Ann Thorac Surg* 1995;**60**:1081–6.

3 Practice guidelines for perioperative transesophageal echocardiography. A report by the American Society of Anesthesiologists and the Society of Cardiovascular Anesthesiologists Task Force on Transesophageal Echocardiography. *Anesthesiology* 1996;**84**:986–1006.

4 Heidenreich PA, Stainback RF, Redberg RF, Schiller NB, Cohen NH, Foster E. Transesophageal echocardiography predicts mortality in critically ill patients with unexplained hypotension. *J Am Coll Cardiol* 1995;**26**:152–8.

5 Netter F. *The Ciba Collection of medical illustrations, Heart.* Vol 5, Rochester, New York: The Case-Hoyt Corp, 1981.

6 James TN. Anatomy of the crista supraventricularis: its importance for understanding right ventricular function, right ventricular infarction and related conditions. *J Am Coll Cardiol* 1985;**6**:1083–95.

7 Ochiai Y, Morita S, Tanoue Y, Kawachi Y, Tominaga R, Yasui H. Use of transesophageal echocardiography for postoperative evaluation of right ventricular function. *Ann Thorac Surg* 1999;**67**:146–152.

8 Weyman AE. *Principles and practice of echocardiography, 2nd edn.* Philadelphia: Lea & Febiger, 1994, 829.

9 Poelaert JI, Visser CA, Everaert JA, De Deyne CS, Decruyenaere J, Colardyn FA. Doppler evaluation of right ventricular outflow impedance during positive-pressure ventilation. *J Cardiothorac Vasc Anesth* 1994;**8**:392–7.

10 Mansencal N, Joseph T, Vieillard-Baron A, *et al.* Comparison of different echocardiographic indexes secondary to right ventricular obstruction in acute pulmonary embolism. *Am J Cardiol* 2003; **92**:116–9.

11 Jardin F, Dubourg O, Bourdarias JP. Echocardiographic pattern of acute cor pulmonale. *Chest* 1997;**111**:209–17.

12 Maslow AD, Regan MM, Panzica P, Heindel S, Mashikian J, Comunale ME. Precardiopulmonary bypass right ventricular function is associated with poor outcome after coronary artery bypass grafting in patients with severe left ventricular systolic dysfunction. *Anesth Analg* 2002;**95**:1507–18.

13 Jardin F. Echocardiographic evaluation of the right ventricular function [in French]. In: *L'évaluation hémodynamique non invasive au lit du patient par échocardiographie-Doppler.* Paris: Masson; 1995, p 44.

14 Kaul S, Tei C, Hopkins JM, Shah PM. Assessment of right ventricular function using two-dimensional echocardiography. *Am Heart J* 1984;**107**:526–31.

15 Ghio S, Recusani F, Klersy C, *et al.* Prognostic usefulness of the tricuspid annular plane systolic excursion in patients with congestive heart failure secondary to idiopathic or ischemic dilated cardiomyopathy. *Am J Cardiol* 2000;**85**:837–42.

16 Meluzin J, Spinarova L, Bakala J, *et al.* Pulsed Doppler tissue imaging of the velocity of tricuspid annular systolic motion; a new, rapid, and non-invasive method of evaluating right ventricular systolic function. *Eur Heart J* 2001;**22**:340–8.

17 Alam M, Wardell J, Andersson E, Samad BA, Nordlander R. Right ventricular function in patients with first inferior myocardial infarction: assessment by tricuspid annular motion and tricuspid annular velocity. *Am Heart J* 2000;**139**:710–5.

18 Bowers TR, O'Neill WW, Grines C, Pica MC, Safian RD, Goldstein JA. Effect of reperfusion on biventricular function and survival after right ventricular infarction. *N Engl J Med* 1998;**338**: 933–40.

19 Klein AL, Leung DY, Murray RD, Urban LH, Bailey KR, Tajik AJ. Effects of age and physiologic variables on right ventricular filling dynamics in normal subjects. *Am J Cardiol* 1999;**84**:440–8.

20 Klein AL, Hatle LK, Burstow DJ, *et al.* Comprehensive Doppler assessment of right ventricular diastolic function in cardiac amyloidosis. *J Am Coll Cardiol* 1990;**15**:99–108.

21 Nagueh SF, Kopelen HA, Zoghbi WA. Relation of mean right atrial pressure to echocardiographic and Doppler parameters of right atrial and right ventricular function. *Circulation* 1996;**93**:1160–9.

22 Mishra M, Swaminathan M, Malhotra R, Mishra A, Trehan N. Evaluation of right ventricular function during CABG: transesophageal echocardiographic assessment of hepatic venous flow versus conventional right ventricular performance indices. *Echocardiography* 1998;**15**:51–8.

23 Nomura T, Lebowitz L, Koide Y, Keehn L, Oka Y. Evaluation of hepatic venous flow using transesophageal echocardiography in coronary artery bypass surgery: an index of right ventricular function. *J Cardiothorac Vasc Anesth* 1995;**9**:9–17.

24 Galderisi M, Severino S, Cicala S, Caso P. The usefulness of pulsed tissue Doppler for the clinical assessment of right ventricular function. *Ital Heart J* 2002;**3**:241–7.

25 Nageh MF, Kopelen HA, Zoghbi WA, Quinones MA, Nagueh SF. Estimation of mean right atrial pressure using tissue Doppler imaging. *Am J Cardiol* 1999;**84**:1448–51.

26 Sundereswaran L, Nagueh SF, Vardan S, *et al.* Estimation of left and right ventricular filling pressures after heart transplantation by tissue Doppler imaging. *Am J Cardiol* 1998;**82**:352–7.

27 Tei C, Ling LH, Hodge DO, *et al.* New index of combined systolic and diastolic myocardial performance: a simple and reproducible measure of cardiac function: a study in normals and dilated cardiomyopathy. *J Cardiol* 1995;**26**:357–66.

28 Eidem BW, O'Leary PW, Tei C, Seward JB. Usefulness of the myocardial performance index for assessing right ventricular function in congenital heart disease. *Am J Cardiol* 2000; **86**:654–8.

29 Nishimura E, Ikeda S, Naito T, *et al.* Evaluation of right-ventricular function by Doppler echocardiography in patients with chronic respiratory failure. *J Int Med Res* 1999;**27**:65–73.

30 Yeo TC, Dujardin KS, Tei C, Mahoney DW, McGoon MD, Seward JB. Value of a Doppler-derived index combining systolic and diastolic time intervals in predicting outcome in primary pulmonary hypertension. *Am J Cardiol* 1998;**81**:1157–61.

31 Michaux I, Filipovic M, Wang JS, Skarvan K, Seeberger M. Right ventricular function during coronary surgery: feasibility of the Tei index. *Eur J Anaesthesiol* 2003;**20(suppl 29)**:14.

32 Ryan J, Podgoreanu M, Veeken C, Booth J, Newman M, Mathew J. Quantification of right ventricular function with Doppler tissue imaging [abstract]. *Anesth Analg* 2003;**96**:114.

33 Yoshifuku S, Otsuji Y, Takasaki K, *et al.* Pseudonormalized Doppler total ejection isovolume (Tei) index in patients with right

ventricular acute myocardial infarction. *Am J Cardiol* 2003;**91**:527–31.

34 Harada K, Tamura M, Toyono M, Yasuoka K. Comparison of the right ventricular Tei index by tissue Doppler imaging to that obtained by pulsed Doppler in children without heart disease. *Am J Cardiol* 2002;**90**:566–69.

35 Stevenson JG. Comparison of several noninvasive methods for estimation of pulmonary artery pressure. *J Am Soc Echocardiogr* 1989;**2**:157–71.

36 Hatle L, Angelsen BA, Tromsdal A. Non-invasive estimation of pulmonary artery systolic pressure with Doppler ultrasound. *Br Heart J* 1981;**45**: 157–65.

37 Prakash R, Matsukubo H. Usefulness of echocardiographic right ventricular measurements in estimating right ventricular hypertrophy and right ventricular systolic pressure. *Am J Cardiol* 1983;**51**:1036–40.

38 Rabinovitch MA, Elstein J, Chiu RC, Rose CP, Arzoumanian A, Burgess JH. Selective right ventricular dysfunction after coronary artery bypass grafting. *J Thorac Cardiovasc Surg* 1983; **86**:444–6.

39 Christakis GT, Fremes SE, Weisel RD, *et al.* Right ventricular dysfunction following cold potassium cardioplegia. *J Thorac Cardiovasc Surg* 1985;**90**:243–50.

40 Baslaim GM, Huynh TT, Stewart JA, Benny C, Cusson D, Morin JF. Assessment of right ventricular function postretrograde cardioplegia by transesophageal echocardiography. *J Card Surg* 1998;**13**:32–6.

41 Rafferty T, Durkin M, Harris S, *et al.* Transesophageal two-dimensional echocardiographic analysis of right ventricular systolic performance indices during coronary artery bypass grafting. *J Cardiothorac Vasc Anesth* 1993;**7**:160–6.

42 Pinto FJ, Wranne B, St Goar FG, *et al.* Systemic venous flow during cardiac surgery examined by intraoperative transesophageal echocardiography. *Am J Cardiol* 1992;**69**:387–93.

43 Wranne B, Pinto FJ, Hammarstrom E, St Goar FG, Puryear J, Popp RL. Abnormal right heart filling after cardiac surgery: time course and mechanisms. *Br Heart J* 1991;**66**:435–42.

44 Gardeback M, Settergren G, Brodin LA. Hepatic blood flow and right ventricular function during cardiac surgery assessed by transesophageal echocardiography. *J Cardiothorac Vasc Anesth* 1996;**10**:318–22.

45 Jugdutt BI, Sussex BA, Sivaram CA, Rossall RE. Right ventricular infarction: two-dimensional echocardiographic evaluation. *Am Heart J* 1984;**107**:505–18.

46 Shinomiya H, Fukuda N, Takeichi N, *et al.* Echocardiographic assessment of right atrial function in patients with myocardial infarction with reference to obstructive lesions of the coronary arteries. *Jpn Circ J* 1998;**62**:393–8.

47 Lopez-Sendon J, Lopez de Sa E, Roldan I, Fernandez de Soria R, Ramos F, Martin Jadraque L. Inversion of the normal interatrial septum convexity in acute myocardial infarction: incidence, clinical relevance and prognostic significance. *J Am Coll Cardiol* 1990;**15**:801–5.

48 Jacobs AK, Leopold JA, Bates E, *et al.* Cardiogenic shock caused by right ventricular infarction: A report from the SHOCK registry. *J Am Coll Cardiol* 2003;**41**:1273–9.

49 Zornoff LA, Skali H, Pfeffer MA, *et al.* Right ventricular dysfunction and risk of heart failure and mortality after myocardial infarction. *J Am Coll Cardiol* 2002;**39**:1450–5.

50 Jardin F, Brun-Ney D, Hardy A, Aegerter P, Beauchet A, Bourdarias JP. Combined thermodilution and two-dimensional echocardiographic evaluation of right ventricular function during respiratory support with PEEP. *Chest* 1991;**99**:162–8.

51 Vieillard-Baron A, Page B, Augarde R, *et al.* Acute cor pulmonale in massive pulmonary embolism: incidence, echocardiographic pattern, clinical implications and recovery rate. *Intensive Care Med* 2001;**27**:1481–6.

52 Jardin F, Lacombe P, Dubourg O, Delorme G, Hardy A, Beauchet A. Quantitative two-dimensional echocardiography in acute pulmonary embolism [in French]. *Presse Med* 1991;**20**:2085–9.

53 Yoshinaga T, Ikeda S, Nishimura E, *et al.* Diagnostic value of pulsed Doppler echocardiography in acute pulmonary thromboembolism: comparison with pulmonary angiography and pulmonary artery pressure. *Jpn Circ J* 2001;**65**: 171–6.

54 Vieillard-Baron A, Schmitt JM, Augarde R, *et al.* Acute cor pulmonale in acute respiratory distress syndrome submitted to protective ventilation: incidence, clinical implications, and prognosis. *Crit Care Med* 2001;**29**:1551–5.

55 Weyman AE. *Principles and Practice of Echocardiography, 2nd edn.* Philadelphia: Lea & Febiger, 1994, p1293 .

56 Lambert-Lintner A. *Referenzwerte für intraoperative transösophageale Echokardiographie. Inaugural dissertation.* Thesis, Medical Faculty, University of Basel, 1997.

9 Thoracic aorta

Raimund Erbel, Steven N Konstadt

Introduction

This chapter describes the anatomy of the thoracic aorta. It then discusses the role of echocardiography in acute aortic syndromes including aortic dissection, intramural haematoma, discrete aortic dissection, aortic plaque rupture, and traumatic/iatrogenic aortic dissection, which are true medical emergencies. Aortic dissection is less common than other acute coronary syndromes, but it occurs more frequently than pulmonary embolism and it often necessitates immediate surgical repair. Key to instituting appropriate therapy in acute aortic syndromes, therefore, is accurate and rapid diagnosis and anatomical assessment of the aorta, including classification of the subtype of disease. Finally, degenerative diseases of the aorta are described. They are found in an increasing number of patients, mainly because of ageing of the general population. Atheroembolic phenomena are a predominant cause of adverse neurological outcomes in this patient population, and atheromatous disease of the thoracic aorta is a significant risk factor for neurological injury after cardiopulmonary bypass. Echocardiography may help to identify the patients at risk and hence permit institution of risk reduction strategies.

Anatomy and techniques

The aortic wall is composed of intimal, medial, and adventitial layers. The intima is a thin layer of endothelium. The media consists of a thick layer of elastic tissue and smooth muscle. The adventitia is a looser layer of tissue containing collagen, lymphatics, and the vasa vasorum. The medial layer accounts for up to 80% of the aortic wall thickness and is responsible for its strength and elasticity.[1]

The thoracic aorta can be divided into three anatomical segments: ascending, transverse, and descending aorta. The ascending aorta is approximately 5 cm long and originates at the aortic valve annulus, extends rightward around the main pulmonary trunk, crosses the right pulmonary artery anteriorly, and ascends rightward and anteriorly until it meets the aortic arch at the level of the second intercostal space. The diameter of the ascending aorta increases with age and is smallest at the annulus and largest at the sinuses of Valsalva, varying from 2 to 3·7 cm in adults (< 2·1 cm/m^2). The ascending aorta superior to the sinuses of Valsalva (sinus portion) is referred to as the "tubular portion". There are no echocardiographic distinctions between the sinus and tubular portions of the aorta; however, occasionally a sclerotic ridge at the sinotubular junction can be mistaken for a mass or an intimal flap.[2]

The ascending aorta can be imaged using transoesophageal echocardiography (TOE) by positioning the probe approximately 20 cm from the lip. Transverse scanning at this level images the aortic valve annulus and the sinotubular junction; however, superiorly, a large blind spot is created by the interposition of the trachea and left mainstem bronchus between the oesophagus and the aorta. Biplane and multiplane scanning have allowed us to overcome some of the limitations imposed by this blind spot and have significantly enhanced our ability to image the ascending aorta. As the probe is advanced 1–2 cm inferiorly to the level of the aortic valve, a longitudinal planar of view images are obtained the ascending aorta for a variable distance (depending on the location of air filled structures; Figure 9.1). Despite these advances, TOE has been shown to image only 50–80% of the entire ascending aorta accurately, and it was only able to identify the aortic cannulation site in 1 of 27 patients.[3] Because of the limitations inherent to TOE (i.e. the poor reliability of imaging the distal ascending aorta and the proximal aortic arch), patients at high risk for ascending aortic atherosclerosis – because of age or extensive disease of the descending aorta – should have their ascending aorta imaged using intraoperative epicardial echocardiography, computed tomography (CT), or magnetic resonance tomography.

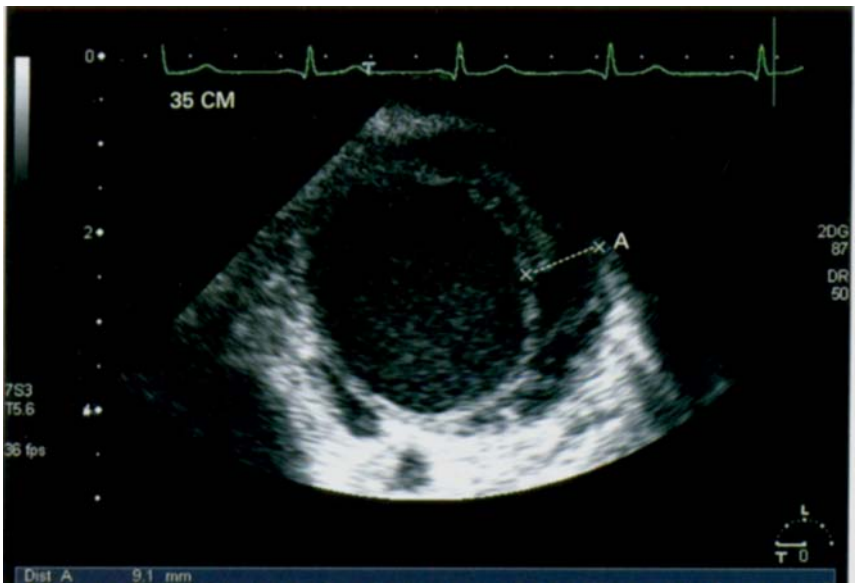

Figure 9.1 Transoesophageal echocardiographic cross sectional image of an intramural haematoma/haemorrhage of the aorta (class 2 aortic dissection), identified by the wall thickening and echo lucent areas within this part of the aortic wall, which is otherwise normal in size and structure.

The epicardial examination is performed using a high frequency linear or phased array probe (7–10 MHz), which is placed directly on the ascending aorta. The major advantage of the linear scanning epicardial probe includes superior image quality for near structures such as the anterior aortic wall; however, a relatively large acoustic window is required. Phased array transducers offer the advantage of a smaller "footprint", or surface area of transducer in contact with the patient, but the entire face of the transducer must be in contact with the patient or image distortion will occur. With the epicardial probe attached to the TOE machine, the probe is placed in a sterile gel-containing plastic cover, and the entire apparatus is placed on the surface of the ascending aorta. After decreasing the field depth, imaging of the ascending aorta can be performed. The anterior wall is an area of intense interest because it is manipulated during cannulation, cross-clamping, induction of cardioplegia, declamping, and proximal vein graft anastomosis. Because of the proximity of the probe to the anterior ascending aortic wall, phased array systems have difficulty imaging this important portion of the aorta because of near field dropout. In order to enhance images of anterior aorta, the pericardium can be filled with fluid or a gel standoff; alternatively, a sterile fluid-filled glove can be placed between the probe and the anterior wall of the aorta. Multiple transverse and longitudinal views can be obtained as the probe traverses the entire ascending aorta from the aortic valve to the innominate artery.

The transverse aorta is a curved structure measuring 4·5 cm in length and 2·5–3·5 cm in diameter. As with the ascending aorta, the trachea can interfere with TOE imaging of this portion of the aorta, especially using monoplane scanning. TOE of the transverse aorta is most easily performed starting at the junction of the transverse and descending aorta. Using transverse and longitudinal or multiplanar scanning, the probe is rotated throughout the visible length of the arch to evaluate for atherosclerotic disease. The site of insertion of the ligamentum arteriosum into the aorta is a common site for atherosclerosis, and a plaque is sometimes imaged in this region. As the descending aorta curves and forms the transverse aorta, the transverse imaging plane through the inferior wall of the aorta is oblique to the aortic wall. This normal curvature can be mistaken for a plaque protruding into the aortic lumen. This artefact can be differentiated from true plaque by the utilisation of multiple scanning planes. A true plaque of the transverse aorta is shown in Figure 9.2.

The descending thoracic aorta originates to the left of the vertebral column and moves rightward as it descends. The diameter of the descending aorta varies between 2 and 2·5 cm, and it is somewhat larger in individuals with atherosclerotic disease. Because of the proximity of the oesophagus to the descending aorta, TOE provides accurate unobstructed images of the size and pathology of the descending thoracic aorta.[4] The descending aorta can be imaged by rotating the TOE probe posteriorly and leftward until the

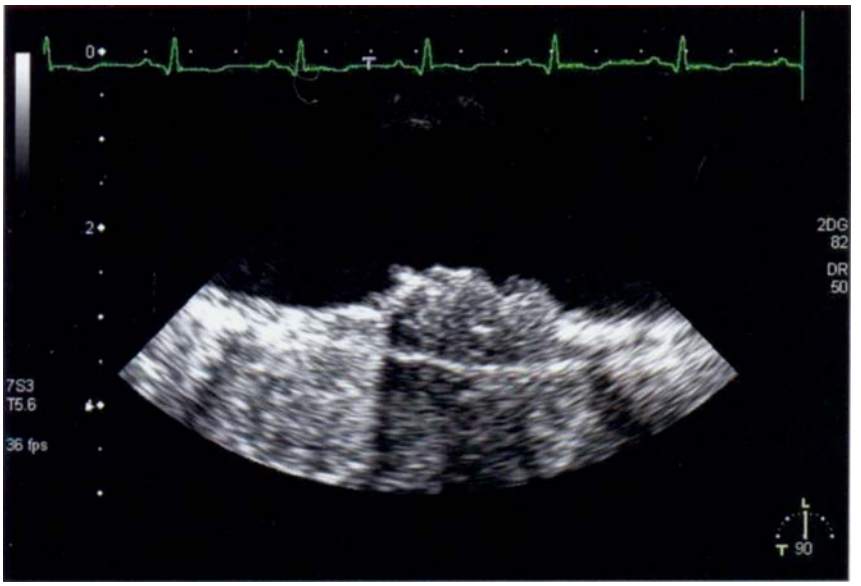

Figure 9.2 Transoesophageal echocardiographic longitudinal image of severe aortic sclerosis with protruding atheroma and beginning ulceration.

transverse cross-section of the aorta is visualised. The probe is advanced slowly into the stomach until the image of the descending aorta is no longer seen. Slowly withdrawing the probe brings the descending aorta into view throughout its entire length, until the probe has been withdrawn to approximately 15 cm from the incisors, where the aortic arch is visualised. The location of the arch will be evident because the transverse image (cross-sectional image) of the descending aorta will no longer be circular as it is in the descending segment of the aorta. Because the scanning plane is parallel to the direction of the arch, a transverse image at this level will appear elongated. Decreasing the depth or using the "zoom" feature of the TOE machine will facilitate evaluation of the intimal surface of the descending aorta.

Acute aortic syndrome

Pathophysiology

All diseases that involve the aortic wall can lead to a weakening in wall tension and result in aortic aneurysm formation, dissection, and rupture due to increased wall stress.[5] Furthermore, this wall stress will increase with extension in aortic diameter. Certain hereditary diseases have a particular tendency to manifest in the aorta, including Marfan's syndrome and Ehlers-Danlos syndrome, as well as bicuspid valve disease and idiopathic ectasia of the ascending aorta.

All mechanisms that damage the adventitia of the aortic wall stimulate pain receptors in the adventitia and induce severe chest pain, typically back pain. Such damage may be caused by iatrogenic procedures such as ballooning of the coarctation of the aorta, by over-expansion of an aortic aneurysm, or by inflammatory processes that involve the aortic wall, such as can occur in syphilis.[5]

According to the Task Force on Diagnosis and Management of Aortic Dissection of the European Society of Cardiology,[5] acute aortic syndromes can be subdivided into five classes (Figure 9.3): aortic dissection (class 1), intramural haematoma/haemorrhage (class 2), discrete/subtle dissection (class 3), plaque rupture (class 4), and traumatic/iatrogenic dissection (class 5). Class 1–5 disease my result in class 1 dissection but can also heal. All subtypes may result in aortic rupture with acute blood loss into the mediastinum, pericardial/pleural space, or abdomen.

Aortic syndrome class 1: aortic dissection

Blood accumulation in the medial layer is the characteristic feature of classic aortic dissection. Dissection of the medial layer may be localised or it may split longitudinally. The plane of dissection usually courses along the greater

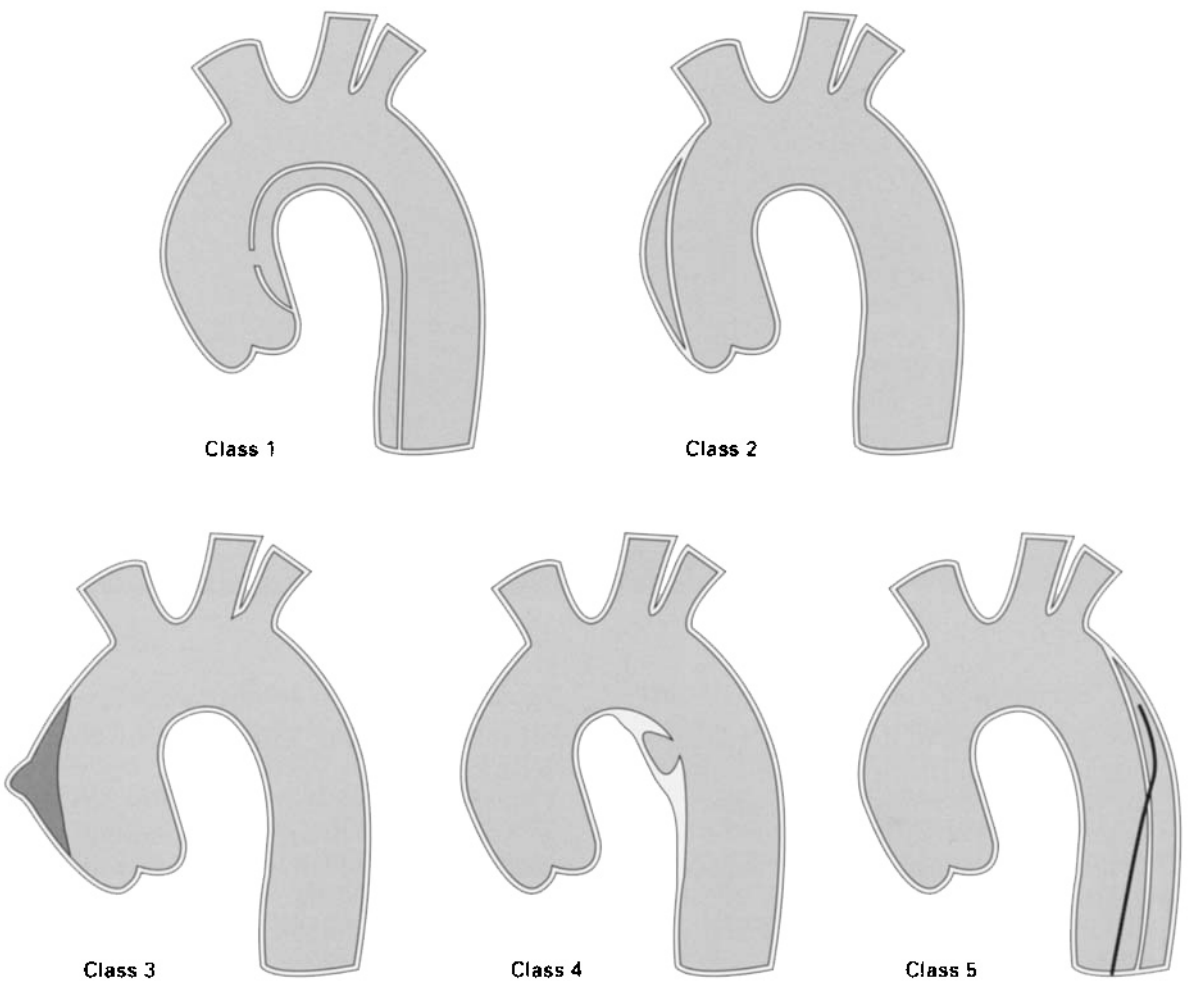

Figure 9.3 Differentiation of classes 1–5 of aortic dissection. Class 1: classic aortic dissection with true and false lumina without communication between the two. Class 2: intramural haemorrhage of haematoma. Class 3: subtle or discrete aortic dissection with bulging of the aortic wall. Class 4: ulceration of aortic plaque following plaque rupture. Class 5: iatrogenic or traumatic aortic dissection, illustrated by a catheter induced separation of the intima. (Modified from Erbel *et al.*,[5] in accordance with the report of Svensson *et al.*[6] American Heart Association; reproduced with permission).

curvature of the ascending aorta and arch of the aorta, whereas in the descending aorta it is mainly located lateral to the true lumen but it may also spiral along its longitudinal axis. The dissection usually does not occupy more than about half of the circumference of the aorta. Most often (70–80%) the dissection starts at a tear (rent) in the intimal layer, which allows blood to flow between the intimal and medial/adventitial layers. The dissection usually propagates distally from the intimal tear, but proximal propagation can also occur. One or more secondary (re-entry or exit) tears may also be present distally. Also, a dissection can occur without any evidence of an intimal tear. It is proposed that this type of aortic dissection is due to medial layer weakness and haemorrhage of vessels in the vasa vasorum.

Aortic syndrome class 2: intramural haematoma/haemorrhage

Intramural bleeding due to rupture of vasa vasorum may lead to intramural haematoma (localised blood accumulation) or intramural haemorrhage (diffuse blood penetration) without intimal rupture in a circumscript part of the ascending or descending aorta. With modern imaging techniques this subtype is found in up to 25% of patients with an acute aortic syndrome, but it would have been overlooked in

many such patients before the advent of these techniques.

Aortic syndrome class 3: discrete/subtle dissection

Discrete bulging of the aortic wall may lead to an acute aortic syndrome caused by localised stretching of the wall; this is often found in Marfan's syndrome and in aneurysm formation. Tears may be present but without bleeding into the aortic wall. This subtype is now more frequently observed following its recent first description, but it may be overlooked using angiography.

Aortic syndrome class 4: plaque rupture

Atherosclerosis of the aortic wall leads to plaque formation (i.e. atheroma and fibroatheroma), which may rupture, leading to ulceration and weakening of the wall. Erosion of the adventitia may occur, as may intramural bleeding, also called penetrating aortic ulcer. This type of acute aortic syndrome occurs in 5–10% and is more common in older patients.

Aortic syndrome class 5: traumatic/iatrogenic dissection

Both traumatic injury (blunt chest trauma) and iatrogenic causes of damage to the aortic wall (mainly catheter based interventions, but surgical procedures as well) can lead to emergency situations involving transection of the aortic wall. The International Registry of Aortic Dissection (IRAD) recently showed that iatrogenic aortic dissections are not as rare as was previously believed.

Incidence

The incidence of aortic dissection is about 5–20 per million of population per year. Predisposing factors include arterial hypertension, age, connective tissue disorders (Marfan's syndrome), congenital lesions (bicuspid aortic valve and coarctation of the aorta), aortic aneurysms, iatrogenic causes (cardiac catheterisation, intra-aortic balloon counterpulsation, and aortic cannulation), trauma, inflammation, and pregnancy. The disease predominantly affects men (male : female ratio 3 : 1), with an average age of onset from the fifth to the seventh decades of life.

Location of aortic dissection

Aortic dissection location may be described using either the DeBakey or the Stanford classification system. In DeBakey types I and II the dissection originates in the ascending aorta, whereas in type III the dissection begins in the descending aorta. The DeBakey type I dissection extends from the ascending aorta and arch to the descending aorta, whereas type II dissections are limited to the ascending aorta. The Stanford system simplified the classification into two groups: type A and type B. Type A includes those dissections that involve the ascending aorta, regardless of the origin of the tear or the extent of dissection (DeBakey types I and II are both included in this category). Type B dissections involve only the descending aorta. Many clinicians have adopted the simplified Stanford classification because it delineates two distinct risk groups and therapeutic approaches. Stanford type A accounts for 50–85% of cases of aortic dissection and is associated with a mortality of 90–95% without surgical intervention. The acute mortality rate with a Stanford type B dissection is about 40%, and accordingly the therapeutic approach is more conservative. At each location, the different aortic dissection classes 1–5 can be observed. The description should therefore include type and class dissection.

Clinical presentation

The typical presentation of acute aortic dissection is the onset of sudden, acute chest pain (proximal dissections) or interscapular pain (distal dissections), which is described as tearing or ripping in nature (aortic pain). The pain usually remains constant and its intensity is maximal from the onset, but it can change in location as the dissection progresses.[7] Other symptoms are related to leaking of blood through the medial/adventitial layer into contiguous areas (for example, pericardial tamponade or hypovolaemia and pulmonary atelectasis) or are caused by the aorta compressing adjacent structures (e.g. stridor or superior vena cava syndrome). Additionally, the dissection may occlude vessels originating from the aorta. Thus, one of the major complications of aortic dissection is ischaemia or infarction of the myocardial, cerebral, mesenteric, renal, or limb tissues, or a combination of these. A careful search for pulse loss is important and may be a key feature in the diagnosis. The aortic root can become dilated or the dissection may extend and

cause mechanical displacement of the aortic valve leaflets, leading to acute aortic insufficiency. Severe aortic insufficiency may cause congestive heart failure, pulmonary oedema, and a low cardiac output state. Patients may also present with shock due to hypovolaemia secondary to leaking of the aneurysm, myocardial ischaemia, myocardial infarction, or pericardial tamponade.

Diagnostic modalities

Because urgent surgical repair plays such a pivotal role in the treatment of type A aortic dissections, it is imperative that a rapid diagnosis be established in any case in which there is a high index of suspicion. The diagnostic aims are as follows:

- confirm the diagnosis
- classify the dissection
- differentiate true/false lumen
- localise intimal tears
- determine whether there is side branch involvement
- detect and grade aortic regurgitation
- detect pleural/pericardial or abdominal fluid extravasation.

Physical examination

The physical examination may reveal signs that are consistent with dissection. Chest auscultation may reveal the murmur of aortic regurgitation. Dyspnoea and haemoptysis are more common in cases of chronic dissection, but they can be seen with an acute dissection that impinges on the tracheobronchial tree. The acute onset of differential or absent pulses in the extremities is a powerful indicator of the presence of an acute dissection.[8] One of a number of clinical manifestations can occur if blood flow to the brain, spinal cord, mesenteric, or renal circulations is compromised. The physical examination, however, can only raise the suspicion of an acute aortic dissection, and calls for further diagnostic work-up to confirm the diagnosis. A clue to the diagnosis is provided by the location of symptoms in vessel territories such as head, thorax, abdomen, or legs.

Chest radiography

The chest radiograph may reveal widening of the mediastinum, changes in the aortic knob, or a pleural effusion (haemothorax). Mediastinal widening is sensitive but not specific for aortic dissection. However, aortic pain, pulse loss, and mediastinal widening are the most sensitive and specific signs for the diagnosis of aortic dissection.

Aortography

The "gold standard" for diagnosing aortic dissections has long been aortography (angiography) via retrograde catheterisation of the femoral artery. Aortography is an extremely helpful tool in locating the sites of intimal disruptions (especially the distal extent of the dissection), in demonstrating involvement of the ascending aorta, in delineating the effects of the dissection on the principal arterial trunks arising from the aorta (including the coronary arteries), in determining the extent and patency of the false lumen, and in assessing the degree of aortic regurgitation. However, this procedure does suffer from certain drawbacks. It is time consuming, invasive, and requires the injection of radiographic contrast media, which is associated with a small but definite potential for morbidity and mortality. False negative findings may result from the following: thrombosis of the false lumen; simultaneous and equal opacification of the true and false lumina, resulting in the appearance of a single lumen in the contrast study; and the presence of aortic syndrome class 2 (see Figure 9.3), which involves the aortic wall and not the lumen. With the advent of more accurate and less invasive diagnostic studies, more institutions are performing aortography only when the results of other studies are inconclusive, when evaluation of the coronary arteries and other major branches of the aorta is deemed necessary, or when an interventional procedure – either fenestration or stent implantation – is planned.

Computed tomography

A CT scan, especially with contrast image enhancement, can aid in determining the extent of dissection and in detecting the true and false lumina. It can also detect aortic wall thickness and calcium deposits within the aortic wall. The CT scan can also be used to visualise the pericardial and pleural spaces to reveal whether there are collections suggestive of leakage of blood or compression of major structures. The test is relatively rapid and non-invasive, and it is therefore used in the IRAD registry in more than

60% of the patients as the first diagnostic test; it received a class I recommendation.[9] However, this procedure carries risks for contrast dye reactions and dye induced renal insufficiency, and aortic regurgitation cannot be analysed. It is also impractical to perform CT scanning in critically ill patients who are haemodynamically unstable.

Magnetic resonance imaging

Magnetic resonance imaging (MRI) produces unrestricted, high resolution views of the aorta in the transverse, sagittal, and coronal planes. Because of its higher quality images, MRI provides better delineation of the origin and extent of aortic dissection. Like CT scanning, MRI can obtain images of structures surrounding the aorta that may be acutely affected by the dissection process. Cine MRI is able to detect aortic insufficiency. MRI has overcome some of the drawbacks of CT scanning in that it is minimally invasive and does not require contrast dye. In the IRAD registry it was shown that, currently, fewer than 10% of the hospitals are using this technique. For acute aortic syndrome it received a class IIa recommendation, but it received a class I recommendation for chronic aortic diseases. The major limitations are that it is time consuming and that the facilities are not always available or on site. MRI may prove very difficult for patients who are haemodynamically unstable or who are in respiratory failure, who must be transported with appropriate monitoring. During the study, only limited access to the patient for examination is possible because they are required to lie within the small housing of the MRI machine and for an extended period of time. Patients who have implantable pacemakers or other internal devices that contain metal are not candidates for MRI scanning.

Transoesophageal echocardiography

TOE has overcome many of the major disadvantages of the diagnostic modalities above. It is a minimally invasive procedure that has a proven safety record.[10] An examination can be performed within about 15–20 minutes in the emergency room but also in the operating theatre or intensive care unit. The close anatomical relationship of the oesophagus to the aorta and the heart allows TOE to provide excellent, high quality images without significant interference from the overlying structures (lungs and chest wall). With the introduction of biplane and multiplane TOE probes, more complete definition of the distal ascending aorta and aortic arch is possible. TOE is performed in real time, which facilitates its unique ability to provide functional and haemodynamic information. This enables evaluation of the aortic valve for regurgitation, of the pericardial space for tamponade, and of the left ventricle for evidence of dysfunction.

- Visualisation of the intimal flap confirms a diagnosis of aortic syndrome class 1 (dissection).
- In class 2 circumscript echolucent areas with wall thickening are typical signs of intramural haematoma. Intramural haemorrhage may only present with a wall thickness increase of more than 7 mm and an increase in the distance from the aorta to the oesophagus of more than 10 mm. This increase in wall thickness is usually not circular but presents as a scale, involving part of the aorta.
- In class 3 bulging of the aortic wall is best seen with aortography, but it can also be detected as a localised enlargement of the aorta using TOE.
- In class 4 plaque formation is present; fibrous caps may be detected. Multiple plaque ruptures sites are commonly found. Thrombus formation can occur, and free floating intimal flaps may be observed.
- In class 5 the degrees of injury can be subdivided into three types: intimal flaps, medial dissection, and aortic transection.

Flow in both the true and false lumina can be analysed using Doppler colour flow imaging and pulsed wave or continuous wave Doppler, providing an alternative technique with which to identify intimal tears when they are not directly visualised using two-dimensional imaging. Doppler echocardiography can show the flow direction as a flow from the true to the false lumen (entry tear), a flow from the false to the true lumen (re-entry tear), or a flow from the true to the false lumen and back. Even multiple flow directions may be observed, indicating a communicating dissection. Flow in the false lumen exhibits a delayed, reversed, or absent flow, allowing differentiation between antegrade and retrograde dissection. More than 20% of type A dissections involve a tear in the descending aorta with retrograde dissection into the ascending aorta, which may have major

therapeutic implications. The coronary arteries can be observed for possible involvement in the dissection process.

In the IRAD study TOE was used frequently and was the second choice method in those cases in which second opinion was needed. It received a class I recommendation for acute syndromes, but it received a class IIa recommendation for chronic diseases because of certain limitations. There is still a risk (albeit small) that the probe will cause damage to the oropharynx, oesophagus, or stomach. Hypotension and/or hypertension can occur rapidly secondary to complications from the aortic dissection (i.e. tamponade) or from stimulation of the oropharynx by the TOE probe, respectively; therefore, continuous monitoring is usually indicated. In addition, because of the risk for aspiration of gastric contents in this patient population, endotracheal intubation should be considered in those who are in shock. This is recommended for all patients with haemodynamic instability; in such cases TOE can be done in the emergency ward or, even better, in the operating theatre just before surgery. TOE is limited in its view of the distal ascending aorta and aortic arch, despite the advantages that biplane and multiplane probes have over the monoplane probe. This is because of the interposition of the trachea and right mainstem bronchus between the oesophagus and the aorta at this location. Also, the abdominal aorta and flow to the major vessels that branch from the aorta are not clearly imaged.

Comparison of diagnostic modalities

Several studies have compared the use of aortography, CT, and MRI and TOE for diagnosing acute aortic dissection. In 1989 Erbel *et al.*[11] compared monoplane TOE with CT and aortography, and found that TOE can provide an accurate diagnosis in a relatively short period of time. Of the 164 patients studied, who had suspected acute aortic dissections, only one false negative finding and two false positive findings occurred with TOE, yielding a sensitivity of 99%, a specificity of 98%, and positive and negative predictive values of 98% and 99%, respectively. CT scan had a slightly higher specificity (100%) but lower sensitivity (83%) and negative predictive value (86%) than did TOE. Angiography did not perform as well as TOE with respect to sensitivity, specificity, and positive or negative predictivity. Those investigators stated that reverberations in the region of the ascending aorta were the main cause for the two false positive examinations with TOE.[11]

Two years later, Ballal *et al.*[12] reported on the value of TOE for diagnosing acute aortic dissections; they used aortography, surgery, and/or autopsy to confirm their findings. Once more TOE was shown to be a highly accurate diagnostic test, having a sensitivity, specificity, and positive and negative predicative values of 97%, 100%, 100%, and 96%, respectively. In a study conducted by Nienaber and associates published in 1992,[13] monoplane TOE was compared with MRI for diagnosing acute aortic dissection. The sensitivity was 100% for both TOE and MRI, but MRI had a better specificity than TOE (100% versus 68%). Transthoracic echocardiography (TTE) did not perform as well as either of those modalities. The lower specificity (higher incidence of false positives) of TOE compared with MRI was again attributed to reverberations in the ascending aorta or to extensive plaque formations in this region. In 1993, Nienaber *et al.*[14] reported on their experience of 110 patients and confirmed the excellent sensitivity of TOE (98%), irrespective of the location of the dissection. As in their previous study, TOE had a lower specificity than MRI (77% versus 100%, respectively; six false positive findings for TOE), which is discordant with the high specificity found in the studies conducted by Erbel *et al.* and Ballal *et al.* In a study conducted by Simon *et al.*[15] it was again confirmed that TOE is an excellent test for identifying aortic dissections (sensitivity and specificity 100%). It can be seen from that study, however, that the ability of TOE to ascertain the type (location) of dissection correctly caused a decrease in specificity for type A dissections (86%; one false positive finding) and a decrease in the sensitivity for type B dissections (88%).

It thus appears that the accuracy of TOE depends on the location of the dissection within the aorta. Nevertheless, recent studies have reiterated that TOE is an accurate test for diagnosing acute aortic dissections, and they support its use as the first test to be done in the acute setting because TOE is minimally invasive, it requires no contrast, it permits real-time analysis of the cardiovascular system, it can be performed at the bedside in critically ill patients, and it can be performed in a short period of time.[16,17] Despite the many advocates of using

TOE as the first diagnostic test, it appears that MRI, when practical, is a more sensitive and specific test for locating the exact location and extent of an aortic dissection. However, the more widely used technique is CT (> 60%), followed by TOE, but even now MRI is used in only a small number of patients in the emergency situation (< 10%).

Limitations

A common denominator in the earlier studies was the decreased specificity of TOE in diagnosing dissections accurately in the ascending aorta and its inferior ability to detect type B dissections in comparison with MRI. It is generally agreed that the former problem was mainly due to artefacts generated in the ascending aorta. Appelbe *et al.*[18] described an in vitro model that could predict a curvilinear artefact emulated by reverberations in the ascending aorta at predictable distances from the transducer. The distance between the transducer and the left atrial wall that abuts the aorta was equal to the distance from this portion of the left atrial wall to the artefact. In their retrospective analysis of in vivo TOE examinations, it was demonstrated that this artefact was primarily limited to those patients whose aortic diameter exceeded the distance of the left atrium. In these cases, the reverberation artefact appeared to lie within the lumen of the aorta, mimicking an intimal flap. As for the decreased ability of TOE to detect dissections of the descending abdominal aorta, this appears to be secondary to the anatomical divergence of the aorta from the oesophagus in the abdomen.

It is also important to note that many of those studies were limited because the authors mainly used monoplane (transverse) TOE probes, which offer only limited views of the ascending aorta. Biplane or multiplane probes can provide additional tomographic images of the ascending aorta, and their use might have improved the specificity of the earlier studies. Despite these additional views, however, visualisation of the distal ascending aorta to the mid-transverse aortic arch is somewhat limited because of the interposition of the trachea and the right mainstem bronchus between the oesophagus and the aorta.[19] TTE in the suprasternal window may allow visualisation of this region when TOE fails. Nevertheless, in subsequent studies, TOE has continued to compare favourably with MRI and appears to perform better than CT, TTE, and angiography in its ability to diagnose acute aortic dissections rapidly.

Secondary diagnoses

In addition to revealing the presence and extent of an aortic dissection, special features of TOE can be used to diagnose and define several important aspects of the dissection (Box 9.1). TOE is among the best methods for accurate identification of the structural and functional status (using colour flow and continuous wave Doppler) of the aortic valve, which has important surgical implications. TOE is also valuable for assessing the degree of involvement and integrity of the coronary arteries in aortic dissection. TOE visualises approximately 70–88% and 25–50% of the left and right coronary artery ostia, respectively. Of the seven cases with proven involvement of the coronary ostium in the study conducted by Ballal *et al.*,[12] six were correctly diagnosed by TOE. There are situations, however, in which coronary angiography is required to define the need for coronary artery bypass grafting or coronary angioplasty (e.g. ascending aortic dissection with an acute myocardial infarct). Aortography should clearly be performed if cardiac catheterisation is planned. Flow patterns of the true and false lumina and the location of intimal tears can be further assessed using colour flow and pulsed wave Doppler. This can lead to identification of patients at risk for malperfusion. The diagnosis of a left pleural or pericardial effusion, or even blood clots in the pericardium can be made more rapidly with TOE than with CT or MRI. TOE can also provide real-time analysis of cardiac function, which is critical for medical, surgical, and anaesthetic management. Furthermore, rare complications of aortic dissections have been reported that were diagnosed by TOE and missed by other modalities. An example is aortic intussusception, in which the intimal flap partially or totally separates from the aorta and migrates distally, causing obstruction of blood flow to extremities or major organs (see Figure 9.1).[20]

Aortic atherosclerosis

Clinical significance

Arteriosclerosis of the aortic wall begins with the development of fatty streaks, with

Presence of an aortic dissection

- Intimal membrane
- Intimal tears: entry and exit site(s); communication between true and false lumina; flow in the false lumen (using CW Doppler or DCFI) – spontaneous echo contrast, thrombus, or no flow
- Extent of dissection

Other important features of aortic dissection detected by transoesophageal echocardiography

- Involvement of coronary arteries
- Involvement of cerebral vessels (malperfusion)
- Functional status of the aortic valve
- Presence of pleural or pericardial (blood clot) effusions
- Cardiac function

CW = continuous wave; DCFI = Doppler colour flow imaging

Box 9.1 Characteristic findings in aortic dissection detected by transoesophageal echocardiography

intermediate lesions being found in children and young adults. In autopsy studies up to 15% of the latter group have been found to have advanced lesions such as atheroma and fibroatheroma. The severity and extent of aortic sclerosis increases exponentially beyond the age of 60 years. The prevalence of atheromas in the aortic arch is 20–30% in stroke patients and 9–13% in control individuals. Thus, the presence of arteriosclerosis of the aorta in stroke patients is as high as the prevalence of atrial fibrillation (18–30%) and carotid artery disease. If plaque thickness exceeds 4 mm, then the risk increases, with an odds ratio as high as 13·8, whereas plaque thickness in the range 1–3·9 mm has an odds ratio of only 3·9; plaque formation of thickness under 1 mm is regarded as normal, with an odds ratio of 1. Protruding plaques with ulcerations are associated with a particularly increased risk for stroke.[21]

Cardiopulmonary bypass (CPB) procedures are fraught with clinical complications, of which the most prevalent fall into the category of neurological dysfunction, either in the form of subtle neuropsychological defects or overt stroke. It is unclear which factor or factors are primarily responsible for this neurological injury after CPB; however, cerebral embolisation and cerebral hypoperfusion continue to be the major foci of study. Because the aetiology of neurological dysfunction is multifactorial, attempts to reduce as many potential risk factors as possible should be undertaken. For example, the watershed zones of infarction in the brain are areas thought to be at high risk for ischaemic injury from decreases in perfusion pressure because of their position at the border of two distinct territories of perfusion. Because these areas rely on small arteriolar connections, they are subject to malperfusion resulting from decreased perfusion pressure, but they are also susceptible to embolic events because of their small calibre and their location as branches of major arteries. Retinal microvascular lesions as well as pathological subcapillary arteriolar dilations in the brain have been demonstrated after CPB.

Attempts to refine the conduct of CPB, such as the introduction of membrane oxygenators and arterial line filtration, have succeeded in reducing the numbers of detectable emboli to the central nervous system. However, patients undergoing CPB are at a greater risk for cerebral injury than are patients with a similar spectrum of risk factors but who are not undergoing CPB.[22]

Prior investigations that focused on cerebral hypoperfusion, non-pulsatility, and air embolisation as the major aetiological factors for stroke have been supplanted by studies of atheroemboli, which are now believed to be responsible for the majority of cerebral embolic events during open or closed cardiac procedures.[23–27] Valvular surgery and open cardiac procedures were once thought to carry greater risk for microembolisation and macroembolisation because of the entrainment of air into cardiac chambers and the potential for embolisation of calcific and thrombotic debris.[27] Atherosclerosis of the ascending thoracic aorta and aortic arch is now recognised as one, if not the major, predictor of postoperative stroke after cardiac surgery due to the cross-clamping that is necessary before cannulation of the aorta.[28] As the median age of our population increases, so too will the prevalence of aortic atherosclerosis.

Despite a progressive decline in perioperative mortality, as a result of improved myocardial preservation, surgical, and perfusion techniques, the overall incidence of perioperative stroke remains unchanged at 1–2% and the incidence increases with age. The incidence of early neuropsychological dysfunction may be as high as 80% immediately after surgery and progressively declines to approximately 40% by

the time of hospital discharge.[29] As the median age of our cardiac surgical population continues to increase, the incidence of age related adverse events will also increase unless appropriate preventive or therapeutic measures can be instituted.

When aortic instrumentation is planned, the presence of ascending, transverse, and descending aortic atheromatous disease is a harbinger of potential cerebral embolisation. Using echocardiographic techniques, aortic atherosclerosis can and should be diagnosed before anticipated instrumentation. Ascending aortic plaque is often soft, friable, and not able to be palpated by the cardiac surgeon. A number of investigations have shown that palpation underestimates the incidence of aortic plaque when compared with diagnosis using echocardiographic techniques.[30,31] Its presence may only be recognised after it is seen oozing from an aortotomy site. After aortotomy, the embolisation of atherosclerotic debris may have already occurred, with resultant adverse sequelae. Thus, the preoperative identification of aortic plaque, made possible by improved echocardiographic technologies, has become an area of intense interest and research.

Risk factors

In order to assess accurately the clinical risk for the development of stroke (stroke having an incidence of only 1%), sufficient numbers of patients must be studied to attain statistical power. For this reason, many of the studies that identified risk factors were necropsy studies, retrospective chart reviews, or prospective multicentre studies. Additionally, use of various criteria for diagnosis and assessment renders comparison of studies quite difficult. Gardner *et al.*[32] retrospectively reviewed 3279 patient records over a 10 year period and conducted a case–control analysis comparing stroke victims with comparable control patients. They identified five factors that were specifically associated with increased stroke. These were age greater than 60 years, pre-existing cerebrovascular disease, severe atherosclerosis of the ascending aorta, prolonged CPB time, and profound perioperative hypotension. An autopsy study reported by Blauth *et al.*[33] ($n = 221$) revealed atheroemboli to be more common after coronary revascularisation than after valvular procedures ($P = 0{\cdot}008$). Peripheral vascular disease and ascending aortic atherosclerosis were significant independent risk factors for atheroemboli. A direct correlation between age and ascending aortic atherosclerosis was found, as was a high correlation between ascending aortic atherosclerosis and atheroembolic events.

In a multicentre prospective observational study in 2108 patients undergoing coronary bypass surgery, Roach *et al.*[34] identified risk factors associated with both overt stroke (type I neurological outcome) and neuropsychological dysfunction (type II neurological outcome). In a multivariate analysis, those investigators determined that independent predictors of type I events included age, preoperative history of neurological disease, and the detection of proximal aortic atherosclerosis by surgical palpation. Age was also an independent predictor of type II neurological events but proximal atherosclerosis was not independently associated. This indicates that stroke is perhaps due to embolisation of large, easily palpated aortic plaque and that subtle dysfunction is the result of smaller peripheral emboli. More likely, however, is that the incidence of proximal aortic atherosclerosis was underestimated in that study because of the insensitivity of surgical palpation as a diagnostic technique. If more sensitive tests such as TOE were employed, then aortic atherosclerosis might have also been independently associated with type II neurological events.

TOE evidence of thoracic aortic atherosclerosis has been shown to be a good predictor of the presence of ascending aortic atherosclerosis as seen by epicardial echocardiography, and may thus be a useful screen for patients at risk for cerebral embolisation.[35] Furthermore, a negative TOE examination for atherosclerosis is helpful in excluding the possibility of ascending atherosclerosis by epicardial examination. Descending aortic atherosclerosis is a risk factor for embolic complications during aortic surgery.[36] Its presence alone may also pose a risk to patients undergoing CPB procedures because these patients undergo extracorporeal perfusion with potential femoral cannulation and femoral instrumentation.[37,38]

The detection of aortic atherosclerosis by TOE may be important because it can be a marker for significant coronary artery disease.[39] Because atherosclerosis plays a major role in the genesis of aortic diseases such as aneurysm and dissection, prevention of such disease progression should involve early detection of the atherosclerotic process.

In a series of patients referred for TOE examination, Konecky *et al.*[40] attempted to define the demographical variables associated with quantity of plaque measured using echocardiographic techniques. The variables analysed included plasma levels of homocysteine, vitamin B_6, vitamin B_{12}, folate, and various pre-existing medical conditions. In a stepwise multivariate analysis, those investigators identified age, sex, and smoking as predictive of the amount of aortic plaque. Plasma homocysteine level further enhanced the ability of this model to predict atherosclerosis and was also an independent predictor itself. Blankenhorn and Kramsch[41] suggested that the study of aortic atherosclerosis should differentially evaluate atherosis and sclerosis. Atherosis is the fatty degeneration that affects the intimal wall and sclerosis is a measure of the elasticity or stiffness of the arterial wall. Because TOE provides such superb images of the intimal wall, Nishino *et al.*[42] used TOE to measure the maximum thickness of the intima–media complex as an index of atherosis and a stiffness parameter (β) as an index of sclerosis. They found that age, cholesterol level, and diabetes mellitus were independently associated with atherosis, and that age and hypertension were significantly associated with sclerosis. Age had the strongest association with both components of atherosclerosis.

Severe atherosclerotic disease of the thoracic aorta is prevalent in elderly patients[43] and is probably an underestimated source of cerebral emboli during cardiac surgery.[44] The presence of aortic knob calcification on radiographic films correlates well with atherosclerotic disease detected by echocardiographic means and should be considered a specific marker for atherosclerotic disease.[45,46]

TOE has been instrumental in detecting atherosclerotic disease of the ascending and transverse aorta. Tunick *et al.* used TOE to identify the presence of mobile atheromatous material in the aortic arch in patients with neurological events and signs of systemic arterial embolisation.[47] The same group of investigators conducted a case–control study and confirmed that the risk for embolic symptoms in patients with protruding atheromas of the thoracic aorta was 3·2 times greater than that of control patients matched for age and sex.[48] When known risk factors for stroke (hypertension and diabetes) were added to the model, the presence of protruding atheromas remained an independent risk factor for embolism. Hypertension was also independently associated with embolic symptoms but diabetes was not. Examples of a protruding atheroma of the descending thoracic aorta can be seen in Figure 9.2. In a prospective study of patients undergoing cardiac surgery, Katz *et al.*[49] identified only aortic arch atheroma as predictive of stroke with an odds ratio of 5·8. Other variables such as the presence of pre-existing cerebrovascular disease, presence of aortic calcification, age, or duration of CPB[50] were not found to be predictive of stroke.

Davila-Roman *et al.*[51] relied heavily on epiaortic ultrasonography to detect aortic atherosclerosis in high risk patients. Those investigators divided the ascending aorta into three equal segments between the aortic root and the innominate artery. Mild atherosclerosis was defined as intimal thickening (< 3 mm) involving only one segment of the ascending aorta, moderate atherosclerosis as intimal thickening (> 3 mm) in one or two segments, and severe atherosclerosis as marked intimal thickening (> 3 mm) in all three segments or circumferentially around the aorta. As expected, palpation of the ascending aorta significantly underestimated the severity and incidence of severe atherosclerosis. An analysis of preoperative variables that are known to correlate with atherosclerosis revealed that age and diabetes were the only significant independent predictors of severe atherosclerosis of the ascending aorta, as identified by epiaortic ultrasonography.

Based on their findings with epiaortic ultrasonography, those investigators devised an algorithm that allowed revision of the planned surgical procedure to avoid areas of moderate or severe atherosclerosis.[52] In a descriptive uncontrolled study, the algorithm was as follows. In patients with moderate aortic disease, potential alterations in the surgical procedure included femoral artery cannulation, change in the site for the aortic cross-clamp, avoidance of aortic cross-clamp using fibrillatory arrest, alteration of site of vein graft anastomoses, relocation of the cardioplegia needle, and avoidance of antegrade cardioplegia by using retrograde cardioplegia. In patients with severe atherosclerotic disease, techniques included femoral artery cannulation with or without graft replacement of the ascending aorta using hypothermic circulatory arrest. Although permanent neurological deficits occurred in 1% of the patients overall, no permanent neurological deficits were present in those patients with severe atherosclerotic disease

in whom aggressive modifications to surgical technique were made. Patients with moderate or severe atherosclerotic disease who underwent only minor modifications to surgical procedure still had a 6·3% stroke rate. There were no strokes in the patients with severe carotid occlusive disease who underwent concomitant carotid endarterectomy and cardiac surgical procedures.

Using historical controls, other investigators have reported similar success when employing measures to avoid instrumentation of the atherosclerotic ascending aorta based on the results of palpation[53] and/or ultrasonography.[54–57] Various strategies have been employed to prevent potential atheroembolism from the ascending aorta; however, studies in larger numbers of patients or randomised trials are necessary to determine whether the incidence of stroke can truly be reduced.

Implications

From the data presented above and from expert consensus, it can be concluded that both TOE and CT are highly accurate and should be considered among the first diagnostic studies to be performed in the initial evaluation of suspected aortic dissections. MRI and aortography also have a solid place in the armamentarium of diagnostic modalities. Each diagnostic test offers distinct advantages and disadvantages. In order to justify the use of any one of these tests, each case must be evaluated on an individual basis, and individual practitioner and institutional preferences should also be considered. Irrespective of this, it seems logical to include TOE in nearly all cases. Most important is that a standard strategy be incorporated into the institutional recommendations and that a team of experts is regularly involved. TOE can be performed rapidly, is portable, and can be safely conducted in haemodynamically unstable patients at the bedside or in the operating theatre. Furthermore, the diagnosis is generally obtained within minutes of the examination. If there is a type A dissection and the primary physicians are satisfied with the information obtained by TOE, then the patient can be operated upon without further delay. If the TOE shows a type B dissection, then medical therapy can be instituted. Additional diagnostic tests can be performed at a later time in order to assess the extent of the dissection with greater accuracy. If the TOE is equivocal, then another diagnostic test can be performed. Therefore, the advantages and limitations of TOE and other modalities (i.e. CT, MRI, and aortography) must be considered in the diagnostic evaluation of the patient with suspected aortic dissection.

Aortic atherosclerosis is a main risk factor for stroke, in addition to atrial fibrillation and carotid artery disease, and its prevalence increases with age. Cerebral dysfunction after cardiac surgery remains a major source of morbidity despite advances in surgical, medical, and perfusion techniques. Although the aetiology of stroke and neuropsychological dysfunction is multifactorial, evidence has been presented that a large component of cerebral dysfunction is a result of embolism of atherosclerotic debris from the thoracic aorta. Various modalities of diagnosis, monitoring, and treatment of severe atherosclerotic disease of the aorta have been proposed. TOE is a sensitive and relatively non-invasive method for detecting atherosclerotic plaque in the thoracic aorta. If TOE monitoring is available, then patients at high risk for atherosclerotic disease of the ascending aorta can be identified both from historical data and by echocardiographic imaging. Once a patient is identified as being at high risk, epiaortic ultrasonography should be performed to delineate further the sites of severe atherosclerosis so that surgical modifications can be made.

References

1 Orihashi K, Sisto DA. Aorta. In: Oka Y, Goldiner PL, eds. *Transesophageal echocardiography*. Philadelphia, PA: Lippincott-Raven, 1992. pp. 189–225.

2 Weyman AE, Caldwell RL, Hurwitz RA, *et al.* Cross-sectional echocardiographic characterization of aortic obstruction. I. Supravalvularaortic stenosis and aortic hypoplasia. *Circulation* 1978;**57**:491–9.

3 Konstadt SN, Reich DL, Quintana C, Levy M. The ascending aorta: how much does transesophageal echocardiography see? *Anesth Analg* 1994;**78**: 240–4.

4 Mintz GS, Kotler MN, Segal BL, Parry WR. Two-dimensional echocardiographic recognition of the descending thoracic aorta. *Am J Cardiol* 1979;**44**: 232–8.

5 Erbel R, Alfonso F, Boileau C, *et al.*, Task Force on Aortic Dissection of the European Society of Cardiology. Diagnosis and management of aortic dissection. *Eur Heart J* 2001;**22**:1542–81.

6 Svensson LG, Labib SB, Eisenhauer AC, Butterly JR. Intimal tear without hematoma. *Circulation* 1999;**99**:1331–6.

7 Lindsay J Jr, DeBakey ME, Beall AC. Diagnosis and treatment of diseases of the aorta. In: Schlant RC, Alexander RW, *et al.*, eds. *Hurst's: the heart, 8th ed.* New York: McGraw-Hill, 1994. pp. 2170–5.

8 Reich DL. Echocardiographic assessment of aortic dissection. In: Oka Y, Konstadt SN, eds. *Clinical transesophageal echocardiography: a problem-oriented approach.* Philadelphia, PA: Lippincott-Raven, 1996. pp. 101–11.

9 Moore AG, Eagle KA, Bruckmann D, *et al.* Choice of computed tomography, transesophageal echocardiography, magnetic resonance imaging, and aortography in acute aortic dissection: International Registry of Acute Aortic Dissection. *Am J Cardiol* 1001;**89**:1235–8.

10 Daniel WG, Erbel R, Kasper W, *et al.* Safety of transesophageal echocardiography: a multicenter survey of 10 419 examinations. *Circulation* 1991; **83**:817–21.

11 Erbel R, Daniel W, Visser C, *et al.* Echocardiography in diagnosis of aortic dissection. *Lancet* 1989;**1**:457–69.

12 Ballal RS, Nanda NC, Gatewood R, *et al.* Usefulness of transesophageal echocardiography in assessment of aortic dissection. *Circulation* 1991;**84**:1903–14.

13 Nienaber CA, Spielmann RP, von Kodolitsch, *et al.* Diagnosis of thoracic aortic dissection: magnetic resonance imaging versus transesophageal echocardiography. *Circulation* 1992;**85**:434–47.

14 Nienaber CA, von Kodolitsch Y, Nicolas V, *et al.* The diagnosis of thoracic aortic dissection by non-invasive imaging procedures. *N Engl J Med* 1993;**1**:328.

15 Simon P, Owen AN, Havel M, *et al.* Transesophageal echocardiography in the emergency surgical management of patients with aortic dissection. *J Thorac Cardiovasc Surg* 1992; **103**:1113–18.

16 Chirillo F, Cavallini C, Longhini C, *et al.* Comparative diagnostic value of transesophageal echocardiography and retrograde aortography in the evaluation of thoracic aortic dissection. *Am J Cardiol* 1994;**74**:590–5.

17 Laissy JP, Blanc F, Soyer P, *et al.* Thoracic aortic dissection: diagnosis with transesophageal echocardiography versus MR imaging. *Radiology* 1995;**194**:331–6.

18 Appelbe AF, Walker PG, Yeoh JK, *et al.* Clinical significance and origin artefacts in transesophageal echocardiography of the thoracic aorta. *J Am Coll Cardiol* 1993;**21**:754–60.

19 Konstadt SN, Reich DL, Quintana C, *et al.* The ascending aorta: how much does the transesophageal echocardiography see? *Anesth Analg* 1994;**78**:240–44.

20 Hudak AM, Konstadt SN. Aortic intussusception: a rare complication of aortic dissection. *Anesthesia* 1995;**82**:1292–4.

21 Tunick PA, Kronzon I. Atheromas of the thoracic aorta: clinical and therapeutic update. *J Am Coll Cardiol* 2000:**35**:545–54

22 Shaw PS, Bates B, Cartlidge NEF, *et al.* Neurologic and neuropsychological morbidity following major surgery: comparison of coronary artery bypass and peripheral vascular surgery. *Stroke* 1987;**18**:700–7.

23 Yao FS, Barbut D, Hager DN, Trifiletti RR, Gold JP. Detection of aortic emboli by transesophageal echocardiography during coronary artery bypass surgery. *J Cardiothorac Vasc Anesth* 1996;**10**:314–17.

24 Barbut D, Gold JP. Aortic atheromatosis and risks of cerebral embolization. *J Cardiothorac Vase Anesth* 1996;**10**:24–9.

25 Lynn GM, Stefanko K, Reed JF III, Gee W, Nicholas G. Risk factors for stroke after coronary artery bypass. *J Thorac Cardiovasc Surg* 1992;**104**:1518–23.

26 Breuer AC, Furlan AJ, Hanson MR, *et al.* Central nervous system complications of coronary artery bypass graft surgery: prospective analysis of 421 patients. *Stroke* 1983;**14**:682–7.

27 Nussmeier NA. Adverse neurologic events: risks of intracardiac versus extracardiac surgery. *J Cardiothorac Vasc Anesth* 1996;**10**:31–7.

28 Bull DA, Neumayer LA, Hunter GC, *et al.* Risk factors for stroke in patients undergoing coronary artery bypass grafting. *Cardiovasc Surg* 1993;**1**:182–5.

29 Mora CT, Henson MB, Weintraub WS, *et al.* The effect of temperature management during cardiopulmonary bypass on neurological and neuropsychological outcomes in coronary revascularization patients. *J Thorac Cardiovasc Surg* 1996;**112**:514–22.

30 Marschall K, Kanchuger M, Kessler K, *et al.* Superiority of transesophageal echocardiography in detecting aortic arch atheromatous disease: identification of patients at increased risk of stroke during cardiac surgery. *J Cardiothorac Vasc Anesth* 1994;**8**:5–13.

31 Duda AM, Letwin LB, Sutter FP, Goldman SM. Does routine use of aortic ultrasonography decrease the stroke rate in coronary artery bypass surgery? *J Vasc Surg* 1995;**21**:98–109.

32 Gardner TJ, Horneffer PJ, Manolio TA, *et al.* Stroke following coronary artery bypass grafting: a ten-year study. *Ann Thorac Surg* 1985;**40**:574–81.

33 Blauth CI, Cosgrove DM, Webb BW, *et al.* Atheroembolism from the ascending aorta. An emerging problem in cardiac surgery. *J Thorac Cardiovasc Surg* 1992;**103**:1104–12.

34 Roach GW, Kanchuger M, Mangano CM, *et al.* Adverse cerebral outcomes after coronary bypass surgery. *N Engl J Med* 1996;**335**:1857–63.

35 Konstadt SN, Reich DL, Kahn R, Viggiani RF. Transesophageal echocardiography can be used to screen for ascending aortic atherosclerosis. *Anesth Analg* 1995;**81**:225–8.

36 Kassirer JP. Atheroembolic renal disease. *N Engl J Med* 1969;**280**:812–18.

37 Karalis DG, Chandrasekaran K, Victor MF, *et al.* Recognition and embolic potential of intra-aortic atherosclerotic debris. *J Am Coll Cardiol* 1991;**17**:73–8.

38 Hartman GS, Yao FS, Bruefach M III, *et al.* Severity of aortic atheromatous disease diagnosed by transesophageal echocardiography predicts stroke and other outcomes associated with coronary artery surgery: a prospective study. *Anesth Analg* 1996;**83**:701–8.

39 Fazio GP, Redberg RF, Winslow T, Schiller NB. Transesophageal echocardiographically detected atherosclerotic aortic plaque is a marker for coronary artery disease. *J Am Coll Cardiol* 1993;**21**: 144–50.

40 Konecky N, Malinow MR, Tunick PA, *et al.* Correlation between plasma homocyst(e)ine and aortic atherosclerosis. *Am Heart J* 1997;**133**: 534–40.

41 DH, Kramsch DH. Reversal of atherosis and sclerosis: the two components of atherosclerosis. *Circulation* 1989;**79**:1–7.

42 Nishino M, Masugata H, Yamada Y, *et al.* Evaluation of thoracic aortic atherosclerosis by transesophageal echocardiography. *Am Heart J* 1994;**127**:336–44.

43 Mitchell MM, Frankville DD, Weinger MB, Dittrich HC. Detection of thoracic aortic atheroma with transesophageal echocardiography in patients without symptoms of embolism. *Am Heart J* 1991;**122**:1768–71.

44 Simons AJ, Carlson R, Hare CL, *et al.* The use of transesophageal echocardiography in detecting aortic atherosclerosis in patients with embolic disease. *Am Heart J* 1992;**123**:224–6.

45 Witteman JCM, Kannel WB, Wolf PA, *et al.* Aortic calcified plaques and cardiovascular disease (The Framingham Study). *Am J Cardiol* 1990;**66**:1060–4.

46 Toyoda K, Yasaka M, Nagata S, Yamaguchi T. Aortogenic embolic stroke: a transesophageal echocardiographic approach. *Stroke* 1992;**23**: 1056–61.

47 Tunick PA, Kronzon I. Protruding atherosclerotic plaque in the aortic arch of patients with systemic embolization: a new finding seen by transesophageal echocardiography. *Am Heart J* 1990; **120**:658–60.

48 Tunick PA, Perez JL, Kronzon I. Protruding atheromas in the thoracic aorta and systemic embolization. *Ann Intern Med* 1991;**115**:423–7.

49 Katz ES, Tunick PA, Rusinek H, *et al.* Protruding aortic atheromas predict stroke in elderly patients undergoing cardiopulmonary bypass: experience with intraoperative transesophageal echocardiography. *J Am Coll Cardiol* 1992;**20**:70–7.

50 AC, Furlan AJ, Hanson MR, *et al.* Central nervous system complications of coronary artery bypass graft surgery: prospective analysis of 421 patients. *Stroke* 1983;**14**:682–7.

51 Davila-Roman VG, Barzilai B, Wareing TH, *et al.* Intraoperative ultrasonographic evaluation of the ascending aorta in 100 consecutive patients undergoing cardiac surgery. *Circulation* 1991;**84**:III47–53.

52 Wareing TH, Davila-Roman VG, Daily BB, *et al.* Strategy for the reduction of stroke incidence in cardiac surgical patients. *Ann Thorac Surg* 1993;**55**:1400–8.

53 Bar-El Y, Goor DA. Clamping of the atherosclerotic ascending aorta during coronary artery bypass operations. *J Thorac Cardiovasc Surg* 1992;**104**:469–74.

54 Ribakove GH, Katz ES, Galloway AC, *et al.* Surgical implications of transesophageal echocardiography to grade the atheromatous aortic arch. *Ann Thorac Surg* 1992;**53**:758–63.

55 Hosoda Y, Watanabe M, Hirooka Y, *et al.* Significance of atherosclerotic changes of the ascending aorta during coronary bypass surgery with intraoperative detection by echography. *J Cardiovasc Surg* 1991;**32**:301–6.

56 Swanson SJ, Cohn LH. Excision of focal aortic arch atheroma using deep hypothermic circulatory arrest. *Ann Thorac Surg* 1995;**60**:457–8.

57 Ohteki H, Itoh T, Natsuaki M, *et al.* Intraoperative ultrasonic imaging of the ascending aorta in ischemic heart disease. *Ann Thorac Surg* 1990;**50**:539–42.

10 Haemodynamics

Jan Poelaert, Ruggero Amà, Karl Skarvan

Introduction

Transoesophageal echocardiography (TOE) is a highly efficient diagnostic and monitoring tool in the perioperative setting.[1–3] It allows fastidious assessment of both cardiac structure and function. Most anaesthetists and critical care specialists still have the impression that echocardiography can provide only qualitative data. However, two-dimensional TOE in conjunction with various Doppler techniques provides pivotal information that, in addition to invasively obtained pressures and cardiac output, can be very helpful in evaluating haemodynamic function. Those who are used to monitoring just pressures find flow measurements cumbersome and the correlation between pressures and flows difficult to interpret. Nevertheless, flow measurements allow a better understanding and better assessment of the various parameters of cardiovascular function.

In principle, all important haemodynamic data can be obtained by Doppler echocardiography. These include preload, afterload, intracavitary, and intravascular pressures and pressure gradients, as well as load dependent and load independent measures of myocardial contractility (see Chapter 3). Hence, Doppler TOE provides a complete set of haemodynamic data in a non-invasive manner, often online, and much quicker than is possible with invasive monitoring. The major disadvantage of the technique, however, is the impossibility of continuous monitoring and the need for elaborate education (see Chapter 15). It was suggested that TOE should be the initial investigation, particularly in haemodynamically unstable patients, and that continuous haemodynamic monitoring can then be initiated whenever justified by TOE findings.[4]

Several issues that are important in analysing the cause of haemodynamic instability are discussed in other chapters. Here, haemodynamics are addressed within the context of information presented in those chapters. The purpose of this chapter is to demonstrate the relationship between pressures and flows in a comprehensible manner, in order to build a bridge between traditionally obtained data and the additional information provided by echocardiography. A typical example is the combination of the interpretation of the arterial trace and Doppler flow parameters, as illustrated in Figure 10.1. The various echocardiographic parameters often provide the missing pieces of the puzzle presented by the haemodynamically unstable patient, and allow that puzzle to be solved in a short period of time. The following issues are discussed:

- determination of haemodynamic parameters using two-dimensional echocardiography, M-mode, and the various Doppler techniques
- the relationship between pressure gradients and volume flow
- the relationship between Doppler flow velocity patterns and filling pressures
- the benefits and limitations of TOE in haemodynamic assessment.

The cardiac cycle

The energy necessary to circulate the blood through the cardiopulmonary vascular bed is provided by the heart, which acts as a double serial pump. The mechanical energy exerted by this pump is induced by an electrical impulse. Direct links between mechanical and electrical signals must be understood because of the close relationship between concomitant pressure and flow changes involving the different cardiac chambers. In order to illustrate this relationship, the events in the left and right heart are discussed step by step below.

At the end of diastole, atrial contraction (marked by the P wave in the electrocardiogram) causes atrial pressure to rise. This increase in pressure manifests as the a wave of the right atrial or pulmonary capillary wedge pressure (PCWP), and coincides with acceleration of the blood flow from the atrium into the ventricle across the atrioventricular valve at end-diastole. The corresponding flow velocity can be recorded by pulsed wave Doppler as the A wave. In the left

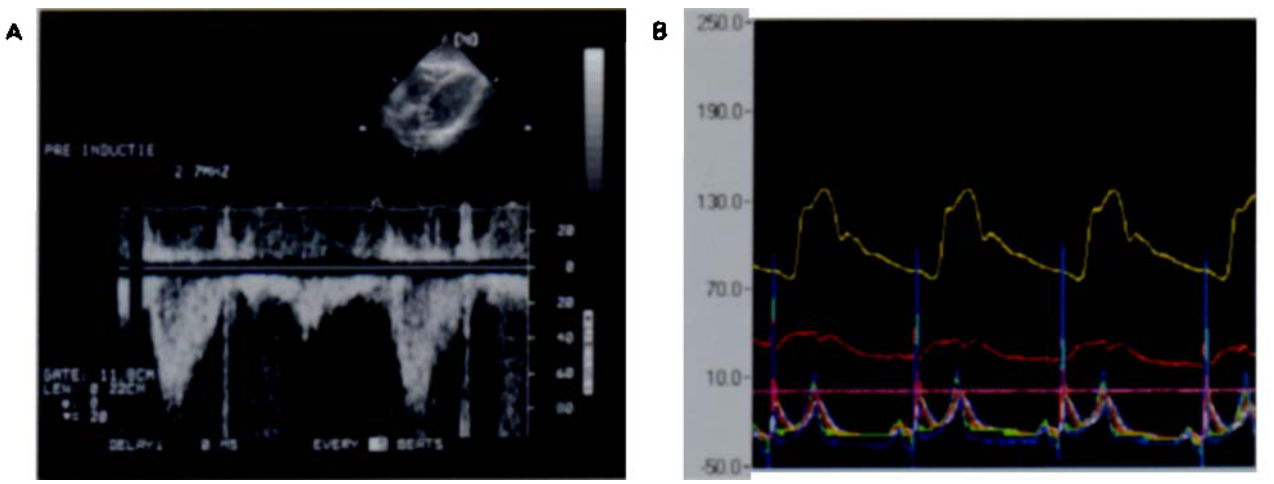

Figure 10.1 A combination of (**A**) Doppler flow and (**B**) invasive haemodynamic monitoring provides important information in the critically ill patient. Automatic acquisition of these signals and digital analysis considerably reduces the workload of the clinician.

ventricle at this moment the mitral valve is maximally opened; this contrasts with the aortic valve, which is closed throughout diastole. After the QRS complex, which marks the onset of electrical activation of the myocardium on the electrocardiogram, ventricular contraction (systole) follows. The intraventricular pressure rises, and this results in the closure of the mitral valve. The isovolumic contraction period is the time between closure of the mitral valve and opening of the aortic valve. The latter opens when the pressure in the ventricle exceeds the pressure in the aorta, and starts the ejection phase of systole. The isovolumic contraction time can be measured by Doppler echocardiography by placing the sample volume between the mitral valve and the left ventricular (LV) outflow tract (either in the four or five chamber mid-oesophageal [MOE four/five chamber] view, or in the deep transgastric long-axis [deep TG LAX] view, both in transverse plane). The time interval between the end of the A wave and the onset of LV ejection is measured.

Once the aortic valve is open, blood is ejected swiftly into the ascending aorta. The extent of opening of the cusps of the aortic valve is directly related to the volume flow across this valve, and hence to cardiac output.[5,6] The time required for ejection of blood across the aortic valve is called the ejection period. This time period is defined as the interval between the onset and the end of systolic blood flow across the aortic valve, and it can be measured by Doppler echocardiography in the deep TG LAX, which permits one to measure flow without a significant intercept angle.[7] The aortic blood flow velocity recorded by pulsed wave or continuous wave Doppler is determined by the following:

- LV preload
- LV afterload (and hence aortic valve resistance also)
- LV contractility.

The slope of the aortic pressure rise and of the aortic flow velocity waveform is dependent on the force developed by the ventricular pump during ejection, and hence on the force of LV contraction. It must be noted that aortic pressure rises slower to its peak value than does flow, even if the delay owing to the use of fluid filled catheters is taken into consideration.[8]

Eventually, LV pressure starts to decline, and once it has fallen below the pressure in the aorta the aortic valve cusps close. Then, the isovolumetric relaxation period begins. It is characterised by an absence of volume change in the left ventricle and lasts until the moment when LV pressure falls below left atrial pressure (LAP) and causes the mitral valve to open. Measurement of the isovolumetric relaxation time is again easily performed by Doppler echocardiography (placing the sample volume between the mitral valve and the LV outflow tract) or by Doppler myocardial imaging at the mitral annular level (as the time interval between the end of the systolic

Table 10.1 Comparison of different Doppler methods of determination of cardiac output

Site	n	Failure	Doppler approach	r	Reference
PA	45	24	CW short-axis	0·93	85
PA	99	29	PW short-axis	0·65	86
PA	15	13	PW short-axis	0·83	87
PA	19	10	PW short-axis	0·95	88
MV	65	NA	Four chamber view	NA	89
LVOT	57	12	CW transverse long-axis	0·91	7
LVOT	109	2	CW transverse long-axis	0·98	12
LVOT	33	12	PW longitudinal long-axis	0·91	90
LVOT	64	9	PW transverse long-axis	0·95	91
LVOT	82	9	PW/CW	Variable*	10
AA	28	7	PW transverse long-axis	0·98	77
RVOT	45	16	PW longitudinal long-axis	0·98	92
LVOT	33	3	CW multiplane long-axis	0·98	11

*In this study, PW and CW Doppler were compared in both transverse and longitudinal planes, using the method of measurement of the diameter; the *r* varied between 0·84 and 0·87. AA = ascending aorta, CW = continuous wave Doppler echocardiography, Failure = not possible to measure, LVOT = left ventricular outflow tract, MV = mitral valve, NA = not available, PA = pulmonary artery, PW = pulsed wave Doppler echocardiography, RVOT = right ventricular outflow tract.

wave and the onset of the early diastolic wave; see Figure 11.4). The opening of the mitral valve marks the onset of the LV filling period and is associated with an abrupt increase in blood flow velocity, which is noted on the Doppler recording as the early filling velocity, or E wave. This early wave E is physiologically higher than the atrial contraction wave A. With advancing age, however, the E velocity decreases whereas the A velocity increases, with a consequent fall in E/A ratio. Apart from the effect of age, the relative changes in the early to late flow wave ratio are governed by LV preload and by LV diastolic function characteristics (see Chapter 4). In order to diminish the impact of filling conditions on the E wave, new techniques such as colour M-mode Doppler propagation flow velocity of early filling and tissue Doppler imaging[9] have been introduced into the practice of echocardiography.

Assessment of stroke volume and cardiac output

Determination of stroke volume (SV) is extensively reviewed in Chapter 3. Briefly, for the assessment of SV two steps are necessary: measurement of flow velocity and determination of the area through which the flow is pushed forward. For the first step, the area under the Doppler velocity waveform is measured. This gives us the velocity time integral (VTI), which is expressed in centimetres. VTI represents the distance a red blood cell is projected forward during one cardiac cycle, and is therefore directly related to the systolic function of the left or right ventricle, depending on the location of the sample volume (see Figure 10.1A). The second step is determination of the cross-sectional area of the vessel or heart chamber at the site of flow velocity measurement. The area can either be calculated from the diameter(s), assuming a circular shape, or it can be determined by direct planimetry. Table 10.1 provides an overview of the different sites at which the sample volume can be placed for measurement of diameters. It was shown in earlier studies that the diameter of the *pulmonary artery* is often difficult to measure, although measurement of flow within the pulmonary artery is often easy. This may account for the poorer correlation between Doppler and thermodilution cardiac outputs observed in those studies.

The diameter of the *mitral valve* is even more difficult to measure because the mitral annulus changes its shape and size throughout the cardiac cycle. In addition, the mitral valvular annulus is not a circle. Measurement of blood flow velocity across the *aortic valve* or in the *LV outflow tract* therefore remains the third and most reliable option for Doppler assessment of SV and cardiac output, provided that aortic stenosis is absent. This measurement can be performed in transgastric or deep transgastric (TG LAX or deep TG LAX) views. The rotating imaging array facilitates

alignment of the Doppler beam with blood flow across the aortic valve or through the LV outflow tract. To permit measurement of the diameter of the aortic valve, a longitudinal mid-oesophageal image (MOE AV LAX) should be obtained (see Figure 2.9 in Chapter 2). It has been demonstrated by various investigators that greater accuracy can be achieved by direct measurement (e.g. planimetry) of the effective aortic valve opening area. The latter can be performed with the probe at a mid-oesophageal position and by rotating the multiplane probe transducer towards 25–40° (MOE AV SAX; see Figure 2.9 in Chapter 2).

Hence, the SV can be calculated from the following formulae:

$$SV = VTI \times 0{\cdot}7854 \times D^2$$

(if the method employing measurement of the diameter [D] is used)

$$SV = VTI \times AVA$$

(if the method employing the mean effective aortic valve opening area [AVA] is chosen)

In clinical practice, the method based on measurement of the diameter at the level of the aortic valve provides an adequate estimation of SV.[10,11] If greater accuracy is needed, however, then the method of the effective aortic valve opening area is preferable.[12]

Finally, cardiac output is calculated by multiplying the Doppler derived SV by the heart rate.

Assessment of left ventricular preload: relationship between pressure and flow

Over many years anaesthetists have become accustomed to working with pressures, and thus are able to approximate indirectly the physiologically relevant determinants of ventricular function, namely contractility, preload, and afterload. In Chapter 3 these three factors are extensively elaborated. Although right heart catheterisation has proved useful in guiding optimal fluid therapy in critically ill patients,[13] the risks and drawbacks of invasive pressure monitoring must be appreciated.[14,15] In this respect it cannot be over-emphasised that the efficiency of the monitoring tool in obtaining haemodynamic information should be taken into consideration. Echocardiography provides quick and instantaneous information on the cause of haemodynamic instability, which cannot be offered by any invasive or non-invasive monitoring technique, although it is providing central venous pressure or pulmonary artery pressures. LV end-diastolic area (EDA) serves as the basis for assessment of LV preload (see Chapter 3). From the same view, a qualitative evaluation of global and regional ventricular function can be conducted. However, in various situations the validity of LVEDA as a descriptor of preload is questionable, as discussed extensively in Chapter 3. The most striking example is the patient with a dilated cardiomyopathy, in whom the absolute value of LVEDA will not help to determine the most appropriate preloading condition.

In the literature, preload and fluid responsiveness have been mixed up. Preload and fluid responsiveness are completely different features and must be defined correctly in order to allow proper interpretation. Whereas preload can be defined in physiological terms as the end-diastolic sarcomere length, it can only be translated into clinical terms as LV end-diastolic volume (EDV) or LVEDA. For many years it was believed that LVEDA is a good estimate of LVEDV.[16] A small LVEDA is indeed a sign of either a low preloading condition or an increased inotropic state of the left ventricle. However, in patients with low ejection fraction, dilated cardiomyopathy, right ventricular (RV) failure and/or LV diastolic dysfunction, LV end-diastolic dimensions provide little information about preloading conditions. In these patients two-dimensional TOE should be completed by measurements of transmitral and pulmonary venous flow velocities (vide infra). TOE offers an excellent window for making these measurements.[17–19] In patients with low ejection fraction and a dilated left ventricle, it is evident that administration of fluid could lead to acute overfilling and pulmonary oedema. Therefore, the safest way to determine whether cardiac preload is optimal is to evaluate fluid responsiveness without fluid challenge by assessing respiratory systolic pressure/SV variation.

Regional ventricular function in patients with cardiac disease is difficult to assess because of the inability of human eye to analyse moving objects faster than every 60–80 ms. Furthermore, proper interpretation of myocardial thickening requires

an experienced observer, and even then measurements will be time consuming and subjective. To overcome these problems, colour coded myocardial Doppler imaging was recently introduced. With this technology it is possible to assess the low velocity, high amplitude Doppler shifts of colour coded myocardial velocities.[20] The reader is referred also to Chapter 11.

Underway to TOE diagnosis and subsequent clinical decision making, both pressures and flows should be evaluated. Doppler echocardiography allows estimation of various intracardiac pressures with reasonable accuracy and reproducibility, provided that following general principles are borne in mind.[17]

- The Doppler beam must be aligned to the direction of blood flow, with a maximal permissible degree of intercept being 20°. The resulting error, albeit still acceptable, will then be ± 6% (cosine 20°).
- The sample volume must be placed in the middle of the flow profile, decreasing the risk for turbulence, which is often seen at the boundaries of the vessel or valvular annulus.
- Whenever high velocities are expected, then continuous wave Doppler should be used.
- Other limitations in the determination of pressures are the quality of the Doppler signal and the presence of valvular or subvalvular stenosis.

Left atrial pressure

As described above, the transmitral flow pattern is directly related to the filling of the left ventricle. Briefly, the normal pattern is displayed as a biphasic tracing with an early and rapid filling wave E, followed by a diastasis period with minimal or no flow, and finally a late filling wave A caused by atrial contraction. Velocities of the respective flow waves and their corresponding VTIs are important characteristics of LV filling.[21] Another easily calculated parameter is the ratio of the peak flow velocities (E/A). A normal flow velocity ratio is in the range 0·8:1–1·4:1. It must again be recalled that the E/A ratio is strongly age dependent; with increasing age the E wave diminishes in favour of the late filling wave A, resulting in progressive diminution of the E/A ratio. Other factors also determine the transmitral flow pattern, including left atrial contractility and compliance, mitral valve function, LV relaxation and compliance, and pulmonary venous return.[22] In addition, mechanical ventilation as well as external constraint affect LV filling. Because of these interfering factors, it is conceivable that there is poor correlation between the early filling velocity and left sided filling pressure.[23] As long as left atrial pressure is normal, such as in dilated cardiomyopathy, E will also remain normal and the E/A ratio will not significantly change. With progression of heart failure and a progressive increase in LV filling pressure in these patients, the E velocity will increase and cause the E/A ratio to increase as well. The higher E wave will have shorter deceleration time, reflecting decreased ventricular compliance.[17] For more detail, the reader is referred to Chapter 4.

When present, mitral regurgitation can also be used to estimate LV filling when the peak velocity of the mitral regurgitation jet is measured by continuous wave Doppler. LAP can than be calculated using the following formula:

$$LAP = SBP - (4 \times V^2_{TMF})$$

where V_{TMF} is the peak mitral regurgitant velocity and SBP is the systolic blood pressure. This method is based on the assumption that there is no pressure gradient between the left ventricle and ascending aorta.

Pulmonary vein flow velocities have been recognised as parameters of LV function. In addition, these Doppler velocities offer useful information on diastolic function of the left ventricle and on LV filling.[24] Again, a detailed description of the significance of the various components of this flow pattern is provided in Chapter 4. Briefly, atrial contraction causes a small, reverse flow wave (a). This is followed by a larger forward systolic flow wave (S), which can exhibit two peaks – S1 and S2. The first is linked to atrial relaxation and the second to downward movement of the mitral annulus.[24] Finally, the diastolic flow wave (D) follows. When a low filling state (hypovolaemia) is present the systolic flow wave is typically biphasic, suggesting that the mitral annular descent lasts longer than the atrial relaxation. Whereas the absence of this biphasic systolic flow pattern is not in itself an indicator of normal filling, the presence of this feature is very suggestive of low filling; with low LAP, the time between atrial contraction and systolic filling is longer, resulting in a biphasic pattern of the systolic flow wave. Table 10.2 provides an overview of the relationships between

Table 10.2 Relationship between left heart pressures and various Doppler parameters

Characteristic	*Relationship*	*Correlation coefficient*	*Reference*
Atrial reverse flow velocity (pulmonary vein)	PCWP	0·81	20
S/D if normal LV function	LAP	0·64	19
VTI-S/(VTI-S + VTI-D)	Mean LAP	−0·88	25
E/A	Change of mean LAP	−0·68	23
Change in VTI-S/(VTI-S + VTI-D)	Change of mean LAP	−0·78	23
Duration a > duration A	LAP >15 mmHg		22
E/Ea	PCWP	0·86	33,34

A = atrial contraction flow velocity wave at the transmitral level, a = atrial contraction flow velocity wave at the pulmonary vein level, E = early flow velocity filling wave at the transmitral level, Ea = early diastolic mitral annulus velocity, LAP = left atrial pressure, PCWP = pulmonary capillary wedge pressure, S = systolic flow velocity wave, VTI-D = velocity-time integral of the diastolic flow velocity (pulmonary vein), VTI-S = velocity–time integral of the systolic flow velocity (pulmonary vein).

various Doppler parameters and left sided filling pressure. The atrial flow velocity in the pulmonary vein (a wave) correlates well with the PCWP.[18] In the absence of LV systolic dysfunction, the ratio of systolic to diastolic flow velocities can be used as an estimate of LAP.[24] With volume infusion, it was shown that an increase in LVEDA or LVEDV correlated with an increase in the systolic-to-diastolic flow velocity ratio in the pulmonary veins in patients with normal systolic LV function. The increase in the late systolic flow velocity (S2) was responsible for the increase in this ratio; the early systolic flow wave (S1) did not change significantly. Another approach is assessment of the systolic fraction of the pulmonary venous flow (i.e. the VTI of the S wave, which is related to the sum of the VTIs of both S and D flow velocity waves), which has been demonstrated to correlate closely with mean LAP ($r = -0{\cdot}88$).[25] In patients with severely depressed LV function, the S flow velocity wave decreases significantly, with a S/D ratio of less than 1.

When cardiac function is depressed with a consequent rise in LAP, the correlation between the ratio of the systolic and diastolic flow velocities and the LAP disappears.[24] Although the systolic component of the pulmonary venous flow is dependent on several other factors,[19,26–29] a systolic flow wave velocity of less than 0·4 m/s is suggestive of an elevated LV end-diastolic pressure.[30] The most important limitation to the use of pulmonary venous flow pattern for evaluation of LV filling is the presence of mitral regurgitation (see below). It should be borne in mind that all of these characteristics are only indirect descriptors of filling status and at best can only approximate the directly measured values.

In summary, LAP can be estimated using three different Doppler methods:

- pulsed wave Doppler echocardiography of the transmitral flow pattern
- continuous wave Doppler measurement of velocity of the mitral regurgitation jet
- pulsed wave Doppler echocardiography of pulmonary venous flow.

The LAP value relative to right atrial pressure (RAP) can be estimated from the shape of the interatrial septum. In the presence of an elevated LAP, the interatrial septum bulges toward the right atrium (see below).

Left ventricular end-diastolic pressure

In analogy to the estimation of LAP from the mitral regurgitation velocity, LV end-diastolic pressure can also be determined from the velocity of aortic regurgitation if present:

$$\text{LV end-diastolic pressure} = \text{DBP} - (4 \times V^2_{AR})$$

where DBP is the diastolic blood pressure and V_{AR} is end-diastolic velocity of the aortic regurgitant jet. This method is based on the assumption of comparable values of diastolic pressure in the aortic root and the brachial or radial artery.

In severe mitral regurgitation, a systolic reverse flow (regurgitation) into one or more pulmonary veins is a characteristic phenomenon. This finding is very helpful in the assessment of severity of mitral regurgitation, for instance during mitral reconstructive procedures to evaluate intraoperatively the effectiveness of the repair.[18,19] Various investigators have examined the relationship between pulmonary venous systolic flow wave and LAP in the presence of mitral regurgitation. It could be demonstrated that there is a significant correlation between changes in the LAP, the amplitude of the v wave, and the a to v ratios of the LAP on the one hand and the pulmonary venous systolic to diastolic flow velocity ratios on the other.[18,19] Although the mechanisms of these relationships are complex,[26] the severity of mitral regurgitation appears to be reflected not only by alterations in LAP waveform but also by alterations in pulmonary venous flow pattern.

Other investigators related a prolonged duration of the pulmonary venous atrial reverse flow (a wave), caused by left atrial contraction, to an increase in LV end-diastolic pressure. Also, the difference in the duration of reverse flow into the pulmonary veins during atrial contraction and the duration of the transmitral A wave was shown to correlate with LV end-diastolic pressure.[30] Pulmonary venous flow reversal duration exceeding the duration of the mitral A wave was predictive of LV end-diastolic pressure greater than 15 mmHg, with a sensitivity of 85% and a specificity of 79%.[30] In clinical practice, this information can be obtained at a glance. Because the onset of the mitral A and pulmonary venous a waves is simultaneous, the termination of these waves can be referred to the QRS complex of the electrocardiogram, allowing rapid determination of the relative duration of both waves.

Thus, abnormalities in various Doppler variables may indicate clinically relevant abnormalities in LV filling. Combining left atrial size, left atrial ejection fraction, and the above mentioned Doppler characteristics can provide independent qualitative parameters of LV filling, as has been shown in patients with coronary artery disease.[31] It must be noted that a reliable measurement of the left atrial size by TOE is not always possible, which contrasts with the transthoracic approach.

Estimation of LV filling in patients with atrial fibrillation can be also difficult. Multilinear regression analysis revealed that the best model for predicting LV filling pressure in patients with atrial fibrillation includes peak acceleration of the transmitral flow velocity wave and isovolumetric relaxation time.[32]

It follows from this discussion that for correct estimation of LV filling it is necessary to combine two-dimensional and Doppler echocardiography.

There are, however, certain clinical situations in which Doppler echocardiography fails to predict filling pressures (for example, in sinus tachycardia, in atrial fibrillation, and in cardiac transplant patients). In this respect colour coded Doppler tissue imaging may provide the required information[33] where routine Doppler echocardiography fails. Although the early transmitral filling wave E closely reflects myocardial relaxation, it is also highly preload dependent. In contrast, the early diastolic velocity Ea, obtained by Doppler tissue imaging, behaves as a relative load independent index of LV relaxation. It was shown that the ratio of E and Ea can be used to estimate filling pressures with reasonable accuracy.[33,34]

Afterload

Among authorities there is much controversy on how afterload should be measured and quantified. Arterial pressure measured in the aorta is considered an index of afterload. Because ejection pressure is defined not only by the aortic impedance but also by the left ventricle, the left ventricle itself determines in part its own afterload.

Some of the important concepts regarding afterload and echocardiography are elaborated in Chapter 3. These can be compiled as global indices of afterload, with respect to the relevance to the performance of the coupling of the left ventricle and the arterial system in normal and pathological conditions.[35]

Regional mechanical properties of the aorta can also be described using echocardiography. In this respect, the relationship between aortic pressure, flow, and dimensions must be investigated closely. Routine evaluation of regional mechanical properties of the aorta has been troubled by technical difficulties (measurement of regional aortic pressure, flow, and dimension changes). Therefore, initial assessments were limited to animal experiments. With the introduction of the impedance catheter, pressure–volume loops could be created, as well as diameter pressure data with variable load. Pulse wave velocity,

measured over a limited aortic segment, provided information about average stiffness over a particular part of the artery through which the pulse travels.[36] The problem is the measurement of local pressure and the assessment of information on local vessel geometry.

Advances in echocardiographic technology permit acquisition of vessel dimensions non-invasively and continuously. Furthermore, regional aortic pressures will allow calculation of regional aortic elastic properties.[37] Dimensional changes of the descending aorta can easily be recorded in a transverse plane utilising acoustic quantification. Acoustic quantification allows automated border detection and instantaneous real time measurements of dimensional changes in the descending aorta. The echocardiograph automatically generates area–time curves, which must be linked with invasive aortic trace signals. Central aortic pressures can be estimated non-invasively from calibrated carotid or subclavian pulse signals[38] – a model that has been further improved on an individual basis.[39]

Although this technique is appealing, much work is yet to be done, not least regarding the technical difficulties associated with acquiring real-time data sets in critically ill patients.

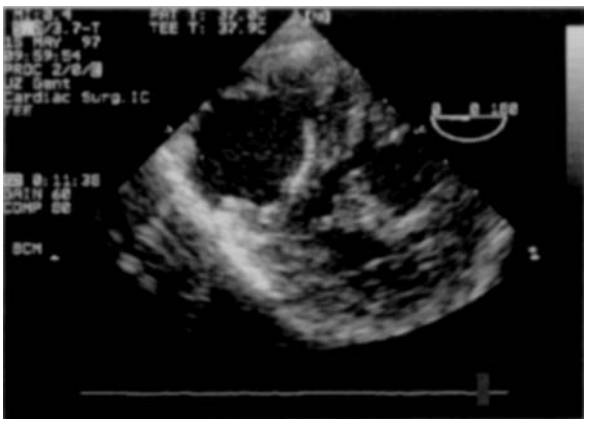

Figure 10.2 Short-axis view in a transverse plane. Right ventricular dilation at the left side is clearly seen.

Estimation of preload of the right heart and the relation between pressure and flow

Volume and pressure

The right heart analogue of LVEDA, the RV end-diastolic area (RVEDA), can be used as an index of RV preload. Because of the complex geometry of the right ventricle, this parameter may be difficult to measure (Figure 10.2). Many studies have attempted to estimate RV volumes using two-dimensional echocardiography. For instance, an ellipsoidal subtraction model was developed to estimate RV volume from cardiac dimensions.[40] A significant linear relationship between the RV free wall to septum dimension and RV volume was demonstrated. More recently multislice magnetic resonance imaging with summation of cavity areas of the right ventricle, a widely accepted methodology, was compared with echocardiography.[41] The investigators concluded that the ellipsoidal shell model of the right ventricle (as shown in Figure 8.1C) provides a simple area–length formula, similar to the formula for the LV volume:

$$RVEDV = \tfrac{2}{3} \times A \times D$$

where A is the area at end-diastole of the right ventricle, excluding the papillary muscles; D the anteroposterior diameter of the right ventricle; and RVEDV is the calculated volume of the right ventricle at end-diastole.

In spontaneously breathing patients it was shown that the RAP is positively related to the diameter of the inferior vena cava.[42] During spontaneous inspiration, the caval vein will collapse or its diameter will reduce by at least 50%. This finding is associated with RAP below 10 mmHg. When this sign is absent or less pronounced, the RAP is probably elevated. Doppler measured RV inflow velocities and superior caval vein flow are in general higher during inspiration than during expiration or apnoea,[29] reflecting the inspiratory increase in venous return.

During mechanical ventilation, preload will decline in parallel with the elevated intrathoracic pressure. The forward blood flow in the caval veins and RV inflow velocities representing the venous return will decrease;[43,44] the lower the filling status, the greater the effects of increased intrathoracic pressures during mechanical ventilation. During hypovolaemia, marked variation in both diastolic and systolic blood velocities can be observed. The haemodynamic effects of increased intrathoracic pressure are less pronounced in patients with low pulmonary

compliance. For more detail regarding the use of TOE to evaluate right heart structure and function, the reader is referred to Chapter 8.

Interatrial septum

The directional movement of the interatrial septum and its curvature (Figure 10.3) reflect the balance between RAP and LAP.[45] The interatrial septum bows to the right during atrial contraction at end-diastole, whereas during mid-systole the septum has a variable shape, and finally, at end-systole, the interatrial septum is usually again directed toward the right atrium.[45] Various investigators studied whether pressure gradients or volume alterations can explain these septal movements.[45–47] The strong relationship of the shape of the interatrial septum to the interatrial pressure gradient in the study conducted by Kusumoto *et al.*[45] suggests that pressure differences between right and left atria are indeed responsible for the septal movements during the cardiac cycle. The useful information offered by interrogating the interatrial septum is related to its shape and motility. The motility of the interatrial septum decreases with increasing filling pressures; vice versa, an exaggerated septal motion is a valuable sign of hypovolaemia. The shape and curvature of the interatrial septa reflects the actual pressure difference between the atria, as mentioned above. In this respect, Figure 10.3 demonstrates a clear example of increased LAP in relation to RAP.

Decreased or absent movement of the interatrial septum is frequently seen in patients with elevated LV or RV filling pressure (RAP and/or PCWP > 15 mmHg). A bulging of the interatrial septum is typically observed in patients with chronic mitral regurgitation or mitral stenosis as a consequence of increased LAP and subsequent decreased left atrial volume changes. In mitral stenosis a permanent bulging of the interatrial septum into the right atrium occurs, whereas in mitral regurgitation the rightward bulging is limited to systole. Similarly, there is a leftward directed systolic movement of the septum in the presence of tricuspid regurgitation and a permanent bulging into the left atrium with RV pressure overload, for example in severe pulmonary hypertension.

The movement of the interatrial septum cannot be used to obtain information about the relative pressure differences between right and left atria in the presence of tricuspid valve pathology.

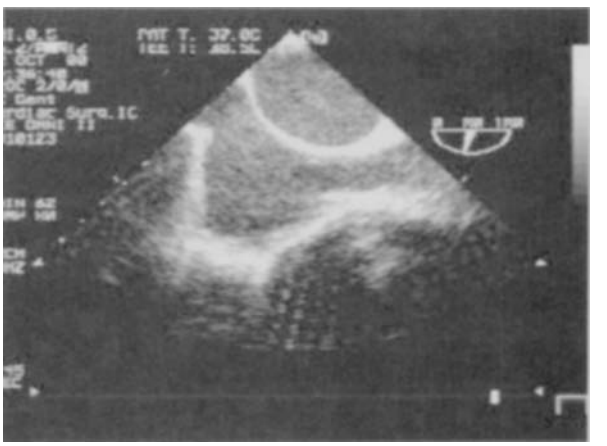

Figure 10.3 Example in which left atrial pressure is markedly increased, with a consequent permanent shift of the interatrial septum towards the right side.

Pressure versus volume overload

For a discussion of this area, the reader is referred to Chapter 8.

Left ventricular interdependence

Under physiological conditions, the interventricular septum is convex toward the right ventricle. In patients with systolic pressure overload of the right ventricle, an early diastolic leftward shift with concomitant flattening of the interventricular septum is observed with a convexity directed toward the left ventricle.[48] When diastolic RV volume overload is present, a late diastolic leftward shift of the interventricular septum may be found. Changes in LV volume significantly influence RV geometry because of the diastolic ventricular interdependence.[40] Conversely, changes in RV volume affect LV volume and geometry. For instance, marked dilation of the right ventricle, particularly in association with a RV pressure overload, will impair LV filling. Ventricular interdependence is also operative during systole. The contraction of the left ventricle contributes significantly to the pump function of the right ventricle.

Estimation of pulmonary artery pressures

Traditionally, anaesthetists measure and monitor pulmonary artery pressures by means of

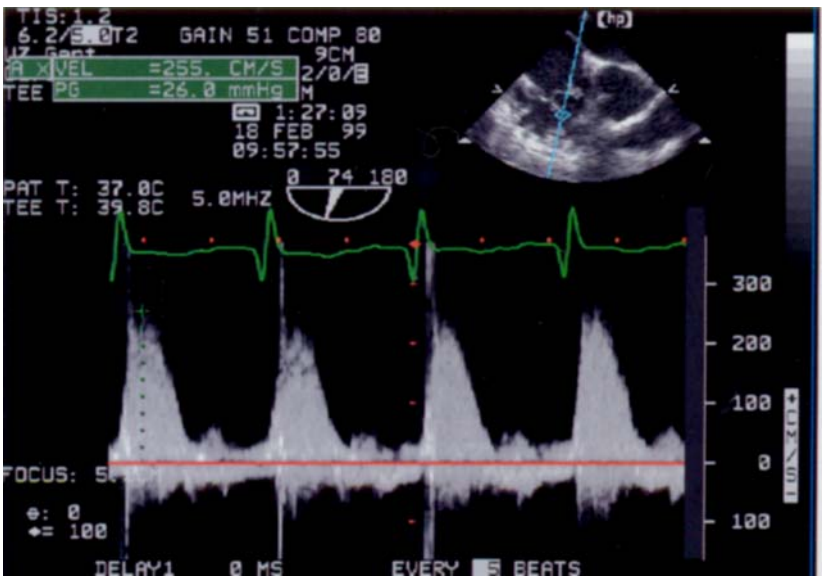

Figure 10.4 Continuous wave Doppler pattern across the tricuspid valve. Estimation or direct measurement of peak velocities allows calculation of right ventricular systolic pressure, utilising the modified Bernoulli equation.

pulmonary artery catheterisation. Pulmonary hypertension and its therapy still play important roles in the context of cardiac and respiratory failure. Therefore, the knowledge of actual pressures and resistances in the pulmonary circulation is helpful for therapeutic decision making and adjustment to therapy. Pulsed wave Doppler measurements of blood flow velocity in the pulmonary artery allowed diagnosis of pulmonary hypertension in a variety of congenital[49] and acquired cardiac diseases. Both transthoracic echocardiography and TOE can be used to measure flow velocities in the pulmonary artery,[50–52] as well as gradients across the tricuspid valve,[53,54] in a non-invasive manner. Non-invasive assessment of pulmonary artery pressure by continuous wave Doppler measurement of tricuspid regurgitation velocity has become a standard component of any echocardiographic study (Figure 10.4). The fact that it can predict morbidity and mortality in patients with ischaemic or idiopathic cardiomyopathy emphasises the clinical relevance of this modality.[55]

Normal and abnormal Doppler patterns of the pulmonary artery flow

For analysis of pulmonary artery Doppler signals, the sample volume must be positioned within 2 cm of the pulmonary valve in the middle of the vessel.[56] Several time intervals can be derived from the Doppler signal of the pulmonary artery flow velocity (see Figure 10.5). The pre-ejection period is the time (in milliseconds) between the start of the QRS complex of the electrocardiogram and the beginning of the pulmonary artery flow. The ejection period is the time (in milliseconds) between the onset of ejection and its end. The acceleration time is defined as the time between the onset of ejection and that at peak flow velocity. In a comparative study including patients with normal and increased pulmonary artery pressures (i.e. mean pulmonary artery pressure below and above 20 mmHg, respectively), peak flow was reached earlier in the patient group with pulmonary arterial hypertension.[52] The Doppler pattern in the latter group also exhibited a mid-systolic notching and a reduction in peak flow velocity. Both acceleration time and the ratio of acceleration time to ejection period decreased with increase in mean pulmonary artery pressure. The ratio of the acceleration time to the RV ejection period correlated well with the logarithm of the mean pulmonary arterial pressure.[52]

The pre-ejection period becomes longer during inspiration and shortens during expiration. This parameter reflects not only afterloading conditions but also RV contractility and preload.[50,51] Both pre-ejection and ejection periods depend on heart rate and should be corrected for heart rate in the presence of marked tachycardia. An increasing

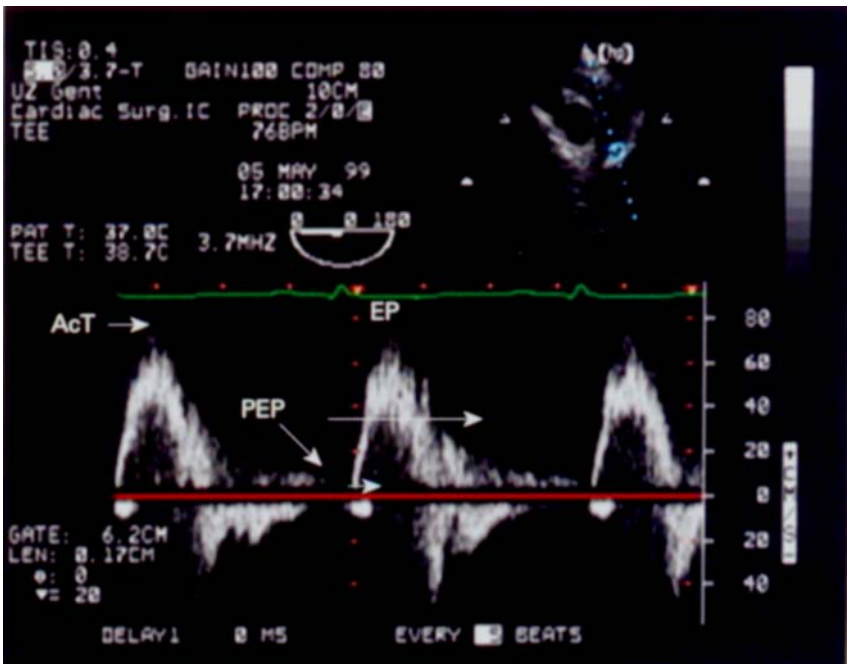

Figure 10.5 Pulmonary artery flow (pulsed wave Doppler) in the main stem of the pulmonary artery. AcT = acceleration time, EP = ejection period, PEP = pre-ejection period.

pre-ejection period in association with a decreasing ejection period points to an elevated pulmonary artery pressure and development of RV dysfunction with decreasing SV.

Tricuspid regurgitant flow and pulmonary hypertension

In the presence of tricuspid regurgitation, the pressure gradient between the right ventricle and the right atrium during systole can be assessed by measuring the maximal velocity of the tricuspid valve regurgitant flow (Figure 10.5). Systolic pulmonary arterial pressure can then be estimated from this pressure gradient added to the RAP, according the modified Bernoulli equation (as described in Chapter 1):[57]

$$PASP = RAP + 4V^2_{TTF}$$

where PASP is the pulmonary artery systolic pressure and V_{TTF} is the maximal regurgitant trans-tricuspid flow velocity. This method is only valid if there is no additional pressure gradient across the pulmonary valve. In the presence of pulmonary stenosis it is the RV systolic pressure that is measured using this method.

The introduction of multiplane technology has facilitated visualisation of the tricuspid valve by TOE, particularly from lower oesophageal and gastro-oesophageal junction views (see Chapters 2 and 8). A close correlation between the trans-tricuspid Doppler gradient and the pulmonary artery systolic pressure measured during right heart catheterisation has repeatedly been reported. Correction for RAP was not found to be necessary.[58]

Similarly, pulmonary artery diastolic pressure can be estimated by summation of mean RAP and the end-diastolic pressure gradient across the pulmonary valve. Box 10.1 summarises the various items that must be consecutively evaluated if the right ventricle is to be excluded as a cause of haemodynamic instability. One begins with the morphology and function of the right ventricle and proceeds with evaluation of the right sided cardiac valves. Finally, pulmonary artery pressure and pulmonary vascular resistance are estimated by measuring the peak transvalvular gradients and by analysing the Doppler waveform of the pulmonary artery blood flow velocity. However, the diagnostic efficacy of TOE with regard to RV function is dependent on the presence of tricuspid and/or pulmonary valve regurgitation. Fortunately, in significant pulmonary hypertension and RV dysfunction, both valves are usually insufficient.

- Is the right ventricle large or small?
- How is its global and regional function alike?
- Morphology and function of the tricuspid valve?
- Trans-tricuspid flow and hepatic venous flow pattern (pulsed wave Doppler)?
- Morphology and function of the pulmonary artery valve?
- Estimated systolic pulmonary artery pressure (from the tricuspid regurgitation flow velocity)?
- Estimated pulmonary artery diastolic pressure (from pulmonary regurgitation flow velocity)
- Pulmonary artery flow profile (systolic time intervals)?

Box 10.1 Steps in transoesophageal echocardiography evaluation of right heart haemodynamics

Haemodynamic instability: differential diagnosis of hypotension and low cardiac output

Haemodynamic instability, including low cardiac output and severe hypotension, is an emergency that must be treated as soon as possible in order to improve cardiovascular function and prevent secondary organ dysfunction. Prompt and appropriate treatment requires immediate and reliable diagnosis of the cause of the haemodynamic disorder. Both invasive pressure measurement and cardiac imaging can be used for online assessment of cardiovascular function.

In this section, the sensitivity and specificity of both transthoracic echocardiography and TOE in the management of haemodynamically unstable patients are addressed. The additional value of the echocardiography beyond the information obtained from pulmonary artery catheterisation data is discussed. Finally, a quick reference guide is proposed that describes the deployment of TOE in critically ill and haemodynamically unstable patients.

Transthoracic versus transoesophageal echocardiography

In assessing the cause of systemic hypotension, both transthoracic echocardiography and TOE can play a central role. However, transthoracic echocardiography remains the first choice, being the least invasive and the quickest method. It provides instantaneous information on global LV contractility, filling of the left ventricle and, when imaging is adequate, regional wall motion abnormalities of the left ventricle. Diagnosis of a pericardial effusion can be easily and more accurately done by the transthoracic approach,[59] although whenever tamponade must be excluded TOE may offer a significant advantage.[60–62] Local haematomas after chest trauma, after cardiac surgery, or an interventional cardiac procedure are better diagnosed with TOE, particularly when classic signs such as respiratory variation in intracardiac flow velocities and pulsus paradoxus are absent.[63] Furthermore, rapid and accurate diagnosis of some intracardiac pathological conditions, such as ventricular septal defect (VSD), can be difficult with the transthoracic approach. Transthoracic echocardiography correctly diagnosed VSD in only four out of 17 cases of postinfarction VSD diagnosed by catheterisation, autopsy, or surgery.[64] TOE, in conjunction with colour Doppler and contrast echocardiography, provided the correct diagnosis in all cases. Also, in ventilated patients, the transthoracic approach is often insufficient. Box 10.2 summarises situations in which TOE provides substantial benefit over transthoracic echocardiography. This summary lists not only diagnoses but also important advantages in patients who are otherwise difficult to evaluate.

- Acute perioperative haemodynamic instability
- Ventilated patients, prone position, chest drains and dressings
- Intra-operative haemodynamic monitoring (global and regional function, contractility, preload and afterload)
- Examination of prosthetic valves (morphology, function)
- Exclusion of endocarditis
- Diagnostic imaging in the evaluation of suspected aortic dissection or traumatic rupture
- Exclusion of a cardiac source of embolism
- Cardiac tamponade (in particular atrial compression, upper mediastinum)
- Minimally invasive cardiac surgery: haemodynamic monitoring
- Detection of perioperative myocardial ischaemia

Box 10.2 Situations in which transoesophageal echocardiography offers advantages over transthoracic echocardiography

When the diagnosis has been made, TOE should be used as a haemodynamic monitor until

the patient's haemodynamic function is stabilised. This requires that one TOE probe and the ultrasound apparatus be temporarily attached to the patient, and hence are not available for deployment elsewhere. In addition, the available information must be interpreted correctly, requiring the participation of an echocardiographer with a rigorous knowledge of physiology and pathophysiology, adequate training, and continuous experience in echocardiography (see Chapters 17 and 18). With these requirements fulfilled, the major advantage of TOE in comparison with invasive and non-invasive monitoring is revealed, namely its ability to provide additional, sometimes unexpected, but very important information on structure and function of the heart and the great vessels. Inherently, in the perioperative setting TOE is always both a diagnostic and a monitoring tool, permitting efficient differential diagnosis of any underlying cardiovascular pathology.

Invasive haemodynamic monitoring versus transoesophageal echocardiography

Once haemodynamic function is stabilised and treatment initiated, continuous haemodynamic monitoring can be instituted. Both the arterial pressure tracing and the indirectly obtained intracardiac pressures have always provided the critical care clinician with important information about filling status and pump function of the ventricles. Newer developed invasive techniques, such as double indicator dilution, offer interesting data on the intravascular volume status (Table 10.3) by measurement of intrathoracic blood volume.[65] The correlation of intrathoracic blood volume with the effective preload in the presence of altered chamber compliance, however, has yet to be proven.

In mechanically ventilated patients, systolic pressure variation was shown to provide a good estimate of preloading conditions and of the response of the heart to volume loading.[66,67] The presence of systolic respiratory blood pressure variation (i.e. the difference between maximal and minimal systolic blood pressure values during one mechanical breath) is a very sensitive but not such a specific sign of hypovolaemia. The systolic pressure variation can be quantified as the pressure difference between apnoeic and minimum systolic blood pressure, and is known as "delta down". A delta down value of more than 5 mmHg indicates that the SV would increase in response to a fluid challenge (positive and negative predictive values 95% and 93%, respectively). A significant difference between responders and non-responders to delta down guided volume management was found in LVEDA and systolic pressure variation, but not in pulmonary artery occlusion pressure.

Table 10.3 *Various bedside haemodynamic monitoring techniques*

Parameter	Pulmonary artery catheter	TOE	Double dye dilution technique
Preload	(+)	+	+
Afterload	(+)	+	(+)
Contractility	–	+	–

Shown is a comparison between various bedside haemodynamic monitoring techniques, to demonstrate their capability to assess separately the determinants of the Frank–Starling mechanism. TOE = transoesophageal echocardiography.

In an intraoperative study of the performance of five community based, full time cardiac anesthesiologists, who used both TOE and a pulmonary artery catheter intraoperatively, TOE provided useful information on volume status of the patients significantly more frequently, and it was more reliable in guiding fluid therapy (in 30%).[68] Even a more sophisticated and expensive thermodilution catheter equipped with a fast transistor, which measures RV ejection fraction and provides RVEDVs, failed to ensure optimal volume management because of systematic underestimation of LV preload.[69] Detection of acute blood losses using TOE measurements of LVEDA was found to be of comparable accuracy to measurements of central venous pressure or PCWP.[70] A linear decrease in LVEDA and PCWP during controlled withdrawal of up to 15 % of estimated blood volume was found. Even mild reductions in blood volume can be identified by visual assessment alone ("eye balling"), which proved to be adequate for clinical purposes. This implies that online measurements are not always necessary.[71] Using the indocyanine green dye dilution technique, Hinder *et al.*[72] showed that changes in LVEDA and intrathoracic blood volume correlated closely ($r = 0{\cdot}87$). However, other determinants of ventricular function such as afterload and contractility cannot be, or at best only indirectly, estimated by dye dilution (see Table 10.3).

Both retrospective and prospective[73] studies confirmed that TOE is a useful monitoring and diagnostic tool, with direct impact on management and therapy. In one study conducted in intensive care unit (ICU) patients monitored

Table 10.4 Evaluation of the hypotensive patient

Diagnosis	LV EDA	LV FAC	RV dilation	E/A	S/D
Hypovolaemia	↓	↑		<1	>1
Cardiogenic shock	↑	↓	↑	<1	<1
Distributive shock	↓	↑	↑	<1 or >1	>1
Combined cardiogenic and septic shock	↑	↑ or ↓	↑	<1	<1
Tamponade	↓	↓		<1	>1
RV infarction	↓	↔	↑		
Pulmonary emboli	↔	↔	↑		
Hypertrophic cardiomyopathy	↓	↑	↔	<1 or >1	<1

E/A = early to late diastolic filling across the mitral valve, LVEDA = left ventricular end-diastolic area, LVFAC = left ventricular fractional area contraction, RV = right ventricular, S/D = systolic to diastolic pulmonary venous flow velocity ratio, ↓ = decrease, ↑ = increase, ↔ = indifferent.

with a pulmonary artery catheter, therapy had to be changed in 44% of the patients after a TOE examination. The therapeutic recommendations based on pulmonary artery data differed in 58% of the patients from the recommendations based on unambiguous TOE findings,[73] which eventually resulted in a change to management.

Transoesophageal echocardiography and hypotension

In this section several common causes of hypotension and haemodynamic instability are summarised, including the impact of echocardiography on decision making in these often critical situations. Relevant changes in various parameters, as assessed by echocardiography, are shown in Table 10.4; this table can serve the reader as a quick reference, which is useful in daily practice.

Tamponade

Cardiac tamponade is a life-threatening situation, although a timely intervention can normalise haemodynamics within seconds and save a patient's life. Clinical features include low cardiac output, hypotension, tachycardia, pulsus paradoxus, and increased RAP and LAP. Pulsus paradoxus (exaggerated inspiratory fall in arterial pressure > 10 mmHg during spontaneous breathing) is explained by a marked reduction in transmitral flow, LV filling, and SV during spontaneous inspiration. In contrast, during mechanical ventilation the filling of the LV and its output increases during inspiration. When the clinical presentation is not quite convincing, additional investigations are necessary before intervention (see Table 10.4). In this respect, echocardiography is the diagnostic tool of choice. An echo-free space (≥ 10 mm) around the cardiac chambers with diastolic compression or invagination of the right ventricle and right atrium, associated with an "empty" left ventricle, are the characteristic findings. Compared with transthoracic echocardiography, TOE can better detect localised fluid accumulation or a clot compressing the right ventricle or one or both atria. This mechanism of cardiac tamponade is frequent after cardiac surgery. If in doubt, another characteristic finding, namely that of marked respiratory variation of transmitral or transtricuspid blood flow velocity, can positively support the diagnosis of a tamponade.[74,75] In the transmitral flow pattern a shift from the early to the late phase of LV filling and consequent increase in atrial flow wave velocity was described. This shift has been related to inspiratory decrease in LV compliance during tamponade.[75] A similar pattern can be expected at the right side, with a prominent X descent with no or little Y descent on the central venous pressure tracing.[60] In practice, however, this finding is of no great value. The pattern of dominant A wave is normal in older patients as well as during tachycardia.[28] Moreover, the control pattern in the patients studied during emergency situations, which is where tamponade commonly occurs, is usually not available. Finally, echocardiography, be it transthoracic or transoesophageal, is used to guide pericardiocentesis.

Cardiogenic shock

In most conditions, TOE is able to identify the cause of a cardiogenic shock, which is characterised by hypotension with high filling pressures, low cardiac output, and peripheral vasoconstriction. The TOE evaluation is based on transgastric short-axis and long-axis views, where global and regional LV function and LV filling status can be assessed online. The search for the extent of dysfunctional myocardium is facilitated by multiplane probe, which allows one to interrogate all segments of the LV wall.[76] In addition, valvular abnormalities and dysfunction or shunts, which are other possible causes of shock states, can be detected.

Distributive shock

The problem of sepsis and septic shock has become increasingly important, and for the past several years has been the highest ranking in the list of most common causes of death in the ICU. Septic shock is a prototype of distributive shock; it is a circulatory shock, which is characterised by hypotension with normal or low filling pressures, high cardiac output, and low peripheral resistance. Estimation and subsequent optimisation of preload is a cornerstone of haemodynamic monitoring. In this respect, it was found that stroke index and ejection fraction, measured as fractional area contraction of the left ventricle, were closely related.[77] However, myocardial dysfunction and impaired global pump function may sometimes occur. Notwithstanding, in the majority of patients the left ventricle is hyperdynamic and inadequately filled, whereas the right ventricle may be dilated in response to the development of pulmonary hypertension and increasing RV afterload. TOE is helpful in estimating cardiac output in patients without a pulmonary artery catheter and in guiding fluid therapy.[78] Furthermore, TOE can exclude endocarditis, myocardial or major vascular abscesses (Figure 10.6),[79] and (septic) thrombi (Figure 10.7) as causes of septic shock.

Right ventricular failure

The right ventricle is well recognised as a major cause of cardiogenic shock. RV failure is characterised by hypotension, high right sided and normal left sided filling pressures, low cardiac output, and clear lung fields on chest radiography. Pulmonary artery pressure is usually high when RV failure develops secondary to severe pulmonary hypertension.[80] Pulmonary

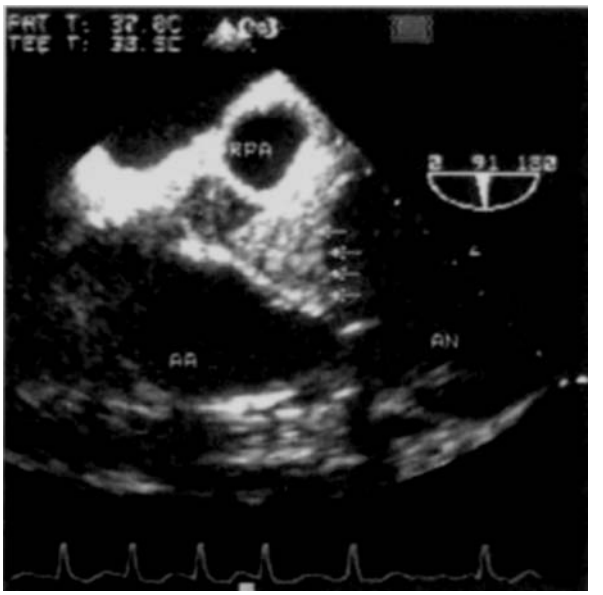

Figure 10.6 Example of a periaortic abscess (arrows). AA = aortic arch, AN = aneurysmic dilation of the aortic arch, RPA = right pulmonary artery.

artery pressures may only be mildly elevated when a failing right ventricle cannot generate sufficient pressure. Tricuspid and pulmonic regurgitation are common, and therefore TOE can be used to estimate pressures in the pulmonary circulation (vide supra). Again, multiplane technology allows one to diagnose correctly both tricuspid and pulmonary valve insufficiencies. Whereas tricuspid regurgitation is relatively easily assessed in a mid-oesophageal view (see Figures 2.6 and 2.7 in Chapter 2), visualisation and quantitative estimation of pulmonary regurgitation is rather difficult (see Figure 8.5C,D). In this manner it is possible to differentiate between pulmonary hypertension (presence of pulmonary valve regurgitation and tricuspid regurgitation) and RV pressure/volume overload (presence of tricuspid valve regurgitation solely). Box 10.1 summarises the different steps necessary for the evaluation of right heart function. A great deal of evidence confirms the important role played by the right heart and its function in the critically ill patients. For instance, the development of a RV infarction increases early mortality to 30%.[81] Frequent follow up of RV function is necessary.

Pulmonary embolism

Pulmonary embolism is a life threatening condition that challenges RV contractile reserve.

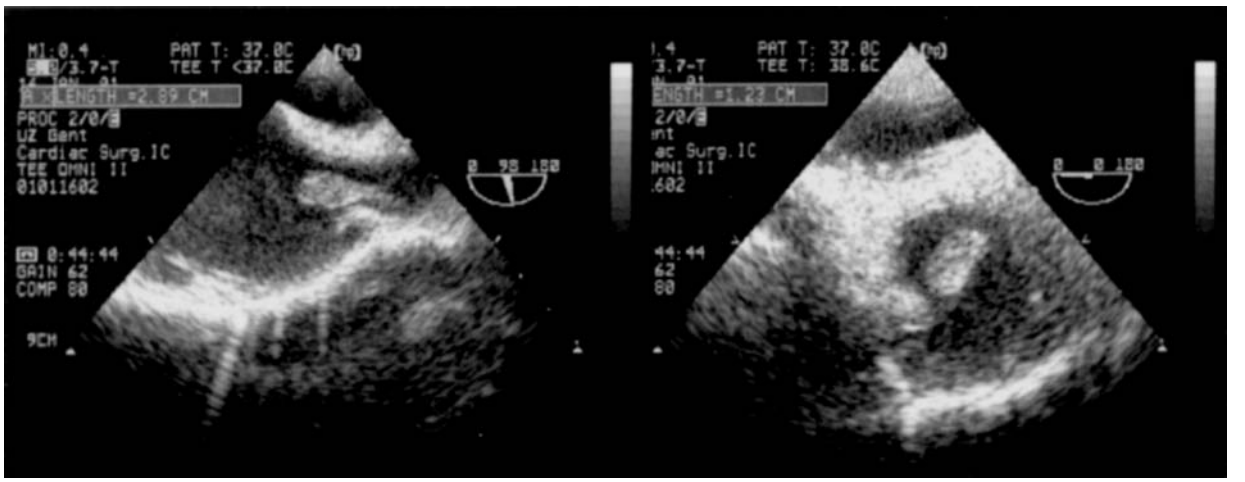

Figure 10.7 Example of septic thrombus in the right atrium, just at the connection with the superior caval vein.

TOE is helpful in the diagnosis of pulmonary embolism because emboli can be found in the main and right pulmonary artery, at its bifurcation, but also in the right ventricle and right atrium. TOE cannot usually detect emboli in the left pulmonary artery or in the lobar arteries.[80] Even in the absence of central emboli the signs of a RV pressure overload are helpful in the diagnostic process, and actual RV function has an important impact on the choice of therapy. Furthermore, TOE provides valuable follow up information, for instance on the effects of lysis or of surgical removal of the clots, on recurrent emboli, and on recovery of RV function. The sensitivity and specificity of TOE in diagnosing acute pulmonary embolism in patients with RV dilation can be as high as 92% and 100%, respectively.[82]

Left ventricular outflow tract obstruction

A refractory hypotension can also be caused by dynamic obstruction of the LV outflow tract, occasionally developing in patients with high sympathetic tone, hypovolaemia and/or LV hypertrophy. TOE shows an acceleration of LV outflow with subaortic pressure gradient and systolic anterior motion of the mitral valve. The therapy is based on administration of fluids and beta blockade.

Intraoperative decision making

It is not always easy to investigate the cost–benefit ratio of a given method or procedure in a prospective randomised manner. This is also true for the TOE. Nevertheless, some studies addressed this issue and suggested that the benefit associated with the use of TOE exceeds the risk and the cost. Benson *et al.*[83] demonstrated a favourable cost–benefit ratio of TOE in both valvular and congenital heart surgery. Although the benefit of TOE in myocardial revascularisation surgery was less clear in that study, other investigators did find a favourable impact of intraoperative TOE on the outcome of aortocoronary bypass surgery. The most frequent interventions based on TOE findings were fluid administration (30%) and institution of anti-ischaemic therapy (21%) or of inodilatory support (6%).[68] The development of new wall motion abnormalities after cardiopulmonary bypass may be due to myocardial stunning, infarction, or coronary or mammary artery spasm. TOE findings can prompt the surgeon to return to the pump if problems with the arterial and venous conduits and their anastomoses are suspected. In future, the availability of contrast echocardiography may facilitate these diagnostic and therapeutic decisions. A retrospective analysis confirmed the data reported by Bergquist *et al.*:[84] routine intraoperative TOE may reduce the cost per operated cardiac surgical patient by about 230 €.

Conclusion

Rapid evaluation of cardiovascular structure and function in haemodynamically unstable patients is the domain of transthoracic echocardiography. In certain situations (for

example, ventilated, critically ill patients, patients after thoracotomy, and patients with increased intra-abdominal pressure) and indications (such as exclusion and evaluation of aortic dissection or traumatic aortic rupture), TOE represents the method of first choice. It can also be deployed when transthoracic echocardiography has failed to achieve a conclusive diagnosis. TOE has proven to be safe, non-invasive, and to provide reliable and rapid information at the bedside.

The first question regarding the cardiac or extracardiac origin of haemodynamic instability can be answered with two-dimensional echocardiography alone. For a complete assessment of the cardiovascular function, Doppler echocardiography, and in the future newer techniques such as tissue Doppler imaging, should be added. No bedside technique other than TOE allows separate determination of RV and LV function and their determinants, namely preload, afterload, and contractility. With such information at hand, the physician is able to improve significantly the quality of care in critically ill patients. The value of the TOE in echocardiography laboratories is not always comparable with the value of TOE in the perioperative setting. In the laboratory, TOE is a secondary diagnostic tool that is used to address specific questions. Intraoperatively, and in the ICU, TOE primarily serves as a monitor of haemodynamic and ventricular function. At the same time it works as an invaluable diagnostic tool, with important impact on quality and efficiency of care both intraoperatively and in the ICU.

TOE represents a life and cost saving technique and has become an essential cornerstone of acute medicine in general and of perioperative medicine in particular. Future developments (such as transnasal miniprobe, new methods of flow and tissue velocity measurements) will shift the role of this tool from its use primarily in diagnosis toward monitoring. Use of such systems to provide continuous information on the function of the cardiovascular system at the bedside will further improve the quality of perioperative management of critically ill patients.

References

1 Seward JB, Khandheria BK, Freeman WK, *et al.* Multiplane transesophageal echocardiography: Image orientation, examination technique, anatomic correlations and clinical applications. *Mayo Clin Proc* 1993;**68**:523–51.

2 Sheikh KH, de Bruijn NP, Rankin JS, Stanley T, Wolfe WG, Kisslo J. The utility of transesophageal echocardiography and Doppler color flow imaging in patients undergoing cardiac valve surgery. *J Am Coll Cardiol* 1990;**15**:363–72.

3 Cahalan M, Ionescu P, Melton H, Adler S, Kee L, Schiller N. Automated real-time analysis of intraoperative transesophageal echocardiograms. *Anesthesiology* 1993;**78**:477–84.

4 Poelaert J, Schmidt C, Colardyn F. Transoesophageal echocardiography in the critically ill. *Anaesthesia* 1998;**53**:55–68.

5 Thubrikar M, Harry R, Nolan SP. Normal aortic valve function in dogs. *Am J Cardiol* 1977;**40**: 563–8.

6 Higashidate M, Tamiya K, Beppu T, Imai Y. Regulation of the aortic valve opening: in vivo dynamic measurement of aortic valve orifice area. *J Thorac Cardiovasc Surg* 1995;**110**:496–503.

7 Katz WE, Gasior TA, Quinlan JJ, Gorcsan J III. Transgastric continuous-wave Doppler to determine cardiac output. *Am J Cardiol* 1993;**71**: 853–57.

8 Schmidt C, Roosens C, Struys M, *et al.* Contractility in humans after coronary artery surgery. Echocardiographic assessment with preload-adjusted maximal power. *Anesthesiology* 1999;**91**:58–70.

9 Garcia M, Thomas J, Klein A. New Doppler echocardiographic applications for the study of diastolic function. Review article. *J Am Coll Cardiol* 1998;**32**:865–75.

10 Poelaert J, Schmidt C, Van Aken H, Hinder F, Mölhoff T, Loick M. A comparison of transoesophageal echocardiographic Doppler across the aortic valve and thermodilution technique for estimating cardiac output. *Anaesthesia* 1999;**54**:128–36.

11 Perrino A Jr, Harris S, Luther M. Intraoperative determination of cardiac output using multiplane transesophageal echocardiography. A comparison to thermodilution. *Anesthesiology* 1998;**89**:350–7.

12 Darmon PL, Hillel Z, Mogtader A, Mindich B. Thys D. Cardiac output by transesophageal echocardiography using continuous-wave Doppler across the aortic valve. *Anesthesiology* 1994;**80**: 796–805.

13 Pinsky M, Desmet J, Vincent J. Estimating left ventricular filling pressure during positive end-expiratory pressure in humans. *Am Rev Respir Dis* 1991;**143**:25–31.

14 Practice guidelines for pulmonary artery catheterisation. A report by the American Society of Anesthesiologists task force on pulmonary artery catheterization. *Anesthesiology* 1993;**78**: 380–94.

15 Weil M. The assault on the Swan Ganz catheter. A case history of constrained technology, constrained

bedside clinicians, and constrained monetary expenditures. *Chest* 1998;**113**:1379–86.

16 Leung JM, Levine EH. Left ventricular end-systolic cavity obliteration as an estimate of intraoperative hypovolemia. *Anesthesiology* 1994;**81**:1102–9.

17 Nishimura RA, Miller FA Jr, Callahan MJ. Doppler echocardiography: theory, instrumentation, technique and application. *Mayo Clin Proc* 1985;**60**:321–43.

18 Nishimura R, Abel M, Hatle L, Tajik A. Relation of pulmonary vein to mitral flow velocities by transesophageal Doppler echocardiography. Effect of different loading conditions. *Circulation* 1990;**81**:1488–97.

19 Klein A, Tajik A. Doppler assessment of pulmonary venous flow in healthy subjects and in patients with heart disease. *J Am Soc Echocardiogr* 1991;**4**:379–92.

20 Sutherland G, Stewart M, Groundstroem K, *et al.* Color Doppler myocardial imaging: a new technique for the assessment of myocardial function. *J Am Soc Echocardiogr* 1994;**7**:441–58.

21 Courteois M, Mechem CJ, Barzilai B, Guterriez F, Ludbrook PA. Delineation of determinants of left ventricular early filling. Saline versus blood infusion. *Circulation* 1994;**90**:2041–50.

22 Appleton A, Hatle L, Popp R. Relation of transmitral flow velocity patterns to left ventricular diastolic function: new insights from a combined hemodynamic and Doppler echocardiographic study. *J Am Coll Cardiol* 1988;**12**:426–40.

23 Courteois M, Mechem C, Barzilai B, Ladbrook P. Factors related to end-systolic volume are important determinants to peak early diastolic transmitral flow velocity. *Circulation* 1992;**85**: 1132–8.

24 Hoit B, Shao Y, Gabel M, Walsh R. Influence of loading conditions and contractile state on pulmonary venous flow. Validation of Doppler velocimetry. *Circulation* 1992;**86**:651–9.

25 Kuecherer HF, Muhiudeen IA, Kusumoto FM, *et al.* Estimation of mean left atrial pressure from transesophageal pulsed Doppler echocardiography of pulmonary venous flow. *Circulation* 1990;**82**: 1127–39.

26 Klein A, Stewart W, Bartlett J, *et al.* Effects of mitral regurgitation on pulmonary venous flow and left atrial pressure: an intraoperative transesophageal echocardiographic study. *J Am Coll Cardiol* 1992;**20**:1345–52.

27 Klein A, Bailey A, Cohen G, *et al.* Importance of sampling both pulmonary veins in grading mitral regurgitation by transesophageal echocardiography. *J Am Soc Echocardiogr* 1993;**6**:115–23.

28 Klein A, Abdalla I, Murray D, *et al.* Age independence of the difference in duration of pulmonary venous atrial reversal flow and transmitral A-wave flow in normal subjects. *J Am Soc Echocardiogr* 1998;**11**:458–65.

29 Klein A, Leung D, Murray R, Urban L, Bailey K, Tajik A. Effects of age and physiologic variables on right ventricular filling dynamics in normal subjects. *Am J Cardiol* 1999;**84**:440–8.

30 Rossvoll O, Hatle L. Pulmonary venous flow velocities recorded by transthoracic Doppler ultrasound: relation to left ventricular diastolic pressures. *J Am Coll Cardiol* 1993;**21**:1687–96.

31 Appleton C, Galloway J, Gonzalez M, Gaballa M, Basnight M. Estimation of left ventricular filling pressures using two-dimensional and Doppler echocardiography in adult patients with cardiac disease. Additional value of analyzing left atrial size, left atrial ejection fraction and the difference in duration of pulmonary venous and mitral flow velocity at atrial contraction. *J Am Coll Cardiol* 1993;**22**:1972–82.

32 Nagueh S, Kopelen H, Quinones M. Assessment of left ventricular filling pressures by Doppler in the presence of atrial fibrillation. *Circulation* 1996;**94**:2138–45.

33 Nagueh S, Mikati I, Kopelen H, Middleton M, Quinonens M, Zoghbi W. Doppler estimation of left ventricular filling pressure in sinus tachycardia. A new application of tissue Doppler imaging. *Circulation* 1998;**98**:1644–50.

34 Sundereswaran L, Nagueh S, Vardan S, *et al.* Estimation of left and right ventricular filling pressures after heart transplantation by tissue Doppler imaging. *Am J Cardiol* 1998;**82**:352–7.

35 Kelly R, Ting C-T, Yang T-M, *et al.* Effective arterial elastance as index of arterial vascular load in humans. *Circulation* 1992;**86**:513–21.

36 Latham R, Westerhof N, Sipkema P, Rubal B, Reuderink P, Murgo J. Regional wave travel and reflections along the human aorta: a study with six simultaneous micromanometric pressures. *Circulation* 1985;**72**:1257–69.

37 Cholley B, Shroff S, Korcarz C, Lang R. Aortic elastic properties with transesophageal echocardiography with automated border detection: validation according to regional differences between proximal and distal descending thoracic aorta. *J Am Soc Echocardiogr* 1996;**9**:539–48.

38 Sharir T, Marmor A, Ting C-T, *et al.* Validation of a method for noninvasive measurement of central aortic pressure. *Hypertension* 1993;**21**:74–82.

39 Segers P, Carlier S, Pasquet A, *et al.* Individualizing the aorto-radial pressure transfer function: feasibility of a model-based approach. *Am J Physiol Heart Circ Physiol* 2000;**279**:H452–9.

40 Feneley M, Elbeery J, Graynor J, Gall S, Davis J, Rankin J. Ellipsoidal shell substraction model of right ventricular volume. Comparison with regional free wall dimensions as indexes of right ventricular function. *Circ Res* 1990;**67**:1427–36.

41 Denslow S, Wiles HB. Right ventricular volumes revisited: a simple model and simple formula for echocardiographic determination. *J Am Soc Echocardiogr* 1998;**11**:864–73.

42 Kircher B, Himelman R, Schiller N. Right atrial pressure estimation from respiratory behavior of the inferior vena cava. *Circulation* 1988;**78**:II-550.

43 Pinsky M. Cardiovascular effects of ventilatory support and withdrawal. *Anesth Analg* 1994;**79**: 567–76.

44 Pinsky M. Breathing exercise: the cardiovascular response to weaning from mechanical ventilation. *Intensive Care Med* 2000;**26**:1164–6.

45 Kusumoto F, Muhiudeen I, Kuecherer H, Cahalan M, Schiller N. Response of the interatrial septum to transatrial pressure gradients and its potential for predicting pulmonary capillary wedge pressure: an intraoperative study using transesophageal echocardiography in patients during mechanical ventilation. *J Am Coll Cardiol* 1993;**21**:721–8.

46 Tei C, Tanaka H, Kashima T, Kakao S, Tahara M, Kanehisa T. Echocardiographic analysis of interatrial septal motion. *Am J Cardiol* 1979;**44**: 472–8.

47 Matsuzaki M, Tohma Y, Anno Y. Esophageal echocardiographic analysis of atrial dynamics. *Am Heart J* 1985;**109**:355–62.

48 Louie E, Rich S, Levitsky S, Brundage B. Doppler echocardiographic demonstration of the differential effects of right ventricular pressure and volume overload on left ventricular geometry and filling. *J Am Cardiol* 1992;**19**:84–90.

49 Kosturakis D, Goldberg S, Allen H, Loeber C. Doppler echocardiographic prediction of pulmonary arterial hypertension in congenital heart disease. *Am J Cardiol* 1984;**53**:1110–5.

50 Hirschfeld S, Meyer R, Schwartz D, Korfhagen J, Kaplan S. The echocardiographic assessment of pulmonary artery pressure and pulmonary vascular resistance. *Circulation* 1975;**52**:642–50.

51 Riggs T, Hirschfeld S, Borkat G, Knoke J, Liebman J. Assessment of the pulmonary vascular bed by echocardiographic right ventricular systolic time intervals. *Circulation* 1978;**1978**:939–47.

52 Kitabatake A, Inoue M, Assao M, *et al.* Noninvasive evaluation of pulmonary hypertension by a pulsed technique. *Circulation* 1983;**68**:302–9.

53 Yock P, Popp R. Noninvasive estimation of right ventricular systolic pressure by Doppler ultrasound in patients with tricuspid regurgitation. *Circulation* 1984;**70**:657–62.

54 Currie P, Seward J, Chan K-L, *et al.* Continuous wave Doppler determination of right ventricular pressure: a simultaneous Doppler catheterization study in 127 patients. *J Am Coll Cardiol* 1985;**6**:750–6.

55 Abramson S, Burke J, Kelly J, *et al.* Pulmonary hypertension predicts mortality and morbidity in patients with dilated cardiomyopathy. *Ann Intern Med* 1992;**116**:888–95.

56 Gardin J, Sung H-W, Yoganathan A, Ball J, McMillan S, Henry W. Doppler flow velocity mapping in an in vitro model of the normal pulmonary artery. *J Am Coll Cardiol* 1988;**12**: 1366–76.

57 Hatle L, Angelsen B. *Doppler Ultrasound in Cardiology. Physical Principles and Clinical Application.* Philadelphia: Lea & Febiger, 1982, 113–6.

58 Berger M, Haimowitz A, Van Tosh A, Berdoff R, Goldberg E. Quantitative assessment of pulmonary hypertension in patients with tricuspid regurgitation using continuous wave Doppler ultrasound. *J Am Coll Cardiol* 1985;**6**:359–65.

59 Vignon P, Mentec H, Terré S, Gastinne H, Guéret P, Lemaire F. Diagnostic accuracy and therapeutic impact of transthoracic and transesophageal echocardiography in mechanically ventilated patients in the ICU. *Chest* 1994;**106**:1829–34.

60 Zhang S, Kerins DM, Byrd BF III. Doppler echocardiography in cardiac tamponade and constrictive pericarditis. *Echocardiography* 1994; **11**:507–21.

61 Tsang T, Freeman W, Barnes M, Reeder G, Packer D, Seward J. Rescue echocardiographically guided pericardiocentesis for cardiac perforation complicating catheter-based procedures. *J Am Coll Cardiol* 1998;**32**:1345–50.

62 Dardas P, Tsikaderis D, Makrigiannakis K, Saripoulos P, Toumbouras M. Complete left atrial obliteration due to localized tamponade after coronary artery perforation during PTCA. *Cathet Cardiovasc Diagn* 1998;**45**:61–3.

63 Joffe I, Douglas P. Cardiac tamponade in association with an atrial septal defect: echocardiographic Doppler and hemodynamic observations. *J Am Soc Echocardiogr* 1996;**9**: 909–14.

64 Zotz R, Dohmen G, Genth S, Erbel R, Dieterich H, Meyer J. Transthoracic and transesophageal echocardiography to diagnose ventricular septal rupture: importance of right heart infarction. *Coron Artery Dis* 1993;**10**:911–7.

65 Hoeft A, Schorn B, Weyland A, *et al.* Bedside assessment of intravascular volume status in patients undergoing coronary bypass surgery. *Anesthesiology* 1994;**81**:76–86.

66 Coriat P, Vrillon M, Perel A, Baron JF, Le Bret F, Saada M, Viars P. A comparison of systolic blood pressure variations and echocardiographic estimates of end-diastolic left ventricular size in patients after aortic surgery. *Anesth Analg* 1994;**78**: 46–53.

67 Tavernier B, Makhotine O, Lebuffe G, Dupont J, Scherpereel P. Systolic pressure variation as a guide to fluid therapy in patients with sepsis-induced hypotension. *Anesthesiology* 1998;**89**: 1313–21.

68 Bergquist BD, Bellows WH, Leung JM. Transesophageal echocardiography in myocardial revascularisation: II. Influence on intraoperative decision making. *Anesth Analg* 1996;**82**:1139–45.

69 Kraut E, Owings J, Anderson J, Hanowell L, Moore P. Right ventricular volumes overestimate left

ventricular preload in critically ill patients. *J Trauma* 1997;**42**:839–45.

70 Cheung A, Joseph S, Weiss S, Aukburg S, B. JA. Echocardiographic and hemodynamic indexes of left ventricular preload in patients with normal and abnormal ventricular function. *Anesthesiology* 1994;**81**:376–87.

71 Reich D, Konstadt S, Nejat M, Abrams H, Bucek J. Intraoperative transesophageal echocardiography for the detection of cardiac preload changes induced by transfusion and phlebotomy in pediatric patients. *Anesthesiology* 1993;**79**:10–5.

72 Hinder F, Poelaert J, Schmidt C, Hoeft A, Möllhoff T, Loick H, Van Aken H. Assessment of cardiovascular volume status by transoesophageal echocardiography and dye dilution during cardiac surgery. *Eur J Anaesth* 1998;**15**:633–40.

73 Benjamin E, Griffin K, Leibowitz A, *et al.* Goal-directed transesophageal echocardiography performed by Intensivists to assess left ventricular function: comparison with pulmonary artery catheterization. *J Cardiothor Vasc Anesth* 1998;**12**: 10–5.

74 Hoit B, Sahn D, Shabetai R. Doppler-detected paradoxus of mitral and tricuspid valve flows in chronic lung disease. *J Am Coll Cardiol* 1986;**8**: 706–709.

75 Leeman D, Levine M, Come P. Doppler echocardiography in cardiac tamponade: exaggerated respiratory variation in transvalvular blood flow velocity integrals. *J Am Coll Cardiol* 1988;**11**:572–8.

76 Rouine-Rapp K, Ionescu P, Balea M, Foster E, Cahalan M. Detection of intraoperative segmental wall-motion abnormalities by transesophageal echocardiography: the incremental value of additional cross sections in the transverse and longitudinal planes. *Anesth Analg* 1996;**83**: 1141–8.

77 Vieillard Baron A, Schmitt JM, Beauchet A, Augarde R, Prin S, Page B, Jardin F. Early preload adaptation in septic shock? A transesophageal echocardiographic study. *Anesthesiology* 2001;**94**: 400–6.

78 Fujii J, Yazaki Y, Sawada H, Aizawa T, Watanabe H, Kato K. Noninvasive assessment of left and right ventricular filling in myocardial infarction with a two-dimensional Doppler echocardiographic method. *J Am Coll Cardiol* 1985;**5**:1155–60.

79 Poelaert J, Poortmans G, Heerman J, Roosens C. Fistulized mycotic aneurysm of the aortic arch. *J Cardiothor Vasc Anesth* 2002;**16**:207–10.

80 Vieillard-Baron A, Prin S, Chergui K, Dubourg O, Jardin F. Echo-Doppler demonstration of acute cor pulmonale at the bedside in the medical intensive care unit. *Am J Respir Crit Care Med* 2002;**166**: 1310–9.

81 Zehender M, Kasper W, Kauder E. Right ventricular infarction as an independent predictor of prognosis after acute inferior myocardial infarction. *N Engl J Med* 1993;**328**:981–8.

82 Krivec B, Voga G, Zuran I, Skale R, Pareznik R, Podbregar M, Noc M. Diagnosis and treatment of shock due to massive pulmonary embolism. Approach with transesophageal echocardiography and intrapulmonary thrombosis. *Chest* 1997;**112**: 1310–6.

83 Benson MJ, Cahalan MK. Cost-benefit analysis of transesophageal echocardiography in cardiac surgery. *Echocardiography* 1995;**12**:171–83.

84 Fanshawe M, Ellis C, Habib S, Konstadt S, Reich D. A retrospective analysis of the costs and benefits related to alterations in cardiac surgery from routine intraoperative transesophageal echocardiography. *Anesth Analg* 2002;**95**:824–7.

85 Savino JS, Troinaos CA, Aukburg S, Weiss R, Riechek N. Measurement of pulmonary blood flow with transesophageal two-dimensional and Doppler echocardiography. *Anesthesiology* 1991;**75**: 445–51.

86 Muhiudeen IA, Kuecherer HF, Lee E, Cahalan MK, Schiller NB. Intraoperative estimation of cardiac output by transesophageal pulsed Doppler echocardiography. *Anesthesiology* 1991;**74**:9–14.

87 Gorcsan J, Gasior T, Mandarino W, Deneault L, Hattler B, Pinsky M. On-line estimation of changes in left ventricular stroke volume by transesophageal echocardiographic automated border detection in patients undergoing coronary artery bypass grafting. *Am J Cardiol* 1993;**72**:721–7.

88 Izzat MB, Regragui IA, Wilde P, Angelini GD, Bryan AJ. Transesophageal echocardiographic measurements of cardiac output in cardiac surgical patients. *Ann Thorac Surg* 1994;**58**:1486–9.

89 Shimamoto H, Kito H, Kawazoe K, Fujita T, Shimamoto Y. Transoesophageal Doppler echocardiographic measurement of cardiac output by the mitral annulus method. *Br Heart J* 1992;**68**:510–5.

90 Feinberg MS, Hopkins WE, Davila-Roman VG, Barzilai B. Multiplane transesophageal echocardiographic Doppler imaging accurately determines cardiac output measurements in critically ill patients. *Chest* 1995;**107**:769–73.

91 Owen AN, Simon P, Moidl R, *et al.* Measurement of aortic flow velocity during transesophageal echocardiography in the transgastric five-chamber view. *J Am Soc Echocardiogr* 1995;**8**:874–8.

92 Maslow A, Comunale ME, Haering JM, Watkins J. Pulsed wave Doppler measurement of cardiac output from the right ventricular outflow tract. *Anesth Analg* 1996;**83**:466–71.

11 Myocardial ischaemia

Manfred D Seeberger, Karl Skarvan, Michael K Cahalan

Introduction

Complications of coronary artery disease (CAD) are a major source of perioperative morbidity and mortality,[1,2] and myocardial ischaemia is a predictor of perioperative cardiac complications.[3–7] Therefore, detection of perioperative myocardial ischaemia is crucial for identification and appropriate management of surgical patients at high risk for cardiac complications.

Electrocardiography (ECG) is the standard monitoring tool for detection of myocardial ischaemia in the operating room and the intensive care unit. However, ECG changes occur later and with less consistency during myocardial ischaemia than do changes in diastolic and systolic ventricular function (Figure 11.1). Therefore, echocardiographic monitoring of ventricular function improves detection of ischaemia in surgical patients at high risk for coronary disease.[8,9] Such monitoring is highly feasible during surgery by using a transoesophageal probe. This chapter describes practice, and reviews the advantages and limitations of two-dimensional and pulsed wave Doppler transoesophageal echocardiography (TOE) for detection of perioperative myocardial ischaemia. In addition, newer echocardiographic technologies for detecting myocardial ischaemia, such as colour kinesis, ultrasonic tissue characterisation, Doppler tissue imaging and contrast echocardiography, are discussed.

Systolic left ventricular function and myocardial ischaemia

Segmental wall motion analysis

Tennant and Wiggers first described the association of segmental wall motion abnormalities and ischaemia in 1935.[10] Within seconds after ligation of a coronary artery, normal systolic inward motion and wall thickening of the affected myocardial area decreased and progressed to failure of contraction, followed by paradoxical wall motion. The diagnostic value of echocardiography for detecting these ischaemic changes in segmental wall motion was established by Pandian and coworkers[8,9] in a canine model of severe coronary stenosis during acutely raised myocardial oxygen requirements. Subsequently, four studies

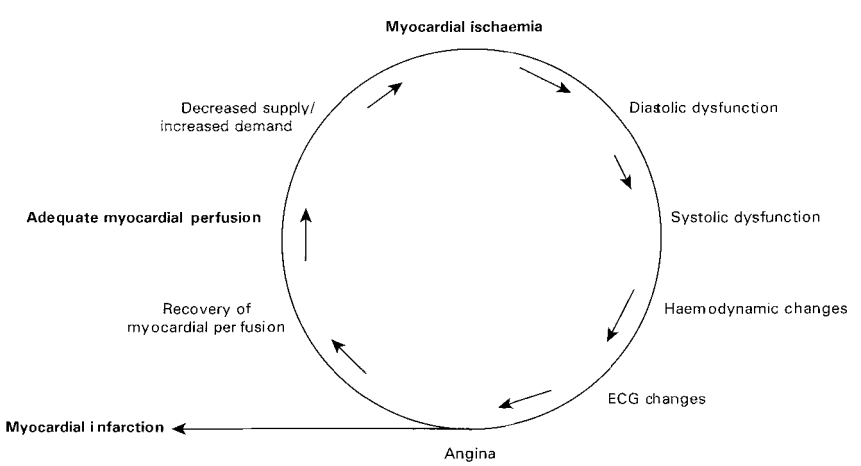

Figure 11.1 Pathophysiological sequence during developing myocardial ischaemia.[66–68] ECG = electrocardiogram.

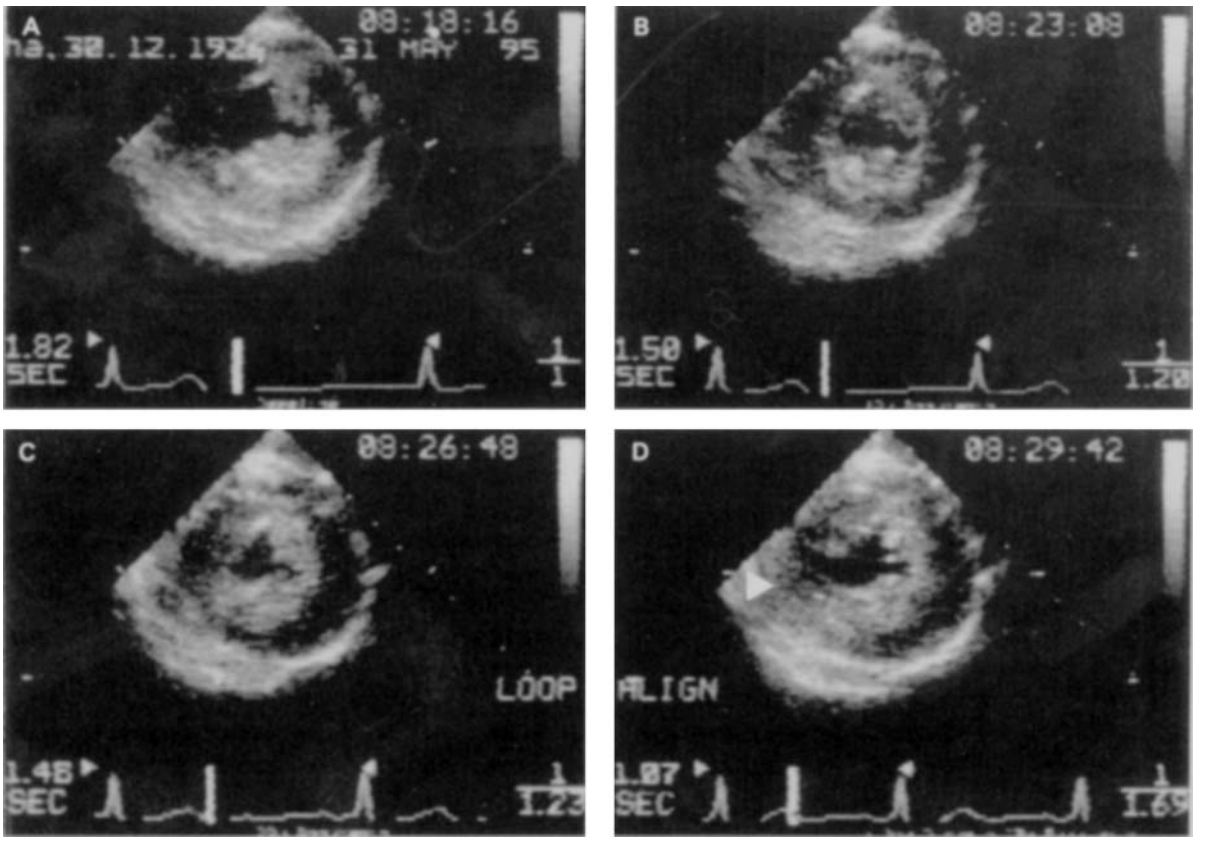

Figure 11.2 Segmental left ventricular contraction during dobutamine stress echocardiography in a patient anaesthetised with isoflurane-fentanyl.[16] Echocardiographic images captured at end-systole in the mid-papillary short-axis cross-section show baseline segmental contraction during general anaesthesia **(A)**, and contraction during gradually increased dobutamine infusion (3 minutes each) at **(B)** 10 μg/kg per min, **(C)** 20 μg/kg per min, and **(D)** 40 μg/kg per min. Segmental contraction improved or remained normal during dobutamine infusion in the inferior wall, the lateral wall, and the anterior wall. By contrast, induced myocardial ischaemia caused akinesia of the septum at 40 μg/kg per min (arrow).

compared TOE and 12-lead ECG with respect to their ability to detect ischaemia during stress testing, and confirmed the existence of CAD independently by arteriography.[11–14] In all four studies, TOE was more sensitive for detecting significant CAD than was 12-lead ECG (mean sensitivity 90% [range 83–93%] versus 52% [range 43–63%]), and in three of the studies TOE was more specific than the ECG (mean specificity 97% [range 93–100%] versus 84% [range 67–100%]).

In two studies of stress testing in anaesthetised patients with severe CAD, the sensitivity of TOE for detecting ischaemia was lower than in the previously discussed studies of awake patients.[15,16] However, TOE sensitivity was still greater than ECG sensitivity in both studies: 75% versus 50% during rapid atrial pacing,[15] and 74% versus 61% during dobutamine stress echocardiography (Figure 11.2).[16] Moreover, the lower sensitivity found in patients during general anaesthesia might be due to the protective effects of anaesthetics[17] and ongoing medication with β-adrenergic antagonists.[18]

Thus, studies conducted during stress testing demonstrate the value of echocardiography for detecting "demand" ischaemia. By using coronary angioplasty as an alternative model of transient ischaemia in awake patients, other studies demonstrated that echocardiography (transthoracic in these studies) is also more sensitive for detecting "supply" ischaemia than multilead ECG.[19,20] Hauser *et al.*[19] found that interruption of coronary blood flow produced new segmental wall motion abnormalities in the distribution of the occluded coronary artery in 86% of the dilations, but did not alter wall motion when highly collateralised areas of myocardium were involved or when there was pre-existing absence of wall motion (i.e. baseline

Table 11.1 Transoesophageal echocardiographic segmental wall motion analysis systems

*Intraoperative scale**	*Radial shortening*†	*Myocardial thickening*‡	*Cardiological scale***
0: No view	–	–	–
1: Normal motion or hyperkinesia	≥30%	+++	1: Normal motion or hyperkinesia
2: Mild hypokinesia	10–30%	++	2: Hypokinesia
3: Severe hypokinesia	>0%, <10%	+	
4: Akinesia	0	0	3: Akinesia
	Systolic lengthening	Systolic thinning	4: Dyskinesia
5: Dyskinesia	Permanent elongation	Thinning	5: Aneurysm

*Scale recommended by the American Society of Echocardiography Council for Intraoperative Echocardiography and the Society of Cardiovascular Anesthesiologists Task Force for Certification in Perioperative Transesophageal Echocardiography.[53] Note: ischaemia is diagnosed if a two-class worsening in segmental wall motion is observed.

† Radial shortening is defined as the decrease in length during systole of an imaginary radius from the endocardium to the centre of the left ventricular cavity. A floating reference system is used.

‡ Myocardial thickening is defined as the increase in distance between the endocardial and epicardial borders during systole.

**Scale recommended in 1989 by the American Society of Echocardiography Committee on Standards, Subcommittee on Quantitation of Two-Dimensional Echocardiograms.[55] Note: ischaemia is diagnosed if a one-class worsening of segmental wall motion is observed.

akinesia). Segmental wall motion abnormalities were apparent approximately 19 ± 8 seconds after coronary artery occlusion and began to resolve within 17 ± 8 seconds (mean ± standard deviation) after reperfusion. In contrast, using seven ECG leads (three limb leads, three augmented leads, and V_5), there were ST-segment changes in only 30% of dilations occurring approximately 30 seconds after coronary artery occlusion. In a subsequent comparison of standard 12-lead ECG and echocardiography during coronary angioplasty, Wohlgelernter and colleagues[20] reported similar findings; segmental wall motion abnormalities became apparent within 12 ± 5 seconds after balloon occlusion in all patients, and full recovery was found within 43 ± 17 seconds after balloon deflation. Again, the onset of ST-segment changes lagged behind the onset of wall motion abnormalities, with evidence of ischaemia on the 12-lead ECG in only 64% of patients after 20 seconds of inflation and in 86% of patients after 60 seconds.

Together, these studies demonstrate that segmental wall motion abnormalities are an earlier and more sensitive indicator of both demand and supply ischaemia than the ECG. Segmental wall motion abnormalities can occur in the absence of surface ECG changes during mild ischaemia, and can precede ECG changes during moderate to severe ischaemia.

The first report on the intraoperative use of TOE for detection of myocardial ischaemia in surgical patients was reported by Smith *et al.*[21] in 1985. That study confirmed the high diagnostic value of echocardiography for detecting ischaemia in anaesthetised patients undergoing coronary artery or major vascular surgery. Monoplane TOE and multilead ECG (three limb leads, three augmented leads, and V_5) studies revealed new segmental wall motion abnormalities diagnostic of myocardial ischaemia (as defined in Table 11.1) in 24 out of 50 study patients during surgery, as compared with ST-segment changes diagnostic of ischaemia (> 0·1 mV deviation) in only six patients. Segmental wall motion abnormalities occurred minutes before ECG changes in three of these six patients, and no ST-segment change was observed before or without new segmental wall motion abnormalities. In addition, all three patients who sustained intraoperative myocardial infarctions developed segmental wall motion abnormalities that persisted until the end of surgery in the corresponding area of myocardium, but only one of them had ischaemic ST-segment changes. Of 10 study patients without coronary disease, none had ST-segment changes or segmental wall motion abnormalities.

Several subsequent studies confirmed these initial results in patients undergoing coronary

artery bypass surgery.[4,22,23] Leung *et al.*[4] used continuous TOE and two-lead Holter recordings, and found major adverse outcomes in six of the 50 study patients (two deaths from cardiac causes, three myocardial infarctions, and one ventricular failure). All patients with an adverse cardiac outcome developed new postbypass wall motion abnormalities that persisted to the conclusion of surgery. Only two of these six patients had new ischaemic ST-segment changes, and three other patients had uninterpretable ST segments because of bundle branch block or ventricular pacing. Patients without new postbypass wall motion abnormalities had uncomplicated courses. The findings of that study illustrate the value of TOE for detection of ischaemia when the ECG is uninterpretable, as is frequently the case in patients undergoing cardiac surgery. Another study, conducted by van Daele *et al.*,[22] similarly found that TOE was a more sensitive method for detection of myocardial ischaemia than was continuous two-lead Holter ECG or standard 12-lead ECG in anaesthetised patients scheduled for coronary artery bypass graft surgery. In the most recent study, Comunale *et al.*[23] again found that TOE monitoring was more sensitive for detecting ischaemia than Holter ECG monitoring, and it was twice as predictive of patients with perioperative myocardial infarction.[23]

By contrast, the high diagnostic value of echocardiography for detecting ischaemia was not confirmed in one study that investigated non-cardiac surgical patients at moderate risk for CAD. By comparing TOE, continuous two-lead Holter ECG, and continuous 12-lead ECG monitoring, Eisenberg *et al.*[24] found that two-lead Holter detected almost twice as many episodes of ischaemia as the 12-lead ECG or TOE. Concordance in the diagnosis of myocardial ischaemia was poor, with only 10% concordance for all three monitors, 16% between TOE and two-lead Holter or 12-lead ECG, and 37% between two-lead Holter and 12-lead ECG. The investigators concluded that routine monitoring for myocardial ischaemia with TOE or 12-lead ECG during non-cardiac surgery has little incremental clinical value in identifying patients at high risk for perioperative ischaemic outcomes, when compared with preoperative clinical data and intraoperative monitoring with two-lead ECG.

The apparently superior sensitivity of two-lead Holter and greater concordance between the two ECG techniques are probably due to differences between the TOE and ECG protocols and the patient populations. For example, the two-lead Holter and 12-lead ECG were monitored continuously whereas TOE was evaluated only intermittently. Second, TOE images were analysed by review of videotape recordings, and not by cine loop analysis. The latter technique is standard for stress echocardiography studies and is now becoming standard in the operating room too. It permits side-by-side viewing of individual cardiac cycles (for example, juxtaposing of baseline and subsequent recordings), to facilitate the diagnosis of changes in segmental wall motion and thickening. Third, only one TOE cross-section, the short-axis cross-section, was monitored, which does not provide an inclusive view of left ventricular wall motion.[25] Thus, TOE evaluation was performed for only a fraction of the time of ECG evaluation, using a relatively insensitive analysis technique and only one cross-section. Additionally, only about half of these patients had proven CAD, which is a critical factor in interpreting the results because decreased prevalence of a disease in a population is invariably linked to an increased risk for false-positive findings. For example, two-lead Holter reveals ST-segment changes that are commonly regarded as diagnostic of ischaemia (horizontal or descending ST-segment depression of at least 0·1 mV) in 7% of healthy young adults and in 26% of healthy young adults given digitalis (as was the case in 13% of the patients in the study just described).[26,27] Therefore, in healthy patients without CAD, two-lead Holter monitoring will reveal more apparent episodes of myocardial ischaemia (false positives) than monitors with greater specificity and equal or even greater sensitivity. TOE monitoring for myocardial ischaemia (similar to Holter monitoring) was concluded to be of value only in patients with proven or high probability of CAD. In addition, several limitations of TOE wall motion analysis must be considered (Table 11.2).

Limitations of TOE wall motion analysis for detection of myocardial ischaemia

Most perioperative TOE studies conducted during the 1980s and early 1990s used just one TOE cross-section – the mid-papillary short-axis cross-section. Although this is the most sensitive single cross-section for detecting ischaemia (because all three major coronaries supply the

Table 11.2 Limitations of transoesophageal echocardiographic wall motion analysis for detection of myocardial ischaemia

Inclusive evaluation of wall motion?	Time requirements for repeated evaluation of multiple cross-sections Imaging of apical wall Reproducibility of identical cross-sections with changed loading conditions
Artefacts	Translation Discoordination Anisotropy Change in cross-section
Segmental wall motion abnormalities not caused by ischaemia	Stunning Tethering Preload Afterload
Reproducibility of wall motion readings	Qualitative, subjective reading system Online analysis versus off-line analysis

myocardium viewed in this cross-section), it fails to detect ischaemia caused by distal stenoses of coronary arteries. Shah *et al.*[28] demonstrated that the addition of the long-axis cross-section to the standard mid-papillary short-axis cross-section increased TOE sensitivity for detection of myocardial ischaemia by over 40%. Rouine-Rapp *et al.*[25] studied nine cross-sections, including the mid-papillary short-axis cross-section, and found that only 17% of all segmental wall motion abnormalities detected by TOE were visible in the mid-papillary short-axis cross-section.[25] Therefore, if multiple TOE cross-sections are used, then TOE is markedly more sensitive for detection of myocardial ischaemia than was initially found by studies in which only the mid-papillary short-axis cross-section was monitored. However, three limitations still must be noted. First, unless additional personnel are available, repeated analysis of wall motion in multiple cross-sections is time consuming and may not always be feasible, given the many other intraoperative tasks of anaesthetists. In fact, one study reported that TOE use increased the anaesthetist's workload and possibly decreased his vigilance.[29] Second, even if multiple cross-sections are studied, imaging of apical segments is frequently not successful with TOE and this fact may result in failure to detect localised apical ischaemia.[25] Finally, assessing exactly the same cross-sections during surgery as those assessed at baseline may be difficult because of surgical retraction near the heart, changes in patient position, or changes in cardiac filling. Assessing exactly the same cross-sections is important because the boundary between segmental wall motion abnormalities, especially old infarctions, and normal myocardium may be just millimetres. Thus, if a slightly different cross-section is used for comparison, then a new segmental wall motion abnormality may be missed or an old injury falsely interpreted as a new episode of ischaemia.

Feasibility of TOE has also been questioned in patients undergoing off-pump coronary artery bypass surgery[30,31] because the vicinity between TOE probe and heart is reduced by pericardial retraction, lap pad placement below the heart, and vertical displacement of the heart. In fact, transgastric views are lost or become distorted in most patients after vertical displacement of the heart. However, in a recently completed study in 60 patients undergoing off-pump coronary revascularisation, we found that TOE remains highly feasible during off-pump revascularisation if echocardiographic monitoring is based on the mid-oesophageal views.[32] Based on the 16 segment model of the left ventricle (see below), the feasibility of TOE was defined by the percentage of readable segments compared with the total number of left ventricular segments. Feasibility of TOE at baseline was 98%. After displacement of the heart, feasibility was 90% each during revascularisation of the left anterior descending and the left circumflex coronary arteries, and 96% during revascularisation of the right coronary artery. These findings indicate that TOE is highly feasible during off-pump coronary surgery and may allow for early detection of ischaemia and other factors that may induce severe haemodynamic instability during displacement of

the heart and positioning of the epicardial stabiliser. Early detection of these factors should help to initiate and guide appropriate therapeutic steps to improve outcome. Moreover, Moises *et al.*[33] previously showed that new segmental wall motion abnormalities persisting at the end of off-pump surgery may predict a complicated postoperative course.

Even when an area of myocardium can be clearly imaged, segmental wall motion can be difficult to evaluate if the entire heart rotates or translates markedly during systole, or if discoordinated contraction occurs because of bundle branch block or ventricular pacing. Therefore, one must first compensate for global motion of the heart (typically by using a "floating" frame of reference) before evaluating segmental wall motion by analysing both segmental endocardial motion and myocardial thickening. Unfortunately, there is still no automated system available that can compensate for rotational and translational movements of the heart, and assess segmental wall motion more reliably and objectively than the human eye.

Discoordinated contraction patterns complicate interpretation of wall motion, especially in the septal segments. As a rule, however, the septum is viable and non-ischaemic if it thickens appreciably during systole, even if its inward motion begins slightly before or after inward motion of the other ventricular segments. Thus, new segmental wall motion abnormalities can be detected even in the presence of bundle branch block, ventricular pacing, and marked global movements of the heart, if both endocardial motion and myocardial thickening are appropriately assessed.

Because of biological differences between normal patients, not all hearts contract normally, and not all parts of the same heart contract to the same degree.[34] Consequently, not all inhomogeneities of contraction are indicative of myocardial ischaemia. For example, previous myocardial infarction or myocarditis can cause segmental wall motion abnormalities in the absence of ischaemia. However, an acute change in regional wall motion and thickening, compared at identical cross-sections, is almost always due to myocardial ischaemia.

One exception to this rule is myocardial stunning, that is, prolonged, postischaemic ventricular dysfunction.[35] When ischaemia has been prolonged, full restoration of blood flow may occur minutes to hours before return of normal segmental contraction. The differentiation between stunning and ischaemic dysfunction is important when a new segmental wall motion abnormality is observed immediately after cardiopulmonary bypass; inadequate revascularisation may require placement of additional grafts, whereas stunned myocardium requires only supportive measures until function returns. However, we do not yet have a diagnostic technique for differentiating between these two aetiologies. Echocardiographic contrast agents can be used to assess myocardial perfusion and have been evaluated in studies for more than a decade, but their clinical usefulness in the perioperative setting has not yet been established.[36–40] Stress echocardiography may be an alternative approach; low dose dobutamine stress echocardiography has been used to differentiate between stunned myocardium and irreversibly damaged myocardium in non-surgical patients,[41–43] but there are no studies on its diagnostic value in anaesthetised patients immediately after cardiopulmonary bypass. Most recently, ultrasonic tissue characterisation has been suggested for identification of viable myocardium,[44] but its value during the perioperative period is unknown. Given the current lack of definitive diagnostic methods, graft status should be re-evaluated (for example, by direct epicardial Doppler flow velocity measurement) and segmental myocardial function closely monitored for signs of improvement when new segmental wall motion abnormalities are detected following cardiopulmonary bypass. If the graft status is questionable, if segmental wall motion further deteriorates, or if the haemodynamic situation is unstable, then additional revascularisation should be provided whenever possible.

Tethering is another commonly cited cause of "artifactual" segmental wall motion abnormalities, and describes non-ischaemic myocardium with impairment of systolic thickening in regions adjacent to ischaemic or infarcted myocardium.[45] Tethering probably accounts for the consistent overestimation of infarct size or severely ischaemic area by up to 1 cm,[46] but it does not mimic new segmental wall motion abnormalities in the absence of acute myocardial ischaemia. Therefore, tethering is not a diagnostic problem, and indeed might facilitate echocardiographic detection of localised ischaemia.

By contrast, marked decreases in preload may induce acute segmental wall motion abnormalities

in the absence of myocardial ischaemia. In a stress study of anaesthetised patients, immediate recovery (within one beat) of severe wall motion abnormalities was observed when rapid atrial pacing was abruptly stopped and preload simultaneously recovered to the pre-pacing baseline.[15] This rapid recovery made myocardial ischaemia an highly unlikely cause for the new wall motion abnormalities, and a subsequent study in fact confirmed that acute decreases in preload can induce new segmental wall motion abnormalities in the absence of ischaemia.[47] This finding challenges the validity of new segmental wall motion abnormalities as markers of myocardial ischaemia during acute hypovolaemia, and it reaffirms the appropriateness of standard clinical priorities; analysis of segmental wall motion should not be performed unless acute hypovolaemia is corrected.

A marked increase in afterload might also produce the appearance of segmental wall motion abnormality, as suggested by Buffington and Coyle,[48] based on findings in a dog model. However, the changes they detected by using piezoelectric crystals were so minimal that they are unlikely to be detected by TOE. In addition, even if detected, they would not fulfil established echocardiographic criteria of ischaemic wall motion abnormalities, that is, marked changes in segmental contraction (as defined in Table 11.1). Nevertheless, marked changes in afterload should be corrected for safety reasons before they provoke myocardial ischaemia.

A more serious limitation of conventional assessment of segmental systolic wall motion is that it relies on subjective qualitative (or semiquantitative at best) visual interpretation (see Table 11.1) rather than quantitative measurements. This limitation applies to offline analysis[49,50] and even more so to real-time analysis in the operating room. In an intraoperative TOE study that compared real-time analysis of segmental wall motion by experienced anaesthetist/echocardiographers with offline analysis of cine loops, the overall sensitivity and specificity for real-time detection of ischaemia were both 76%.[51] Better standardisation of image acquisition and reading criteria, and the use of a more detailed 16 segment model have been proposed for improving inter-reader agreement,[49,50] but will not eliminate all of the limitations of an essentially qualitative analysis. A variety of quantitative techniques has been developed based on repeated manual offline tracing of the myocardial borders, but these time-consuming methods are impractical for routine clinical use and require the subjective definition of endocardial and epicardial borders.[52] One method that allows automated quantification of segmental wall motion in real-time is colour kinesis – a technique based on acoustic quantification.

The 16-segment model

Repeated analysis of regional wall motion and thickening is a highly sensitive and specific method for detecting myocardial ischaemia only if identical segments are being compared. For this purpose, the use of an appropriate model of the left ventricle is necessary. Originally, the transgastric mid-papillary short-axis view divided into four segments was widely applied both in research and in intraoperative monitoring.[21] Although this single view offers quick and valuable information and is often used for continuous monitoring, it has been replaced by a 16 segment model that allows a comprehensive evaluation of regional wall motion of the entire left ventricle.[53] The three mid-oesophageal cross-sections are required for the analysis and are presented in Figure 11.3, together with the transgastric mid-papillary short-axis, and the segmental subdivisions. Most recently, a 17 segment model has been proposed, defining the apical cap beyond the left ventricular cavity as the 17th segment.[54] This model may be advantageous for transthoracic myocardial perfusion studies and for comparison of findings obtained by echocardiography and by nuclear cardiological evaluations. However, imaging of the true left ventricular apex by TOE is frequently difficult, which may limit the usefulness of the 17 segment model in the perioperative setting.

In all visualised segments, the systolic thickening of the left ventricular wall and the direction and extent of the systolic movement of the endocardium are assessed visually, and a score is assigned to each segment according to a grading scale (see Table 11.1). This scale, recommended in the guidelines for intraoperative TOE of the American Society of Echocardiography (ASE) and the Society of Cardiovascular Anesthesiologists (SCA),[53] distinguishes four grades of wall motion abnormality, including mild and severe hypokinesia. This is in contrast to the scale recommended by the ASE Standards Committee and used by cardiologists[55,56] (see footnote at the bottom of Table 11.1). The latter

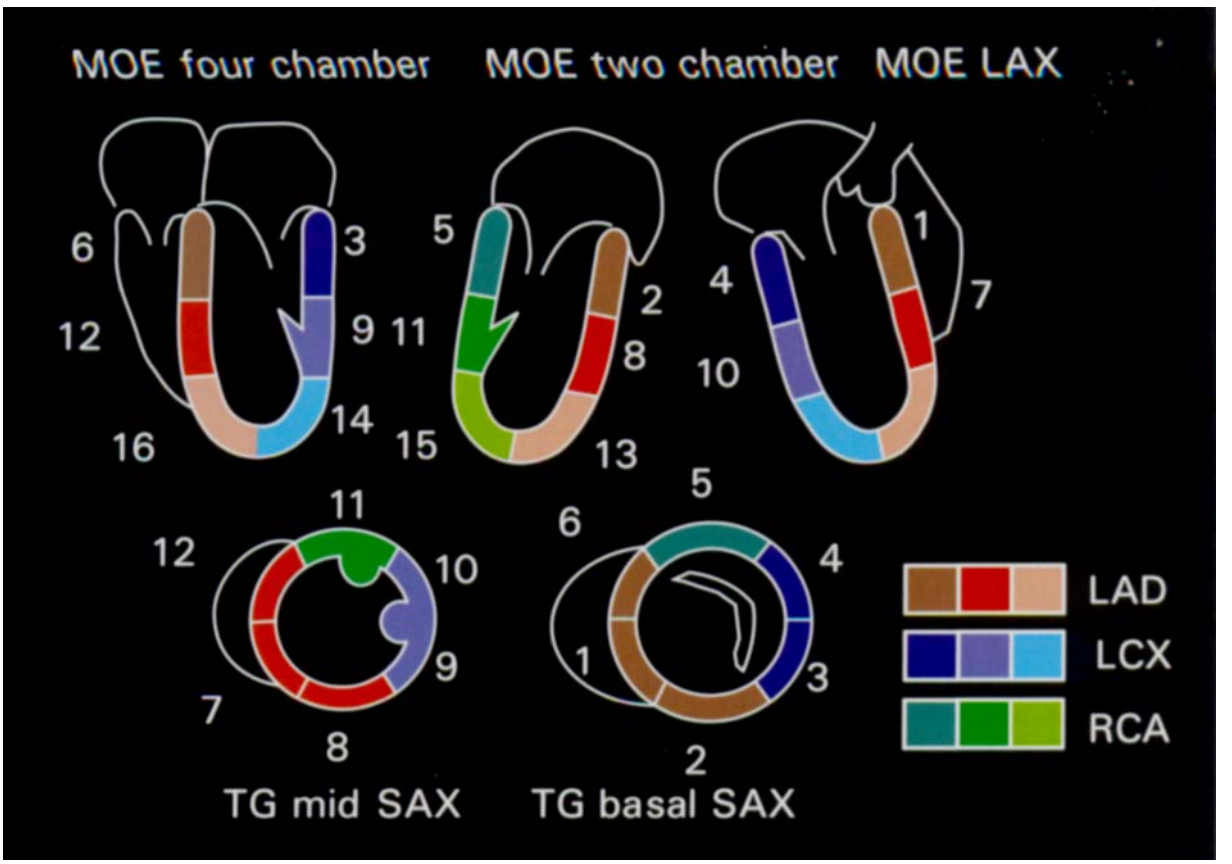

Figure 11.3 The 16 segment model of the left ventricle.[53] This model is now widely used for evaluation of left ventricular regional wall motion and detection of myocardial ischaemia. All segments can be monitored using the three mid-oesophageal (MOE) cross-sections (MOE four chamber, MOE two chamber, and MOE long-axis [MOE LAX] cross-sections). The left ventricular wall is divided into six circumferential parts (anterior, lateral, posterior, inferior, septal, and anteroseptal), as illustrated for the transgastric mid-papillary short-axis view (TG mid SAX), and into three longitudinal levels (basal, mid-papillary, and apical). This division results in six basal (1–6), six mid-papillary (7–12), and four apical (13–16) segments. The model permits easy identification of the culprit coronary artery (left anterior descending coronary artery [LAD], left circumflex coronary artery [LCX], or right coronary artery [RCA]) according to the localisation of the segmental wall motion abnormalities.

scale does not differentiate between mild and severe hypokinesia and includes wall aneurysm as the highest grade. Neither scale rates hyperkinesia that occurs quite often during the perioperative period as a separate grade. However, a normal segment, when compared with a hyperkinetic one, can be erroneously classified as abnormal. Using the ASE/SCA scale, ischaemia is diagnosed when the wall motion worsens by two grades or more, whereas using the ASE scale a worsening of one grade or more would be compatible with ischaemia. One may speculate that the ASE/SCA scale, which has predominantly been used in studies reported by anaesthetists, entails lower sensitivity but better specificity.

Until now, no study comparing the respective virtues of both methods for online intraoperative evaluation of left ventricular wall motion based on the 16 segment model has been published. Offline evaluation of videotaped left ventricular short-axis views using the ASE scale exhibited excellent interobserver and intraobserver agreement,[57] but this may not apply to online evaluation. A study limited to two transgastric views and nine segments and that used the ASE/SCA scale demonstrated that the sensitivity of real-time assessment of ischaemia ranged from

50% to 100%, and specificity from 67% to 82% among five anaesthetists experienced in TOE.[51] In that study, only 79% of akinetic segments were recognised as akinetic or severely hypokinetic in real-time, and there was also a noticeable variability in the differentiation between normal to mild hypokinetic segments and between mild to severe hypokinetic segments. This is not surprising in view of the qualitative ("eyeball") assessment of endocardial motion and myocardial thickening, the limited resolution of the human eye, and the large overlap of myocardial velocities and wall thickening in neighbouring segments with different grades of wall motion abnormality. In fact, the very existence of two different scales points out the imprecise nature of the information they are intended to describe.[58] With regard to the importance of perioperative myocardial ischaemia, and consequently of the correct interpretation of left ventricular wall motion in real time, a high priority should be given to both training and quality control in real-time TOE performance in every institution.

Other echocardiographic indicators of ischaemia related systolic dysfunction

New or increased mitral regurgitation[59,60] and acutely decreased global systolic function, as indicated by area ejection fraction,[61] are other echocardiographic indicators of acute myocardial ischaemia. Area ejection fraction has the advantage that it can be reliably analysed continuously using a semiautomated technique.[62] However, both area ejection fraction and mitral regurgitation are much less specific for acute ischaemia than are new segmental wall motion abnormalities, because both are dependent on multiple factors including mitral valve anatomy, preload, afterload, and contractility.[63–65]

Diastolic left ventricular function and myocardial ischaemia

Although diastolic myocardial relaxation requires a markedly smaller amount of high energy phosphates than does systolic contraction, diastolic dysfunction occurs earlier after onset of ischaemia (see Figure 11.1) and may be present in the absence of systolic dysfunction during mild ischaemia.[66–68] Doppler echocardiography allows detection of ischaemic diastolic dysfunction by analyses of transmitral flow velocities[68–70] and by tissue Doppler imaging (see below).

Physiologically, two waves of transmitral blood flow velocity are detected by Doppler echocardiography. After opening of the mitral valve, the pressure gradient between atrium and ventricle in early diastole results in rapid filling of the ventricle, detected as the early (E) Doppler wave. Under normal conditions the major part of ventricular filling occurs during the early rapid filling period, and peak velocity as well as time velocity integral of the E wave are larger than the corresponding values of the second Doppler wave in late diastole. The late Doppler wave of transmitral flow is caused by the contraction of the atrium, and it is therefore called the A wave. During ischaemia, diastolic function is altered markedly because myocardial relaxation depends on active, energy consuming reuptake of calcium from the cytosol into the sarcoplasmatic reticulum. Reuptake of calcium is mandatory for release of ionised calcium from its binding site on troponin C and for dissociation of actin–myosin cross-bridges. Therefore, impaired myocardial relaxation during ischaemia results in a "stiffer" ventricle, in abnormalities of left ventricular filling, and consequently in changed Doppler waves of transmitral flow.

The most frequently described ischaemia induced change in transmitral Doppler flow is a marked decrease in the ratio between peak E and peak A flow velocities. In a dog study, changed E/A ratio correlated closely with negative dP/dt after occlusion of the left anterior coronary artery.[69] In patients undergoing coronary angioplasty, a marked decrease in the ratio between peak E and peak A flow velocities was found within 15 seconds of coronary artery occlusion, and preceded segmental wall motion abnormalities that required a mean time of 29 seconds after coronary artery occlusion to be detectable by two-dimensional echocardiography.[68] After reperfusion, peak E/A ratio normalised to baseline values within 15 seconds, and segmental wall motion within 21 seconds.

The E/A ratio of peak flow velocities has the advantage of being easily available for online analysis in daily clinical practice. More sophisticated Doppler indicators of myocardial ischaemia include decreases in the ratio of E/A diastolic time velocity integrals,[68] total diastolic time–velocity integral, or E acceleration and deceleration time.[71] However, these indicators require time consuming analyses and are rarely used in acute care settings.

The crucial question is whether Doppler monitoring of diastolic function adds incremental value to monitoring of systolic function alone for the detection of myocardial ischaemia in surgical patients. Such value has been hypothesised based on previous observations and on theoretical considerations, but there is increasing evidence that Doppler monitoring of diastolic transmitral flow is not useful for detecting ischaemia in surgical patients. Kolev *et al.*[72] postulated that a combination of several Doppler parameters of diastolic transmitral flow improved the detection of ischaemic episodes during surgery. However, they did not have an independent "gold standard" to provide convincing evidence for the presence of myocardial ischaemia when it was diagnosed based on the Doppler criteria, and neither did they investigate whether the diagnosed ischaemic episodes were of any prognostic value.

The value of monitoring diastolic transmitral flow by intraoperative Doppler echocardiography was questioned by Wang *et al.*[73] in a study recently published in abstract form. Those investigators studied 24 patients during off-pump revascularisation of the left anterior descending coronary artery (LAD) and used 1 mm or greater ST-segment shifts on a seven lead ECG and/or marked new segmental wall motion abnormalities (worsening more than two grades based on the five grade scale in at least two segments supplied by the LAD) as indicators of ischaemia. Twelve patients fulfilled the predefined criteria for the diagnosis of ischaemia during transient coronary occlusion (ischaemia group) and 12 patients did not (no ischaemia group). Surprisingly, the E/A ratio did not decrease during coronary occlusion in any group, but it increased in the ischaemia group as well as in the no ischaemia group. E deceleration time, another reported indicator of ischaemia in awake patients,[71] also did not change in any group. These preliminary data fundamentally question the value of Doppler monitoring of diastolic transmitral flow for detection of myocardial ischaemia in surgical patients.

Several factors may limit the value of monitoring transmitral flow for detection of ischaemia in surgical patients or may even prevent it from being clinically useful. These confounding factors that may affect transmitral flow by themselves include changes in heart rate,[74] preload,[75] and afterload[76] – changes that frequently occur during major surgery in patients at high cardiac risk. These haemodynamic changes were not similarly present when the value of Doppler monitoring for detection of induced ischaemia was documented during coronary angioplasty.[68] Therefore, changes described as typical of acute ischaemia during coronary angioplasty may be specific for ischaemia in surgical patients as long as haemodynamics are stable. For example, we have occasionally observed these ischaemia related changes in transmitral Doppler flow in haemodynamically stable surgical patients when ischaemic episodes were induced by minimally invasive coronary artery bypass surgery. However, when the haemodynamic situation is not stable, as is frequently the case in surgical patients undergoing major surgery, the diagnostic value of these changes in transmitral Doppler flow is questionable.

Heart rate, preload, and afterload may also be altered by vasoactive drugs, which are frequently needed when patients at high cardiac risk undergo major surgery. In addition, vasoactive drugs may confound Doppler parameters of diastolic transmitral flow because they directly influence diastolic relaxation.[77–79] No published studies have analysed the previously described Doppler indicators of ischaemia in patients treated with vasoactive drugs, but data from dobutamine stress echocardiographic studies question their diagnostic value in this clinical situation also. That is, in awake patients, one study found that Doppler parameters of transmitral flow were more sensitive to ischaemia induced by increasing doses of dobutamine than were new wall motion abnormalities,[71] but a second study failed to confirm a diagnostic value of these Doppler parameters.[80] In anaesthetised patients, two studies failed to find diagnostic value of the published Doppler parameters for detecting ischaemia during dobutamine stress echocardiography.[81,82] Therefore, published Doppler parameters of diastolic transmitral flow are unreliable indicators of ischaemia during high dose dobutamine infusion, and their value in surgical patients treated with positive inotropic drugs at clinical doses remains uncertain.

Newer echocardiographic technologies

Colour kinesis

Real-time evaluation of regional wall motion remains the mainstay of intraoperative detection

for myocardial ischaemia. At the present time wall motion is assessed visually, and at best by comparing control cine loops with the real-time images. The quality of this online assessment depends strongly on the experience of the observer and it exhibits significant interobserver variability. Whereas several automated and computerised methods that can quantify endocardial excursion and wall thickening are impractical for routine use in the operating theatre, the recently introduced colour kinesis is relatively easy to use.

Colour kinesis is based on the method of endocardial border detection by acoustic quantification and provides a colour coded image of timing and magnitude of the systolic endocardial excursion in real time.[83] During standard perioperative two-dimensional imaging, the left ventricular short-axis is best suited to this purpose. After a fixed delay from the R wave of the ECG, the baseline endocardial borders are detected and displayed during the systolic inward movement every 33 ms until 11 "onion skin" rings have been recorded, representing complete systolic motion. The space between the subsequent rings is coded from red–orange over yellow and green to blue and purple–blue, according to the displayed colour bar. The occurrence of the last (11th) purple–blue colour code superimposed on the two-dimensional image would indicate that the systolic inward motion of the endocardium lasted 363 ms. In normal persons, however, the normal contraction is shorter and varies in different regions of the left ventricular wall.[83] The appearance of 9–11 colours with a width of the colour rim in excess of 5 mm corresponds to normal wall motion. The appearance of eight to four colours corresponds to mild hypokinesia, and that of three to one colours corresponds to severe hypokinesia.[84] In the absence of endocardial movement (akinesia) there is no colour coding. In addition, a dyskinetic movement is coded by red colour. The display is updated every beat. The end-systolic colour kinesis image is valuable because it represents the time motion history of the systolic endocardial excursion.

An initial transthoracic echocardiographic study found that colour kinesis provided highly consistent information on segmental wall motion in normal persons and that it detected segmental wall motion abnormalities as accurately as expert readers in a small group of selected patients.[83] A subsequent study demonstrated the feasibility of intraoperative colour kinesis used with TOE in 60 patients with CAD undergoing non-cardiac surgery.[84] A total of 600 left ventricular segments were analysed both by colour kinesis and by expert readers, and colour kinesis correctly detected 60 out of 61 segments with wall motion abnormalities. However, it falsely diagnosed abnormal systolic movement in another 57 segments with normal segmental wall motion. These findings resulted in a positive predictive value of 51% and negative predictive value of 100% for detection of abnormal segmental wall motion. The intertechnique variability between the conventional interpretation of two-dimensional images and colour kinesis was 26%.

Translational and rotational movement of the heart and papillary muscle interference accounted for many of the false-positive diagnoses. Other factors that may limit the value of colour kinesis include insufficient quality of the two-dimensional echocardiographic images and pre-existing abnormal septal wall motion (left bundle branch block, diastolic flattening secondary to right ventricular volume/pressure overload). Another limitation is that colour kinesis solely analyses systolic endocardial movement, whereas both endocardial movement and myocardial thickening are important for evaluation of systolic wall motion.[83] Finally, another study found that interobserver variability for analysing systolic wall motion was only slightly less when colour kinesis software was used compared with conventional two-dimensional analysis,[85] showing that colour kinetic analysis is not purely objective. These limitations question the view that colour kinesis is "a useful aid for the less experienced",[84] and indicate the need for additional studies on its usefulness in clinical practice.

Ultrasonic tissue characterisation

Structural changes in myocardial muscle can be studied by analysing the ultrasound signal backscattered from tissue. Animal studies found characteristic changes in the backscattered ultrasound beam during ischaemia, including a reduction in the physiological cardiac cycle dependent variation in the backscatter power levels and an increase in the time averaged integrated backscatter.[86–89] The degree of these backscatter changes was related to the severity of ischaemia,[90] and recovery of backscatter changes after reperfusion was detectable before

simultaneous segmental wall motion abnormalities normalised.[91]

Human studies found similarly characteristic, reversible changes in the backscattered ultrasound beam during transient ischaemia induced by coronary angioplasty[92] or exercise.[93] In patients undergoing thrombolytic therapy for acute myocardial infarction, ultrasonic tissue characterisation identified areas with persisting wall motion abnormalities but early recovery of cyclic variation of integrated backscatter. Because recovered backscatter characteristics were found only in areas with patent coronary artery shown by subsequent angiography, the authors hypothesised that backscatter evaluations might identify viable myocardium that will recover following coronary artery reperfusion.[94] This hypothesis is supported by a more recent human study comparing backscatter characteristics of left ventricular myocardium and inotropic response to low dose dobutamine infusion in ischaemic segments with dysfunctional wall motion.[44] Resting cyclic variations of integrated backscatter closely paralleled contractile reserve in these patients with chronic ischaemic dysfunction, and this suggests that backscatter tissue characterisation could be a useful method for identification of viable but dysfunctional myocardium.

Sensitivity and specificity of the reported backscatter changes for detection of myocardial ischaemia and the comparative predictive value of these changes have not yet been defined. Also, the technique of ultrasonic tissue characterisation must be better standardised in order to ensure its general reproducibility.[93] In addition, whether findings in non-surgical patients can be applied to surgical patients in the operating theatre and intensive care unit must be studied. These studies should assess the value of ultrasonic tissue characterisation for detection of perioperative ischaemia and for differentiation between dysfunctional but viable myocardium and irreversibly damaged myocardium, for instance, immediately after cardiopulmonary bypass in patients undergoing cardiac surgery.

Tissue Doppler imaging

The physical principles of tissue Doppler imaging (TDI) are described in Chapter 1 (see Figures 1.18–1.20). This section focuses on the use of TDI for quantification of regional ventricular function and detection of myocardial ischaemia.

In experimental studies the changes in myocardial contractility provoked by ischaemia can be precisely measured by microsonometry. In clinical echocardiography, however, one must still rely on visual assessment of wall motion, which is highly observer dependent. TDI is a novel promising technique that allows quantification of wall motion and may assist or even replace the "naked eye" in intraoperative monitoring of myocardial ischaemia.

At present the following modalities of myocardial TDI are being developed:

- spectral pulsed wave tissue Doppler
- colour tissue Doppler
- strain rate and strain imaging
- tissue tracking.

Principles of tissue Doppler imaging

Spectral pulsed wave tissue Doppler imaging

Spectral pulsed wave TDI measures the instantaneous velocities of the myocardium throughout the cardiac cycle, with excellent temporal resolution. The main velocity waves are isovolumic contraction velocity, early and late systolic waves (S1 and S2), and early and late diastolic waves (Figure 11.4). The peak and mean velocities can be readily measured online; the systolic velocity time interval provides the wall thickening or displacement. In addition, time intervals such as isovolumic contraction and relaxation periods, and time to peak velocity can also be measured, and postsystolic shortening, if present, can be detected. Optimal alignment of the ultrasound beam with the moving myocardium is a prerequisite for accurate measurements. Even then, one must recognise that the measured axial velocity (radial, longitudinal, or circumferential) is influenced to a varying degree by other velocities and represents a spatial summation of all of them. Velocities other from axial velocity can be caused by translation and rotation (twist) of the entire heart and, in the case of abnormal wall motion, by the tethering action of adjacent myocardial fibres. A practical method for reducing the effects of overall heart motion is the measurement of mitral annular velocities. During systole, the base of the ventricle descends toward the stationary apex whereas during diastole it moves back. The annular velocities are related to the sum of longitudinal displacement produced by all myocardial fibres contracting between the base and the apex. The

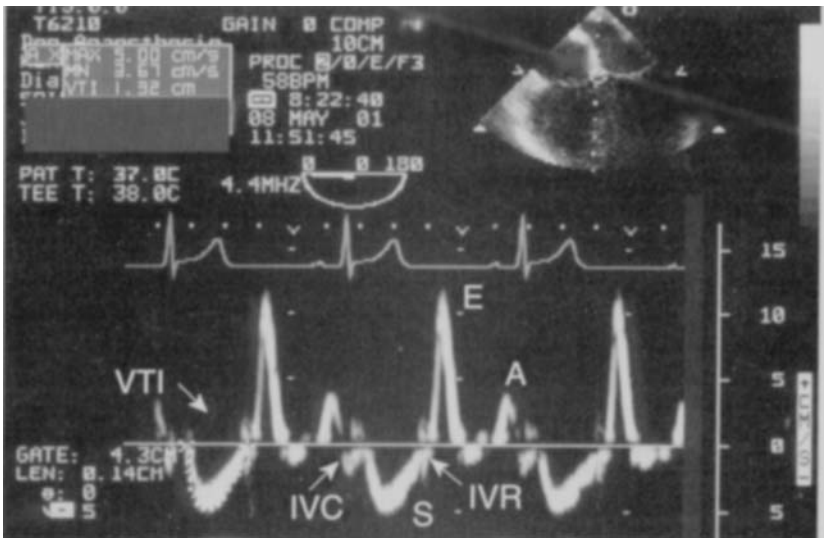

Figure 11.4 *Pulsed wave tissue* Doppler recording of mitral annulus velocities in a patient with coronary artery disease. The sampling volume is placed at the junction of the annulus and the interventricular septum, in the mid-oesophageal four chamber view. Velocities of isovolumic contraction (IVC), systolic shortening (S), isovolumic relaxation (IVR), early (E) and late (A) diastolic filling were recorded. Planimetry of the ejection phase of the velocity profile (first beat) gives a peak and mean velocity of 5·0 cm/s and 3·7 cm/s, respectively, and a velocity time integral of 1·32 cm. The *latter value equals the displacement of* the septal annulus. The early diastolic velocity is distinctly greater than the late diastolic velocity. All of these measurements are within the range of normal values.

measurement of velocities at different sites of the annulus provides information on regional systolic and diastolic function in the corresponding ventricular wall. Mitral annular systolic descent velocity varies between 9·5 ± 1·5 cm/s (anteroseptal wall) and 11·9 ± 2·5 cm/s (lateral wall) according to the recording site at the annulus. The early diastolic velocity (E) is also lower in the septum (12·9 ± 3·1 cm/s) than in the lateral annulus (16·5 ± 4·0 cm/s) or other sites.[95,96]

Colour tissue Doppler

Similar to colour Doppler mapping of blood flow, colour TDI processes the frequency shifts arriving from the moving myocardium and encodes computed velocities into colours (Figure 11.5). The colour coded myocardial map is superimposed on either an M-mode or a two-dimensional image. The myocardium moving toward the transducer is coded red, whereas that moving away from the transducer is coded blue. The colour becomes brighter with increasing velocity, and the maximum brightness corresponds to the upper limit of the measurable velocity range. However, such colour maps are of only limited utility in practice. Fortunately, by means of dedicated software, the colour coded information can be converted into velocity values and velocity profiles can be displayed from any site of interest within the ventricular wall.[97,98]

The mean velocity is the average of myocardial velocities along each M-mode scan line through the full thickness of the ventricular wall, and peak mean velocity is the maximum value of the mean velocity during a particular phase of the cardiac cycle.[99,100] The reported interobserver variability in offline measurements of longitudinal peak systolic velocity in the basal and mid-ventricular segments is 9–24% at rest and 11–28% during maximal dobutamine stress.[101] With the goal of eliminating errors related to the translational motion of the heart, the measurement of myocardial velocity gradient (MVG) was introduced. It is defined as the difference in myocardial velocity between the endocardium and epicardium divided by myocardial wall thickness:

$$MVG = (V_{endo} - V_{epi})/(L \times \cos \theta)$$

where L equals wall thickness and θ Doppler angle of incidence.[102] MVG is calculated as the slope of a regression line obtained by plotting the transmural velocities against the distance between epicardium and endocardium. Because the translational motion equally affects subendocardium and subepicardium, its effect on the local velocities is eliminated.

Peak velocity gradient is the maximum value of the velocity gradient over the duration of a particular phase of the cardiac cycle, and it reflects the peak velocity of radial thickening. Velocity gradients are expressed as positive when the endocardium is moving faster than the epicardium, and as negative when the epicardium is moving faster. The gradient is 0 when there is no difference in endocardial and epicardial

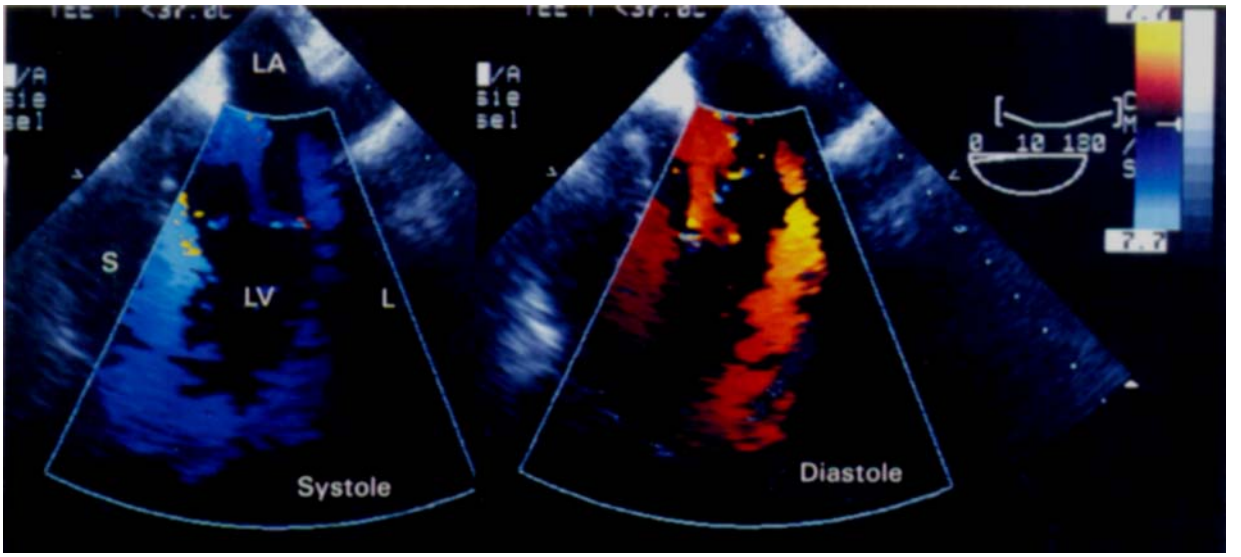

Figure 11.5 Myocardial colour tissue Doppler imaging of the left ventricle (LV) in mid-oesophageal four chamber view. A colour coded velocity map is superimposed on the two-dimensional image. During systole, the shortening of longitudinal fibres results in a motion that is directed toward the apex, away from the transducer, and is therefore coded blue. During diastole the myocardium moves back toward the base of the LV and is coded red. The greater the velocity, the brighter the colour. The encoded velocity information can be extracted from any site of interest and displayed as a time–velocity waveform.

velocities. The velocity gradients are useful for quantifying radial thickening and thinning in stress echocardiography.[103]

Strain rate and strain imaging

In the beating heart, the myocardium undergoes cyclic deformation. The extent of this deformation can be expressed as strain. The local rate of deformation or strain of the myocardium is called strain rate (SR). SR is defined as a difference in velocities measured at two sites (V1 and V2) within the myocardium, divided by the distance L (usually 8–10 mm) between the measuring points: $SR = (V1 - V2)/L$, or $SR = dV/dL$ (unit/s). The SR profile resembles the velocity curve from which it is derived and shows systolic and early and late diastolic peaks (Figure 11.6). SR applied to measurement of radial deformation (systolic thickening and diastolic thinning) corresponds to MVG and is, like the latter, independent of extrinsic motion. In the longitudinal direction, SR reflects the rate of systolic shortening and diastolic lengthening. By convention, positive SR represents radial thickening or longitudinal lengthening, whereas negative strain represents radial thinning or longitudinal shortening of the myocardium.[104] SR can be calculated online and displayed in real-time as a colour coded SR map superimposed on M-mode or two-dimensional images.[105] Apart from its role as a measure of regional function, SR is used to calculate myocardial strain.

In physiological terms, strain is tissue deformation as a function of applied force or stress. In physical terms, there are two types of strain (ε): Lagrangian strain, in which the deformation is expressed relative to a constant unstressed initial length ($\varepsilon = [l_0 - l]/l_0$); and natural strain, in which the deformation is calculated locally as a time integral of the SR

$$\text{Strain } \varepsilon = \int_{t0}^{t} \text{SR}dt$$

and is expressed as a percentage. Natural ε values are smaller than Lagrangian strain values. Natural ε is independent of the unstressed length; it is less sensitive to the exact timing of the systolic interval and is therefore used in current systems.[106] Within the ventricular wall, ε can be determined in a radial, longitudinal, or circumferential direction. In longitudinal views and in accordance with the orientation of SR, positive ε represents diastolic lengthening and negative ε represents systolic shortening of the examined myocardium. The difference between regional end-systolic and end-diastolic ε corresponds to regional wall thickening obtained by M-mode echocardiography. SR is relatively independent of heart rate and closely follows

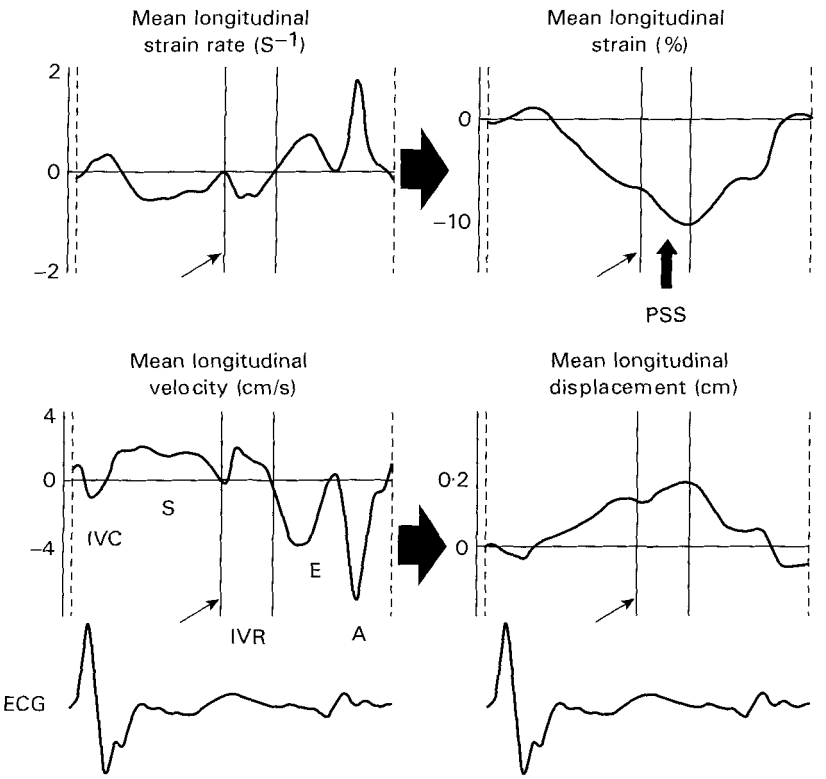

Figure 11.6 Profiles of longitudinal strain rate, strain, mean velocity, and mean displacement derived from infarcted mid-septal segment by postprocessing of myocardial colour Doppler data. The individual phases of the profiles are as follows: isovolumic contraction (IVC), systolic shortening (S), isovolumic relaxation (IVR), and early (E) and late (A) diastolic filling. Small arrows indicate end-systole. Large arrows indicate that strain and displacement were obtained by integration of strain rate and velocity, respectively. All four tissue Doppler imaging indexes of systolic septal function are abnormally low, and there is a significant amount of postsystolic shortening (PSS) during IVR. *ECG = electrocardiogram.* (*Reproduced from* Jamal *et al.* 2002,[125] by permission of the American Society of Echocardiography.)

changes in inotropy, correlating significantly with left ventricular + dp/dt. In contrast, ε, which reflects the amount of local deformation without taking into account the time factor, correlates better with left ventricular ejection fraction and stroke volume.[104,107]

Tissue tracking

This is a promising new ultrasound technique for evaluating regional wall motion. It is also based on colour TDI and provides information on longitudinal myocardial velocities and regional myocardial displacement. The colour Doppler myocardial images are superimposed on two-dimensional images. During systole endocardial inward motion is shown, whereas during diastole the colour coded integrals of the systolic velocity–time curves in the different regions are shown. The motion distances (regional displacement) in the different regions can be read from the simultaneously displayed colour scale.[108] The advantage of this technique is that it provides quantitative information on regional wall motion in real-time without the need for any time consuming offline processing. There are also potential disadvantages that may limit its applicability in the setting of cardiac surgery. It may not be feasible in patients with conduction abnormalities and ventricular dyssynchrony. It is also not suitable for detecting and quantifying postsystolic shortening. In comparison with myocardial SR imaging, the tissue tracking appears to be more affected by translational and rotational motions of the whole heart.

Clinical applications of tissue Doppler imaging

Normal findings

Radial velocities, SR, and ε can be recorded in transthoracic short-axis and parasternal long-axis views (anterior, inferior, septal, and posterior walls) and in transoesophageal transgastric short-axis, two chamber, and long-axis views. Longitudinal variables are recorded using the transthoracic or the transoesophageal approach in four chamber, two chamber, and long-axis views (anterior, inferior, and posterior wall, and

septum). Thus, in theory, all segments of the standard 16 segment model are accessible to TDI. In practice, however, measurement in apical segments is often not feasible. By extracting the velocities from varying depths of the left ventricular wall, different myocardial fibres are interrogated; the circumferential fibres are located in the mid-wall whereas the longitudinal fibres make up the subendocardial and subepicardial layers. The velocities of radial thickening are significantly greater than the velocities of longitudinal shortening. In the normal myocardium, shortening of the longitudinal fibres predominates during early systole, whereas the circumferential fibres predominate over the longitudinal fibres during ejection.[109] Subendocardial fibres are known to be particularly sensitive to ischaemia, emphasising the utility of longitudinal TDI. Transthoracic TDI studies describe physiological heterogeneity of myocardial velocities in the left ventricle; the systolic velocities decrease from the base toward the apex, and this basal–apical gradient is more pronounced in the septum and in the anterior wall. The systolic velocities in the inferior and posterior walls are greater than in the septum and the anterior wall. The greatest early diastolic velocity is consistently found in the lateral wall.[110,111] Finally, the subendocardium moves faster than the subepicardium, creating a transmural velocity gradient described above.

Myocardial ischaemia

Experimental studies

The value of TDI in myocardial ischaemia was investigated in a standard model of coronary artery occlusion. In open chest pigs, myocardial velocities were measured in the interventricular septum during graded reductions in blood flow in the LAD and compared with the changes in regional function measured by ultrasonic crystals.[112] During coronary artery occlusion, the systolic velocities abruptly fell and became negative, corresponding to the paradoxical outward motion revealed by sonomicrometry. At the same time, the velocities during isovolumic contraction and relaxation increased. Furthermore, the velocity during rapid early filling decreased whereas the late filling velocity increased, resulting in a reduction in the ratio of early to late filling velocities. In addition, the inner–outer myocardial velocity gradient disappeared. The changes in systolic velocity during ischaemia and reperfusion correlated closely with the changes in systolic shortening obtained by microsonometry and with the percentage decrease in regional myocardial blood flow measured by radioactive microspheres.[112] A brief (20 second) occlusion of a coronary artery in a closed chest animal model causes a marked fall in systolic velocity, displacement, SR, and ε in the territory of this artery. Analysis of the systolic SR and ε changes reveals a delayed onset and marked reduction in thickening, end-systolic thinning, and postsystolic thickening of the ischaemic myocardium.[113] In addition, there are decreases in velocity, SR and ε, and the time to their respective peaks is delayed. Marked changes also occur during dobutamine challenge in an animal model with subtotal coronary stenosis and absent coronary flow reserve; postsystolic shortening increases significantly whereas ε tends to decrease.[113] Reperfusion following severe ischaemia is associated with preferential recovery of myocardial velocity in the subepicardium, resulting in a persistent reduction in SR. Reperfusion after ischaemia and non-transmural infarction results in complete recovery of reduced SR, which is not the case after transmural infarction.[114] Simultaneous contrast (perfusion) echocardiography and TDI may allow for the distinction between persisting ischaemia or necrosis and stunning after reperfusion.[115]

Clinical findings at rest

Systolic tissue velocities, SR, and ε decrease in hypokinetic and akinetic segments compared with normokinetic segments of the same ventricle or with corresponding areas in healthy controls. Such decreases in TDI values are found both in akinetic and hypokinetic segments and even in normokinetic segments of the left ventricle with segmental wall motion abnormalities.[105,116–118] However, the clinical applicability of these changes for diagnosing either the presence or the degree of wall motion abnormality is limited because of the considerable overlap of the velocity values. For instance, neither SR nor ε can distinguish normokinetic from hypokinetic segments of the same left ventricle.[105] Dyskinetic segments, however, exhibit inverted velocities and can easily be recognised.[105,116]

Positive inotropic stimulation (stress tests)

In normal human myocardium, dobutamine or exercise stress induces an overall increase in myocardial velocities and SR.[107] The physiological base–apex gradient is preserved at any stage of stress. The ε shows a biphasic behaviour: an early increase, followed by a plateau at high levels of stress, possibly related to shortened filling time and reduced stroke volume. Myocardial ischaemia during dobutamine challenge is detected as a markedly blunted increment in systolic shortening velocity, SR, or strain. The peak systolic velocities in the segments that respond to dobutamine by a worsening in wall motion are significantly lower than in normal segments.[119,120] In addition, the early diastolic velocity, which increases in normal segments during dobutamine stress test, decreases in ischaemic segments.[121] TDI is more sensitive to dobutamine increments than is standard two-dimensional imaging. The dobutamine stress test complemented by TDI distinguishes viable from non-viable segments.[116] Viable segments exhibit either a sustained improvement (increase in systolic velocity), worsening (decrease in velocity), or a biphasic response (increase followed by decrease in velocity) during dobutamine infusion, whereas non-viable myocardium shows no change in velocity.[122]

Percutaneous transluminal coronary angioplasty

Occlusion of the LAD during balloon angioplasty causes a marked reduction in early and late systolic velocities.[123] A reversal of the velocity direction indicating paradoxical motion and postsystolic shortening occurs in a significant proportion of patients. The velocities of remote myocardium increase or decrease depending on the patency of the supplying artery. During successful reperfusion, the velocities exceed baseline values.[124] In contrast to SR and ε, which are able to detect ischaemia in normal as well as in abnormal segments, velocity measurements may fail to detect ischaemic changes in segments with abnormal wall motion at baseline.[118]

Acute myocardial infarction

The effects of experimental coronary occlusion are reproduced by acute myocardial infarction in patients. SR and ε analyses revealed the following abnormalities in infarcted segments: early systolic isovolumic shortening is replaced by lengthening; onset of systolic shortening is delayed and its extent reduced; myocardial lengthening during isovolumic relaxation is replaced by postsystolic shortening; and there is a decrease in early diastolic filling.[125] Although the peak velocities failed to differentiate hypokinetic and akinetic from normal segments in the acutely infarcted ventricle, this differentiation was possible with SR and ε.

Intraoperative TDI

Recently, TDI data obtained in patients undergoing aortocoronary bypass surgery were reported. With few exceptions, the myocardial velocities obtained by intraoperative TOE are comparable to velocities obtained preoperatively by transthoracic imaging.[126,127] The proportion of successful TDI analyses obtained with either transthoracic echocardiography or TOE is similar and ranges between 50% and 86% of all possible basal and mid-ventricular segments, but it is lower in the apical segments.[126] Interobserver coefficients of variation of repeated measurements by TOE varies between 4·4% and 8·5% (velocities), 12·7–22·5% (displacements), 10·7–28·2% (strain), and 11·8–15·9% (SR). The TOE and transthoracic echocardiography interobserver variabilities appear to be comparable.[126] In the transgastric short-axis, velocity, displacement, ε, and SR of the anterior wall are $4{\cdot}0 \pm 1{\cdot}4$ cm/s, $7{\cdot}2 \pm 2{\cdot}8$ mm, $0{\cdot}36 \pm 0{\cdot}10$%, and $1{\cdot}58 \pm 0{\cdot}63$/s, respectively. In the septum, a longitudinal velocity gradient was recorded with basal, mid-ventricular, and apical velocity of $3{\cdot}6 \pm 0{\cdot}7$ cm/s, $2{\cdot}8 \pm 0{\cdot}8$ cm/s, and $2{\cdot}1 \pm 0{\cdot}5$ cm/s, respectively. The longitudinal displacement is also greater at the base ($6{\cdot}1 \pm 1{\cdot}3$ mm) and decreases at the apical level to $1{\cdot}5 \pm 1{\cdot}1$ mm.[126] A similar basal–apical velocity and displacement gradient is found in the inferior wall, whereas ε and SR do not exhibit any longitudinal variation.

In a TDI study of myocardial ischaemia induced by occlusion of the LAD during off-pump revascularisation surgery, a marked change in peak systolic strain was found in mid-septum and apical septum (from $-13{\cdot}7 \pm 5{\cdot}7$% to $2{\cdot}2 \pm 13{\cdot}4$% and from $-9{\cdot}8 \pm 11{\cdot}9$% to $11{\cdot}0 \pm 8{\cdot}0$%, respectively). The change from negative to positive systolic strain reflects a paradoxical lengthening of the ischaemic septal segments during systole and occurred in all but one patient.[128] In a comparison between TDI and standard visual wall motion assessment before and after off-pump cardiac surgery, regional wall

motion scoring failed to detect a change that was evidenced by velocity, SR, and ε measurements in 50% of the segments.[129] Immediately after on-pump aortocoronary bypass surgery, an overall trend toward greater myocardial velocities was found; this increase was significant in mid-posterior and mid-anteroseptal short-axis segments (+ 33–42%) as well as in longitudinal basal lateral and basal anterior segments (+ 25–32%).[127] Such findings appear to be related to the effect of endogenous and exogenous catecholamines, and confirm a successful revascularisation.

The operating theatre environment can give rise to electrical interference and artefacts, and these occasionally prevent performance of TDI. Because SR data are derived from the velocity gradient, they are more susceptible to artefacts than ε, which is obtained by integration of the SR and is therefore less affected. Neither sternotomy nor pericardiotomy affects the TDI variables, except for basal and mid-septum where a reduced displacement was recorded following an opening of the pericardium.[126]

Although the initial experience with TDI in the setting of cardiac surgery seems promising, additional research is needed to determine the true value of TDI for monitoring myocardial ischaemia during anaesthesia and in the intensive care unit. Correctly applied TDI can already provide useful information and assist anaesthetists in their visual assessment of regional left ventricular function.

Contrast echocardiography

A rapid central venous injection of manually agitated saline for detection of intracardiac shunts or abnormal venous connections is a well known example of contrast echocardiography in its simple form. The method is based on the delivery of ultrasound scattering particles into cardiac cavities or the myocardium. These particles must have acoustic impedance that clearly differs from that of blood or myocardium if they are to act as strong ultrasound reflectors. The intensity of the backscatter is proportional to the sixth power of the particle radius, but the size of the particles must permit their safe passage through pulmonary and systemic capillaries. That means that their size must be less than 5 μm. The resonant frequency of such small bubbles is 1·5–7·0 MHz. The prerequisite for clinical utility of contrast agents, apart from non-toxicity and lack of haemodynamic alterations, is sufficient persistence in the bloodstream. In the first generation of contrast agents, air microbubbles were encapsulated by albumin (Albunex®) or by adherence to microparticles (Levovist®; air-filled galactose/palmitic acid shell). The replacement of air by low solubility gas (for example, fluorocarbon) is characteristic of the second generation of contrast agents (Optison®, pentafluoropeptan filled albumin; and SonoVue™, sulphur hexafluoride in a phospholipidic shell). The composition of the shell has an important influence on the acoustic properties of the microbubbles, and the poor solubility of the gases is responsible for the slow diffusion out of the bubbles and, therefore, for prolonged contrast effect. EchoGen® differs from the agents mentioned above because it exists in the circulation as free dodecafluoropentane microbubbles.[130,131]

In parallel with the development of new contrast agents, remarkable progress has been made in the field of imaging technology. Harmonic imaging makes use of the property of microbubbles to oscillate in response to ultrasound waves and to remit sound waves at multiples of the insonating (fundamental) frequency. The reception and processing of ultrasound waves at twice the fundamental frequency (the so-called second harmonic) have a more favourable signal to noise ratio and a better acoustic contrast between the agent and the surrounding structures. Subharmonic imaging operates at a receiving frequency that is one half the fundamental frequency, and the ultraharmonic imaging at a frequency that is one and a half the fundamental frequency.[132]

Microbubbles are sensitive to pressure, because even an increase in pressure during injection can decrease their size and contrast effect. Therefore, as expected, ultrasound waves destroy microbubbles by their acoustic pressure. The effect that ultrasound waves have on microbubbles depends on their energy. With increasing power, the ultrasound waves induce linear oscillation, then non-linear oscillation, and finally destruction of the microbubbles. It is the non-linear oscillation that is responsible for the generation of harmonics, and thus it forms the basis of harmonic contrast imaging. The intensity of ultrasound power is expressed as the mechanical index, which is defined as the peak

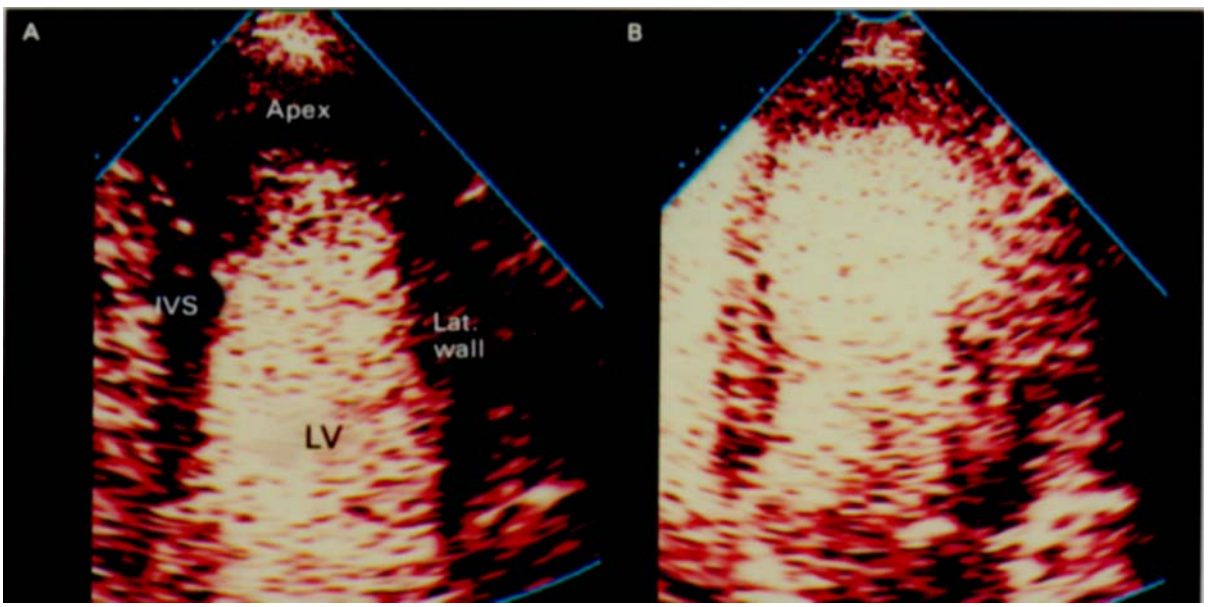

Figure 11.7 Myocardial contrast perfusion echocardiography. **(A)** Image of the left ventricle after peripheral venous bolus injection of ultrasound contrast agent (Optison® 0·3 ml followed by 10 ml saline) shows opacification of the left ventricular cavity. This allows assessment of wall motion and global systolic function, even in patients with poor image quality and/or dropouts of the endocardial borders. **(B)** After the injection, as the contrast agent passes through myocardial capillaries, the myocardium also becomes opacified. The intensity of the ultrasound reflected from the myocardium depends on the amount of microbubbles present in the microcirculation, and consequently on myocardial blood volume and perfusion. The changes in contrast density with time (wash-in and wash-out) are related to myocardial blood flow velocity and can be measured by video densitometry in selected regions of interest. IVS = interventricular septum, Lat. wall = lateral wall, LV = left ventricle. (Image courtesy of Dr. Michel Zuber, Kantonsspital Lucerne, Switzerland.)

rarefactional (negative) pressure in the scanned medium divided by the square root of the ultrasound frequency. The capacity of ultrasound to disrupt microbubbles increases with peak negative pressure and decreases with frequency. Consequently, a low mechanical index (for example, 0·1–0·5) protects the microbubbles, whereas a high mechanical index (for example, 1·5) destroys them.[132]

Conventional contrast echocardiography uses agitated saline as the contrast medium. Because the air bubbles in the air–saline mixture are too large to traverse the pulmonary circulation, this technique is mostly used for detection of intracardiac shunts (for example, patent foramen ovale), for identification of abnormal structures (persistent left superior vena cava), and for enhancement of weak Doppler signals (tricuspid or pulmonary regurgitation). Administration of crystalloid cardioplegia into the aortic root also produces a weak contrast enhancement that is dependent on its distribution in the left ventricular myocardium. This allows the surgeon to identify myocardial segments that are at the greatest risk for intraoperative injury and to adjust the surgical plan accordingly.[37] With the present technology of harmonic imaging and with the second generation contrast agents, it is possible to obtain excellent opacification of the left heart after an intravenous injection of contrast agent (Figure 11.7A). This is particularly useful in cases where image quality is poor and in stress echocardiography, where it improves detection of regional wall motion abnormalities.

The ultimate goal of contrast echocardiography has always been the non-invasive assessment of myocardial perfusion. In the past, contrast agents had to be injected into aortic root, coronary arteries,

or aortocoronary venous grafts, and accordingly studies have been limited to catheterisation laboratories and operating theatres. Recent advances in imaging technology permit imaging the contrast microbubbles during their passage through the myocardial capillary bed even after an intravenous injection of the microbubbles (myocardial contrast perfusion imaging). One of these novel techniques is intermittent power Doppler imaging. The images are not acquired continuously but at adjustable intervals (1–8 beats) and with use of high power (high mechanical index). During the recording of one frame, the microbubbles present within the myocardial capillaries are destroyed. Normally, the microbubbles reappear in the myocardium before the next imaging cycle. The time (or number of cardiac cycles) to full replenishment of the myocardial capillaries roughly correlates with myocardial blood flow.[133]

Pulse inversion and power modulation are techniques that produce a cancellation of echoes returning from the cardiac tissues and enhance the harmonics reflected by the microbubbles. This allows a separation of contrast echoes from the tissue echoes and imaging at very low mechanical index, which protects the microbubbles from destruction. The contrast can be administered by intravenous infusion and the myocardial perfusion imaged in real-time, both at rest and during pharmacological stress (Figure 11.7B). The existing relationship between microbubble concentration in the myocardium and the myocardial blood volume and flow on the one hand, and the video intensity on the other is the basis for quantification of myocardial perfusion by video densitometry.[133]

The applications of myocardial contrast echocardiography in patients with acute and chronic CAD are numerous and will expand rapidly when a reliable non-invasive transpulmonary imaging technique is developed.[130,131,134] Intraoperative contrast echocardiography has been used to evaluate the success of bypass graft surgery.[135,136] Contrast echocardiography may also be helpful in assessment of the area at risk, localisation and size of myocardial infarction, collateral circulation, microvascular perfusion pattern, coronary flow reserve, myocardial viability, and evaluating the success of interventional or surgical revascularisation. Contrast defects found immediately after thrombolytic therapy of acute myocardial infarction may represent an indication for rescue angioplasty. Despite successful reopening of the affected vessel, an absent or heterogeneous microvascular perfusion (no or low reflow phenomenon) can be demonstrated by contrast echocardiography in the infarcted region in a significant proportion of patients. This finding is associated with poor recovery of regional function and thereby a worse prognosis.[137]

References

1 Mangano DT. Perioperative cardiac morbidity. *Anesthesiology* 1990;**72**:153–84.

2 Mangano DT. Adverse outcomes after surgery in the year 2001: a continuing odyssey. *Anesthesiology* 1998;**88**:561–4.

3 Slogoff S, Keats AS. Does perioperative myocardial ischemia lead to postoperative myocardial infarction? *Anesthesiology* 1985;**62**:107–14.

4 Leung JM, O'Kelly B, Browner WS, Tubau J, Hollenberg M, Mangano DT. Prognostic importance of postbypass regional wall-motion abnormalities in patients undergoing coronary artery bypass graft surgery. SPI Research Group. *Anesthesiology* 1989;**71**:16–25.

5 Smith RC, Leung JM, Mangano DT. Postoperative myocardial ischemia in patients undergoing coronary artery bypass graft surgery. SPI Research Group. *Anesthesiology* 1991;**74**:464–73.

6 Mangano DT, Browner WS, Hollenberg M, London MJ, Tubau JF, Tateo IM. Association of perioperative myocardial ischemia with cardiac morbidity and mortality in men undergoing noncardiac surgery. The Study of Perioperative Ischemia Research Group. *N Engl J Med* 1990;**323**:1781–8.

7 Raby KE, Barry J, Creager MA, Cook EF, Weisberg MC, Goldman L. Detection and significance of intraoperative and postoperative myocardial ischemia in peripheral vascular surgery. *JAMA* 1992;**268**:222–7.

8 Pandian NG, Kerber RE. Two-dimensional echocardiography in experimental coronary stenosis. I. Sensitivity and specificity in detecting transient myocardial dyskinesis: comparison with sonomicrometers. *Circulation* 1982;**66**:597–602.

9 Pandian NG, Kieso RA, Kerber RE. Two-dimensional echocardiography in experimental coronary stenosis. II. Relationship between systolic wall thinning and regional myocardial perfusion in severe coronary stenosis. *Circulation* 1982;**66**: 603–11.

10 Tennant R, Wiggers C. The effect of coronary occlusion on myocardial contraction. *Am J Physiol* 1935;**112**:351–61.

11 Lambertz H, Kreis A, Trumper H, Hanrath P. Simultaneous transesophageal atrial pacing and transesophageal two-dimensional echocardiography: a new method of stress echocardiography. *J Am Coll Cardiol* 1990;**16**:1143–53.

12 Zabalgoitia M, Gandhi DK, Abi-Mansour P, Yarnold PR, Moushmoush B, Rosenblum J. Transesophageal stress echocardiography: detection of coronary artery disease in patients with normal resting left ventricular contractility. *Am Heart J* 1991;**122**:1456–63.

13 Agati L, Renzi M, Sciomer S, *et al.* Transesophageal dipyridamole echocardiography for diagnosis of coronary artery disease. *J Am Coll Cardiol* 1992;**19**:765–70.

14 Kamp O, De Cock CC, Kupper AJ, Roos JP, Visser CA. Simultaneous transesophageal two-dimensional echocardiography and atrial pacing for detecting coronary artery disease. *Am J Cardiol* 1992;**69**: 1412–6.

15 Seeberger MD, Cahalan MK, Chu E, *et al.* Rapid atrial pacing for detecting provokable demand ischemia in anesthetized patients. *Anesth Analg* 1997;**84**:1180–5.

16 Seeberger MD, Skarvan K, Buser P, *et al.* Dobutamine stress echocardiography to detect inducible demand ischemia in anesthetized patients with coronary artery disease. *Anesthesiology* 1998;**88**:1233–9.

17 Tarnow J, Markschies H, Schulte S. Isoflurane improves the tolerance to pacing-induced myocardial ischemia. *Anesthesiology* 1986;**64**:147–56.

18 Skopicki HA, Abraham SA, Weissman NJ, *et al.* Factors influencing regional myocardial contractile response to inotropic stimulation. Analysis in humans with stable ischemic heart disease. *Circulation* 1996;**94**:643–50.

19 Hauser AM, Gangadharan V, Ramos RG, Gordon S, Timmis GC. Sequence of mechanical, electrocardiographic and clinical effects of repeated coronary artery occlusion in human beings: echocardiographic observations during coronary angioplasty. *J Am Coll Cardiol* 1985;**5**:193–7.

20 Wohlgelernter D, Cleman M, Highman HA, *et al.* Regional myocardial dysfunction during coronary angioplasty: evaluation by two-dimensional echocardiography and 12 lead electrocardiography. *J Am Coll Cardiol* 1986;**7**:1245–54.

21 Smith JS, Cahalan MK, Benefiel DJ, *et al.* Intraoperative detection of myocardial ischemia in high-risk patients: electrocardiography versus two-dimensional transesophageal echocardiography. *Circulation* 1985;**72**:1015–21.

22 van Daele M, Sutherland GR, Mitchell MM, *et al.* Do changes in pulmonary capillary wedge pressure adequately reflect myocardial ischemia during anesthesia? A correlative preoperative hemodynamic, electrocardiographic, and transesophageal echocardiographic study. *Circulation* 1990;**81**:865–71.

23 Comunale ME, Body SC, Ley C, *et al.* The concordance of intraoperative left ventricular wall-motion abnormalities and electrocardiographic S-T segment changes: association with outcome after coronary revascularization. Multicenter Study of Perioperative Ischemia (McSPI) Research Group. *Anesthesiology* 1998;**88**:945–54.

24 Eisenberg MJ, London MJ, Leung JM, *et al.* Monitoring for myocardial ischemia during noncardiac surgery. A technology assessment of transesophageal echocardiography and 12-lead electrocardiography. The Study of Perioperative Ischemia Research Group. *JAMA* 1992;**268**:210–6.

25 Rouine-Rapp K, Ionescu P, Balea M, Foster E, Cahalan MK. Detection of intraoperative segmental wall-motion abnormalities by transesophageal echocardiography: the incremental value of additional cross sections in the transverse and longitudinal planes. *Anesth Analg* 1996;**83**: 1141–8.

26 Mooss AN, Prevedel JA, Mohiuddin SM, Hilleman DE, Sketch MH Sr. Effect of digoxin on ST-segment changes detected by ambulatory electrocardiographic monitoring in healthy subjects. *Am J Cardiol* 1991;**68**:1503–6.

27 Voller H, Andresen D, Bruggemann T, Jereczek M, Becker B, Schroder R. Transient ST segment depression during Holter monitoring: how to avoid false positive findings. *Am Heart J* 1992;**124**:622–9.

28 Shah PM, Kyo S, Matsumura M, Omoto R. Utility of biplane transesophageal echocardiography in left ventricular wall motion analysis. *J Cardiothorac Vasc Anesth* 1991;**5**:316–9.

29 Weinger MB, Herndon OW, Gaba DM. The effect of electronic record keeping and transesophageal echocardiography on task distribution, workload, and vigilance during cardiac anesthesia. *Anesthesiology* 1997;**87**:144–55; discussion 29A–30A.

30 Gayes JM. The minimally invasive cardiac surgery voyage. *J Cardiothorac Vasc Anesth* 1999;**13**: 119–22.

31 Platt MJ, Davies S, Riedel BJ, Slaughter TF, Mehta SM. Case 4–2002 Near-fatal pulmonary embolism in the immediate postoperative period after off-pump coronary artery bypass graft surgery. *J Cardiothorac Vasc Anesth* 2002;**16**:502–7.

32 Seeberger M, Wang J, Filipovic M, Skarvan K. Feasibility of transoesophageal echocardiography during coronary surgery without cardiopulmonary bypass. *Eur J Anaesth* 2001;**18(suppl 22)**:A33.

33 Moises VA, Mesquita CB, Campos O, *et al.* Importance of intraoperative transesophageal echocardiography during coronary artery surgery without cardiopulmonary bypass. *J Am Soc Echocardiogr* 1998;**11**:1139–44.

34 Pandian NG, Skorton DJ, Collins SM, Falsetti HL, Burke ER, Kerber RE. Heterogeneity of left ventricular segmental wall thickening and excursion in 2-dimensional echocardiograms of normal human subjects. *Am J Cardiol* 1983;**51**: 1667–73.

35 Braunwald E, Kloner RA. The stunned myocardium: prolonged, postischemic ventricular dysfunction. *Circulation* 1982;**66**:1146–9.

36 Moore CA, Smucker ML, Kaul S. Myocardial contrast echocardiography in humans: I. Safety – a comparison with routine coronary arteriography. *J Am Coll Cardiol* 1986;**8**:1066–72.

37 Goldman ME, Mindich BP. Intraoperative cardioplegic contrast echocardiography for assessing myocardial perfusion during open heart surgery. *J Am Coll Cardiol* 1984;**4**:1029–34.

38 Ismail S, Johnson SH, Utsunomiya H, Craig D, Kisslo JA, Smith PK. Safety and efficacy of sonicated albumin microspheres in perfusion and vein graft patency assessments. *Clin Cardiol* 1991;**14**:V29–32.

39 Aronson S, Lee BK, Wiencek JG, *et al.* Assessment of myocardial perfusion during CABG surgery with two-dimensional transesophageal contrast echocardiography. *Anesthesiology* 1991;**75**:433–40.

40 Kaul S. Myocardial contrast echocardiography: 15 years of research and development. *Circulation* 1997;**96**:3745–60.

41 Salustri A, Elhendy A, Garyfallydis P, *et al.* Prediction of improvement of ventricular function after first acute myocardial infarction using low-dose dobutamine stress echocardiography. *Am J Cardiol* 1994;**74**:853–6.

42 Sawada S, Elsner G, Segar DS, *et al.* Evaluation of patterns of perfusion and metabolism in dobutamine-responsive myocardium. *J Am Coll Cardiol* 1997; **29**:55–61.

43 Belardinelli R, Georgiou D, Purcaro A. Low dose dobutamine echocardiography predicts improvement in functional capacity after exercise training in patients with ischemic cardiomyopathy: prognostic implication. *J Am Coll Cardiol* 1998;**31**:1027–34.

44 Pasquet A, D'Hondt AM, Melin JA, Vanoverschelde JL. Relation of ultrasonic tissue characterization with integrated backscatter to contractile reserve in chronic left ventricular ischemic dysfunction. *Am J Cardiol* 1998;**81**:68–74.

45 Lima JA, Becker LC, Melin JA, *et al.* Impaired thickening of nonischemic myocardium during acute regional ischemia in the dog. *Circulation* 1985;**71**:1048–59.

46 Force T, Kemper A, Perkins L, Gilfoil M, Cohen C, Parisi AF. Overestimation of infarct size by quantitative two-dimensional echocardiography: the role of tethering and of analytic procedures. *Circulation* 1986;**73**:1360–8.

47 Seeberger MD, Cahalan MK, Rouine-Rapp K, *et al.* Acute hypovolemia may cause segmental wall motion abnormalities in the absence of myocardial ischemia. *Anesth Analg* 1997;**85**:1252–7.

48 Buffington CW, Coyle RJ. Altered load dependence of postischemic myocardium. *Anesthesiology* 1991;**75**:464–74.

49 Badano L, Stoian J, Cervesato E, *et al.* Reproducibility of wall motion score and its correlation with left ventricular ejection fraction in patients with acute myocardial infarction. *Am J Cardiol* 1996;**78**:855–8.

50 Hoffmann R, Lethen H, Marwick T, *et al.* Analysis of interinstitutional observer agreement in interpretation of dobutamine stress echocardiograms. *J Am Coll Cardiol* 1996;**27**:330–6.

51 Bergquist BD, Leung JM, Bellows WH. Transesophageal echocardiography in myocardial revascularization: 1. Accuracy of intraoperative real-time interpretation. *Anesth Analg* 1996;**82**:1132–8.

52 Nidorf SM, Weyman AE. Left ventricle, II: quantification of segmental dysfunction. In: Weyman AE, ed. *Principles and practice of echocardiography*. Philadelphia: Lea & Febiger, 1994.

53 Shanewise JS, Cheung AT, Aronson S, *et al.* ASE/SCA guidelines for performing a comprehensive intraoperative multiplane transesophageal echocardiography examination: recommendations of the American Society of Echocardiography Council for Intraoperative Echocardiography and the Society of Cardiovascular Anesthesiologists Task Force for Certification in Perioperative Transesophageal Echocardiography. *J Am Soc Echocardiogr* 1999;**12**:884–900.

54 Cerqueira MD, Weissman NJ, Dilsizian V, *et al.* Standardized myocardial segmentation and nomenclature for tomographic imaging of the heart: a statement for healthcare professionals from the Cardiac Imaging Committee of the Council on Clinical Cardiology of the American Heart Association. *Circulation* 2002;**105**:539–42.

55 Schiller NB, Shah PM, Crawford M, *et al.* Recommendations for quantitation of the left ventricle by two- dimensional echocardiography. American Society of Echocardiography Committee on Standards, Subcommittee on Quantitation of Two-Dimensional Echocardiograms. *J Am Soc Echocardiogr* 1989;**2**:358–67.

56 Gardin JM, Adams DB, Douglas PS, *et al.* Recommendations for a standardized report for adult transthoracic echocardiography: a report from the American Society of Echocardiography's Nomenclature and Standards Committee and Task Force for a Standardized Echocardiography Report. *J Am Soc Echocardiogr* 2002;**15**:275–90.

57 Couture P, Denault AY, Carignan S, Boudreault D, Babin D, Ruel M. Intraoperative detection of segmental wall motion abnormalities with transesophageal echocardiography. *Can J Anaesth* 1999;**46**:827–31.

58 Shiga T, Ogawa R, Shanewise JS. Five-grade scoring system is still confusing: does ASE/SCA set up a double standard? Response. *Anesth Analg* 2000;**90**:1248–9.

59 Nishimura RA, Holmes DR Jr, Reeder GS, Tajik AJ, Hatle LK. Doppler echocardiographic observations during percutaneous aortic balloon valvuloplasty. *J Am Coll Cardiol* 1988;**11**:1219–26.

60 Sheikh KH, Bengtson JR, Rankin JS, de Bruijn NP, Kisslo J. Intraoperative transesophageal Doppler color flow imaging used to guide patient selection and operative treatment of ischemic mitral regurgitation. *Circulation* 1991;**84**:594–604.

61 Koolen JJ, Visser CA, David GK, *et al.* Transesophageal echocardiographic assessment of

systolic and diastolic dysfunction during percutaneous transluminal coronary angioplasty. *J Am Soc Echocardiogr* 1990;**3**:374–83.

62 Cahalan MK, Ionescu P, Melton HJ, Adler S, Kee LL, Schiller NB. Automated real-time analysis of intraoperative transesophageal echocardiograms. *Anesthesiology* 1993;**78**:477–85.

63 Borgenhagen DM, Serur JR, Gorlin R, Adams D, Sonnenblick EH. The effects of left ventricular load and contractility on mitral regurgitant orifice size and flow in the dog. *Circulation* 1977;**56**:106–13.

64 Miller DC, Daughters GT, Derby GC, *et al.* Effect of early postoperative volume loading on left ventricular systolic function (including left ventricular ejection fraction determined by myocardial marker) after myocardial revascularization. *Circulation* 1985; **72(suppl II)**:207–15.

65 Konstadt SN, Louie EK, Shore-Lesserson L, Black S, Scanlon P. The effects of loading changes on intraoperative Doppler assessment of mitral regurgitation. *J Cardiothorac Vasc Anesth* 1994;**8**:19–23.

66 Sigwart U, Grbic M, Payot M, Goy J, Essinger A, Fischer A. Ischemic events during coronary artery balloon obstruction. In: Rutishauser W, Roskamm H, eds. *Silent myocardial ischemia.* Berlin: Springer-Verlag, 1984:29–36.

67 Iskandrian AS, Bemis CE, Hakki AH, Heo J, Kimbiris D, Mintz GS. Ventricular systolic and diastolic impairment during pacing-induced myocardial ischemia in coronary artery disease: simultaneous hemodynamic, electrocardiographic, and radionuclide angiographic evaluation. *Am Heart J* 1986;**112**:382–91.

68 Labovitz AJ, Lewen MK, Kern M, Vandormael M, Deligonal U, Kennedy HL. Evaluation of left ventricular systolic and diastolic dysfunction during transient myocardial ischemia produced by angioplasty. *J Am Coll Cardiol* 1987;**10**:748–55.

69 Fischer DC, Voyles W, Sikes W, Greene ER. Left ventricular filling patterns during ischemia: an echo/Doppler study in open chest dogs. *J Am Coll Cardiol* 1985;**5**:426–31A.

70 Rinder ML, Courtis MR, Perez JE, Brasiliai B, Ludbrook PA. Alterations in Doppler indexes of diastolic function following coronary artery reperfusion. *Circulation* 1986;**74(suppl II)**:47–53.

71 El Said ES, Roelandt JR, Fioretti PM, *et al.* Abnormal left ventricular early diastolic filling during dobutamine stress Doppler echocardiography is a sensitive indicator of significant coronary artery disease. *J Am Coll Cardiol* 1994;**24**:1618–24.

72 Kolev N, Berkemeier H, Ihra G, Mayer N, Zimpfer M. A new scoring system, using Doppler transmitral diastolic measurement, identifies transient myocardial ischaemia. *Eur J Anaesthesiol* 1996;**13**:49–55.

73 Wang J, Filipovic M, Bernet F, *et al.* The diagnostic value of changes in transmitral flow velocities for detecting ischaemia in anaesthetised patients during cardiac surgery. *Eur J Anaesth* 2002; **19(suppl 27)**:13.

74 Oniki T, Hashimoto Y, Shimizu S, Kakuta T, Yajima M, Numano F. Effect of increasing heart rate on Doppler indices of left ventricular performance in healthy men. *Br Heart J* 1992;**68**:425–9.

75 Choong CY, Herrmann HC, Weyman AE, Fifer MA. Preload dependence of Doppler-derived indexes of left ventricular diastolic function in humans. *J Am Coll Cardiol* 1987;**10**:800–8.

76 Nishimura RA, Abel MD, Housmans PR, Warnes CA, Tajik AJ. Mitral flow velocity curves as a function of different loading conditions: evaluation by intraoperative transesophageal Doppler echocardiography. *J Am Soc Echocardiogr* 1989;**2**:79–87.

77 Bernardi L, Perlini S, Soffiantino F, *et al.* Acute haemodynamic effects of ibopamine and dopamine on isovolumic relaxation. *Eur J Pharmacol* 1989;**164**:415–24.

78 Niwa H, Hirota Y, Sibutani T, *et al.* The effects of epinephrine and norepinephrine administered during local anesthesia on left ventricular diastolic function. *Anesth Prog* 1991;**38**:221–6.

79 Parker JD, Landzberg JS, Bittl JA, Mirsky I, Colucci WS. Effects of beta-adrenergic stimulation with dobutamine on isovolumic relaxation in the normal and failing human left ventricle. *Circulation* 1991;**84**:1040–8.

80 Colon P, Milani R, Richards D, *et al.* The clinical utility of assessing diastolic function during dobutamine stress echocardiography [abstract]. *J Am Soc Echocardiogr* 1996;**9**:399.

81 Seeberger MD, Filipovic M, Rohlfs R, *et al.* The diagnostic value of Doppler echocardiographic indexes of diastolic filling for detecting demand ischemia in anesthetized patients. *Int J Cardiol Imaging* 2000;**16**:437–46.

82 Filipovic M, Seeberger MD, Rohlfs R, *et al.* Doppler indices of diastolic transmitral flow velocity are invalid indicators of myocardial ischaemia during high-dose dobutamine infusion in anaesthetized patients. *Eur J Anaesthesiol* 2002;**19**:789–95.

83 Lang RM, Vignon P, Weinert L, *et al.* Echocardiographic quantification of regional left ventricular wall motion with color kinesis. *Circulation* 1996;**93**:1877–85.

84 Hartmann T, Kolev N, Blaicher A, Spiss C, Zimpfer M. Validity of acoustic quantification colour kinesis for detection of left ventricular regional wall motion abnormalities: a transoesophageal echocardiographic study. *Br J Anaesth* 1997;**79**:482–7.

85 Vitarelli A, Sciomer S, Schina M, Luzzi MF, Dagianti A. Detection of left ventricular systolic and diastolic abnormalities in patients with coronary artery disease by color kinesis. *Clin Cardiol* 1997;**20**:927–33.

86 Barzilai B, Madaras EI, Sobel BE, Miller JG, Perez JE. Effects of myocardial contraction on ultrasonic backscatter before and after ischemia. *Am J Physiol* 1984;**247**:H478–83.

87 Rasmussen S, Lovelace DE, Knoebel SB, Ransburg R, Corya BC. Echocardiographic detection of ischemic and infarcted myocardium. *J Am Coll Cardiol* 1984;**3**:733–43.

88 Sagar KB, Rhyne TL, Warltier DC, Pelc L, Wann LS. Intramyocardial variability in integrated backscatter: effects of coronary occlusion and reperfusion. *Circulation* 1987;**75**:436–42.

89 Fitzgerald PJ, McDaniel MD, Rolett EL, Strohbehn JW, James DH. Two-dimensional ultrasonic tissue characterization: backscatter power, endocardial wall motion, and their phase relationship for normal, ischemic, and infarcted myocardium. *Circulation* 1987;**76**:850–9.

90 Wickline SA, Thomas LJd, Miller JG, Sobel BE, Perez JE. Sensitive detection of the effects of reperfusion on myocardium by ultrasonic tissue characterization with integrated backscatter. *Circulation* 1986;**74**:389–400.

91 Milunski MR, Mohr GA, Wear KA, Sobel BE, Miller JG, Wickline SA. Early identification with ultrasonic integrated backscatter of viable but stunned myocardium in dogs. *J Am Coll Cardiol* 1989;**14**:462–71.

92 Lythall DA, Gibson DG, Kushwaha SS, Norell MS, Mitchell AG, Ilsley CJD. Changes in myocardial echo amplitude during reversible ischemia in humans. *Br Heart J* 1992;**67**:368–76.

93 Vitale DF, Bonow RO, Gerundo G, *et al.* Alterations in ultrasonic backscatter during exercise-induced myocardial ischemia in humans. *Circulation* 1995;**92**:1452–7.

94 Milunski MR, Mohr GA, Perez JE, *et al.* Ultrasonic tissue characterization with integrated backscatter. Acute myocardial ischemia, reperfusion, and stunned myocardium in patients. *Circulation* 1989;**80**:491–503.

95 Fukuda K, Oki T, Tabata T, Iuchi A, Ito S. Regional left ventricular wall motion abnormalities in myocardial infarction and mitral annular descent velocities studied with pulsed tissue Doppler imaging. *J Am Soc Echocardiogr* 1998;**11**:841–8.

96 Alam M, Wardell J, Andersson E, Samad BA, Nordlander R. Characteristics of mitral and tricuspid annular velocities determined by pulsed wave Doppler tissue imaging in healthy subjects. *J Am Soc Echocardiogr* 1999;**12**:618–28.

97 Sutherland GR, Stewart MJ, Groundstroem KW, *et al.* Color Doppler myocardial imaging: a new technique for the assessment of myocardial function. *J Am Soc Echocardiogr* 1994;**7**:441–58.

98 Palka P, Lange A, Fleming AD, Sutherland GR, Fenn LN, McDicken WN. Doppler tissue imaging: myocardial wall motion velocities in normal subjects. *J Am Soc Echocardiogr* 1995;**8**: 659–68.

99 Gorcsan JD, Gulati VK, Mandarino WA, Katz WE. Color-coded measures of myocardial velocity throughout the cardiac cycle by tissue Doppler imaging to quantify regional left ventricular function. *Am Heart J* 1996;**131**:1203–13.

100 Palka P, Lange A, Fleming AD, *et al.* Age-related transmural peak mean velocities and peak velocity gradients by Doppler myocardial imaging in normal subjects. *Eur Heart J* 1996;**17**:940–50.

101 Fraser AG, Payne N, Madler CF, *et al.* Feasibility and reproducibility of off-line tissue Doppler measurement of regional myocardial function during dobutamine stress echocardiography. *Eur J Echocardiogr* 2003;**4**:43–53.

102 Uematsu M, Miyatake K, Tanaka N, *et al.* Myocardial velocity gradient as a new indicator of regional left ventricular contraction: detection by a two-dimensional tissue Doppler imaging technique. *J Am Coll Cardiol* 1995;**26**:217–23.

103 Tsutsui H, Uematsu M, Shimizu H, *et al.* Comparative usefulness of myocardial velocity gradient in detecting ischemic myocardium by a dobutamine challenge. *J Am Coll Cardiol* 1998;**31**:89–93.

104 Weidemann F, Eyskens B, Mertens L, *et al.* Quantification of regional right and left ventricular function by ultrasonic strain rate and strain indexes after surgical repair of tetralogy of Fallot. *Am J Cardiol* 2002;**90**:133–8.

105 Voigt JU, Arnold MF, Karlsson M, *et al.* Assessment of regional longitudinal myocardial strain rate derived from Doppler myocardial imaging indexes in normal and infarcted myocardium. *J Am Soc Echocardiogr* 2000;**13**:588–98.

106 D'Hooge J, Konofagou E, Jamal F, *et al.* Two-dimensional ultrasonic strain rate measurement of the human heart in vivo. *IEEE Trans Ultrason Ferroelectr Freq Control* 2002;**49**:281–6.

107 Davidavicius G, Kowalski M, Williams RI, *et al.* Can regional strain and strain rate measurement be performed during both dobutamine and exercise echocardiography, and do regional deformation responses differ with different forms of stress testing? *J Am Soc Echocardiogr* 2003;**16**:299–308.

108 Borges AC, Kivelitz D, Walde T, *et al.* Apical tissue tracking echocardiography for characterization of regional left ventricular function: Comparison with magnetic resonance imaging in patients after myocardial infarction. *J Am Soc Echocardiogr* 2003;**16**:254–62.

109 Oki T, Tabata T, Mishiro Y, *et al.* Pulsed tissue Doppler imaging of left ventricular systolic and diastolic wall motion velocities to evaluate differences between long and short axes in healthy subjects. *J Am Soc Echocardiogr* 1999;**12**:308–13.

110 Galiuto L, Ignone G, DeMaria AN. Contraction and relaxation velocities of the normal left ventricle using pulsed-wave tissue Doppler echocardiography. *Am J Cardiol* 1998;**81**:609–14.

111 Pai RG, Gill KS. Amplitudes, durations, and timings of apically directed left ventricular myocardial velocities: I. Their normal pattern and coupling to ventricular filling and ejection. *J Am Soc Echocardiogr* 1998;**11**:105–11.

112 Derumeaux G, Ovize M, Loufoua J, *et al.* Doppler tissue imaging quantitates regional wall motion

during myocardial ischemia and reperfusion. *Circulation* 1998;**97**:1970–7.

113 Jamal F, Kukulski T, Strotmann J, *et al.* Quantification of the spectrum of changes in regional myocardial function during acute ischemia in closed chest pigs: an ultrasonic strain rate and strain study. *J Am Soc Echocardiogr* 2001;**14**:874–84.

114 Derumeaux G, Loufoua J, Pontier G, Cribier A, Ovize M. Tissue Doppler imaging differentiates transmural from nontransmural acute myocardial infarction after reperfusion therapy. *Circulation* 2001;**103**:589–96.

115 Garot P, Pascal O, Simon M, *et al.* Usefulness of combined quantitative assessment of myocardial perfusion and velocities by myocardial contrast and Doppler tissue echocardiography during coronary blood flow reduction. *J Am Soc Echocardiogr* 2003;**16**:1–8.

116 Palka P, Lange A, Ferrington C, Fox KA. Mean myocardial velocity mapping in quantifying regional myocardial contractile reserve in patients with impaired left ventricular systolic function: Doppler myocardial imaging study. *J Am Soc Echocardiogr* 2000;**13**:96–107.

117 Pasquet A, Armstrong G, Beachler L, Lauer MS, Marwick TH. Use of segmental tissue Doppler velocity to quantitate exercise echocardiography. *J Am Soc Echocardiogr* 1999;**12**:901–12.

118 Kukulski T, Jamal F, D'Hooge J, Bijnens B, De Scheerder I, Sutherland GR. Acute changes in systolic and diastolic events during clinical coronary angioplasty: a comparison of regional velocity, strain rate, and strain measurement. *J Am Soc Echocardiogr* 2002;**15**:1–12.

119 Katz WE, Gulati VK, Mahler CM, Gorcsan J III. Quantitative evaluation of the segmental left ventricular response to dobutamine stress by tissue Doppler echocardiography. *Am J Cardiol* 1997;**79**:1036–42.

120 Armstrong G, Pasquet A, Fukamachi K, Cardon L, Olstad B, Marwick T. Use of peak systolic strain as an index of regional left ventricular function: comparison with tissue Doppler velocity during dobutamine stress and myocardial ischemia. *J Am Soc Echocardiogr* 2000;**13**:731–7.

121 von Bibra H, Tuchnitz A, Klein A, Schneider-Eicke J, Schomig A, Schwaiger M. Regional diastolic function by pulsed Doppler myocardial mapping for the detection of left ventricular ischemia during pharmacologic stress testing: a comparison with stress echocardiography and perfusion scintigraphy. *J Am Coll Cardiol* 2000;**36**:444–52.

122 Rambaldi R, Poldermans D, Bax JJ, *et al.* Doppler tissue velocity sampling improves diagnostic accuracy during dobutamine stress echocardiography for the assessment of viable myocardium in patients with severe left ventricular dysfunction. *Eur Heart J* 2000;**21**:1091–8.

123 Edvardsen T, Aakhus S, Endresen K, Bjomerheim R, Smiseth OA, Ihlen H. Acute regional myocardial ischemia identified by 2-dimensional multiregion tissue Doppler imaging technique. *J Am Soc Echocardiogr* 2000;**13**:986–94.

124 Bach DS, Armstrong WF, Donovan CL, Muller DW. Quantitative Doppler tissue imaging for assessment of regional myocardial velocities during transient ischemia and reperfusion. *Am Heart J* 1996;**132**:721–5.

125 Jamal F, Kukulski T, Sutherland GR, *et al.* Can changes in systolic longitudinal deformation quantify regional myocardial function after an acute infarction? An ultrasonic strain rate and strain study. *J Am Soc Echocardiogr* 2002;**15**:723–30.

126 Simmons LA, Weidemann F, Sutherland GR, *et al.* Doppler tissue velocity, strain, and strain rate imaging with transesophageal echocardiography in the operating room: a feasibility study. *J Am Soc Echocardiogr* 2002;**15**:768–76.

127 Williams RI, Haaverstad R, Sianos G, Vourvouri E, Fraser AG. Perioperative tissue Doppler echocardiography and bypass graft flowmetry in patients undergoing coronary revascularization: predictive power for late recovery of regional myocardial function. *J Am Soc Echocardiogr* 2002;**15**:1202–10.

128 Skulstad H, Andersen K, Edvardsen T, *et al.* Strain Doppler echocardiography as a means for detecting myocardial ischaemia: assessment during off-pump coronary bypass surgery. *Eur Heart J* 2000;**335**:P1798.

129 Dupont FW, Lam NT, Heller LB, Drum M, Aronson S. Intraoperative TEE using tissue Doppler modalities vs. regional wall motion scoring in the short axis view. *Anesthesiology* 2002;**96**:A140.

130 Kasprzak JD, Ten Cate FJ. New ultrasound contrast agents for left ventricular and myocardial opacification. *Herz* 1998;**23**:474–82.

131 Main ML, Grayburn PA. Clinical applications of transpulmonary contrast echocardiography. *Am Heart J* 1999;**137**:144–53.

132 Stewart MJ. Contrast echocardiography. *Heart* 2003;**89**:342–8.

133 Becher H, Burns PN. LV function and myocardial perfusion. In: *Handbook of contrast echocardiography*. Berlin: Springer Verlag, 2000:2–44.

134 Kaul S. Myocardial contrast echocardiography in coronary artery disease: potential applications using venous injections of contrast. *Am J Cardiol* 1995;**75**:61D–8D.

135 Mudra H, Zwehl W, Klauss V, *et al.* Intraoperative myocardial contrast echocardiography for assessment of regional bypass perfusion. *Am J Cardiol* 1990;**66**:1077–81.

136 Kabas JS, Kisslo J, Flick CL, *et al.* Intraoperative perfusion contrast echocardiography. Initial experience during coronary artery bypass grafting. *J Thorac Cardiovasc Surg* 1990;**99**:536–42.

137 Greaves K, Dixon SR, Fejka M, *et al.* Myocardial contrast echocardiography is superior to other known modalities for assessing myocardial reperfusion after acute myocardial infarction. *Heart* 2003;**89**:139–44.

12 Congenital heart disease

Pierre-Guy Chassot, Dominique Bettex

Introduction

Major advances made over the past 30 years in cardiac surgery have resulted in an increased number of children with congenital heart disease who survive for long period of time. Of babies born with heart disease, 85% are expected to reach adulthood, and this population is growing at a rate of 5% each year.[1] Any anaesthesiologist might therefore encounter one of these patients in their daily practice and may rely on transoesophageal echocardiography (TOE) in three different circumstances:

- to assess and manage haemodynamics during non-cardiac surgery performed in patients with corrected or uncorrected congenital heart defects
- to diagnose unexpected findings in symptomatic or asymptomatic patients
- to assess anatomical abnormalities and their surgical repair during cardiac surgery.

This chapter provides a brief review of the indications for perioperative TOE, followed by an overview of the anatomical nomenclature of congenital heart disease. Finally, the chapter describes characteristic TOE images for the main congenital pathologies as they appear in adults, along with particular findings seen after their surgical correction.

Indications and impact of transoesophageal echocardiography

Various task forces have reported practice guidelines for TOE in paediatrics, anaesthesiology, and cardiology.[2–4] They advocate the following indications for TOE:

- procedures that are dependent on TOE examination to achieve adequate correction, such as ventricular outflow tract reconstruction or valve repair
- immediate detection of residual pathology after surgical correction, such as residual shunts or flow limitation through anastomoses
- monitoring ventricular function
- guiding and controlling percutaneous interventions during catheterisation procedures.

Echocardiographic examination of adults with congenital heart diseases is a difficult task; the anatomy is grossly abnormal, and the long-lasting haemodynamic constraints have resulted in significant remodelling of the cardiac chambers. All possible planes and angles must be used in order to visualise properly the different structures. TOE offers fewer acoustic windows than does transthoracic echocardiography, but it provides important additional information on posterior structures such as pulmonary venous return, atrial anatomy, atrioventricular (AV) junction, left ventricular outflow tract (LVOT), or descending aorta.[5] Some areas and structures are not properly imaged by TOE, including posterior wall of the left atrium (too close to the transducer), apical muscular ventricular septum (because of far field attenuation), distal ascending aorta, distal pulmonary artery (PA), and aortic arch (because of main bronchus interposition).[6] TOE offers an outstanding assessment of right and left ventricular function, and a qualitative evaluation of cardiac filling.[7] For quantification of volume or ejection fraction, the use of Simpson's rule is recommended rather than the usual geometrical approximations such as Teichholz formula because the ventricles are frequently dysmorphic. Anaesthesia, intermittent positive pressure ventilation, high inspired oxygen concentration, and opening of the pericardium have important impact on haemodynamic status, and may substantially modify assessment of valvular regurgitations or intracardiac shunts. These modifications must be appreciated in order to interpret the post-correction data.

In cardiac surgery, modifications to surgical management because of unexpected findings from the pre-bypass examination occur in up to 7% of cases.[8–10] After bypass, immediate assessment of the surgical repair offers a unique opportunity to correct possible residual defects during the same

operation. Although most of the outcome studies in congenital heart defects are directed at paediatric patients, it seems reasonable to assume that their conclusions are valid for adult surgery as well.[11] The rate of immediate surgical revision following post-bypass TOE examination is 3–10%.[8–10,12] The procedures that benefit most are valvular repairs, outflow tract reconstructions, and complex AV discordances.[13] The sensitivity and specificity of TOE in determining the need for reoperation are 89% and 100%, respectively.[14,15] Post-bypass TOE can also reveal residual defects that do not require surgical revision. The rate of these "acceptable" defects has been estimated at between 15% and 38%.[8,10,12] This high incidence of findings without surgical or haemodynamic significance is a drawback of the exquisite sensitivity of TOE.

In performing a complete post-bypass examination, attention must be paid to specific details for each corrected lesion.[16] A careful analysis of segmental wall motion will detect any impairment in coronary flow. When the issue of returning to bypass is raised, the appropriate decision can only be made when the surgeon (who is aware of the feasibility of further repair) and the echocardiographer (who appreciates the limitations of the technique) are working together in close cooperation. In the case of persistent doubt, direct intraoperative measurements of gradients and oxymetry should be taken. Patients who leave the operating room with significant residual defects tend to have a poorer outcome than do those with immediate complete correction.[8,12] Post-bypass ventricular performance is in itself an important predictor of survival; patients with severely diminished ventricular function have a greater incidence of early death than do those with preserved function (35% versus 4%).[17]

Should TOE be routinely employed in correction of adult congenital cardiac defects? Institutional surgical abilities and echocardiographic experience impact directly on clinical impact.[18] In complex cases, routine TOE results in a significant decrease in hospital costs because it decreases the rate of residual defects, and therefore the rate of delayed reoperation.[10,12,19,20] The economic implications of intraoperative echocardiography are currently of great importance, but they should not obscure other significant facts. Unexpected but significant intraoperative findings, with an incidence of 3–7% of cases, cannot be predicted to occur only in certain categories of patients; only routine TOE can discover them.[15] Moreover, perioperative haemodynamic management (ventricular function, volaemia) is more accurate with TOE, which has a "medical" impact reaching 25%.[9,10,13] Finally, TOE is an excellent teaching instrument for anaesthesiologists who need to learn the haemodynamic behaviour of congenital cardiopathies.

Anatomical nomenclature

The extreme diversity of congenital heart disease calls for a structural classification. The basic concept of this classification is a segmental approach; the heart is considered in terms of three segments (atria, ventricles, and arterial trunks) connected via two junctions (AV and ventriculo-arterial; Figure 12.1).[21,22] The definition of the segments is based on their intrinsic morphology because the usual criteria of size and position are not relevant in congenital disease.[23]

In the sequential analysis, five criteria are used to determine the anatomical structures of the heart:[24]

- situs: it can be solitus (normal) or inversus; because it is concordant with abdominal status, the situs is mainly defined by the position of the right atrium
- concordance or discordance of successive segments: instead of following each other normally (concordance), the various anatomical segments can be in an inappropriate relative position (discordance)
- segmental connections: the junctional parts between segments are the AV canal between atria and ventricles, and the infundibulum (or conus arteriosus) between ventricles and arterial trunks
- spatial relationships: these define what is right, left, anterior, posterior, and inferior
- associated abnormalities: dysmorphic chamber structures, obstructive lesions, or septal defects.

The TOE examination of patient with congenital heart disease must be conducted in a logical sequence:[25]

- four chamber view: relative size, shape, and position of each cardiac cavity
- atrial segment: situs, location, arrangement, identity, and venous connections

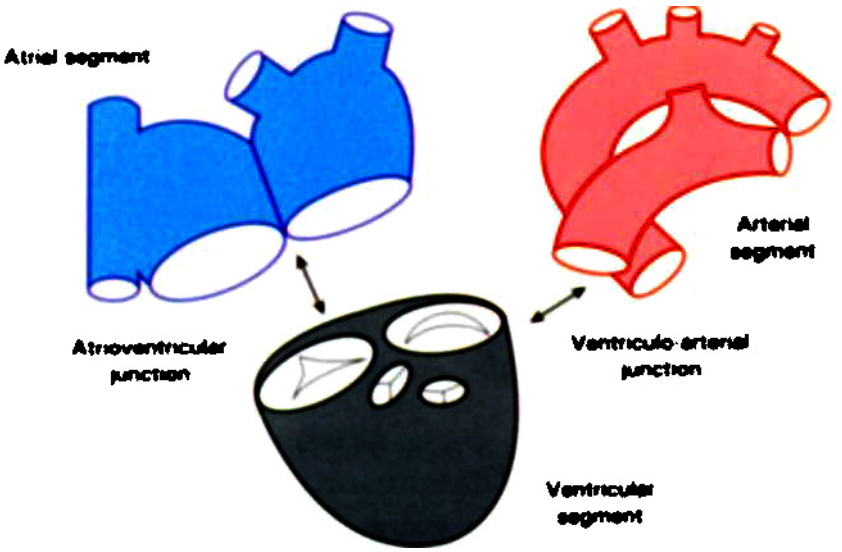

Figure 12.1 Segmental analysis. The heart is divided into three segments, connected through two junctions. The atrioventricular valves belong to the ventricular segment.

- AV connection: valvular status, univentricular, uniatrial, and single inlet
- ventricular segment: number, size, orientation, and identity
- ventriculo-arterial connection: double outlet, single outlet, outflow tract, and valvular status
- arterial segment: great vessel orientation and identity
- presence and direction of intracardiac shunts.

Four-chamber view

The TOE examination should begin with an overview of all four cavities in order to appreciate the relative development and remodelling of each cardiac structure. In case of atresia or stenosis of a valve, structures situated downstream do not receive sufficient blood to develop normally and become involuted and hypoplastic. Conversely, the structures situated upstream sustain a volume and pressure overload. Volume overload also results from a shunt or a regurgitation, and it induces chamber dilation; pressure overload due to an obstruction or high vascular resistance leads to hypertrophy. Both of these phenomena can occur together. Because defects and remodelling are related, it is important to search for the consequences of a primary defect or the causes of a secondary effect.[26] Timing of rapid events is facilitated by M-mode studies.

Atrial segment

Cardiac situs is determined by the position of the atria. The abdominal situs is concordant with the cardiac situs in the vast majority of patients; transdiaphragmatic discordance is extremely rare, and leads to complex congenital anomalies that are never seen in adults. The inferior vena cava (IVC) is the best criterion to identify the right atrium. In the rare cases of absence of the IVC, the suprahepatic veins drain directly into the right atrium. The superior vena cava (SVC) can enter either atrium or can be duplicated, and is therefore of little help in atrial orientation. The pulmonary veins draining into the morphological left atrium is not a constant feature.

The auricular appendages are the most consistent components of the atria.[27] The right appendage is short, blunt, broad based, and pyramidal. The left appendage is long and finger-like; it is crenated by the pectinate muscles and has a narrow junction with the left atrium. When both appendages are the same, this situation is termed isomerism, and is defined as right or left depending upon the morphology of the appendages.

Other anatomical landmarks can help to define each atrium. The right surface of the interatrial septum contains the fossa ovalis and receives the insertion of the Eustachian valve. The crista terminalis runs from the base of the right appendage to the orifice of the SVC and down to the IVC. The left atrial septal surface includes the flap valve of the fossa ovalis. In the case of difficulty in identification, the systemic venous return can be verified by a contrast study, which is easily obtained with the forceful injection of a few millilitres of hand-agitated normal saline through an intravenous cannula. The receiving chamber is then flooded with echo-dense microbubbles.

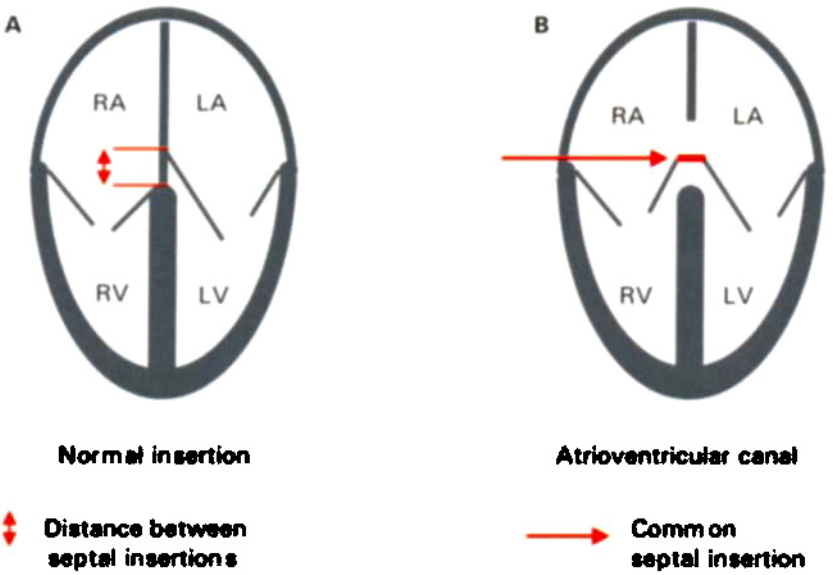

Figure 12.2 Insertion of the septal leaflets of the tricuspid and mitral valves. **(A)** In normal anatomy the tricuspid valve is inserted on the muscular part of the interventricular septum, whereas the mitral valve is inserted on the membranous part of the septum; the distance between the insertions is less than 10 mm. **(B)** In atrioventricular canal, or endocardial cushion defect, both atrioventricular valves are inserted at the same level. LA = left atrium, LV = left ventricle, RA = right atrium, RV = right ventricle.

Atrioventricular connections

The internal cardiac crux is the anatomical junction of atrial septum, ventricular septum, and septal portions of the mitral and tricuspid valves. On the four chamber view (0°) the septal leaflet of the tricuspid valve is inserted slightly (5–10 mm) below the anterior leaflet of the mitral valve (Figure 12.2).[28] The anatomical landmark of the crux is useful for differentiating ventricular and AV–valvular abnormalities. In patients with endocardial cushion defect, both AV valves are at the same level.

AV connections are either concordant (when atria are connected to their appropriate ventricles) or discordant (when atria are connected to the inappropriate ventricle). In the case of discordance, AV valves remain connected to their corresponding ventricle. When both atria are connected to only one ventricle, this is called double-inlet ventricle. Overriding of the valve describes the opening of the valvular orifice into both ventricles; tension apparatus of an AV valve inserted into both ventricles across a ventricular septal defect is called straddling (Figure 12.3).

Ventricular segment

A ventricle has three components: the inlet, the trabecular apex, and the outlet. Of these, the trabecular component is the most consistent feature. A chamber is considered a ventricle if it receives more than 50% of the ventricular inlet or fibrous ring of an AV valve;[25] below this value, the cavity is termed a rudimentary chamber.

Position, shape and wall thickness are misleading features for determining which ventricle is morphologically right or left in congenital heart diseases. Various criteria are used to identify them.

- The mitral valve is always associated with the morphological left ventricle and the tricuspid valve with the morphological right ventricle.
- The septal leaflet of the tricuspid valve inserts inferiorly to the insertion of the anterior leaflet of the mitral valve with the exception of the AV canal.
- The number and orientation of papillary muscles are important features. The anatomical left ventricle has two papillary muscles of equal size, which arise from the posteromedial and anterolateral walls, but never from the septum. The anatomical right ventricle has three papillary muscles of varying size, one of which has chordal insertions on the interventricular septum.
- The apical trabeculations of the right ventricle are much coarser, and a large muscular moderator

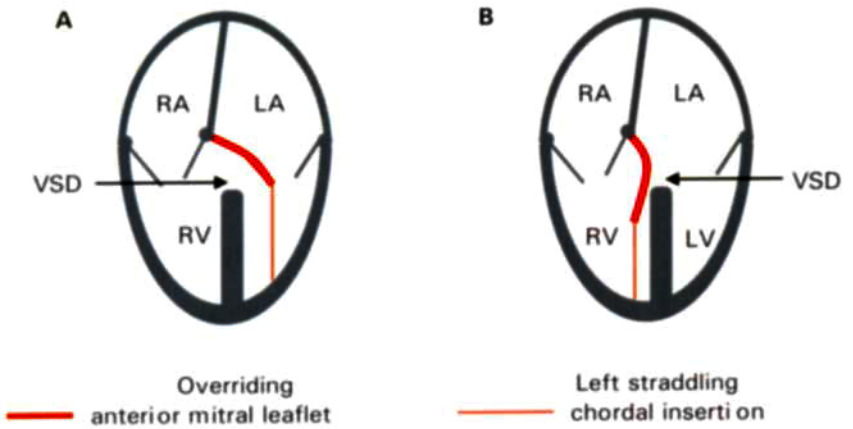

Figure 12.3 Atrioventricular junction. **(A)** Overriding. The mitral valve overlaps the septum; the orifice is committed to both ventricles, but the subvalvular apparatus belongs to the same ventricle as the valve. **(B)** Straddling. The subvalvular apparatus of the atrioventricular valve (the mitral valve) is inserted into both ventricles across the interventricular septal defect (VSD). LA = left atrium, LV = left ventricle, RA = right atrium, RV = right ventricle.

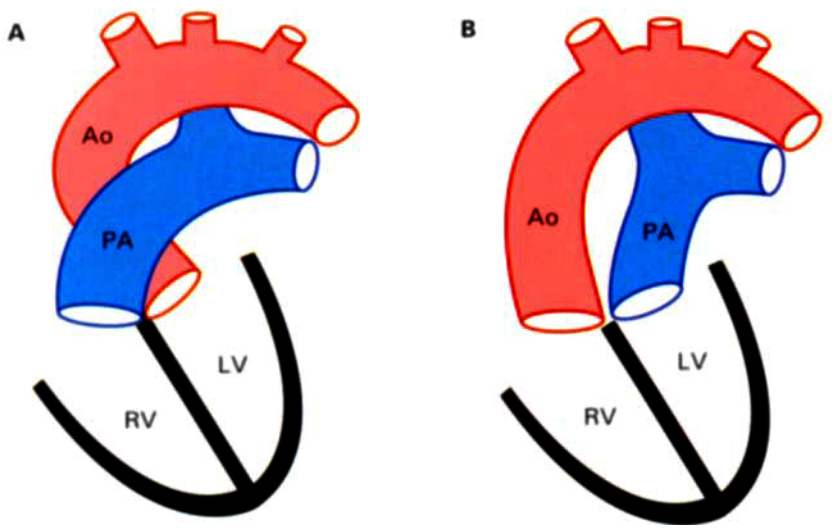

Figure 12.4 Ventriculo-arterial discordance. **(A)** Normal concordant connection. The pulmonary artery (PA) is positioned in front of the aorta (Ao). **(B)** In discordant connection (transposition of the great arteries), both vessels are parallel; the anatomical right ventricle (RV) is subaortic, and the anatomical left ventricle (LV) is subpulmonary.

band crosses the right ventricular cavity from the lower interventricular septum to the anterior free wall. The left ventricular trabeculations are fine, and its endocardial surface is smooth.

- The outlet of the right ventricle is completely muscular, with a prominent supraventricular crest; the outlet of the left ventricle has a fibrous continuity between arterial (normally aortic) and AV (normally mitral) valves.

Ventriculo-arterial connections

Normally, the right ventricular outflow tract (RVOT) lies anterior to the aorta and intersects it at a 45° angle. It continues posteriorly into the PA. Four possible types of ventriculo-arterial connections exist. Concordance and discordance are described when the arterial trunks are connected to their morphologically appropriate or inappropriate ventricles, respectively (Figure 12.4). A double outlet ventricle is characterised by connection of more than 50% of both arterial valves to the same ventricle, which may be right, left, or solitary. A single outlet ventricle is diagnosed when only one arterial trunk can be traced to the ventricle. One or both arterial valves can override. They cannot straddle because they have no tension apparatus.

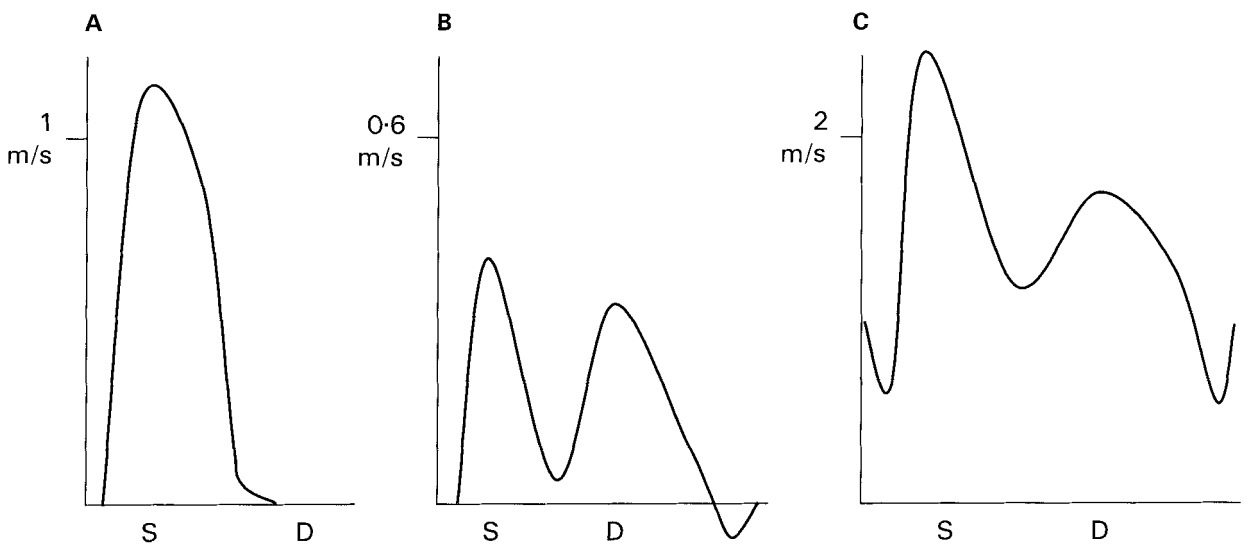

Figure 12.5 Spectral display of flows. **(A)** Arterial flow trace. The flow is systolic. V_{max} is about 1 m/s for aorta and 0·7 m/s for pulmonary artery. **(B)** Venous flow. The flow is systolo-diastolic. It returns to baseline between each cardiac cycle, with a slight backward flow during atrial contraction. V_{max} is about 0·4 m/s. **(C)** Shunt flow. The flow is systolo-diastolic with higher velocity during systole. It does not reach baseline. The V_{max} depends on the pressure gradient between upstream and downstream chambers; it is usually 1–4 m/s. D = diastole, S = systole.

Arterial segment

Two great vessels exit from the heart. When they normally cross at their origin, the anterior vessel is the PA and the posterior vessel is the aorta; the PA runs toward the left side of the aorta. If they are transposed, both vessels maintain a parallel orientation (see Figure 12.4). Both appear circular in the short axis (0°) and parallel in the long axis (90°). Identification of both vessels is based on their branching patterns;[29] the PA bifurcates shortly after its origin, whereas the aorta ascends into the neck without branching before the aortic arch, which lies outside the field of the transoesophageal images.

Septal defects: intracardiac shunts

A loss of continuity in a septal barrier on the two-dimensional image demonstrates the presence of an intracardiac shunt; however, this can be missed when the septum is parallel to the axis of the ultrasound beam. The striking echocardiographic appearance is the enlargement of the receiving chambers; isolated defects situated upstream from the AV valves cause right sided chamber dilation, whereas lesions downstream from the AV junctions mostly induce left sided chamber dilation. Confirmation of the diagnosis is based on the presence of an abnormal continuous colour flow through the area of echo dropout. Pulsed wave or continuous wave Doppler can assess the timing of complex or bidirectional flows with precision. Contrast studies are particularly useful when Doppler sensitivity is poor or shunt is small. When the shunt is predominantly right-to-left or presents with a right-to-left component, the microbubbles of hand-agitated normal saline injected into a systemic vein, preferably central, appear secondarily in the left sided receiving cavity.[30] In patients with a predominant left-to-right shunt, some passage may be observed during short periods of right-to-left shunting. When the shunt is strictly left-to-right the study may still be useful because of the effect of "negative contrast"; non-contrast-containing blood passing through the shunt displaces the contrast-containing blood.[31]

The instantaneous direction of a shunt depends upon its dimension and pressure gradient. A restrictive shunt creates a significant pressure gradient across the defect; the flow velocity is high, and aliasing is obvious. A non-restrictive shunt does not impede blood flow, resulting in an absence of significant gradient and low velocity without aliasing. On spectral display the shunt flow is systolic and diastolic, and does not return to baseline between cardiac cycles; its velocity is usually between 1 and 4 m/s. This pattern can be differentiated from arterial or central venous flows (Figure 12.5).

Flow and pressure calculations

The flow (Q) in a vessel can be calculated from the product of the cross-sectional area of this vessel (A) and the maximal velocity (V_{max}) obtained by pulsed wave or continuous wave Doppler at the same position:

$$Q\ (cm^3/s) = A\ (cm^2) \times V_{max}\ (cm/s)$$

The stroke volume (SV), or the volume flowing through the area for the duration of measurement, is the product of the cross-sectional area (A) and the velocity–time integral (VTI):

$$SV\ (cm^3) = A\ (cm^2) \times VTI\ (cm)$$

The systemic-to-pulmonary shunt (Qp/Qs) can be estimated by measuring the stroke volume through the PA trunk in the basal transverse plane, and through the aorta or the LVOT in the deep retroflexed transgastric view. In the shunt equation, maximal flow velocity (V_{max}) values can be substituted for VTIs. Different sites can be used for measuring flow, with mitral orifice methods potentially being the least accurate. The main sources of errors are inaccuracy in the measurement of vessel diameter and failure to collect the data simultaneously.

Assuming that an atrial septal defect (ASD) is a circular orifice of surface A, and the pulsed Doppler sample is parallel to the supposedly uniform flow, then the shunt can be directly calculated at this level:[32]

$$SV_{ASD}\ (cm^3) = A_{ASD}\ (cm^2) \times VTI_{shunt}\ (cm)$$

The simplified Bernoulli equation may be used to evaluate PA systolic pressure (PAP_s) if the V_{max} of tricuspid regurgitation ($V_{max}TR$) is known:

$$PAPs = 4\ (V_{max}TR)^2 + RAP$$

In the absence of pathology of the RVOT and the pulmonary valve, the systolic right ventricular pressure is equal to the PAP_s, which equals the sum of the systolic pressure gradient between the right ventricle and the right atrium, and the right atrial pressure (RAP). This assumption is not valid in the presence of a VSD; the upstream pressure is then the left ventricular pressure.

In the case of pulmonary regurgitation, the PA diastolic pressure (PAP_d) can be estimated from the pressure gradient trough the pulmonary valve in diastole; if we take the right ventricular diastolic pressure to be equal to the RAP, then the formula becomes:

$$PAP_d = 4\ (V_{max}PR)^2 + RAP$$

Pathological approach

Usually, congenital heart defects are classified according to their impact on pulmonary blood flow, leading to cyanotic or non-cyanotic pathologies. In this chapter, however, we review the different pathologies in accordance with the segmental approach mentioned above.

Anomalous systemic venous return

Persistence of a left SVC is found in 0·1% of the general population.[33] The left SVC drains into an enlarged coronary sinus in 90% of cases. On the transverse plane, it lies close to the lateral wall of the left atrium, between the left upper pulmonary vein and the left atrial appendage; the coronary sinus is dilated (Figure 12.6). Other possible sites of connection of the left SVC are the roof of the left atrium and the pulmonary venous atrium. A microbubble injection into an upper left-sided vein permits one to follow the drainage of the anomalous system. In the presence of a left SVC, the right SVC may be absent.

In the absence of an IVC, the blood from the lower half of the body is rerouted into the SVC via the azygos vein, which appears as a dilated venous channel on the right side of the spine. The hepatic veins are visualised as they exit the liver and enter separately or by way of a common hepatic vein directly into the right atrium.

Anomalous pulmonary venous connections

Access of TOE to the pulmonary venous return is excellent, with the exception of the right lower pulmonary vein, which is imaged inconsistently. In partial anomalous pulmonary venous drainage, one or two pulmonary veins drain into the systemic venous return. It is frequently associated with a sinus venosus ASD, but it occurs in up to 20% of patients with an intact interatrial septum. The right cavities exhibit echocardiographic evidence of volume overload. The most common form is the anomalous drainage of the right upper pulmonary vein into the right atrium or into the base of the SVC (Figure 12.7A).

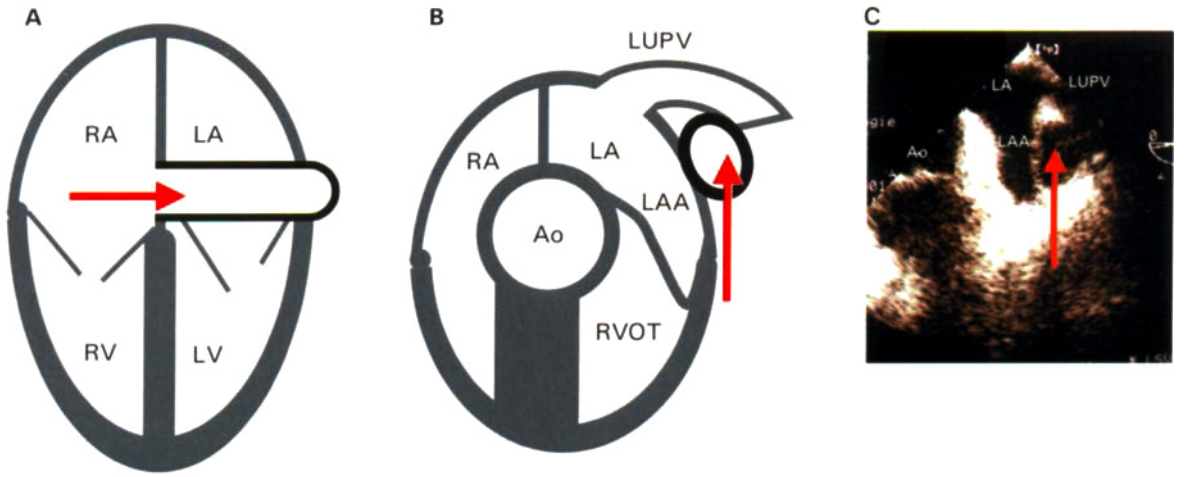

Figure 12.6 Left superior vena cava (SVC). **(A)** Enlarged coronary sinus (arrow). **(B)** Position of the left SVC (arrow) at the atrial level (transverse basal view 0°), between left atrial appendage (LAA) and left upper pulmonary vein (LUPV). **(C)** TOE image of the left SVC (arrow) on a transverse basal 0° view. Ao = aorta, LA = left atrium, RVOT = right ventricular ouflow tract.

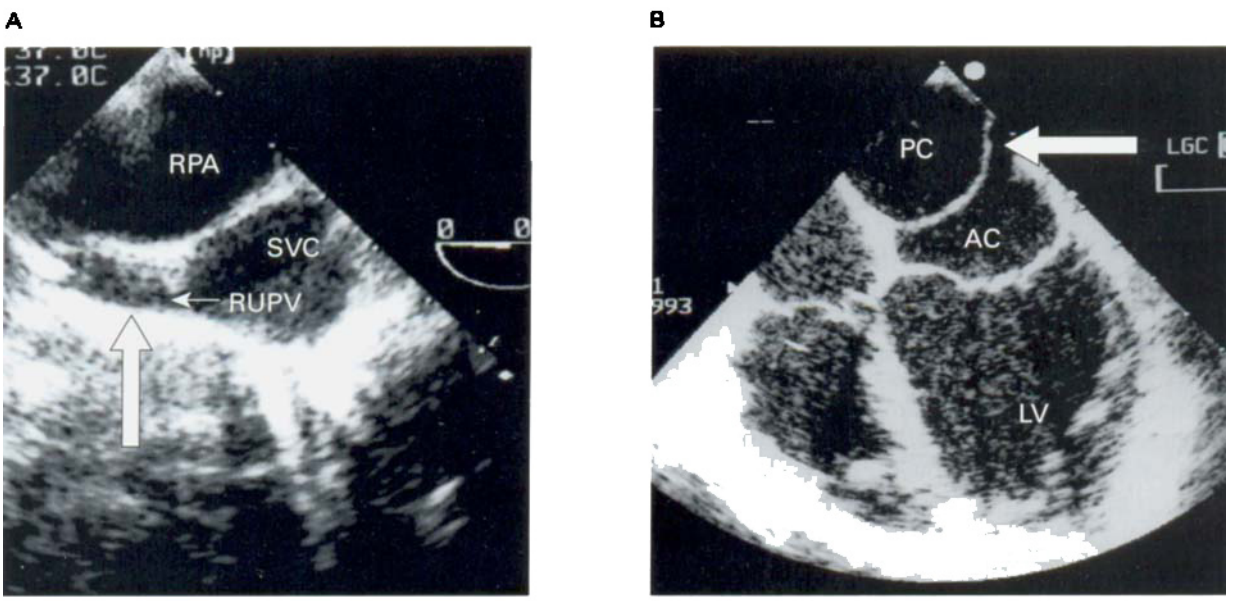

Figure 12.7 Inflow anomalies. **(A)** Partial anomalous pulmonary venous return. The right upper pulmonary vein (RUPV) drains into the superior vena cava (SVC). **(B)** Cor triatriatum sinister. A membrane (arrow) divides the left atrium into a posterior chamber (PC), collecting the pulmonary venous drainage, and an anterior chamber (AC), opening to the mitral valve. LV = left ventricle, RPA = right pulmonary artery.

After correction of caval or pulmonary venous return, demonstration of continuous aliasing flow at the level of the anastomosis is highly indicative of restriction. On the spectral display, the flow trace presents with a continuous non-phasic flow pattern and does not return to baseline between each cardiac cycle. Peak velocity of 2 m/s or greater is indicative of restriction.[34]

Cor triatriatum sinister

A fibromuscular membrane separates the left atrial chamber into a posterior compartment receiving the pulmonary veins, and an anterior compartment communicating with the mitral valve and the left atrial appendage (Figure 12.7B). The size of the communication between the posterior

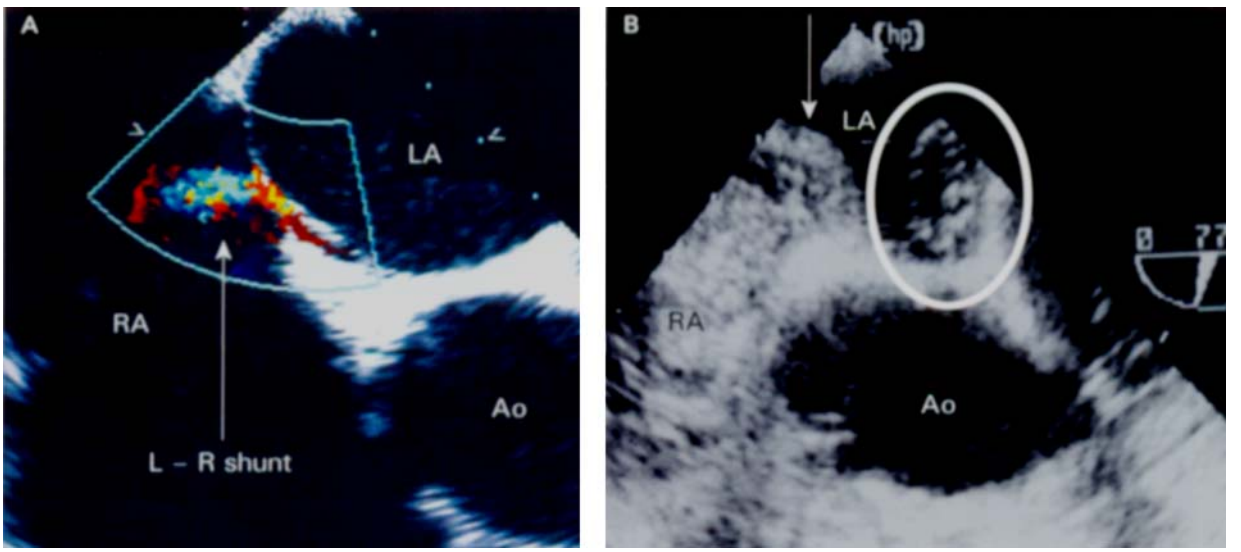

Figure 12.8 Patent foramen ovale (PFO). **(A)** 90° view of the fossa ovalis membrane, the distal part of which is not attached to the interatrial septal wall. The colour flow shows the left-to-right (L–R) shunt. **(B)** Microbubble test. Microbubbles have filled the right atrium, the interatrial septum is bulging toward the left atrium (LA; arrow), and many bubbles are visible in the LA (circle). Ao = aorta, RA = right atrium.

and anterior chambers determines the clinical picture. When the orifice is tight, the symptomatology is similar to that in mitral stenosis; the colour flow exhibits a turbulent pattern. Interatrial communications may be present between either chamber and the right atrium.

Patent foramen ovale

Patent foramen ovale (PFO) is a common finding in the adult population: its incidence varies from 5% at echocardiographic examination to 27% at autopsy.[35–38] The flap occluding the foramen ovale usually closes during the first years of life by fusion with the interatrial wall. When it only overlaps the septum on the left atrial side, the orifice may reopen if the RAP becomes greater than the left atrial pressure (LAP). The patency of the foramen ovale is best demonstrated in a longitudinal plane (90°). The bidimensional image of PFO should be confirmed by colour flow and contrast studies (Figure 12.8). Injection of microbubbles, which is best performed into a central line, must be synchronous with the release of endothoracic pressure.[39] The normal pressure gradient between the atria is reversed, and the bubbles, even in small number, appear in the left cavities during the next four systoles;[40] they are best observed near the roof of the left atrium and in the ascending aorta. If their appearance is delayed by five cardiac cycles or more, then this is caused primarily by transpulmonary passage. The test is considered positive when more than five bubbles cross the septum during a single cardiac cycle.

Atrial septal defect

ASDs account for 7% of all congenital heart disease and for 30% of congenital heart disease in the adult population; in the latter group it is the second most common congenital defect.[41] The interatrial septum may present with four types of defect (Figure 12.9):

- ostium secundum: defect at the level of the fossa ovalis, accounting for 69% of cases
- sinus venosus: associated with an abnormal caval or pulmonary venous connection
- coronary sinus defect: unroofing of the coronary sinus into the left atrium
- ostium primum: defect in the AV septum.

The volume overload due to the mostly left-to-right shunt induces a dilation of the right atrium, a dilated hypertrophy of the right ventricle, and an increase in size of the PA (Figure 12.10D). In the basal short-axis view the diameter of the PA is greater than that of the aorta, and the flow velocity is increased in PA and pulmonary veins. A tricuspid regurgitation is frequently present.

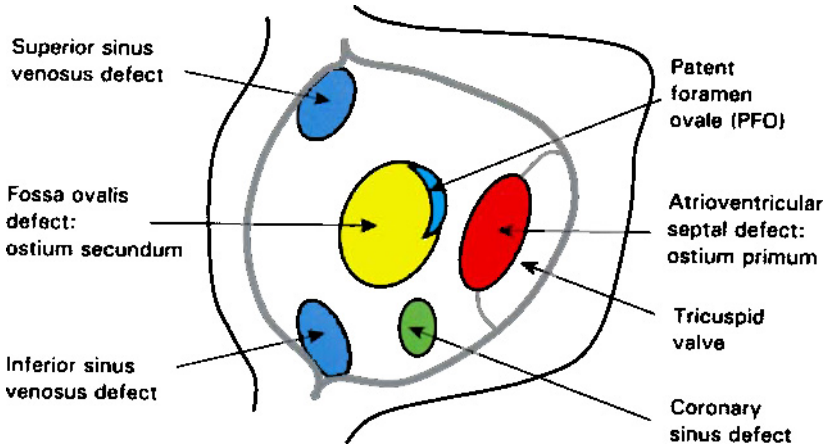

Figure 12.9 Atrial septal defects. The view of the interatrial septum is taken from the right atrium; the different types of atrial septal defect are depicted.

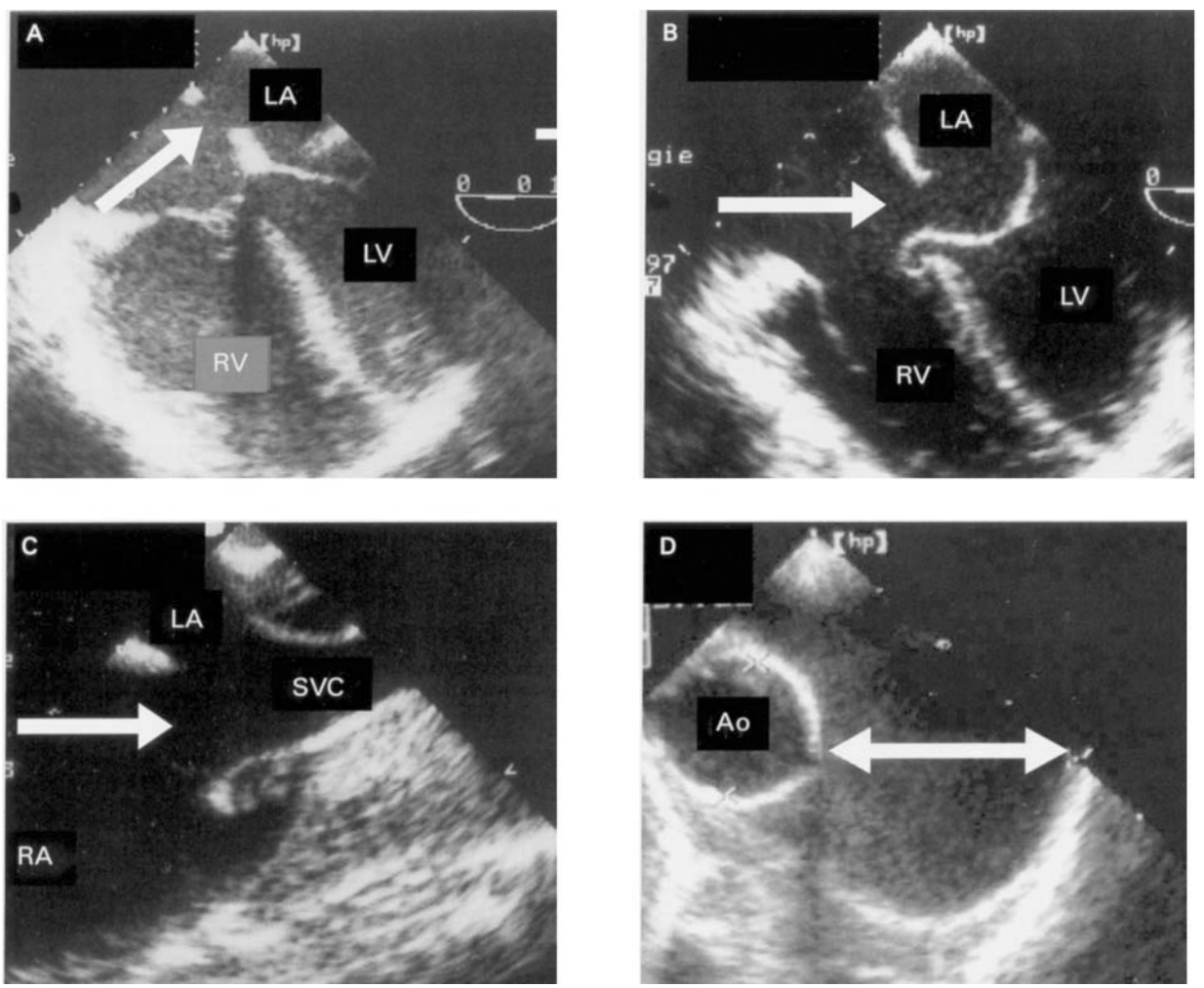

Figure 12.10 Atria septal defects. **(A)** Ostium secundum defect (arrow) in the middle part of the septum; the right ventricle (RV) is enlarged. **(B)** Ostium primum defect (arrow), contiguous to the tricuspid annulus. A curled portion of the septal leaflet of the tricuspid valve is occluding a small ventricular septal defect (atrioventricular canal). **(C)** Sinus venosus defect close to the superior vena cava (SVC; 90° plane). **(D)** Enlargement of the pulmonary artery, the diameter of which is 1·5 times the diameter of the ascending aorta (Ao). LA = left atrium, LV = left ventricle, RA = right atrium.

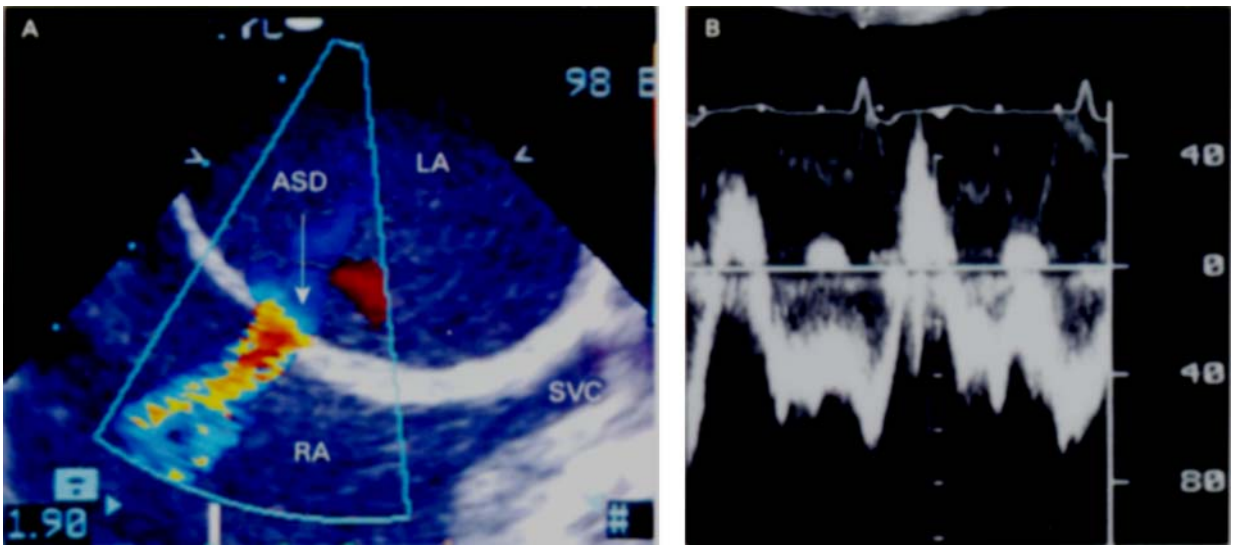

Figure 12.11 Atrial septal defect (ASD) flow. **(A)** Colour flow through an ASD (left-to-right shunt). **(B)** Pulsed wave Doppler spectral display of the ASD flow. Although the flow is predominantly left-to-right (below baseline), there are two right-to-left components (above baseline) – one during systole and one during diastole. LA = left atrium, RA = right atrium, SVC = superior vena cava.

The orientation and the position of the septum renders TOE an important tool in the investigation of ASD.[42] The defect appears as discontinuities or areas of focal dropout in the normal linear band (Figure 12.10). The edges of the defect are usually of increased echogenicity, except in fenestrated defects. Ostium primum and secundum defects are best identified in the retrocardiac transverse plane (0°), whereas sinus venosus defects, like the entry site of the pulmonary veins, are better detected in longitudinal basal imaging (90–110°).[6,43]

Doppler analysis is mandatory for confirmation of the diagnosis. Colour flow mapping is very sensitive and is useful for distinguishing between a true defect and an artefactual echo dropout; it appears as a bright continuous systolo-diastolic flow (Figure 12.11). The caval flow may be confused with an interatrial shunt, particularly when it is made turbulent by a prominent Eustachian valve. The optimal flow velocity recordings are obtained with the pulsed Doppler sample volume positioned immediately distal to the orifice. Because the pressure difference between atria is small, the V_{max} through the shunt is low, in the 0·5–1·5 m/s range. A V_{max} greater than 2 m/s is indicative of a restrictive defect. The volume overflow through the right heart increases the blood velocities through the tricuspid valve and PA. The normal ratio of 0·6 between right and left heart velocities is more than doubled.

Spectral Doppler reveals the cyclic flow pattern of the shunt. Variations are related to the cardiac cycle and to respiration. There is a typical biphasic left-to-right flow; one peak of flow occurs during late systole and early diastole ("v" wave), and one peak occurs during the atrial contraction ("a" wave). A short period of right-to-left shunt can usually be recorded during early systole and mid-diastole.[44,45] This flow pattern is consistent with the instantaneous cyclic pressure differences between left and right atria (Figure 12.12).[46] The most important shunt reversal is observed in proto-systole when the mitral annulus descent abruptly increases the left atrial volume and therefore decreases its pressure.[47] The pressure gradient between atria is modified by ventricular compliance and distensibility, by systemic and pulmonary venous capacitance, and by AV regurgitation.

The right-to-left component of shunt flow is increased when RAP is higher than LAP; this happens when the intrathoracic pressure drops suddenly (increased venous return to the right atrium and decreased venous return to the left atrium), as occurs during spontaneous inspiration, the relaxing phase of a Valsalva manoeuvre, or during a Mueller manoeuvre.[48] The RAP increases when the afterload of the right ventricle is elevated or during intermittent positive pressure ventilation or positive end-expiratory pressure (> 15 cmH_2O; Figure 12.13). With a large ASD, the longstanding pulmonary overflow increases progressively the

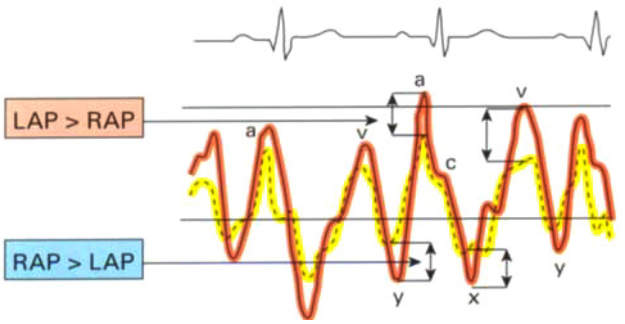

Figure 12.12 Simultaneous recordings of the right atrial pressure (RAP) and the left atrial pressure (LAP). The amplitude of the pressure variations is greater in the left atrium than in the right atrium; LAP is greater than RAP during "a" and "v" peaks of pressure, but lower during nadirs of pressure "x" and "y". This fact accounts for the two right-to-left components of the shunt. (Adapted from Bettex and Chassot.[48])

RV afterload. A pressure overload is added to the well-tolerated volume overload. The pulmonary hypertension increases the R-L component of the shunt, and the patient might become hypoxemic.

A residual shunt can be observed after surgical repair of an ASD or a PFO. This raises two critical questions: how large is the shunt and is a reoperation indicated? Minimal residual shunting across the suture line, appearing as a small flame-like jet, may be found and is without significance; it frequently disappears with protamine injection. A large dehiscence is an indication for immediate surgical revision. Contrast study and blood oxymetry may help to determine the difference.

Atrioventricular canal

Endocardial cushion defect is a lack of central septation of the heart. In the complete form, the AV canal presents with a large ostium primum ASD, a large ventricular septal defect (VSD) extending anteriorly into the membranous septum, and a five leaflet AV valve surrounding the common orifice (Figure 12.14).[49] The posterior leaflet of the mitral valve makes up less than one-third of the annulus (normally two-thirds); the septal anterior leaflet is made of two components separated by a mitral cleft, and may be attached to both right and left ventricles. The inferolateral and anterosuperior leaflets of the tricuspid valve are normal, but the septal leaflet is divided into two parts joining the mitral cleft. The tricuspid and the mitral valves appear inserted at the same level on the septum in the four chamber view

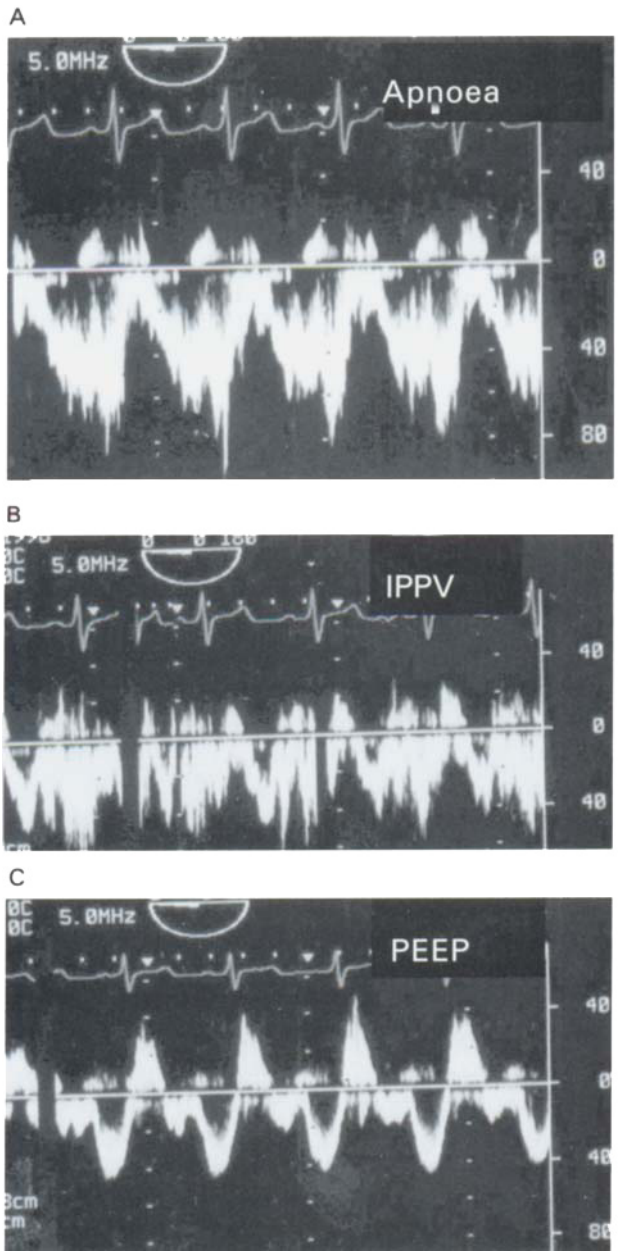

Figure 12.13 Atrial septal defect (ASD) shunt flow modifications with different ventilatory patterns. **(A)** Apnoea. The shunt is almost exclusively left-to-right. **(B)** With intermittent positive pressure ventilation (IPPV), the right-to-left component becomes significant. **(C)** With 15 cmH_2O positive end expiratory pressure (PEEP), both components are almost equal.

(see Figure 12.2). The colour flow is composite and may take various configurations: shunt between left and right atria, shunt between left and right ventricles, shunt between left ventricle and right atrium, or mitral or tricuspid regurgitation.

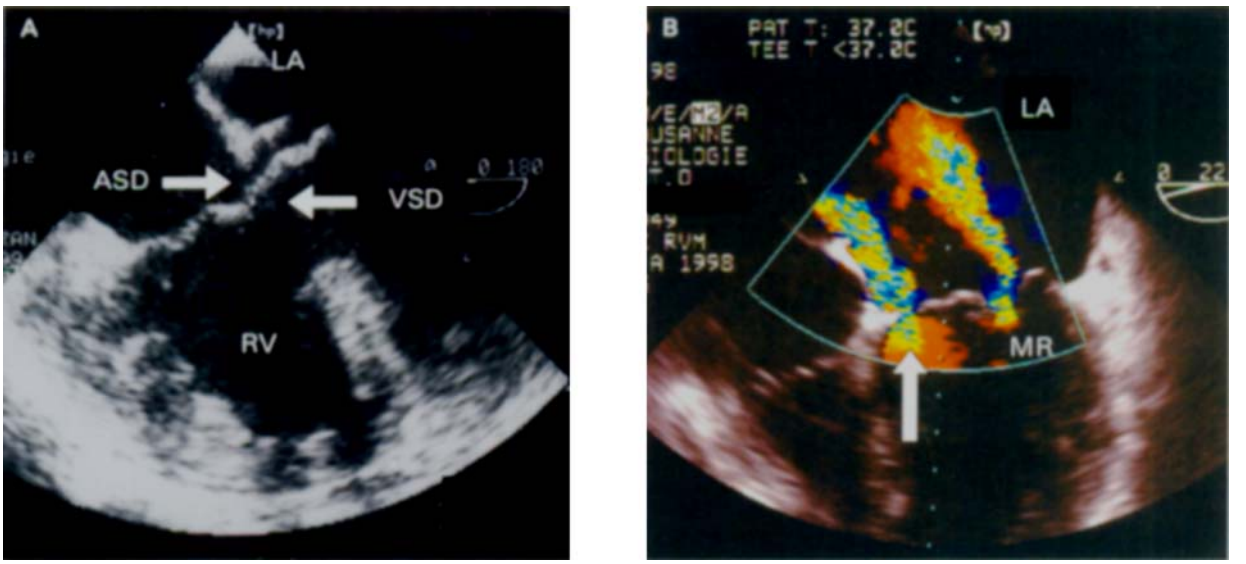

Figure 12.14 Atrioventricular (AV) canal defect (or endocardial cushion defect). **(A)** The ostium primum defect (ASD) is accompanied by a membranous ventricular septal defect (VSD); both mitral and tricuspid leaflets are inserted at the same level. **(B)** Regurgitant flow through the mitral cleft of an AV canal (arrow), which is distinguishable from the mitral commissural regurgitation (MR). LA = left atrium, RV = right ventricle.

The surgical correction of AV canal consists of ASD and VSD closure, with or without patch, and AV valve repair. The postoperative echocardiographic assessment should address the competence of the AV valve and search for residual septal defects or LVOT obstruction. Small jets of AV regurgitation or residual shunts are frequently encountered after correction of the AV canal; they mostly disappear after protamine administration and haemodynamic stabilisation. The dense and echogenic prosthetic material shields the right cavities on retrocardiac imaging. Deep transgastric transverse and longitudinal planes offer better views for finding jets from residual shunt and for measuring LVOT flow velocity. Contrast echocardiography often allows better semiquantification of residual shunts than do colour flow studies. A small amount (2–5 ml) of normal saline is injected under pressure by the surgeon into the left atrium. Cross-sectional images of the aorta and the RVOT are obtained in the short-axis view, and the relative amount of contrast on each side is evaluated. If the density of contrast in the right ventricle is more than 50% of the density in the left ventricle, then the patch must be surgically completed.[50]

Ebstein's anomaly

Ebstein's anomaly is characterised by an apical displacement by more than 10 mm of the insertion of the tricuspid leaflets from the tricuspid annulus into the right ventricle; the septal and posterior leaflets are most commonly involved and progressively exhibit impaired mobility because of chordae shortening, tethering, or fibrosis (Figure 12.15). The right ventricular cavity is smaller, and its inlet portion is atrialised; the right atrium is enlarged. The tricuspid valve may be regurgitant, stenotic, or both. There is a poor correlation between the morphological findings and the resultant severity of the lesion.[51]

TOE findings with potential implications for surgical repair include leaflet size and mobility, presence or absence of restriction, and size and function of the right ventricle. After surgical repair, the examination includes measurement of tricuspid anterograde flow velocity, looking for possible restriction (acceptable mean gradient < 5 mmHg); quantification of residual regurgitation; and evaluation of right ventricular function.

Congenital lesions of the mitral valve

The mitral valve orifice can be separated in two smaller orifices of equal or unequal size by a bridge of tissue, creating a stenotic or incompetent valve. It is a rare anomaly and sometimes without any clinical significance. The congenital mitral stenosis is a developmental abnormality of mitral leaflets, commissures, annulus, interchordal spaces,

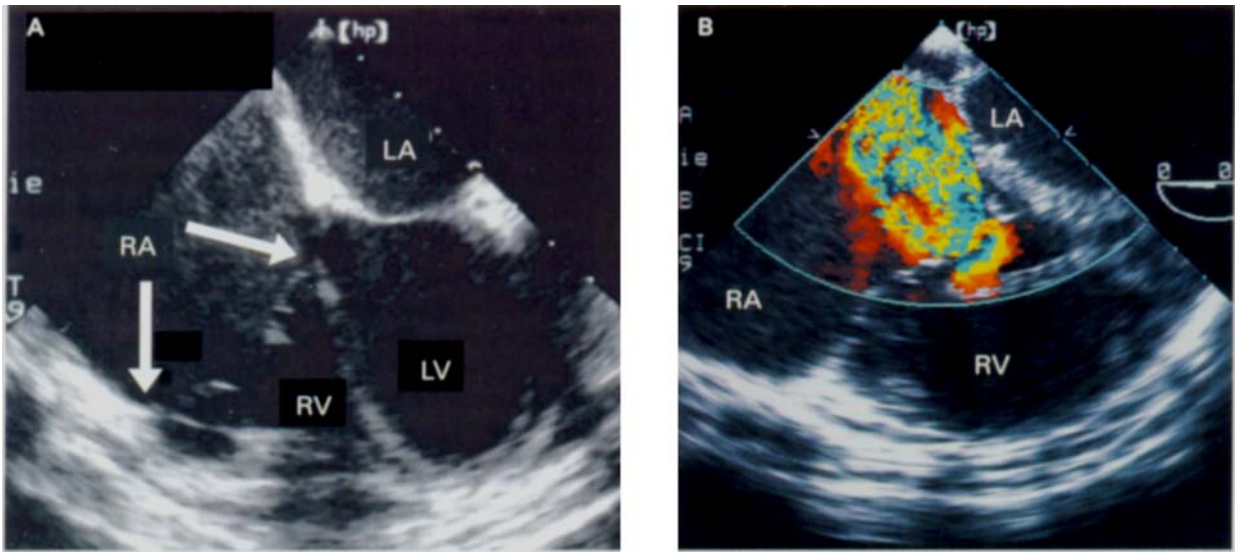

Figure 12.15 Ebstein's anomaly. **(A)** Four chamber view, with posterior and septal leaflets of the tricuspid valve (arrows) inserted low inside the right ventricular cavity. The right ventricle (RV) is decreased in size, whereas the right atrium (RA) is very large, because of the atrialisation of the right ventricular inlet. **(B)** Severe tricuspid regurgitation through the low inserted tricuspid valve. LA = left atrium, LV = left ventricle.

or papillary muscles that produce obstruction to left ventricular filling.[52] The typical stenosis consists of hypoplasia and thickening of the valve leaflets; the orifice is smaller and often eccentric. In the parachute mitral valve, the chordae from both leaflets insert into a single papillary muscle, usually causing a mitral stenosis with or without regurgitation.

Intraoperative examination after valve repair must exclude significant residual regurgitation; however, its quantification remains complex. The usual criteria of acceptable residual mitral regurgitation (grade < 2) should be used with caution in congenital heart defects and viewed within the context of the patient's global haemodynamic status. Regurgitation that occurs only during early systole and is highly dependent on loading conditions can be ignored. The decision to attempt further repair depends on the anatomy of the valve, understanding of the mechanism of regurgitation, feasibility of repair, and the patient's global haemodynamic status.[53]

Ventricular septal defects

VSDs represent 10% of cases of congenital heart disease in adults. The interventricular septum is normally concave toward the left ventricle on the short-axis plane, but it has a complex twisted crescent shape on the longitudinal plane. It is mainly muscular, with the exception of a small membranous segment located at its superior border just beneath the right and non-coronary cusps of the aortic valve. The defect can be present in four different parts of the interventricular septum (Figure 12.16):

- membranous or perimembranous VSD (68% of all cases; Figure 12.17): it can be progressively closed by marked septal hypertrophy surrounding the defect or by redundancy of tricuspid valve septal leaflet[54]
- inlet VSD is part of an endocardial cushion defect (see Figure 12.14): it appears between the mitral and tricuspid leaflets
- supracristal VSD, immediately below the pulmonary valve: infundibular or doubly committed subarterial defect
- muscular VSD: these are less frequent among congenital defects – up to 40% close spontaneously during the first years of life (see Figure 12.17).

There are four clinical groups of adult patients: those with spontaneously or surgically closed VSD and no shunt; those with a small VSD, small shunts, and normal pulmonary pressures; those with a moderate shunt and slightly elevated pulmonary pressure; and those with large shunts and

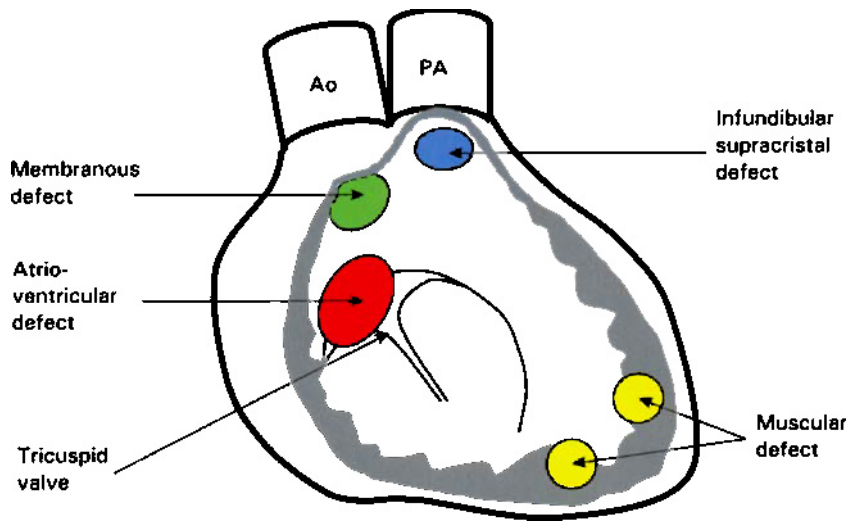

Figure 12.16 Ventricular septal defects. The view of the interventricular septum is taken from the right ventricle. The most common congenital ventricular septal defects are situated close to the right ventricular outflow tract. Ao = aorta, PA = pulmonary artery.

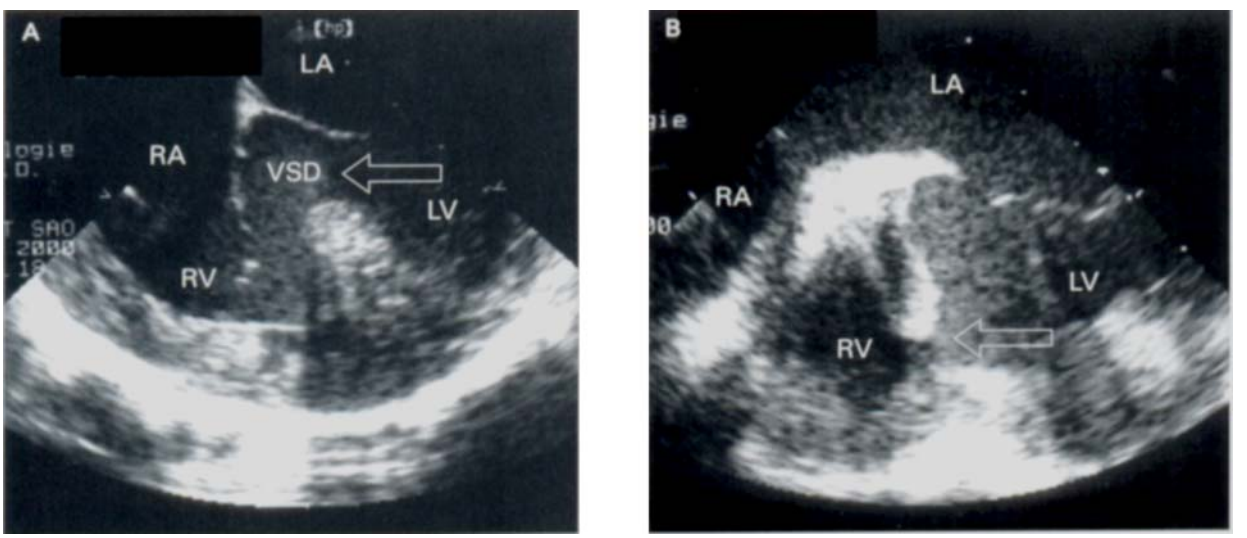

Figure 12.17 Ventricular septal defects (VSDs). **(A)** Perimembranous VSD. **(B)** Large clear-cut muscular VSD. This image is unusual, with most VSDs being oblique and trabeculated. LA = left atrium, LV = left ventricle, RA = right atrium, RV = right ventricle.

Eisenmenger's syndrome. The latter syndrome is defined as a shunt reversal caused by severe or progressive pulmonary hypertension.

Multiple echocardiographic sections are required to locate the position of a VSD and to identify the relationship of the defect with the central fibrous part of the septum, the arterial valves, and the AV valves. The PA is dilated because it is the receiving chamber for the shunted flow; left sided cavities are enlarged because of volume overload. The most frequent congenital VSDs are located close to the RVOT; the blood ejected by the left ventricle almost directly into the PA bypasses the right ventricular cavity, which may remain normal.

In the transverse plane, the membranous part is almost parallel to the ultrasound beam; a false positive echo dropout may be created. The defect is better identified on the longitudinal plane. The perimembranous VSD has a superior margin formed by fibrous continuity between the AV valves or between an AV valve and an arterial valve. A common feature of the perimembranous defect is the presence of tissue tags derived from

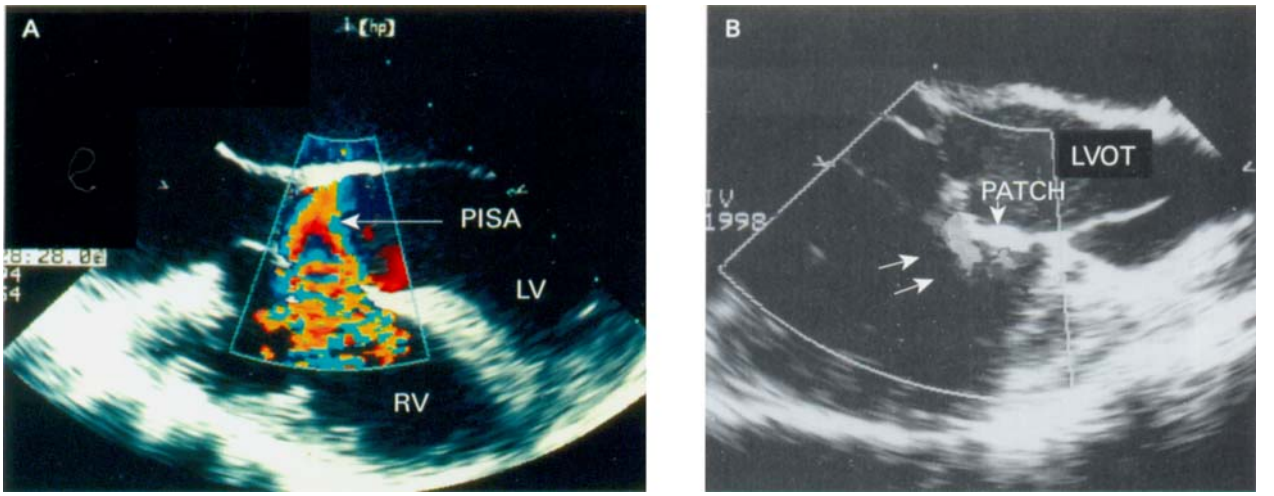

Figure 12.18 Ventricular septal defect flow. **(A)** The colour flow shows the left-to-right shunt. The convergence acceleration zone on the left ventricular side creates a proximal isovelocity surface area (PISA), which is typical of a high velocity shunt. **(B)** Small non-significant residual shunt after correction of a ventricular septal defect with a prosthetic patch. LV = left ventricle, LVOT = left ventricular outflow tract, RV = right ventricle.

the tricuspid valve, which may partially close the defect and create an aneurysm of the septum. Overriding and straddling of an AV valve are uncommon but have important surgical implications. The characteristic feature of a supracristal defect is a superior margin formed by the fibrous continuity between both arterial valves. A prolapse of the right coronary cusp of the aortic valve is often present and may produce aortic incompetence. It is better delineated in the longitudinal plane.

The trabecular muscular VSDs are mostly antero-apical and less well visualised. In the four chamber view the apex is truncated; to profile the apical septum better, the probe should be advanced deep into the fundus of the stomach and strongly retroflexed. Trabecular VSDs are mostly serpentiginous and rarely appear as a loss of continuity on the bidimensional image. Occasionally, the septum may contain multiple sieve-like fenestrations (Swiss cheese septum). Colour flow mapping will reliably identify the defect by imaging the characteristic systolic, or both systolic and diastolic, flow jet within the right ventricle, and by visualising the flow convergence area on the left ventricular side (Figure 12.18); the dimension of the proximal converging flow field is a good estimate of the size of the VSD.[55] With high volume left-to-right shunts these colour images appear both during systole and diastole, whereas the shunt flow is recorded only during early systole in small muscular VSDs. When the jet is properly aligned with the continuous wave Doppler beam, the systolic pressure difference between right and left ventricles can be calculated from the jet V_{max} using the Bernoulli equation. In the absence of aortic or subaortic pathology, the subtraction of the pressure gradient (ΔP) from the peripheral systolic blood pressure (BP_s) gives an accurate assessment of right ventricular systolic pressure (RVP_s):

$$RVP_s = BP_s - \Delta P$$

Minimal residual shunting across the suture line of the patch, appearing as small flame-like jets, are frequently found after surgical repair of a VSD and are without significance; only large dehiscence of the patch is an indication for immediate surgical revision (see Figure 12.18). The area of the orifice between the ventricles can be estimated by the diameter of the colour flow jet through the septal wall; defects less than 2 mm in diameter are usually considered non-significant,[6] whereas those that are greater than 3 mm require an immediate redo.[56] The presence of a flow convergence zone in the upstream chamber is a reliable sign of significant residual shunt. Unfortunately, the extent of the VSD jet into the right ventricular cavity is difficult to appreciate because of ultrasound attenuation by prosthetic material. Simultaneous occurrence of a RVOT

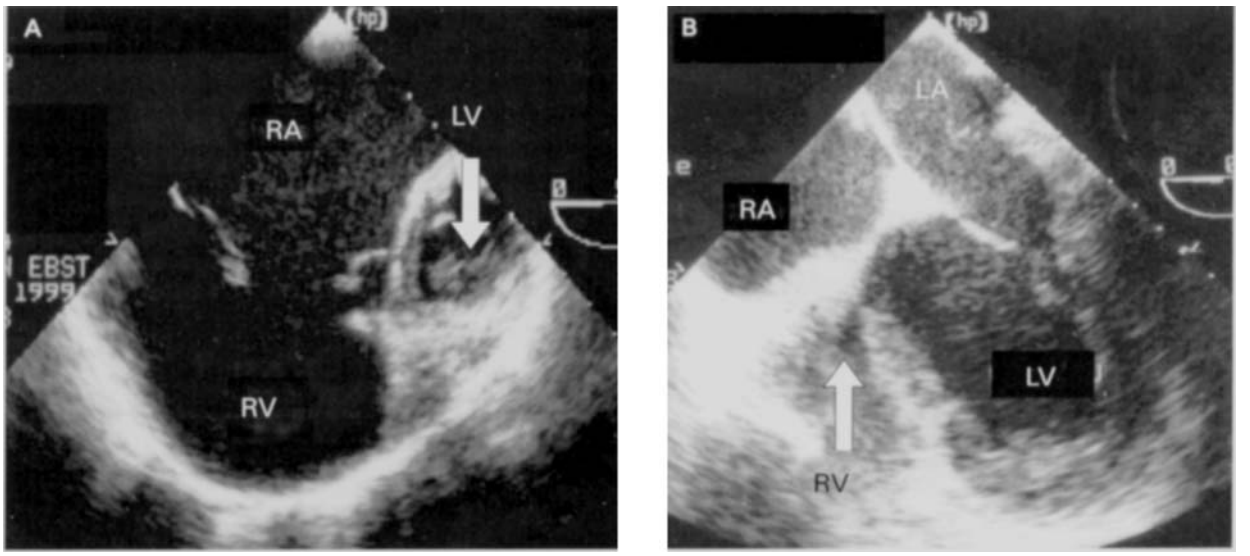

Figure 12.19 Hypoplastic ventricles. **(A)** Hypoplastic left ventricle (LV), appearing as a small posterior chamber. **(B)** Hypoplastic right ventricle (RV). The rudimentary RV is positioned anteriorly. The tricuspid valve is atretic. LA = left atrium, RA = right atrium.

obstruction may also induce turbulence in the right ventricular cavity. If doubt exists, then a contrast study through the left atrium can be conducted.[50] An assessment of the tricuspid valve is important because tethering of the septal leaflet is possible during perimembranous VSD closure. The right coronary cusp of the aortic valve should be checked for the same reason.

Hypoplastic right/left heart syndromes

The ventricular segment may present with variable degrees of hypoplasia and marked asymmetry, even the absence of one ventricle (univentricular heart). An anteriorly positioned accessory chamber is a rudimentary right ventricle, whereas a posteriorly positioned one is a remnant of the left ventricle (Figure 12.19). The degree of morphological alteration of the main chamber – more or less circular – is a useful predictor of postoperative ventricular function.[57] Shunting at the atrial level is crucial for survival. Children with hypoplastic ventricles do not survive into adulthood without palliative surgery. Various operations have been designed to correct these anomalies. They lead to special haemodynamic situations.

The Fontan operation consists of rerouting the systemic venous flow directly into the PA; this can be achieved using a wide range of procedures, such as end-to-side anastomosis of the SVC to the right PA (Glenn procedure), atriopulmonary connection, and/or interposition of a conduit between systemic venous return and pulmonary circulation (Figure 12.20).[58] Critical issues in these reconstructions are adequacy of the pulmonary bed, low PA resistances, AV valvular competency, and systemic ventricular function. The pulmonary flow drive relies entirely on the gradient between central venous pressure and LAP, which should be in the range 5–8 mmHg. A slightly turbulent flow at the site of the anastomosis or in the receiving pulmonary vessel may be found, as well as small retrograde diastolic and turbulent flow in the main pulmonary trunk.

The pulsed wave Doppler flow profile through the venopulmonary anastomosis or in the conduit exhibits a biphasic forward pattern of moderate velocity (0·2–0·5 m/s), which reaches the baseline between each cardiac cycle.[59,60] A higher flow velocity (> 1·5 m/s), without cyclic variations and not reaching baseline during the cardiac and/or respiratory cycle, is suggestive of a significant obstruction.[50] Documentation of only to-and-fro flow within a pulmonary vein is highly suggestive of diminished or absent blood flow within the corresponding PA.[61] The flow pattern is highly dependant on respiration. To be accurate, the Doppler studies must be obtained during spontaneous breathing or apnoea. Flow attenuation or even reversal has been demonstrated during the positive pressure phase of intermittent positive

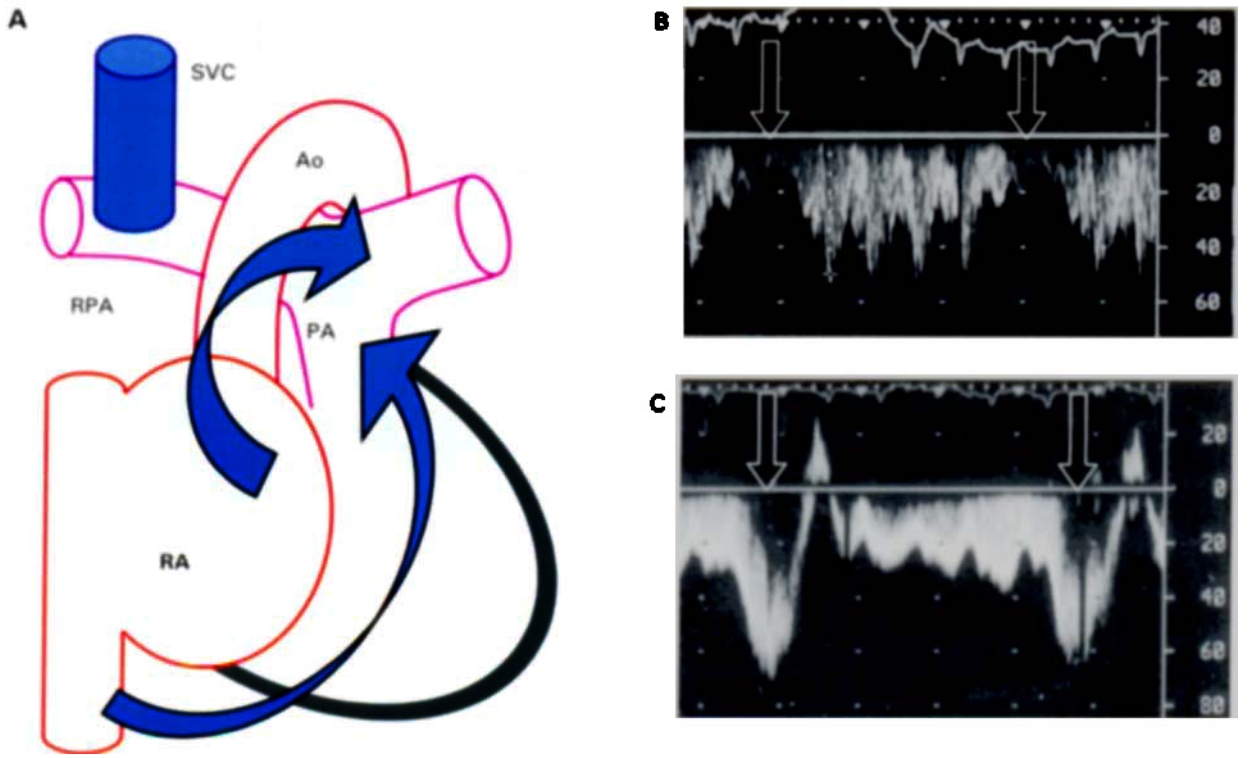

Figure 12.20 Fontan procedures. **(A)** Schematic drawing of the right ventricular bypass by the Glenn procedure (superior vena cava [SVC] to right pulmonary artery [RPA] anastomosis) and the Fontan reconstructions (anastomoses or conduits between the right atrium [RA] or the inferior vena cava and the main pulmonary artery [PA]). **(B)** The flow through a Fontan conduit is similar to a central vein flow; it is highly dependent on the systemic venous pressure. During intermittent positive pressure ventilation, it is interrupted when the intrathoracic pressure raises with each mechanical inspiration. **(C)** In spontaneous respiration the flow is increased during inspiration when the negative intrathoracic pressure aspirates blood into the PA. Ao = aorta.

pressure ventilation.[62] Under those circumstances, TOE may be used to manage properly the ventilatory pattern of the patient. A chronic low flow through the Fontan circulation may induce blood stagnation with spontaneous contrast and thrombus formation in the right atrium.

Tetralogy of Fallot and pulmonary stenosis/atresia

Tetralogy of Fallot (TOF) is the third most common lesion encountered in adults. Although TOF comprises four anomalies (VSD, RVOT stenosis, overriding aorta, and right ventricular hypertrophy), the basic abnormality is under-development of the right pulmonary infundibulum; malalignment and deviation of the parietal band result in an obstruction to pulmonary outflow and in a large subaortic VSD.[63] The right ventricular hypertrophy is secondary to the increased afterload. The subvalvular muscular narrowing has an important dynamic component; it is associated with variable degrees of pulmonary valvular stenosis and thickening, and hypoplastic pulmonary arteries. The aortic valve is enlarged and competent in children, but progressive aortic dilation may occur with ageing, mostly in unoperated patients, leading to some degree of aortic regurgitation. In 25% of cases a secundum ASD creates a pentalogy. Patients who survive into adulthood have either a mild degree of pulmonary flow restriction or a pulmonary blood flow maintained through multiple aortopulmonary collaterals originating anywhere in the thoracic arterial system.

In the transverse mid-oesophageal plane, the large aortic valve is a striking feature. It opens to both ventricles by a large subaortic defect located between the right and non-coronary cusps (Figure 12.21). The blood flows through the VSD from both ventricular chambers toward the aorta; there is no clear-cut shunt from the left ventricle

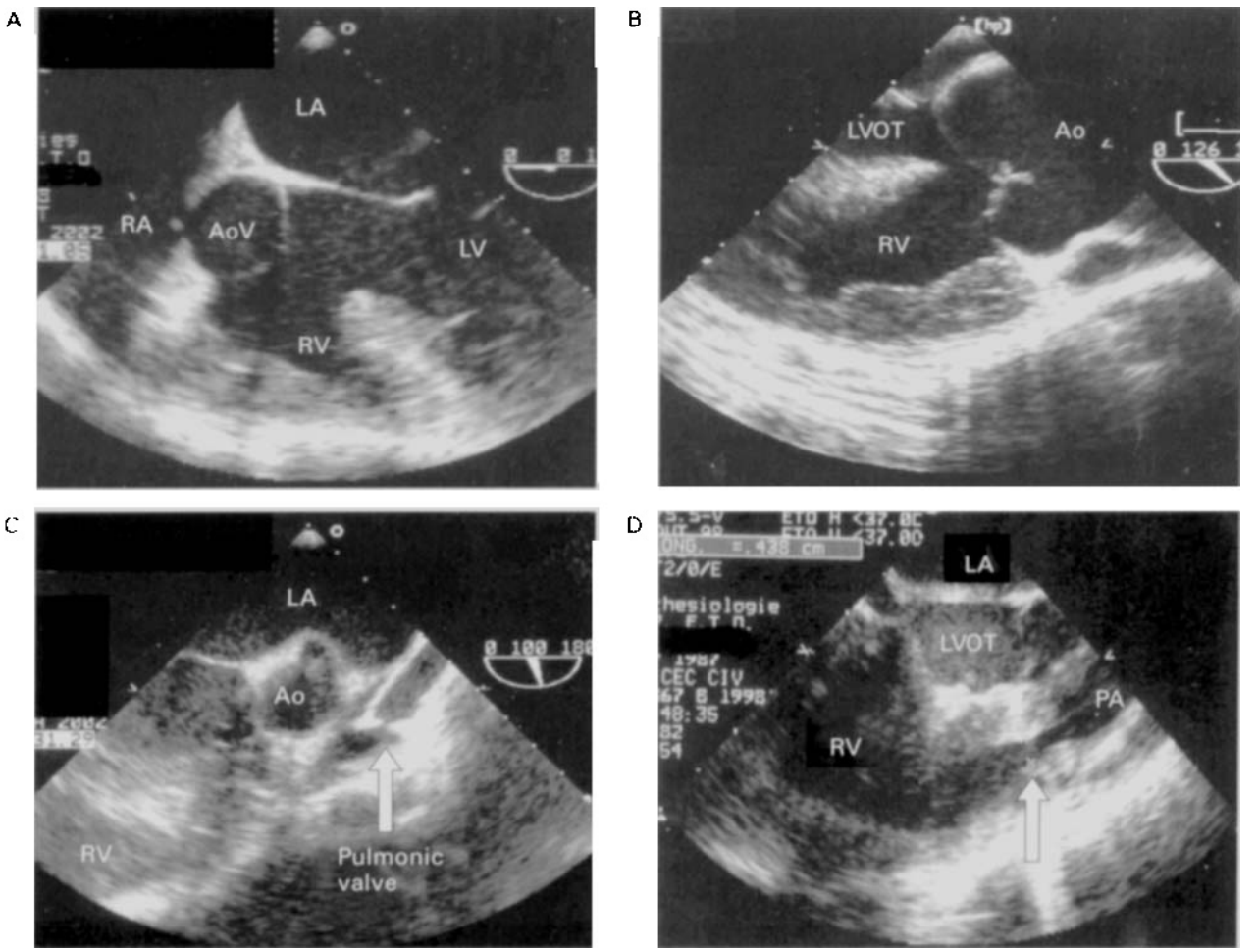

Figure 12.21 Tetralogy of Fallot. **(A)** Large membranous ventricular septal defect with overriding aorta (0° view). **(B)** Aorta overriding the ventricular septal defect at 120° view. **(C)** Atretic pulmonary valve and artery, with hypertrophied right ventricle (RV). The pulmonary flow is maintained by large aortopulmonary collaterals. **(D)** Right ventricular hypertrophy with muscular stenosis of the right ventricular outflow tract (arrow). Ao = aorta, LA = left atrium, LVOT = left ventricular outflow tract.

to the right. The RVOT is best visualised in mid-oesophageal view from 60° to 110°, but the flow direction is best aligned with the ultrasound beam in deep transgastric views. With colour Doppler, an intense turbulent flow with aliasing is demonstrated at the stenotic area; it might be at subvalvular level (dynamic or membranous stenosis), at the valvular level (fibrosis and stenosis of the pulmonary valve), or in the pulmonary tree (combined stenoses and membranes). Usually, the maximal velocity (3 m/s) peaks in early systole in case of fibrous stenosis, whereas it appears later in systole in cases of dynamic muscular obstruction.

Some degree of pulmonary stenosis is found in 10% of adult patients with congenital heart disease.[64] If major collateral arteries can preserve a sufficient pulmonary flow, then children with severe pulmonary stenosis or atresia can survive until adolescence or adulthood. Anatomically, the image is close to that of a TOF. In order to maintain enough pulmonary flow, many patients have undergone surgically implemented shunts in infancy. With colour Doppler, these shunts appear as continuous systolo-diastolic aliasing flow images in the posterior mediastinum; they can sometimes be traced from aorta to pulmonary vessel.

Surgical correction of the TOF consists of patching the VSD and enlarging the RVOT and PA. When necessary, a valved conduit is placed from the right ventricle to the main PA. After total correction, the presence of residual left-to-right shunt at the margins of the patch must be sought. Systolic turbulences in the RVOT may be caused

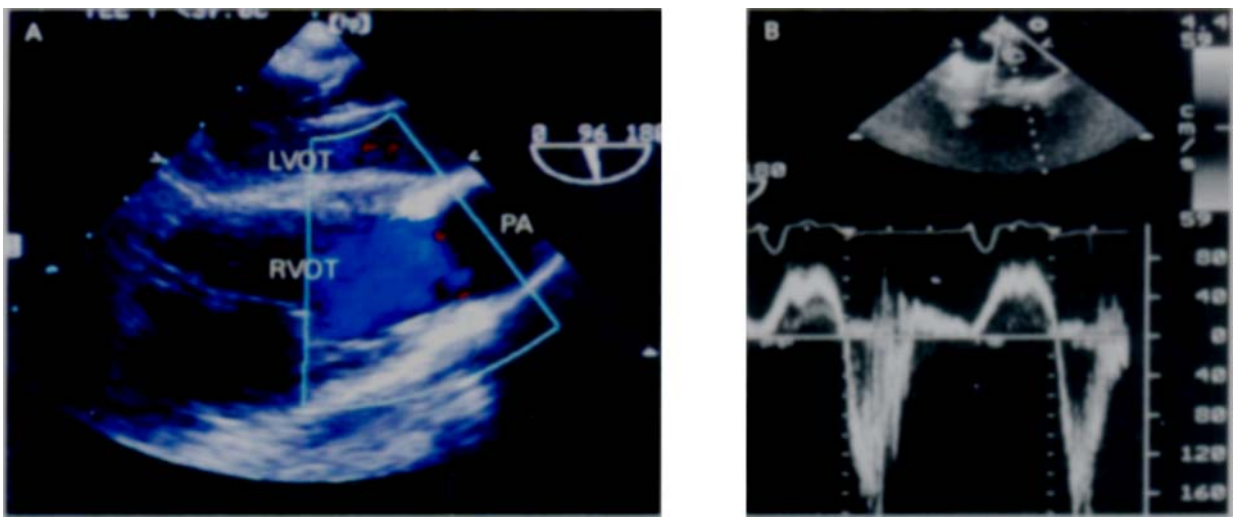

Figure 12.22 Pulmonary regurgitation after correction of tetralogy of Fallot in childhood. **(A)** dilation of right ventricle (RV) and right ventricular outflow tract (RVOT) with massive pulmonary valve regurgitation (blue flow). **(B)** Flow in the pulmonary artery (PA; basal 0° view). The severe pulmonary regurgitation leads to a massive backflow during diastole (below the baseline). LVOT = left ventricular outflow tract.

by residual outflow obstruction, and not just by shunt flow. Patching the pulmonary valve annulus induces a regurgitation proportional to the relief of obstruction. The surgical result is therefore a compromise between minimal regurgitation and some residual gradient. Assessment of residual stenosis is based on colour Doppler flow during mid-systole and on gradient measurement with continuous Doppler. With a retrocardiac or transgastric probe position, it is possible to interrogate the peak flow velocity of the PA or conduit; a peak gradient up to 20 mmHg is considered as normal. V_{max} greater than 3 m/s and gradients above 40 mmHg indicate significant stenosis.[6] The maximal gradient may represent an overestimation due to pressure recovery in the case of a tubular narrowing or due to an associated pulmonary regurgitation. The finding of a moderate or severe organic fixed obstruction that could easily be resected favours immediate revision, but dynamic obstructions are more difficult to evaluate. They are likely to resolve completely during the early postoperative period with re-equilibration of loading conditions and sympathetic tone. On the other hand, the dynamic obstruction arising at the entrance of ventriculo-arterial conduits are due to systolic occlusion of the anastomosis, and do not improve spontaneously.[50]

Some degree of pulmonary regurgitation is present in the majority of patients. It is important to quantify this pulmonary regurgitation; it is the single most important factor determining the degree of right ventricular dilation and performance with time.[65] In adult cases that were corrected during childhood the pulmonary regurgitation can become the main pathology; when pulmonary regurgitation becomes severe, the right ventricle sustains a volume overload, dilates, and finally fails (Figure 12.22). In the absence of residual shunt, the right ventricular systolic pressure can be assessed through the tricuspid regurgitation jet.

Left ventricular outflow tract obstruction

Stenosis of the LVOT can be dynamic or static. In the former, the situation is analogous to the dynamic obstruction of hypertrophic idiopathic subaortic stenosis. On two-dimensional images, the outflow tract appears hypertrophied and the channel is obviously narrowed. On Doppler analysis the velocity peaks in late systole. In the latter case, a fixed membrane is visible in the middle of the outflow tract as a more or less circular fibrous thickening; this ridge or diaphragm of fibromuscular tissue extends from the interventricular septum to the anterior leaflet of the mitral valve (Figure 12.23). A turbulent flow appears below the valve, which is frequently hypoplastic. Both pathologies may accompany a stenosis or regurgitation of the valve itself. The velocity can be recorded using continuous Doppler from a deep transgastric view at 0° or 120°.

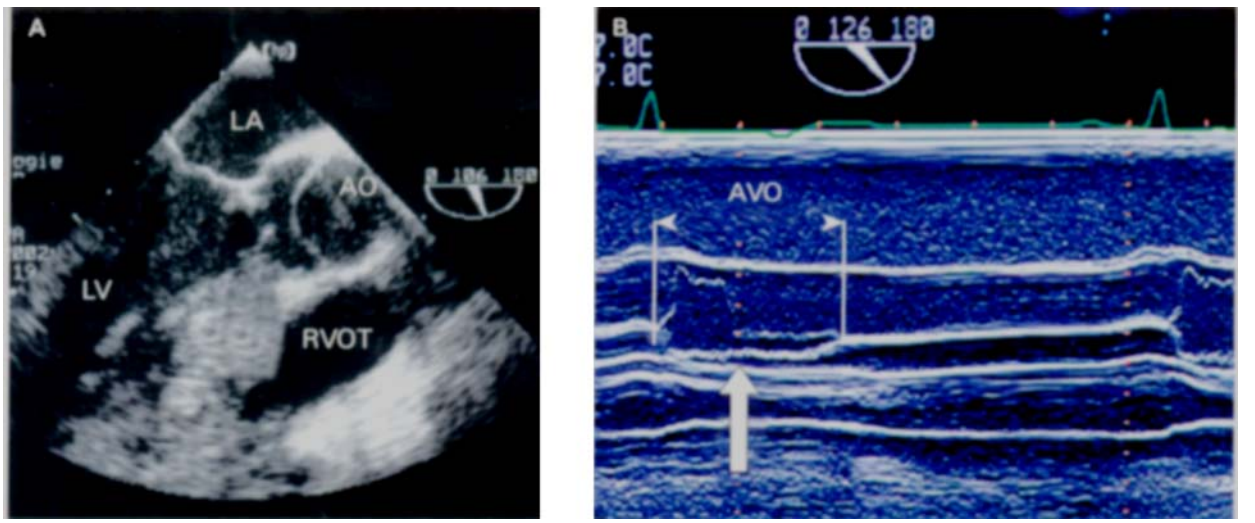

Figure 12.23 Subaortic stenosis. **(A)** A fibrous ring is visible in the left ventricular outflow tract (arrow) on the septum and below the anterior mitral leaflet. **(B)** In case of dynamic stenosis, the M-mode analysis of the aortic valve demonstrates an early closure of the valve during mid-systole (arrow). Ao = aorta, AVO = aortic valve opening during systole, LA = left atrium, left ventricle, RVOT = right ventricular outflow tract.

After LVOT reconstruction, TOE examination must detect potential remnants of fibromuscular membrane or residual muscular ridge. M-mode study through the aortic valve permits exclusion of an early closure of the valve, which is a sensitive sign of a residual obstruction (Figure 12.23B). Care must be taken to exclude an iatrogenic VSD and an injury to the mitral or aortic valve. The velocity can still be increased at the septal bulge depending on haemodynamic conditions, and this may impact on the need for reoperation.[66] The impact of TOE examination on surgical results of LVOT reconstruction is very high: in 12–55% of cases an immediate surgical revision is indicated by post-bypass examination.[8,14,15,53,66]

Bicuspid aortic valve

Bicuspid aortic valve is the commonest congenital cardiac anomaly; its incidence is 2% in the global population.[67] It is identified by two cusps of unequal size, the larger of which may have a fibrous raphe at the site of fusion. It presents as a fish mouth opening in the short axis, and a characteristic doming on long-axis view during systole (Figure 12.24). Rarely, the valve may be unicuspid with a central hole generating stenosis and incompetence simultaneously. With continuous stress over the years, the valve may become calcified and stenotic, usually after the age of 40 years; by annular dilation it can also loose tensile strength and become incompetent. The restriction to flow is characterised by a mean gradient greater than 50 mmHg in the case of severe stenosis and normal left ventricular function. The valve area is calculated by direct planimetry or by the continuity equation. Bicuspid aortic valve is frequently associated with aortic coarctation and perimembranous VSD.

In the Ross procedure, the pulmonary valve is transposed in the aortic position and substituted by a homograft or a heterograft. The pre-bypass TOE examination allows measurement of the dimensions of the aortic and pulmonary annulus, the diameter of the sinotubular junction, and the thickness of the subpulmonary interventricular muscular septum (Figure 12.25). The examination should also address the functional status of the pulmonary valve because it will have to withstand the systemic pressures. Shortly after unclamping of the aorta, an acute left ventricular dilation secondary to an aortic regurgitation should be excluded. A slight leak in the transposed valve (grade < 2) can be considered acceptable. Doppler flow velocities through the pulmonary homograft are usually recordable in a transgastric view; the echogenicity of the material prevents a basal transverse examination. An iatrogenic VSD should be excluded.

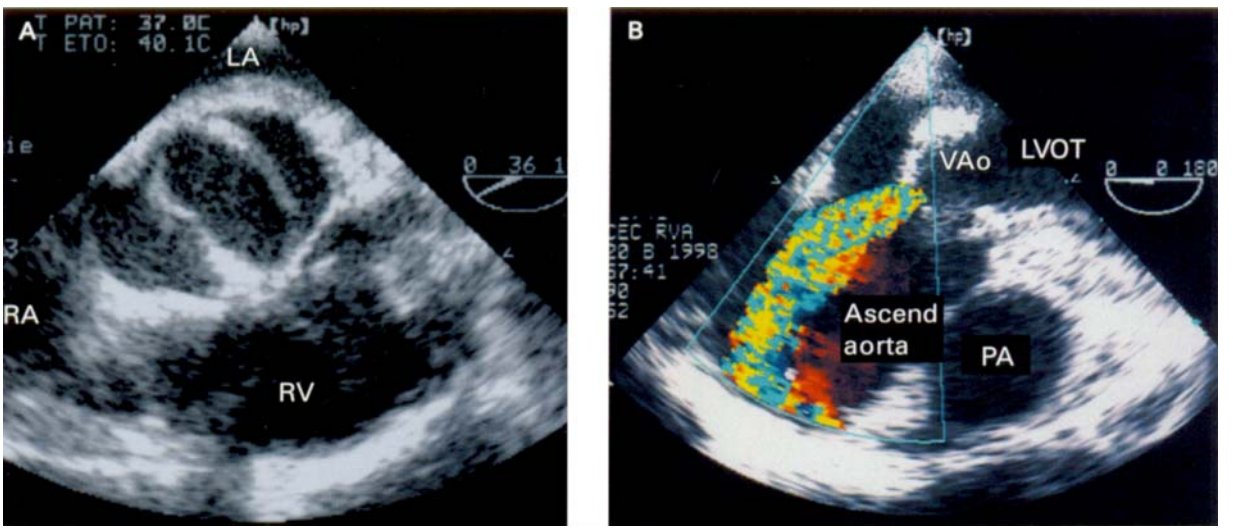

Figure 12.24 Bicuspid aortic valve. **(A)** Short-axis view. The opening is elliptical. **(B)** In systole, the long-axis view reveals a typical "doming" of the valve into the ascending aorta. The high velocity jet indicates a stenosis. LA = left atrium, PA = pulmonary artery, RA = right atrium, RV = right ventricle.

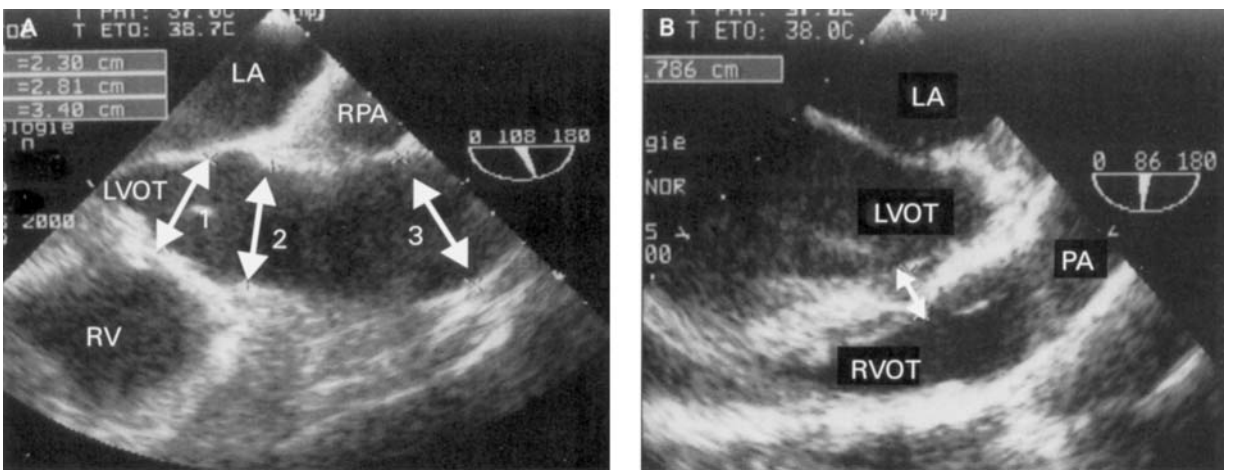

Figure 12.25 Ross procedure. **(A)** Before reconstruction it is important to measure three diameters: (1) the aortic annulus, (2) the sinotubular junction, and (3) the ascending aorta at the crossing of the right pulmonary artery. **(B)** The explantation of the pulmonary valve requires removal of a sleeve of the muscular outflow tract. The thickness of the interventricular septum at the level of the right ventricular outflow tract (RVOT; arrow) must be measured. LA = left atrium, LVOT = left ventricular outflow tract, PA = pulmonary artery.

Transposition of the great arteries

AV concordance and ventriculo-arterial discordance occur in complete transposition of the great arteries. The aorta arises from the anatomical right ventricle, and the PA originates from the anatomical left ventricle. On the longitudinal plane, the great arteries arise in parallel at the base of the heart. In the transverse view both semilunar aortic and pulmonary valves appear in the same plane on cross-section. The aortic valve is anterior, to the right, and slightly superior to the pulmonary valve (D transposition). The PA originates directly above the LVOT with fibrous continuity between mitral and pulmonic valves. An ASD allows mixing between the pulmonary and systemic circuits. A VSD is present in 30–40% of patients.

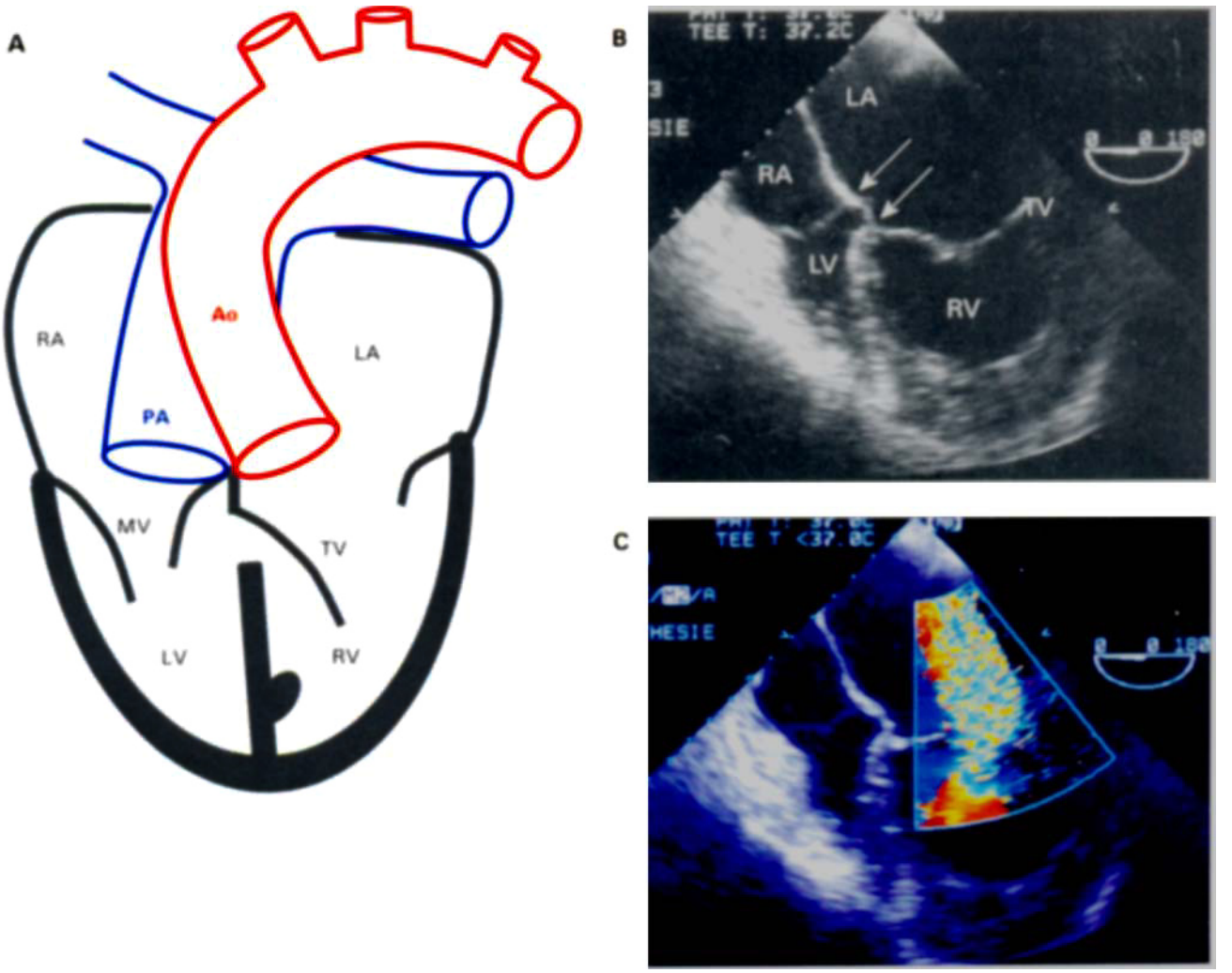

Figure 12.26 Anatomically corrected transposition of the great arteries. **(A)** The atrioventricular and the ventriculo-arterial junctions are discordant. The anatomical left ventricle (LV), with the mitral valve (MV), is on the right side and connected to a pulmonary artery (PA). The anatomical right ventricle (RV), with the tricuspid valve (TV) and a septal papillary muscle, is on the left side and connected to the aorta (Ao). **(B)** Four chamber view. The septal insertions of the MV and the TV (arrows) show that the MV is connected to the right atrium (RA) and the TV to the left atrium (LA). The enlarged anatomical RV is on the left side. The small triangular LV is on the right side. **(C)** Severe tricuspid regurgitation of the dilated subaortic ventricle.

Two main therapeutic approaches govern surgical treatment: redirecting the venous return at the atrial level (Mustard or Senning procedures), and switching the great arteries during the first 2–3 weeks of life. Examination of adult patients with previous arterial switch procedure should be close to normal. However, RVOT or LVOT obstruction, AV and semilunar valve regurgitation, possible residual shunt, or left ventricular dysfunction may be found.[11]

After Mustard or Senning operations, the echocardiographic images are more complex. The intra-atrial repair divides the bi-auricular cavity into an anterior and a posterior chamber, with a baffle redirecting the systemic venous return to the mitral valve (anterior chamber) and the pulmonary venous flow to the tricuspid valve (posterior chamber), wrapping in horseshoe fashion around the mid-atrial systemic venous channel where the flow should remain biphasic, mirroring the atrial pressure trace.[68] A contrast study with saline injected into a systemic vein helps in the evaluation of cardiac anatomy. In the case of obstruction, the Doppler analysis reveals a loss of phasic pattern,

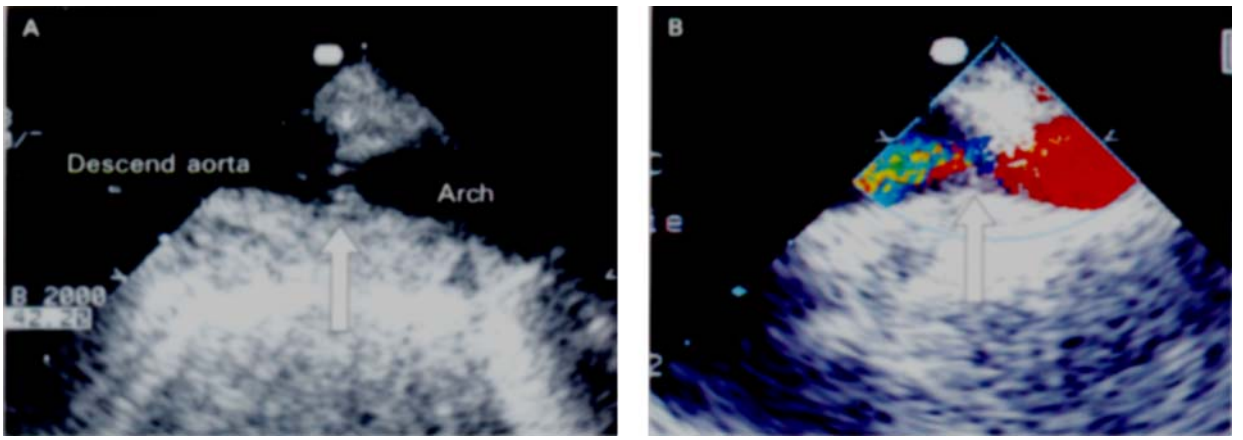

Figure 12.27 Coarctation of the aorta. **(A)** Circular ridge at the level of the isthmus (90° view of descending aorta). **(B)** The colour flow shows turbulences starting at the level of the coarctation.

an increased flow velocity (> 1·5 m/s), and a turbulent flow on colour mapping. Tricuspid regurgitation and progressive right ventricular dilation and dysfunction are frequently encountered in adulthood, as the right ventricle assumes the systemic work. The left ventricle is small and squashed by the right ventricle because of septum encroachment on the left ventricular cavity. A dynamic LVOT obstruction, which is most frequently encountered by patients with intact septum, may occur progressively with advancing age because of the low resistance PA bed being connected to an anatomical left ventricular chamber. Left ventricular dilation and failure may supervene in case of increased pulmonary vascular resistance.

Congenitally corrected transposition

In such cases, the great vessels are transposed (ventriculo-arterial discordance) but the circulation is physiologically corrected because the ventricles are inverted (AV discordance). The position of the infundibulum is such that the aorta arises anteriorly and to the left of the PA. There is a fibrous continuity between mitral and pulmonary valves (Figure 12.26). The anatomical right ventricle is in a left sided position, and the anatomical left ventricle stays on the right side of the heart. Nearly 80% of the patients have a perimembranous VSD, 50% mitral abnormalities, and 30% tricuspid regurgitation.[69] The tricuspid valve may be abnormally displaced toward the apex of the ventricle (Ebstein-like anomaly). A pulmonary outflow tract obstruction is frequent because it lies in an oblique position because of the malalignment of the interventricular septum.

Each ventricle is recognised from its anatomical features. In the four chamber view, the normal right atrium is followed by a bileaflet, high inserted mitral valve connected to a more or less triangular ventricle with two papillary muscles and fine trabeculations. On the left side, the left atrium is connected to a tricuspid, low inserted AV valve and a round-shaped ventricle with coarse trabeculations and three papillary muscles. The great arteries are positioned as in transposition of the great arteries and run parallel. Most adult patients present with progressive deterioration of systemic right ventricular function accompanied by tricuspid regurgitation.

Arterial anomalies

In coarctation of the aorta, the endo-aortic area is usually ill-defined and restricted just distal to the left subclavian artery; in young patients, a ridge of dense tissue that narrows the lumen may be observed (Figure 12.27). The aortic arch above the lesion is dilated and highly pulsatile, whereas the descending aorta distal to the coarctation exhibits much less expansion in systole. The flow through the stenotic area is turbulent. Aortic coarctation is frequently associated with bicuspid aortic valve and left ventricular concentric hypertrophy. After surgical correction, TOE examination should determine the degree of residual narrowing. Even if the coarctation has been corrected in childhood, it may recur in adulthood.

Coronary arteries may present with an anomalous origin from various aortic coronary sinuses or from a single common trunk, and anomalous termination into the right ventricle or the PA. This situation leads to a fistula or a shunt between left and right ventricles. A turbulent flow appears in the right ventricle or in the PA in diastole. The effective shunt (Qp/Qs) is usually around 1·6.[70] A direct interrogation of flow with colour and pulsed Doppler is frequently possible in left anterior descending and right main coronary arteries. A biventricular dysfunction is frequently present.

Conclusion

Echocardiography in congenital heart disease is particularly challenging for the anaesthetist. The success of haemodynamic management and surgical outcome relies on their experience and competence. This is demonstrated by a rate of 14% of non-diagnosed residual defects after cardiac surgery when an inexperienced echocardiographer is in charge.[71]

References

1 Moodie DS. Adult congenital heart disease. *Curr Opin Cardiol* 1994;**9**:137–42.

2 Fyfe DA, Ritter SB, Snider AR, *et al.* Guidelines for transesophageal echocardiography in children. *J Am Soc Echocardiogr* 1992;**5**:640–4.

3 Thys D, Abel M, Bollen B, *et al.* Practice guidelines for perioperative transesophageal echocardiography. *Anesthesiology* 1996;**84**:986–1006.

4 Cheitlin M, Alpert J, Armstrong W, *et al.* ACC/AHA guidelines for clinical application of echocardiography: a report of the ACC/AHA Task Force on Practice Guidelines (Committee on clinical application of echocardiography). *Circulation* 1997;**95**: 1686–744.

5 Marelli AJ, Child JS, Perloff JK. Transesophageal echocardiography in congenital heart disease in adult. *Cardiol Clin* 1993;**11**:505–20.

6 Weintraub R, Shiota T, Elkadi T, *et al.* Transesophageal echocardiography in infants and children with congenital heart disease. *Circulation* 1992;**86**:711–22.

7 Ramamoorthy C, Lynn AM, Stevenson JG. Pro: Transesophageal echocardiography should be used routinely for pediatric open cardiac surgery. *J Cardiothorac Vasc Anesth* 1999;**13**:629–31.

8 O'Leary PW, Hagler DJ, Seward JB, *et al.* Biplane intraoperative transesophageal echocardiography in congenital heart disease. *Mayo Clinic Proc* 1995;**70**:317–26.

9 Bernath MA, Sekarski N, Hurni M, Payot M, Chassot PG. Impact of intraoperative transesophageal echocardiography in surgical repair of congenital heart disease in children. Third World Conference on Pediatric Cardiology and Cardiac Surgery, Toronto, 2001.

10 Bettex DA, Schmidlin D, Bernath MA, Prêtre R, Hurni M, Chassot PG. Intraoperative transesophageal echocardiography in pediatric congenital heart surgery: a two-center observational study. *Anesth Analg* 2002;**93**:1275–82.

11 Miller-Hance WC, Silverman NH. Transesophageal echocardiography (TEE) in congenital heart disease with focus on the adult. *Cardiol Clin* 2000; **18**:861–92.

12 Ungerleider RM, Kisslo JA, Greeley WJ, *et al.* Intraoperative echocardiography during congenital heart operations: experience from 1000 cases. *Ann Thorac Surg* 1995;**60**:S539–42.

13 Randolph GR, Hagler DJ, Connolly HM, *et al.* Intraoperative transesophageal echocardiography during surgery for congenital heart defects. *J Thorac Cardiovasc Surg* 2002;**124**:1176–82.

14 Stevenson JG, Sorensen GK, Gartman DM, Hall DJ, Rittenhouse EA. Transesophageal echocardiography during repair of congenital cardiac defects: Identification of residual problems necessitating reoperation. *J Am Soc Echocardiogr* 1993;**6**: 356–65.

15 Rosenfeld HM, Gentles TL, Wernkovsky G, *et al.* Utility of intraoperative echocardiography in the assessment of residual cardiac defects. *Pediatr Cardiol* 1998;**19**:346–51.

16 Muhiudeen IA, Cahalan MK, Silverman NH. Intraoperative transesophageal echocardiography in patients with congenital heart disease. In: Greeley WJ, ed. *Perioperative management of patients with congenital heart disease.* SCA Monograph. Baltimore: Williams & Wilkins, 1996. pp. 43–66.

17 Ungerleider RM, Greeley WJ, Sheikh KH. The use of intraoperative echo with Doppler color flow imaging to predict outcome after repair of congenital cardiac defects. *Ann Surg* 1989;**210**:526–33.

18 McGowan FX, Laussen PC. Con: Transesophageal echocardiography should not be used routinely for pediatric open cardiac surgery. *J Cardiothor Vasc Anesth* 1999;**13**:632–4.

19 Benson MJ, Cahalan MK. Cost-benefit analysis of transesophageal echocardiography in cardiac surgery. *Echocardiography* 1995;**12**:171–83.

20 Siwik ES, Spector ML, Patel CR, Zahka KG. Costs and cost-effectiveness of routine transesophageal echocardiography in congenital heart surgery. *Am Heart J* 1999;**138**:771–6.

21 Van Praagh R. Terminology of congenital heart disease. Glossary and commentary. *Circulation* 1977;**56**:139–43.

22 Shinebourne EA, Macartney FJ, Anderson RH. Sequential chamber localization. Logical approach to diagnosis in congenital heart disease. *Br Heart J* 1976;**38**:327–40.

23 Lev M. Pathologic diagnosis of positional variations in cardiac chambers in congenital heart diseases. *J Lab Invest* 1954;**3**:71–81.

24 Dupuis C, Kachaner J, Payot M. *Cardiologie pédiatrique.* Paris: Flammarion, 1991. pp. 137–42.

25 Weyman AE. Complex congenital heart disease I: diagnostic approach. In: Weyman AE, ed. *Principle and practice of echocardiography.* Philadelphia: Lea & Febiger, 1994. pp. 979–1001.

26 Linker DT. *Practical echocardiography of congenital heart disease from fetus to adult.* New York: Churchill Livingstone, 2001.

27 Ho SY, Anderson RH. Nomenclature. In: Roelandt JRTC, ed. *Cardiac ultrasound.* Edinburgh: Churchill-Livingstone, 1993. pp. 621–9.

28 Tajik AJ. Two-dimensional real-time ultrasonic imaging of the heart and great vessels: technique, image orientation, structure identification and validation. *Mayo Clin Proc* 1978;**53**:271–9.

29 Bierman FZ, Williams RG. Prospective diagnosis of D-transposition of the great arteries in neonates by subxyphoid, two-dimensional echocardiography. *Circulation* 1979;**60**:1496–9.

30 Valdez-Cruz LM, Pieroni DR, Roland JMA, *et al.* Echocardiographic detection of intracardiac right-to-left shunts following peripheral vein injection. *Circulation* 1976;**54**:558–61.

31 Wyman AE. Negative contrast echocardiography: a new method for detecting left-to-right shunts. *Circulation* 1979;**59**:498–500.

32 Mehta RH, Helmecke F, Nanda NC, *et al.* Transesophageal Doppler color flow mapping assessment of atrial septal defect. *J Am Coll Cardiol* 1990;**16**:1010–3.

33 Stümper O. Intraoperative monitoring of surgical repair. In: Stümper O, Sutherland GR. *Transesophageal echocardiography in congenital heart disease.* London: Edward Arnold, 1994. pp. 163–83.

34 Vick GW. Pulmonary venous and systemic ventricular inflow obstruction in patients with congenital heart disease: detection by combined two-dimensional and Doppler echocardiography. *J Am Coll Cardiol* 1987;**9**:580–4.

35 Hagen PT, Scholtz DG, Edwards WD. Incidence and size of patent foramen ovale during the first ten decades of life. *Mayo Clin Proc* 1984;**59**:17–22.

36 Konstadt SN, Louie EK, Black S. Intraoperative detection of foramen ovale by transesophageal echocardiography. *Anesthesiology* 1991;**74**:212–6.

37 Berkompas DC, Sagar KB. Accuracy of color Doppler transesophageal echocardiography for diagnosis of patent foramen ovale. *J Am Soc Echocardiogr* 1994;**7**:253–6.

38 Schneider B, Zienkiewicz T, Jansen V, Hofman T, Naltenius H, Meinertz T. Diagnosis of patent foramen ovale by transesophageal echocardiography and correlation with autopsy findings. *Am J Cardiol* 1996;**77**:1202–9.

39 Stollberger C, Schneider B, Abzieher F, Wallner T, Meinertz T, Slany J. Diagnosis of patent foramen ovale by transesophageal contrast echocardiography. *Am J Cardiol* 1993;**71**:604–6.

40 Nacht A, Kronzon I. Intracardiac shunts. *Crit Care Clin* 1996;**12**:295–319.

41 Brecker SJD, Redington A, Shore D, Oldershaw P. Atrial septal defects. In: Redington A, ed. *Congenital heart disease in adults. A practical guide.* London: WB Saunders Co Ltd, 1994. pp. 104–10.

42 Schwinger ME, Gindea AJ, Freeberg RS, Kronzon I. The anatomy of the interatrial septum: A transesophageal echocardiographic study. *Am Heart J* 1990;**119**:1401–5.

43 Muhiudeen-Russel IA, Miller-Hance WC, Silverman NH. Intraoperative transesophageal echocardiography for pediatric patients with congenital heart disease. *Anesth Analg* 1998;**87**:1058–76.

44 Lin FC, Fu M, Yeh SH, Wu D. Doppler atrial flow patterns in patients with secundum atrial septal defects. Determinants, limitations, and pitfalls. *J Am Soc Echocardiogr* 1988;**1**:141–5.

45 Jaffe RA, Pinto FJ, Schnittger I, Siegel LC, Wranne B, Brock-Ufne JG. Aspects of mechanical ventilation affecting interatrial shunt flow during general anesthesia. *Anesth Analg* 1992;**75**:484–8.

46 Levin AR. Atrial pressure-flow dynamics in atrial septal defects (secundum type). *Circulation* 1968; **37**:476–9.

47 Louie EK, Konstadt SN, Rao TL. Transesophageal echocardiographic diagnosis of the right to left shunting across the foramen ovale in adults without prior stroke. *J Am Coll Cardiol* 1993;**21**:1231–7.

48 Bettex D, Chassot PG. Malformations congénitales de l'adulte. In: *Echocardiographie transoesophagienne en anesthésie-réanimation.* Paris: Pradel–Masson, Williams & Wilkins, 1997. pp. 171–87.

49 Piccoli GP. Morphology and classification of complete atrioventricular defects. *Br Heart J* 1979; **42**:633–9.

50 Stümper O. Intraoperative ultrasound in surgery for congenital heart disease. In: Roelandt JRTC, ed. *Cardiac ultrasound.* Edinburgh: Churchill-Livingstone, 1993. pp. 809–19.

51 Shiina A, Seward JB, Edwards WD, Hagler DJ, Tajik AJ. Two-dimensional echocardiographic spectrum of Ebstein's anomaly: detailed anatomic assessment. *J Am Coll Cardiol* 1984;**3**:356–70.

52 Sutherland GR, Sreeram N. Congenital anomalies of the atrioventricular valves. In: Stümper O, Sutherland GR, eds. *Transesophageal echocardiography in congenital heart disease.* London: Edward Arnold, 1994. pp. 89–105.

53 Bengur AR, Li JS, Herlong JR, Jaggers J, Sanders SP, Ungerleider RM. Intraoperative transesophageal echocardiography in congenital heart disease. *Semin Thorac Cardiovasc Surg* 1998;**10**:255–64.

54 Flanagan MF, Foran RB, Van Praagh R, Jonas R, Sanders SP. Tetralogy of Fallot with obstruction of the ventricular septal defect: spectrum of echocardiographic findings. *J Am Coll Cardiol* 1988;**11**: 386–92.

55 Moises VA, Maciel BC, Homberger LK, *et al.* A new method for non-invasive estimation of ventricular septal defect shunt flow by color Doppler flow mapping: imaging of the laminar flow convergence region on the left septal surface. *J Am Coll Cardiol* 1991;**18**:824–32.

56 Tee SDG, Shiota T, Weintraub R, *et al.* Evaluation of ventricular septal defect by transesophageal echocardiography: Intraoperative assessment. *Am Heart J* 1994;**127**:585–92.

57 Matsuda H. Problems in the modified Fontan operation for univentricular heart of the right ventricular type. *Circulation* 1987;**76**(suppl III):III-45.

58 Fontan F, Baudet E. Surgical repair of tricuspid atresia. *Thorax* 1971;**26**:240–8.

59 Disessa TG, Child JS, Perloff JK, *et al.* Systemic venous and pulmonary arterial flow patterns after Fontan's procedure for tricuspid atresia or single ventricle. *Circulation* 1984;**70**:898–902.

60 Stümper O, Sutherland GR, Geuskens R, Roelandt JR, Bos E, Hess J. Transesophageal echocardiography in evaluation and management after a Fontan procedure. *J Am Coll Cardiol* 1991;**17**:1152–60.

61 Stümper O, Hess J. Evaluation of Fontan-type procedures. In: Stümper O, Sutherland GR, eds. *Transesophageal echocardiography in congenital heart disease.* London: Edward Arnold, 1994. pp. 261–75.

62 Fyfe DA, Kline CH, Sade RM, Greene CA, Gillette PC. The utility of transesophageal echocardiography during and after Fontan operations in small children. *Am Heart J* 1991;**122**:1403–15.

63 Van Praagh R. Tetralogy of Fallot: underdevelopment of the pulmonary infundibulum and its sequelae. *Am J Cardiol* 1970;**47**:1279.

64 Kaplan S, Adolph RJ. Pulmonary valve stenosis in adults. *Cardiovasc Clin* 1979;**10**:327–33.

65 Redington A, Shore D, Oldershaw P. *Congenital heart disease in adults. A practical guide.* London: WB Saunders Co Ltd, 1994.

66 Stevenson JG, Sorensen GK, Gartman DM, Hall DG, Rittenhouse EA. Left ventricular outflow tract obstruction: an indication for intraoperative transesophageal echocardiography. *J Am Soc Echocardiogr* 1993;**6**:525–35.

67 Friedman WF. Aortic stenosis. In: Emmanoulides GC, ed. *Moss and Adams's heart disease in infants, children and adolescents, including the fetus and young adult.* Baltimore: Williams & Wilkins, 1995. p. 1087.

68 Chin AJ, Sanders SP, Williams RG, Lang P, Norwood WI, Castaneda AC. Two-dimensional echocardiographic assessment of caval and pulmonary venous pathways after the Senning operation. *Am J Cardiol* 1983;**52**:118–26.

69 Anderson R, Ho SH. Echocardiographic diagnosis and description of congenital heart disease: Anatomic principles and philosophy. In: St John Sutton MG, ed. *Textbook of echocardiography and Doppler in adults and children.* Cambridge (MA): Blackwell Science, 1996. pp. 711–43.

70 Bishop A. Coronary artery anomalies. In: Redington A, ed. *Congenital heart disease in adults. A practical guide.* London: WB Saunders Co Ltd, 1994. pp. 153–60.

71 Stevenson JG. Adherence to physician training guidelines for pediatric transesophageal echocardiography affects the outcome of patients undergoing repair of congenital cardiac defects. *J Am Soc Echocardiogr* 1999;**12**:165–72.

13 Cardiac masses, air, and foreign bodies

Kazumasa Orihashi, Yasu Oka

Introduction

During surgical procedures various types of intracardiac mass may be visualised in the heart and great vessels with transoesophageal echocardiography (TOE), including thrombus, tumour, and air. The former two are related to the pathology of the disease and are moderately echogenic, whereas air is highly echogenic and its presence is related to the operative procedure. TOE is particularly suited to the intraoperative assessment of all of these entities. The appearance of such intracardiac masses may change during surgery or they may cause considerable complications unless they are properly identified and managed. In addition, various types of catheters and other foreign bodies that are used for monitoring or treatment (for example, vascular prostheses) may be visualised in the cardiac chambers and great vessels. They are encountered in the operating theatre as well as in the intensive care unit and catheterisation laboratory. TOE may be used to minimise complications by guiding placement of devices and treatment, but special considerations in interpreting the images are required. This chapter describes the roles of TOE in the intraoperative assessment of cardiac masses, air, and foreign bodies.

Thrombus and tumour

The appearance of thrombus and tumour may vary with respect to shape, size and location, and they have various underlying pathologies. A common clinical problem is potential systemic or pulmonary embolism. Both massive embolisation to the pulmonary artery and small embolisations to vital organs such as brain, heart, and visceral artery are often fatal or lead to a considerable deterioration in the postoperative course. Thus, early detection and appropriate treatment based on accurate information is important. The roles of TOE in patients with potential emboli are as follows:[1,2]

- to detect the emboli
- to locate the emboli accurately
- to assess the fragility of emboli
- to guide and immediately evaluate surgical resection.

Thrombus

Thrombus formation may occur in the left atrium and left ventricle, among other structures, and is closely associated with stagnant blood flow where spontaneous echo contrast is depicted. Thromboembolism in the pulmonary artery can occur during the perioperative period.

Left atrial thrombus is predominantly found in patients with mitral stenosis and/or atrial fibrillation, in which blood stagnates in the left atrium. Spontaneous echo contrast is apparent in the dilated left atrium, exhibiting slowly whirling movement. The left atrial appendage, which forms an inlet structure, is the most common site of thrombus formation. Thrombus can also be found on the posterior wall of the left atrium. Formation of thrombus is less common in patients with mitral regurgitation because blood in the left atrium is agitated by regurgitant jets.[3]

Thrombus appears as an echogenic mass. The shape varies a great deal (thrombi may be flat, sessile, pedicled, or floating; Figure 13.1),[4,5] as does the size. When the thrombus is vascularised, colour Doppler imaging reveals multiple small vessels with blood flow in the thrombus. Small mobile thrombi may be found on the surface of a thrombus.

It is not easy to differentiate a small thrombus in the left atrial appendage from the pectinate muscles. The latter usually form a ridge-like structure, whereas the former does not. Sequential scanning of left atrial appendage is necessary for differentiation. Another pitfall in

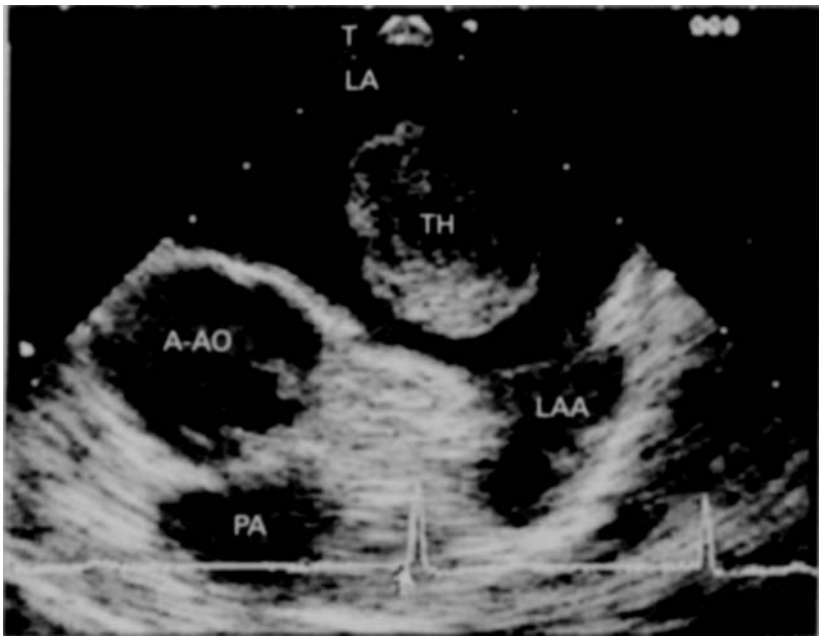

Figure 13.1 Transoesophageal echocardiogram showing left atrial thrombus (ball-like). A-AO = ascending aorta, LA = left atrium, LAA = left atrial appendage, PA = pulmonary artery, TH = thrombus.

diagnosing thrombus in the left atrial appendage is a sigmoid wall, often caused by pericardial effusion or lobulation of the appendage. When the wall is scanned tangentially, a thrombus-like image appears in the appendage. Perpendicular scan images are useful for accurate diagnosis.

Left ventricular thrombus is often associated with myocardial infarction and/or left ventricular aneurysm.[6] Stagnant blood in the aneurysm, loss of wall motion, and damaged intima are responsible for thrombus formation. The thrombus usually has a smooth surface and partially fills the cavity. Echogenicity is rather homogeneous.

Unlike thrombus in the left atrium and left ventricle, pulmonary thrombus is the result of embolism from the inferior vena cava and/or veins in the pelvis and lower extremities. It occurs in the operating theatre after extubation or within a few days after surgery. Acute embolism is often associated with critical circulatory and respiratory failure. Ventricular fibrillation may necessitate cardiopulmonary resuscitation or use of circulatory assist,[7] although the former may be less effective because of obstruction of the pulmonary circulation. Thus, immediate diagnosis followed by restoration of systemic circulation without delay is mandatory.

The right ventricle is enlarged because of pressure and volume overload, with the interventricular septum compressed toward the left ventricle. Thrombus is depicted as an echogenic mass that occupies a large space in the pulmonary artery (Figure 13.2). Colour Doppler imaging shows narrowing and deviation of blood flow. TOE is advantageous for diagnosing pulmonary embolism at the bedside, even in critically ill patients.[8] Thrombi at the main or right pulmonary artery can be clearly visualised.[9] However, visualisation of thrombi in the left pulmonary artery or lobar arteries is limited.[10,11] There are two solutions to this problem. Visualisation of left pulmonary artery is interrupted by the left main bronchus, which is situated between the oesophagus and left pulmonary artery. Because the bronchus is about 1 cm wide, further withdrawal of the TOE probe with mild anteflexion and counterclockwise rotation permits visualisation of the distal portion of the left pulmonary artery. It can also be visualised through the short-axis or long-axis view of the aortic arch, which provides an excellent acoustic window. Slight retroflexion is usually needed with this approach. This view depicts the left lobar arteries and thrombus within (Figure 13.3).

Tumour

There are a number of types of tumour found in the heart and large vessels. They may be primary or secondary, and may be histologically benign or malignant. Whatever the type of tumour, the risk

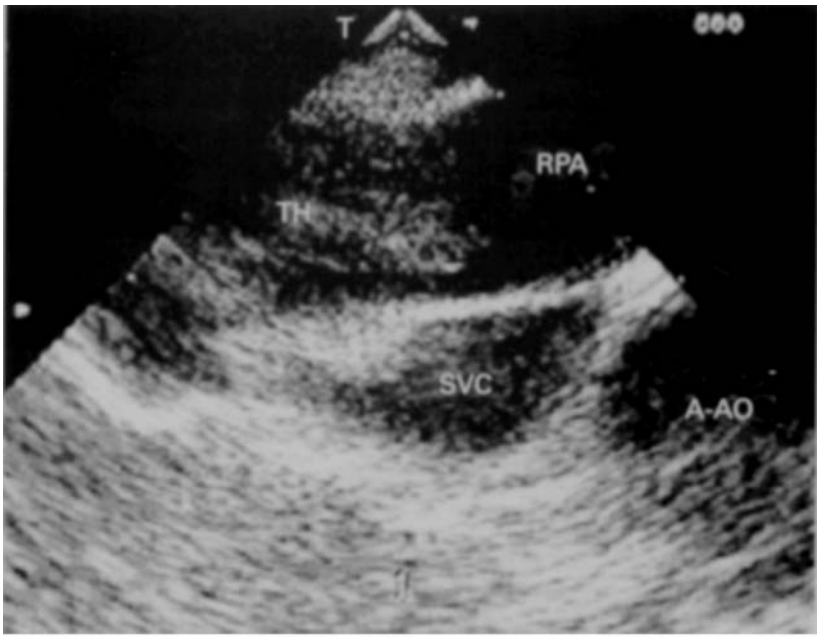

Figure 13.2 Transoesophageal echocardiogram showing pulmonary embolism. A-AO = ascending aorta, RPA = right pulmonary artery, SVC = superior vena cava, TH = thrombus.

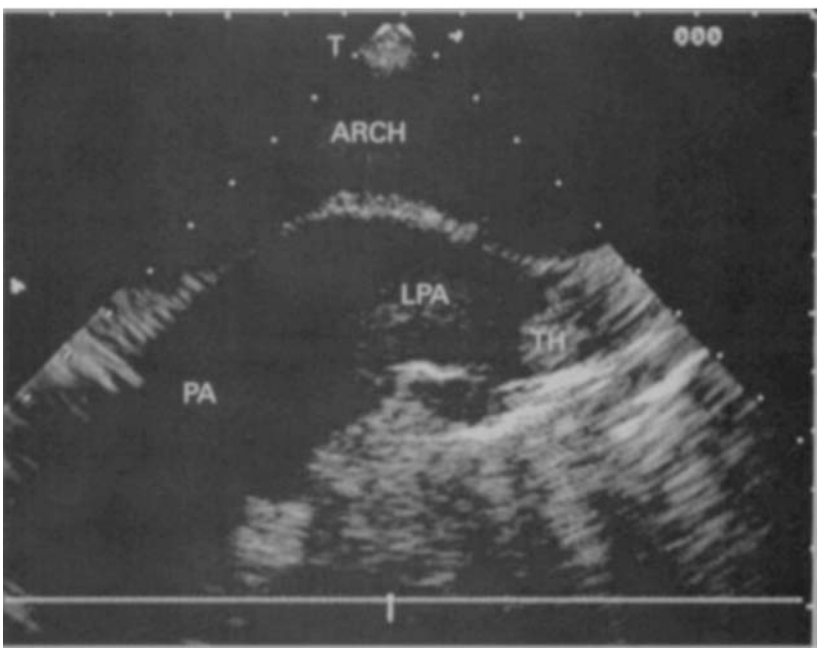

Figure 13.3 Transoesophageal echocardiogram showing thrombus in the left pulmonary artery (LPA). PA = pulmonary artery, TH = thrombus.

for possible detachment and embolisation is clinically important.

Primary tumour of the heart is rare. The most common form is myxoma.[12,13] Although pathologically benign, it is fragile and can detach, resulting in systemic embolisation. Myxoma often arises in the left atrium and has an attachment to the interatrial septum. TOE shows a soft and mobile mass. It contains a speckled pattern and moves in the bloodstream during the cardiac cycle (Figure 13.4). Myxoma less commonly arises in the right atrium.[14] Other primary tumours include lipoma, papillary fibroelastoma, angiosarcoma, and rhabdomyosarcoma.

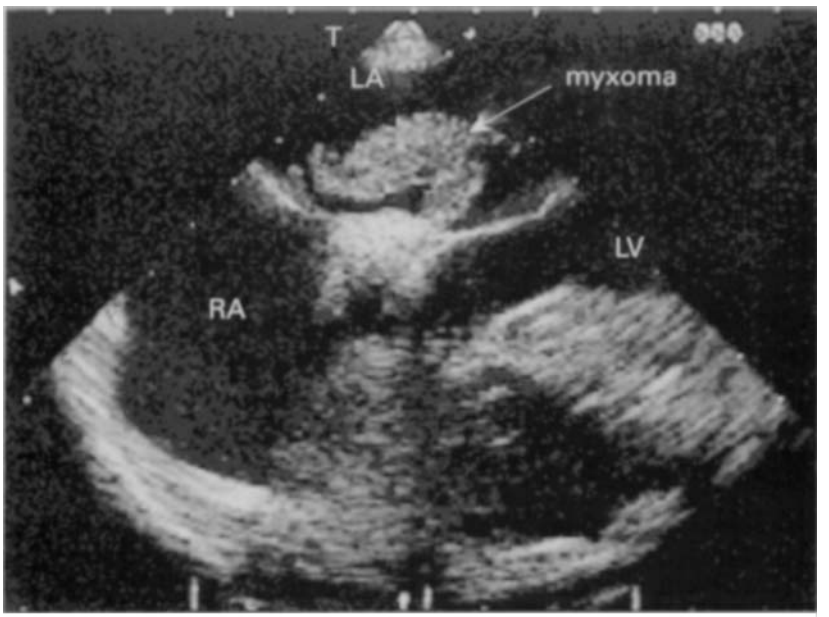

Figure 13.4 Transoesophageal echocardiogram showing left atrial myxoma. RA = right atrium, LA = left atrium, LV = left ventricle.

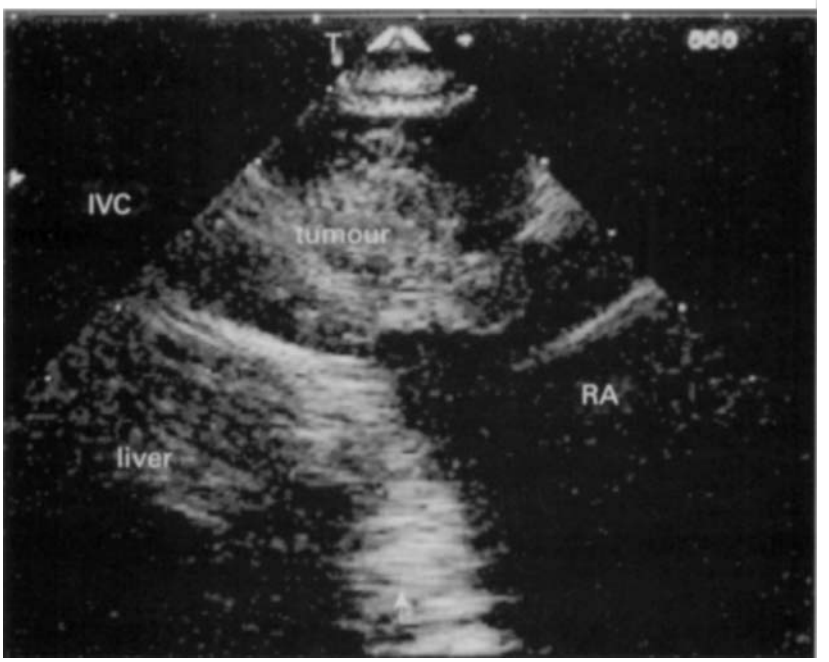

Figure 13.5 Transoesophageal echocardiogram showing renal cell carcinoma extending into the inferior vena cava (IVC) up to the right atrium (RA).

Tumours that originate in other organs may extend into the heart. Renal cell carcinoma and hepatocellular carcinoma occasionally grow into the inferior vena cava and right atrium (Figure 13.5). Not only do they disturb venous return but also they can cause acute pulmonary embolism preoperatively or during surgical manipulation. Surgical strategy varies according to the extent of tumour and between institutions.

TOE is used to:[15–17]

- assess extension of tumour to the inferior vena cava and cardiac chambers
- monitor the mobility of tumour during surgical dissection
- guide safe placement of catheters near the tumour
- detecting residual tumour on the caval wall.

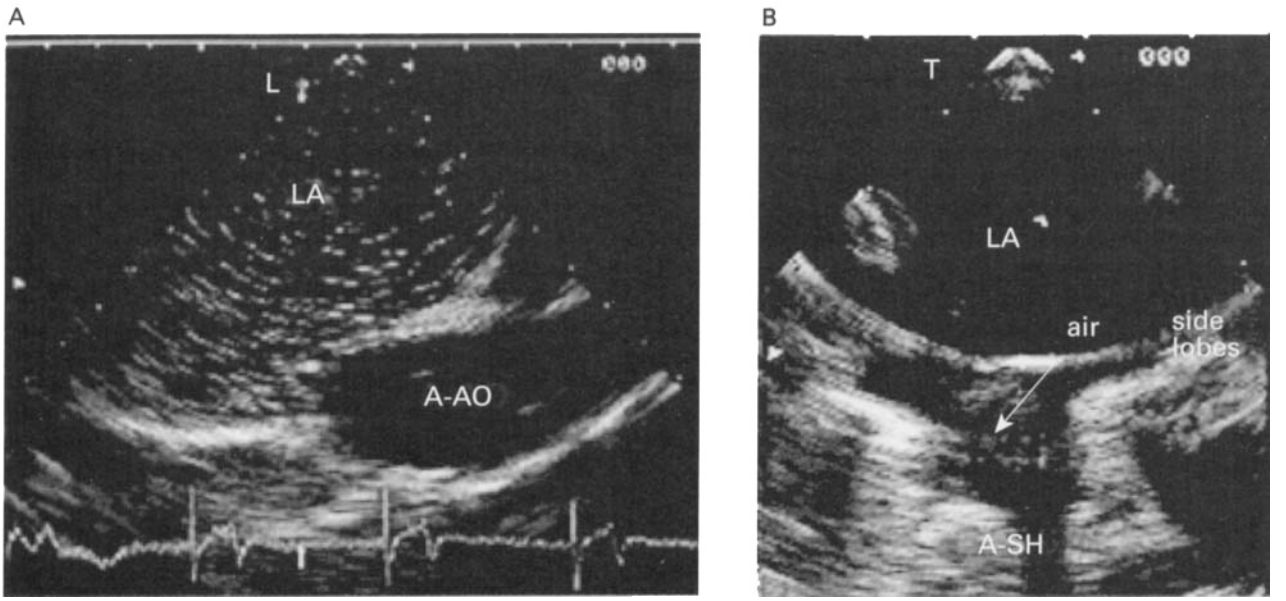

Figure 13.6 Transoesophageal echocardiogram showing retained intracardiac air: **(A)** bubble form and **(B)** pooled form. A-AO = ascending aorta, A-SH = acoustic shadow, LA = left atrium.

Tumour is visualised as a space-occupying mass in the inferior vena cava. It simply expands in the lumen or invades the caval wall. When blood flow is depicted around the tumour, this portion of caval wall is free from invasion. Unless tumour is resected under circulatory arrest in a bloodless field, tumour can remain and local recurrence may result, making prognosis poor. In the case of sudden circulatory derangement during surgical dissection, the pulmonary artery should be checked immediately for tumour embolus and the right ventricle for acute distention.[18]

Lung tumour can extend to the pulmonary vein and left atrium.[19–21] It can result in systemic embolisation during surgical procedures. TOE is advantageous because it provides real-time information in the operating theatre and permits clear visualisation of the pulmonary veins, which are close to the transducer. Tumour is visualised as a mass in the pulmonary vein. In such cases TOE is used to:[22]

- determine whether cardiopulmonary bypass is required for safe resection
- guide operative procedures
- assess the result immediately.

Rarely, mediastinal tumour invades the cardiac chambers or great vessels. It can occlude the superior vena cava, leading to superior vena cava syndrome or pericardial effusion may appear.

Intracardiac air

Air embolism has been a catastrophic occurrence throughout the history of cardiac surgery. Embolism to the cerebral artery and coronary artery results in considerably poorer clinical outcome. As long as the cardiac chamber is opened, air may be retained in the heart. Various procedures have been routinely carried out to eliminate air retention as completely as possible. TOE studies have shown that air retention is a common occurrence despite meticulous attempts to eradicate it.[23–26] TOE was found to be helpful in detecting and removing air, and thus in preventing embolic events.

Visualisation

Retained air exhibits unique TOE findings. It is never static but changes dynamically. It appears in two forms: in bubble form and in pooled form.

Bubbles are visualised as highly echogenic dots in the cardiac chambers (Figure 13.6A). They are laterally oblong because of side lobes, and are usually not accompanied by acoustic shadow. They are highly mobile and appear to be flying around with blood flow. When blood stagnates, these dots begin to move toward the highest place in each chamber and collect there, viewed as a bright line along the wall and often associated with reverberations.

In 1993, we reported the TOE findings and behaviour of "pooled air".[24] This air is important because it amounts to several millilitres and it can cause a bolus embolism. Like bubbles, pooled air is visualised as strongly echogenic, accompanied by side lobes (Figure 13.6B). What is different is the wide acoustic shadow, which disturbs visualisation of the cardiac structures below. The appearance of pooled air is different from that of air bubbles; pooled air stays along the wall that is at the highest level in the chamber, and moves toward the next chamber along the ceiling. When the pooled air is agitated, numerous bubbles pop up. In contrast to bubbles, pooled air is visualised as smaller than it actually is. The entire pool is not visualised, but rather the strong echo is reflected only from that part of the pool's surface that is perpendicular to the ultrasound beam. The actual width of the pooled air is almost equal to the width of the acoustic shadow. Thickness corresponds to the distance between the strong echo and the cardiac wall, which is masked by the acoustic shadow.

Sites of air retention

Although bubbles are diffuse in their appearance, pooled air collects discretely at limited sites. Common sites of air retention in the heart and in the corresponding TOE view are summarised in Table 13.1 (illustrated in Figure 13.7). Retained air can be examined in the three chamber view, two chamber view (longitudinal scan), transgastric two chamber view (longitudinal scan), and TG short-axis view.

Table 13.1 Common sites of air retention

Side	Site
Left	Right upper pulmonary vein
	Left upper pulmonary vein
	Left atrial appendage
	Left atrium
	Left ventricular apex
	Right coronary sinus
	Ascending aorta
Right	Right atrium
	Right ventricular outflow tract
	Right pulmonary artery

The left ventricle can hold several millilitres of air. It is found at the apical region and is strongly echogenic with an acoustic shadow. After mitral valve replacement, however, visualisation of the left ventricular apex is impaired by the prosthetic valve. In this situation, the transgastric approach is helpful for detecting air.

The right upper pulmonary vein can also hold a large amount of air. When air fills the pulmonary vein up to the atrial orifice (several millilitres), strong echo is found at the atrial orifice and visualisation of pulmonary vein is disturbed by acoustic shadow. As the heart is agitated or pulmonary circulation resumes, air bubbles pop up into the left atrium or pooled air moves to the left atrium along the wall. A longitudinal scan is helpful for visualising the air

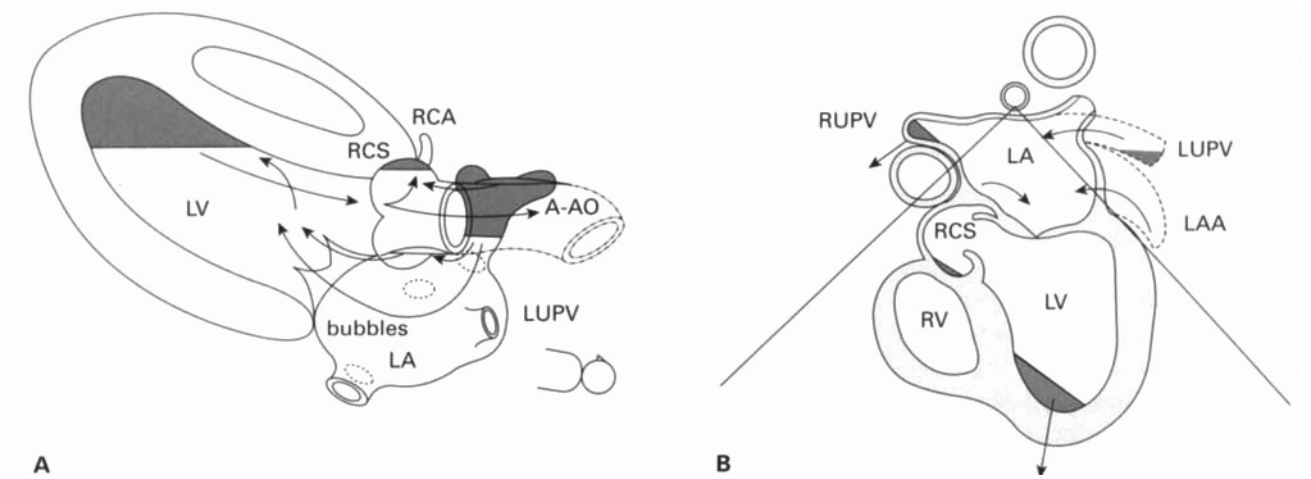

Figure 13.7 **(A)** common sites of air retention and **(B)** corresponding sites visualised in the transoesophageal echocardiographical view and route of air removal. A-AO = ascending aorta, LA = left atrium, LAA = left atrial appendage, LUPV = left upper pulmonary vein, LV = left ventricle, RCA = right coronary artery, RCS = right coronary sinus, RUPV = right upper pulmonary vein, RV = right ventricle.

in a more distal portion of the pulmonary vein. Air tends to remain deep within the pulmonary vein until the venous return into the left atrium becomes adequate. Air can retain in the right upper pulmonary vein not only in mitral valve surgery but also in atrial septal defect closure, aortic valve replacement, or replacement of ascending aorta. As the blood in the left ventricle is evacuated, air retrogradely enters the left atrium and even the right upper pulmonary vein, which has its orifice at the highest level among the four pulmonary veins.

The left atrium can form a shallow air pocket at the superior aspect and can hold a small amount of air, which moves from the right upper pulmonary vein to the left ventricle.[25] Air may be found in the left atrial appendage and left upper pulmonary vein. Because the orifice is situated dorsally (at a lower level in the supine position), air enters there only when the blood in the left atrium is totally aspirated.

At the ceiling of right coronary sinus there is the ostium of the right coronary artery, resembling a chimney on a roof. Air in the right coronary sinus readily enters the right coronary artery. By contrast, the ostium of the left coronary artery is situated at a lower level, and entry of air at that site is unlikely to occur. It should be noted that air at the left ventricular apex or in the ascending aorta readily moves to the right coronary sinus and enters the right coronary artery.

The appearance of bubbles in the right heart is not uncommon in laparoscopic procedures,[27,28] in neurosurgery conducted in the sitting position,[29] and in liver transplantation. Pooled air is found in cardiac surgery with right sided cardiotomy, such as resection of tumour in the inferior vena cava and tricuspid valve surgery. During cardiac arrest air collects at the right ventricular outflow tract, which is at the highest level. As pulmonary circulation resumes, air is stirred up and bubbles pop up toward the pulmonary artery. Unless air is aspirated, it moves to and is retained at the right pulmonary artery. Because the left pulmonary artery is directed posteriorly, air preferentially enters the right pulmonary artery.

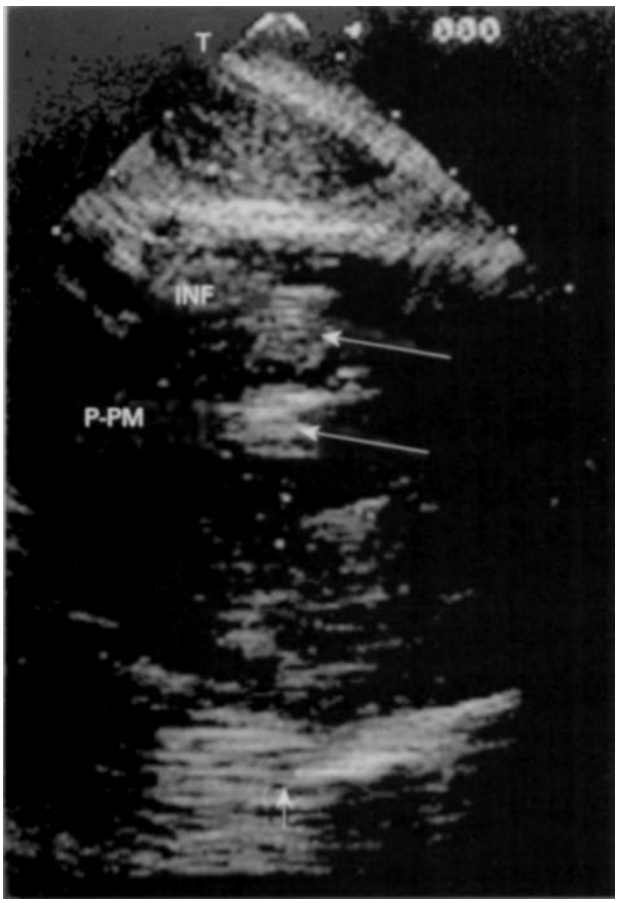

Figure 13.8 Transoesophageal echocardiogram showing echogenic dots (arrows) in the inferior wall (INF) and posteromedial papillary muscle (P-PM).

Retained air, and cardiac and neurological events

Various cardiac events are encountered intraoperatively, especially during weaning from bypass. They include arrhythmia and conduction disturbances (for example, block, arrest, and ventricular fibrillation), and left ventricular dysfunction (for example, asynergy and ST segment elevation). These events are related to the presence of pooled air in the left heart or to an appearance of gross dots of strong echo in the myocardium, found predominantly at the inferior wall, posteromedial papillary muscle, and interventricular septum near the mitral annulus (Figure 13.8).[30] These appear immediately after pooled air and/or bubbles enter the right coronary artery (Figure 13.9).

At the time of declamping the aorta, the patient is routinely put into a head-down position in order to prevent entry of air into the innominate artery. With this manoeuvre, however, the right coronary sinus becomes situated at the highest level, facilitating entry of air into the coronary artery.[30] An acute onset of cardiac arrest or block after a change of posture during the immediate

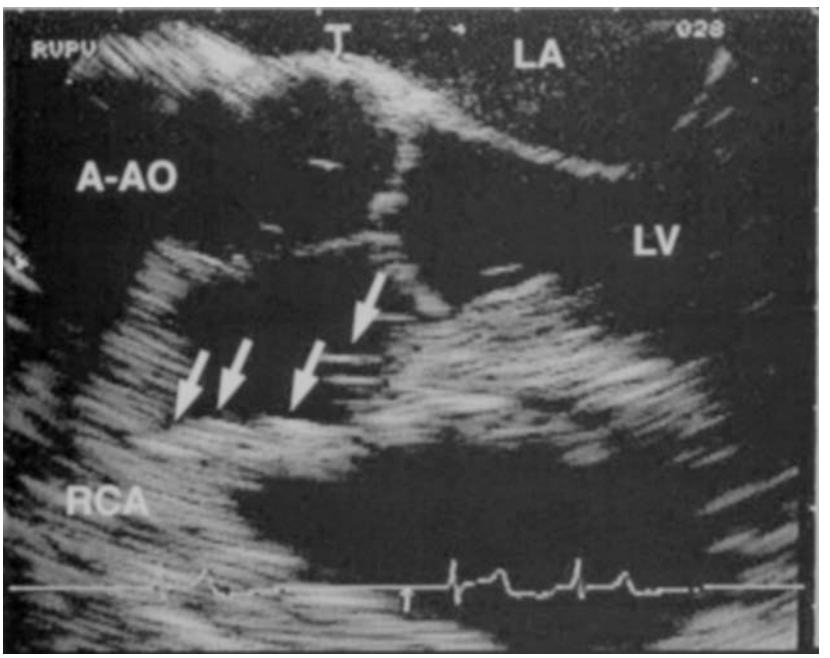

Figure 13.9 Transoesophageal echocardiogram showing air entering the right coronary artery (RCA).
A-AO = ascending aorta, LA = left atrium, LV = left ventricle.

postoperative period would be diagnosed as "cardiac event of unknown cause". Retained pooled air may be responsible for these events. If the air in the right upper pulmonary vein or left ventricle is not aspirated, then it remains at these sites in the supine position. Air can then be suddenly expelled to the ascending aorta as a bolus and enter the right coronary artery, possibly leading to acute cardiac arrest.

The presence of abundant bubbles may result in neurological complications. Detection of bubbles with TOE may be associated with detection of emboli in the cerebral arteries by means of transcranial Doppler. Abnormal Doppler signals of high intensity are detected. Massive cerebral infarction is seldom encountered. Small but multiple embolisms may be associated with postoperative brain dysfunction, such as cognitive disorder.

Quantitative analysis

When retained air is found with TOE, the next question is how much air there is. As mentioned above, bubbles appear to be larger than they actually are. In the operating theatre we often find bubbles smaller than 1 mm after TOE indicates the presence of bubbles that are 2–3 mm. Although each bubble is small, the total amount can be large when numerous bubbles are present.

The amount of pooled air can be estimated by measuring the thickness and width of the pool. A good correlation between the estimated amount and real volume was achieved in one of our studies.[31] In the clinical setting, however, it is not important to estimate precisely the amount of air, but rather to determine whether the amount of air is so large that it must be aspirated or so small that it may be allowed to remain. Air of width 1 cm corresponds approximately to a volume of 0·5 ml.

Removal of air

TOE is helpful for:[30,32]

- locating the air
- guiding aspiration
- evaluating immediately whether the attempt at aspiration was successful.

Figure 13.7 shows the appropriate route for removing air at each retention site. Visualisation of digital compression helps the surgeon to locate the air accurately and to minimise the number of aspirations. As soon as the air is removed, it is visualised as smaller or it may even disappear.

Air in the left upper pulmonary vein, left atrial appendage, and left atrium are moved to the left ventricle by shaking or agitating the heart; it is

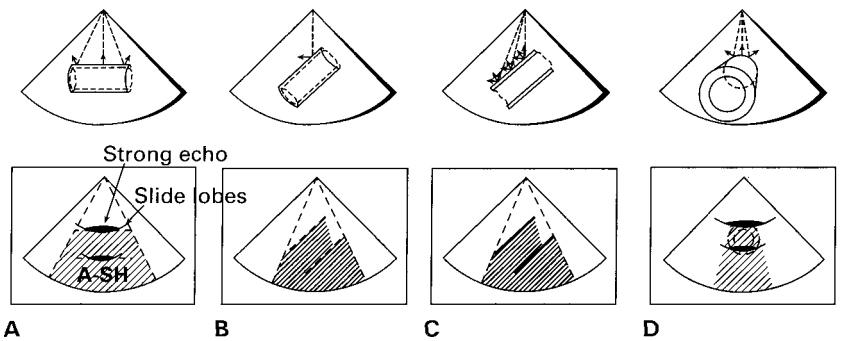

Figure 13.10 Echocardiographic expression of catheters. A-SH = acoustic shadow.

then aspirated through the left ventricular vent tube or by direct puncture of the left ventricular apex. However, it is difficult to remove the air in the right upper pulmonary vein. This vein appears as an inverted tube. Once the blood is replaced with air, it tends to remain in the vein because of buoyancy, in spite of agitation. Inflation of the lung to squeeze the air out of the pulmonary vein is often unsuccessful while the pulmonary vein is flat. With a direct puncture, one can aspirate only blood because the needle passes beyond the air. Instead, several needle holes at the roof of pulmonary vein are needed to allow the air to escape. With the operating table tilted to lower the right side of the patient, the venous return is transiently increased by partially clamping the venous cannula, and the lung is inflated. Air comes out of the holes or bubbles appear in the left atrium.

In minimally invasive cardiac surgery, evacuation of air is more difficult than in conventional surgery because the available space is not sufficient to agitate or mobilise the left ventricular apex or to aspirate the air from the apex. In such cases, the role played by TOE in removing the air is more important.

Catheters

Various types of catheters are increasingly being used in cardiovascular surgery, including pulmonary artery catheters, arterial and venous cannulas, vent tubes, cardioplegic catheters, and intra-aortic balloon pump catheters. TOE is used to:

- guide placement procedures and adjustment of catheter position
- evaluate the function of the catheter
- detect complications related to the placement or manipulation of the catheter.

For these purposes, a simultaneous side-by-side display of transverse and longitudinal views is helpful because it provides both long-axis and short-axis views at the same time. Real-time, three-dimensional TOE will be preferable in such situations once it is developed for clinical use.

Visualisation of catheter and guidewire

A catheter is composed of the catheter portion with or without a balloon, and it is placed with the use of a guidewire. The catheter portion reflects ultrasound at its surface and is basically echogenic. The echogenicity of the catheter within the echo image depends on the state of the surface and the incidence angle of ultrasound (Figure 13.10).[33]

When the surface is smooth and lies perpendicular to the ultrasound beam, it reflects a large portion of ultrasound and is echogenic, accompanied by side lobes and acoustic shadow. When the smooth surface is oblique to the ultrasound, it deflects ultrasound elsewhere and generates no strong echo. Only acoustic shadow indicates the presence of the catheter. The width of the acoustic shadow corresponds to the length of the catheter crossing the scanning plane. When the surface is irregular, the ultrasound beam is randomly reflected and a portion returns to the transducer. Then, the entire portion of catheter in the scanning plane can be visualised, even though it is oblique to the ultrasound beam.

The balloon may either be filled with gas (for example, air or helium) or fluid (for example, saline). The former causes strong echo at its surface. Because the incidence angle of ultrasound is always 90° at some portion of the

round surface of the balloon, it consistently causes strong echo, accompanied by side lobes and acoustic shadow as wide as the balloon. The latter is visualised as a circle with a thin wall. The lumen is echo free and catheter is seen inside. Acoustic shadow and side lobes are usually absent.

A guidewire is usually echogenic. Because its surface is irregular, the entire portion in the scanning plane is visualised. In the long-axis view the guidewire is visualised as an echogenic line, and the short-axis view as a dot.

Pulmonary artery catheter

A pulmonary artery catheter is composed of a catheter portion and a balloon at its tip. The balloon is strongly echogenic, accompanied by a wide acoustic shadow. It moves in a to-and-fro manner ("shuttle movement") in the bloodstream. This characteristic finding enables one to locate the catheter tip within the heart. TOE is used for monitoring and guiding placement of the pulmonary artery catheter in the operating theatre as well as in the intensive care unit, where routine fluoroscopic guidance is not practical.[34]

As the guidewire is inserted, it can be visualised as it enters the right atrium. This finding rules out an extravasation of the guidewire or entry of the guidewire into a branch vein or even the carotid artery.[35] As the catheter is inserted, the balloon appears in the superior vena cava and then enters the right atrium, which is best visualised with a longitudinal scan (Figure 13.11A). Advancement of the balloon into the right ventricle is monitored in the four chamber view (transverse scan; Figure 13.11B). When the balloon fails to enter the right ventricle:

- it may migrate into the inferior vena cava (balloon in the inferior vena cava)
- the catheter may become entangled within the right atrium (multiple strong echoes in the right atrium)
- the balloon may become wedged in the right atrial appendage (balloon in the appendage).

Next, as the balloon advances to the pulmonary artery, TOE shows the balloon to move from the right ventricle to the right ventricular outflow tract, and then to the pulmonary artery, visualised in the long-axis view of the right ventricular outflow tract (longitudinal scan; Figure 13.11C). The balloon can occasionally become stuck at the right ventricular apex, which is identified on the basis of loss of shuttle movement of the balloon at the apex. As the balloon enters the pulmonary artery, the pulmonary artery view (transverse scan) is helpful for visualising movement of the balloon into the right pulmonary artery (Figure 13.11D). As the balloon is wedged in the distal pulmonary artery, the catheter portion loses its swinging motion and is stretched tight (anchoring). Throughout the above mentioned process, pressure monitoring shows compatible changes in accordance with the position of the balloon.

Arterial cannula

An arterial cannula is placed at the distal ascending aorta. It is difficult to visualise this portion of the aorta. On starting to pump, a jet stream appears in the aortic arch, which may be visualised in colour Doppler mode. As the jet stream is traced proximally, the catheter tip may be shown. In visualising this portion, rightward bending of the probe tip is necessary to direct the ultrasound beam past the trachea.

Possible complications related to placement of arterial cannula include development of aortic dissection at the cannulation site and detachment of atheromatous plaque at the cannulation site or by the jet stream. The ascending aorta should be checked for the presence of atheroma before cannulation. When the presence of atheromatous plaque or aneurysmal change is detected at the aortic arch, the cannula tip may be directed toward the aortic valve.

Venous cannula

Venous cannulas are inserted from the right atrium, superior vena cava, femoral vein, pulmonary artery, or left atrial appendage. Inadequate drainage is indicated if the drained chamber is dilated.

A two-staged cannula may be inserted from the right atrium into the inferior vena cava. The reinforcement coil is clearly visualised as multiple echogenic parallel arcs, whereas the cannula surface is not echogenic unless the cannula is perpendicular to the ultrasound beam. A wide acoustic shadow indicates the presence of the cannula. A caval cannula is visualised in the inferior and superior vena cava as echogenic, accompanied by an acoustic shadow.

A venous cannula can also be inserted from the femoral vein. For safe insertion, a guidewire is

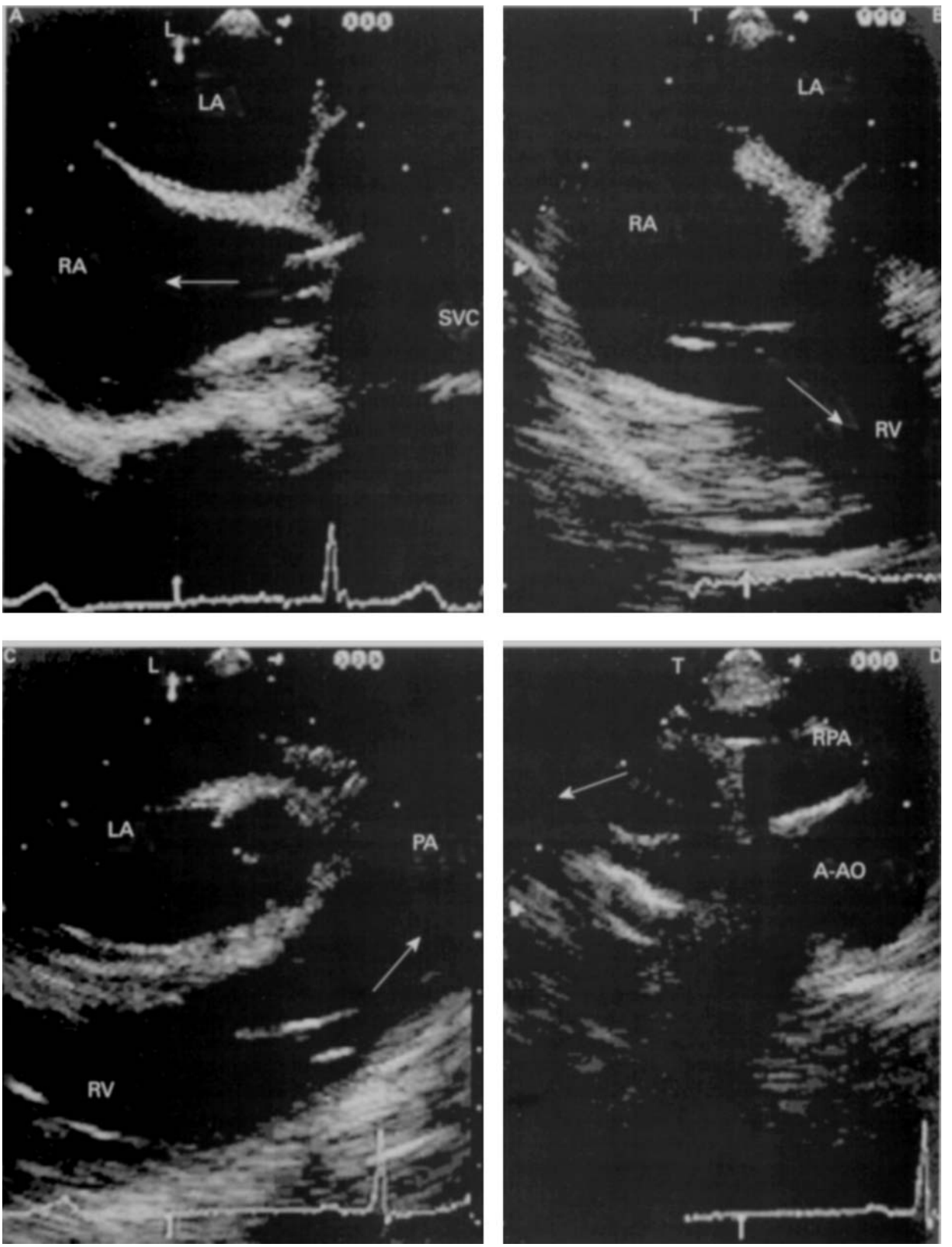

Figure 13.11 Transoesophageal echocardiogram showing process of pulmonary artery (PA) catheter placement: **(A)** from superior vena cava (SVC) to right atrium (RA); **(B)** from RA to right ventricle (RV); **(C)** from RV to PA; and **(D)** advancement in the right pulmonary artery (RPA). A-AO = ascending aorta, LA = left atrium.

first advanced into the right atrium. Entry of the guidewire can be confirmed by TOE. Failure to identify the guidewire in the inferior vena cava suggests migration of the guidewire into the contralateral iliac vein or other branch veins, even in the absence of unusual resistance. In such cases, another attempt is necessary. As the cannula is advanced to the right atrium along the guidewire, the guidewire is replaced with thick cannula. The tip is placed in the right atrium or proximal superior vena cava under TOE guidance in order to achieve maximal efficacy of drainage. Side holes of the cannula are visualised as defects in the cannula wall. Blood flow through the holes is depicted in colour Doppler mode.

A venous cannula may be placed in the pulmonary artery or left atrium for partial bypass in surgery of the descending aorta. A pulmonary artery cannula is inserted from the main pulmonary artery toward the right pulmonary artery. It is visualised as echogenic lines. When the cannula tip is too deeply inserted into the right pulmonary artery, drainage efficacy is impaired. A left atrial cannula is inserted from the left atrial appendage and is shown in the left atrium. When the cannula tip reaches the right pulmonary vein, the venous cannula sucks the venous wall and drainage becomes inadequate.

Vent cannula

A vent cannula is commonly inserted from the right upper pulmonary vein into the left atrium or left ventricle. It is depicted in the left atrium as echogenic, accompanied by acoustic shadow. Because only a portion exhibits strong echo, it is difficult to locate the cannula tip. The three chamber view is not suitable for confirming entry of the cannula into the left ventricle. Rather, the ventricular short-axis view is better because the cannula is almost perpendicular to the ultrasound beam and causes strong echo, whereas the acoustic shadow is discrete. Inadequate venting causes a distended cavity of the left ventricle.

Cardioplegic cannula

Either antegrade or retrograde cardioplegia, or both, may be applied. Adequate cardioplegia is essential in patients with coronary artery disease, left ventricular hypertrophy, or poor left ventricular function.

Antegrade cardioplegia is given from the ascending aorta. The jet stream from the cannula tip toward the posterior wall is apparent in colour Doppler mode. The needle tip is depicted as echogenic. Perfusion of cardioplegic solution into the coronary artery is visualised in colour Doppler mode. A considerable portion of cardioplegic solution may be lost when aortic regurgitation is present. The development of dissection must be ruled out when haematoma is found around the cannula.

The retrograde cardioplegic cannula is placed in the coronary sinus through the right atrial wall. The cannula is depicted as parallel echogenic lines in the coronary sinus (Figure 13.12). The roles of TOE are to:[36,37]

- rule out unusual morphology of coronary sinus
- guide safe insertion of the cannula
- detect accidental decannulation during operative procedures.

The size of the coronary sinus varies between individuals. Leakage of cardioplegic solutions around the cuff is visualised as flow toward the right atrium.

In surgery to the descending aorta, a balloon catheter may be advanced into the ascending aorta to administer the cardioplegic solution antegradely with endo-aortic clamp by an inflated balloon. In port access cardiac surgery, an endo-aortic clamp is used for occlusion of the ascending aorta, delivery of cardioplegic solution, and aortic root venting.[38] Its placement from the femoral artery can be clearly visualised and facilitated by TOE guidance, with or without fluoroscopic guidance.[37,38] The balloon is depicted in the ascending aorta as an echogenic ellipse. TOE is used in such cases to confirm appropriate inflation of the balloon and endoclamp of the aorta (adequate contact of balloon to the aortic wall without leakage around the balloon), while preventing intimal damage caused by over-distension of the balloon; and to detect distal migration of balloon,[38] which may lead to injection of cardioplegic solution into the cerebral branches and loss of effective cardioplegic solution.

Intra-aortic balloon pump catheter

An intra-aortic balloon pump catheter is composed of the shaft portion and the balloon portion. A balloon is visualised as an echogenic

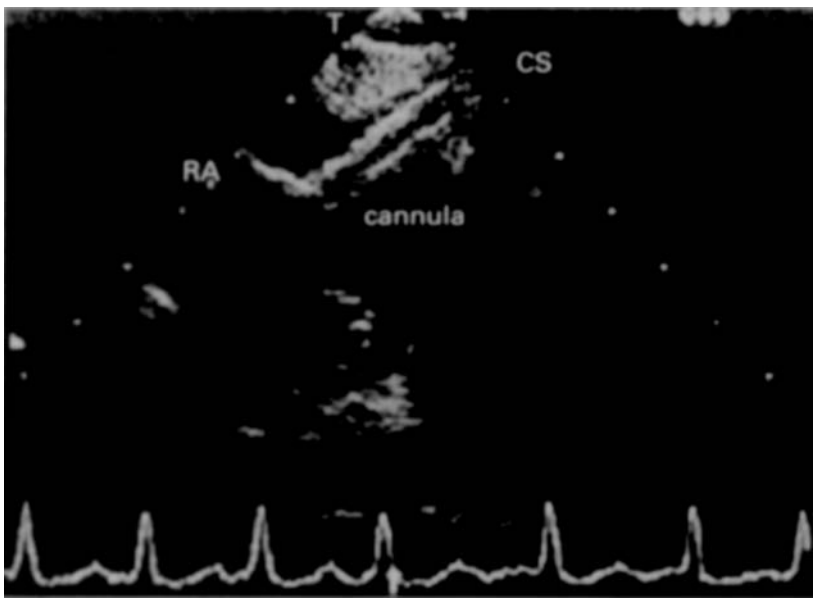

Figure 13.12 Transoesophageal echocardiogram showing coronary sinus (CS) cannula for retrograde cardioplegia. RA = right atrium.

area that fills the aortic lumen during inflation, accompanied by reverberations, whereas the shaft is depicted as an echogenic line with acoustic shadow during deflation. Periodic inflation of the balloon is apparent and indicates adequate pumping.

In placing the catheter, a guidewire is inserted first, which can be clearly visualised using TOE as an echogenic dot (short-axis view) or line (long-axis view). It is important to confirm the appearance of the guidewire in order to prevent its entry into the contralateral iliac artery, visceral branches, or even inferior vena cava in the puncture method. As the catheter is advanced along the guidewire, it appears in the descending aorta (Figure 13.13). By measuring the difference in depth of the TOE probe tip between the level of the catheter tip and the aortic arch, the catheter can be placed at the appropriate depth.[39,40] This is feasible in the operating theatre before starting pumping and much earlier than with confirmation by means of postoperative radiography. As soon as the catheter is inserted, dissection should be ruled out with TOE.

When atheromatous plaque is present adjacent to the catheter tip, it is best to retreat the catheter slightly to prevent dislodgement of plaque.[41,42] As pumping starts, adequate inflation is confirmed by TOE findings as well as by pressure monitoring. The augmentation effect can be confirmed by measuring blood flow at the aortic arch, subclavian artery, and coronary artery. Later, improved contraction of the left ventricle is monitored using TOE.[43] When the augmentation effect is not clear on pressure monitoring, check that the balloon is adequately inflated and that the catheter tip is appropriately positioned, and rule out gas leakage. Inadequate inflation indicates the presence of a kink at any portion of the catheter or malfunction of the driving system.

Catheter intervention

Percutaneous transvenous mitral commissurotomy has become one of the routine options for treating mitral stenosis. Fluoroscopic guidance has been used in this procedure. TOE has proved to be useful for visualising and guiding catheter manipulation.[44,45] It has the following advantages.

- It may detect left atrial thrombus.
- It can be used to visualise both catheter and cardiac structures such as the interatrial septum and mitral valve.
- It avoids the use of contrast media.
- It permits immediate evaluation of commissurotomy and detection of complications (mitral regurgitation).
- It limits exposure to radiation and procedure time.[46]

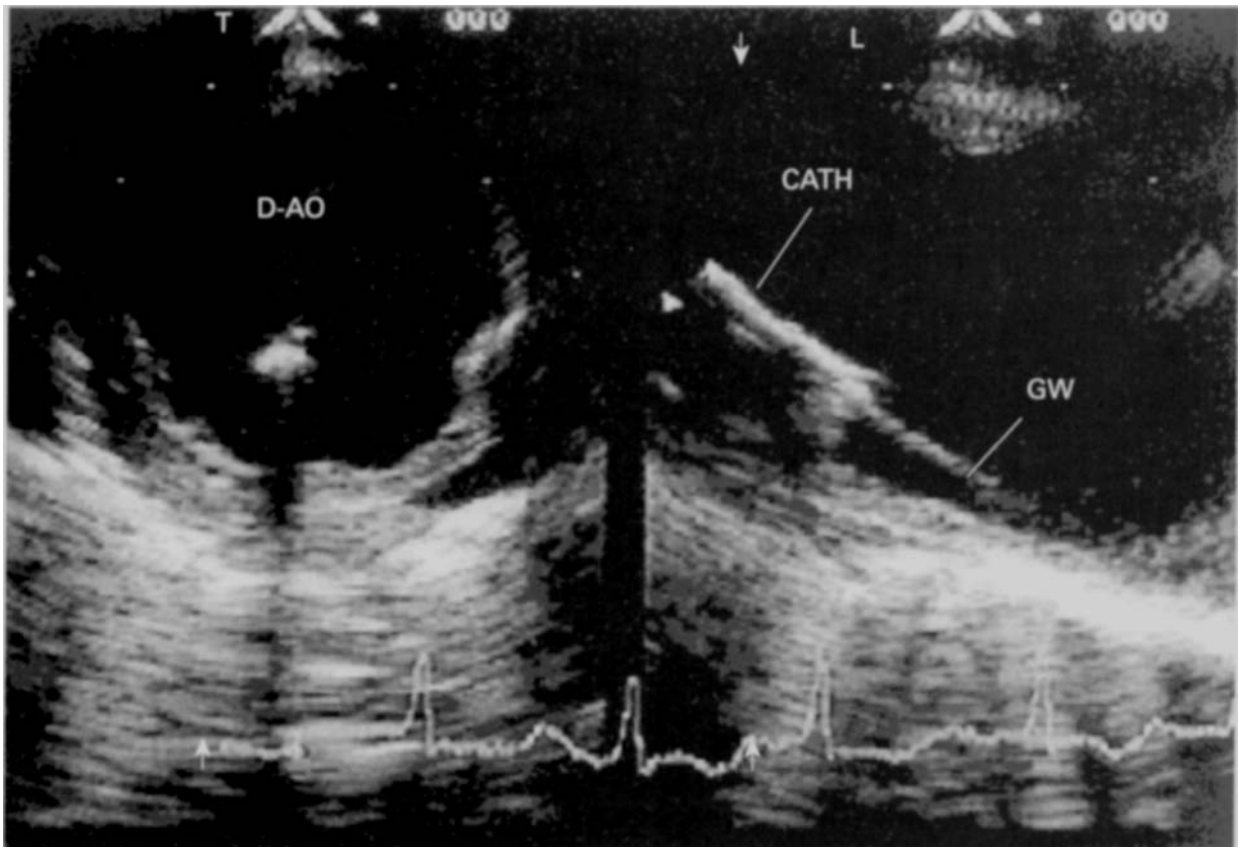

Figure 13.13 Transoesophageal echocardiogram showing placement of intra-aortic balloon pump catheter (CATH) in the descending aorta (D-AO). The catheter is being advanced along the guidewire (GW).

TOE has also applied in transseptal left heart catheterisation for radiofrequency ablation[47] and transcatheter ventricular septal defect closure.[48]

Aortic graft

Recently, placement into the descending aorta of an aortic prosthesis incorporating a self-expandable stent was attempted both surgically (Figure 13.14) and by catheter intervention. In this context, TOE is useful for[49,50]:

- evaluating the suitability of the aorta for this procedure
- determining the appropriate graft size
- clearly visualising the catheter and the aorta, facilitating precise placement of the graft
- evaluating immediately the result of the procedure (i.e. adequate contact of the graft with the aortic wall, without endoleakage)
- detection of complications such as dissection and dislodgement of atheromatous plaque.

Limitations of transoesophageal echocardiography

TOE has certain limitations in the applications referred to above. First, TOE images are two dimensional, not three dimensional. One must resolve the three-dimensional structure by accumulating planar images. Real-time, three-dimensional TOE is being developed. Second, an object that is not in the scanning plane is not visualised; thus, for any given object, the scanning plane must be manipulated to encompass the object if it is to be visualised. Furthermore, TOE is not non-invasive, but semi-invasive, and inappropriate manipulation may result in complications. Thus, the technique of TOE manipulation is important and a learning curve exists. Finally, TOE is subject to every limitation of ultrasound, including marked attenuation of ultrasound by calcification, air, metal, and so on.

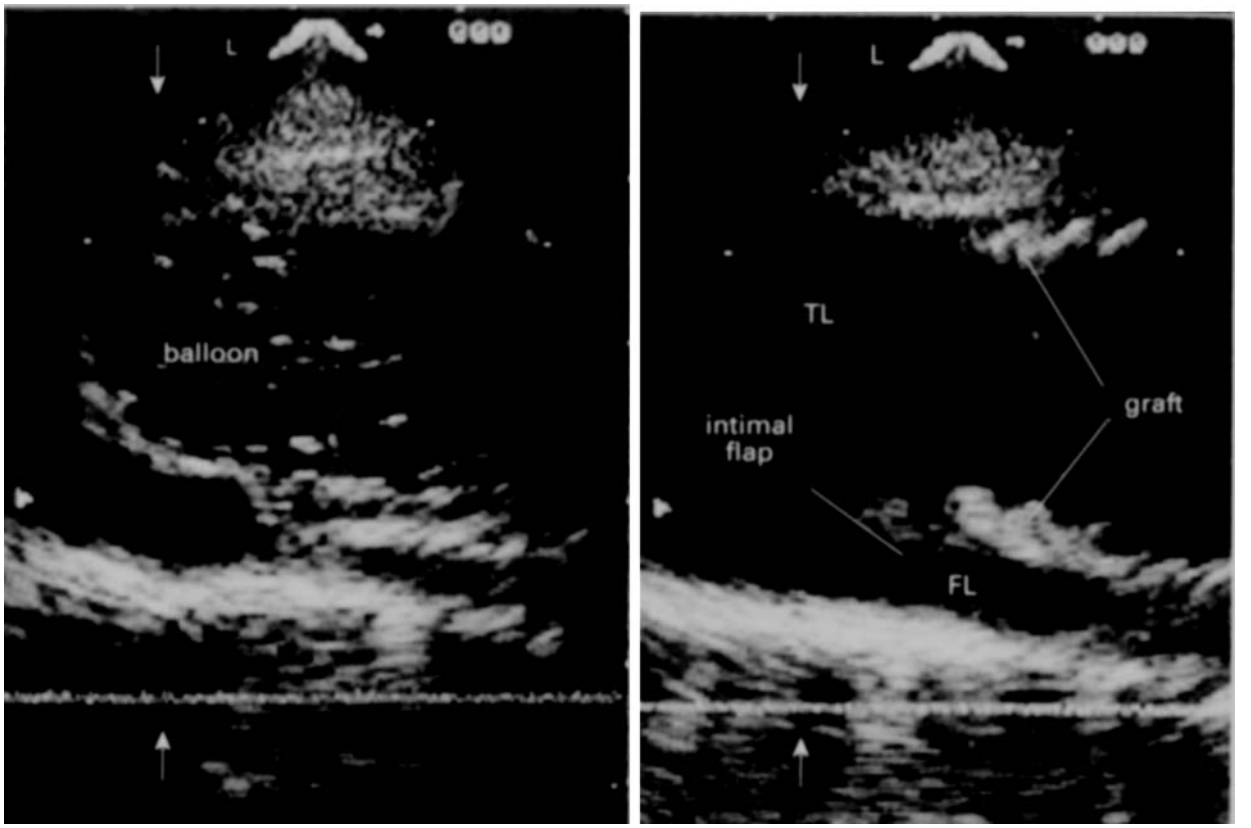

Figure 13.14 Transoesophageal echocardiogram showing placement of an aortic graft incorporated with self-expandable stent in a case of aortic dissection. The graft fills the true lumen (TL). FL = false lumen.

Conclusion

In conclusion, TOE provides clinically important information in real time, including morphological and haemodynamic parameters, and static and dynamic data. Appropriate utilisation of TOE in the applications mentioned above is of tremendous value intraoperatively, and it is associated with minimal complications. An understanding of the appropriate use of TOE and of its limitations is mandatory for obtaining the best results.

References

1 McNamara RL, Lima JA, Whelton PK, Powe NR. Echocardiographic identification of cardiovascular sources of emboli to guide clinical management of stroke: a cost-effectiveness analysis. *Ann Intern Med* 1997;**127**:775–87.

2 Manning WJ. Role of transoesophageal echocardiography in the management of thromboembolic stroke. *Am J Cardiol* 1997;**80**:19D–28D; discussion 35D–9D.

3 Nakagami H, Yamamoto K, Ikeda U, Mitsuhashi T, Goto T, Shimada K. Mitral regurgitation reduces the risk of stroke in patients with nonrheumatic atrial fibrillation. *Am Heart J* 1998;**136**:528–32.

4 Alkan LM, Yalcin R, Timurkaynak T, *et al.* Left atrial free floating thrombus. Diagnosis by two dimensional and M-mode echocardiography. *Jpn Heart J* 1995;**36**:399–404.

5 Harpaz D, Menahemi D, Dolev E, Kishon Y. Free-floating left atrial thrombus: medical management directed by transoesophageal echocardiography. *Am Heart J* 1996;**132**:1311–3.

6 Vaitkus PT. Left ventricular mural thrombus and the risk of embolic stroke after acute myocardial infarction. *J Cardiovasc Risk* 1995;**2**:103–6.

7 van der Wouw PA, Koster RW, Delemarre BJ, de Vos R, Lampe-Schoenmaeckers AJ, Lie KI. Diagnostic accuracy of transoesophageal echocardiography during cardiopulmonary resuscitation. *J Am Coll Cardiol* 1997;**30**:780–3.

8 Krivec B, Voga G, Zuran I, *et al.* Diagnosis and treatment of shock due to massive pulmonary embolism: approach with transoesophageal echocardiography and intrapulmonary thrombolysis. *Chest* 1997;**112**:1310–6.

9 Pruszczyk P, Torbicki A, Pacho R, *et al.* Noninvasive diagnosis of suspected severe pulmonary embolism: Transoesophageal echocardiography vs spiral CT. *Chest* 1997;**112**:722–8.

10 Steiner P, Lund GK, Debatin JF, *et al.* Acute pulmonary embolism: value of transthoracic and transoesophageal echocardiography in comparison with helical CT. *AJR Am J Roentgenol* 1996;**167**:931–6.

11 Vieillard-Baron A, Qanadli SD, Antakly Y, *et al.* Transesophageal echocardiography for the diagnosis of pulmonary embolism with acute cor pulmonale: a comparison with radiological procedures. *Intensive Care Med* 1998;**24**:429–33.

12 Law DA, Dulaney JJ, Graeber G. Left atrial myxoma: a case presentation and review of the literature. *W V Med J* 1995;**91**:95–7.

13 Ponduri K, Alam M, Keohane M, Jafri S, Paone G. Left atrial myxoma presenting with embolism to the aorta. *J Am Soc Echocardiogr* 1997;**10**:381–3.

14 De Carli S, Sechi LA, Ciani R, Barillari G, Dolcetti G, Bartoli E. Right atrial myxoma with pulmonary embolism. *Cardiology* 1994;**84**:368–72.

15 Rousou JA, Tighe DA, Rifkin RD, *et al.* Echocardiography allows safer venous cannulation during excision of large right atrial masses. *Ann Thorac Surg* 1998;**65**:403–6.

16 Singh I, Jacobs LE, Kotler MN, Ioli A. The utility of transoesophageal echocardiography in the management of renal cell carcinoma with intracardiac extension. *J Am Soc Echocardiogr* 1995;**8**:245–50.

17 Koide Y, Mizoguchi T, Ishii K, Okumura F. Intraoperative management for removal of tumour thrombus in the inferior vena cava or the right atrium with multiplane transoesophageal echocardiography. *J Cardiovasc Surg (Torino)* 1998;**39**:641–7.

18 Nagasaka S, Taniguchi S, Kobayashi S, *et al.* Successful treatment of intraoperative pulmonary tumour embolism from renal cell carcinoma. *Heart Vessels* 1997;**12**:199–202.

19 Gandhi AK, Pearson AC, Orsinelli DA. Tumor invasion of the pulmonary veins: a unique source of systemic embolism detected by transoesophageal echocardiography. *J Am Soc Echocardiogr* 1995;**8**:97–9.

20 Brandt RR, Rubin J, Reeder GS. Intracardiac extension of a lung tumour causing left ventricular inflow obstruction. *J Am Soc Echocardiogr* 1995;**8**:930–3.

21 Heslin MJ, Casper ES, Boland P, Gold JP, Burt ME. Preoperative identification and operative management of intraatrial extension of lung tumours. *Ann Thorac Surg* 1998;**65**:544–6.

22 O'Keefe PA, Jin XY, Jenkins M, Amadi AA, Bennett JG. Unidentified retained left atrial myxoma: intraoperative detection by transoesophageal echocardiography. *Eur J Cardiothorac Surg* 1995;**9**:599–601.

23 Oka Y, Moriwaki KM, Hong Y, *et al.* Detection of air emboli in the left heart by M-mode transoesophageal echocardiography following cardiopulmonary bypass. *Anesthesiology* 1985;**63**: 109–13.

24 Orihashi K, Matsuura Y, Hamanaka Y, *et al.* Retained intracardiac air in open heart operation examined by transoesophageal echocardiography. *Ann Thorac Surg* 1993;**55**:1467–71.

25 Wellford AL, Lawrie G, Zoghbi WA. Transesophageal echocardiographic features and management of retained intracardiac air in two patients after surgery. *J Am Soc Echocardiogr* 1996;**9**:182–6.

26 Tingleff J, Joyce FS, Pettersson G. Intraoperative echocardiographic study of air embolism during cardiac operations. *Ann Thorac Surg* 1995;**60**: 673–7.

27 Derouin M, Couture P, Boudreault D, Girard D, Gravel D. Detection of gas embolism by Transoesophageal echocardiography during laparoscopic cholecystectomy. *Anesth Analg* 1996;**82**:119–24.

28 O'Sullivan DC, Micali S, Averch TD, *et al.* Factors involved in gas embolism after laparoscopic injury to inferior vena cava. *J Endourol* 1998;**12**:149–54.

29 Mammoto T, Hayashi Y, Ohnishi Y, Kuro M. Incidence of venous and paradoxical air embolism in neurosurgical patients in the sitting position: detection by transoesophageal echocardiography. *Acta Anaesthesiol Scand* 1998;**42**:643–7.

30 Orihashi K, Matsuura Y, Sueda T, Shikata H, Mitsui N, Sueshiro M. Pooled air in open heart operations examined by transoesophageal echocardiography. *Ann Thorac Surg* 1996;**61**:1377–80.

31 Orihashi K, Matsuura Y. Quantitative echocardiographic analysis of retained intracardiac air in pooled form: an experimental study. *J Am Soc Echocardiogr* 1996;**9**:567–72.

32 Dalmas JP, Eker A, Girard C, *et al.* Intracardiac air clearing in valvular surgery guided by transoesophageal echocardiography. *J Heart Valve Dis* 1996;**5**:553–7.

33 Orihashi K, Oka Y. Cannulae. In: Oka Y, Goldiner PL, eds. *Transesophageal echocardiography.* Philadelphia, PA: J.B. Lippincott Company, 1992.

34 Orihashi K, Nakashima Y, Sueda T, Yamanoue T, Yuge O, Matsuura Y. Usefulness of Transoesophageal echocardiography for guiding pulmonary artery catheter placement in the operating room. *Heart Vessels* 1994;**9**:315–21.

35 Applebaum RM, Adelman MA, Kanschuger MS, Jacobowitz G, Kronzon I. Transesophageal echocardiographic identification of a retrograde dissection of the ascending aorta caused by inadvertent cannulation of the common carotid artery. *J Am Soc Echocardiogr* 1997;**10**:749–51.

36 Orihashi K, Matsuura Y, Sueda T, Shikata H, Mitsui N, Sueshiro M. Findings of transoesophageal echocardiographic images in placing the coronary sinus perfusion catheter. *Hiroshima J Med Sci* 1994;**43**:169–73.

37 Applebaum RM, Cutler WM, Bhardwaj N, *et al.* Utility of transoesophageal echocardiography during port-access minimally invasive cardiac surgery. *Am J Cardiol* 1998;**82**:183–8.

38 Siegel LC, St Goar FG, Stevens JH, *et al.* Monitoring considerations for port-access cardiac surgery. *Circulation* 1997;**96**:562–8.

39 Orihashi K, Hong YW, Chung G, Sisto D, Goldiner PL, Oka Y. New applications of two-dimensional transoesophageal echocardiography in cardiac surgery. *J Cardiothorac Vasc Anesth* 1991;**5**:33–9.

40 Nishioka T, Friedman A, Cercek B, *et al.* Usefulness of transoesophageal echocardiography for positioning the intraaortic balloon pump in the operating room. *Am J Cardiol* 1996;**77**:105–6.

41 Karalis DG, Quinn V, Victor MF, *et al.* Risk of catheter-related emboli in patients with atherosclerotic debris in the thoracic aorta. *Am Heart J* 1996;**131**:1149–55.

42 Orihashi K, Oka Y. Intraluminal projection of descending thoracic aorta and intraaortic balloon pump catheter examined by transoesophageal echocardiography in patients undergoing coronary artery bypass surgery. *Hiroshima J Med Sci* 1991;**40**:119–6.

43 Cheung AT, Savino JS, Weiss SJ. Beat-to-beat augmentation of left ventricular function by intraaortic counterpulsation. *Anesthesiology* 1996;**84**:545–54.

44 Orihashi K, Matsuura Y, Ishihara H, *et al.* transvenous mitral commissurotomy examined with transoesophageal echocardiography. *Heart Vessels* 1988;**3**:209–13.

45 Saleh MA, El Fiky AA, Fahmy M, Farag N, Khashaba AA. Use of biplane transoesophageal echocardiography as the only imaging technique for percutaneous balloon mitral commissurotomy. *Am J Cardiol* 1996;**78**:103–6.

46 Poirier P, Champagne J, Alain P, *et al.* Mitral balloon valvuloplasty in pregnancy: limiting radiation and procedure time by using transoesophageal echocardiography. *Can J Cardiol* 1997;**13**:843–5.

47 Tucker KJ, Curtis AB, Murphy J, *et al.* Transesophageal echocardiographic guidance of transseptal left heart catheterization during radiofrequency ablation of left-sided accessory pathways in humans. *Pacing Clin Electrophysiol* 1996;**19**:272–81.

48 van der Velde ME, Sanders SP, Keane JF, Perry SB, Lock JE. Transesophageal echocardiographic guidance of transcatheter ventricular septal defect closure. *J Am Coll Cardiol* 1994;**23**:1660–5.

49 Orihashi K, Matsuura Y, Sueda T, *et al.* Echocardiography-assisted surgery in transaortic endovascular stent grafting: role of transesophageal echocardiography. *J Thorac Cardiovasc Surg* 2000;**120**:672–8.

50 Orihashi K, Sueda T, Watari M, Okada K, Ishii O, Matsuura Y. Endovascular stent-grafting via the aortic arch for distal aortic arch aneurysm: an alternative to endovascular stent-grafting. *Eur J Cardiothorac Surg* 2001;**20**:973–8.

14 Minimally invasive and minimal access cardiac surgery

Fiona Clements

Introduction

The age of minimally invasive cardiac surgery is upon us. However, "minimally invasive" means different things to different people. In coronary artery surgery (coronary artery bypass grafting [CABG]) this might mean simply doing without cardiopulmonary bypass (CPB). "OPCAB", for example, generally means "off-pump coronary artery bypass grafting", and is done with a standard median sternotomy. The term "MIDCAB", on the other hand, implies an off-pump CABG through a small incision, generally confined to a left internal mammary artery graft to the left anterior descending coronary artery (LAD).

Coronary grafting has been attempted through a variety of small thoracotomy incisions, depending upon the vessels to be grafted and the conduits to be used. Surgical techniques that permit coronary grafting without needing to support the circulation with CPB are becoming more and more successful. At the same time, techniques that allow for smaller incisions are being advanced through development of innovative suturing techniques, videoscopy, and robotics.

With off-pump techniques, transoesophageal echocardiography (TOE) allows us to see how well the left ventricle is tolerating the procedure, which inevitably involves manipulation of the heart by the surgeon, especially for grafting of the circumflex coronary. Eversion of the heart out of the chest can be accompanied by difficulty with left ventricular filling, systolic dysfunction, and mitral insufficiency. The profound change in the axis of the heart makes the electrocardiogram uninterpretable and probably irrelevant, because the issue is not so much whether there is ischaemia but rather whether the left ventricle can maintain adequate circulation during grafting. Once grafting has been accomplished TOE can tell us something about the recovery process and, particularly, the recovery of function in those areas of the myocardium supplied by the grafted coronary artery. Although not yet in clinical use, contrast agents may yet play a role in helping to assess the quality of the new graft. Certainly, to be effective in utilising TOE to monitor these procedures, the user must have a thorough understanding of the segmental anatomy of the left ventricle in order to relate segmental dysfunction to the various coronary arteries and, indeed, to make sense of preoperative stress echo studies that would be relevant.

Intracardiac procedures are also being done with minimally invasive techniques. These include, but are not limited to, valve surgery and atrial septal defect repairs. They may be done under direct vision or with the assistance of videoscopic equipment. In any event, the surgical view is confined to the immediate target of the procedure, and the surgeon is unable to see or feel much of the cardiac chambers. In these circumstances, TOE acts as a substitute for the direct vision and palpation of the heart, which are traditionally available to the surgeon and anaesthetist with open chest procedures.

For minimally invasive procedures requiring CPB and cardioplegia, a number of catheters and cannulae have been developed that fulfil these needs in the absence of a median sternotomy. Port-Access™ procedures developed by the Heartport Company (Redwood, California, USA) might be considered the prototype for a system that allows cardiac surgery to be accomplished through a 5–8 cm incision with circulatory support and conventional myocardial protection.

In this chapter, we first consider off-pump procedures (OPCAB and MIDCAB), in which segmental left ventricular function is of particular relevance. We then consider on-pump procedures, in which TOE has multiple and specific uses.

Off-pump coronary surgery

In off-pump coronary surgery, TOE has value in assessing the following:

- global left ventricular function during grafting
- regional left ventricular function before, during, and after grafting
- position related valvular insufficiency.

Global left ventricular function

Left ventricular (LV) function during off-pump coronary surgery is compromised by the stabilisation devices used by the surgeon for coronary anastomoses and by the elevation of the heart out of the chest, which is required for anastomoses of the circumflex coronary system. The more spectacular surgical manoeuvres are better tolerated by a heart that is well filled, and this can be accomplished by steep head-down positioning and by fluid administration. Even hearts with low ejection fractions will tolerate the surgery provided that adequate preload is provided.

Regional left ventricular function

Even in the presence of adequate overall LV function, regions or segments of the LV may exhibit systolic dysfunction. These are collectively termed systolic wall motion abnormalities (SWMAs) and refer to some abnormality of myocardial contraction in the segment of interest. Normal myocardium thickens by about 30% during systole. A segment that thickens less than this is termed hypokinetic. Of course, where a myocardial infarction has previously taken place the myocardium will have become scarred. The segment then appears thin in comparison with adjacent normal myocardial tissue and will fail to contract at all during systole. This is termed akinesia. When the segment appears to bulge outward during systole, the segment is described as dyskinetic. During off-pump CABG, most attention should be paid to segments that develop new regional SWMAs, because these are most likely to represent new changes in coronary blood supply and should be restored to normal function with restoration of blood flow.

Moises and colleagues[1] examined the incidence and significance of new SWMAs occurring in 27 patients undergoing off-pump CABG. TOE was used intraoperatively, and transthoracic echo was used preoperatively and 7 days postoperatively for comparison. There were 48 coronary artery anastomoses, 31 of which were accompanied by new SWMAs. By the end of surgery, 16 of the 31 SWMAs had completely recovered, 10 had partially recovered, and 5 were persistent. By the postoperative day 7, only eight of the ten partially recovered segments had returned to normal, and the five persistent SWMAs at the end of surgery remained the same. The seven patients with persistent SWMAs were found to have had a significantly higher incidence of surgical problems intraoperatively (71·4%) than had patients without (20%). Four of the seven patients developed evidence of perioperative myocardial infarction, whereas none of the patients without persistent SWMAs did so.

Interestingly, the 17 coronary anastomoses that were not associated with new SWMAs occurred in patients who had previously suffered a myocardial infarction in the corresponding area of the left ventricle. In that report, three lead electrocardiographic monitoring showed ST-T wave abnormalities during only nine anastomoses, all involving the right coronary artery (RCA).

Most studies reporting off-pump CABG have involved single grafts of the left internal mammary artery to the LAD. Since the introduction of stabilization devices, LAD anastomoses are accomplished more easily and with little ventricular compromise. Jurmann *et al.*,[2] in a study of 28 patients, found that anterior placement of the stabilization device itself lead to negligible changes in LV geometry. With LAD occlusion, however, segmental hypokinesia was usual, with some reduction in LV function and increase in LV diameter. However, overall function was generally adequate (Table 14.1).

As in many centres, these authors did a 5 minute test occlusion of the LAD before beginning the anastomosis. The test occlusion is generally done for two purposes: first, if it is associated with severe regional dysfunction or life threatening dysrhythmias, then the procedure may be converted to an on-pump CABG; and second, it has been shown that a brief coronary occlusion results in better tolerance of subsequent ischaemia, as may be expected during a 15–20 minute coronary anastomosis. The test occlusion is known as "ischaemic preconditioning". Jurmann

Table 14.1 Haemodynamic variables related to cardiac function during MIDCAB[2]

Variable	Baseline	Stabiliser	Ischaemia	Recovery
Cardiac index (l/min per m^2)	2·14 ± 0·49	2·09 ± 0·51	1·0 ± 0·54	2·8 ± 0·6
PCWP (mmHg)	12·7 ± 2·6	12·9 ± 2·7	13·8 ± 3·1	12·1 ± 4·2

PCWP = pulmonary capillary wedge pressure. (Data from Jurmann *et al.*[2])

et al.[2] found that TOE evidence of severe LV compromise during the test occlusion was very helpful in making the decision to use CPB. Other authors have noted that segmental wall motion abnormalities are generally seen only with test occlusion when the native vessel is less than 75% occluded to begin with.[3] Test occlusions are not done when the native vessel is known to be 100% occluded.

Bonatti and colleagues[4] looked at myocardial damage after off-pump CABG. They attempted to correlate echocardiographic and electrocardiographic evidence with biochemical evidence of myocardial ischaemia. Ten of the fifteen patients studied had echocardiographic and/or electrocardiographic evidence of ischaemia intraoperatively and/or postoperatively. One of these died with a myocardial infarction. Six of the patients had transient intraoperative ischaemia. In three of these patients, ischaemia appeared postoperatively as well and in a further three it was seen only during the postoperative period, possibly related to coronary or left internal mammary artery spasm. Of the ten patients demonstrating some echo or ECG evidence of ischaemia, five had elevated cardiac troponin levels, and three of these had a clinical correlate (one lethal myocardial infarction, two symptomatic LAD stenoses). All patients without ischaemia by echocardiography and electrocardiography also had normal enzymes and good clinical outcomes. Therefore, echocardiographic and electrocardiographic evidence of ischaemia in this study was sensitive, but not specific, for myocardial damage. This is in agreement with previously published work regarding regional wall motion abnormalities detected by echocardiography.[5,6]

The quantitative assessment of SWMAs has been extensively reviewed elsewhere and is beyond the scope of this chapter. In clinical practice it is more useful that the anaesthetist has a good understanding of LV segmental terminology and of the relationship of the coronary arterial blood supply to those segments. In this way, the anaesthetist can interpret the preoperative stress echo findings and correlate them with the intraoperative coronary occlusion.

Left ventricular segmentation

The left ventricle is considered generally to be a bullet-shaped structure, from mitral valve annulus to apex, and the long axis dimension of the left ventricle is divided into three roughly equal portions (Figure 14.1): basal, mid, and apical. The prevailing system divides the basal and mid portions into six segments, and the apex into four. This provides 16 segments, which can be found by three short-axis views or by various long-axis views that may be obtained using a multiplane transducer. Although the precise angulation varies according to the exact orientation of the heart with respect to the transducer in the oesophagus, it can be seen that as the angle is rotated from 0° (Figure 14.2) upward (Figures 14.3 and 14.4) the LV free wall seen on the right side of the image progresses from the lateral wall toward the anterior and anteroseptal segments. These segments would usually correspond with the circumflex and LAD coronary distribution. In the four chamber long-axis view at 0°, the left (septal) wall of the left ventricle is the septal segment (served by the LAD and right coronary), progressing as the angle is increased to the inferior and posterior segments. The inferior and septal segments would usually be served by the RCA, with posterior segments being in the territory of the circumflex coronary artery. Apical segments are generally served by the LAD. However, the apical inferior segment may be supplied by the posterior descending coronary, which normally comes from the right coronary. Accordingly, if the apical inferior segment is abnormal, then

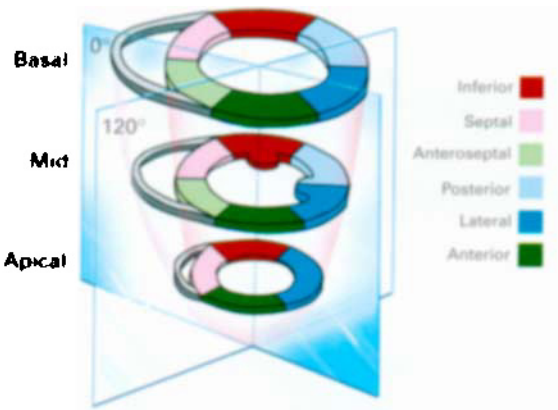

Figure 14.1 Left ventricular segmentation

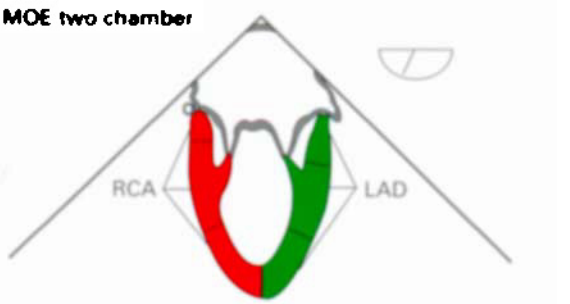

Figure 14.3 Mid-oesophageal (MOE) two chamber view. LAD = left anterior descending coronary artery, RCA = right coronary artery.

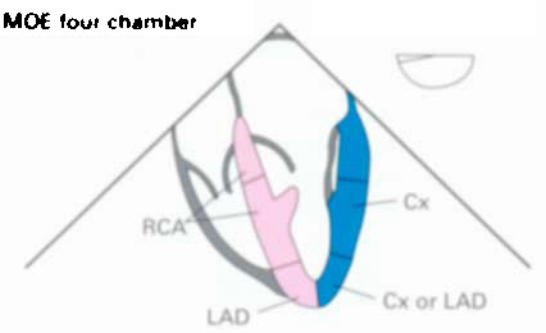

Figure 14.2 Mid-oesophageal (MOE) four chamber view. Cx = circumflex coronary, LAD = left anterior descending coronary artery, RCA = right coronary artery.

Figure 14.4 Mid-oesophageal long-axis (MOE LAX) view. Cx = circumflex coronary, LAD = left anterior descending coronary artery, RCA = right coronary artery.

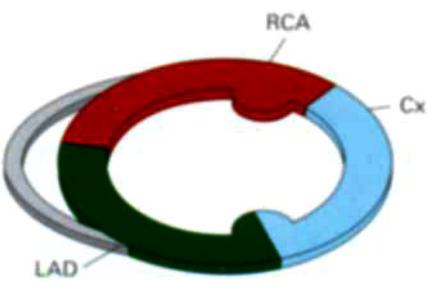

Figure 14.5 Short-axis view of the left ventricle at a mid-papillary muscle level, showing the coronary artery supply. Cx = circumflex coronary, LAD = left anterior descending coronary artery, RCA = right coronary artery.

evidence of other LAD or RCA related segmental dysfunction should be sought. If, for example, there was also coexisting apical septal dysfunction, implicating LAD disease, then this would suggest that the LAD was also supplying the inferior apex. Likewise, the apical lateral segment may be served by either the LAD or the circumflex. When this segment is abnormal, other abnormal segments should be sought. If the apical septal segment is normal but the mid-level lateral segments are abnormal, suggesting circumflex disease, then the apical lateral segment would also be assigned to the circumflex coronary artery.

SWMAs are most readily appreciated on a mid-papillary short-axis view, in which both endocardium and epicardium can be clearly seen. At this level all coronary arteries are normally represented (Figure 14.5). During off-pump CABG, however, a short-axis view may be unobtainable, especially during elevation of the heart to do a circumflex graft. In this case the ventricle can be scanned using the various long axis views to examine all segments, as shown in Figures 14.2–14.4.

In all off-pump CABGs there has been considerable concern about graft patency where surgical anastomoses are performed on a moving target. Stabilisation devices have done much to

encourage the surgeon to feel that they have achieved a technically good result. However, in many institutions confirmation of graft patency by angiography would be desirable, to justify the departure from the conventional and proven on-pump CABG. Through the use of contrast agents that can be injected directly into a graft, we may find that intraoperative TOE will find a role in providing evidence of adequate blood flow. However, this is as yet speculative. Preliminary work with intraoperative stress echo also indicates that this may be a feasible method for assessing the surgical result, independently or in conjunction with contrast agents.[7]

Position-related valvular insufficiency

Occasionally, mitral valvular insufficiency will be a problem during off-pump CABG. A patient with pre-existing mitral annular dilation due either to inferior wall myocardial infarction or to global LV dilation may be more prone to severe mitral insufficiency during elevation of the heart to do a circumflex anastomosis. Similarly, temporary occlusion of the RCA may result in posterior papillary muscle dysfunction and transient mitral insufficiency. This may be enough of a problem to warrant putting the patient on bypass. We have only found this to be a problem during elevation of the heart, and then only in patients with pre-existing myocardial dysfunction. A majority of patients undergoing off-pump multivessel CABG do so without serious haemodynamic compromise.

Port-Access™ procedures

Port-Access procedures were developed by a group of physicians from Stanford University, and subsequently through the Heartport company, as an innovative solution to the problem of doing cardiac surgery through a small incision without sacrificing the options of CPB, cardioplegic arrest, and LV venting. With this technique, the bloodless field and arrested heart provide the same optimal surgical conditions as do conventional surgery, which should allow for optimal technical results.

It can be seen from Figure 14.6 that the bypass cannulae are removed to the femoral vessels. The venous cannula is advanced from the femoral vein as far as the junction of the right atrium and the superior vena cava (SVC). The system is

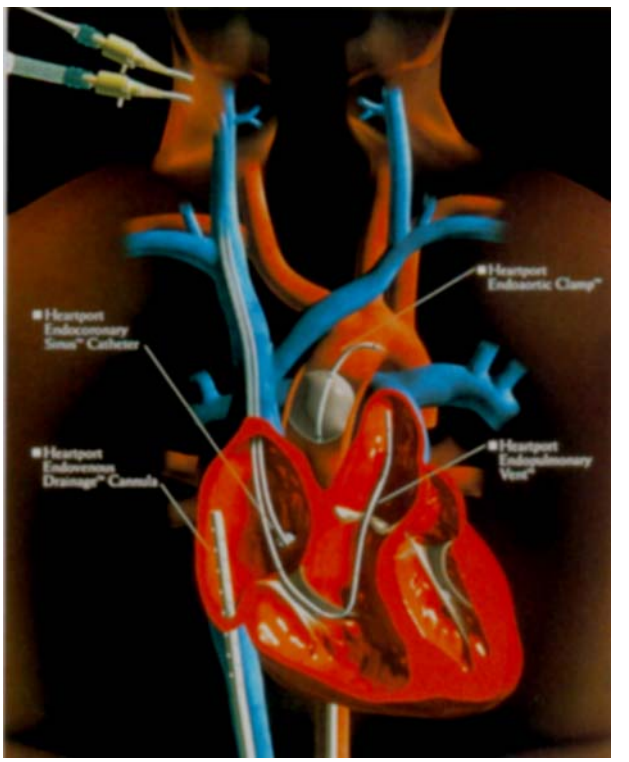

Figure 14.6 The Port-Access system. (Reproduced with permission from the Heartport Company, Redwood, California, USA.)

designed to use assisted venous drainage, meaning that venous drainage is not simply gravity fed, but rather that negative pressure is applied to the venous cannula. Assisted venous drainage is coming back into vogue as manufacturers provide smaller venous cannulae for CPB. Many of these can now be inserted percutaneously.

The arterial cannula differs from the usual femoral arterial cannula in having a "Y" form that allows for passage of the endoaortic clamp (EAC; also known as an aortic occlusion balloon catheter) via the side arm, through the cannula, and up into the aorta. An alternative, central aortic cannula, has now been developed for insertion via a port in the first or second interspace on the operative side of the chest into the ascending or transverse aorta. As with the femoral cannula, the EAC can be passed through it. The balloon occlusion of the aorta, replacing the aortic clamp, is a main feature of the Port-Access system. The central lumen of the balloon-tipped catheter provides for antegrade cardioplegia delivery and, when not in use, for aortic root venting. A parallel and separate

channel in the catheter allows for aortic root pressure measurement. Proper positioning of the balloon in the aortic root is a prime concern for the whole operative team. Migration of the inflated balloon into the aortic arch can occlude the innominate artery; migration to the aortic valve, or through it into the left ventricle, can impair cardioplegia delivery and maintenance of a cold, arrested, and empty heart. The central aortic cannula has an advantage here in that the inflated balloon can be stabilised against the cannula and migration is much less likely to be a problem.

The pulmonary artery vent is placed by the anaesthetist and serves two purposes. First, by collecting any excess blood volume from the pulmonary artery, it contributes to effective emptying of the cardiac chambers. Second, the amount of blood vented provides a check on the effectiveness of the venous cannula, which, when draining properly, should be accompanied by a vent flow rate of less than 50 ml/minute.

The coronary sinus (CS) catheter is also placed by the anaesthetist, via an 11Fr introducer that is usually placed in the right internal jugular vein. A 2-ml balloon provides CS occlusion during cardioplegia delivery and a separate channel in the catheter allows for pressure monitoring.

Conceived as a complete system, Port-Access requires specific training, especially in fluoroscopy and TOE, for placement and positioning of the various catheters and cannulae involved. A pre-existing knowledge of TOE has proved to be invaluable to the anaesthetist, and indeed TOE is integral to the success of the technique. In many institutions familiar with Port-Access procedures and in which TOE expertise is readily available, fluoroscopy is now seldom used.

The role of TOE in Port-Access procedures can be considered threefold (Table 14.2):

- special diagnostic
- cannula/catheter placement
- monitoring.

Special diagnostic

This concerns the TOE examination for specific diagnoses that have a bearing on the conduct of the operation. A number of diagnoses that may go undetected before surgery can pose special problems for the use of assisted venous drainage, femoral arterial cannulation, and passage of a catheter up the length of the aorta.

Table 14.2 The roles of transoesophageal echocardiography Port-Access procedures

Role	Details
Special diagnostic	Aorta Interatrial septum Aortic valve competence
Cannula/catheter placement	Coronary sinus catheter Pulmonary vent Femoral venous cannula and guidewire Femoral aortic cannula and guidewire Endoaortic clamp catheter and guidewire; balloon inflation
Monitoring	Left ventricule filling and function Endoaortic clamp balloon position Venous cannula position Intracardiac air

Evaluation of the aorta

Any cardiac procedure that involves cannulation of the aorta carries with it a risk for aortic dissection. With passage of an aortic cannula into the relatively small femoral artery, the risk for dissection is somewhat higher. Early in the experience of Port-Access procedures a number of dissections were reported. It was also recognised that preoperative cardiac catheterisation is associated with a 3% incidence of aortic dissection or intramural haematoma formation, and that patients arriving for surgery may have some catheterisation related trauma to their aortic or femoral vessels. Therefore, the initial diagnostic TOE examination performed after induction of anaesthesia should pay special attention to the entire visible aorta, as far down into the abdominal region as possible.

In addition to looking for intimal flaps and intramural haematomas, a careful examination for atherosclerotic plaques should be done. At Duke University we have certainly abandoned plans for femoral artery cannulation after finding large protuberant atheromata, that were entirely unexpected, in the descending aorta. The best view for evaluating such atheromata is a cross-sectional plane of the aorta as seen at 0° (Figure 14.7). With this view, any irregularity can be evaluated more accurately than with a tangential view that slices through the aortic wall at an angle. In the arch some transducer angulation will be required to maintain this cross-sectional view. Because of the risk for dislodging atheromatous plaques with guidewires and intra-aortic catheters, some

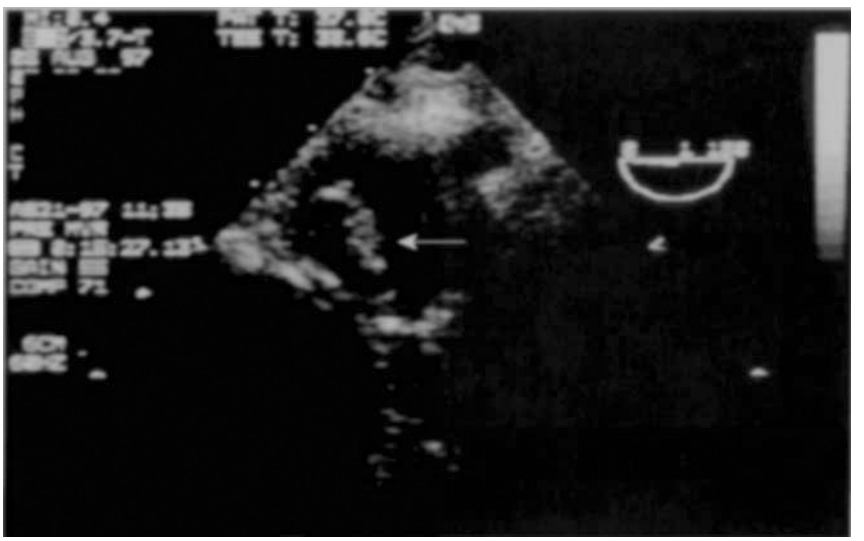

Figure 14.7 Short-axis view of the descending aorta, showing a protruding atheroma that was unsuspected and changed the surgical plan from femoral to central aortic cannulation.

institutions have specifically obtained aortic run-off angiography at the time of cardiac catheterisation to evaluate the lower aorta and femoral vessels. Others have recommended preoperative spiral computed tomography or magnetic resonance imaging. A TOE examination in the operating room will serve as a final check of the thoracic aorta.

Finally, attention should be paid to tortuosity and dilation of the aorta that may complicate catheter and/or endoaortic balloon placement. Many anaesthetists will measure the diameter of the aortic root just above the sinotubular junction (Figure 14.8). This serves as a guide as to how much volume will be needed in the balloon to occlude the aorta for cardioplegia delivery. A diameter of more than 3·5 cm may be too large. It is also useful to examine the arch; the origin of the left carotid artery is usually visible with a 60–70° angulation, and the origin of the innominate at a 120° angle. If the arch vessels are easily seen it is more probable that TOE will be helpful in detecting cephalad migration of a femorally introduced EAC balloon.

Interatrial septal defects

As many as 25% of cadavers have a probe patent foramen ovale. By TOE examination, with contrast injection and Valsalva manoeuvre to elevate the right atrial pressure above the left, the detection rate should be similar.[8] True atrial

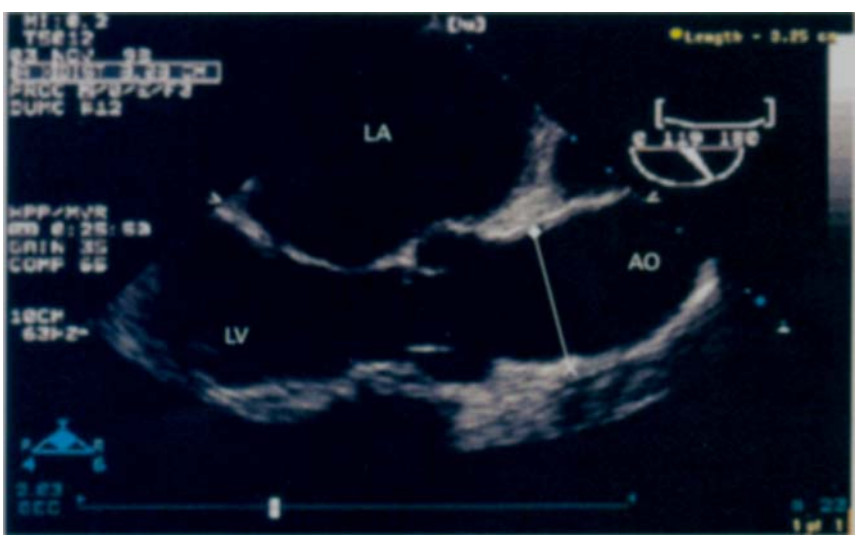

Figure 14.8 Measuring the aortic root diameter. Ao = aorta, LA = left atrium, LV = left ventricle.

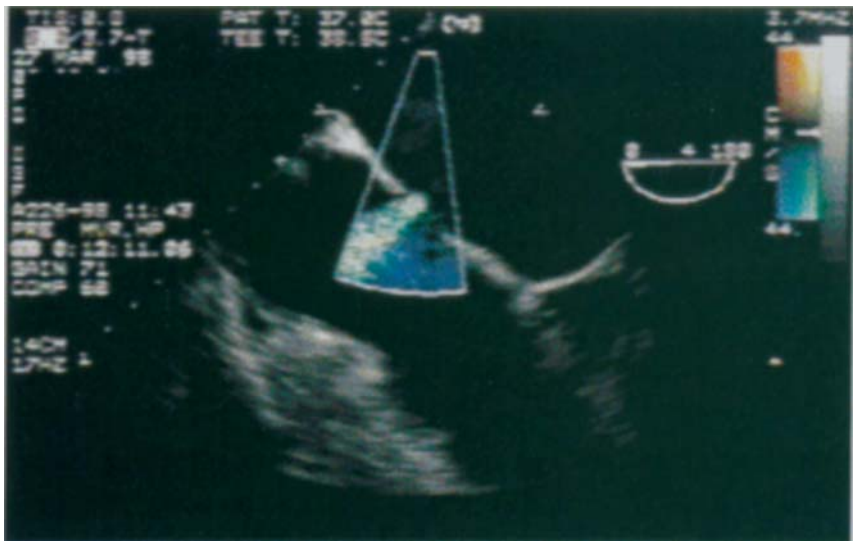

Figure 14.9 Iatrogenic atrial septal defect in a patient with severe mitral stenosis who had undergone balloon mitral valvuloplasty 2 years earlier.

septal defects may also go undetected in the cardiac surgical population because preoperative transthoracic echo studies may not have been done and are not as sensitive as TOE.

The significance of an interatrial communication concerns the use of assisted venous drainage, with which a negative pressure will be applied to the right atrium during CPB. For a closed heart procedure such as CABG, this poses no difficulty. However, if the left atrium is to be opened for a mitral valve procedure, then air can be sucked into the venous cannula, compromising venous drainage.

In patients presenting with mitral stenosis, it should be remembered that the patient may previously have undergone an attempt at balloon dilation of the mitral valve – a procedure that requires the cardiologist to pass a stiff balloon-tipped Brockenbrough catheter across the atrial septum. These procedures frequently result in an iatrogenic atrial septal defect that is small but significant for the purposes of surgery (Figure 14.9).

The presence of an interatrial communication does not preclude a Port-Access mitral valve procedure. If the defect is known to the surgeon then it is simply a matter of placing a few stitches to close it before proceeding with the planned operation.

Aortic insufficiency

Some mild degree of aortic insufficiency is a relatively common finding in the elderly population presenting for CABG or other cardiac surgery. It may be unrecognised and certainly of no significance for the clinical management of the patient, except for the purpose of delivering antegrade cardioplegia. Recognition will alert the operative team to the possibility of LV distension during antegrade cardioplegia administration and may raise the issue of whether a CS catheter should be used to provide retrograde cardioplegia, which might otherwise have been thought unnecessary (Figure 14.10). It should also be noted that it will be useful to know whether the valve was competent before the procedure, in the event of intraoperative balloon migration through the aortic valve. This has been associated with new onset aortic insufficiency of short duration.

Catheter and cannula placement

For safe placement of various catheters in the heart by TOE, it is important to remember that the image is a thin 2-mm, two-dimensional slice. The catheter may pass through this slice and appear as a dot, but the catheter tip may be far ahead of where it should be. TOE guidance demands careful communication between the TOE operator and the person advancing the catheter or wire, so that the correct imaging planes are used in each region.

Coronary sinus retrograde cardioplegia catheter

The CS can be imaged easily in the 0° plane (Figure 14.11), and with a little more effort in a

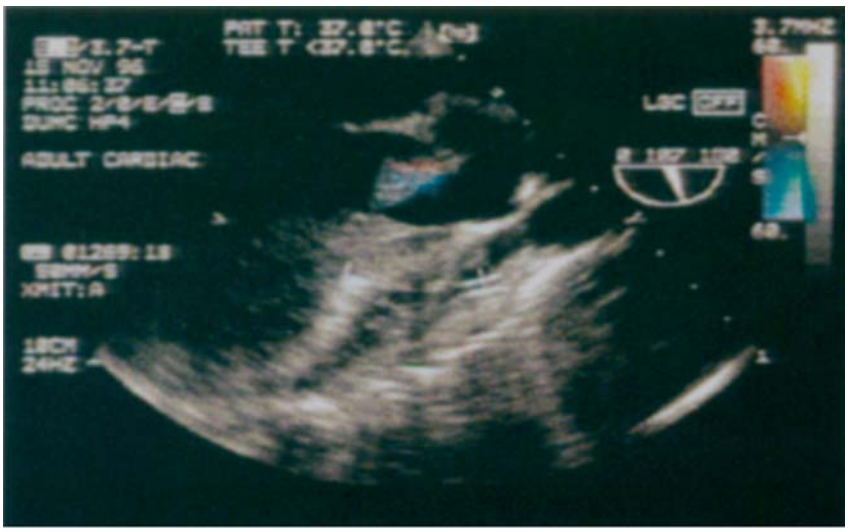

Figure 14.10 Mild aortic insufficiency, which may pose a problem for antegrade cardioplegia delivery.

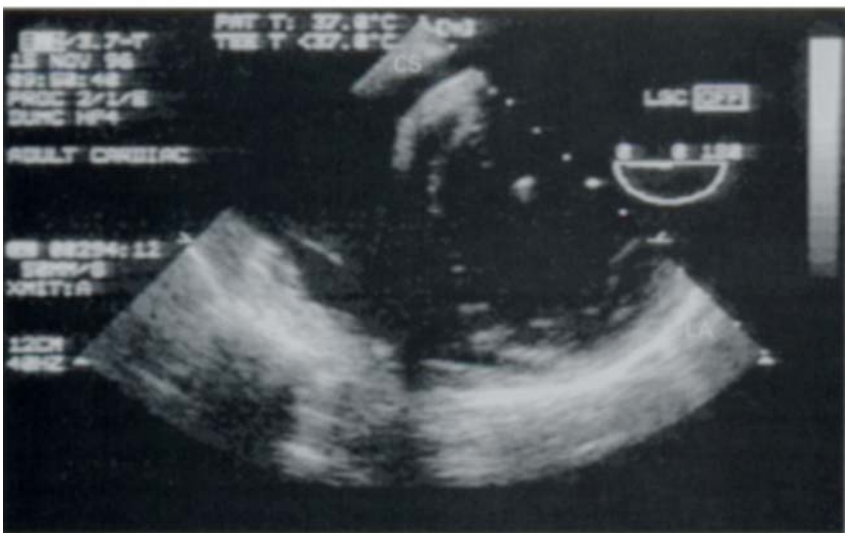

Figure 14.11 0° View of the coronary sinus (CS). LA = left atrium, LV = left ventricle, RA = right atrium.

modified bicaval image of 90–120° (Figure 14.12). It is normally about 8–9 mm in diameter (range 7–15 mm), but if it appears dilated there may be some abnormal drainage into it, such as a persistent left superior vena cava (SVC), which occurs in 0·5% of the general population[9]. A persistent left SVC would preclude the use of retrograde cardioplegia. More commonly, a large coronary sinus will be associated with an enlarged heart and with right atrial volume overload.

In order to pass the catheter, the modified bicaval view is sought, with the goal of having the orifices of both the SVC and the CS in the same image. In general the best view will be obtained at about 110°. Special attention must be given to correct identification of the IVC and the CS, which have their orifices adjacent to each other, with the CS lying on the left side of the IVC. The IVC is twice as broad in diameter as the CS, and it can be followed into the liver with some clockwise rotation of the probe, whereas the CS is followed around the left atrioventricular groove, where it appears as a circle, by anticlockwise rotation of the TOE probe (Figure 14.13).

The curved CS catheter is passed through the introducer with its tip facing posteriorly and slightly medially, toward the 7 o'clock position (Figure 14.14). At about 25–30 cm it should

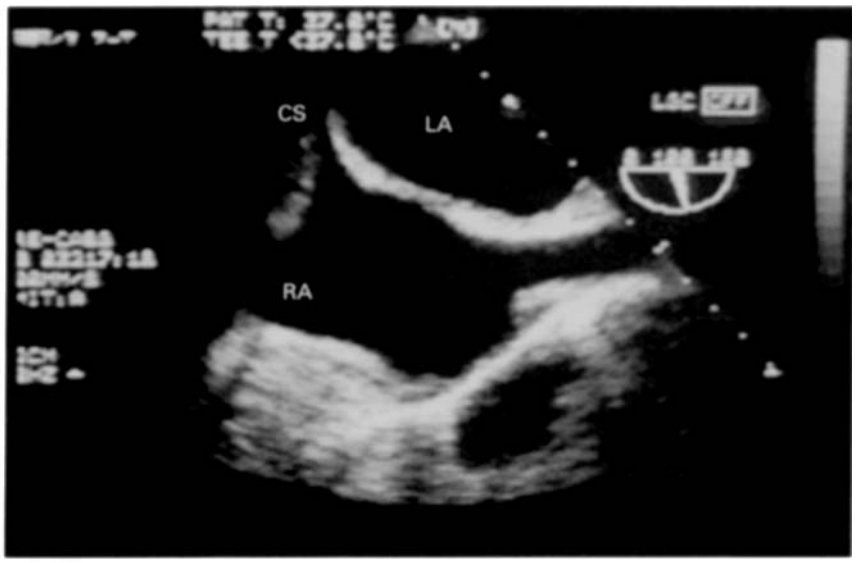

Figure 14.12 Modified bicaval image showing the coronary sinus. (Reproduced with permission from Clements *et al.*[9])

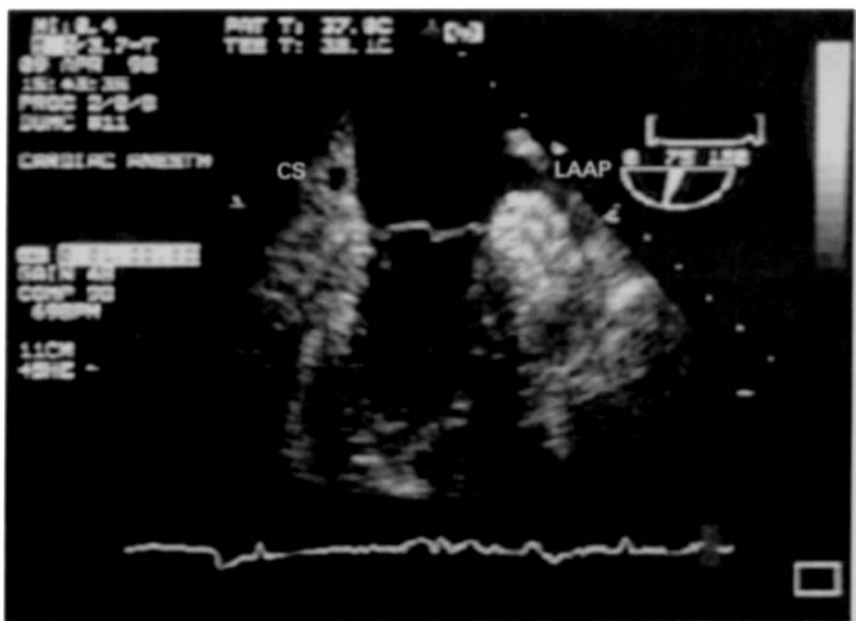

Figure 14.13 The coronary sinus (CS) appears as a circle in a cross-section as the transoesophageal echocardiography probe is rotated anticlockwise.

appear on the TOE image at the junction of the SVC and the right atrium. The pressure monitoring port should be connected and flushed so as to provide a readable pressure tracing during the advancement process. Because the imaging plane connects the SVC and the CS, the properly directed catheter should appear as a long line, with its tip clearly visible (Figure 14.15A). If it does not do so, then it is not aligned correctly to enter the CS and its direction should be adjusted. The distance that the catheter has been advanced should always be borne in mind, because after arriving at the right atrium a further 5 cm should bring it to the CS orifice. Upon entering the CS the distance should again be noted because it is expected to require another 2–5 cm advancement. As the catheter is advanced into the CS, the line of the catheter will be clearly visible on the TOE image and its degree of curvature should remain the same. If it bends or bows then it has encountered some resistance and should be withdrawn (Figure 14.15B). A slight change in angle may help in advancing the catheter to the desired depth.

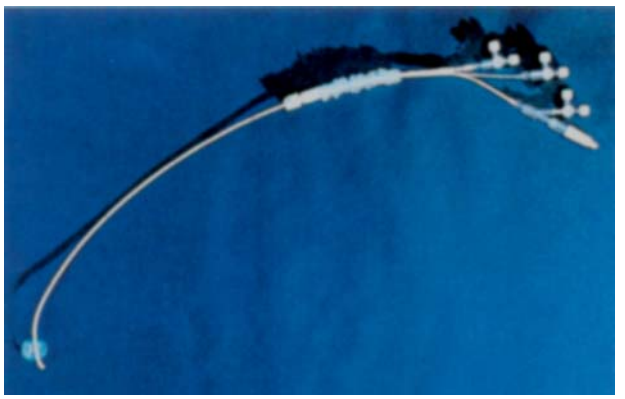

Figure 14.14 Coronary sinus catheter for retrograde cardioplegia delivery, shown with balloon inflated. (Reproduced with permission from the Heartport Company, Redwood, California, USA.)

When the catheter has been advanced about 3 cm into the CS, the balloon should be gently inflated while observing the pressure waveform. If the waveform changes, resembling a right ventricular trace, then CS occlusion has been achieved (Figure 14.16). If this change occurs with only 0·5 ml of balloon inflation, then it may inferred that the catheter is well into the CS and may safely be withdrawn by half a centimetre or so. If the balloon takes 2 ml before the waveform changes, then it may be desirable to deflate the balloon and advance the catheter a little further.

Some centres prefer to use only fluoroscopy or to use fluoroscopy in conjunction with TOE, as we previously recommended[9] (Figure 14.17). Our decision to use TOE alone saves the time and expense associated with fluoroscopy and allows

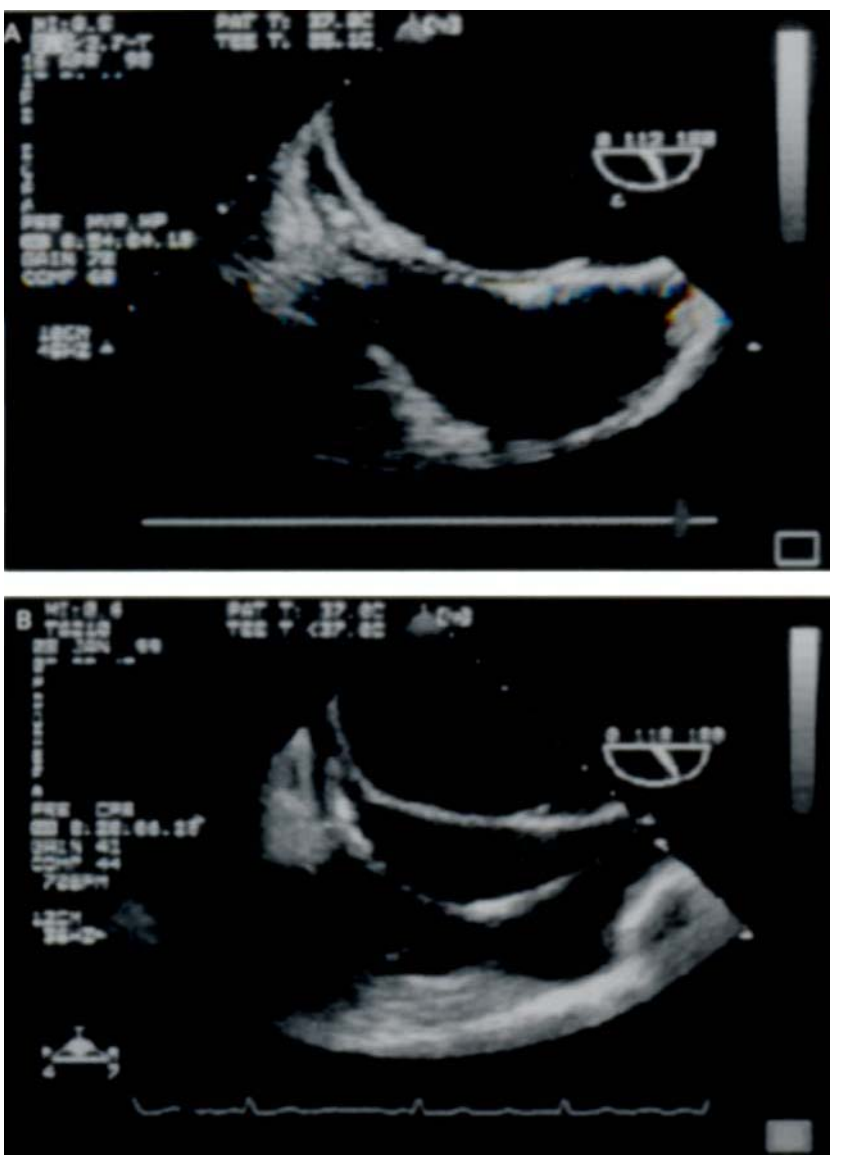

Figure 14.15 Insertion of coronary sinus (CS) catheter. **(A)** CS catheter correctly aligned, entering the coronary sinus. **(B)** "Buckling" of the catheter as it encounters an obstruction. LA = left atrium.

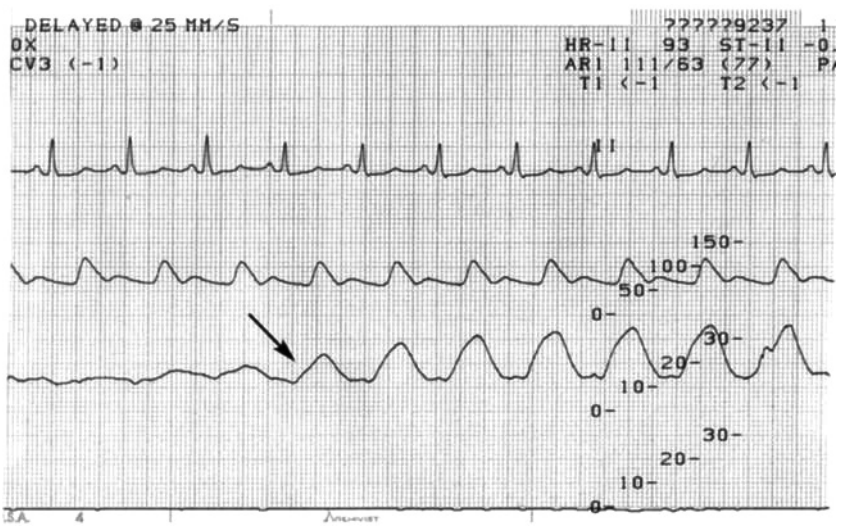

Figure 14.16 Pressure waveform associated with balloon occlusion of the coronary sinus (CS). BP = systemic blood pressure.

us to insert the catheter while the surgeon is proceeding with skin preparation and exposure of the heart. However, we also recognise that a difficult CS catheterisation may have to be abandoned without fluoroscopy, and feel that a guidewire technique is not feasible unless fluoroscopy is to be used; TOE imaging cannot reliably follow a small guidewire along a substantial length of the CS.

Pulmonary artery vent

The pulmonary artery vent can be positioned by pressure waveform, in the same way that a conventional pulmonary artery catheter is. TOE can be helpful in defining the position but it is not essential.

Femoral venous cannulation

The venous cannula is advanced from the femoral vein over a dilator and a guidewire. Preferably, the whole assembly will be advanced from the right femoral vein, which provides a direct path up to the right atrium. When the cannula must be passed from the left femoral vein, there is more likely to be difficulty in getting the relatively stiff cannula to cross the vertebral column. In either case it is important that the TOE operator image the wire as it enters the right atrium from the inferior vena cava (IVC), and can see it passing as a straight line into the SVC (Figure 14.18). The surgeon will have a good idea of how far in the wire should be from the femoral access point by having previously laid the wire across the patient's torso from the groin to the right

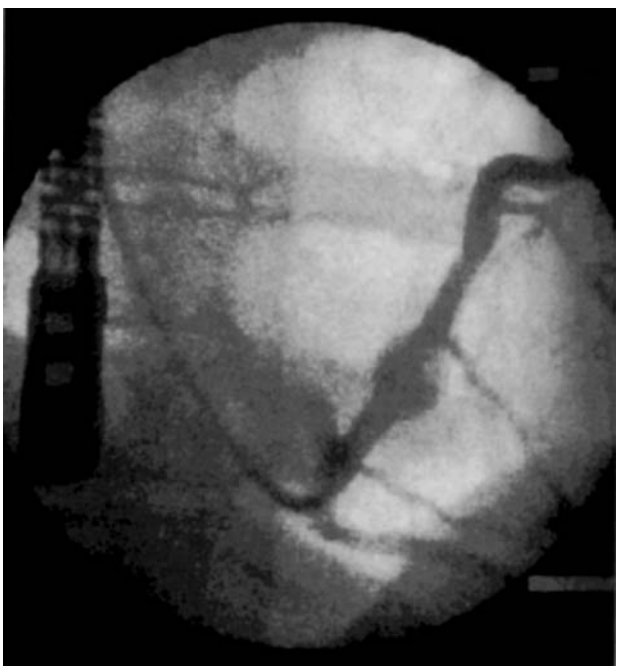

Figure 14.17 30° RAO fluoroscopy image of the coronary sinus, with contrast injection. The TOE probe is seen on the left. (Reproduced with permission from Clements *et al.*[9])

chest wall to measure the distance. If the wire is not seen in the right atrium by the expected distance, then it should be withdrawn and a second pass made. If the wire does not follow a straight course to the right atrium and SVC, then injury may result when the stiffer dilator and cannula are passed over it. In particular, if the wire makes a loop through the right atrium or the right ventricle that is not recognised, then a right atrial or vena caval tear may occur. All being well, the

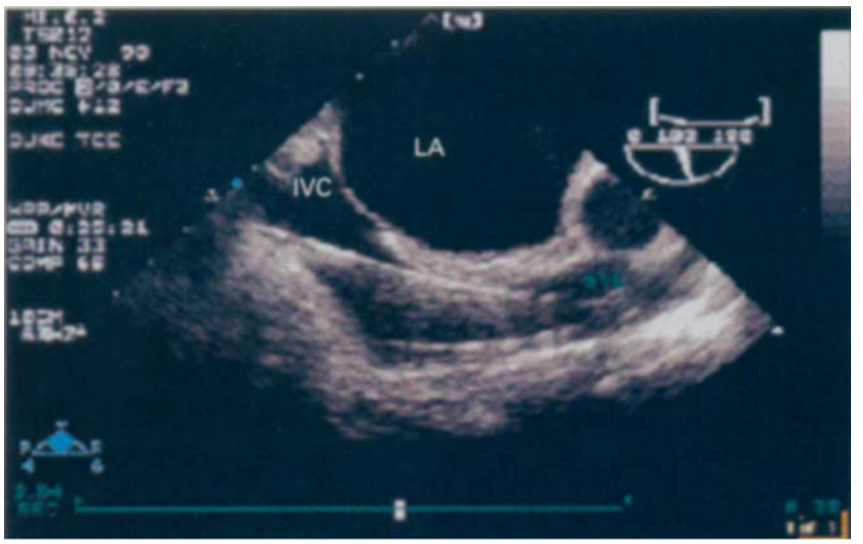

Figure 14.18 Imaging the venous cannula guidewire.

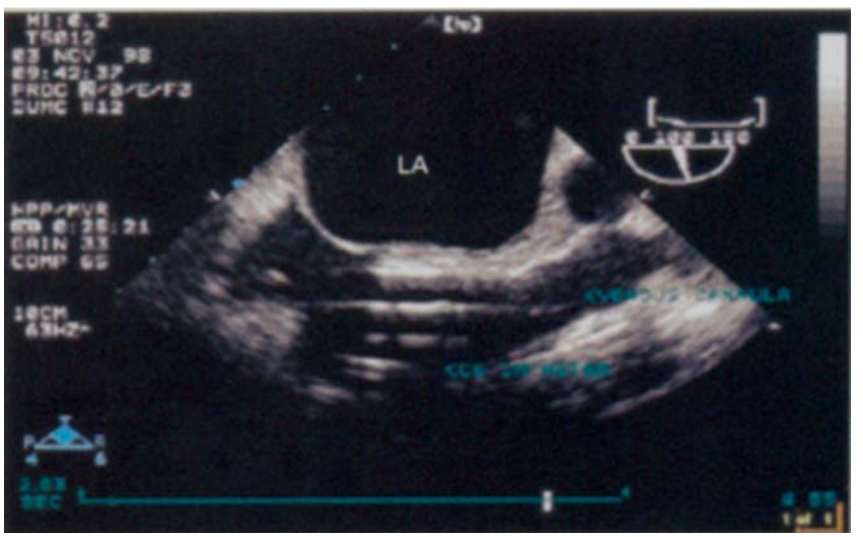

Figure 14.19 Positioning the venous cannula.

cannula tip should come to rest just inside the SVC. There are multiple holes along its distal 15 cm, as well as the large orifice at the tip. These multiple perforations can clearly be seen and may be mistaken for the actual tip of the cannula (Figure 14.19). If there are also other catheters in the right atrium, masking and reverberation artefacts may further confuse the picture. Therefore, passage of the cannula should be done slowly and carefully to give the TOE operator time to distinguish the various pieces of hardware.

Aortic cannula

The femoral aortic cannula itself is fairly short and will usually not be seen by TOE. However, the cannula is passed over a wire that may be passed far enough up the descending aorta for it to come into view. This wire should be seen to be free-floating within the aortic lumen. If it lies along the aortic wall, then rotation of it at the groin by the surgeon should displace it away from the wall, so that there is no question of it being intraluminal, and not in a subintimal dissection plane.

Endoaortic clamp

When passed through a femoral cannula, the balloon-tipped catheter (EAC) is passed over a long wire that can be clearly followed up the aorta as far as the aortic root. (Figure 14.20). The EAC

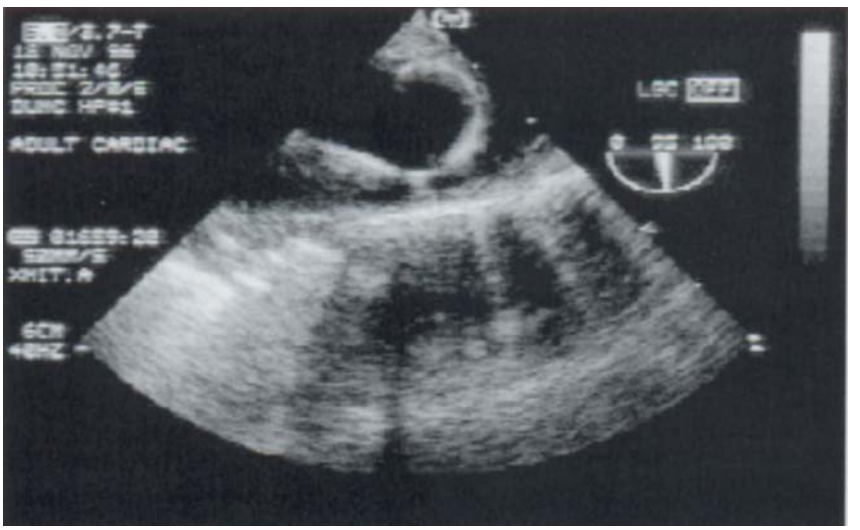

Figure 14.20 Transoesophageal echocardiography image of the guidewire for the endoaortic clamp in the descending aorta.

A

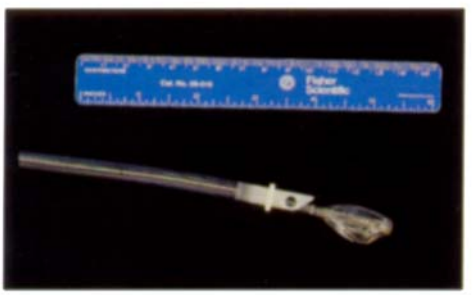

B

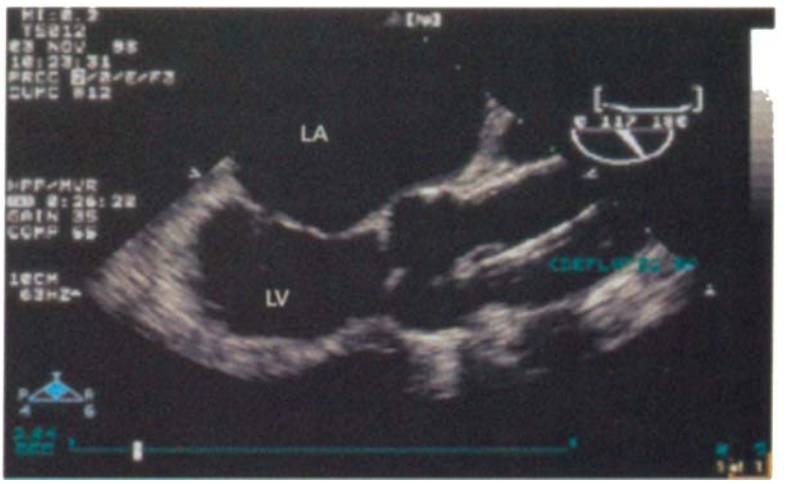

should be advanced over this as far as the aortic root and will be visible in the 120° view just above the aortic valve leaflets. When the central aortic cannula is used, the tip is directed toward the aortic valve and the deflated balloon catheter passed through the cannula (Figure 14.21). The inflated balloon should lie between the sinotubular junction and the innominate artery (Figure 14.22). If the central aortic cannula is too close to the aortic valve, then there may be insufficient aortic length for full balloon inflation above the sinotubular junction. However, the balloon can be retracted up against the cannula tip (Figure 14.22A) so that it is unable to migrate. Arterial inflow is then maintained through two large side holes proximal to the cannula tip. This balloon stability represents a considerable advantage over the femorally introduced EAC, which is prone to migration.

Monitoring

It has been recommended for Port-Access procedures that CPB be initiated very slowly in order to adjust properly the assisted venous drainage and ensure reasonable line pressures through the arterial cannula. At this time, imaging of the descending aorta can be done to verify the absence of aortic dissection as retrograde aortic inflow begins. We have often observed at this

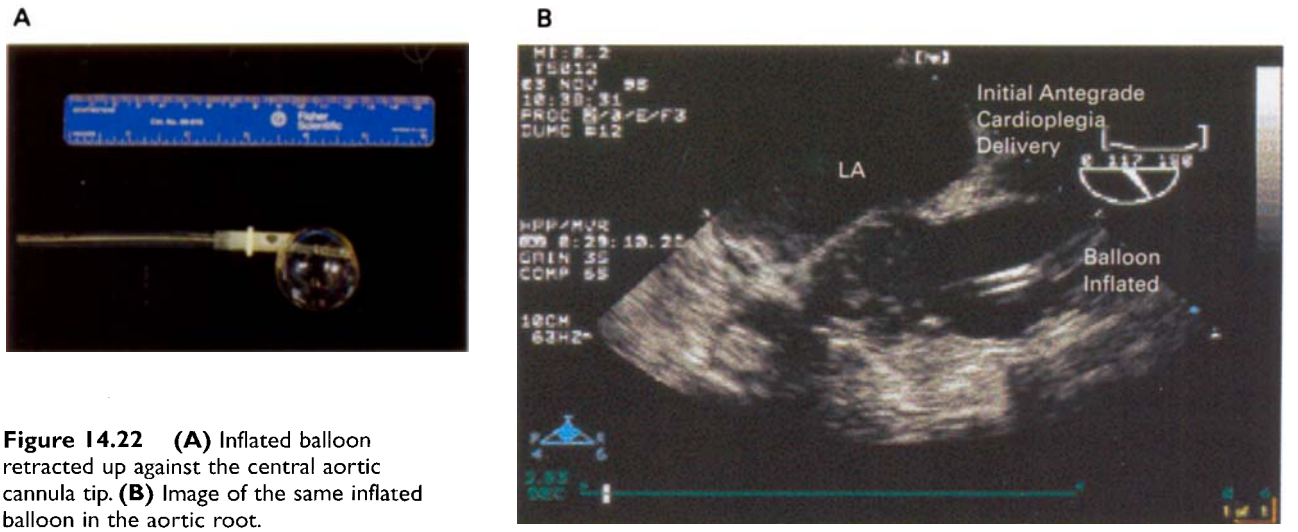

Figure 14.22 **(A)** Inflated balloon retracted up against the central aortic cannula tip. **(B)** Image of the same inflated balloon in the aortic root.

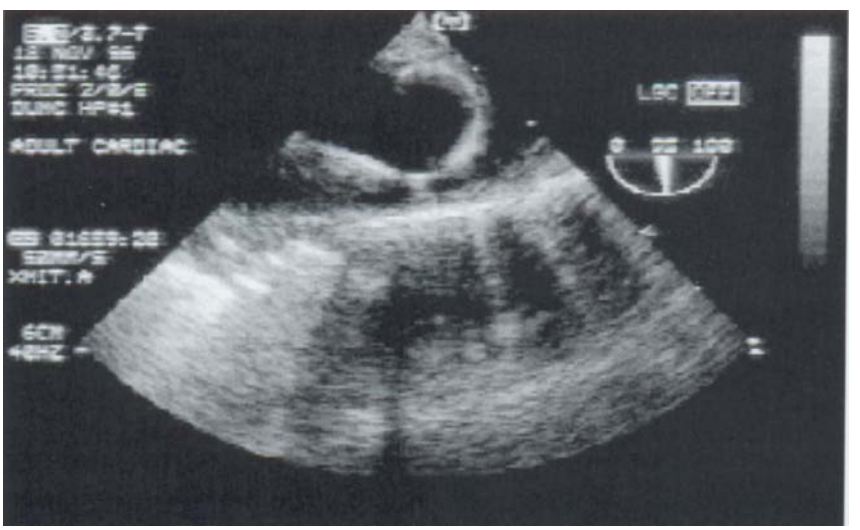

Figure 14.23 Image of the aortic flow channelling that can take place with slow onset of retrograde flow at the beginning of cardiopulmonary bypass, mimicking an aortic dissection.

time a channelling of aortic flow as the retrograde, crystalloid pump prime collides with blood ejected antegrade by the left ventricle into the descending aorta (Figure 14.23). This may take the appearance of a dissection, briefly, before LV ejection ceases and the retrograde aortic flow takes over. This phenomenon appears to be associated with very gradual initiation of CPB.[10]

As full flow is reached on CPB, TOE imaging will reveal how empty the heart has become. In fact, as the heart empties, the imaging planes are lost and orientation becomes difficult. Thus, if the chambers can no longer be identified, then this is a good indication that the heart is effectively empty. During CPB and cardioplegia delivery, it is desirable to keep an eye on the ascending aorta in the 120° view to confirm balloon position, especially with a femorally introduced EAC, and to look for evidence of aortic insufficiency and LV distension.

The sudden onset of LV distension and ventricular fibrillation during ischaemic arrest may indicate EAC balloon rupture, or migration into the left ventricle, both of which would be associated with loss of aortic occlusion and immediate warming of the heart. Balloon rupture is most likely to occur during mitral valve surgery when the surgeon is placing sutures through the anterior portion of the mitral valve annulus. A balloon situated too low, in the sinuses of Valsalva, is pressed very close to the mitral valve annulus and easily punctured by the suture needle. Surgery can be completed during fibrillation, with the inconvenience of blood in the field, or another balloon can be inserted.

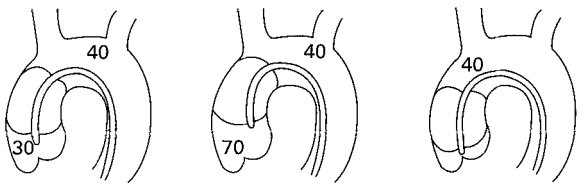

A Clamping B Cardioplegia C Venting

Figure 14.24 Pressure measurements for **(A)** clamping, **(B)** cardioplegia, and **(C)** venting. (Reproduced with permission from the Heartport Company, Redwood, California, USA.)

It is especially important to image the EAC balloon during delivery of cardioplegia because this is when it is most likely to migrate. The femorally introduced EAC balloon is tethered by a long catheter, secured only by a screw clamp on the side arm of the femoral cannula. As the balloon is inflated the pump flow is reduced to try to keep the pressures on either side of the balloon fairly similar so that the balloon remains in one place (Figure 14.24A.). Slight tension is applied to the femoral end of the catheter to stabilise the balloon. However, during cardioplegia delivery the pressure proximal to the balloon will tend to displace it toward the aortic arch (Figure 14.24B). During LV venting the pressure proximally will be lower, and a high systemic pressure is apt to displace the balloon toward the aortic valve (Figure 14.24C). Migration toward the arch can be difficult to identify with TOE alone. However, by keeping the aortic root under observation, and by following the right radial artery pressure tracing, most instances of migration will be promptly detected. Doppler monitoring of intracranial blood flow provides additional safety. However, it seems likely that the central aortic cannula will be preferable for a majority of cases, and the problem of balloon migration is then largely solved.

Conclusion

Progression of cardiac surgical techniques in the direction of minimally invasive surgery will ensure and enhance the role of TOE. Lessons learned with Port-Access can be applied to other minimally invasive techniques and vice versa.

References

1 Moises VA, Mesquita CG, Campos O, *et al.* Importance of intraoperative transesophageal echocardiography during coronary artery surgery without cardiopulmonary bypass. *J Am Soc Echocardiogr* 1998;**11**:1139–44.

2 Jurmann MJ, Menon AK, Haeberle L, *et al.* Left ventricular geometry and cardiac function during minimally invasive coronary artery bypass grafting. *Ann Thorac Surg* 1998;**66**:1082–6.

3 Westaby S, Benetti FJ. Less invasive coronary surgery: consensus from the Oxford meeting. *Ann Thorac Surg* 1996;**62**:924–31.

4 Bonatti J, Hangler H, Hoermann C, *et al.* Myocardial damage after minimally invasive coronary artery bypass grafting on the beating heart. *Ann Thorac Surg* 1998;**66**:1093–6.

5 Smith JS, Cahalan MJ, Benefiel DJ, *et al.* Intraoperative detection of myocardial ischaemia in high-risk patients: electrocardiography versus 2-dimensional transesophageal echocardiography. *Circulation* 1985;**72**:1015–21.

6 Clements F, de Bruijn NP. Perioperative evaluation of regional wall motion by transesophageal two-dimensional echocardiography. *Anesth Analg* 1987;**66**:249–61.

7 Seeberger MD, Skarvan K, Buser P, *et al.* Dobutamine stress echocardiography to detect inducible demand ischemia in anesthetized patients with coronary artery disease. *Anesthesiology* 1998;**88**:1233–9.

8 Konstadt SN, Louie EK, Black S, *et al.* Intraoperative detection of patent foramen ovale by transesophageal echocardiography. *Anesthesiology* 1991;**74**:212–5.

9 Clements F, Wright S, de Bruijn NP. Coronary sinus catheterization made easy for port access minimally invasive cardiac surgery. *J Cardiothorac Vasc Anesth* 1998;**12**:96–101.

10 Watke C, Clements F, Glower D, *et al.* False positive diagnosis of aortic dissection by transesophageal echocardiogaphy during initiation of heartport cardiopulmonary bypass. *Anesthesiology* 1998;**88**: 1119–21.

15 Circulatory assist devices, artificial heart, and heart and lung transplantation

Joachim M Erb

Transoesophageal echocardiography and circulatory assist devices

The cardiac anaesthesiologist will almost inevitably take care of patients supported by some form of circulatory assist device. Complex procedures with long ischaemic times increase the likelihood of postcardiotomy heart failure. New generation circulatory assist devices have found wider indications for use, including intraoperative short-term applications and as bridges to transplantation, or as long-term palliative therapy in patients with congestive heart failure. The spectrum of devices ranges from the temporarily placed intra-aortic balloon pump (IABP) and axial flow pumps across modified heart–lung machine pumps to partial or total implantable left ventricular, right ventricular, or biventricular assist devices, and total artificial hearts designed for long-term or permanent use. Patients requiring a circulatory assist device are at high risk and should always be monitored intraoperatively with transoesophageal echocardiography (TOE). Therefore, the anaesthesiologist must have an understanding of the device used and be familiar with the echocardiographic appearance and special aspects of echocardiographic evaluation.

This chapter provides a basic understanding of currently used circulatory assist devices, their echocardiographic appearance, and special aspects that are critical to the echocardiographic evaluation. Although specific devices and manufacturers are mentioned, the chapter provides neither a complete listing nor a recommendation or rating. Technical aspects of devices are only explained in as much detail as is necessary to support the diagnostic approach using TOE. For more detailed information, the reader should refer to specific literature on this topic.[1] Whenever standard TOE views are mentioned, this refers to the American Society of Echocardiography/Society of Cardiovascular Anesthesiologists intraoperative TOE guidelines.[2]

When discussing mechanical circulatory support, devices are usually grouped into short-term or long-term support systems, single (left or right) ventricular or biventricular systems, and external or implantable systems. This is useful in matching the appropriate system to the individual clinical indication.

In echocardiographic evaluation, it is most useful to differentiate three groups of circulatory assist devices:

- intra-aortic balloon counter-pulsation (which operates in the descending aorta)
- microaxial pumps (which operate in the heart but are introduced semi-invasively through the vascular system)
- systems that require inflow and outflow cannulae positioned in the heart and great vessels.

In contrast, the total artificial heart requires explantation of the native heart, similar to orthotopic heart transplantation. This approach will be used in the following text, with some remarks made regarding the specifics of left, right, and biventricular use, and pulsatile versus non-pulsatile flow where it impacts on the echocardiographic examination. For the remainder of the chapter, "inflow" refers to the blood flow into the circulatory assist device, and "outflow" is defined as the blood flow from the device into the patient's vascular system.

Intra-aortic balloon counter-pulsation

The IABP, which is the most widely used circulatory assist device, is a long catheter with

an inflatable, tubular balloon mounted at the end. The balloon section is positioned in the descending thoracic aorta, just distal to the aortic arch and the offspring of the left subclavian artery. The IABP is inserted using a Seldinger technique retrograde via the femoral artery; alternatively, it can be inserted surgically antegrade through the ascending aorta.[3] A driving console inflates the balloon with helium during ventricular diastole and deflates it during systole, and is triggered by electrocardiography or intra-aortic pressure measured at the catheter tip.

The IABP supports patients with coronary insufficiency or predominant left ventricular failure by increasing diastolic perfusion pressure and coronary blood flow during diastolic inflation and decreasing ventricular afterload during systolic deflation, reducing myocardial oxygen demand through a decrease in ventricular systolic wall stress and improving global left ventricular systolic function.[4–7] Right heart function may improve by means of improved coronary perfusion.

Before implantation of the intra-aortic balloon pump

The TOE evaluation starts before placement of the IABP with a comprehensive examination. Special focus is placed on baseline biventricular function and the exclusion of thoracic aortic disease. Aneurysms, dissections, intramural haematomas, and severe atheromatous or calcific changes (in particular with mobile lesions or thrombi) represent contraindications to IABP use. Aortic valve patency must be confirmed, because insufficiency that is more than trivial/mild excludes the use of the IABP.

During implantation of the intra-aortic balloon pump

During implantation, the appearance of the guidewire in the aortic lumen is confirmed to the surgeon, and correct positioning of the balloon section in the descending aorta is guided by TOE. For this purpose, the aortic arch and the descending thoracic aorta are best visualised in both transverse and longitudinal imaging planes. The echocardiographic appearance of the catheter, a highly echogenic, well defined reflection with a characteristic echo dropout, resembles that of a wire, whereas the balloon section exhibits irregular boundaries with soft reflections and side lobe artefacts. This allows identification and differentiation of the balloon section from the catheter itself (Figure 15.1).

In the femoral approach, TOE identification of the catheter tip just at the transition of the aortic arch into the descending aorta, at the level of the inferior margin of the aortic arch, ensures optimal IABP placement, with the balloon section just distal to the aortic arch. It must be confirmed that the catheter is not entering the aortic arch or any of the main arch vessels, with special attention given to the left subclavian artery. The echocardiographic evaluation is challenging with IABP insertion through the ascending aorta, because the catheter section is always visible in the aortic arch and the correct position can only be confirmed by identification of the balloon section in the descending aorta according to the above-mentioned characteristics (Figure 15.2). Inflation of the balloon with resulting movement of the catheter will create strong reflections and reverberation artefacts, which help in the discrimination of the balloon section but make it difficult to evaluate the descending aorta itself. Finally, before the IABP is continuously started, the aortic intima is examined carefully to exclude any injury caused by the guidewire or catheter tip, and for the ascending aortic approach the entrance site in the ascending aorta is screened for signs of dissection or intimal changes.

During use of the intra-aortic balloon pump

During use, effective left ventricular support is demonstrated by an increase in left ventricular ejection fraction and stroke volume following IABP augmentation, which can be directly measured by an increase in transaortic velocity and velocity–time integral by pulsed wave Doppler.[8] Common problems during use are displacement of the IABP, which can easily be recognised and corrected using the approach described above, and damage to the balloon with gas leakage or rupture, which is identified by small gas bubbles in the aorta. If assessment of optimal timing by means of the resulting arterial pressure is difficult (fast heart rate, insufficient pressure recording), then transthoracic parasternal imaging of the ascending and descending thoracic aortae in M-mode has the advantage of simultaneously recording aortic valve motion and balloon inflation and deflation, allowing precise adjustment to the timing.[9,10]

Table 15.1 gives a checklist for echocardiographic evaluation during implantation and use of an IABP.

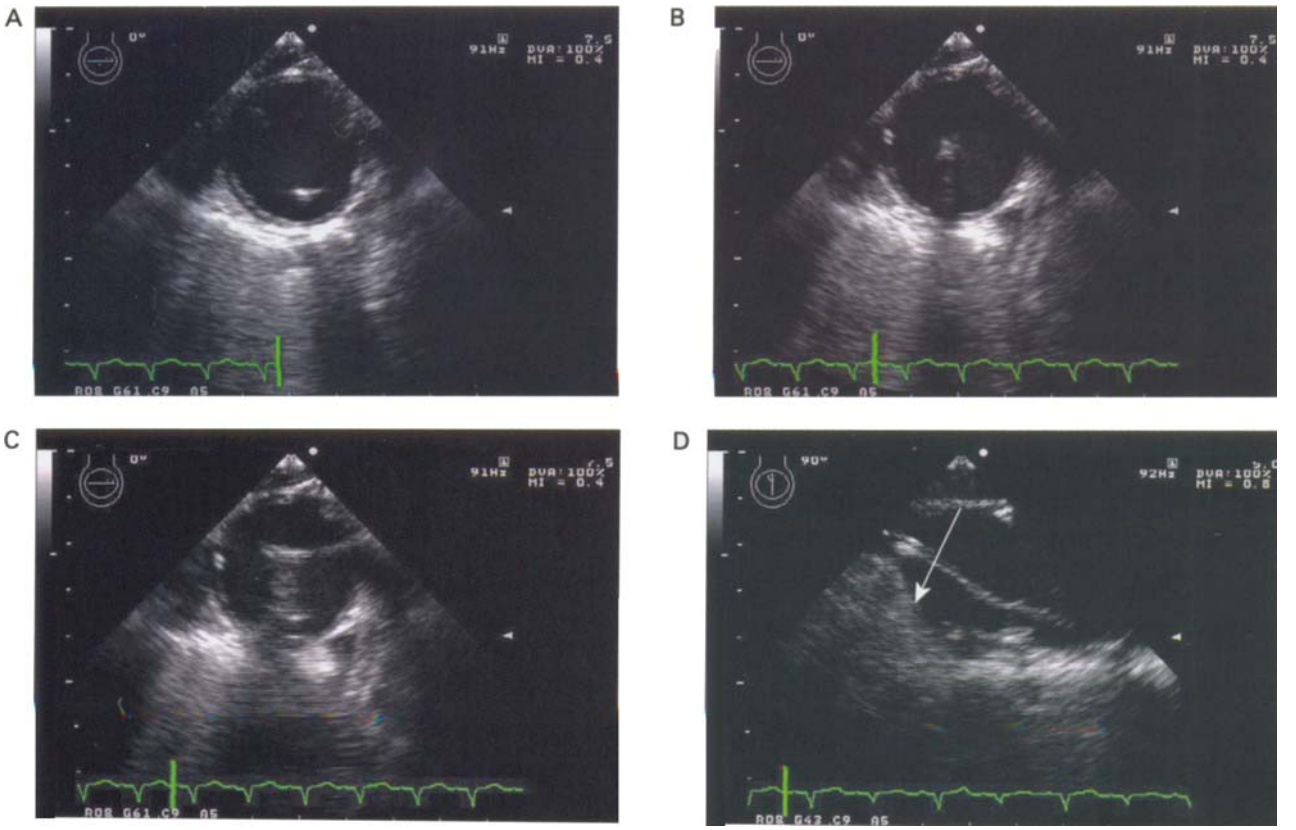

Figure 15.1 Femoral intra-aortic balloon pump (IABP) placement. Cross-sectional views of the descending aorta with the guidewire advanced **(A)**, and the IABP catheter with the balloon deflated **(B)** and the IABP balloon inflated **(C)**, giving characteristic reflections. **(D)** The IABP tip with the inflated balloon (arrow) in the descending aorta in the longitudinal view.

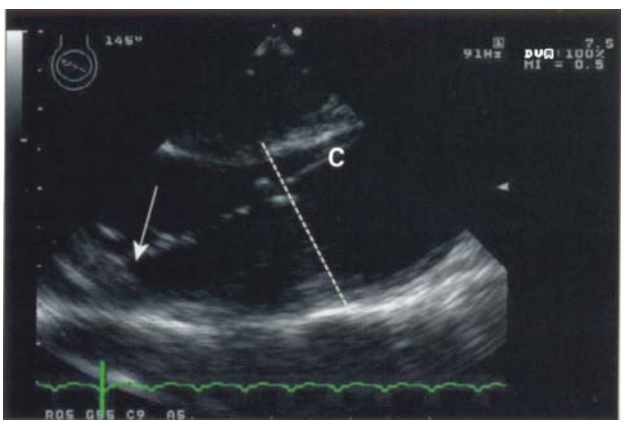

Figure 15.2 Thoracic intra-aortic balloon pump (IABP) placed surgically through the ascending aorta imaged in a oblique plane. The catheter (C) is visible on its passage from the aortic arch into the descending aorta. The arrow indicates where the balloon section starts, and the dashed line marks the transition of the aortic arch into the descending aorta.

Axial flow pumps

The Impella® pump (Impella Cardiotechnik AG, Aachen, Germany) and the Hemopump® (DLP, Medtronic, Grand Rapids, Michigan, USA) are intracardial microaxial centrifugal pumps mounted on a catheter connected to an external driving console. The Impella® comes in configurations for left sided or right sided cardiac support, and the Hemopump® is a left sided assist device with cannulae for direct femoral, percutaneous, or sternotomy insertion. For left heart support, the pump is inserted into the aorta or a large peripheral artery and advanced retrograde through the aortic valve into the left ventricular cavity, positioning the inflow section in the ventricular cavity and the outflow portion in the ascending aorta, thus propelling blood from the left ventricular cavity into the ascending aorta. For right heart support, the device is inserted into the right atrium or a large peripheral vein and floated with the help of an inflatable balloon through the tricuspid and pulmonic valve to position the tip with the outflow in the main pulmonary artery while the inflow rests in the right atrium, thus propelling blood from the right atrium into the pulmonary artery. Depending on

Table 15.1 Checklist for echocardiographic evaluation during intra-aortic balloon pump implantation and use

Stage	Details
Before IABP implantation	Comprehensive examination with focus on: • Baseline ventricular function • Thoracic aortic pathology (contraindications to IABP use) • Aortic valve patency
During IABP implantation	• Correct guide wire position • Guidance of IABP advancement along guidewire into correct position • Confirmation of optimal IABP positioning
During IABP use	• Changes in ejection fraction, regional wall motion, and ventricular volumes • Confirmation of correct position • Confirmation of function, exclusion of leakage • Correct timing using TTE approach

IABP = intra-aortic balloon pump, TTE = transthoracic echocardiography.

the adjusted rotational speed, the axial flow pumps generate a non-pulsatile flow of up to 4·5–5 l/min, thus directly unloading the ventricle. The intraoperative use of axial flow pumps to support the heart during minimal invasive coronary surgery is finding increasing application.[11–13] With their support, cardiac output can be maintained even if extreme positioning of the heart is required, and therefore axial flow pumps present an alternative to conversion into cardiopulmonary bypass. In addition, they can be used for short term (postoperative) support during heart failure for up to 7 days.[14]

Before implantation of the axial flow pump

The TOE evaluation before device placement includes detailed biventricular functional assessment and focuses on the status and function of the valves crossed by the device, as well as on the anatomy of cardiac cavities, outflow tract, and ascending aorta and/or pulmonary artery. Depending on whether a left sided or right sided pump is used, the aortic valve or pulmonary valve, respectively, must be patent or exhibit only mild insufficiency, because otherwise sufficient support cannot be achieved. Abnormalities in the outflow tract can interfere with device placement and must therefore be recognised.

During implantation of the axial flow pump

TOE guidance is helpful during placement, especially on the left side, where passage through the aortic valve is difficult, requiring appropriate systolic timing, and often leads to entrapment of the device tip in the coronary cusps. Correct placement of the left sided device is confirmed by TOE identification of the inflow area in the middle of the left ventricular cavity and the outflow area in the ascending aorta. The mid-oesophageal long-axis view shows the axial pump entering from the ascending aorta through the aortic valve and the left ventricular outflow tract, and into the left ventricular cavity, all in one imaging plane. The rotator chamber of the device gives a characteristic, double lined echo reflection of about 6·5 mm in width and can easily be distinguished from the catheter portion. The inflow of the left sided device is located at the tip and can be identified by interruptions in the outline echo, which correspond to the inflow openings (Figure 15.3). Care should be taken that the inflow end is not buried in the ventricular wall, the papillary muscles, or the chords or leaflets of the mitral valve, but rather is centred freely in the ventricular cavity. The outflow section is located at the catheter end of the rotator chamber, which is identified distal to the aortic valve in the ascending aorta.

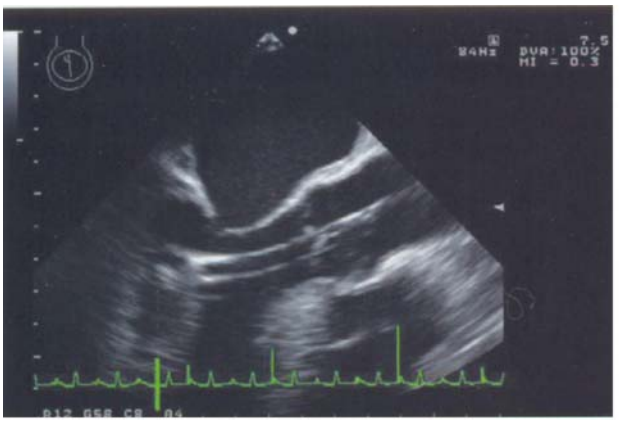

Figure 15.3 Mid-oesophageal long-axis view showing a left ventricular Impella® axial flow pump in the correct position. The arrow indicates the inflow openings at the pump tip.

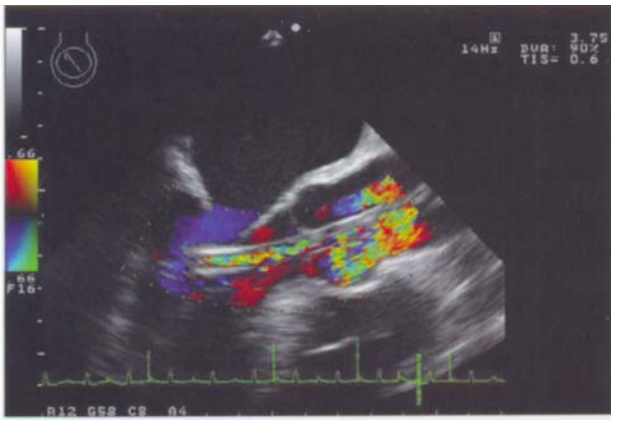

Figure 15.4 Mid-oesophageal long-axis view showing a left ventricular Impella® axial flow pump in the correct position with colour flow Doppler. Note the laminar flow toward the openings at the pump tip, and the turbulent flow in the rotator chamber and at the outflow positioned in the ascending aorta. The arrow indicates the outflow openings of the pump.

To assist in determining whether the device is correctly placed, the high velocity flow generated by the centrifugal pump can easily be visualised by colour flow Doppler. Around the inflow section, the previous laminar flow is converted through a zone of three-dimensional flow acceleration into a turbulent flow, which can be followed through the rotator chamber along to the outflow of the chamber, where the entry of the pump flow into the ascending aorta can clearly be identified from the resulting turbulent flow mosaic (Figure 15.4). Correct placement of the right sided device can be confirmed with TOE by identification of the inflow area in the middle of the right atrium and the outflow area in the pulmonary artery, for which the right ventricular inflow–outflow tract view is the optimal imaging plane. If positioning of the right ventricular device is difficult to visualise by TOE, then epicardial echocardiography has been shown to be helpful.[15] During intraoperative use, TOE permits detection of changes in device position (which occur frequently with surgical manipulation of the heart) and monitoring of ventricular volumes in order to avoid obstruction to pump inflow by the collapsing ventricular walls of a hypovolaemic ventricle.

During use of the axial flow pump

Optimal support by the axial flow pump will result in marked reduction in systolic blood flow velocity in the ventricular outflow tract and aortic and/or pulmonary valve opening is reduced, which is identified by a decrease in systolic leaflet separation. If the device is used to support an impaired left ventricle, then TOE monitoring of right ventricular function is essential if changes in right ventricular performance and a tendency toward right sided volume overload are to be detected early, because with the improved systemic circulation supported by the assist device a coexisting right ventricular dysfunction may be unmasked. Similarly, left ventricular function and volume status must be monitored closely by TOE if the device is used to provide right ventricular support. In biventricular use, TOE guided maintenance of balanced ventricular volume is most helpful. Inadequate pump flow is usually due to insufficient preload or dislocation of the device, both of which can easily be detected by TOE. In any case, the aortic intima must be checked, because rarely an ascending aortic intimal flap or dissection can cause device failure.

If the support of the axial flow pump is no longer necessary, then weaning is performed by gradual reduction in pump flow during TOE monitoring of global and regional ventricular function and volume status. After removal of the axial flow pump, TOE examination of the valves is required to exclude or document any changes caused by the device, and the ascending aortic entry side is examined again to exclude intimal changes, dissection, or stenosis after closure of the entry side.

Table 15.2 gives a checklist for echocardiographic evaluation during the various stages of axial flow pump use.

Table 15.2 Checklist for echocardiographic evaluation during the various stages of axial flow pump use

Stage	Details
Before device implantation	Comprehensive examination with focus on: • Biventricular function • Status of valves passed by device • Outflow tract and ascending aorta/pulmonary artery
During device implantation	Guiding of correct placement and optimal positioning: • Inflow in cavity of left ventricle or right atrium • Outflow in ascending aorta or pulmonary artery • Exclusion of flow obstruction
During device use	• Confirmation of correct positioning during changes in heart position • Monitoring of volume status • Monitoring of ventricular function and stroke volume of the unsupported ventricle
After device explantation	• Documentation of unimpaired valvular integrity • Inspection of intima and lumen of ascending aorta

Ventricular assist devices

Of all the various ventricular assist devices (VADs) available, centrifugal pumps (designed for short term use) are the most commonly used; they are the least expensive and are relatively simple to use. By rotation of impellers, blades, or concentric cones, centrifugal pumps produce a non-pulsatile flow, and can provide left ventricular (LVAD), right ventricular (RVAD), or biventricular (BVAD) assistance. Extracorporeal pneumatic or electromechanical systems, which consist of a blood filled flexible sac enclosed in a case that is compressed and decompressed, thereby generating a pulsatile flow, can be used to provide intermediate or long-term univentricular or biventricular support. The currently available intracorporeal implantable LVADs are pulsatile, electromechanical pumps; implantable, non-pulsatile systems that employ the principle of the Archimedes' screw are in clinical trial. All implantable devices are intended to provide long term support as a bridge to transplant or as a bridge to recovery, and are designed to allow maximal patient mobility. VADs are connected to the heart with cannulae that drain the chambers (atrium or ventricle), and the blood is pumped back through cannulae into the great vessels (aorta or pulmonary artery). The type and position of the inflow and outflow cannulae vary depending on the indication, coexisting cardiac and vascular pathologies, surgical preference, and long term strategy pursued. Table 15.3 provides an overview of currently used VADs.

Before implantation of the ventricular assist device

Before VAD implantation, a comprehensive intraoperative TOE examination is conducted to document biventricular baseline function, including an assessment of size and regional wall motion, especially if single ventricular support (mostly LVAD) is planned. This is because the significant incidence of postimplantation failure of the unsupported ventricle (commonly the right ventricle) creates a need to plan supportive medical therapy. Proper VAD function requires sufficient ventricular and/or atrial filling volumes; this depends on adequate flow generated by the unsupported ventricle, which in the right ventricle might be limited in the presence of pulmonary hypertension and reduced baseline ventricular function. A right ventricular fractional area change of less than 20% renders

Table 15.3 Overview on ventricular assist devices currently in use

VAD location	*Extracorporeal*		*Intracorporeal*	
Pump types	*Centrifugal pumps*	*Pneumatic or electromechanical pumps*	*Electromechanical pumps*	*Electromagnetic axial flow pumps*
Systems currently in use	• Sarns™ centrifugal system (Terumo Corp., Tokyo, Japan)* • Lifestream centrifugal pump (Livestream Int., Haverhill, MA, USA) • Bio-Medicus BIO-Pump (Medtronic Bio-Medicus Inc., Eden Prairie, MN, USA) • Nikkiso centrifugal pump (Nikkiso Co. Ltd., Shizuoka, Japan)	• Abiomed BVS® 5000 (ABIOMED Inc., Danvers. MA, USA)† • Thoratec® VAD (Thoratec Corp., Woburn, MA, USA) • Berlin Heart EXCOR (Berlin Heart AG, Berlin, Germany) • Medos VAD® (Medos Medizintechnik AG, Stolberg, Germany)	• Novacor® LVAS (Worldheart Inc., Oakland, CA, USA) • HeartMate® LVAS (Thoratec Corp., Woburn, MA, USA) • *LionHeart*™ (Arrow International Inc., Reading, PA, USA)‡	• *Berlin Heart INCOR* (Berlin Heart AG, Berlin, Germany) • *MicroMed DeBakey* VAD® (MicroMed Technology Inc., Houston, TX, USA) • *Jarvik 2000 Heart* (Jarvik Heart Inc., New York, NY, USA) • *HeartMate® II LVAD* (Thoratec Corp., Woburn, MA, USA) • *CorAide*™ (Arrow International Inc., Reading, PA, USA)
VAD flow	Non-pulsatile (+ pulsatile*)	Pulsatile	Pulsatile	Continuous, non-pulsatile
Use as	LVAD, RVAD, BVAD	LVAD, RVAD, BVAD	LVAD	LVAD
Cannulation sites	Usually atrium to ascending aorta/pulmonary artery	Atrium or ventricular apex to ascending aorta/pulmonary artery	Ventricular apex to ascending aorta	Ventricular apex to ascending or descending aorta
Indication	Short term support (days)	Short† to intermediate term support (months) Bridge to transplant or recovery	Intermediate to long term support (months to years) Bridge to transplant or recovery	Long term support (years) Bridge to transplant or recovery
Connection to patient	Cannulae	Cannulae	Power line No connection (transcutaneous power supply)‡	Power line
External parts	Pumps and driving console	Pumps and driving console	Battery pack	Battery pack

Devices in *italics* are in clinical trial. BVAD = biventricular assist device, LVAD = left ventricular assist device, RVAD = right ventricular assist device. *Of all the centrifugal pumps, the Sarns™ centrifugal system is the only one that can do non-pulsatile (as can all) and pulsatile flow. †The Abiomed BVS 5000 is a short term system, whereas the others in this category are intermediate term systems. ‡LionHeart™ is the only device that has no connection (transcutaneous power supply).

patients more likely to suffer right ventricular failure when LVAD support is started.[16]

Examination of the cardiac chambers and great vessels focuses on the locations where inflow and outflow cannulae will be positioned. Atrial and ventricular thrombi are likely to be present in dilated cardiomyopathy and ventricular aneurysms, often with spontaneous echo contrast as a sign of

low flow velocities in atrial and ventricular cavities. Attention should be paid to the left ventricular apex in cardiomyopathy, to areas of previous infarction, and to the atrial appendages, especially in atrial fibrillation, because mobilisation of thrombi is a known cause of thromboembolic complications in these patients. Calcification, haematoma, and atheromatous changes in the aorta must be excluded in those areas where cannulation is planned.

The cardiac valves must be inspected to document insufficiency or stenoses. Moderate or severe regurgitation of the aortic and pulmonary valves creates a need for valvular reconstruction or replacement surgery before LVAD and RVAD placement, respectively. This is because ventricular unloading increases the retrograde artery-to-ventricle gradient across the permanently closed valve and leads to an increase in regurgitation volume. This would increase VAD preload, thereby increasing VAD pump flow volume, while effective forward blood flow to the patient's circulation is reduced. The presence of mitral stenosis contraindicates placement of a left ventricular apical cannula or a transmitral cannula, and left atrial cannulation should be done instead, whereas mitral regurgitation usually decreases with LVAD placement and does not impair LVAD function. Mild tricuspid insufficiency is seen in most patients receiving a VAD, and a considerable amount present with moderate to severe tricuspid regurgitation. Although for most patients receiving a LVAD the pulmonary artery pressure drops with left ventricular unloading, tricuspid regurgitation often does not decrease and can progress to severe tricuspid regurgitation with the increase in volume load of the right ventricle that occurs with institution of LVAD function.[17,18]

It is mandatory to exclude the presence of intracardiac shunts such as a patent foramen ovale (PFO) or atrial and ventricular septal defects, preferably by combining colour flow Doppler (Figure 15.5) and pulse wave Doppler examination with contrast echocardiography during intravenous injection of agitated colloid or crystalloid solutions or blood. Because left atrial pressure usually is increased and markedly exceeds right atrial pressure in patients with cardiac failure, this pressure gradient must be reversed during the contrast study in order to enable the contrast enriched blood to pass from right to left in the presence of a shunt. This is achieved by sustained airway pressure, which reduces left atrial pressures by decreasing blood flow through the lungs, followed by a sudden release during contrast injection, which allows increased blood flow and contrast return to the right atrium because of intrathoracic pressure reduction, further supporting a right-to-left transseptal pressure gradient.[19] If even a small opening remains undetected, then this can lead to significant right-to-left shunt flows of unoxygenated blood once the LVAD achieves left ventricular decompression, which may lead to systemic arterial desaturation with added risk for paradoxical embolism.[20]

During implantation of the ventricular assist device

Intraoperatively, during cardiopulmonary bypass (CPB), surgical cannula positioning is

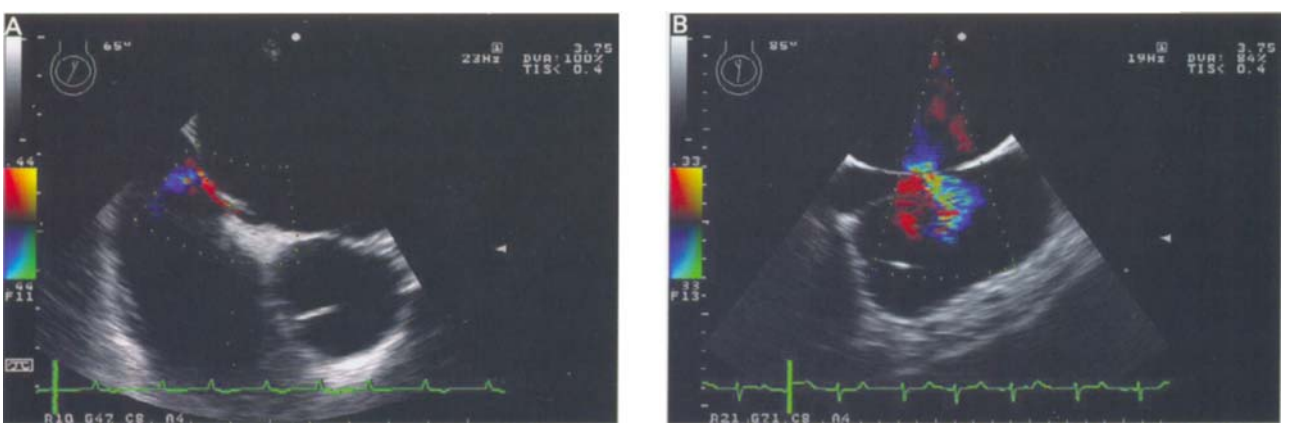

Figure 15.5 Atrial septal patent foramen ovale visualised in the mid-oesophageal **(A)** aortic valve short axis and **(B)** bicaval views. Colour flow Doppler shows left-to-right shunt flow.

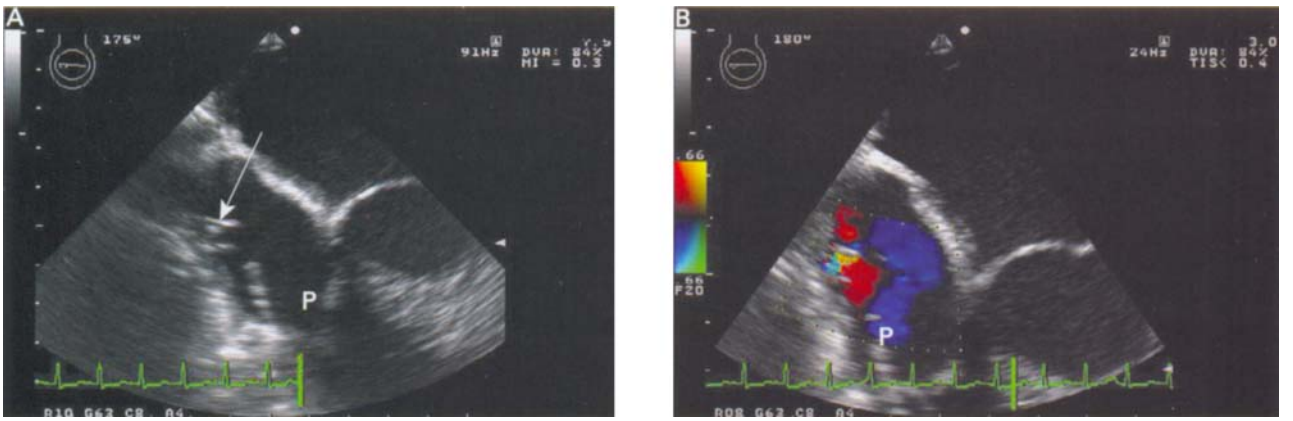

Figure 15.6 Right ventricular assist device (RVAD) inflow cannula placed laterally in the right atrium, visualised in the **(A)** mid-oesophageal four chamber view (arrow). **(B)** Colour flow Doppler shows laminar flow toward the cannula and flow acceleration at the cannula entrance. A pacing wire is visible in the right atrium (P).

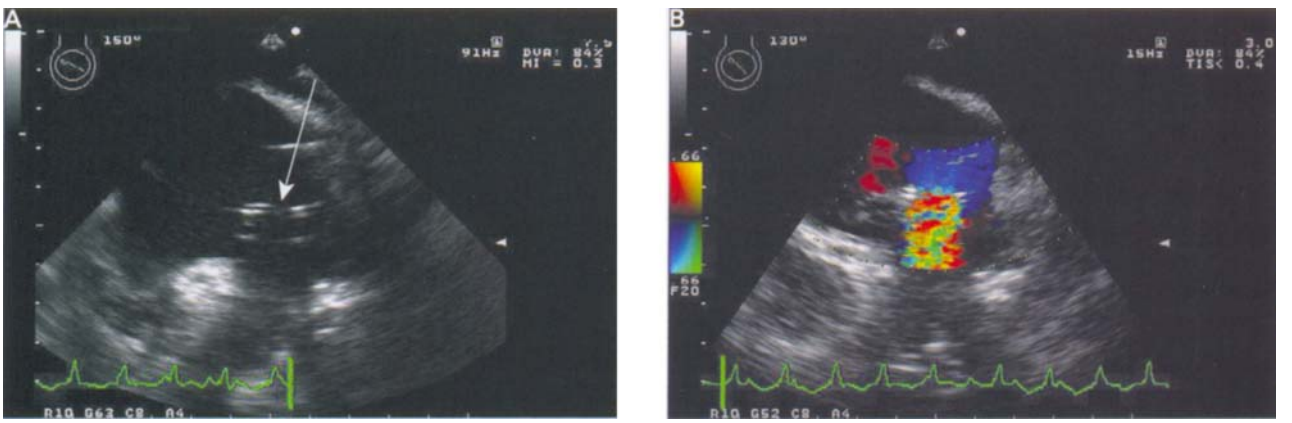

Figure 15.7 Right ventricular assist device (RVAD) inflow cannula placed through the right atrial appendage, visible in the **(A)** mid-oesophageal bicaval view (arrow). **(B)** Colour flow Doppler shows laminar flow toward the cannula and flow mosaic in the cannula entrance.

guided by TOE. To create echocardiographic windows, it is necessary to reduce venous drainage in order to fill the heart at least partially. Atrial cannulae in the adult patient are usually 32–36 French, with a more or less angular tip that is designed as a cage and protrudes 2–2·5 cm into the atrial cavity. The echocardiographic appearance is one of distinct reflections of the large cannula tip, with openings clearly visible as echolucent areas.

The right atrial appendage or the right atrial free wall are the most common cannulation sites for right sided inflow; alternatives are the low right atrium and cannulae placed across the tricuspid valve, whereas bicaval cannulation is rarely done. Right atrial cannulation is best monitored in the mid-oesophageal bicaval and the four chamber views, whereas the right ventricular inflow–outflow view allows the best appreciation of a cannula across the tricuspid valve (Figures 15.6 and 15.7). Apical right ventricular cannulation has been described in the literature;[21] with this approach, the right inflow cannula is best monitored in the mid-oesophageal four chamber and right ventricular inflow–outflow views. With the omniplane probe, the extracardiac portion of the right atrial cannula can often be visualised longitudinally on its passage alongside the right pericardial margin.

The left atrial cannula enters the left atrium either anterior through the atrial appendage or posteromedial close to the junction of the right pulmonary veins with the atrium, whereas connections to the dome of the left atrium are less frequently used. Left atrial cannula position is best visualised in the four chamber, two chamber, or long axis view of the left atrium. If a left transmitral cannula is advanced from the left atrium into the left ventricle, then passage of this

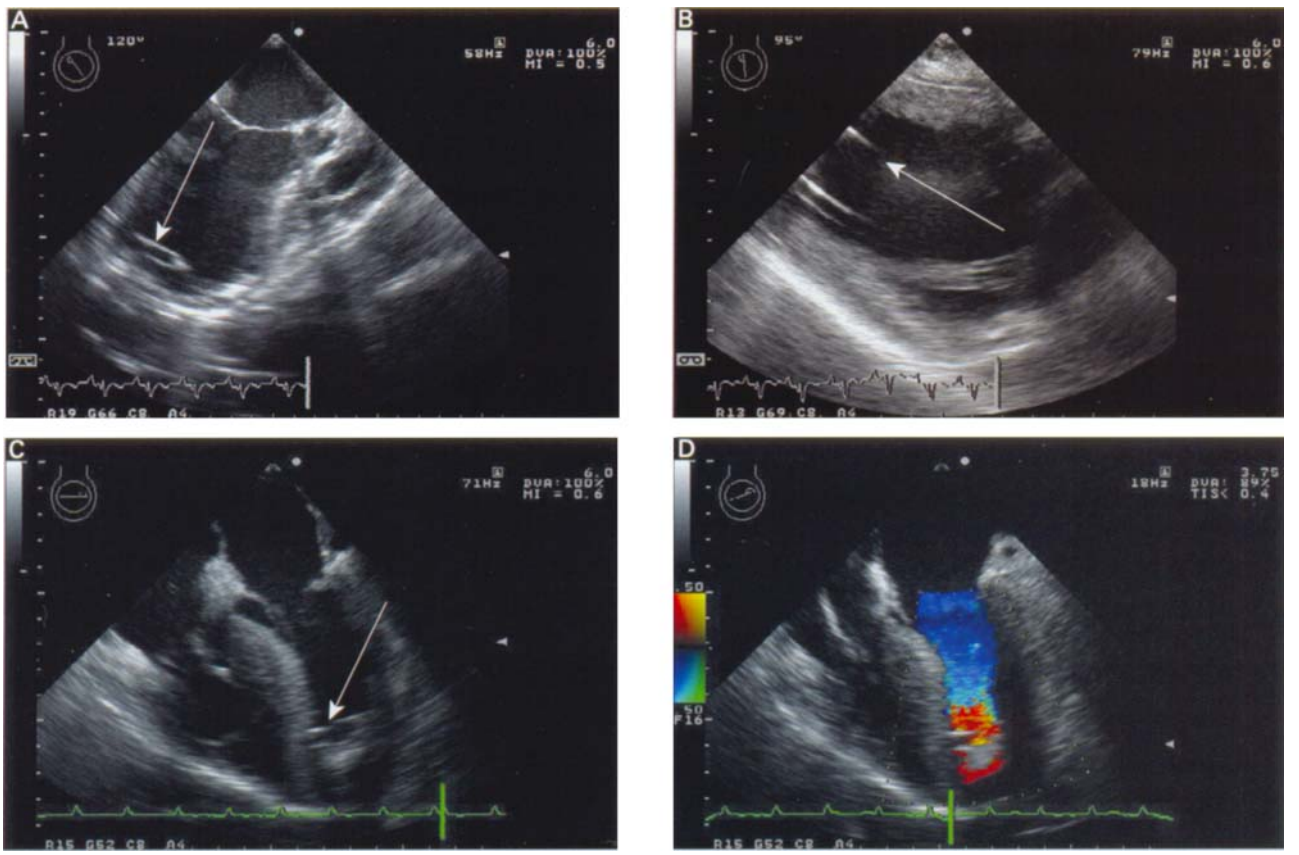

Figure 15.8 Left ventricular assist device (LVAD) inflow cannula positioned in the left ventricular apex (arrows). Shown are **(A)** the circular appearing inflow in the mid-oesophageal long-axis view, **(B)** the centrally orientated cannula in the transgastric two chamber view, and **(C)** the four chamber view with an unloaded left ventricle with the septum convex to the left ventricle. **(D)** Colour flow Doppler shows aliasing as blood flow accelerates on entering the cannula.

cannula through the mitral valve can be demonstrated in all mid-oesophageal ventricular imaging planes. The echocardiographic appearance is one of a double contour of about 16 mm in diameter. Care must be taken that the cannula tip is positioned in the mid-ventricular cavity and is not obstructed by the ventricular wall, the papillary muscles, or the mitral valve chords. If an apical left ventricular inflow cannula is used, then TOE can assist the surgeon in positioning the cannula centrally in the apex, with the orifice directed toward the mitral valve annulus and slightly away from the interventricular septum. The cannula tip is best seen in the mid-oesophageal ventricular imaging planes or in the transgastric two chamber view, and is identified by the double contour of the opening. In an oblique cut, the opening of the cannula can be demonstrated as a near circular structure (Figure 15.8). Care must be taken that the cannula opening is not directed toward any of the ventricular walls, especially the septum, which could be shifted toward the left cavity once left ventricular unloading by the device and right ventricular overload lead to a change in the interventricular pressure relationship. Another but rarely used variant of the left ventricular inflow cannula enters the left ventricle via the ascending aorta retrograde through the aortic valve – a position that is easily monitored using the mid-oesophageal long-axis view.

Centrifugal pumps used as short term VADs are usually connected to aortic cannulae, which protrude into the aorta at a length of about 1 cm and whose tip can be located in the mid-oesophageal long-axis view as a double lined structure (Figure 15.9). Outflow cannulae for longer term VADs usually have a rectangular orientated tip with a basket shaped opening that is sutured side to side to the margin of an appropriately sized ostium in the vessel wall, with no part of the cannula protruding into the vascular lumen. The anastomosis of the outflow cannula of a RVAD to the pulmonary artery main

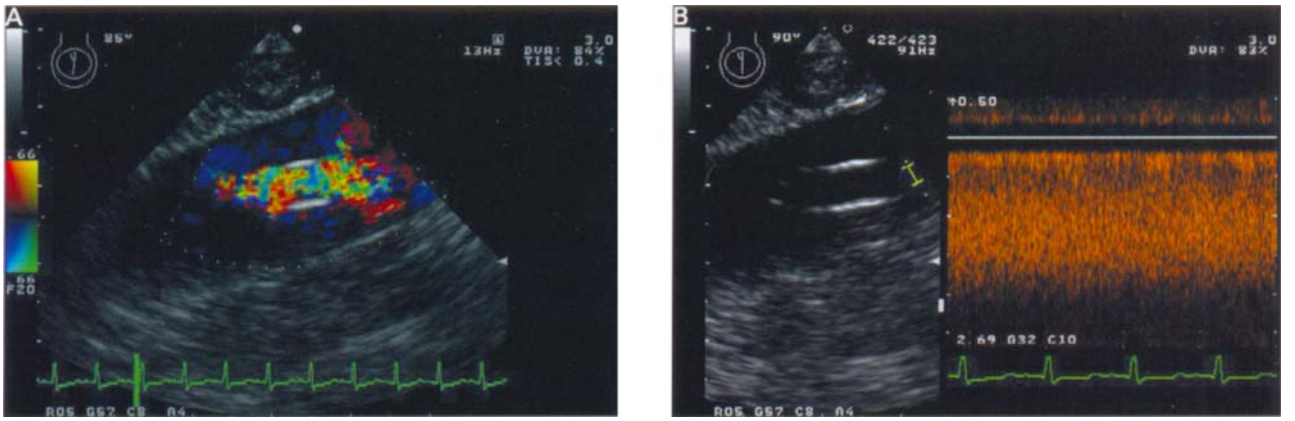

Figure 15.9 Outflow cannula of a centrifugal pump positioned in the ascending aorta, imaged in the long-axis view. **(A)** Colour flow Doppler shows a turbulent outflow velocity profile, whereas **(B)** pulsed wave Doppler recording shows continuous flow with a maximum velocity of 1·6 m/s.

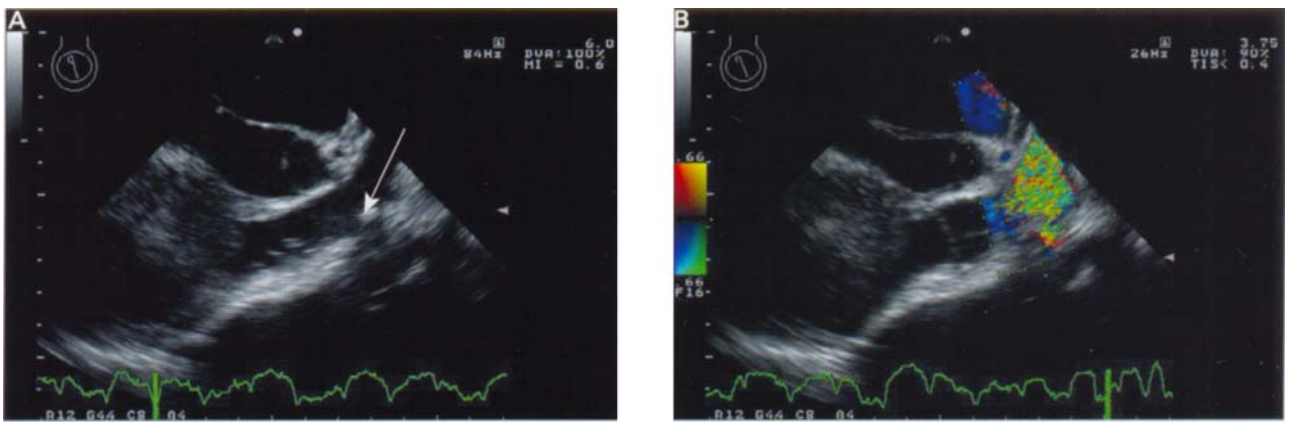

Figure 15.10 Pulmonary artery anastomosis to the outflow cannula of a pulsatile right ventricular assist device (RVAD; arrow), imaged in **(A)** a longitudinal view of the pulmonary artery. **(B)** Colour flow Doppler shows pulsatile flow as a colour mosaic.

stem can best be visualised in the upper oesophageal short-axis view of the aortic arch, which shows the pulmonary artery in a long-axis view (Figure 15.10), but optimal image orientation is often difficult to acquire. Anastomosis of the LVAD outflow cannula to the ascending aorta, which is best viewed from the mid-oesophageal long-axis imaging plane (Figure 15.11), is often obscured by the shadow of the left mainstem bronchus. Alternatively, the LVAD outflow cannula is connected to the descending thoracic aorta, where it is easily visualised in long-axis and short-axis imaging planes, with anatomy, cannula position and diameters, and outflow profile and flow velocities easily accessible using the various echocardiography modes (Figure 15.12).

Before separation from CPB, TOE may be used to confirm that intracardiac air has been completely removed. Air usually collects in the pulmonary veins, along the anterior wall of the left atrium, and is visible just opposite the ascending aorta in the mid-oesophageal long-axis view, as well as along the interventricular septum and in the ventricular apex (Figure 15.13). The device itself, along with the connected cannulae, is also a major source of air bubbles. Air passing through the aortic root can enter the coronary arteries, with the anteriorly directed right coronary ostium being particularly prone to air embolism, leading to ischaemic changes, arrhythmias, and predominant right ventricular failure (Figure 15.14).

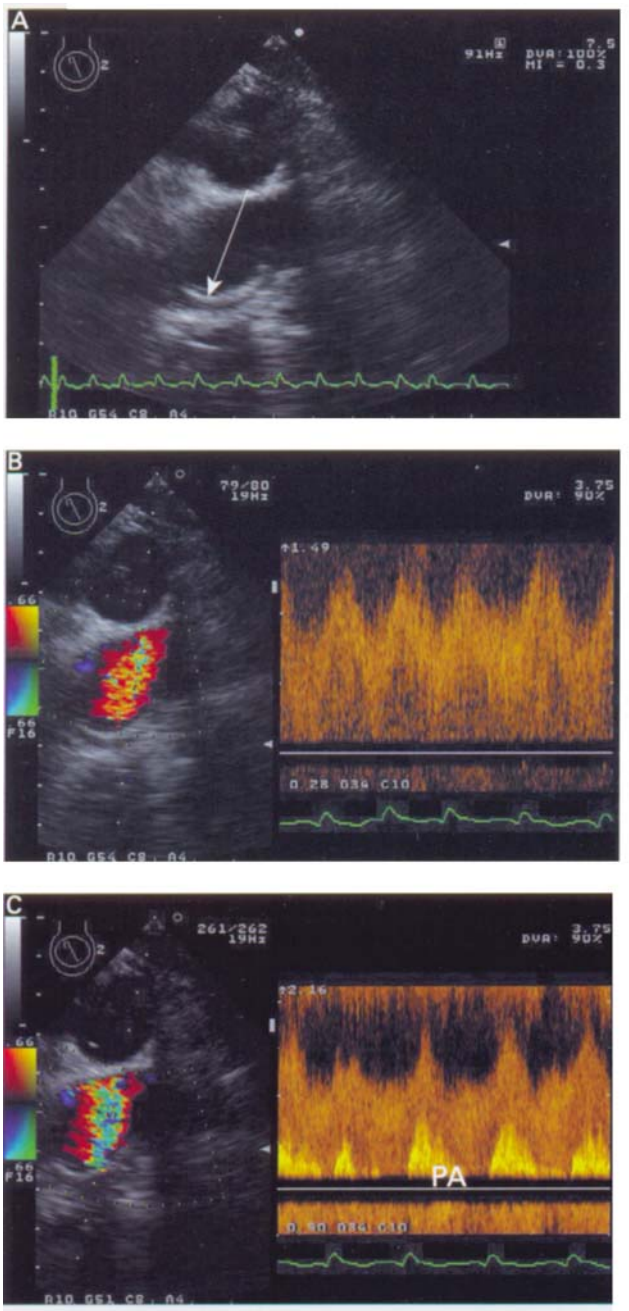

Figure 15.11 Ascending aortic outflow cannula of a non-pulsatile left ventricular assist device (LVAD; arrow), imaged in **(A)** the mid-oesophageal long axis view. **(B)** Pulsed wave Doppler shows continuous but wavelike flow due to left ventricular ejection assisting LVAD filling. **(C)** Continuous wave Doppler shows overlying systolic pulmonary artery flow (PA). Note the time synchrony to the peaks in LVAD outflow velocity.

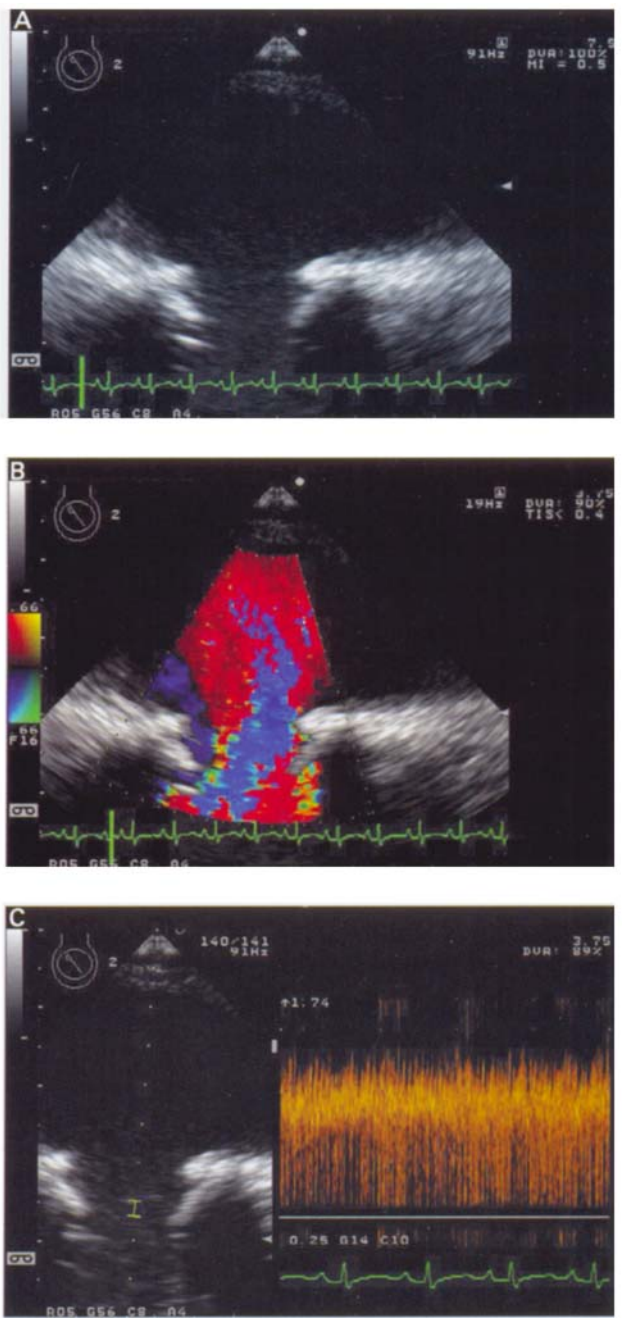

Figure 15.12 The anastomosis of the outflow cannula of a non-pulsatile left ventricular assist device (LVAD) to the descending aorta is imaged in **(A)** the long-axis view of the descending aorta, **(B)** with colour flow Doppler, and **(C)** with pulsed wave Doppler, showing continuous flow without pulsatility.

During use of the ventricular assist device

During separation from CPB, TOE monitoring of ventricular function and volume is indispensable for maintaining a balanced volume status, which is essential for adequate VAD filling. Careful screening for air entry must follow while the assist device is started. This is because residual air in the device or the cannula may be ejected into the circulation and air may be sucked into the heart

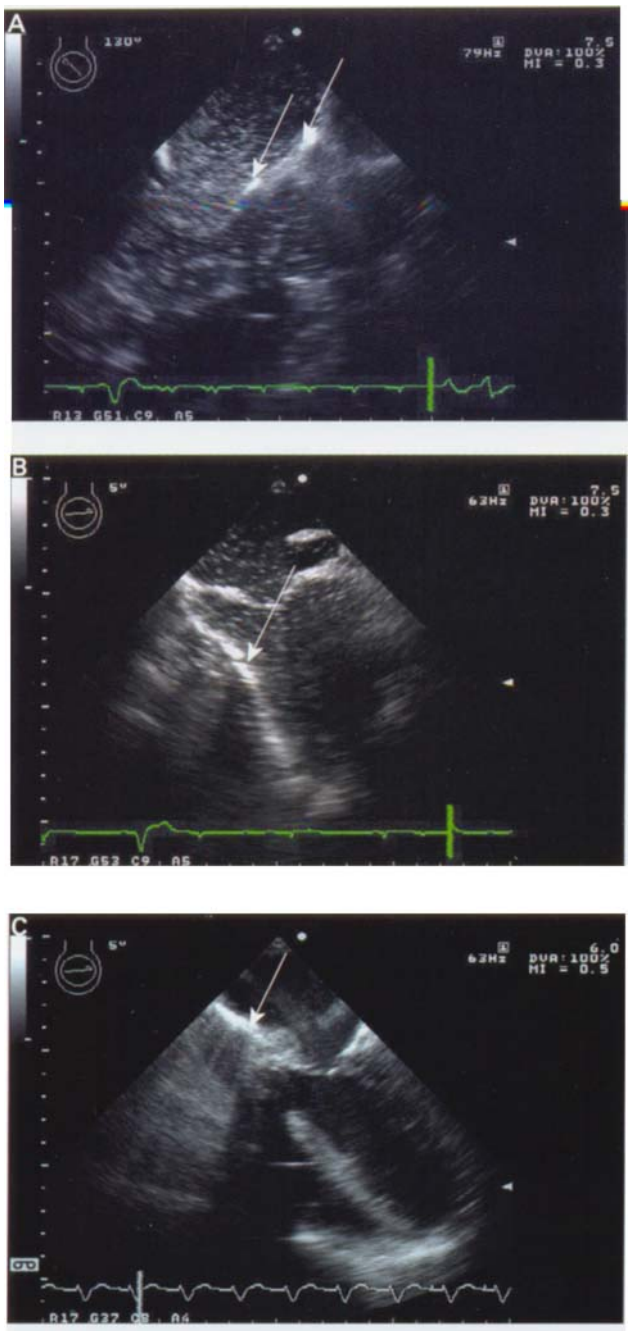

Figure 15.13 Air pockets causing characteristic artefacts (shadowing, reverberation), seen **(A)** in the mid-oesophageal long-axis view along the anterior roof of the left atrium, and in the mid-oesophageal four chamber views along **(B)** the interventricular and **(C)** the interatrial septum (arrows). Small air bubbles are seen floating in the atrium and the ventricle.

along incompletely sealed cannula suture lines if significant negative intracardiac pressure is generated by the cardiac assist device, as occurs with partial cannula obstruction or insufficient intracardiac volume. If air is visualised, then the VAD must be stopped and the outflow cannula clamped immediately, followed by careful and thorough removal of air. If the site of the aortic outflow cannula in the ascending aorta cannot be visualised, then alternatively air can be detected on its passage through the aortic arch and the descending aorta. Increased vacuum to support VAD filling should be avoided in the presence of hypovolaemia because this increases the risk for air entry and can lead to invagination of the atrial appendage and parts of the atrial walls.[22]

With separation from CPB, adequate VAD function leads to complete unloading of the supported ventricle without ventricular ejection, which is confirmed by systolic and diastolic closure of either the aortic or the pulmonary valve, depending on the type of VAD used. With LVAD support, attention must focus on monitoring of the unsupported right ventricle. Beneficial effects of a LVAD on right ventricular function are increased coronary perfusion pressure, which improves contractility, while pulmonary artery pressure and therefore right ventricular afterload might decrease due to a decrease in left atrial pressure. The leftward septal shift during left ventricular unloading might increase right ventricular diastolic compliance, but it will impair right ventricular global contraction, which is very dependent on the septal contribution. Unfortunately, in the patient with high pulmonary vascular resistance, the increased circulatory volume increases pulmonary artery pressures, and in combination with the increased venous return the right ventricle may be driven into failure.[23] Signs on TOE will be dilation of the right ventricle with onset of severe tricuspid regurgitation, as well as hypovolaemia of the left sided chambers because of the reduced transpulmonary flow with left atrial and ventricular collapse and consequent LVAD dysfunction. Apart from pharmacological support of right ventricular contractility and decrease in right ventricular afterload, this situation requires careful adjustment of volume status and LVAD output, which is guided by TOE monitoring.

After separation from CPB, cannula anastomoses at locations that are difficult to visualise, not identified previously with B-mode, can at least be estimated from the colour flow Doppler signal, which gives an estimate through the characteristics of the flow profile if correct position was achieved. Cannula inflow and outflow at all locations must be repeatedly documented with colour flow Doppler, and the

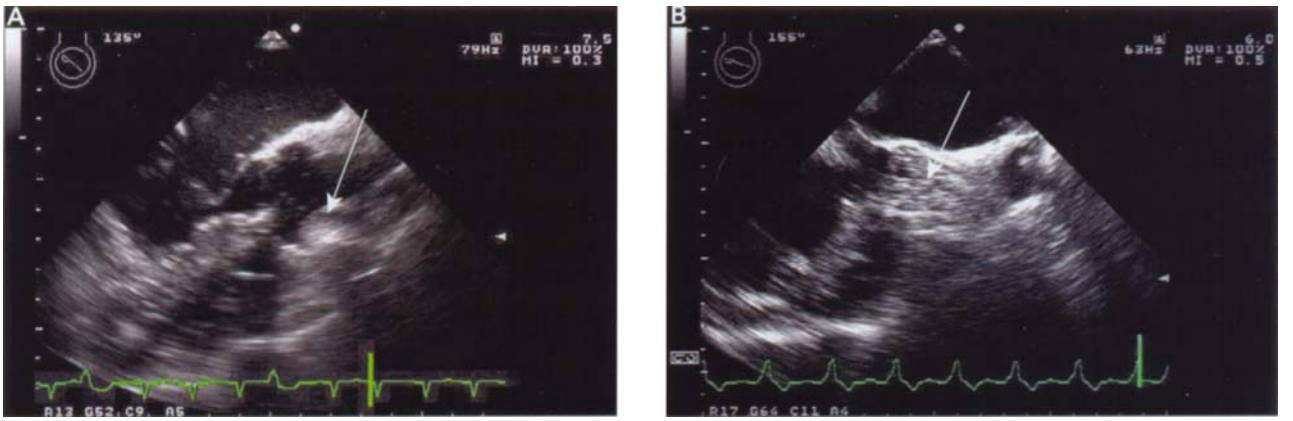

Figure 15.14 Insufficient removal of air from a left ventricular assist device (LVAD) device. With TOE, air is visualised **(A)** entering through the VAD outflow cannula into the ascending aorta; **(B)** the ascending aorta is then filled with air after one test beat (arrows).

information from the pulsed wave Doppler signal is used whenever adequate parallel image alignment to the flow direction can be obtained. With colour flow Doppler, unobstructed cannula inflow shows a laminar flow convergence zone toward the cannula orifice, with aliasing depending on the adjusted Nyquist limit (see Figures 15.6–15.8). The pulsed wave Doppler inflow signal will allow discrimination between a pulsatile and non-pulsatile VAD. With pulsatile flow, inflow velocity is only measured in VAD diastole (Figure 15.15), whereas with non-pulsatile flow the inflow velocities are continuously recorded. The non-pulsatile flow velocity profile is not necessarily flat, as might be expected, but will exhibit a waveform that depends on the amount of ventricular contraction still provided by the supported ventricle. With a closed aortic or pulmonary valve, the ventricular contraction increases intraventricular pressure, thereby supporting VAD filling and augmenting filling velocities in systole. Likewise, the additional placement of an IABP in a patient with a non-pulsatile LVAD will lead to an wave-like inflow curve on pulsed wave Doppler, because axial flow pump output is very dependent on afterload, which increases periodically with IABP inflation. Maximum inflow velocities measured with pulsed wave Doppler are usually within the range of 1·0–2·0 m/s, depending on whether gravity drainage only or suction is used to fill the VAD. High velocity, turbulent flow is a sign of cannula obstruction, and maximal velocities can be measured using continuous wave Doppler, with inflow velocities greater than 2·5 m/s usually reported in cases of inflow obstruction.[16] Cannula outflow usually appears as a colour mosaic on colour flow Doppler because of the increased flow velocities, and pulsatility can easily be distinguished from the continuous flow in non-pulsatile devices, which again might exhibit a flat or wave-like flow profile depending on the amount of ventricular contraction preserved (Figure 15.16; also see Figures 15.9–15.12).

The use of pulsed wave Doppler, in combination with a knowledge of the area (πr^2) of the cannula orifice, allows the assist device flow to be quantified, which should be routinely measured and compared with thermodilution cardiac output and intrinsic flow measurements of the assist device.[24] With stabile haemodynamics and LVAD function, the presence of a PFO must again be excluded, because with the reversed right-to-left pressure gradient a previously undetected PFO could now be unmasked. Once more, the function of all valves is checked. On chest closure attention must be directed at detecting potential changes in cannula position because of shifts in device position, which is most likely with implantable LVADs. Again, flow is documented by colour flow Doppler and pulsed wave Doppler in order to ensure that no significant changes have occurred during chest closure.

Postoperatively, TOE is important for guiding optimal VAD adjustment and for determining the cause of unstable haemodynamics, which may result from or lead to VAD malfunction. The most frequent reasons for low pump flow rates are

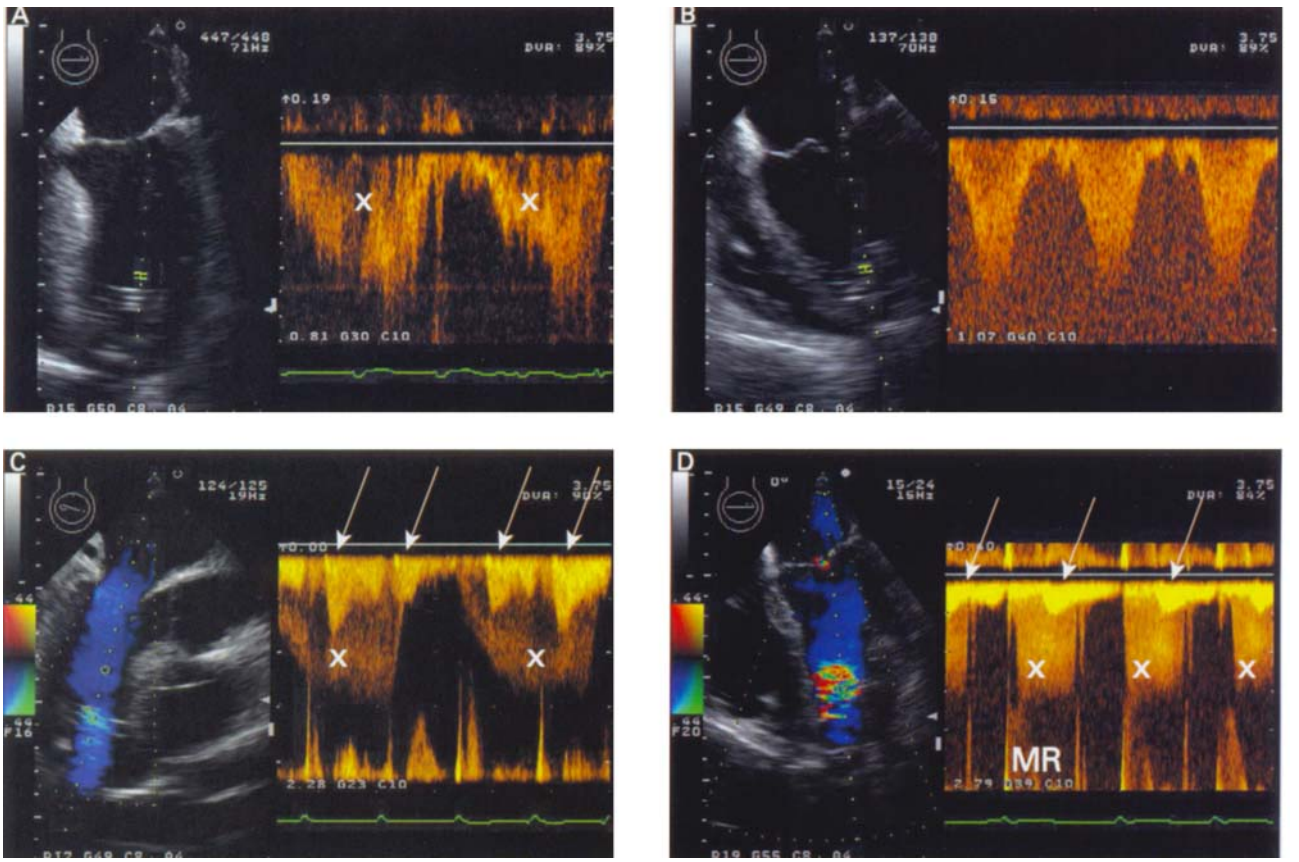

Figure 15.15 **(A, B)** Pulsed wave Doppler and **(C, D)** continuous wave Doppler recording at the inflow cannula of a pulsatile left ventricular assist device (LVAD), showing the electrocardiographically asynchronous LVAD filling velocities (x), in panels A and C with a low pump frequency. Continuous wave Doppler simultaneously shows the electrocardiographically synchronous inflow through the mitral valve (arrows) and a mitral regurgitation jet (MR).

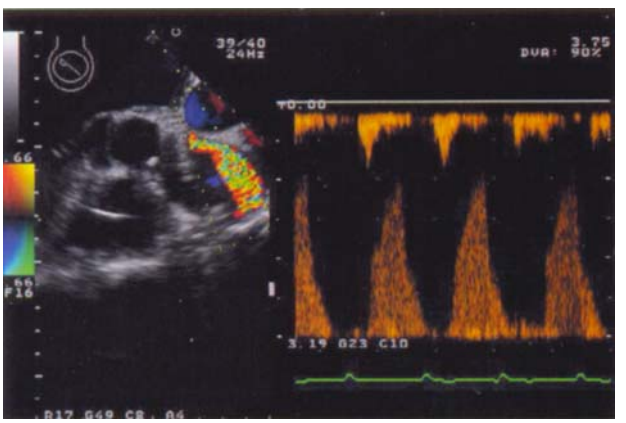

Figure 15.16 Outflow cannula of a pulsatile left ventricular assist device (LVAD) positioned in the ascending aorta, imaged in the mid-oesophageal long-axis view. Colour flow Doppler shows turbulent flow, and continuous wave Doppler shows unobstructed pulsatile flow with a maximum velocity of 2 m/s.

hypovolaemia, right ventricular failure, and inflow cannula obstruction through malposition.[25] Thrombus formation may cause inflow cannula obstruction that is detectable on TOE (Figure 15.17). Pericardial tamponade may be difficult to diagnose, with coagulated blood retained locally and obscured by artefacts from the cannula or device. Small collections may be haemodynamically significant, and standard Doppler signs of tamponade do not apply. Spontaneous echo contrast (smoke) in the ventricle is a sign of blood stagnation and has been shown to correlate with high risk for ventricular thrombus formation, creating a source of pulmonary and systemic embolisation.[26] Pulmonary embolus should be suspected with sudden right ventricular failure and rises in pulmonary artery pressures, with careful inspection of the pulmonary artery and its bifurcation into the right and left mainstem in the

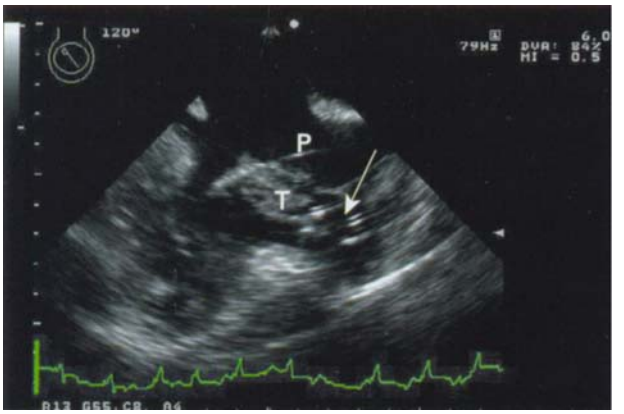

Figure 15.17 Thrombus (T) originating from a pacing wire lead (P) that is partially obstructing a right ventricular assist device inflow cannula (arrow) placed through the right atrial appendage (mid-oesophageal bicaval view).

longitudinal and cross-sectional imaging planes. In any case of systemic desaturation, especially if other causes have been ruled out, intermittent or new onset right-to-left shunting through a previously undetected or newly opened PFO should be sought.[27,28] High LVAD flow rates should prompt careful examination of the aortic valve, because newly occurring regurgitation might be caused by infective endocarditis. If high VAD flow rates do not match the patient's effective circulation, then dysfunction and regurgitation of the inflow or outflow valve of the VAD might be the cause. Careful examination of the flow profile at the inflow and outflow cannula with colour flow Doppler and pulsed wave Doppler will reveal pump rate synchronous bidirectional instead of unidirectional flow, with the leaking portion visible at the inflow cannula during VAD systole and at the outflow cannula in diastole.[29]

Table 15.4 gives a checklist for echocardiographic evaluation during implantation and use of a VAD.

Transoesophageal echocardiography and total artificial hearts

The total artificial heart (TAH) is a biventricular pulsatile pump that is attached to the patient's atria after removal of the native heart, similar to the technique of orthotopic heart transplantation. The CardioWest TAH (CardioWest Technologies Inc., Tucson, Arizona, USA) – a device in clinical trial in the USA and occasional clinical use in Europe – has prosthetic ventricles made of polyurethane and Medtronic Hall valves and is connected to a driving console by power lines. Another TAH in clinical trial – the AbioCor™ implantable replacement heart (ABIOMED Inc., Danvers, Massachusetts, USA) – is a fully implantable device with transcutaneous power supply, whose ventricles and valves are manufactured from polyurethane.

Echocardiographic assessment of the TAH is difficult because of its prosthetic nature, with limitations caused by inadequate penetration and artefact generation. In general, the patient's atria and the anastomosis can be visualised, whereas the TAH itself is difficult to image because of artefacts caused by the prosthetic valves, but the function of the left and right sided inflow valves can usually be assessed by B-mode and colour flow Doppler and pulsed wave Doppler echocardiography. Simon *et al.*[30] reported flow velocities of 1·0–1·2 m/s for the left and 0·8–0·9 m/s for the right inflow valve. The positions of the left and right outflow cannulae in the ascending aorta and the pulmonary artery are similar to those in a BVAD and are examined as described above.

Transoesophageal echocardiography and heart transplantation

Echocardiographic evaluation of the donor heart is mandatory for pretransplantation assessment, with TOE having a higher yield of abnormal findings than transthoracic echocardiography.[31] Comprehensive screening includes assessment of atria, ventricles and valves, pulmonary veins, interatrial septum, venae cavae, pulmonary artery and ascending aorta, including precise description of global and regional biventricular function. Moderate wall motion abnormalities, which are frequently found in donors without coronary artery disease, have been shown to be reversible shortly after transplantion.[32,33] Maintenance of donor haemodynamic stability is often challenging during explantation, and TOE monitoring will detect changes in regional wall motion as signs of myocardial ischaemia and guide volume replacement.

Table 15.4 Checklist for echocardiographic evaluation during the various stages of VAD implantation and use

Stage	*Details*
Before VAD implantation	Comprehensive examination with focus on: • Ventricular function, size, and regional wall motion abnormalities, especially of the unsupported ventricle • Chamber and vessel anatomy, especially at cannulation sites • Presence of intracavitary thrombi • Valvular anatomy and function, especially aortic valve competence • Presence of patent foramen ovale, atrial septal defect, or ventricular septal defect or other shunts Guidance of haemodynamic management before CPB
During VAD implantation and activation	Examination of cannula position: • Anatomically correct orientation • Free of obstruction • Normal Doppler flow profile Confirmation of sufficient removal of air: • Exclusion of intracardiac and intravascular air enclosures • Monitoring of device outflow at VAD start for residual air (VAD stop if air present!) Guidance of volume adjustments and VAD flow to ensure optimal function during and after CPB separation • Adequate ventricular unloading Exclusion of aortic/pulmonary valve regurgitation
During VAD use	Adequate VAD function: • Sufficient ventricular unloading • Permanently closed aortic/pulmonary valve • Unobstructed optimal cannula position • Flow characteristics across all cannulae • TOE calculation of VAD flow/output Presence of newly appearing shunt flow Exclusion of air embolism or air drawing with VAD suction Ventricular function and volume: • Response to pharmacological support • Need for mechanical assist
TOE signs of VAD dysfunction	• Aortic/pulmonary valve opening • Forward flow in outflow tract • Incomplete ventricular unloading • Increased Doppler velocities across inflow and outflow cannulae • Turbulence and regurgitation on colour flow Doppler at the inflow cannula • Mismatch between Doppler derived cardiac output across outflow tract of unsupported ventricle and device output • Abnormal inflow cannula orientation
Troubleshooting low VAD pump flow rates	• Hypovolaemia • Failure of the unsupported ventricle (usually right ventricle) • Inflow and outflow cannula obstruction • Pericardial tamponade • Ventricular thrombus formation (smoke), pulmonary artery embolism • Cannula malposition
Troubleshooting high VAD pump flow rates	• Shunt flow • Aortic valve insufficiency (LVAD), pulmonic valve insufficiency (RVAD) • Inflow and/or outflow valve incompetence

BVAD = biventricular assist device, CPB cardiopulmonary bypass, LVAD = left ventricular assist device, RVAD = right ventricular assist device, TOE = transoesophageal echocardiography.

Heart transplant recipients present with severe cardiopulmonary dysfunction, possibly supported by some form of circulatory assist device. Maintenance of haemodynamic stability during induction of anaesthesia and surgical preparation can be very challenging, and intraoperative TOE monitoring to guide volume management and titration of inotropic medications is essential. TOE evaluation will reveal a dilated left ventricle with severe global ventricular hypokinesis and varying degrees of mitral insufficiency caused by annular dilation. In the presence of pulmonary hypertension, the right ventricle is hypertrophic while still compensated, but will exhibit enlargement with decompensation. With tricuspid regurgitation present in virtually all recipients, systolic pulmonary artery pressure can be calculated non-invasively by Doppler echocardiography. A complete TOE examination should identify intracardiac thrombi, for which these patients are at risk, in order to prevent systemic embolisation through surgical manipulation. Signs of right ventricular adherence to the sternum should be recognised in patients with previous sternotomy.

In orthotopic heart transplantation, the venous anastomoses are performed first by atrial or bicaval technique. Thereafter, the pulmonary artery anastomosis is performed, and finally the ascending aortic anastomosis is completed before removal of the arterial cross clamp. At this point, thorough removal of intracardiac air is important and guided by TOE (see the section entitled Ventricular assist devices, above). After opening of the cross-clamp, adequate decompression of the left and right ventricles by the vent during the reperfusion period is confirmed echocardiographically. Distortion of the aortic valve with resulting aortic insufficiency must be excluded to prevent left ventricular dilation. Prior to separation from CPB, myocardial global and regional function is assessed by TOE to help in the titration of inotropic support needed for separation from CPB. Persistent marked regional wall motion abnormalities should prompt an evaluation to determine whether flow in the main coronary arteries is adequate, using the mid-oesophageal aortic cross-sectional imaging plane just above the aortic valve. At this point, severe tricuspid and mitral valve dysfunction must be excluded.

During and immediately after separation from CPB, TOE monitoring will focus on biventricular systolic and diastolic function and volume status. A typical scenario is a vigorously pumping, small left ventricle that appears hypertrophied because of myocardial oedema with signs of diastolic dysfunction (see Chapter 4), whereas the right ventricle exhibits impaired function with global hypokinesis, thin walls, dilation, and paradoxical systolic septal motion. The donor right heart, which is not adapted to the increased recipient pulmonary vascular resistance, is at high risk for progressing to right ventricular failure, with early right ventricular dysfunction recovering in the majority of patients with adequate treatment.[34] Biventricular global and segmental myocardial function is precisely evaluated and an estimate of systolic pulmonary artery pressure obtained through Doppler echocardiographic measurement of a tricuspid regurgitation jet. Echocardiography plays an important role in guiding the titration of inotropic support of the right ventricle, in reducing pulmonary artery resistance with intravenous and inhaled vasodilatory drugs, and in managing the patient's volume status. With adequate preload, the atrioventricular valves are examined carefully. Mitral and especially tricuspid regurgitation can result from distortion of the valve annulus, which is most likely to happen if a considerable size mismatch between donor and recipient organ is present and if the atrial anastomosis technique is used.[35,36] Tricuspid regurgitation, if severe, will further aggravate right ventricular dysfunction, and therefore tricuspid reconstruction must be considered.[37] In this case, a precise description of the cause and severity of regurgitation will support the surgical procedure. Inflow Doppler velocity profiles across the atrioventricular valves will exhibit variations depending on the presence, extent, and timing of atrial activity of the donor and recipient atria. Effective atrial contraction, which is often difficult to determine electrocardiographically in heart transplant recipients, can be demonstrated with pulsed wave Doppler or colour flow Doppler (Figure 15.18).

With circulatory stability reached, a comprehensive examination is conducted to evaluate the suture lines, excluding stenosis, by way of colour flow Doppler or pulsed wave Doppler. With the atrial suture technique, the resulting atrium is built from recipient atrium in the dorsal part and donor atrium in the ventral sections, resulting in biatrial enlargement, and prominent suture lines in the left but also in the right atrium are regularly seen and can appear as masses. This gives an hourglass appearance to the atria, also called "snowman" configuration (Figures 15.19 and 15.20).[35,38] Stenosis at the line of

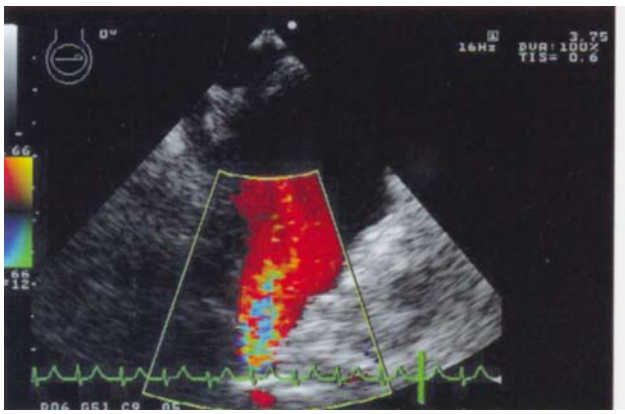

Figure 15.18 Colour flow Doppler of left atrial appendage after heart transplantation showing effective atrial contraction.

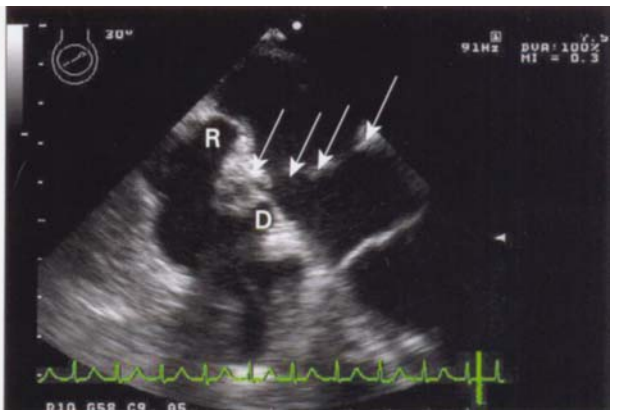

Figure 15.19 Atrial anastomosis after heart transplantation, imaged in the mid-oesophageal four chamber view. The arrows indicates the suture line, which is visible through the left atrium. The interatrial septum is thickened at the suture line, and two fossae ovalis are visible, one from the donor atrium (D) and the other from the remnants of the recipient atrium (R).

the atrial anastomosis (acquired cor triatriatum) has been reported,[39–42] which manifests as high velocity flows on colour flow Doppler across the suture line, a significant trans-stenotic gradient, and diastolic fluttering of the mitral leaflets, suggesting high velocity diastolic flow. Atrial septal pseudoaneurysms are found in approximately one third of patients, variation in thickness of the donor versus recipient atrial septum is seen,[43] and often two fossa ovalis regions can be identified in the interatrial septum (see Figures 15.19 and 15.20), which should be checked for patency (see the section entitled Ventricular assist devices, above), because the usually increased right atrial pressure will make paradoxical embolism more likely. Spontaneous echocardiographic contrast or smoke-like echo, a sign of haemostasis, can appear in the enlarged double atrium (see Figure 15.20),[44] and should be monitored at close intervals because these patients have been shown to be at increased risk for atrial thrombus formation.[45]

Studies comparing standard orthotopic (atrial technique) with total orthotopic (bicaval technique) heart transplantation have found spontaneous echo contrast in the left atrium in about 55% of patients after standard orthotopic heart transplantation, with thrombi in the left atrial appendage (Figure 15.21), the posterior wall, or on the suture line detected by TOE in about 25% and signs of systemic embolism in 15% of patients,[46–48] requiring systemic anticoagulation. Another, although rare, finding

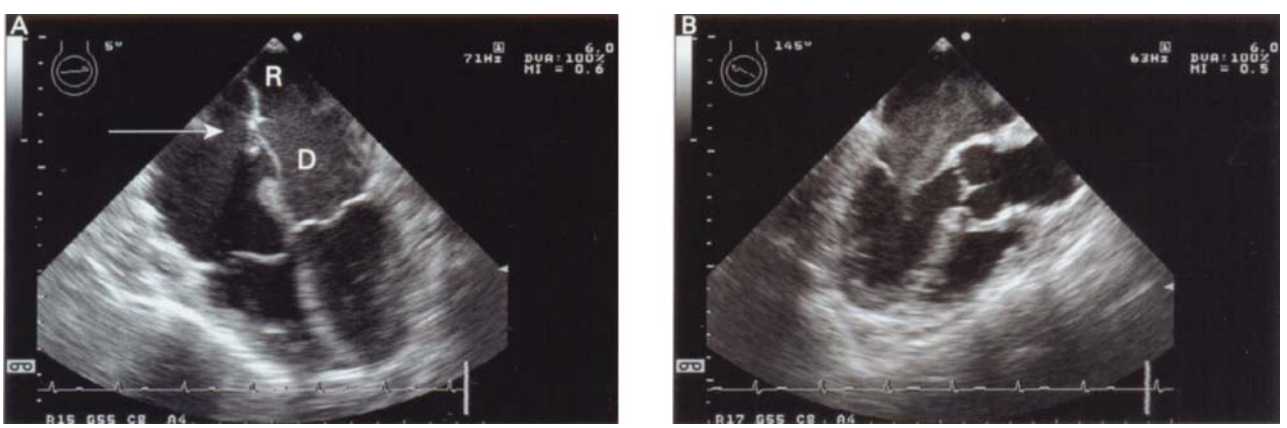

Figure 15.20 Biatrial enlargement after heart transplantation, imaged in the midoesophageal **(A)** four chamber and **(B)** long-axis views. The arrow indicates the suture line, which is visible at the interatrial septum. Two fossae ovalis are visible, one from the donor atrium (D) and the other from the recipient atrium (R). The increased right atrial pressure pushes the interatrial septum to the left, and the recipient fossa ovalis appears as a pseudoaneurysm. Note that "smoke" is visible in the left atrium and that the right ventricle appears dilated.

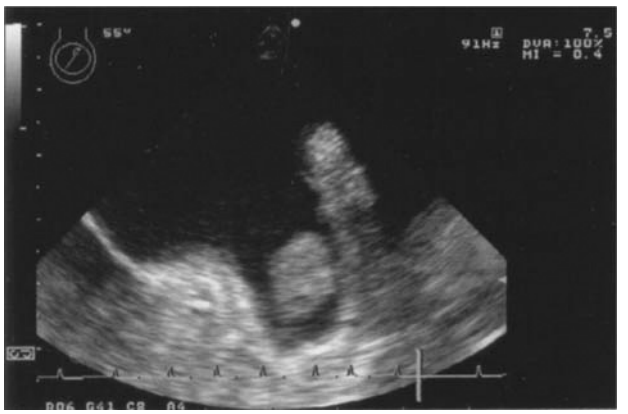

Figure 15.21 Thrombus in the left atrial appendage.

at the left atrial suture line is the appearance of diastolic flow on colour flow Doppler and pulsed wave Doppler from atrial arteries branching off the circumflex coronary artery, entering into the atrial lumen after completion of the anastomosis.[49] If the bicaval surgical technique, including pulmonary venous anastomosis, is used then unobstructed caval and pulmonary venous inflow must be confirmed by laminar flow on colour flow Doppler and normal caval and pulmonary venous inflow velocities (0·4–0·6 m/s) by pulsed wave Doppler, because size mismatch can lead to distortion with ensuing increased velocities and turbulent flow profile.[50] The pulmonary artery as well as the ascending aorta must be examined carefully at the valvular level as well as at the anastomosis site by way of B-mode and Doppler to document unobstructed valve opening and patency, because distortion at the anastomosis can result in impaired valvular function, and supravalvular stenosis at the level of the anastomosis may be present.[51] If flow appears turbulent with colour flow Doppler, then continuous wave Doppler measurements must be obtained to calculate gradients across the anastomosis.

Postoperatively, TOE is important in determining the cause of low cardiac output states. Hypovolaemia, right ventricular failure, and cardiac tamponade as the major differential diagnoses are discussed above. Another cause is temporary diastolic dysfunction with a restrictive filling pattern, which is usually present in the early postoperative period (see Chapter 4).[52]

Table 15.5 provides a checklist for TOE evaluation during the various stages of heart and lung transplantation.

Table 15.5 Checklist for echocardiographic evaluation during the various stages of transplantation

Stage	Details
Before transplantation	• Ventricular function, valvular status, volume, haemodynamic guidance • Doppler derived pulmonary artery pressure calculation • Exclusion of intracavitary thrombus
During transplantation	• Monitoring of sufficient removal of air • Ventricular unloading during reperfusion • Global and regional ventricular function • Valvular function and anatomy • Screening of anastomoses to exclude stenosis
After transplantation	Differential diagnosis of low cardiac output: • Hypovolaemia • (Right) ventricular failure • Pericardial tamponade • Diastolic dysfunction • Anastomotic stenosis

Transoesophageal echocardiography and lung transplantation

Single or double lung transplantation is a very challenging procedure that carries a high risk for haemodynamic instability and respiratory deterioration, especially during the period of single lung ventilation, which is necessary if the operation is to be performed without the support of CPB. This renders TOE essential for the management of such cases.

A thorough baseline examination, as described in the sections above, is mandatory. Points to concentrate on are the baseline ventricular size and function, including valvular anatomy and function, with a focus on the right ventricle and exclusion of a PFO. At this point it is also advisable to image the pulmonary arteries and pulmonary veins in order to obtain a baseline impression of the anatomy at these areas. If the transplantation is performed without the support of CPB, TOE monitoring during the procedure will focus on the right ventricular function

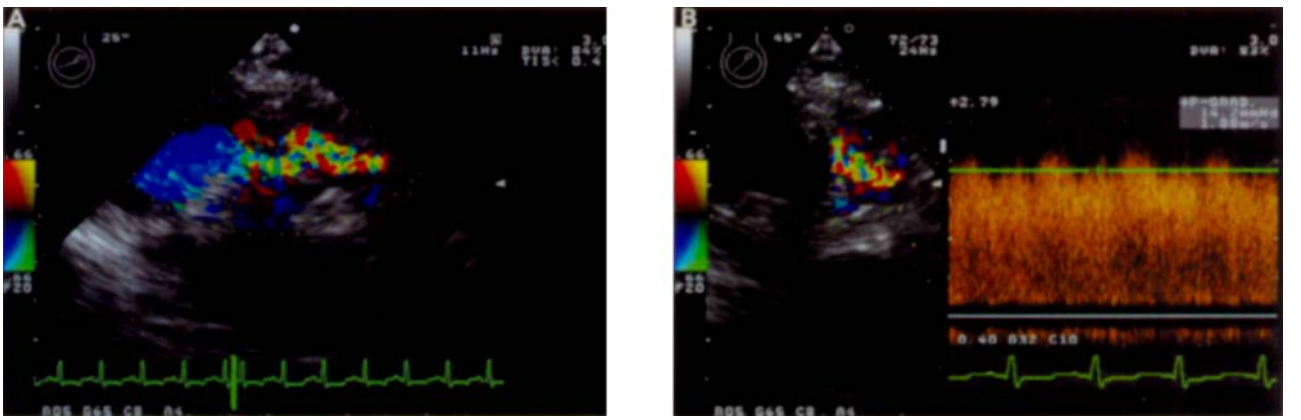

Figure 15.22 Anastomosis of left upper pulmonary vein after lung transplantation showing distortion and flow diversion in an S configuration, with a turbulent flow profile on **(A)** colour flow Doppler, which is indicative of stenosis. **(B)** Pulsed wave Doppler shows continuous flow of increased velocity without the characteristic pulmonary vein flow pattern. The calculated pressure gradient across the stenosis is 14 mmHg.

because the risk for developing right ventricular dysfunction (see sections above and Chapter 8), including advanced degrees of tricuspid and pulmonary valve regurgitation, is very high with the institution of single lung ventilation. Severe hypoxaemia during the procedure should trigger a repeated search for a PFO, including contrast studies (see the section entitled Ventricular assist devices, above), because an increase in right ventricular afterload creates high right atrial pressures with the potential of opening a previously closed foramen ovale.

Toward the end of the procedure, echocardiographic assessment of all vascular anastomoses is performed. The pulmonary vein anastomoses can nearly always be visualised by TOE from the mid-oesophageal approach, preferably in a longitudinal imaging plane.[53,54] The diameter of the anastomosis should be comparable to the pulmonary vein diameter proximal to it, and narrowing or distortion as well as thrombus formation must be excluded. Colour flow Doppler should reveal laminar, unobstructed blood flow into the left atrium, and pulsed wave Doppler should show the characteristic pulmonary flow velocity profile (S wave and D wave), with peak velocities recorded usually elevated up to 1 m/s. Signs of pulmonary venous obstruction are a mosaic pattern on colour flow Doppler, combined with a significant increase in the velocity of the pulsed wave Doppler tracing, which will lose the characteristic pulmonary inflow profile and show a continuous signal of high flow velocity (> 1·5 m/s) recorded instead (Figure 15.22).[54,55] Because the incidence of pulmonary vein complications reported in the literature is up to 30%, with significant impact on morbidity and mortality, intraoperative TOE detection of any abnormality at the anastomosis site is very important for initiating and guiding timely surgical intervention.[56]

Echocardiographic imaging of the pulmonary artery anastomoses is best achieved in the horizontal imaging plane at the level of the aortic and pulmonary valves, giving a longitudinal cut of the pulmonary artery and its bifurcation, from where the left and right pulmonary artery can be followed distally. Whereas the right pulmonary artery anastomosis can nearly always be imaged, the left pulmonary artery anastomosis is more difficult to visualise, with 0% to 70% success reported in the literature.[53,54] The region of the anastomosis should show no narrowing in vessel diameter, and distortion should be excluded. Colour flow Doppler may show localised areas of turbulent flow at the site of the anastomosis, especially if cardiac output is increased, but unless a significant increase in flow velocity is measured with pulsed wave or continuous wave Doppler, this is not indicative of a stenosis. If significant narrowing of the pulmonary artery anastomosis is suspected and TOE visualisation of the anastomosis is not possible, then indirect signs such as right ventricular distension, failure, and paradoxical septal motion in combination with left ventricular hypovolaemia are valuable signs in guiding further diagnostic and therapeutic interventions.

References

1 Goldstein DJ, Oz MC. *Cardiac assist devices.* Armonk NY: Futura Publishing Company, 2000.

2 Shanewise JS, Cheung AT, Aronson S, *et al.* ASE/SCA guidelines for performing a comprehensive intraoperative multiplane transesophageal echocardiography examination: recommendations of the American Society of Echocardiography Council for Intraoperative Echocardiography and the Society of Cardiovascular Anesthesiologists Task Force for Certification in Perioperative Transesophageal Echocardiography. *Anesth Analg* 1999;**89**:870–84.

3 Kaplan LJ, Weiman DS, Langan N, Sokil AB, Whitman GJR. Safe intraaortic balloon pump placement through the ascending aorta using transesophageal ultrasound. *Ann Thorac Surg* 1992;**54**:374–5.

4 Williams DO, Korr KS, Gewirtz H, Most AS. The effect of intraaortic balloon counterpulsation on regional myocardial blood flow and oxygen consumption in the presence of coronary artery stenosis in patients with unstable angina. *Circulation* 1982;**66**:593–7.

5 Kern MJ, Aguirre FV, Tatineni S, *et al.* Enhanced coronary blood flow velocity during intraaortic balloon counterpulsation in critically ill patients. *J Am Coll Cardiol* 1993;**21**:359–68.

6 Reichert CLA, Koolen JJ, Visser CA. Transesophageal echocardiographic evaluation of left ventricular function during intraaortic balloon pump counterpulsation. *J Am Soc Echocardiogr* 1993;**6**:490–5.

7 Cheung AT, Savino JS, Weiss SJ. Beat-to-beat augmentation of left ventricular function by intraaortic counterpulsation. *Anesthesiology* 1996;**84**:545–54.

8 Werner GS, Sold G, Andreas S, Wiegand V, Kreuzer H. Doppler-echocardiographic evaluation of left ventricular function during intra-aortic balloon counterpulsation. *Z Kardiol* 1990;**79**:8–14.

9 Minich LL, Tani LY, McGough EC, Shaddy RE, Hawkins JA. A novel approach to pediatric intraaortic balloon pump timing using M-mode echocardiography. *Am J Cardiol* 1997;**80**:367–9.

10 Pinkney KA, Minich LL, Tani LY, *et al.* Current results with intraaortic balloon pumping in infants and children. *Ann Thorac Surg* 2002;**73**:887–91.

11 Lönn U, Peterzén B, Granfeldt H, Caismir-Ahn H. Coronary artery operation with support of the Hemopump cardiac assist system. *Ann Thorac Surg* 1994;**58**:519–23.

12 Meyns B, Ozaki S, Sergeant P, Nishimura Y, Flameng W. Circulatory support during minimally invasive coronary surgery. *Perfusion* 1998;**13**:265–71.

13 Meyns B, Sergeant P, Nishida R, Perek B, Zietkiewicz M, Flameng W. Micropumps to support the heart during CABG. *Eur J Cardiothorac Surg* 2000;**17**:169–74.

14 Meyns BP, Sergeant PT, Daenen WJ, Flameng WJ. Left ventricular assistance with the transthoracic 24F Hemopump for recovery of the failing heart. *Ann Thorac Surg* 1995;**60**:392–7.

15 Ender J, Anwar N, Brose S, Engel M, Retry A, Autschbach R. Epicardial echocardiography for correct placement of the intracardial biventricular assist device (Impella®). *Thorac Cardiovasc Surg* 2002;**50**:92–4.

16 Scalia GM, McCarthy PM, Savage RM, Smedira NG, Thomas JD. Clinical utility of echocardiography in the management of implantable ventricular assist devices. *J Am Soc Echocardiogr* 2000;**13**:754–63.

17 Holman WL, Bourge RC, Fan P, Kirklin JK, Pacifico AD, Nanda NC. Transplantation, cardiomyoplasty, long-term support: influence of left ventricular assist on valvular regurgitation. *Circulation* 1993; **88**:II309–18.

18 Holman WL, Bourge RC, Fan P, Kirklin JK, Pacifico AD, Nanda NC. Influence of longer term left ventricular assist device support on valvular regurgitation. *ASAIO J* 1994;**40**:M454–9.

19 Konstadt SN, Louie EK, Black S, Rao TLK, Scanlon P. Intraoperative detection of patent foramen ovale by transesophageal echocardiography. *Anesthesiology* 1991;**74**:212–6.

20 Baldwin RT, Duncan JM, Frazier OH, Wilansky S. Patent foramen ovale: a cause of hypoxemia in patients on left ventricular support. *Ann Thorac Surg* 1991;**52**:865–7.

21 Arabia FA, Paramesh V, Toporoff B, Arzouman DA, Sethi GK, Copeland JG. Biventricular cannulation for the Thoratec ventricular assist device. *Ann Thorac Surg* 1998;**66**:2119–20.

22 Cokis C, Manikappa S. An unusual transesophageal echocardiographic finding after insertion of a ventricular assist device. *J Cardiothorac Vasc Anesth* 2002;**16**:524–5.

23 Pavie A, Leger P. Physiology of univentricular versus biventricular support. *Ann Thorac Surg* 1996;**61**:347–9.

24 Akosah KO, Song A, Guerraty A, Mohanty P, Paulsen W. Echocardiographic evaluation of patients with a left ventricular device. *ASAIO J* 1998;**44**:M624–7.

25 Snoddy BE, Nanda NC, Holman WL, Kirklin J, Chung SM. Usefulness of transesophageal echocardiography in diagnosing and guiding correct placement of a right ventricular assist device malpositioned in the left atrium. *Echocardiography* 1996;**13**:159–63.

26 Nakatani T, Noda H, Beppu S, *et al.* Thrombus in a natural left ventricle during left ventricular assist: another thromboembolic risk factor. *ASAIO Trans* 1990;**36**:M711–4.

27 Shapiro GC, Leibowitz DW, Oz MC, Weslow RG, Di Tullio MR, Homma S. Diagnosis of patent foramen ovale with transesophageal echocardiography in a patient supported with a left ventricular assist device. *J Heart Lung Transplant* 1995;**14**:594–7.

28 Kilger E, Strom C, Frey L, *et al.* Intermittent atrial level right-to-left shunt with temporary hypoxemia in a patient during support with a left ventricular assist device. *Acta Anaesthesiol Scand* 2000;**44**: 125–7.

29 Moursi M, Nanda NC, Holman W, McGiffin D, Samal A, de Sousa JB. Usefulness of transesophageal echocardiography in diagnosing valve leakage of left ventricular assist device. *Echocardiography* 1998;**15**:703–7.

30 Simon P, Owen AN, Moritz A, *et al.* Transesophageal echocardiographic evaluation in mechanically assisted circulation. *Eur J Cardiothorac Surg* 1991;**5**:492–7.

31 Stoddard MF, Longaker RA. The role of transesophageal echocardiography in cardiac donor screening. *Am Heart J* 1993;**125**:1676–81.

32 Seiler C, Laske A, Gallino A, Turina M, Jenni R. Echocardiographic evaluation of left ventricular wall motion before and after heart transplantation. *J Heart Lung Transplant* 1992;**11**:867–74.

33 Vedrinne JM, Vedrinne C, Coronel B, Mercatello A, Estanove S, Moskovtchenko JF. Transesophageal echocardiographic assessment of left ventricular function in brain-dead patients: are marginally acceptable hearts suitable for transplantation? *J Cardiothorac Vasc Anesth* 1996;**10**:708–12.

34 Hosenpud JD, Norman DJ, Cobanoglu A, Floten HS, Conner RM, Starr A. Serial echocardiographic findings early after heart transplantation: evidence for reversible right ventricular dysfunction and myocardial edema. *J Heart Transplant* 1987;**6**: 343–7.

35 Stevenson LW, Dadourian BJ, Kobashigawa J, Child JS, Clark SH, Laks H. Mitral regurgitation after cardiac transplantation. *Am J Cardiol* 1987;**60**: 119–22.

36 De Simone R, Lange R, Sack FU, Mahmanesh H, Hagl S. Atrioventricular valve insufficiency and atrial geometry after orthotopic heart transplantation. *Ann Thorac Surg* 1995;**60**:1686–93.

37 Haverich A, Albes JM, Fahrenkamp G, Schäfers HJ, Wahlers T, Heublein B. Intraoperative echocardiography to detect and prevent tricuspid valve regurgitation after heart transplantation. *Eur J Cardiothorac Surg* 1991;**5**:41–5.

38 Starling RC, Baker PB, Hirsch SC, Myerowitz PD, Galbraith TA, Binkley PF. An echocardiographic and anatomic description of the donor-recipient atrial anastomosis after orthotopic cardiac transplantation. *Am J Cardiol* 1989;**64**:109–11.

39 Ulstad V, Braunlin E, Bass J, Shumway S, Molina E, Homans D. Hemodynamically significant suture line obstruction immediately after heart transplantation. *J Heart Lung Transplant* 1992;**11**: 834–6.

40 Canivet JL, Defraigne JO, Demoulin JC, Limet R. Mechanical flow obstruction after heart transplantation diagnosed by TEE. *Ann Thorac Surg* 1994;**58**:890–1.

41 Oaks TE, Rayburn BK, Brown ME, Kon ND. Acquired cor triatriatum after orthotopic cardiac transplantation. *Ann Thorac Surg* 1995;**59**:751–3.

42 Law Y, Belassario A, West L, Coles J, Taylor G, Benson L. Supramitral valve obstruction from hypertrophied native atrial tissue as a complication of orthotopic heart transplantation. *J Heart Lung Transplant* 1997;**16**:922–5.

43 Angermann CE, Spes CH, Tammen A, *et al.* Anatomic characteristics and valvular function of the transplanted heart: transthoracic versus transesophageal echocardiographic findings. *J Heart Transplant* 1990;**9**:331–8.

44 Hauptman PJ, Gass A, Goldman ME. The role of echocardiography in heart transplantation. *J Am Soc Echocardiogr* 1993;**6**:496–509.

45 Beppu S, Nimura Y, Sakakibara H, *et al.* Smoke-like echo in the left atrial cavity in mitral valve disease: its features and significance. *J Am Coll Cardiol* 1985;**6**:744–9.

46 Derumeaux G, Habib G, Schleifer DM, *et al.* Standard orthotopic heart transplantation versus total orthotopic heart transplantation. A transesophageal echocardiography study of the incidence of left atrial thrombosis. *Circulation* 1995;**92**:196–201.

47 Bouchart F, Derumeaux G, Mouton-Schleifer D, Bessou JP, Redonnet M, Soyer R. Conventional and total orthotopic cardiac transplantation: a comparative clinical and echocardiographical study. *Eur J Cardiothorac Surg* 1997;**12**:555–9.

48 Riberi A, Ambrosi P, Habib G, *et al.* Systemic embolism: a serious complication after cardiac transplantation avoidable by bicaval technique. *J Cardiothorac Surg* 2001;**19**:307–12.

49 Gascuena R, De Lombera F, Fernancez S, *et al.* Left circumflex coronary artery-to-left atrium fistulas detected by transesophageal echocardiography in heart transplant recipients. *Echocardiography* 2000;**17**:443–5.

50 Lin CP, Chan KC, Chou YM, Wang MJ, Tsai SK. Transesophageal echocardiographic monitoring of pulmonary venous obstruction induced by sternotomy closure during infant heart transplantation. *Br J Anaesth* 2002;**88**:590–2.

51 Rose AG, Park SJ, Shumway SJ, Norton D, Miller LW. Acquired supravalvar aortic stenosis following heart transplantation: report of 2 cases. *J Heart Lung Transplant* 2002;**21**:499–502.

52 Hausmann B, Muurling S, Stauch C, Haverich A, Hirt S, Simon R. Detection of diastolic dysfunction: acoustic quantification in comparison to Doppler echocardiography. *Int J Card Imaging* 1997;**13**:301–10.

53 Hausmann D, Daniel WG, Mügge A, *et al.* Imaging of pulmonary artery and vein anastomoses by transesophageal echocardiography after lung transplantation. *Circulation* 1992;**86**:II251–8.

54 Michel-Cherqui M, Brusset A, Liu N, *et al.* Intraoperative transesophageal echocardiographic

assessment of vascular anastomoses in lung transplantation. *Chest* 1997;**111**:1229–35.

55 Huang YC, Cheng YJ, Lin YH, Wang MJ, Tsai SK. Graft failure caused by pulmonary venous obstruction diagnosed by intraoperative transesophageal echocardiography during lung transplantation. *Anesth Analg* 2000;**91**:558–60.

56 Leibowitz DW, Smith CR, Michler RE, *et al.* Incidence of pulmonary vein complications after lung transplantation: a prospective transesophageal echocardiography study. *J Am Coll Cardiol* 1994;**24**:671–5.

16 Artifacts and pitfalls

Bijoy K Khandheria

Introduction

Transoesophageal echocardiography (TOE) is considered a logical extension of a standard echocardiographic study in certain groups of patients.[1,2] Although the images are consistently of superior quality and can be obtained in the great majority of patients, the technique has limitations because of the limited imaging window within the confines of the oesophagus and stomach, and the difficulty in swapping transducers in special situations. Pitfalls – potential erroneous diagnoses resulting from misinterpretation of normal and abnormal anatomy – are prevalent because of the new topographic presentations and the necessity of using transducers that are not optimised for all diagnostic situations. This chapter critically reviews the current practice of TOE, with particular emphasis on limitations and pitfalls.

Limitations

TOE introduced a new era of semi-invasive ultrasound into the clinical practice of cardiology.[3,4] The concerns associated with this semi-invasive procedure are offset by images that are consistently of high quality. However, in young and elderly patients, TOE has unique considerations and potential limitations. Small children, particularly infants, may require general anaesthesia if they are to undergo the examination.[5–7] Elderly patients are much more sensitive to systemic sedation[8] and have a greater incidence of oesophageal and cervical spine disease that must be specifically addressed with each examination.[9] In our experience of 21 287 consecutive examinations, the procedure was aborted in 1% of patients (because of unsuccessful intubation, patient intolerance, and oesophageal disease).

Learning curve

There is a steep learning curve associated with TOE, and the tomographic anatomy can be confusing initially. The TOE examination is unfamiliar to the beginner, and this may pose limitations with respect to interpretation, demonstration of anatomical relationships, and diagnosis.

Air

It is through the walls of the oesophagus and stomach that the heart and great vessels of the thorax are visualised during TOE examination. The manoeuvrability of the transducer is limited within the lumen of the oesophagus and fundus of the stomach. Because it is impervious to transmission of ultrasound, entrapped air may interfere with certain transducer manoeuvres, particularly retroflexion of the endoscope tip in the mid-oesophagus and imaging from the fundus of the stomach. Air within the upper gastrointestinal system rarely precludes a diagnostic examination, but in any particular examination all areas of the heart may not be imaged with consistent predictability or quality.

Although there is no definitive solution to the problem of interference by entrapped air, some observations may be helpful. First, there is more air in the oesophagus at the beginning of the examination than at the end. Air is continually cleared out by oesophageal and transducer action during the study. Early in the procedure, it is best to use views and endoscopic manipulations that are not as likely to be affected by entrapped air. Anteflexion, movement of the transducer lens into apposition with the oesophageal wall, is preferred over retroflexion, which moves the transducer away from the oesophageal wall. Retroflexion more readily permits entrapped air to move in front of the transducer lens. Early in the examination, the longitudinal transducer or short-axis views with the transverse plane should be used because anteflexion produces the best images. Four chamber views, which require retroflexion, should be obtained later in the examination. Passing the tip of the endoscope into the stomach also tends to clear air from the oesophagus. Additionally, larger endoscopes have

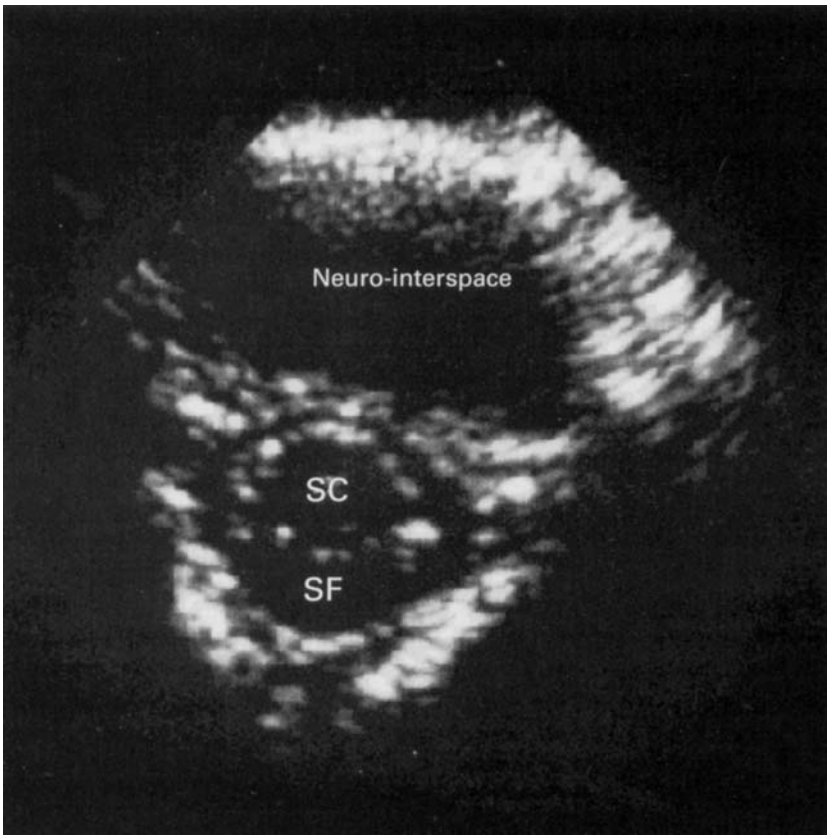

Figure 16.1 Spinal cord (SC). If the transducer is rotated posteriorly, the SC can be visualised at each neuro-interspace of the thoracic spine. Spinal fluid (SF) and the SC can produce a mass-like appearance. This observation can be misinterpreted as an extracardiac mass or tumour. (Reproduced from Seward *et al.* 1992,[20] by permission of the American Society of Echocardiography.)

greater contact with oesophageal mucosal surfaces and hence are associated with less air interference than are smaller endoscope heads.

Trachea and bronchi

The air filled trachea and bronchi consistently interfere with certain tomographic planes of section. These interposed portions of the respiratory tract particularly affect the basal cardiac and aortic arch examinations. This problem can largely be circumvented with multiplanar transducers, which allow off-axis imaging around interfering respiratory structures to areas of interest. Attempts to image the upper ascending aorta with the horizontal plane are limited by a "blindspot" caused by the interposed bronchus between the oesophagus and the upper ascending aorta.[1] Using an anteflexed longitudinal plane that directs the ultrasound beam around the left bronchus[2] can minimise the extent of this limitation. Similarly, the distal left pulmonary artery, which can be obscured by the left bronchus, is best imaged in the off-axis longitudinal plane.

Pitfalls

False masses

TOE vividly images structures that are inaccessible by transthoracic echocardiography. Thus, unfamiliar normal anatomy may be misinterpreted as abnormal (Figures 16.1 and 16.2).

Trabeculations of the atria or atrial appendages

Muscular trabeculations (pectinate muscles) and irregularities are seen in the walls of both atrial appendages, and the examiner should become well acquainted with normal appearances (Figure 16.3). These muscle ridges are usually small and refractile, move in concert with the atrial wall, and are typically multiple. However, thrombus is characteristically of a different texture than the atrial wall; also, it is more echo refractile, is uniform in consistency, is often pedunculated, and typically occurs in conjunction with significant atrioventricular valve disease or low output state. Tumours that extend into the atria or

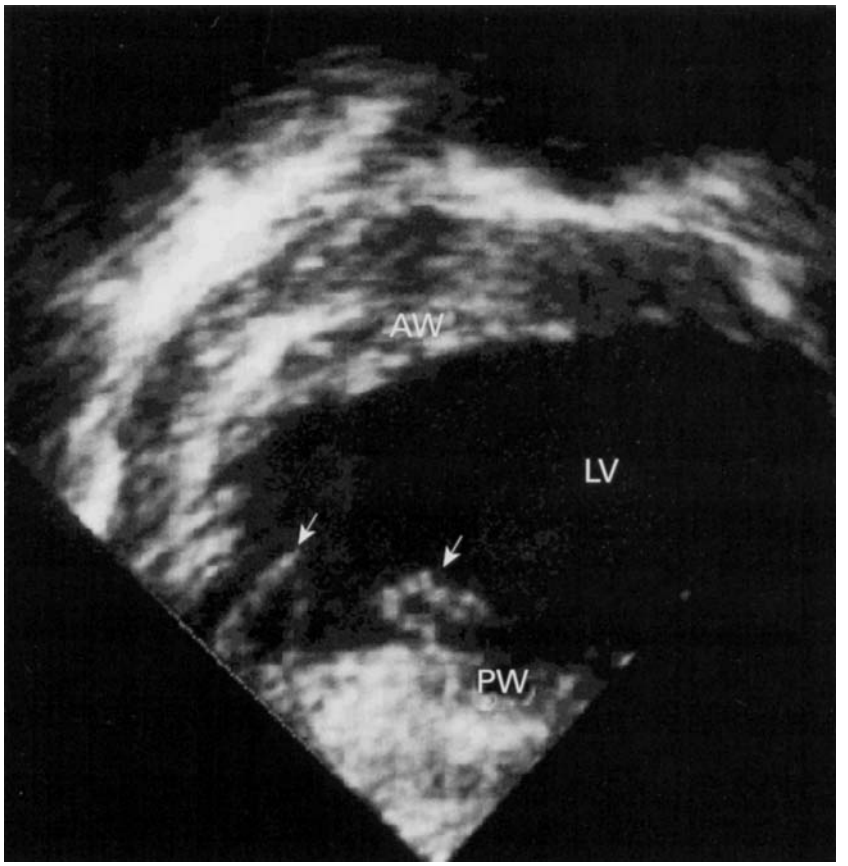

Figure 16.2 Pseudomass. This transgastric long-axis view of the left ventricle is from a patient with a mitral prosthesis. Mobile transected chordae after mitral valve replacement within the left ventricle (arrows) gives a mass effect. These transected chordae may appear multicentric, mobile, and pedunculated – features that are also associated with thrombus. However, there were no significant underlying left ventricular wall motion abnormalities, and the true identity as chordae could be discerned by long-axis and short-axis transgastric images. AW = anterior wall, LV = left ventricle, PW = posterior wall. (Reproduced from Seward *et al.* 1992,[20] by permission of the American Society of Echocardiography.)

atrial appendage are also distinctly different in echo density from normal muscle ridges. We have found that multiplanar imaging is very helpful in identifying pathological conditions involving the atrial appendage and differentiating them from normal muscle ridges.

Within the left atrium, the orifices of the pulmonary veins are encircled by tissue that may appear mass-like in some tomographic planes of section. One of the most frequent mass effects encountered is the common wall separating the left atrial appendage from the left upper pulmonary vein (Figure 16.4). In a tomographic plane of section the terminal portion of this partition appears globular and looks like a mass, especially as it undulates with cardiac motion. This common wall in its mid-portion is thin and the globular end can sometimes be quite large, mimicking a left atrial tumour. Awareness of this common anatomical variant should prevent serious misinterpretation. A persistent left superior vena cava[42] and a potentially fluid-filled recess of the pericardial reflection course within this common wall should not be misinterpreted as a cyst, abscess, or other abnormal structure. Notably, a persistent left superior vena cava is associated with a large coronary sinus, which normally enters the right atrium[1,10] and has colour flow detectable blood movement within the space. Pericardial fluid within the pericardial reflection does not generate a colour flow signal.

In the right atrium at the orifices of the superior and inferior vena cave, muscle bundles can also appear mass-like (see Figure 16.3). In the horizontal plane, at the orifice of the right superior vena cava, an encircling muscle ridge appears ovoid and mass-like. Slow withdrawal of the endoscope to the lumen of the superior vena cava completes visualisation of the muscle ridge around the orifice of the superior vena cava and ensures proper identification. Less commonly, a similar ridge of muscle is visualised at the orifice of the inferior vena cava. In the horizontal plane, advancing the endoscope completes imaging of the encircling eustachian valve. Multiplane imaging consistently eliminates confusion.

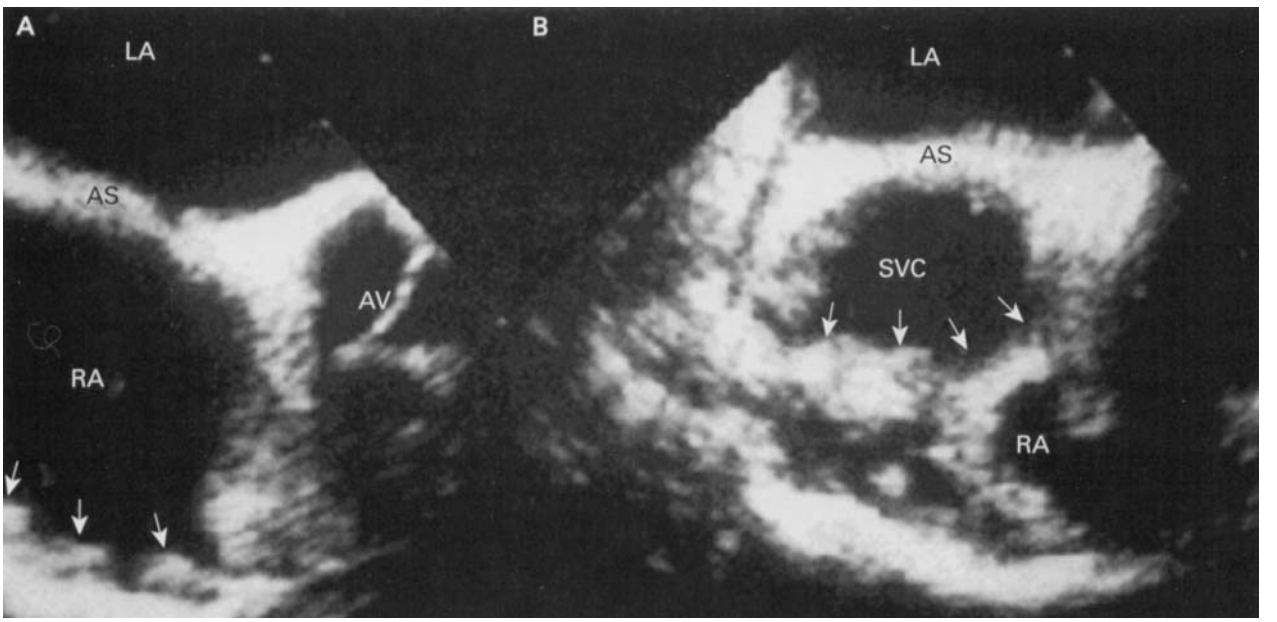

Figure 16.3 Right atrial trabeculations or pectinate muscles (arrowheads) and muscular bands (arrows). The right atrium is more trabeculated (i.e. pectinate muscles) than the left atrium. A highly trabeculated atrial appendage may be difficult to differentiate clearly from thrombus. The example is from a patient with atrial septal defect (not seen in these views) in whom the atrial musculature is hypertrophied. **(A)** A larger muscle band (arrowheads) is commonly visualised at the orifice of the superior vena cava (SVC). **(B)** A normal atrial muscle bundle can be identified by slow withdrawal of the transoesophageal endoscope in the transverse horizontal plane. Normal muscle (arrows) encircles the superior vena caval orifice, separating the SVC and the right atrial appendage (RA). AS = atrial septum. (Reproduced from Seward *et al.* 1992,[20] by permission of the American Society of Echocardiography.)

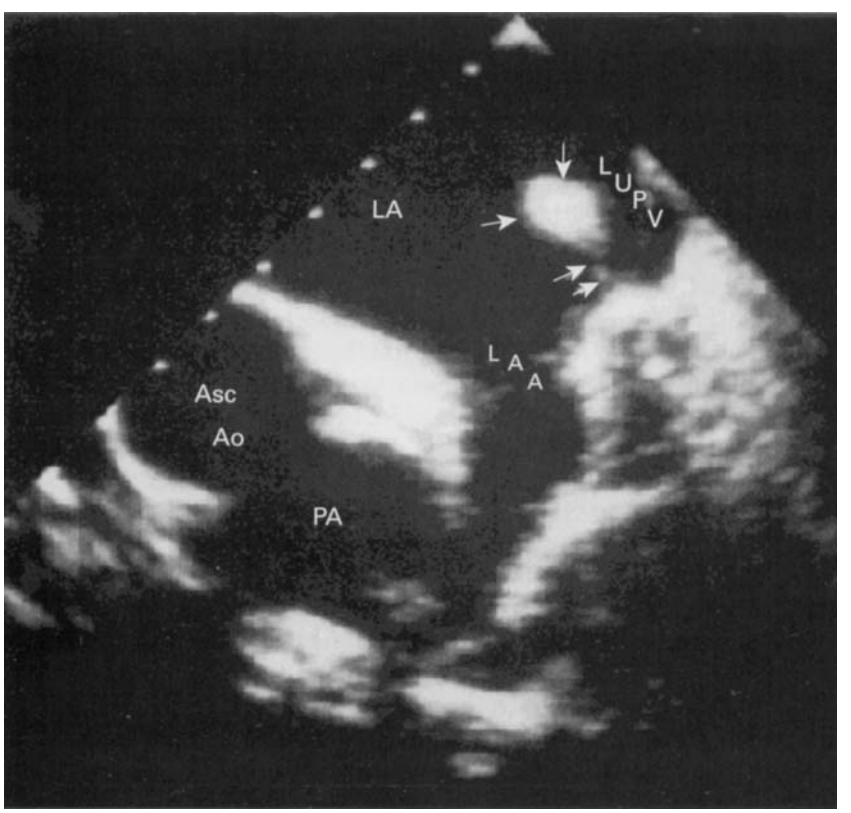

Figure 16.4 Left atrial pseudomass. The normal partition between the left upper pulmonary vein (LUPV) and left atrial appendage (LAA) can be fat laden and appear like a mass (large arrows). The proximal portion of the common wall is usually thin (small arrows) and the distal portion bulbous (large arrows) – features that add to the mass effect. Asc Ao = ascending aorta, LA = left atrium, PA = pulmonary artery. (Reproduced from Seward *et al.* 1992,[20] by permission of the American Society of Echocardiography.)

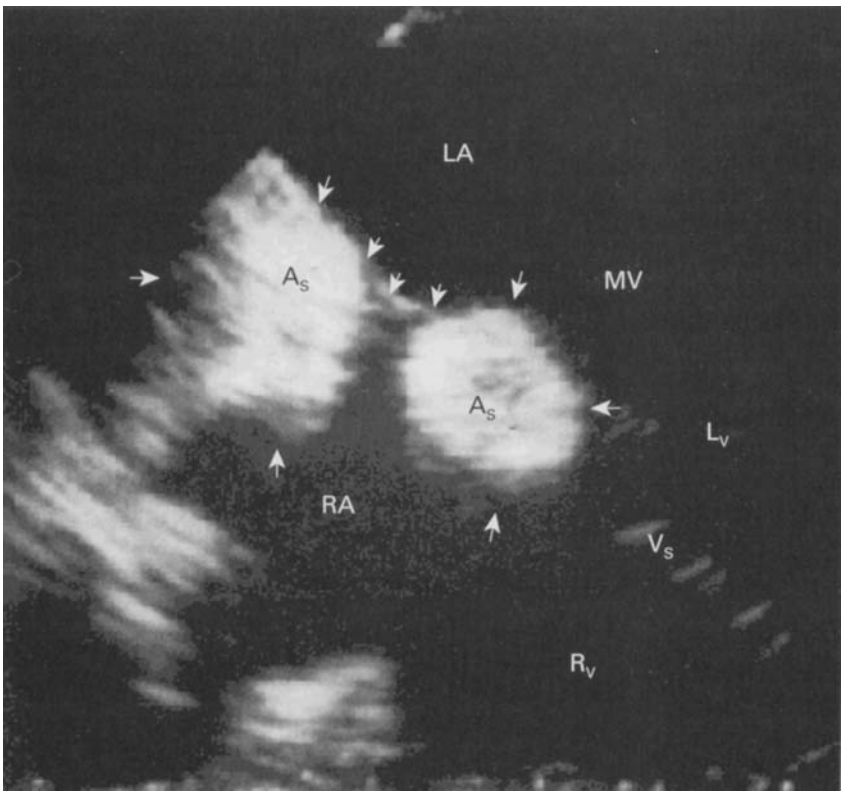

Figure 16.5 Lipomatous atrial septum. The atrial septum (AS) frequently becomes inundated with fatty tissue (lipomatous hypertrophy). A characteristic mass effect is observed. The membrane of the fossa ovalis (small arrows) is spared, but the fatty atrial septum is thickened with hypertrophic fat (large arrowheads). A pathognomonic dumbbell shape of the atrial septum is observed. The amount of fatty infiltrate varies but can be impressive. This condition is usually considered benign. LA = left atrium, LV = left ventricle, MV = mitral valve, RA = right atrium, RV = right ventricle. (Reproduced from Seward *et al.* 1992,[20] by permission of the American Society of Echocardiography.)

Atrial septum

The atrial septum surrounding the centrally located membrane of the fossa ovalis is fat laden and in older patients can be up to 1 cm thick (Figure 16.5). In certain tomographic planes, the limbus of the fossa ovalis can appear like a mass. When excessively thick, it is referred to as lipomatous hypertrophy or atrial septal lipoma.[11] This usually appears as an echo-dense mass of variable size, and consistently may reach large proportions. Confusion arises particularly when the lipomatous hypertrophy of the atrial septum is asymmetrical. This pitfall is more common with monoplane TOE examination, and a multiplane examination clarifies the appearance. The condition is benign but can easily be misinterpreted by an inexperienced examiner.

Tricuspid annulus

Fat or fluid in the tricuspid annulus can produce a mass effect (Figure 16.6), particularly when viewed obliquely in the horizontal tomographic plane. This common observation should not be misinterpreted as a tumour or ring abscess. Magnetic resonance imaging may be diagnostic when the observation remains in doubt.

Mitral valve annulus

The mitral valve annulus usually causes fewer problems. However, annular calcification, and occasionally fat, can be impressive and appear like a mass. Because of the near field location, calcium occasionally does not appear as dense and may be mistaken for a tumour. However, the characteristic location and reflectance of calcium usually allow easy recognition.

Aortic valve

A frequently observed mass effect occurs when a cusp of the aortic valve is cut obliquely in the short-axis or in transitional views from the left ventricular outflow tract. The ovoid appearance of the aortic cusp is often mistaken for an aortic valve vegetation or tumour (Figure 16.7). Similarly, the aortic valve can be incorrectly interpreted as either bicuspid or tricuspid when cut obliquely. These phenomena most often occur with horizontal planar imaging and when

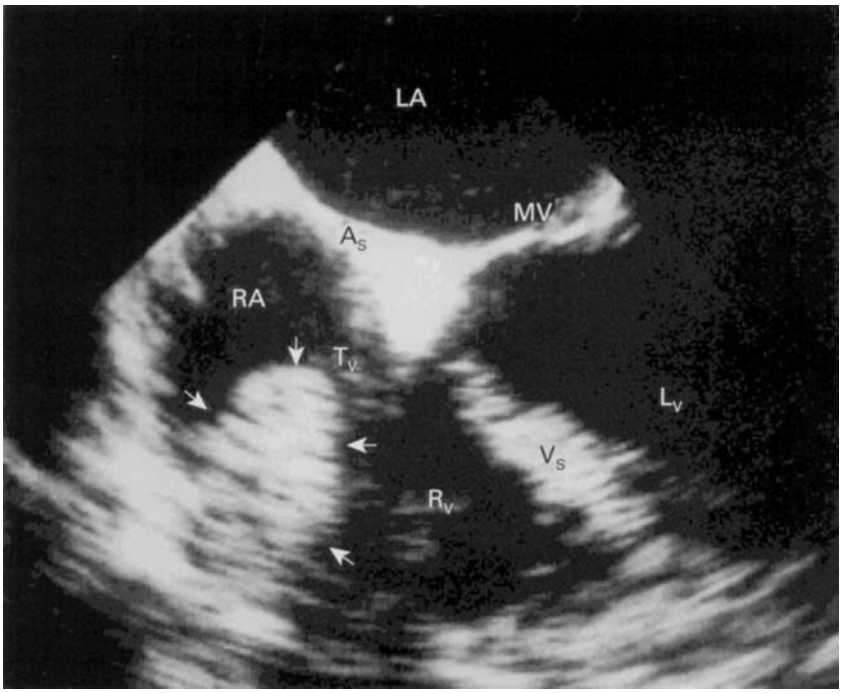

Figure 16.6 Pseudomass of the tricuspid valve annulus (arrows). The tricuspid annulus at the right ventricular and right atrial junction normally contains fat, which can give a mass effect (arrows). This is particularly noticeable in oblique horizontal imaging planes. AS = atrial septum, LA = left atrium, LV = left ventricle, MV = mitral valve, RA = right atrium, RV = right ventricle, TV = tricuspid valve, VS = ventricular septum. (Reproduced from Seward *et al.* 1992,[20] by permission of the American Society of Echocardiography.)

incomplete tomographic analysis is performed. Biplane and multiplane views of the aortic valve eliminate these potential pitfalls, and emphasise the importance of examination within true orthogonal short-axis planes and of confirmation of the analysis in other imaging planes.

Sutures and other materials

Surgical sutures can be visualised at the sewing ring of prosthetic valves or at the margins of prosthetic patch material. The regular spacing and highly refractile appearance of sutures help one to arrive at the correct interpretation. Although redundant suture material moves with the cardiac cycle, these structures should not appear multicentric, irregularly spaced, independently mobile, elongated, or bulbous; these features are more consistent with adherent thrombus or vegetation.

Membranes

Membrane of the fossa ovalis

This membrane portion of the atrial septum can be redundant or aneurysmal, and can exhibit variable undulating motion with each cardiac and respiratory cycle.[12] Occasionally, if the membrane has a large excursion, then it can produce a mass effect in the left atrium, particularly with a monoplane examination. multiplane imaging easily elucidates the true identity of this structure.

Valve of the fossa ovalis

The posterosuperior margin of the fossa membrane overlaps the superior fatty limbus of the atrial septum (i.e. the valve of the fossa ovalis). Non-fusion of these structures results in a patent valve of the fossa ovalis. The overlap between the fatty atrial septum and the fossal membrane in certain tomographic planes (particularly the horizontal plane) appears as a cavity.[10] If the valve of the fossa ovalis is patent, then shunting from one atrium to the other can be observed within this space. Longitudinal planar images best delineate this potentially confusing anatomy.

Eustachian valve

In the right atrium at the orifice of the inferior vena cava, the eustachian valve often appears as a mobile, undulating membrane or mass partially encircling the orifice of the inferior vena cava as it enters the floor of the atrium[13] (Figure 16.8). Accurate identification is readily accomplished with biplane or multiplane imaging.

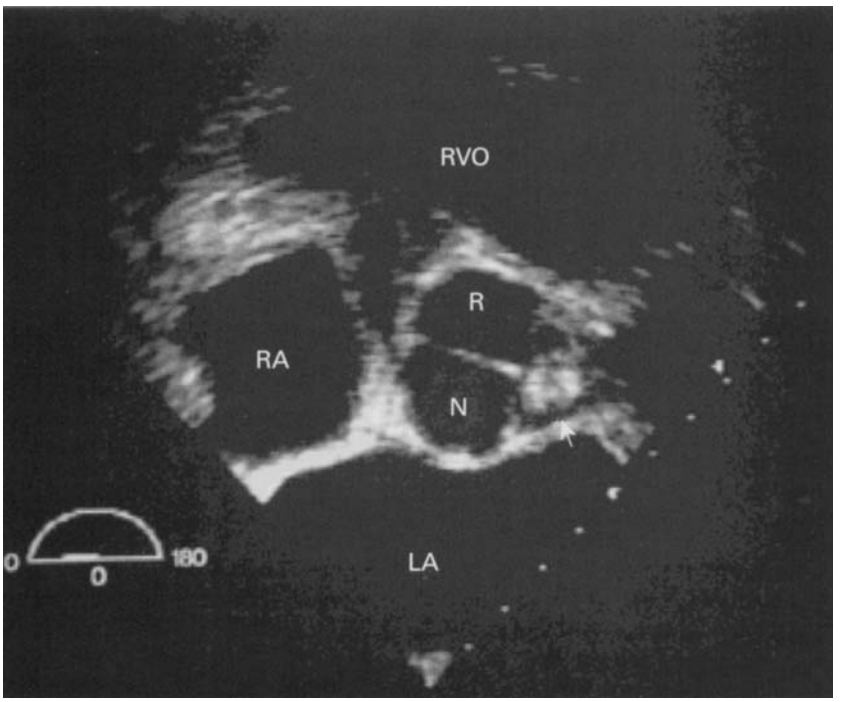

Figure 16.7 Aortic valve pseudomass: off-axis longitudinal plane. The left coronary cusp of the aortic valve is imaged obliquely *en face* and has the appearance of a mass (arrow), which may be incorrectly identified as a tumour or vegetation. This finding was not present in standard short-axis imaging planes of the aortic valve. LA = left atrium, N = non-coronary cusp, R = right coronary cusp, RA = right atrium, RVO = right ventricular outflow tract.

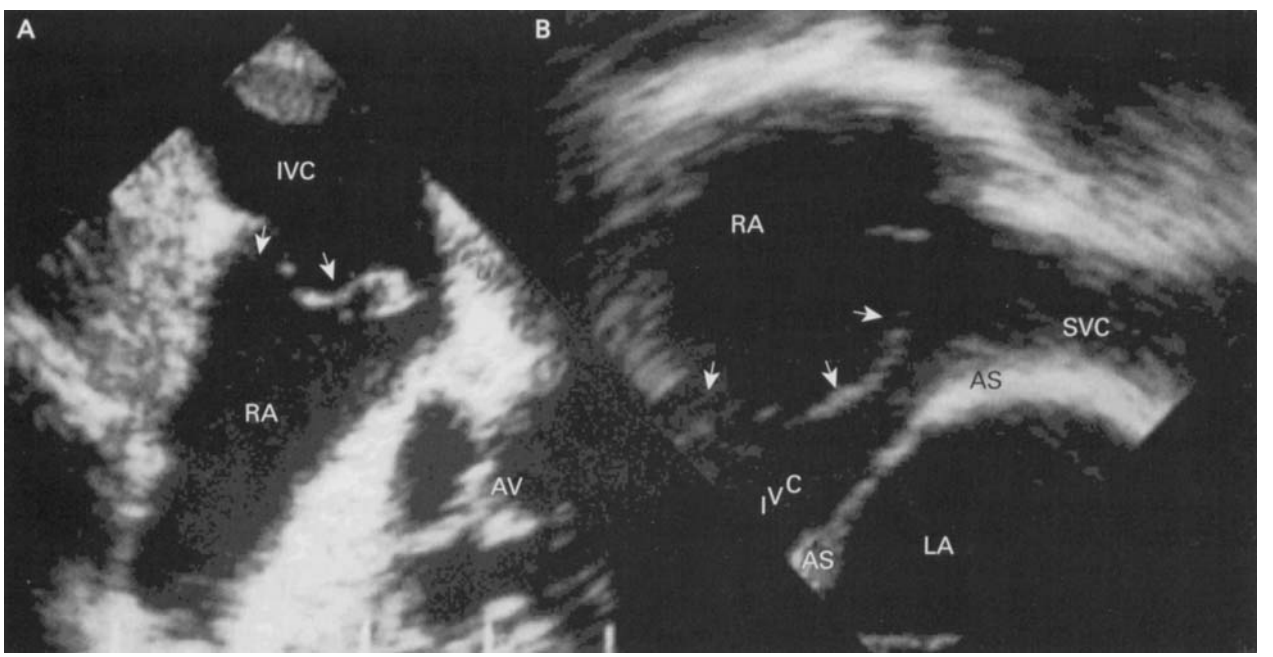

Figure 16.8 Eustachian valve. **(A)** In the horizontal plane with the transducer at the gastro-oesophageal junction, the orifice of the inferior vena cava (IVC) and the body of the right atrium is the eustachian valve (arrows). This structure usually is membranous and undulates throughout the cardiac cycle. **(B)** In the longitudinal plane, the eustachian membrane (arrows) originates from the anterior lip of the inferior vena cava orifice and partially separates the body of the right atrium (RA) and atrial septum (AS). This undulating membrane can be mistaken for a mass or thrombus or even a catheter. AV = aortic valve, LA = left atrium, SVC = superior vena cava. (Reproduced from Seward *et al.* 1992,[20] by permission of the American Society of Echocardiography.)

Echo-free spaces

Transverse sinus

The transverse sinus – a pericardial reflection between the left atrium and the great vessels at the base of the heart – typically contains a small amount of pericardial fluid that produces a small crescent-like, echo-free space between the left atrium and the aorta when visualised in the horizontal plane and a triangular space in the longitudinal planes.[2] When filled with larger amounts of fluid, this space can be misinterpreted as a pathological finding and confused with a cyst or abscess cavity. Within the fluid-filled space, the left atrial appendage, its outpouchings, and attached epicardial fat may appear as mobile cystic or solid masses. multiplane imaging and careful sweeps of the ultrasound beam across the sinus and atrial appendages permit proper identification.

Oblique sinus

The oblique sinus – a posterior pericardial reflection between the pulmonary veins – can appear as a fluid-filled space interposed between the left atrium and the oesophagus. A pericardial cyst can also appear in the same position. Recognition of the pericardial layers usually permits proper identification of the pericardial cyst or the fluid-filled oblique sinus.

Other pericardial reflections

Because of the high resolution tomographic presentation of anatomy, pericardial reflections and recesses are easily visualised and are potentially confusing. A pericardial reflection between the wall separating the left atrial appendage and the left upper pulmonary vein can also appear as a cystic space or mass.

Hiatal hernia

A large hiatal hernia can markedly interfere with a complete TOE examination[14] (Figure 16.9). Occasionally, however, a large fluid-filled or gas-filled hernia becomes interposed between the heart and the oesophageal lumen. When fluid filled, the hiatal hernia can appear as a thick walled cystic mass posterior to the left atrium. When filled with gas the hernia produces the expected problem of interference with ultrasound transmission, causing shadowing of more anterior structures and resulting in a technically difficult TOE examination.

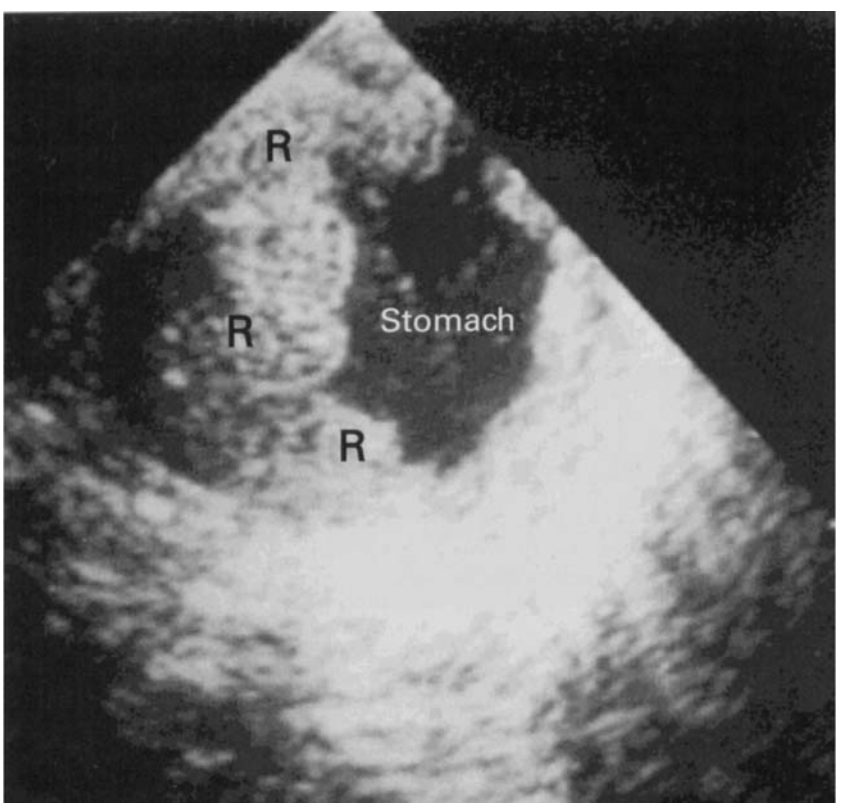

Figure 16.9 Hiatal hernia. Stomach or bowel can herniate into the thorax and become interposed between the normal oesophagus and the heart. Rugal folds (R) within the stomach can be mistaken for a tumour or mass. The heart can be obscured from visualisation, as in this example. (Reproduced from Seward *et al.* 1992,[20] by permission of the American Society of Echocardiography.)

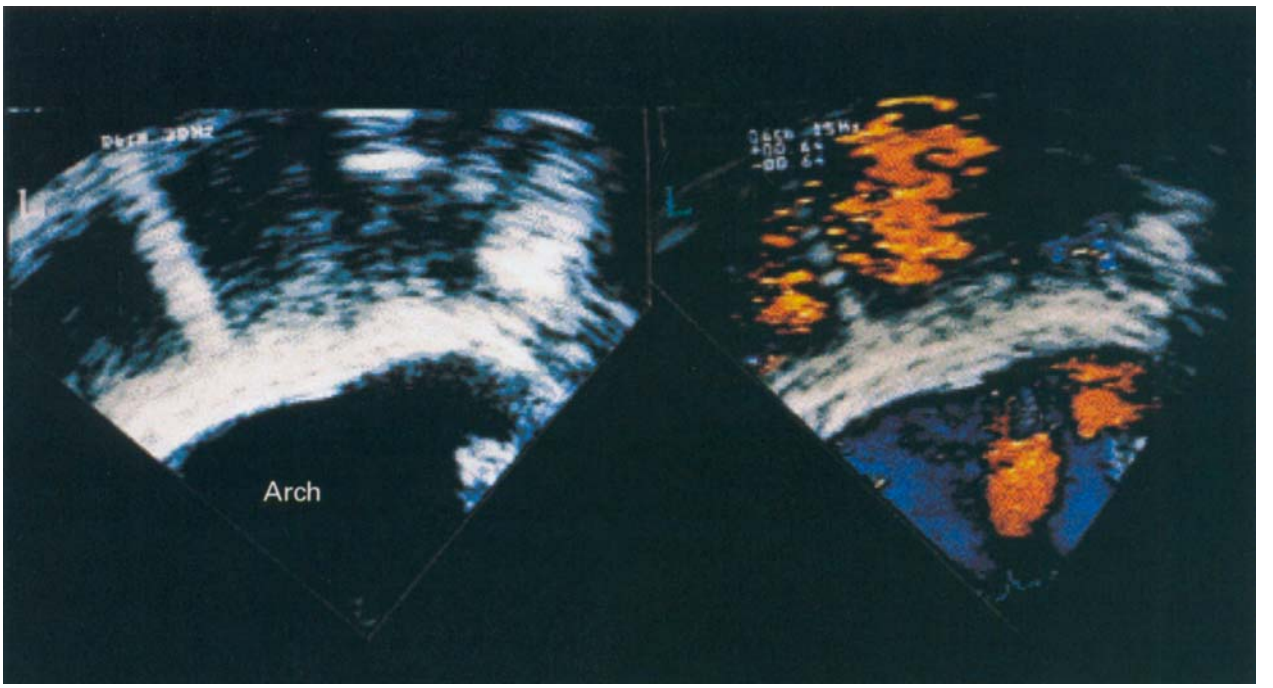

Figure 16.10 Reverberation artefact: arch of aorta. A common reverberation artefact occurs when the ultrasound beam is directed toward air-filled lung, which acts as an ultrasound reflector. Near-field structures are duplicated in the far field as a reverberation artefact. All signals are duplicated, including colour flow Doppler. This artefactual duplication of anatomy and Doppler signal should not be mistaken as a true structure. This example depicts reverberation artefact of the arch of aorta. In the far field, a reverberation artefactual aorta is imaged when the ultrasound beam is directed toward the left lung.

Spontaneous contrast effect

Because of the proximity of the transducer to the atrial cavities and the higher frequency transducers used, visualisation of blood movement within the cardiac chambers is more commonly observed.[15,16] The phenomenon is associated with reduced blood flow and poor clearance of blood from the cardiac chamber.

Reverberations and ghosting

The oesophagus is surrounded by air-filled lung. Reverberation signals or ghost artefacts are common because of the strong ultrasound reflection that results from impedance mismatch between tissue and air. Linear artefacts most frequently occur within the upper ascending aorta and mid-descending thoracic aorta, which have air-filled lung in the immediate far-field image (Figure 16.10). Imaging the thoracic aorta is among the most diagnostic examinations with TOE.[17,18] Linear artefacts often lie in non-anatomical planes, cross normal anatomy, have artificial motion, do not alter Doppler depicted blood flow, and may disappear with change in imaging depth. Nearly perfect duplication of Doppler signal occurs if the field of the view is expanded to accommodate a second signal. The only way to avoid misinterpretation is to be aware of these phenomena and to be careful not to misinterpret atypical anatomy, such as a double thoracic aorta or Doppler signal lying outside the blood-filled aorta or cardiac chambers.

Extracardiac fluid

Accumulations of pleural fluid are easily visualised by TOE. However, loculated fluid may appear ovoid or suspiciously like a normal or abnormal structure. Fibrous bands within the fluid-filled space may give the false appearance of dissection or rupture of the thoracic aorta.[19] It is imperative to track all fluid-filled spaces to their source, for example a ventricular aneurysm to the ventricle, or aortic dissection to the thoracic aorta. Biplanar and multiplanar imaging usually permit proper diagnosis. Difficulty in correct identification may be compounded by colour flow artefacts or ghosting phenomena within the

fluid-filled space. These artefacts are usually of low velocity and should lot be confused with pathological blood movement within the fluid-filled space. Because of the proximity of structures and use of higher frequency transducers, Doppler artefacts are frequently observed within any fluid-filled space. To avoid misinterpretation, one should be cautious when interpreting very low velocity signals and always search for a source of communication. Motion artefacts are very common, whereas pathological communication from aneurysm or aortic dissection is much less frequently observed.

Conclusion

The limitations and pitfalls of TOE are best minimised by experience. Initial training should not be circumvented and maintenance of competency should be strictly monitored. Physicians with echocardiographic training below level II should work in close collaboration with an active echocardiographic laboratory and undergo appropriate review of their standards to ensure that competency is maintained.

Although TOE has been a dramatic step forward in diagnostic imaging, there is potential for serious misinterpretation. This chapter discusses most of these potential problems. However, there will always be unique situations in which the findings must be consistently addressed and differentiated as normal, artefact, new observation, or misinterpretation.

References

1 Seward JB, Khandheria BK, Oh JK, *et al.* Transesophageal echocardiography: technique, anatomic correlations, implementation, and clinical applications. *Mayo Clin Proc* 1988;**63**: 649–80.

2 Seward JB, Khandheria BK, Edwards WD, *et al.* Biplanar transesophageal echocardiography: anatomic correlations, image orientations, and clinical applications. *Mayo Clin Proc* 1990;**65**: 1193–213.

3 Hanrath P, Bleifeld W, Souquet J, eds. *Cardiovascular diagnosis by ultrasound: transesophageal, computerized, contrast, Doppler echocardiography.* The Hague: Martinus Nijhoff, 1982.

4 Erbel R, Khandheria BK, Brennecke R, *et al.* eds. *Transesophageal echocardiography: a new window to the heart.* Berlin: Springer-Verlag, 1989.

5 Cyran SE, Kimball TR, Meyer RA, *et al.* Efficacy of intraoperative transesophageal echocardiography in children with congenital heart disease. *Am J Cardiol* 1989;**63**:594–8.

6 Cyran SE, Myers JL, Gleason MM, *et al.* Application of intraoperative transesophageal echocardiography in infants and small children. *J Cardiovasc Surg (Torino)* 1991;**32**:318–21.

7 Ritter SB. Transesophageal real-time echocardiography in infants and small children with congenital heart disease. *J Am Coll Cardiol* 1991;**18**:569–80.

8 Dundee JW, Halliday NJ, Loughran PG, Harper KW. The influence of age on the onset of anesthesia with midazolam. *Anesthesia* 1985;**40**:441–3.

9 Ofili EO, Rich MW. Safety and usefulness of transesophageal echocardiography in persons aged 70 years. *Am J Cardiol* 1990;**66**:1279–80.

10 Seward JB, Tajik AJ. Transesophageal echocardiography in congenital heart disease. *Am J Card Imaging* 1990;**4**:215–22.

11 Fyke FE III, Tajik AJ, Edwards WD, Seward JB. Diagnosis of lipomatous hypertrophy of the atrial septum by two-dimensional echocardiography. *J Am Coll Cardiol* 1983;**1**:1352–7.

12 Hanley PC, Tajik AJ, Hynes JK, *et al.* Diagnosis and classification of atrial septal aneurysm by two-dimensional echocardiography: report of 80 consecutive cases. *J Am Coll Cardiol* 1985;**6**:1370–82.

13 Goldfarb A, Weinreb J, Daniel WG, Kronzon I. A patient with right and left atrial membranes: the role of transesophageal echocardiography and magnetic resonance imaging in diagnosis. *J Am Soc Echocardiogr* 1989;**2**:350–3.

14 Freedberg RS, Weinreb J, Gluck M, Kronzon I. Paraesophageal hernia may prevent cardiac imaging by transesophageal echocardiography. *J Am Soc Echocardiogr* 1989;**2**:202–3.

15 Daniel WG, Nellessen U, Schröder E, *et al.* Left atrial spontaneous echo contrast in mitral valve disease: an indicator for an increased thromboembolic risk. *J Am Coll Cardiol* 1988;**11**:1204–11.

16 Black IW, Hopkins AP, Lee LCL, Walsh WF. Left atrial spontaneous echo contrast: a clinical and echocardiographic analysis. *J Am Coll Cardiol* 1991;**18**:398–404.

17 Erbel R, Engberding R, Daniel W, *et al.* Echocardiography in the diagnosis of aortic dissection. *Lancet* 1989;**1**:457–61.

18 Karalis DG, Chandrasekaran K, Victor MF, *et al.* Recognition and embolic potential of intraaortic atherosclerosis debris. *J Am Coll Cardiol* 1991;**17**: 73–8.

19 Kronzon I, Demopoulos L, Schrem SS, *et al.* Pitfalls in the diagnosis of thoracic aortic aneurysm by transesophageal echocardiography. *J Am Soc Echocardiogr* 1990;**3**:145–8.

20 Seward JB, Khandheria BK, Oh JK, *et al.* Critical appraisal of transoesophageal echocardiography: limitations, pitfalls, and complications. *J Am Soc Echocardiogr* 1992;**5**:288–305.

17 Training and certification in the USA

Daniel M Thys

Introduction

Although echocardiography has been in clinical use for more than 20 years, it is still a relatively new technique in the practice environment of anaesthesiologists. Although the clinical benefits of perioperative echocardiography are well established, the problems surrounding training and certification are widespread. In some institutions cardiothoracic anaesthesiologists and cardiologists have jointly developed a structured educational programme for education in perioperative echocardiography that includes full time assignment to the echocardiography laboratory.[1] In many institutions, however, the demands of clinical practice preclude full time assignment to the echocardiography laboratory, and more flexible training pathways have been explored. Some experts such as Cahalan and coworkers[2] have suggested that transoesophageal echocardiography (TOE) can be safely and effectively learned "on the job", provided that an expert or "mentor" is available to ensure that essential information is not missed. This apparent lack of consensus in an area that is deemed critical to the growth of anaesthesiology as a profession has stimulated professional anaesthesia organisations to study the issue and to suggest solutions.

The main goal of this chapter is to describe the involvement of the Society of Cardiovascular Anesthesiologists (SCA), in collaboration with the American Society of Anesthesiologists (ASA) and the American Society of Echocardiography (ASE), in the development of guidelines for training, accreditation, and certification in perioperative TOE. The reasons for focusing on the activities of the SCA are that the SCA has played a leading role in the study of these issues in the USA and that I have been privileged to be intimately involved in the process and most of the decision making. Although some of the proposed solutions may suffer from provincial connotations, most are applicable on a broad basis and have widespread implications.

Training

Problems with education in echocardiography have been recognised since the earliest days of the technology. In an editorial published in 1974,[3] Harvey Feigenbaum described the growing demands from clinicians for echocardiographic information, yet deplored the paucity of adequately trained echocardiographers. A similar dilemma exists today for cardiothoracic anaesthesiologists. Many cardiac surgeons and cardiac surgical programmes rely on echocardiography for intraoperative decision making. Cardiothoracic anaesthesiologists are expected to be proficient in all aspects of intraoperative echocardiography but few have benefited from a formal education in the technique. In a recent survey of all active members of the SCA residing in the USA or Puerto Rico, Morewood *et al.*[4] documented that 94% of respondents practised at institutions that use intraoperative echocardiography. Furthermore, 72% of anaesthesiologists working at such institutions indicated that they personally employed TOE during anaesthetic care. Of the anaesthesiologists using TOE, about 70% had undergone training after completion of their residency or fellowship. Most described their training as "self-taught" (22%), "on the job" (27%), and/or consisting of "short courses" (35%). A minority of individuals had obtained experience with TOE during residency (12%) or fellowship (17%).[4]

Over the years, professional organisations of many countries have published recommendations and guidelines concerning training in echocardiography.[5–9] In the USA, the ASE has taken the lead in the development of training guidelines for echocardiography. In 1988, the

ASE Committee for Physician Training in Echocardiography published Guidelines for Optimal Physician Training in Echocardiography.[10] The principal themes of the recommendations were the following:

- The comprehensive evaluation of a patient with heart disease involves the use of several, related diagnostic techniques such as M-mode, two-dimensional, and Doppler echocardiography. Under certain circumstances, these techniques may need to be supplemented with specialised examinations such as contrast echocardiography, stress echocardiography, or invasive echocardiography. All of these techniques are related, usually complementary, and together they define the field of echocardiography. Physicians who take responsibility for the performance and interpretation of echocardiography should therefore have a clear understanding of the fundamental principles of, and practical experience with, all of these techniques.
- Physicians who take responsibility for the performance and interpretation of echocardiography should have a broad background knowledge that spans the physical principles of echocardiography, echocardiographic instrumentation, the experience needed to recognise normal and abnormal information, and experience with other cardiac diagnostic techniques.
- Physicians training in echocardiography ideally should spend a specified period of time in an active echocardiographic laboratory, working under the direction of an experienced echocardiographer who has achieved an advanced level of training. The levels of training were summarised in table format (Table 17.1).
- Techniques in echocardiography evolve rapidly, and therefore physicians responsible for the performance and interpretation of echocardiographic examinations should maintain active and ongoing continuing education in the field.

Subsequently, specific training recommendations were also published for training in paediatric[11,12] and stress echocardiography.[13]

A few years later, the ASE also published guidelines for physician training in TOE.[14] The guidelines again stressed that TOE was only one

Table 17.1 Levels of training in echocardiography

	Objectives	*Duration*	*Number of cases*
Physicians in cardiology training programme			
Level 1	Introductory experience	3 months	150 2D/M-mode examinations 75 Doppler examinations
Level 2	Sufficient experience to take responsibility for echocardiographic studies	3 additional months (beyond level 1)	150 2D/M-mode examinations 150 Doppler examinations
Level 3	Sufficient expertise to direct an echocardiography laboratory	6 additional months (beyond level 2)	450 examinations (using both imaging and Doppler)
Physicians in postcardiology training			
	Responsibility for performance and interpretation of echocardiograms	Variable: level of achievement equivalent to level 2	250–300 patients (2D/M-mode and Doppler examinations)
	Direct echocardiography laboratory in hospital or large group practice	Variable: level of expertise equivalent to level 3	450 patients (2D/M-mode and Doppler examinations)

2D = two-dimensional. (Reproduced from Pearlman *et al.*[10])

Table 17.2 Recommended training components for developing and maintaining skills in transoesophageal echocardiography

Component	Objective	Duration	Number of cases (approximate)
General echocardiography level 2	Background needed for performance and interpretation	6 months or equivalent	300
Oesophageal intubation	TOE probe introduction	Variable	25
TOE examination	Skills in TOE performance and interpretation	Variable	50
Ongoing education	Maintenance of competence	Annual	5–75

TOE = transoesophageal echocardiography. (Reproduced from Pearlman *et al.*[14])

technique in a family of complementary echocardiographic techniques. The training components for developing and maintaining skills in TOE were summarised in a table (Table 17.2). The guidelines recognised that TOE was frequently performed by non-cardiologists and used to guide the immediate management of acutely ill patients. The guidelines warned against the use of TOE for narrowly focused examinations by physicians with limited background or experience. They also recognised that anaesthesiologists often found TOE useful for monitoring of left ventricular volume, and both global and regional function. They stated that because it was not practical for cardiologists experienced in TOE to be continuously present in the operating room during lengthy surgical procedures, anaesthesiologists should develop a close collaborative working relationship with a cardiologist experienced in TOE. The guidelines also stressed that a collaborative relationship that did not provide for immediate consultation to facilitate intraoperative decisions was not in the interest of good patient care.

In 1993, the ASA and the SCA established an Ad Hoc Task Force on Practice Parameters for Transesophageal Echocardiography to develop evidence-based guidelines on the proper indications for performing TOE in the operative setting. To develop its recommendations, the task force reviewed all evidence regarding the effectiveness of TOE in the perioperative setting. Computerised and manual literature searches identified 1844 studies, of which 558 were considered relevant to the perioperative setting. Evidence was considered relevant if it addressed the accuracy and reliability of perioperative TOE, its yield and predictive value, or the effect of perioperative TOE on therapeutic decisions or clinical outcomes. The task force divided its recommendations into three categories based on the strength of supporting evidence or expert opinion that the technology improves clinical outcomes.[15]

Although the primary goal of the task force was to develop recommendations on the indications and contraindications for TOE during the perioperative period, it was also specifically instructed to examine the issues of training and certification for anaesthesiologists. Published training guidelines were analysed and were supplemented with the expert opinions of the members of the task force. Recommendations regarding training and certification were based on the above scientific evidence, as well as on legal, regulatory, and scientific literature and expert opinion. The task force referred to two levels of training in perioperative TOE: basic and advanced. Both basic and advanced TOE training referred to specialised TOE training that extended beyond the minimum exposure to TOE that occurs during normal anaesthesia residency training. Anaesthesiologists with basic training were considered able to use TOE for indications that lie within the customary practice of anaesthesiology. Anaesthesiologists with advanced training were considered, in addition to the above, able to utilise the full diagnostic potential of perioperative TOE (Tables 17.3 and 17.4)

The ASE/SCA training guidelines

In August 2000, the presidents of the ASE and the SCA appointed a joint task force to develop training guidelines for perioperative echocardiography. Each society was represented by four

Table 17.3 Recommended training objectives for basic perioperative echocardiography

Skills	Objectives
Cognitive	• Knowledge of the physical principles of echocardiographic image formation and blood velocity measurement • Knowledge of the operation of ultrasonographs including all controls that affect the quality of data displayed • Knowledge of equipment handling, infection control, and electrical safety associated with the techniques of perioperative echocardiography • Knowledge of the indications, contraindications, and potential complications for perioperative echocardiography • Knowledge of the appropriate alternative diagnostic techniques • Knowledge of the normal tomographic anatomy as revealed by perioperative echocardiographic techniques • Knowledge of commonly encountered blood flow velocity profiles as measured by Doppler echocardiography • Knowledge of the echocardiographic manifestations of native valvular lesions and dysfunction • Knowledge of the echocardiographic manifestations of cardiac masses, thrombi, cardiomyopathies, pericardial effusions, and lesions of the great vessels • Detailed knowledge of the echocardiographic presentations of myocardial ischaemia and infarction • Detailed knowledge of the echocardiographic presentations of normal and abnormal ventricular function • Detailed knowledge of the echocardiographic presentations of air embolisation
Technical	• Ability to operate ultrasonographs including the primary controls affecting the quality of the displayed data • Ability to insert a TOE probe safely in the anaesthetised, tracheally intubated patient • Ability to perform a comprehensive TOE examination and differentiate normal from markedly abnormal cardiac structures and function • Ability to recognise marked changes in segmental ventricular contraction indicative of myocardial ischaemia or infarction • Ability to recognise marked changes in global ventricular filling and ejection • Ability to recognise air embolisation • Ability to recognise gross valvular lesions and dysfunction • Ability to recognise large intracardiac masses and thombi • Ability to detect large pericardial effusions • Ability to recognise common echocardiographic artefacts • Ability to communicate echocardiographic results effectively to health care professionals, the medical record, and patients • Ability to recognise complications of perioperative echocardiography

TOE = transoesophageal echocardiography. (Adapted from the American Society of Anesthesiologists/Society of Cardiovascular Anesthesiologists Task Force on Transesophageal Echocardiography.[15])

members in addition to Michael Cahalan, MD, who was appointed by both societies and served as Chair of the task force. The charge of the task force was to develop a "Guidelines" document that would define the essential principles of training in perioperative echocardiography. Issues that the task force was asked to consider included:

- prerequisite medical knowledge and training
- scope of echo knowledge and skills
- training components and duration
- training environment and supervision
- equivalence and "grandfathering" for individuals who are already in practice.

The task force completed its activities in October 2001, and in May 2002 its recommendations were published simultaneously in *Anesthesia and Analgesia*[16] and in the *Journal of the American Society of Echocardiography*.[17] A summary of the ASE/SCA guidelines is provided in this chapter.

General principles

Although practitioners from different specialties must attain comparable expertise in perioperative echocardiography, different training may be needed to achieve this goal. Thus,

Table 17.4 Recommended training objectives for advanced perioperative echocardiography

Skills	Objectives
Cognitive	• All the cognitive skills defined under basic training (see Table 17.3) • Detailed knowledge of the principles and methodologies of qualitative and quantitative echocardiography • Detailed knowledge of native and prosthetic valvular function including valvular lesions and dysfunction • Knowledge of congenital heart disease (if congenital practice is planned then this knowledge must be detailed) • Detailed knowledge of all other diseases of the heart and great vessels that is relevant in the perioperative period (if paediatric practice is planned than this knowledge may be more general than detailed) • Detailed knowledge of the techniques, advantages, disadvantages, and potential complications of commonly used cardiac surgical procedures for treatment of acquired and congenital heart disease • Detailed knowledge of other diagnostic methods appropriate for correlation with perioperative echocardiography
Technical	• All the technical skills defined under basic training (see Table 17.3) • Ability to acquire or direct the acquisition of all necessary echocardiographic data, including epicardial and epiaortic imaging • Ability to recognise subtle changes in segmental ventricular contraction indicative of myocardial ischaemia or infarction • Ability to quantify systolic and diastolic ventricular function and to estimate other relevant haemodynamic parameters • Ability to quantify normal and abnormal native and prosthetic valvular function • Ability to assess the appropriateness of cardiac surgical plans • Ability to identify inadequacies in cardiac surgical interventions and the underlying reasons for the inadequacies • Ability to aid in clinical decision making in the operating room

(Adapted from the American Society of Anesthesiologists/Society of Cardiovascular Anesthesiologists Task Force on Transesophageal Echocardiography.[15])

although the recommendations provide specific guidelines for training, they were designed to allow enough flexibility to ensure that individual circumstances were appropriately accommodated. Minimum numbers of cases were delineated; however, these numbers were less important than the depth and diversity of the clinical experience and quality of training. The goal of the training must be to provide exposure to the entire spectrum of perioperative echocardiography that a trainee will probably encounter in subsequent practice. While these guidelines should serve equally well for adult or paediatric practices, the delineated minimum requirements are not sufficient for training in both disciplines. The trainee who plans to practise both adult and paediatric perioperative echocardiography should complete appropriate curricula in both.

Like prior published guidelines, these guidelines recognised different levels of expertise in echocardiography and made level specific recommendations for training. Specifically, the guidelines endorsed the concept of a basic level and an advanced level of perioperative echocardiography, and provided training recommendations for each. They also stated that regardless of the level of expertise, all practitioners, even experts, must recognise that timely consultation during perioperative echocardiography may be necessary because of constraints of time or experience. Unlike prior guidelines, the guidelines did not specify the duration of training. Instead, they emphasised the goals of training and the number and diversity of cases required to meet those goals. The time required for perioperative training will vary markedly depending on the volume and diversity of the affiliated cardiac surgical programme.

Prerequisite medical knowledge and training

Trainees in perioperative echocardiography must be licensed physicians enrolled in, or having completed, an accredited residency. The

training objectives outlined in the ASA/SCA Practice Parameters were updated and modified to include epicardial echocardiography and epivascular ultrasonography (see Tables 17.3 and 17.4). Essentially, basic training in perioperative echocardiography should impart a detailed appreciation of when and how to perform perioperative echocardiography, as well as the underlying principles of ultrasound. In addition to these cognitive skills, a basic practitioner should possess the technical skills to use TOE to recognise markedly abnormal cardiac structure and function, severe hypovolemia, large pericardial effusions, and the presence of intracardiac air. As defined in these guidelines, basic training does not prepare the practitioner to influence the surgical plan without the assistance of a physician with advanced training in perioperative echocardiography. Advanced training in perioperative echocardiography should impart the cognitive and technical skills necessary to employ independently the full diagnostic potential of perioperative echocardiography, including the expertise to effect changes in cardiac surgical procedures.

Components of training

Basic training

The essential components of basic training include independent work, supervised activities, and assessment programmes. Through a structured independent reading and study programme, trainees must acquire an understanding of the principles of ultrasound and indications for perioperative echocardiography. This independent work should be supplemented by regularly scheduled didactics such as lectures and seminars designed to reinforce the most important aspects of perioperative echocardiography. Under appropriate supervision (see section entitled Training environment and supervision, below) the trainee learns to place the TOE probe, operate the ultrasonograph, and perform a TOE examination. Subsequently, some clinical work should be performed with progressively more independence. However, a practitioner with advanced training must review every examination performed by the trainee with him or her. The trainee should be encouraged to master the comprehensive examination defined by the ASE and SCA.[18,19] Although not all components of this examination are needed for a basic examination, the basic practitioner should be able to acquire all 20 of the recommended cross-sections in the event they are needed for remote consultation with an advanced practitioner. For basic training, the task force recommends study of 150 complete examinations under appropriate supervision (for a definition of appropriate supervision, see section entitled Training environment and supervision, below). These examinations must include the full spectrum of commonly encountered perioperative diagnoses, and at least 50 comprehensive intraoperative TOE examinations personally performed, interpreted, and reported by the trainee (Table 17.5). The trainee must be taught how to convey and document the results of their examination effectively. Periodic formal and informal evaluations of the trainee's progress should be conducted during training. Trainees should keep a log of examinations performed and reviewed to document the depth and breadth of their training.

Advanced training

For advanced practice, the comprehensiveness of training is paramount. Essential components include independent work, supervised activities, and assessment programmes. The task force recommends study of 300 complete examinations under appropriate supervision (see section entitled Training environment and supervision, below). These examinations must include a wide spectrum of cardiac diagnoses and at least 150 comprehensive intraoperative TOE examinations personally performed, interpreted, and reported by the trainee (see Table 17.5). The trainee must develop the skills to convey and document the results of their examinations effectively and independently. Periodic formal and informal evaluations of the trainee's progress should be conducted during training. The experience and case numbers acquired during basic training may be counted for advanced training provided the basic training was completed in an advanced training environment (see section entitled Training environment and supervision, below).

The task force recognises that trainees from different specialties should use their time in training somewhat differently depending on their varying backgrounds. A cardiologist with little operating room experience will need to spend more time in this environment than a cardiac anaesthesiologist or surgeon to understand cardiac surgical techniques fully. A cardiac

Table 17.5 Numbers of examinations and other key training: recommendations for basic and advanced perioperative echocardiography

	Basic*	Advanced*
Minimum number of examinations†	150	300
Minimum number personally performed‡	50	150
Programme director qualifications	Advanced perioperative echocardiography training	Advanced perioperative echocardiography training plus at least 150 additional perioperative TOE examinations
Programme qualifications	Wide variety of perioperative applications of echocardiography	Full spectrum of perioperative applications of echocardiography

*Totals for basic training may be counted toward advanced training provided the basic training was completed in an advanced training environment. (See text for additional details and explanation of training environments and programme director qualifications.) †Complete echocardiographic examinations interpreted and reported by the trainee under appropriate supervision. May include transthoracic studies recorded by qualified individuals other than the trainee. ‡Comprehensive intraoperative TOE examinations personally performed, interpreted, and reported by the trainee under appropriate supervision.[18,19]

anaesthesiologist or surgeon working in a centre with a limited variety of cardiac surgery will need to spend more time in the echocardiographic laboratory than a cardiologist to understand fully the diagnostic techniques of echocardiography. Like basic trainees, advanced trainees should keep a log of examinations performed and reviewed to document the depth and breadth of their training.

Comparison with previously published guidelines

Training guidelines in basic and advanced perioperative echocardiography are similar to the training guidelines for level I and level II in general echocardiography, except that a greater number of personally performed cases (see above) and a specified number of months are required for training in general echocardiography.[10,14] The task force believes that these differences are justified because the spectrum of cardiac diagnoses is more limited in perioperative echocardiography than in general echocardiography, and because the volume and diversity of the supporting surgical programme is more crucial for attaining training goals in perioperative echocardiography than the absolute duration of training.

Training environment and supervision

Basic training

The director of the echocardiographic training programme should be a physician with advanced training and demonstrated expertise in perioperative echocardiography or equivalent experience. At the start of training, the trainee must be supervised directly as they learn to place the TOE probe, operate the ultrasonograph, and perform a TOE examination. This direct supervision should continue until the trainee can introduce the TOE probe safely and consistently, and perform an appropriate examination. The trainee should have access to a wide variety of surgery in which TOE is performed as an integral part of patient management. The perioperative echocardiography training programme should have an affiliation with an echocardiography laboratory so that basic trainees can gain regular and frequent exposure to teaching and clinical resources within that laboratory.

Advanced training

Advanced training should take place in a training programme specifically designed to accomplish comprehensive training in perioperative echocardiography. The director of the training

programme must be a physician with advanced training and demonstrated expertise in perioperative echocardiography who has performed at least 450 complete examinations, including 300 personally performed intraoperative TOE examinations, or equivalent experience. If the advanced trainee has not already accomplished basic training, then the same initial direct supervision should be provided for the advanced trainee as outlined above for the basic trainee. Subsequently, some clinical work may be performed with progressively more independence, but the immediate availability and direct involvement of an advanced practitioner is an essential component of advanced training. The supporting surgical programme must have the volume and diversity to ensure that the trainee will experience a wide spectrum of diagnostic challenges encountered in perioperative echocardiography. The task force wishes to emphasise the importance of case diversity by noting that practitioners with advanced training must be able to use TOE effectively in all its established perioperative applications.[15] The perioperative echocardiography training programme should have an affiliation with an echocardiography laboratory so that trainees can gain regular and frequent exposure to teaching and clinical resources within that laboratory.

Training within specialty fellowship programmes

Both accredited and non-accredited fellowship programmes may wish to offer training in perioperative echocardiography. This may require revision of their current curricula to accomplish the training goals outlined in this document. Alternatively, the task force recommends the creation of fellowships solely devoted to advanced perioperative echocardiography and offered to graduates of qualifying training programmes.

Training equivalence for specialists who are already in practice

Physicians already in practice can achieve appropriate training in perioperative echocardiography without enrolling in a formal training programme. However, the same prerequisite medical knowledge, medical training, and goals for cognitive and technical skills (see Tables 17.3 and 17.4) apply to them as apply to physicians in formal training programmes. When a physician has already acquired extensive experience in perioperative echocardiography, then this physician should document their experience in detail and be able to demonstrate its equivalence in depth, diversity, and case numbers to the training levels delineated above.

When a physician has no experience in perioperative echocardiography, then they should work with another physician who has advanced TOE training or equivalent experience to achieve the same training goals and case numbers as the training levels delineated above. In addition, the task force recommends that physicians seeking basic training via this pathway should have at least 20 hours of continuing medical education devoted to echocardiography. Physicians seeking advanced training via this pathway should have at least 50 hours of continuing medical education devoted to echocardiography. The continuing medical education in echocardiography should be obtained during the time that the physician is acquiring the requisite clinical experience in TOE.

Accreditation

The organisation that is responsible for evaluating and accrediting residency programmes in the USA is the Accreditation Council for Graduate Medical Education (ACGME). It is a private sector council that operates under the aegis of five medical organisations (the American Board of Medical Specialties, the American Hospital Association, the American Medical Association, the Association of American Medical Colleges, and the Council of Medical Specialty Societies). It evaluates and accredits residency programmes in accordance with established standards and mechanisms designed to ensure that acceptable graduate medical education is provided. The ACGME establishes general procedures for reviewing residency programmes, develops and maintains records on each programme, and informs the programme director and other designated parties of the action taken by the reviewing bodies.

At present there is no accreditation process for cardiothoracic anaesthesiology or perioperative echocardiography. In practice, this means that, in the USA, there are no standardised training requirements for either field and that training programmes are not bound by any published standards. In 1997 the leadership of the SCA

became concerned by the disparity in the quality of educational programmes in cardiothoracic anaesthesiology. An additional concern was the lack of uniformity in the exposure of trainees to the many facets of cardiothoracic anaesthesiology, including exposure to perioperative echocardiography. As a result, the SCA has recommended that accreditation by ACGME of subspecialty training programmes in cardiothoracic anaesthesiology be pursued. As part of this process, an SCA task force is developing standardised requirements for training programmes in cardiothoracic anaesthesiology; once completed they will be published. Some of the training elements that will be considered in the requirements are listed in Table 17.6. Programmes that wish to be accredited by the ACGME for subspecialty training in cardiothoracic anaesthesiology will need to first submit a written application that includes a description of the programme and indicates how the published requirements will be met. After provisional approval, continued accreditation will be contingent on compliance with the published requirements as determined from regularly submitted written descriptions of the programme and onsite surveys by ACGME surveyors. Each ACGME programme review can result in full accreditation, probationary accreditation, or withdrawal of accreditation.

Certification

> "The intent of certification is to provide assurance to the public that a physician specialist who is certified has successfully completed an approved educational program and an evaluation process that includes an examination designed to assess the knowledge, skills and experience required to provide quality patient care in that specialty."[20]

Despite the public's expectations, until recently there was no mechanism to allow a physician to demonstrate or receive recognition for special knowledge, skills, or experience in perioperative echocardiography. In 1993, the ASE appointed a committee to develop an examination that would allow physicians to test and demonstrate their knowledge of echocardiography, based on objective standards.[21] Secondary goals were to provide the medical community with the opportunity to recognise individuals who had successfully completed a voluntary examination, to stimulate continuing education in echocardiography, and to provide training programmes with a mechanism to identify strengths and weaknesses in their curriculum. The first examination (ASEXAM) was conducted in 1996 and annually since then. The examination is open to all physicians and tests knowledge in all areas of echocardiography. Although the examination includes questions on perioperative echocardiography, it is certainly not the principal focus of the test.

Individual anaesthesiologists have explored opportunities to test and demonstrate their knowledge in perioperative echocardiography on an objective basis. In 1996, Konstadt *et al.*[22] published their experience with a test that had been utilised at two institutions. Although they concluded that the test provided a valid measure of competence in intraoperative echocardiography, there were several problems with this conclusion: the body of knowledge that was tested was ill defined; the test consisted of only 30 questions; and the anaesthesia residents who took the test before training in echocardiography obtained high scores and improved little after a year of training.

In response to the concerns of its members, the leadership of the SCA decided that a larger effort was indicated and appointed a Task Force for Certification in Perioperative Transesophageal Echocardiography in 1996.[23] The first assignment of the task force was to define the body of knowledge that would be tested in an examination. A content outline consisting of 23 knowledge categories was compiled by the task force and mailed to all active members of the SCA (Table 17.7). Subsequently, the task force compiled more than 250 multiple choice questions in the various categories of the content outline. It also developed multiple choice questions that were associated with 15 echocardiographic cases, recorded on videotape. The SCA commissioned the National Board of Medical Examiners (NBME), a private organisation specialising in medical examinations, to edit the questions and administer the examination. NBME was also hired to conduct psychometric analyses of the test and item performance, and to present recommendations for the continuing development of the examination process.

On 9 May 1997, a pilot examination of the test was conducted in Baltimore. The main purpose of the pilot examination was to test the examination questions and to provide potential candidates with a practice examination. Ninety-five

Table 17.6 Elements of programme requirements for subspecialty training programmes in cardiothoracic anaesthesiology

Introduction	Definition and description of the subspecialty	
	Duration and scope of education	• Admission prerequisites • Length of programme • Specific description of programme format
	Appointment of residents	• Description of appointment process • Qualifications for delimiting the number of resident positions
Faculty qualifications and responsibilities	Programme director	• Academic and professional qualifications • Certification qualifications
	Responsibilities of programme director	• Leadership qualifications; continuity of leadership • Requirements of scholarly pursuit • Resident evaluation, programme evaluation, and faculty evaluation • Data collection • Other administrative responsibilities
	Number and qualifications of faculty	• Number of faculty (faculty/resident ratio) • Certification requirements • Description of academic and professional qualifications • Statement regarding qualifications for scholarly activity
Facilities and resources		• Space and equipment • Clinical facilities (echo laboratory, ICUs, etc.) • Medical records: medical library • Patient population • Support services

Educational programme	Clinical components	• Requirement regarding number, variety, and classification of patients
		• Requirements regarding educational experiences of residents
		• Statements regarding:
		  • resident responsibility for patient care
		  • resident participation in continuity of care
		  • degree of resident supervision
		  • qualifications for providing graded responsibility to residents

	Didactic components	• Basic science content
		• Specialty content
		• Conferences:
		  • description of types of conferences
		  • comment regarding quality and frequency of conferences
		  • documentation of faculty and resident attendance
		  • requirements for faculty supervision of educational activities

	Other requirements	• Research • Requirements for multidisciplinary care
Internal evaluation	Evaluation of residents	• Policy for resident evaluation • Regularity and frequency of resident evaluations • Description of areas which should be evaluated
	Faculty evaluation	• Policy for faculty evaluation and promotion • Regularity and frequency of faculty evaluations • Description of areas which should be evaluated
	Programme evaluation	• Policy for programme evaluation • Regularity and frequency of program evaluation • Description of areas which should be evaluated

Table 17.7 National Board of Echocardiography content outline for perioperative transoesophageal echocardiography

Principles of ultrasound	• Nature of ultrasound: compression and rarefaction • Frequency, wavelength, tissue propagation velocity • Properties of ultrasound waves • Ultrasound–tissue interactions • Tissue characterisation
Transducers	• Piezoelectric effect • Crystal thickness and resonance • Damping • Sound beam formation • Focusing • Axial and lateral resolution • Arrays
Equipment, infection control, and safety	• Clinical dosimetry • Biological effects of ultrasound • Electrical and mechanical safety • Infection control • TOE probe insertion and manipulation • Contraindications to TOE • Complications of TOE
Imaging	• Instrumentation • Displays • B-mode, M-mode, and two-dimensional echocardiography • Signal processing and related factors
Principles of Doppler ultrasound	• Doppler effect • Doppler equation • Doppler shift frequencies and influencing factors • Nyquist limit • Spectral analysis and display characteristics • Pulsed-wave Doppler • High pulse repetition frequency pulsed wave Doppler • Continuous wave Doppler • Colour flow Doppler • Colour M-mode
Quantitative M-mode and two-dimensional echocardiography	• Edge recognition • Edge components • Temporal resolution • Referencing centroids, fixed and floating axis • Centre line method • Global function; measurements and calculations • Geometric, spectral, and other methods
Quantitative Doppler	• Types of velocity measurements • Volumetric measurements and calculations • Valve gradients, areas, and other measurements • Cardiac chamber and great vessel pressures • Tissue Doppler
Doppler profiles and assessment of diastolic function	• Tricuspid valve and right ventricular inflow • Pulmonary valve and right ventricular outflow • Mitral valve and left ventricular inflow • Aortic valve and left ventricular outflow • Non-valvular flow profiles
Cardiac anatomy	• Imaging planes • Cardiac chambers and walls • Cardiac valves • Cardiac cycle and relation of events relative to electrocardiogram

(Continued)

Table 17.7 *(Continued)*

Pericardium and extracardiac structures: anatomy and pathology	• Pericardium and pericardial space
	• Pulmonary arteries
	• Pulmonary veins
	• Vena cavae and hepatic veins
	• Coronary arteries
	• Aorta and great vessels
	  • anatomy
	  • atherosclerosis
	  • aneurysm
	  • dissection and traumatic injury of the aorta
	• Pleural space

Pathology of the cardiac valves	• Acquired valve diseases
	  • endocarditis
	  • rheumatic
	  • myxomatous
	  • calcific/degenerative
	  • traumatic
	• Tricuspid
	• Pulmonary
	• Mitral
	  • mitral regurgitation
	  • ischemic mitral valve dysfunction
	  • mitral stenosis
	  • systolic anterior motion of mitral valve
	• Aortic
	  • aortic regurgitation
	  • aortic stenosis

Intracardiac masses and devices	• Tumors • Thrombi • Devices and foreign bodies

Global ventricular systolic function	• Normal left ventricular systolic function
	• Abnormal left ventricular systolic function
	  • aetiologies including ischaemia
	  • assessment/ejection fraction
	  • confounding factors
	• Right ventricular systolic function
	• Cardiomyopathies
	  • hypertrophic
	  • restrictive
	  • dilated

Segmental left ventricular systolic function	• Myocardial segment identification
	• Coronary artery distribution and flow
	• Normal and abnormal segmental function
	  • assessment and methods
	  • differential diagnosis
	  • confounding factors
	• Left ventricular aneurysm
	• Left ventricular rupture

Assessment of perioperative events and problems	• Hypotension and causes of cardiovascular instability • Cardiac surgery: techniques and problems

(Continued)

Table 17.7 *(Continued)*

	• assessment of bypass and cardioplegia • cannulae and devices commonly used during cardiac surgery • circulatory assist devices • intracavity air • minimally invasive cardiopulmonary bypass • off-pump cardiac surgery • Coronary surgery: techniques and assessment • Valve surgery: techniques and assessment • valve replacement: mechanical, bioprosthetic, and other • valve repair • Transplantation surgery • heart • lung • liver
Congenital heart disease	• Identification and situs of morphologically left and right structures • Atrial septal defects • Ventricular septal defects • Pulmonary valve and infundibular stenosis • Left atrial and mitral valve conditions • Aortic valve and left ventricular outflow tract abnormalities • Coronary artery anomalies • Patent ductus arteriosus • Coarctation of the aorta • Ebstein's anomaly • Persistent left superior vena cava • Tetralogy of Fallot • Transposition of great arteries • Atrioventricular septal defect – "AV canal" • Conditions with single ventricle physiology
Artefacts and pitfalls	• Imaging artefacts • Doppler artefacts and pitfalls • Structures mimicking pathology
Related diagnostic modalities	• Stress echocardiography • Myocardial perfusion imaging • Epicardial scanning • Contrast echocardiography • Utility of TOE relative to other diagnostic modalities

TOE = transoesophageal echocardiography.

candidates decided to participate in the pilot examination, knowing that no passing score would be associated with their participation. All candidates viewed the same 51-minute videotape and answered the same 43 multiple choice questions related to the video portion of the examination. Subsequently, they were divided into two groups that each responded to a different set of 100 multiple choice questions.

On 24 April 1998, the first formal certification examination in perioperative TOE was conducted in Seattle. The examination was open to all physicians and was administered by the NBME; 243 physicians participated in the examination. A total of 200 items were selected, consisting of 159 non-video questions (72 new, 87 used) and 41 video questions (33 new, 8 used). The examination began with a 50-minute videotape and was followed by the non-video questions. Raw scores were standardised by placing the scores of all examinees on a scale that has a mean of 500 and a standard deviation of 100. The KR_{20} reliability coefficient was 0·93, indicating adequate internal consistency of the scores. The standard error of the mean was ± 26

standard score points. Therefore, an examinee with a true proficiency score of 600 was likely (probability 68%) to score between 574 and 626 on this examination. The final step in defining the pass/fail rate required a standard setting exercise. To that effect, eight members of the SCA certification task force undertook a standard setting study on 30 May 1998. The study had four parts. First, a consistent profile of the borderline candidate (minimally competent) was developed. Next, the complete examination was studied item by item to determine how difficult each item would appear to the "borderline" candidate. The third part required that each panelist rate the relevance of the concept measured by each item after estimating its difficulty. The final part consisted of viewing the examination as a whole and describing views on acceptable percentages of content to be mastered, associated failing rates, and the general relevance of the examination as a whole. In early July 1998 the candidates received a pass/fail score, and detailed results of their examination. Subsequently, examinations have been conducted each year. More than 1200 physicians have taken the examination and more than 70% have passed.[24]

While the SCA Task Force on Perioperative Transesophageal Echocardiography was developing its examination, the leadership of SCA began discussions with ASeXAM Inc. to coalesce the two examination processes. The discussions were successful, and on 1 November 1998 the National Board of Echocardiography (NBE) was established. The NBE is a not-for-profit corporation established to develop and administer examinations in the field of clinical echocardiography, and to recognise those physicians who successfully complete either the Adult Special Competency in Echocardiography Examination or the Perioperative TOE Certification Examination. The leadership of the NBE consists of a board of directors with fixed representations from adult cardiology, paediatric cardiology, and anaesthesiology. Although the NBE is the oversight organisation responsible for the administration of both examinations, the question writing committees remain separate. Both examination committees use the NBME for the administration and scoring of the examinations. Physicians who successfully complete the Adult Special Competency in Echocardiography Examination or the Perioperative TOE Certification Examination are recognised as "testamurs".

In 2000, NBE took the next major step in the certification process by defining criteria for the certification of competency in adult echocardiography. The NBE believes that it is possible to certify physicians as competent in adult echocardiography because of the existence of a well defined body of knowledge, published training guidelines, ACGME approved training programmes, published guidelines for continuing quality improvement,[25] and a mature, well tested examination. The certification process is expected to:

- establish the domain of the practice of echocardiography for the purpose of certification
- assess the level of knowledge demonstrated by a licensed practitioner of echocardiography in a valid manner
- enhance the quality of echocardiography and individual professional growth in echocardiography
- formally recognise individuals who satisfy the requirements set by the NBE
- serve the public by encouraging quality patient care in the practice of echocardiography.

At present, certification is envisioned at various levels consisting of basic echocardiography alone, TOE alone (non-perioperative), basic echocardiography plus TOE (non-perioperative), basic plus stress echocardiography, and comprehensive echocardiography, which encompasses all previous levels. Although the certification is predominantly aimed at specialists in cardiology, other physicians with training in cardiovascular diseases such as cardiothoracic anaesthesiologists and surgeons can also be certified, provided they meet the certification criteria (Boxes 17.1 and 17.2).

Presently, the NBE is developing a certification process for perioperative TOE. As for general echocardiography, requirements for certification will include passage of the NBE perioperative echocardiography examination and documentation of training in perioperative echocardiography.

Competence in echocardiography

In 1998, the American College of Cardiology (ACC)/American Heart Association (AHA)/

1 Current license to practice medicine
2 Current Medical Board Certification
3 Specific training in cardiovascular disease
4 Specific training in Echocardiography
5 Successful completion of the Adult Special Competency in Echocardiography Examination

Box 17.1 Eligibility requirements for certification (general criteria)

6 Meet requirements 1–5 for general criteria (see Box 17.1)
7 Completion of comprehensive training program or show continued maintenance of skills according to one of the following:

- Performance and interpretation of 300 TOEs within training programme (if training completed after 1 July 1998)
- Performance and interpretation of 150 TOEs during training and at least 100 TOE examinations each year for 2 years before application under supervision of level 3 echocardiographer (if training completed prior to 1 July 1998)

TOE = transoesophageal echocardiography.

Box 17.2 Eligibility requirements for transoesophageal echocardiography certification: general adult echocardiography (specific criteria)

American College of Physicians–American Society of Internal Medicine (ACP–ASIM) formed a Task Force on Clinical Competence to develop recommendations for attaining and maintaining the cognitive and technical skills necessary for the competent performance of a specific cardiovascular service, procedure, or technology. In 2002 this task force appointed a writing committee to revise the 1990 ACP/ACC/AHA Clinical Competence in Adult Echocardiography document.[26] The writing committee consisted of recognised experts in echocardiography representing the ACC, AHA, ACP–ASIM, ASE, Society of Pediatric Echocardiography, and the SCA. The writing committee developed a new ACC/AHA Clinical Competence Statement on Echocardiography. The statement has been approved for publication by the governing bodies of the ACC and the AHA,[27,28] and endorsed by the ASE, SCA, and Society of Pediatric Echocardiography.

The document addresses competence in the performance and interpretation of all of the different modalities of echocardiography, including application of echocardiography in the operating room. For each of the applications, there is a brief general overview, a discussion of the cognitive skills required and recommendations on training requirements, proof of competence, and maintenance of competence. Whenever possible, these recommendations are linked to previously published recommendations made by specialty societies. In some situations, however, the writing group provides a set of recommendations that represent the consensus of this body of experts.

The document makes an important distinction between training requirements and documentation of competence. Training requirements represent the minimal training experience that is considered necessary to achieve the skills for performance at a particular level. It is recognised that training is highly individualised and some trainees may require higher volume and more hours of exposure to a particular technique. Proof of competence, on the other hand, consists of a set of requirements that provide some assurance that physicians have gained the expertise needed to perform according to recognised standards.

The sections on training requirements refer primarily to the training needed to achieve specific levels of expertise. Such training is expected to occur under the direct supervision of a qualified level 3 or equivalent physician/teacher, and for the most part occurs during formal fellowship training in either cardiovascular medicine or cardiovascular anaesthesiology. However, the document recognises the fact that physicians trained before the development of these techniques may have properly learned their use while in practice. Thus, whenever possible, the document addresses training requirements and proof of competence for this group of physicians. Maintenance of competence requires the performance of a certain minimal volume of procedures and participation in continuing medical education. This document recommends that physicians practising echocardiography obtain a minimum of 5 hours per year of continuing medical education credits in echocardiography, as recommended recently by the Intersocietal Commission for the Accreditation of Echocardiography Laboratories.[1]

Conclusion

TOE is an intrinsic component of the practice of cardiothoracic anaesthesiology. This chapter focused on the organisational activities that have taken place in the USA to ensure that anaesthesiologists practise echocardiography at a level that is consistent with good patient care. Although many challenges remain, significant progress has been made in the standardisation of the educational objectives and programmes for cardiothoracic anaesthesiology in general and echocardiography more specifically. Training guidelines and an examination process in perioperative TOE are now a reality. While progressing along this road, cardiothoracic anaesthesiologists have gained the respect of other specialists and ensured that, in any decision making surrounding echocardiography, the voice of anaesthesiology will be heard.

References

1 Savage R, Licina M, Koch C, *et al.* Educational program for intraoperative transesophageal echocardiography. *Anesth Analg* 1995;**81**:399–403.

2 Cahalan M, Foster E. Training in transesophageal echocardiography: in the lab or on the job? *Anesth Analg* 1995;**81**:217–8.

3 Feigenbaum H. Editorial: educational problems in echocardiography. *Am J Cardiol* 1974;**34**:741–2.

4 Morewood GH, Gallagher ME, Gaughan JP, Conlay LA. Current practice patterns for perioperative transesophageal echocardiography in the United States. *Anesthesiology* 2001;**95**:1507–12.

5 Anonymous. Recommendations for training in echocardiography [in Spanish]. *Rev Esp Cardiol* 1990;**43**:135–6.

6 Dumesnil JG, Lebeau R, Van Doesberg N, Migneault JD, Roy P, Cote MA. Recommendations for physician training in Doppler echocardiography. *Can J Cardiol* 1991;**7**:281–6.

7 Education and Training Subcommittee of the British Society of Echocardiography. Training in echocardiography. *Br Heart J* 1994;**71(suppl)**: 2–5.

8 Chan KL, Alvarez N, Cujec B, *et al.* Standards for adult echocardiography training. Canadian Cardiovascular Society Committee. *Can J Cardiol* 1996;**12**:473–6.

9 Roudaut R, Touche T, Cohen A, *et al.* Recommendations of the French Society of Cardiology for the training of echocardiographers and performing echocardiograms [in French]. *Arch Mal Coeur Vaiss* 1998;**1(suppl)**:7–14.

10 Pearlman AS, Gardin JM, Martin RP, *et al.* Guidelines for Optimal Physician Training in Echocardiography. *J Am Soc Echocardiogr* 1988;**1**:278–84.

11 Fouron JC, Robertson MA, Sandor G. Standards for training in pediatric echocardiography. Canadian Cardiovascular Society. *Can J Cardiol* 1998;**14**: 899–901.

12 Meyer RA, Hagler D, Huhta J, *et al.* Guidelines for physician training in pediatric echocardiography. Recommendations from the Society of Pediatric Echocardiography Committee on Physician Training. *Am J Cardiol* 1987;**60**:164–5.

13 Popp R, Agatston A, Armstrong W, *et al.* Recommendations for training in performance and interpretation of stress echocardiography. *J Am Soc Echocardiogr* 1998;**11**:95–6.

14 Pearlman AS, Gardin JM, Martin RP, *et al.* Guidelines for Physician Training in Transesophageal Echocardiography: recommendation of the American Society of Echocardiography Committee for Physician Training in Echocardiography. *J Am Soc Echocardiogr* 1992;**5**:187–94.

15 American Society of Anesthesiologists and the Society of Cardiovascular Anesthesiologists Task Force on Transesophageal Echocardiography. Practice guidelines for perioperative transesophageal echocardiography. A report by the American Society of Anesthesiologists and the Society of Cardiovascular Anesthesiologists Task Force on Transesophageal Echocardiography. *Anesthesiology* 1996;**84**:986–1006.

16 Cahalan MK, Abel M, Goldman M, *et al.* American Society of Echocardiography and Society of Cardiovascular Anesthesiologists task force guidelines for training in perioperative echocardiography. *Anesth Analg* 2002;**94**:1384–8.

17 Cahalan MK, Abel M, Goldman M, *et al.* American Society of Echocardiography and Society of Cardiovascular Anesthesiologists task force guidelines for training in perioperative echocardiography. *J Am Soc Echocardiogr* 2002;**15**:647–52.

18 Shanewise JS, Cheung AT, Aronson S, *et al.* ASE/SCA guidelines for performing a comprehensive perioperative multiplane transesophageal echocardiography examination: recommendations of the American Society of Echocardiography Council for Perioperative Echocardiography and the Society of Cardiovascular Anesthesiologists Task Force for Certification in Perioperative Transesophageal Echocardiography. *Anesth Analg* 1999;**89**:870–84.

19 Shanewise JS, Cheung AT, Aronson S, *et al.* ASE/SCA guidelines for performing a comprehensive perioperative multiplane transesophageal echocardiography examination: recommendations of the American Society of Echocardiography Council for Perioperative Echocardiography and the Society of Cardiovascular Anesthesiologists Task Force for Certification in Perioperative

Transesophageal Echocardiography. *J Am Soc Echocardiogr* 1999;**12**:884–900.

20 Statement of the American Board of Medical Specialties. Approved by the ABMS assembly on 3/19/87; revised on 9/23/93.

21 Pearlman AS. ASEXAM: the end of the beginning. *J Am Soc Echocardiogr* 1997;**10**:14A–7A.

22 Konstadt SN, Reich DL, Rafferty T. Validation of a test of competence in transesophageal echocardiography. *J Cardiothorac Vasc Anesth* 1996;**10**:311–3.

23 Aronson S, Thys DM. Training and certification in perioperative transesophageal echocardiography: a historical perspective. *Anes Analg* 2001;**93**: 1422–7.

24 Aronson S, Butler A, Subhiyah R, *et al.* Development and analysis of a new certifying examination in perioperative transesophageal echocardiography. *Anes Analg* 2002;**95**:1476–82.

25 Kisslo J, Byrd BF, Geiser EA, *et al.* Recommendations for continuous quality improvement in echocardiography. *J Am Soc Echocardiogr* 1995;**8(suppl)**:1A–S28.

26 Popp RL, Winters WL Jr. Clinical competence in adult echocardiography. A statement for physicians from the ACP/ACC/AHA Task Force on Clinical Privileges in Cardiology. *J Am Coll Cardiol* 1990;**15**:1465–8.

27 Quiñones MA, Douglas PS, Foster E, *et al.* ACC/AHA clinical competence statement on echocardiography: a report of the American College of Cardiology/American Heart Association/ American College of Physicians–American Society of Internal Medicine Task Force on Clinical Competence (Committee on Echocardiography). *J Am Coll Cardiol* 2003;**41**:687–708.

28 Quiñones MA, Douglas PS, Foster E, *et al.* ACC/AHA clinical competence statement on echocardiography: a report of the American College of Cardiology/American Heart Association/ American College of Physicians–American Society of Internal Medicine Task Force on Clinical Competence (Committee on Echocardiography). *Circulation* 2003;**107**:1068–89.

18 Training and certification in Europe

Karl Skarvan, Clemens-Alexander Greim, Norbert Roewer, John D Kneeshaw, Jan Poelaert

Introduction

Transoesophageal echocardiography (TOE) has become an important diagnostic and monitoring tool in cardiac surgery, and it is now considered an indispensable part of some procedures. Furthermore, in haemodynamically unstable patients TOE can detect with unmatched accuracy the cause of the circulatory failure and guide therapy. If patients are to benefit from this tool, then not only ultrasound machines and probes but also fully trained and experienced physicians must be present at all times in the operating theatre, intensive care unit (ICU), and emergency ward. This can only be achieved through training, certification, continuing education, and quality assurance programmes.

One must applaud what our colleagues in the USA have accomplished on behalf of the Society of Cardiovascular Anaesthesiologists with respect to training and certification of anaesthetists in perioperative TOE.[1–3] Although Europe was the birthplace of TOE, acceptance and introduction of TOE into the practice of anaesthesia have taken much longer here, and the process is evolving quite differently in each country. A brief account of the present state of training and certification in Europe may be useful, particularly for readers who are pursuing certification in TOE, as well as for anaesthetists and intensivists who are about to start certification programmes in their respective countries. It is beyond the scope of this chapter to report in detail the situation in all European countries. Rather, we focus on two existing exemplary accreditation programmes – the German and the UK – and include brief comments based on our own experience as well as that of our colleagues.

Germany

The German Society of Anaesthesiology and Intensive Medicine (DGAI) were among the first to recognise the importance of training and certification in perioperative TOE. A certification committee appointed by the DGAI published practice guidelines for training and defined the requirements for certification in perioperative TOE in 1999 (Box 18.1).[4] To specify the contents of TOE education and to provide rules for training and certification, the guidelines were supplemented by detailed recommendations.[5] The certification committee supervises education programmes and regularly updates the guidelines. The theoretical part of the training takes place in accredited centres (24 accredited centres are presently listed) that organise courses in perioperative TOE. The accredited centres are authorised to impart required knowledge and skills and to confirm their acquisition by the trainees. The courses provide a minimum of 40 hours of teaching spread over a minimum of 4 days. Although the majority of lecturers are anaesthetists who are certified in TOE, cardiologists and cardiac surgeons also present selected topics. Under specified conditions, the certification committee can also accept theoretical lessons completed in a non-DGAI accredited institution, abroad, or in courses held by cardiologists. A maximum of 20 hours of this alternative theoretical education can contribute to the total of 40 hours required by the guidelines.

Every anaesthesia department that is using TOE on a regular basis and is practising it in accordance with the accepted guidelines can provide practical training. The certification guidelines require a total of 200 perioperative TOE

- Attendance at a structured echocardiographic study programme (40 hours)
- 200 perioperative TOE examinations, personally performed under supervision, including 50 TOE studies in cardiac surgical cases
- Regular application of perioperative TOE for more than 1 year
- Board certification in anaesthesiology
- Proof of cognitive and technical skills in an examination (1 hour)

TOE = transoesophageal echocardiography.

Box 18.1 Requirements for certification in perioperative TOE in Germany

examinations under the guidance and supervision of an instructor. The latter is usually a certified anaesthetist, but he or she may also be a cardiologist who is certified in echocardiography. The supervision includes discussing the interpretation of findings and approval of final reports written by the trainee. The reports must be made available to the certification committee on demand. Documentation of the TOE findings varies among training centres, and efforts are currently being undertaken to develop standards that allow quality assurance and benchmarking, particularly in cardiac anaesthesia.[6] Although the duration of training is not specifically limited, the training centres must take appropriate measures to ensure that the trainees can perform the required number of TOE studies in a reasonable period of time. The studies should cover a wide range of pathologies observed in operative medicine, intensive care, and emergency care. Although a minimum of 50 cardiac surgical studies is required, not all of the required 200 studies should be performed in patients undergoing cardiac surgery. To account for the still growing and not yet fully established use of perioperative TOE, the DGAI committee currently considers the validation of practical training on an individual basis.

The supervising instructor or the certified director of the respective department gives confirmation of an individual's practical experience. In accredited centres the anaesthetists can acquire the preconditions for certification in perioperative TOE without any restrictions or controls. The validity of preconditions acquired in non-accredited institutions must be assessed on an individual basis by the certification committee.

Examination

Examinations are conducted in the accredited training centres by examination teams appointed by the certification committee. Each team consists of two examiners from two different training centres. At least one of these centres must be accredited. The candidates cannot be examined in the centres where they have trained. The examination is oral and can include a live study in a patient and/or questions based on a clinical case recorded on videotape. The anaesthetists who successfully complete the examination receive a certificate for "TOE in Anaesthesiology and Intensive Medicine".

To apply for the examination, applications should be submitted to the DGAI (Roritzer Strasse 27, D-90419 Nürnberg, Germany), and the DGAI will then forward them to the permanent certification committee.

United Kingdom

The Association of Cardiothoracic Anaesthetists (ACTA) has played a pivotal role in the development of intraoperative echocardiography in the UK. Under the auspices of the ACTA, eight training centres within the UK are currently offering "hands-on" courses in intraoperative TOE. The scope of intraoperative TOE appears to be extending into intensive care, and consequently the term "perioperative TOE" more accurately reflects this activity. The role of transthoracic echocardiography as a part of the training and certification process in perioperative echocardiography has been discussed and remains controversial. Because many preoperative and postoperative problems in the ICUs can be solved using the transthoracic approach, it would be desirable that the term "perioperative echocardiography" stand for both transthoracic and transoesophageal methods. However, UK anaesthetists have recently rejected the idea of having to conduct transthoracic echocardiography as a part of their accreditation process.

The British Society of Echocardiography (BSE) has developed and runs an accreditation process for transthoracic echocardiography. This successful programme was not intended to result in credentials for echocardiography but to offer a chance for BSE members to demonstrate their level of proficiency. It has awoken great interest in education and has been an important incentive

for the organisation of courses in echocardiography. Based on this experience and in response to increasing demand, the joint TOE accreditation committee of the BSE, including members of the ACTA, formulated a programme for UK accreditation in TOE. This accreditation is designed for all TOE users, including cardiologists, cardiac anaesthetists, echocardiography technicians, intensivists, and others. The accreditation is offered as a means of ensuring standards of training and practice in TOE; it is not intended as a compulsory or regulatory certificate of competence, or is it intended to be a device for the credentialing of individual practitioners. Because this TOE accreditation programme is based on the BSE accreditation for transthoracic echocardiography, it will also be administered by the BSE. Although the accreditation process is involved predominantly with TOE, an understanding of transthoracic echocardiography is also necessary because the two approaches are considered complementary.

Each candidate for accreditation must enrol with a suitable qualified supervisor who will undertake the candidate's training and supervision, and who can arrange for visits to other centres, should difficulties with obtaining an adequate case mix occur locally. The supervisors must be approved by the BSE committee based on their demonstration of competence in echocardiography and evidence of continuing practice in TOE. To maintain supervisor status, it will also be necessary for the supervisor to pass the BSE accreditation process by November 2005. There is currently no mutual recognition with other accreditation systems. Accreditation represents a minimum standard and cannot be regarded as a guarantee of continuing competence. After passing the examination, the physicians are expected to engage in continuing education toward re-accreditation. The re-accreditation process includes evidence of continuing clinical activity, correspondence courses, and attendance at courses and conferences.

The accreditation itself consists of two parts (Box 18.2): first, maintenance and presentation of a log book of activity and retention of images from 10 cases; and, second, attainment of a suitable standard in a multiple choice examination. The log book is collected over a period of up to 18 months and is composed of 150 studies. There are two options for collecting the required number of studies. One option takes into consideration the interests of the anaesthetist because it requires at least 50 perioperative TOE and up to 50 transthoracic studies. However, the minimum possible number of TOE studies is 100, but all 150 studies may be perioperative TOE. The second option favours cardiologists because up to 100 transthoracic studies can be accepted and the minimum of perioperative TOE studies is 10. A letter from the supervisor must be submitted with the completed log book certifying that the studies were completed by the candidate and that the candidate is safe to practice.

- Enrolment in the accreditation process with an approved supervisor
- Completion of a log book (set of copies of signed TOE reports) over a period of 18 months
- At least 150 studies, of which at least 50 must be perioperative TOE studies and up to 50 can be transthoracic studies
- Ten full TOE studies recorded, retained electronically or on video, and available for review at request
- A letter from the supervisor testifying that the candidate has performed and reported the 150 studies and is competent to practice
- Written examination (50 multiple choice questions based on video clips, 50 multiple choice questions based on theory)

TOE = transoesophageal echocardiography.

Box 18.2 Requirements for accreditation in TOE in UK

An example of a minimum portfolio of abnormal TOE studies, covering the most important pathologies, is as follows: at least five mitral valve repairs, two aortic dissections, and 10 left ventricular wall motion abnormalities. Ten full TOE studies with reports must be collected and retained electronically or on video. Views of all four cardiac chambers, including the atrial appendages, the aorta, the right and left pulmonary veins, and the inferior and superior vena cava should be shown. The acquisition of the views must be carried out according to published guidelines.[7,8] A minimum quantitative data set should include left ventricular diameter in systole and diastole, left ventricular wall thickness, and left atrial diameter, with additional measurements provided as appropriate for the pathology. These studies serve as the basis of the supervisor's letter and they must be available for review at the request of the accreditation committee at any time up to 2 years from the date of submitting the log book.

The written examination consists of a total of 100 multiple choice questions covering the

syllabus published by the BSE. The first 50 questions are based on video clips, whereas the second part is based on theory. The log book and images (if required) are assessed by members of a BSE examination board, which includes members of the ACTA. The examination board makes a report to the Chairman of the examination committee of the BSE. In order to achieve accreditation, candidates must satisfy the examiners in both written examination and log book elements.

Candidates should enrol for accreditation on the forms supplied and downloadable (from www.bcs.com/affiliates/bse.html), and send these to the BSE Administrator, 9 Fitzroy Square, London W1P 5AH, UK. Similarly, candidates should register for the examination (using forms downloadable from www.acta.org.uk, where examination dates are also posted).

France

At the present time, there is no national certification/accreditation programme in France for anaesthetists and intensivists in perioperative TOE. There are also no generally accepted guidelines regarding indications and practice of perioperative TOE, and considerable differences exist in application of the technique among the different regions and institutions. The French Society of Cardiology has published recommendations but has not yet taken into consideration the specific needs of anaesthetists and intensivists. Nevertheless, in at least two regions special programmes, including lectures, practical workshops, and a final examination, are regularly organised. In Paris this programme is organised by cardiologists with a common part for both cardiologists and anaesthetists, followed by separate courses for each speciality. In order to complete this programme, candidates must perform and interpret 100 transthoracic echocardiography and 50 TOE studies in an echocardiography laboratory under the supervision of a cardiologist. In certain circumstances, some of these studies can be conducted in an ICU under the supervision of a fully trained consultant. Each echocardiography study must be recorded in a log book and signed by the consultant. The total duration of this programme is 2 years. The trainees are encouraged to attend symposia and national congresses organised by the echocardiographic committee of the French Society of Cardiology. Interestingly, approximately 50% of physicians participating in this programme are anaesthetists (Guarin JP, personal communication, 2003). A special programme is also organised in Lyon by local cardiac anaesthetists. This programme has the same main characteristics as the Parisian one but lasts only 1 year. Our search on the website of the Société Française d'Anesthésie et de Réanimation (www.sfar.org) failed to identify any information on training or accreditation programmes in perioperative TOE.

Italy

Cardiac anaesthetists have been organising courses for TOE in Italy since 1999. In 2002, the Italian Association of Cardiothoracic Anaesthesiologists (IACTA) was founded and assumed responsibility for TOE in the setting of cardiothoracic anaesthesia and intensive care. For this purpose, the IACTA appointed a steering group on TOE, which has organised national courses in perioperative TOE since 2003 (for further information, e-mail cardioanestesia@virgilio.it). These courses include both a basic (3 days) and an advanced (3 days) course, with a wet lab in between. With regard to accreditation, the IACTA opted to follow the future programme that will be developed by joint committees of the European Society of Cardiology (ESC) and the European Society of Cardiothoracic Anaesthesia (EACTA; Ranucci M, personal communication, 2003).

Switzerland

In Switzerland, cardiac anaesthetists began using intraoperative TOE in the late 1980s. They also founded a working group for perioperative TOE, that has been organising courses and educational meetings since 1994. This early educational effort and experience resulted in the first European textbook on perioperative TOE written by anaesthetists and published in 1997.[9] Since 2000 the group has offered a 3 day course, which includes a wet lab and basic hands on experience in transthoracic echocardiography. In the beginning, separate basic courses were provided in German and French. Now both basic and advanced courses are taught in English and they take place at the same time. The information about the date, location, and content of the courses is available on the website of the Swiss Society of Anaesthesiology (Société Suisse d'Anesthésiologie et de réanimation/Schweizerische Gesellschaft für

Anästhesiologie und Reanimation [SGAR/SSAR]; www.sgar-ssar.ch). The working group, which was later promoted to the position of SGAR/SSAR committee for perioperative TOE, has defined the requirements for training of anaesthetists in TOE and proposed a curriculum consisting of both cognitive and practical skills that are prerequisites to taking the examination. The curriculum is based on one advanced level of competency in perioperative TOE that comprises 40 hours of theoretical education, 100 supervised TOE studies with a written report, and a final examination. The proposal was extensively discussed with and finally approved by the Echocardiographic Committee of the Swiss Society of Cardiology. Unfortunately, the board of directors of the SGAR/SSAR rejected the proposal, and it is unlikely in the near future that it will ever receive the necessary majority of votes at the annual assembly of the society. Had this proposal been approved, the physicians who successfully passed the examination would have received a diploma certifying their competency in perioperative TOE. As the situation now stands, at the end of each course a test is taken but no official certification is given.

The Netherlands and Belgium

In The Netherlands and Belgium it was the anaesthetists who began education in perioperative TOE. Initially, this education was limited to lectures combined with some hands on training, but for the past few years there has been a 2 day interdisciplinary and international course with two levels (basic and advanced), including theory lectures, wet lab, and specific sessions on "knobology" and technical explanations. (For information about this course, e-mail J.M.A.A.van.der.Maaten@anest.azg.nl or anne.ducart@ulb.ac.be.) Both the Belgian Society of Anaesthesia and Resuscitation and the Society of Anaesthesiology of The Netherlands acknowledge this course; accredited tests and/or examinations are not organised.

Other countries

It is not surprising that in the central and eastern European countries the perioperative use of TOE is only slowly increasing, and the possibility to become trained and use TOE in the practice of anaesthesia are still very limited. However, the situation is improving rapidly, as shown for instance by the successful organisation in early 2003 of the first course in perioperative TOE in Prague, Czech Republic. These countries may benefit from European training and certification programmes.

In the mid-1990s the EACTA started to prepare a European accreditation programme in perioperative TOE. Unfortunately, the project was abandoned because of a conflict of interests between EACTA and other societies. Recently, the EACTA has resumed its effort to organise the training and certification of anaesthetists in perioperative TOE on a European level. The ESC workgroup in echocardiography and the EACTA have come together and set up a joint group for TOE. The planned accreditation process will consist of two parts. The first part is a written examination on basic sciences and technology relevant to echocardiography, and clinical echocardiography interpretation. The ESC will administer the examination with an examining board drawn from both specialties. Second, there will be an accreditation of practical experience requiring the candidate to submit evidence of training under supervision, case mix, and a series of reports of TOE examinations (Feneck R, personal communication, 2003). Since 2002 the EACTA has organised a course in perioperative TOE, the details of which can be found on the EACTA website (www.eacta.org).

Conclusion

There are distinct differences in the evolving concepts of training and certification in TOE in anaesthesia. The German model is based on the central role of DGAI and its TOE certification committee, and is tailored to the needs of anaesthetists. In contrast, the UK programme was primarily developed and organised by cardiologists, although it is open to candidates from both specialities. The differences in the practice of TOE between cardiologists and anaesthetists were taken into account by including perioperative transthoracic studies. There is no doubt that the transthoracic approach is the method of choice for most preoperative and postoperative diagnostic questions. Consequently, the term "perioperative TOE" should indeed include both alternatives. Whereas the German programme requires participation in approved

courses, the UK programme leaves the acquisition of necessary knowledge to the personal initiative of the candidate. In contrast to the USA, neither the German nor the UK models distinguish between a basic and an advanced level. Furthermore, only the UK accreditation programme has a time limit for completion.

In conclusion, the necessity of training and certification in perioperative TOE in Europe has been universally recognised and has already resulted in a variety of courses, workshops, and training programmes. Cardiac anaesthetists, working in close cooperation with cardiologists, play a central role in this effort. These educational activities have been met with a lively interest among anaesthetists, intensivists, and surgeons involved in perioperative patient care. Unfortunately, many professional societies representing these physicians are not really engaged in this educational process and their support leaves much to be desired. There is no doubt that, in the near future, training in TOE will become an integral part of the curriculum of physicians who are responsible for patients who have been operated on, are traumatised, and are critically ill.

References

1 Aronson S, Thys DM. Training and certification in perioperative transesophageal echocardiography: A historical perspective. *Anesth Analg* 2001;**93**: 1422–7.

2 Cahalan MK, Abel M, Goldman M, *et al.* American Society of Echocardiography and Society of Cardiovascular Anesthesiologists Task Force Guidelines for Training in Perioperative Echocardiography. *Anesth Analg* 2002;**94**:1384–8.

3 Thys DM. Clinical competence in echocardiography. *Anesth Analg* 2003;**97**:313–22.

4 Loick HM, Greim CA, Roewer N, Van Aken H. Richtlinien zur Weiterbildung in der transösophagealen Echokardiographie für Anästhesisten: Indikationen – Ausbildung – zertifizierung "TEE in der Anästhesiologie". *Anasthesiol Intensivmed* 1999;**40**:67–71.

5 Greim CA, Rolf N, Ender J, Goetz A, *et al.* Transösophageale Echokardiographie in der Anästhesiologie und Intensivmedizin. Ueberarbeitete Empfehlungen für die Zertifizierung der Berufsbegleitenden Fortbildung. *Anasthesiol Intensivmed* 2001;**43(suppl)**:97.

6 Sauren B, Wyderka T, Zickmann B. Qualitätssicherung in der transösophagealen Echokardiographie (TEE): Validierung der standardisierten Datenerfassung bei Herzklappenoperationen. *Anasthesiol Intensivmed* 2002;**43 (suppl)**:97.

7 Flachskampf FA, Decoodt P, Fraser AG, *et al.* Recommendations for performing transoesophageal echocardiography. *Eur J Echocardiography* 2001;**2**: 8–21.

8 Shanewise JS, Cheung AT, Aronson S, *et al.* ASE/SCA Guidelines for performing a comprehensive intraoperative multiplane transesophageal echocardiography examination: recommendations of the American Society of Echocardiography Council for Intraoperative Echocardiography and the Society of Cardiovascular Anesthesiologists Task Force for Certification in Perioperative Transesophageal Echocardiography. *Anesth Analg* 1999;**89**:870–84.

9 Bettex D, Chassot PG. *Échocardiographie transoesophagienne en anesthésie-réanimation.* Paris: Masson Williams & Wilkins, 1997.

Index

Page numbers in **bold** type refer to figures; those in *italics* to tables or boxed material